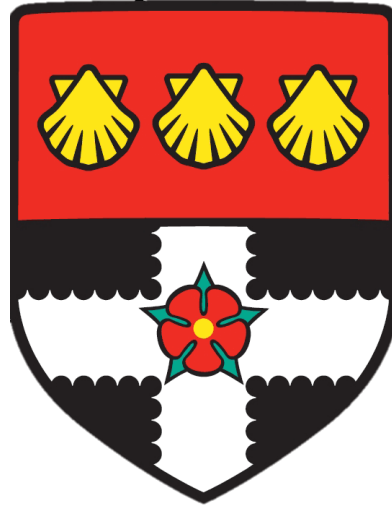


UNIVERSITY OF READING



**The dual kinase and scaffold function of Btk downstream
of GPVI and CLEC-2 in platelets**

A thesis submitted for the degree of Doctor of Philosophy

By Sophie Nock

Institute for Cardiovascular and Metabolic Research

School of Biological Sciences

November 2020

Declaration

I confirm that this is my own work and the use of all material from other sources has been properly and fully acknowledged.

Signed: Sophie Nock

Date: 4/11/2020

Abstract

Background

Bruton's tyrosine kinase (Btk) is a Tec family non-receptor tyrosine kinase found in platelets and B-cells. In platelets, Btk has demonstrated a role in facilitating both ITAM- and hemITAM-mediated platelet activation. Downstream of the B-cell receptor, Btk has been shown to induce signalling independently of its kinase domain, suggesting it may have a role as a scaffold protein.

Aims

To determine if Btk can act as an adaptor protein in platelets and to identify if there are differential roles of Btk downstream of GPVI and CLEC-2.

Methods

Indicators of platelet activity such as aggregometry, granule release and Ca^{2+} mobilisation, along with western blotting were used to study the effect of acalabrutinib, an inhibitor of Btk, downstream of GPVI and CLEC-2 mediated platelet activation. To identify a role for Btk kinase function downstream of GPVI and CLEC-2 signalling an NFAT-Luciferase reporter assay was used, expressing wild type or a kinase dead Btk mutant in Btk-deficient cells. Total Internal Reflection Fluorescence Microscopy (TIRFM) and Stochastic optical reconstruction microscopy (STORM) was used to investigate the co-localisation of Btk with other signalling proteins.

Results

At specific Btk inhibiting concentrations of acalabrutinib, platelet aggregation downstream of GPVI is normal despite loss of Btk pY223, an indicator of Btk activity and PLC γ 2 pY759 (PLC γ 2 active site) phosphorylation. In a cell line model, GPVI mediated signalling is maintained despite inhibition with acalabrutinib or expression of a kinase dead mutant of Btk. However, Btk kinase function is essential for CLEC-2 mediated signalling at submaximal concentrations of rhodocytin in platelets and in a cell line model but can be

overcome at high concentrations of rhodocytin. Btk colocalised more with the transmembrane receptor LAT than either GPVI or CLEC-2 on collagen or rhodocytin, respectively. A proportion of Btk colocalised with GPVI, with the localisation and clustering of Btk unaltered in the presence of acalabrutinib. However, Btk inhibition altered the clustering of GPVI suggesting a kinase dependent role of Btk in the clustering of GPVI.

Conclusions

Platelets can aggregate without Btk pY223 phosphorylation downstream of GPVI showing a scaffolding role for Btk. Furthermore, Btk does not require kinase activity to signal downstream of GPVI in a cell line model. Localisation of Btk does not change when its kinase activity is inhibited with a Btk-specific dose of acalabrutinib, suggesting kinase independent recruitment of Btk, providing further evidence of adaptor protein function downstream of GPVI. However, Btk kinase activity is required for signalling downstream of CLEC-2 at submaximal concentrations, as platelets fail to aggregate when Btk pY223 is lost. At high concentrations of rhodocytin when Btk is inhibited, platelets can still aggregate. Secondary feedback is likely mediating the aggregation of platelets. This demonstrates a novel difference between ITAM and hemITAM signalling.

Acknowledgements

Firstly an absolute massive shoutout to my supervisors. Alice and Craig. Craig and Alice – you guys can choose who goes last. Some people get 1 supervisor – I was lucky enough to get two and two fab ones at that! I am very thankful and appreciative for all the help, support, and time you have given me over the 4 years. Thanks to Alice for consistently telling me there is no such thing as a stupid question when I have always asked them. Thanks for all of the help teaching and explaining me the microscope and coming to me when I often forget 1 little switch. Thankyou for showing that it's possible to be wicked scientist and a mom at the same time, especially during lockdown. A lot of us think you're an such an amazing role model and the queen of always asking great questions in lab meetings. Thanks Craig for always checking my maths and for teaching me cell culture and bacteria way back when I first started. Thanks for all of the experiment advice by rubbish pictures on WhatsApp. Thanks for telling me that if I had a broken leg I would get help – that has really stuck with me and trying to help me think that not everything is my fault all the time. And thanks for running all those miles. 1:40 half soon enough I reckon, then a marathon!

Massive thanks to Mike Tomlinson for all of the Btk constructs, antibodies and emails about DT40's over the years. Big thanks to Johannes Eble for the rhodocytin also.

A huge, huge thankyou to Jon Gibbins and the whole of his lab for all the reagents, blood, and time both past and present. Huge thanks to Alex Bye and Amanda for all their helpful chats, ideas, and antibodies. Thanks to Tanya, Neline, Yasmin, Sez Ryan and Paru for being so kind, helpful and all round lovely!

Massive shoutout to all my other lab pals. In particularly, thanks Renato for laughing at our horrendous westerns together, Safa for always discussing what to wear, Carly for also finding funny platelet shapes when drawing around them in ImageJ too. Eva for being the best person to sit next to and introducing us to a Spanish wedding – I want chants at every wedding now! Marcin for repeatedly telling me the correct time to run an agarose

gel and for being a fab person. Charlotte for being a G-T-Bae and to being the best demonstrators ever! Daniel for dinking' and sinking' everything. Thanks to Jo for all the company whilst on opposite sides of the microscope / or hood -flow cytometer combo.

Huge thanks to my best friends Charl and Gem for being the ladies who lunch, the ladies in labcoats, and using the corridor between Lyle and Harborne as a catwalk. There is an end in friend, but no end in lab partner...For the secret crying stairs, hugs and laughs in and out of the lab I honestly can't thank you both enough. Thanks to Jodie too, for always backing me being a nerd even from school.

Thanks to my mom and dad who have given nothing but love and support, even if you couldn't give blood. Even when you have had no clue what I am going on about most of the time, you have always been at the end of the phone listening. Thanks for always being a phonecall and a 2-hour drive away, anytime. Thanks to Jas and Loz too, and for sending me pictures of baby Alfie when I am on microscope Alfie.

Lastly, a massive thankyou to my absolute better half, Jack. For putting up with so much, being so calm and kind always, and coming to pick me up if it was raining. I didn't dream I'd be writing my thesis with you just a room away, but it's made it a lot better.

Publications

Bye AP, Unsworth AJ, Desborough MJ, Hildyard CAT, Appleby N, Bruce D, Kriek N, **Nock SH**, Sage T, Hughes CE, Gibbins JM. Severe platelet dysfunction in NHL patients receiving ibrutinib is absent in patients receiving acalabrutinib. *Blood Adv.* 2017 Dec 12;1(26):2610-2623. doi: 10.1182/bloodadvances.2017011999. PMID: 29296914; PMCID: PMC5728643.

Nicolson PLR, Hughes CE, Watson S, **Nock SH**, Hardy AT, Watson CN, Montague SJ, Clifford H, Huissoon AP, Malcor JD, Thomas MR, Pollitt AY, Tomlinson MG, Pratt G, Watson SP. Inhibition of Btk by Btk-specific concentrations of ibrutinib and acalabrutinib delays but does not block platelet aggregation mediated by glycoprotein VI. *Haematologica.* 2018 Dec;103(12):2097-2108. doi: 10.3324/haematol.2018.193391. PMID: 30026342; PMCID: PMC6269309.

Nicolson PLR, **Nock SH**, Hinds J, Garcia-Quintanilla L, Smith CW, Campos J, Brill A, Pike JA, Khan AO, Poulter NS, Kavanagh DM, Watson S, Watson CN, Clifford H, Huissoon AP, Pollitt AY, Eble JA, Pratt G, Watson SP, Hughes CE. Low dose Btk inhibitors selectively block platelet activation by CLEC-2. *Haematologica.* 2020 Jan 16;haematol.2019.218545. doi: 10.3324/haematol.2019.218545. PMID: 31949019.

In preparation

Nock SH, Bye AP, Gibbins JM, Hughes CE, Pollitt AY. The regulation of GPVI clustering via Btk catalytic activity.

Presentations

Poster presentation – UK Platelet Group Annual meeting, Bath, UK. September 2017.

Poster presentation – 1ST Platelet Society early career researcher meeting, Manchester UK. July 2018.

Poster presentation – International Society on Thrombosis and Haemostasis, Melbourne, Australia. July 2019.

Poster presentation – Platelet society meeting, Cambridge, UK. September 2019.

Oral communication – European congress on thrombosis and Haemostasis. Glasgow, UK. October 2019.

Abbreviations

ACD - Acid citrate dextrose

ADP - Adenosine diphosphate

ANOVA - Analysis of variance

ATP - Adenosine triphosphate

AU – arbitrary units

BCR - B cell receptor

BLNK - B-cell linker protein

BSA - bovine serum albumin

Btk -Bruton's tyrosine kinase

Ca²⁺ - calcium ion

cAMP – cyclic adenosine monophosphate

CLEC-2 - C-type lectin-like receptor 2

CLL - Chronic lymphocytic leukaemia

COX-1 - Cyclooxygenase enzyme 1

CRISPR - Clustered Regularly Interspaced Short Palindromic Repeats

CRP-XL – cross linked collagen-related peptide

Csk – C-terminal Src Kinase

CVD – Cardiovascular disease

DAG - 1,2-diacyl-glycerol

DIC - Differential Interference Contrast

DioC6 - 3,3'-dihexyloxacarbocyanine iodide

DMSO - Dimethyl sulfoxide

ECM -Extracellular matrix

EC₅₀ – half maximal agonist concentration

EDTA – Ethylenediaminetetraacetic acid

EGTA – Ethylene glycol-bis(□-aminoethyl ether)-N,N,N',N'-tetraacetic acid

FBS - Fetal bovine serum

FcR γ - Fc receptor γ chain

Gads - Grb2 Related Adaptor Protein Downstream of Shc

GFP – Green fluorescent protein

GP - glycoprotein

GPCR - G protein coupled receptor

GPVI - Glycoprotein VI

GPO – Gly-Pro-Hyp

GPRP – Gly-Pro-Arg-Pro

hemITAM - hemi-immunoreceptor tyrosine-based activation motif

IC₅₀ – half maximal inhibitory concentration

Ig – immunoglobulin

IP₃ - inositol-1,4,5-trisphosphate

IS – immune synapse

ITAM - Immunoreceptor tyrosine-based activation motif

ITIM - Immunoreceptor Tyrosine-Based Inhibitory Motif

JAK2 - Janus kinase 2

LAT - Linker of Activated T cells

LTA – light transmission aggregation

M – Molar

mg – Milligram

Mg²⁺ – Magnesium ion

MgCl₂ – Magnesium chloride

Mins – Minutes

mL – Millilitre

μ g – Microgram

μ L – Microliter

μM – Micromolar

NaCl – Sodium chloride

NFAT - Nuclear factor of activated T cells

nm – Nanometre

nM – Nanomolar

NO – Nitric Oxide

ns – Not significant

Orai1 – Calcium-Release Activated Calcium Modulator 1

PBA – plate-based aggregation

PBS - phosphate buffered saline

PCA - Protein fragment Complementation Assay

PCC – Pearson correlation coefficient

PCR – Polymerase Chain Reaction

PECAM-1 - Platelet endothelial cell adhesion molecule-1

PGI₂ - Prostacyclin

PI3K - phosphoinositide 3 -kinase

PIP2 - phosphoinositide-4,5-bisphosphate

PIP3- phosphoinositide-3,4,5-trisphosphate

PH – pleckstrin homology

PKC - Protein kinase C

PLC β – Phospholipase β

PLC γ 2 - Phospholipase C gamma 2

PRP - Platelet rich plasma

PTEN - Phosphatase and tensin homolog

PVDF – polyvinylidene fluoride

pY – phosphotyrosine

R - Resting

RIPA buffer - Radioimmunoprecipitation assay buffer

RPMI – Roswell park memorial institute

SDS – sodium dodecyl sulphate

SDS-PAGE – sodium dodecyl sulphate polyacrylamide gel electrophoresis

SEM- standard error of the mean

SFK – Src family kinase

SH2 - Src homology 2

SH3 - Src homology 3

SHIP - SH2-containing inositol-5 phosphatase-1

SHP-1 – Src homology 2 domain-containing protein tyrosine phosphatase-1

SHP-2 – Src homology 2 domain-containing protein tyrosine phosphatase-2

SLP-76 – SH2 domain containing leukocyte protein of 76kDa

SNARE – soluble NSF attachment protein receptors

STORM – stochastic optical reconstruction microscopy

Syk – spleen tyrosine kinase

TAE - Tris Acetate EDTA

TBST – tris buffered saline with tween

TFK - Tec family kinase

TIRFM - Total internal reflection fluorescence microscopy

TPO – thrombopoietin

TX_{a2} – thromboxane

U46619 – 9,11-Dideoxy-11 α ,9 α -epoxymethanoprostaglandin

U/mL – Unit/millilitre

V -volts

Veh / V – vehicle

v/v – Volume/Volume

VWF – von Willebrand Factor

w/v – Weight/Volume

XID - X-chromosome-linked immune-deficiency

XLA - X-linked agammaglobulinemia

Y – tyrosine

YFP – Yellow fluorescent protein

Table of Contents

| | |
|---|-------|
| List of Figures | xxiii |
| List of Tables | xxvii |
| 1 Introduction | 1 |
| 1. Platelets..... | 1 |
| 1.1.1 Platelets in haemostasis..... | 1 |
| 1.1.2 Platelet ultrastructure..... | 2 |
| 1.2 Common platelet activation and thrombus formation..... | 3 |
| 1.2.1 Calcium release and granule release | 3 |
| 1.2.2 Shape change and spreading..... | 4 |
| 1.2.3 Release of ADP as a secondary mediator | 4 |
| 1.2.4 Thromboxane A2 production and release as a secondary mediator | 5 |
| 1.2.5 Integrin shape change and fibrinogen binding | 5 |
| 1.2.6 Stable thrombus formation..... | 6 |
| 1.3 GPVI and FcRγ..... | 10 |
| 1.3.1 GPVI Ligands..... | 12 |
| 1.3.2 Structure..... | 14 |

| | |
|---|----|
| 1.3.3 Signalling..... | 16 |
| 1.3.4 Non haemostatic functions | 18 |
| 1.4 ITAM signalling in other cells..... | 20 |
| 1.5 CLEC-2..... | 21 |
| 1.5.1 Ligands..... | 21 |
| 1.5.2 Structure..... | 23 |
| 1.5.3 Function in haemostasis..... | 24 |
| 1.5.4 Signalling..... | 26 |
| 1.5.5 Non-hemostatic roles of CLEC-2 | 30 |
| 1.5.5.1 Blood lymphatic development | 30 |
| 1.5.5.2 Inflammation | 30 |
| 1.5.5.3 Cancer | 31 |
| 1.6 Differences in ITAM and HemITAM mediated signalling..... | 32 |
| 1.7 Tec family kinases | 34 |
| 1.7.1 General | 34 |
| 1.7.2 Bruton's Tyrosine Kinase (Btk) | 35 |
| 1.7.3 Clinical relevance of Btk mutations | 40 |
| 1.7.4 Tec..... | 41 |
| 1.8 Btk inhibitors | 43 |
| 1.8.1 Ibrutinib | 43 |
| 1.8.2 Acalabrutinib..... | 45 |
| 1.8.3 Btk inhibitors in non-ITAM mediated signalling events and experiments under flow | 46 |

| | |
|--|----|
| 1.8.4 The platelet function of patients taking ibrutinib and acalabrutinib. | 48 |
| 1.9 Aims and Hypothesis. | 51 |
| 1.9.1 Differences in ITAM and hemITAM signalling | 51 |
| 1.9.2 Btk kinase activity in B cells..... | 51 |
| 1.9.3 Localisation of proteins..... | 52 |
| 1.9.4 Aims and hypothesis | 53 |
| 2.1 Materials and Methods..... | 54 |
| 2.1.1 Agonists and inhibitors | 54 |
| 2.1.2 Antibodies | 54 |
| 2.1.3 Other reagents | 57 |
| 2.2 Methods..... | 58 |
| 2.2.1 Human Washed Platelet Preparation..... | 58 |
| 2.2.2 Light transmission aggregometry..... | 58 |
| 2.2.3 Western blot platelet sample production..... | 59 |
| 2.2.4 Immunoprecipitation | 59 |
| 2.2.5 SDS-PAGE and Immunoblotting..... | 60 |
| 2.2.6 Calcium Flux..... | 61 |
| 2.2.7 Flow cytometry | 61 |
| 2.2.8 Platelet spreading microscopy..... | 62 |
| 2.2.9 Cells and plasmids | 62 |
| 2.2.10 Transfections and luciferase assay..... | 63 |
| 2.2.11 Flow cytometry of DT40 cells..... | 64 |
| 2.2.12 DT40 Lysates and microscopy..... | 64 |

| | |
|---|----|
| 2.2.13 Creation of DT40 CRISPR Btk knockout..... | 65 |
| 2.2.14 Creation of DT40 CRISPR Btk knockins..... | 69 |
| 2.2.15 DT40 DNA extraction and Touchdown PCR..... | 72 |
| 2.2.15.1 DNA extraction..... | 72 |
| 2.2.15.2 Touchdown PCR..... | 72 |
| 2.2.16 Total internal reflection fluorescence microscopy (TIRFM) and Stochastic optical reconstruction microscopy (STORM) sample preparation..... | 73 |
| 2.2.17 TIRFM image analysis..... | 73 |
| 2.2.18 STORM imaging..... | 74 |
| 2.2.19 STORM analysis..... | 74 |
| 2.2.19.1 LAMA..... | 74 |
| 2.2.19.2 Plot profile..... | 75 |
| 2.2.19.3 ClusDoC: Cluster detection with degree of colocalization..... | 75 |
| 2.2.20 Statistical analysis..... | 76 |
| 3 Btk inhibitors inhibit CLEC-2 mediated platelet functions more severely than GPVI mediated function..... | 77 |
| 3.1 Introduction..... | 77 |
| 3.1.1 Btk deficient platelet function downstream of GPVI and CLEC-2..... | 77 |
| 3.1.2 Btk inhibitors downstream of GPVI..... | 78 |
| 3.1.3 Btk inhibitors downstream of CLEC-2..... | 79 |
| 3.2 Aims and hypothesis..... | 82 |
| 3.3 Results..... | 84 |
| 3.3.1 Establishing conditions to assess CLEC-2 signalling in washed platelets..... | 84 |

| | |
|--|-----|
| 3.3.2 Ibrutinib inhibits (hem)ITAM mediated washed platelet responses more severely than acalabrutinib, with hemITAM responses more severely inhibited..... | 87 |
| 3.3.3 Platelets can aggregate at concentrations despite loss of the autophosphorylation site downstream of GPVI..... | 95 |
| 3.3.4 CLEC-2 phosphorylation is only reduced in ADP sensitive washed platelets at high concentrations of ibrutinib, but not acalabrutinib. | 99 |
| 3.3.5 Btk phosphorylation is inhibited downstream of CLEC-2 in washed platelets.... | 103 |
| 3.3.6 ADP Sensitive platelets are less severely inhibited by acalabrutinib downstream of GPVI and CLEC-2..... | 110 |
| 3.3.7 ADP sensitive platelets are less susceptible to inhibition by acalabrutinib downstream of GPVI..... | 114 |
| 3.3.8 Preparation of platelets depends on the degree on inhibition by ibrutinib and acalabrutinib to rhodocytin..... | 118 |
| 3.3.9 CLEC-2 mediated signalling of ADP sensitive platelets is not inhibited by acalabrutinib..... | 123 |
| 3.3.10 Calcium flux downstream of GPVI is only inhibited at the highest concentration of acalabrutinib whereas acalabrutinib dose dependently inhibits calcium flux downstream of CLEC-2. | 127 |
| 3.3.11 Platelets do not spread on fucoidan but spread weakly on rhodocytin. | 133 |
| 3.3.12 Platelet spreading on collagen or rhodocytin is not inhibited by acalabrutinib. | 137 |
| 3.3.13 PI3K inhibition reduces platelet adhesion and spreading on collagen..... | 140 |
| 3.4 Discussion | 145 |
| 3.4.1 Aim - To identify if acalabrutinib causes platelet inhibition to a similar manner to ibrutinib | 145 |

| | |
|--|-----|
| 3.4.1.1 Ibrutinib inhibits both GPVI and CLEC-2 aggregation, granule release and fibrinogen binding more potently than acalabrutinib and CLEC-2 responses are more severely inhibited | 145 |
| 3.4.1.2 The phosphorylation of CLEC-2 is inhibited in the presence of ibrutinib but not acalabrutinib | 148 |
| 3.4.2 Aim - To characterise the effect of acalabrutinib downstream of GPVI and CLEC-2 using platelet aggregation, granule secretion and protein phosphorylation and to investigate where Btk lies in the CLEC-2 signalling cascade | 148 |
| 3.4.2.1 Dose dependent inhibition of platelet responses of acalabrutinib downstream of GPVI..... | 148 |
| 3.4.2.2 Dose dependent inhibition of platelet responses of acalabrutinib downstream of CLEC-2 and elucidating where Btk lies downstream of CLEC-2 | 150 |
| 3.4.3 Aim - To investigate if rhodocytin can support platelet spreading and if it can, to investigate if acalabrutinib can inhibit platelet adhesion and spreading to rhodocytin and to compare this with collagen | 154 |
| 3.4.3.1 Acalabrutinib does not inhibit GPVI or CLEC-2 mediated spreading or adhesion..... | 154 |
| 3.4.3.2 The potential mechanism of Btk playing a dual scaffolding role..... | 155 |
| 3.5 Conclusions | 156 |
| 4 The use of the DT40 B cell line to investigate which functional Btk domains are required to convey GPVI and CLEC-2 signalling..... | 158 |
| 4.1 Introduction | 158 |
| 4.1.1 DT40 cells | 158 |
| 4.1.2 The study of signalling pathways using the NFAT Luciferase assay | 159 |
| 4.1.3 CRISPR-Cas9 | 164 |

| | |
|---|-----|
| 4.1.4 Domains of Btk required for signalling | 167 |
| 4.2 Aims of this chapter | 172 |
| 4.3 Results..... | 173 |
| 4.3.1 WT DT40 cells express Btk and PLC γ 2 whereas Btk Knockout cells only express PLC γ 2..... | 173 |
| 4.3.2 WT DT40 cells express Btk and PLC γ 2 when assessed using microscopy, whereas Btk deficient cells only express PLC γ 2..... | 175 |
| 4.3.3 Btk does not require a functional kinase domain to signal downstream of GPVI. | 178 |
| 4.3.4 Btk requires a functional kinase domain to signal downstream of CLEC-2..... | 182 |
| 4.3.5 Ibrutinib and acalabrutinib do not inhibit GPVI mediated signalling. | 186 |
| 4.3.6 Ibrutinib and acalabrutinib inhibit signalling downstream of CLEC-2..... | 189 |
| 4.3.7 The PH, SH3 and SH2 domain of Btk are required to mediate signalling downstream of GPVI. | 191 |
| 4.3.8 The PH, SH3 and SH2 domain of Btk are required to mediate signalling downstream of CLEC-2. | 197 |
| 4.3.9 Generation of a Btk deficient DT40 cell line using CRISPR-Cas9 gene editing. | 199 |
| 4.3.10 <i>Btk</i> gene is evolutionary conserved and sites for function altering CRISPR-Cas9 knockin mutations are present in Chicken <i>Btk</i> | 205 |
| 4.3.11 Design of CRISPR-Cas9 donor sequence for function altering knockin mutations in Chicken <i>Btk</i> | 208 |
| 4.3.12 CRISPR-Cas9 did not induce function altering knock-ins in the Btk PH, SH3 pr kinase domain..... | 210 |
| 4.3.13 An amino acid deletion in the SH2 domain renders Btk unable to signal downstream of GPVI. | 213 |

| | |
|---|-----|
| 4.4 Discussion | 217 |
| 4.4.1 Aim -To elucidate which domains of Btk are required to mediate NFAT-Luciferase signalling downstream of GPVI and CLEC-2 using an overexpression model | 217 |
| 4.4.1.1 DT40'S as a model for platelet signalling | 217 |
| 4.4.1.2 The use of the NFAT luciferase assay to measure intracellular signalling downstream of GPVI and CLEC-2 | 218 |
| 4.4.1.3 What domains of Btk are needed to mediate signalling? | 219 |
| 4.4.1.4 The PH domain of Btk is required to mediate signalling downstream of GPVI and CLEC-2..... | 220 |
| 4.4.1.5 The SH3 domain of Btk is required to mediate signalling downstream of GPVI and CLEC-2..... | 221 |
| 4.4.1.6 The SH2 domain of Btk is required to mediate signalling downstream of GPVI and CLEC-2..... | 223 |
| 4.4.1.7 The kinase function of Btk is required to mediate signalling downstream of CLEC-2 but not GPVI..... | 224 |
| 4.4.2 Aim - To genetically modify Btk using CRISPR-Cas9 to generate mutants to verify overexpression experimental models. | 225 |
| 4.4.2.1 CRISPR-Cas9 did not induce knock-ins for all the designed guides and donor sequences | 225 |
| 4.4.2.2 CRISPR-Cas9 KI experiments resulted in amino acid deletions in the SH2 domain of Btk, which renders it inactive | 226 |
| 4.5 Conclusions | 228 |
| 5 Total internal reflection fluorescence microscopy to identify the localisation of Btk in relation to GPVI, LAT and CLEC-2. | 229 |
| 5.1 Introduction..... | 229 |

| | |
|---|-----|
| 5.1.1 The location of Btk in platelets and B cells..... | 229 |
| 5.1.2 Total internal reflection fluorescence microscopy | 231 |
| 5.1.3 Colocalisation methods | 233 |
| 5.1.3.1 Pearson correlation coefficient | 234 |
| 5.1.3.2 Manders colocalisation coefficient..... | 235 |
| 5.2 Aims and Hypothesis | 236 |
| 5.3 Results..... | 238 |
| 5.3.1 Btk and GPVI do not colocalise on collagen fibres using TIRFM | 238 |
| 5.3.2 Btk kinase inhibitors do not alter the localisation of Btk..... | 242 |
| 5.3.3 Btk and GPVI are distributed throughout the platelet when spread on CRP-XL, and do not colocalise when imaged in TIRFM | 246 |
| 5.3.4 Btk and phosphotyrosine residues do not colocalise in TIRFM. | 248 |
| 5.3.5 Btk and LAT colocalise when spread on collagen and imaged in TIRFM | 251 |
| 5.3.6 Syk and GPVI colocalise when spread on collagen and imaged in TIRFM | 254 |
| 5.3.7 Btk and CLEC-2 colocalise when imaged in TIRF and spread on rhodocytin.... | 256 |
| 5.3.8 Btk and LAT colocalise when spread on CLEC-2 ligand rhodocytin and imaged in TIRFM..... | 258 |
| 5.4 Discussion | 261 |
| 5.4.1 Aim - To investigate the distribution of Btk in platelets | 261 |
| 5.4.1.1 Btk forms a punctate pattern when imaged in TIRFM..... | 261 |
| 5.4.2 Aim - To establish the localisation of Btk in relation to GPVI, LAT and CLEC-2 at the membrane using TIRFM..... | 262 |
| 5.4.2.1 Distribution of Btk in platelets spread on GPVI ligands..... | 262 |
| 5.4.2.2 Distribution of Btk in platelets spread on a CLEC-2 ligand | 264 |

| | |
|--|-----|
| 5.4.2.3 Possible reasons for the lack of colocalization between of Btk and other proteins in this study | 264 |
| 5.4.3 Aim - To identify changes in Btk localisation in the presence of a Btk inhibitor.. | 266 |
| 5.5 Conclusion | 267 |
| 6 Investigating the localisation and clustering of Btk, GPVI, LAT and CLEC-2 using Stochastic optical reconstruction microscopy..... | 268 |
| 6.1 Introduction | 268 |
| 6.1.1 Protein clustering as a mechanism of regulation..... | 268 |
| 6.1.2 Microscopy techniques and analysis methods used in this study..... | 270 |
| 6.1.2.1 Stochastic optical reconstruction microscopy | 270 |
| 6.1.3 Coordinate based colocalisation | 275 |
| 6.1.4 Density based spatial clustering of applications with noise (DBSCAN) | 277 |
| 6.1.5 Software used in this study..... | 278 |
| 6.1.5.1 ChriSTORM | 278 |
| 6.1.5.2 LocAlisation Microscopy Analyser - LAMA | 278 |
| 6.1.5.3 Cluster detection with a degree of colocalisation -ClusDoC..... | 278 |
| 6.2 Aims and Hypothesis | 280 |
| 6.3 Results..... | 282 |
| 6.3.1 Investigating protein clustering analysis using STORM and LAMA..... | 282 |
| 6.3.1.1 Btk and GPVI cluster on collagen..... | 283 |
| 6.3.1.2 Btk and GPVI cluster on CRP-XL..... | 286 |
| 6.3.1.3 Inhibition of Btk catalytic activity does not impact Btk clustering but does impact GPVI clustering | 289 |
| 6.3.1.4 Btk and LAT cluster on collagen..... | 292 |

| | |
|--|-----|
| 6.3.1.5 Btk and CLEC-2 cluster when platelets spread on rhodocytin | 295 |
| 6.3.1.6 Btk and LAT cluster when platelets spread on rhodocytin | 298 |
| 6.3.2 Colocalisation analysis using plot profile along a collagen fibre or line across a platelet | 301 |
| 6.3.2.1 Syk and GPVI colocalise to collagen fibres when evaluated using plot profile analysis | 303 |
| 6.3.2.2 Btk and GPVI partly colocalise in STORM on collagen..... | 306 |
| 6.3.2.3 Btk kinase inhibition does not change the amount of Btk and GPVI recruited to the collagen fibre | 309 |
| 6.3.2.4 When assessed using plot profile analysis Btk and GPVI do not strongly colocalise in platelets spread of CRP-XL | 312 |
| 6.3.2.5 Btk and LAT partially colocalise at collagen fibres when assessed using plot profile analysis..... | 315 |
| 6.3.2.6 Btk and CLEC-2 look to colocalise when spread on rhodocytin and examined using plot profile analysis..... | 318 |
| 6.3.2.7 Btk and LAT look to colocalise when spread on rhodocytin and examined using plot profile analysis..... | 321 |
| 6.3.3 Investigating the colocalisation of protein clusters | 324 |
| 6.3.3.1 Clusters of GPVI colocalise with Btk more than clusters of Btk with GPVI.. | 324 |
| 6.3.3.2 Btk kinase inhibition does not inhibit the number of GPVI or Btk clusters, or their colocalisation relative to each other. | 327 |
| 6.3.3.3 Btk and GPVI clusters do not colocalise on CRP-XL..... | 330 |
| 6.3.3.4 Btk preferentially localises with LAT when platelets spread on collagen..... | 333 |
| 6.3.3.5 Btk and CLEC-2 do not colocalise when platelets spread on rhodocytin | 336 |
| 6.3.3.6 Btk partially colocalised with LAT when platelets spread on rhodocytin..... | 339 |

| | |
|--|-----|
| 6.3.4 Results summary..... | 342 |
| 6.4 Discussion | 345 |
| 6.4.1 Aim - Investigate the localisation of Btk in relation to GPVI, LAT and CLEC-2 and verify the colocalisation results in chapter 5 | 345 |
| 6.4.2 Aim - To investigate the clustering of Btk on collagen, CRP-XL and rhodocytin..... | 347 |
| 6.4.3 Aim – To confirm if Btk recruitment and clustering is independent of its kinase function downstream of GPVI..... | 348 |
| 6.5 Conclusion | 351 |
| 7 General Discussion..... | 352 |
| 7.1 Summary of results..... | 352 |
| 7.1.1 What domains are important for Btk signalling?..... | 354 |
| 7.1.1.1 The PH domain of Btk is required for GPVI and CLEC-2 signalling..... | 354 |
| 7.1.1.2 The SH3 domain is required for GPVI and CLEC-2 signalling | 355 |
| 7.1.1.3 SH2 domain function is required for GPVI and CLEC-2 signalling..... | 356 |
| 7.1.1.4 The kinase function of Btk downstream of GPVI is not required..... | 357 |
| 7.1.1.5 The kinase domain of Btk is required at low concentrations, but not at high concentrations of CLEC-2 ligation..... | 360 |
| 7.1.2 The localisation of Btk, and differences between analysis methods..... | 363 |
| 7.2 Is Btk a psuedokinase or a scaffold protein?..... | 367 |
| 7.3 Use of Btk inhibition in COVID-19 treatment | 371 |
| 7.4 Conclusion | 377 |
| 8 References | 381 |

List of Figures

| | |
|---|-----|
| Figure 1.2.1 Schematic of haemostasis in response to vascular injury..... | 9 |
| Figure 1.3.1 Platelet GPVI signalling..... | 17 |
| Figure 1.5.1 Platelet CLEC-2 signalling | 29 |
| Figure 1.7.1 Tec family kinase structure..... | 34 |
| Figure 1.7.2 Domain structure of Btk..... | 35 |
| Figure 1.7.3 The interaction of Btk and phosphatidyl lipase signalling..... | 36 |
| Figure 1.7.4 Saratase dimer formation..... | 38 |
| Figure 1.8.1 Structure of acalabrutinib and ibrutinib adapted from Byrd et al., 2016... | 43 |
| Figure 2.2.1 Thermocycling conditions used to phosphorylate and anneal single oligonucleotides | 68 |
| Figure 3.3.1 Washed platelets respond to rhodocytin at high concentrations and 300 seconds is an appropriate time point to assess downstream CLEC-2 phosphorylation. | 86 |
| Figure 3.3.2 only high concentrations of Btk inhibitors inhibit GPVI washed platelets and Ibrutinib inhibits mediated α granule release and α IIb β 3 activation more than acalabrutinib mediated granule release | 92 |
| Figure 3.3.3 ibrutinib and acalabrutinib dose dependently inhibit CLEC-2 mediated platelet functions however ibrutinib is more potent. | 94 |
| Figure 3.3.4 Platelets can still aggregate downstream of GPVI when Btk and PLC γ 2 phosphorylation is lost | 98 |
| Figure 3.3.5 CLEC-2 phosphorylation is reduced in ADP sensitive washed platelets treated with ibrutinib but not acalabrutinib. | 101 |
| Figure 3.3.6 CLEC-2 mediated aggregation can occur where Btk phosphorylation is lost | 107 |
| Figure 3.3.7 Platelets cannot aggregate downstream of 100nM CLEC-2 when Btk phosphorylation is lost and there is a differential pattern of phosphorylation downstream of ibrutinib compared to acalabrutinib | 108 |

| | |
|--|-----|
| Figure 3.3.8 Platelet preparation effects their response to ADP and ADP sensitive platelets are less susceptible to Btk inhibition by acalabrutinib..... | 113 |
| Figure 3.3.9 Platelets can still aggregate downstream of GPVI when Btk and PLC γ 2 phosphorylation is lost | 117 |
| Figure 3.3.10 Platelet preparation effects their responses to rhodocytin in the presence of ibrutinib..... | 120 |
| Figure 3.3.11 Platelet preparation affects the response of their aggregation to rhodocytin in the presence of acalabrutinib | 122 |
| Figure 3.3.12 ADP sensitive washed platelets can aggregate to rhodocytin in the presence of acalabrutinib when Btk phosphorylation is lost..... | 126 |
| Figure 3.3.13 High concentration of acalabrutinib inhibits GPVI mediated calcium flux | 130 |
| Figure 3.3.14 High concentrations of acalabrutinib inhibit CLEC-2 mediated calcium flux | 132 |
| Figure 3.3.15 Platelets spread on collagen and rhodocytin but not fucoidan..... | 136 |
| Figure 3.3.16 Platelet spreading is not inhibited in the presence of acalabrutinib on collagen or rhodocytin..... | 139 |
| Figure 3.3.17 Addition of acalabrutinib does not further inhibit spreading with a PI3K inhibitor | 142 |
| Figure 4.1.1 NFAT-Luciferase reporter assay | 162 |
| Figure 4.1.2 Mechanisms of DNA repair using CRISPR-Cas9 gene editing | 166 |
| Figure 4.3.1 WT DT40's express Btk and PLC γ 2 | 174 |
| Figure 4.3.2 WT DT40's express Btk and PLC γ 2 | 177 |
| Figure 4.3.3 K430E plasmid has the mutation..... | 179 |
| Figure 4.3.4 Kinase dead Btk is sufficient for GPVI signaling | 181 |
| Figure 4.3.5 The kinase domain of Btk is required for CLEC-2 signalling | 184 |
| Figure 4.3.6 A high concentration of ibrutinib inhibits GPVI signalling whereas acalabrutinib does not in a cell line model..... | 188 |
| Figure 4.3.7 Ibrutinib and acalabrutinib inhibit CLEC-2 signalling in a cell line model | 190 |
| Figure 4.3.8 PH, SH3 and SH2 domain mutant plasmids have the mutation expected | 193 |

| | |
|--|-----|
| Figure 4.3.9 The PH, SH3 and SH2 domains of Btk are required to mediate GPVI signalling..... | 195 |
| Figure 4.3.10 The PH, SH3 and SH2 domains of Btk are required to mediate CLEC-2198 | |
| Figure 4.3.11 The CRISPR-Cas9 design strategy to create a Btk knockout | 203 |
| Figure 4.3.12 The cloning of the selected guides into the plasmid and verification by sequencing that the insert is present..... | 203 |
| Figure 4.3.13 CRISPR-Cas9 can be utilised to generate Btk knockouts in DT40 cells and these knockouts behave as other Btk KO's | 204 |
| Figure 4.3.14 Btk is evolutionary conserved and CRISPR-Cas9 target sites are present in chicken Btk | 207 |
| Figure 4.3.15 Donor plasmids contain the designed 300bp insert | 209 |
| Figure 4.3.16 Expression of Btk post transfection with CRISPR-CAS9 R307K plasmids | 211 |
| Figure 4.3.17 R307K KI strategy resulted in two amino acid deletions that render Btk inactive downstream of GPVI..... | 216 |
| Figure 5.1.1 Principles of TIRFM | 232 |
| Figure 5.1.2 Co-occurrence and correlation based colocalisation analysis adapted from Aaron et al., 2018. | 234 |
| Figure 5.3.1 Btk and GPVI weakly colocalise | 240 |
| Figure 5.3.2 Inhibition of the Btk kinase domain does not alter the distribution and colocalisation of Btk using TIRFM..... | 245 |
| Figure 5.3.3 Btk and GPVI do not colocalise on CRP-XL | 247 |
| Figure 5.3.4 Btk and phosphotyrosines colocalise more out of TIRF than in TIRF ... | 250 |
| Figure 5.3.5 Btk and LAT colocalise in platelets when spread on collagen..... | 253 |
| Figure 5.3.6 Syk and GPVI colocalise when platelets are spread on collagen | 255 |
| Figure 5.3.7 Btk and CLEC-2 colocalise when spread on rhodocytin | 257 |
| Figure 5.3.8 Btk and LAT colocalise when spread on rhodocytin | 259 |
| Figure 6.1.1 Principles of STORM..... | 273 |
| Figure 6.1.2 Reconstructed STORM image of platelets | 274 |

| | |
|--|-----|
| Figure 6.1.3 Principles of CBC analysis | 275 |
| Figure 6.1.4 Schematic of DBSCAN | 277 |
| Figure 6.1.5 The analysis workflow taken in this study. ClusDoC workflow from Pajeon et al., 2016..... | 279 |
| Figure 6.3.1 GPVI and Btk cluster on collagen..... | 285 |
| Figure 6.3.2 Btk and GPVI cluster on CRP-XL..... | 288 |
| Figure 6.3.3 High concentrations of acalabrutinib inhibit the number of GPVI but not Btk clusters compared to vehicle control..... | 291 |
| Figure 6.3.4 Btk and LAT cluster on collagen..... | 294 |
| Figure 6.3.5 Btk and CLEC-2 cluster on rhodocytin | 297 |
| Figure 6.3.6 Btk and CLEC-2 cluster on rhodocytin | 300 |
| Figure 6.3.7 Plot profile analysis method | 302 |
| Figure 6.3.8 Syk and GPVI colocalise when spread on collagen and imaged in STORM | 305 |
| Figure.6.3.9 Btk and GPVI colocalise along collagen fibres when imaged using STORM | 308 |
| Figure 6.3.10 Treatment with Btk inhibitors can change the location of Btk and GPVI when analysed using the plot profile method..... | 311 |
| Figure 6.3.11 Plot profile assessment of Btk and GPVI colocalisation in platelets spread of CRP-XL | 314 |
| Figure 6.3.12 Btk can partially colocalise with LAT along collagen fibres when..... | 317 |
| Figure 6.3.13 Btk and CLEC-2 localise together in spread platelets on rhodocytin when analysed using plot profile analysis..... | 320 |
| Figure 6.3.14 Btk and LAT do not look to colocalise when assessed using plot profile when spread on rhodocytin | 323 |
| Figure 6.3.15 Cluster analysis of Btk and GPVI co-clusters | 326 |
| Figure 6.3.16 Acalabrutinib does not alter clustering of Btk and GPVI using ClusDoC329 | |
| Figure 6.3.17 Btk and GPVI do not localise when platelets are spread on CRP-XL . | 332 |
| Figure 6.3.18 Btk preferentially colocalises with LAT | 335 |

| | |
|---|-----|
| Figure 6.3.19 Btk and CLEC-2 do not strongly colocalise | 338 |
| Figure 6.3.20 Btk partially colocalises with LAT when platelets are spread on rhodocytin | 341 |
| Figure 6.3.21 Btk and CLEC-2 colocalise more than Btk and GPVI and there is no difference in the localisation of Btk and LAT on either rhodocytin or collagen. | 344 |
| Figure 7.2.1 Btk's interaction with phospholipid metabolism..... | 371 |
| Figure 7.4.1 Overview of the role of Btk downstream of GPVI and CLEC-2 | 379 |

List of Tables

| | |
|---|-----|
| Table 2.1.1 The primary antibodies used in this study..... | 54 |
| Table 2.1.2 Secondary antibodies used in this study | 57 |
| Table 2.2.1 The primers used in this study..... | 66 |
| Table 2.2.2 Component mixture for oligonucleotide phosphorylation and annealing .. | 67 |
| Table 2.2.3 Donor sequences used in CRISPR-Cas9 Btk KI experiments | 71 |
| Table 3.3.1 Calculated IC ₅₀ values in this study | 143 |
| Table 4.1.1 Describes the Btk domain functions and evidence that they are or not required to mediate signalling | 168 |
| Table 4.3.1 Primers used to sequence Btk plasmids with point mutations in this chapter | 179 |
| Table 4.3.2 Donor sequences for Btk CRISPR-Cas9 knockins | 209 |
| Table 4.3.3 The number of viable cell colonies post stable selection | 211 |

1 Introduction

1. Platelets

1.1.1 Platelets in haemostasis

Platelets are small anucleate cells found in the blood stream. The primary role of platelets is to maintain haemostasis. Without platelets, there is an increased risk of haemorrhage as patients with thrombocytopenia (low platelet count) have an increased risk of bleeding (Lo et al., 2016).

Within the healthy vasculature due to their size, shear forces and the presence of red blood cells, platelets flow near to the vessel wall. Factors including endothelial production of nitric oxide (NO) and prostacyclin (PGI₂) ensure platelets are kept in an inactive state (Whittle et al., 1978). Thrombosis is initiated during the rupture of an atherosclerotic plaque or damage to vessel walls. This exposes extracellular matrix proteins including fibronectin, laminin and collagen which recruit and activate platelets. Plasma circulating von Willebrand factor (VWF) binds to exposed collagen through its A3 domain (Bonney et al., 2006). The A1 domain of VWF then binds to Glycoprotein 1B, (GPIb α), one of the four subunits of the GPIb-IX-V complex upon the platelet surface. This decreases the velocity of the platelets causing them to roll at low speeds over the extracellular matrix (Savage et al., 2002).

Reduced platelet speed increases the likelihood of direct interactions to occur, such as the binding of collagen receptors GPVI and $\alpha_2\beta_1$ to collagen within the sub endothelium matrix. These contacts with collagen are stable and induce a tyrosine kinase signal transduction cascade which is discussed in more detail in Section 1.3.2.

Tyrosine kinase signal transduction results in the mobilisation of calcium (Section 1.2.1), causing granule secretion (Section 1.2.2) which results in a secondary wave of activation, leading to the activation of platelet integrin $\alpha\text{IIb}\beta_3$ (Section 1.2.3). Upon integrin activation

a stable thrombus is formed due to fibrinogen crosslinking between platelets (Ma et al., 2007).

1.1.2 Platelet ultrastructure

Platelets are anucleate cells with a volume of 7-10.5 μm^3 and a diameter of between 1 and 3.5 μm (Giles, 1981, Tocantins, 1938).

Platelet shape is maintained by its cytoskeleton which consists of microtubules and actin filaments. Consisting of α and β tubulins, microtubules are bundles which form a marginal ring, maintaining cell integrity and a resting discoid shape (Schwer et al., 2001).

Furthermore, actin filaments are located outside the microtubule band and are concentrated beneath the plasma membrane further contributing to the discoid shape.

Within the platelet cytoplasm are secretory granules – α -granules and dense granules. α granules are the most abundant type, with approximately 80 per cell. They contain molecules such as fibrinogen, von Willebrand factor (VWF) and P -selectin (Maynard et al., 2007). Furthermore, α granules contain coagulation factors, growth factors, chemokines and intracellular pools of several transmembrane receptors such as GPIb-V-IX and $\alpha\text{IIb}\beta_3$; therefore the levels of these receptors at the plasma membrane increase upon activation (Berger et al., 1996).

Dense granules are far less abundant, with approximately 3-5 per platelet. They are larger and contain ATP, ADP, Ca^{2+} , Mg^{2+} and serotonin (Meyers et al., 1982). The contents of dense granules are involved in regulating paracrine (same platelet) and autocrine (surrounding platelets) activation, resulting in a positive feedback activation loop of platelets.

1.2 Common platelet activation and thrombus formation

1.2.1 Calcium release and granule release

Calcium mobilisation is a downstream event common to all platelet receptors. In resting platelets, cytosolic calcium is maintained at approximately 100nM and this increases upon activation. At 1µM, calcium can initiate several processes within the platelet including, shape change, degranulation and inside-out activation of αIIbβ3 and therefore aggregation (Varga-Szabo et al., 2009). Elevation of calcium occurs from two major sources: release from intracellular stores and extracellular entry.

Both methods require activation of a phospholipase C isoform (PLC), a key family of enzymes in the platelet. Different receptors activate one of the two isoforms within platelets, PLCγ2 and PLCβ. Upon activation of PLCγ2, phosphoinositide-4,5-bisphosphate (PIP2) is hydrolysed to inositol-1,4,5-trisphosphate (IP₃) and 1,2-diacylglycerol (DAG) (Bird et al., 2004). IP₃ induces Ca²⁺ release from its stores in the endoplasmic reticulum by activating the Ca²⁺ permeable ion channel IP₃R. This results in the release of calcium from intracellular stores (O'Rourke et al., 1985). DAG activates protein kinase C (PKC) and together with the increase in calcium leads to degranulation and conformational change of αIIbβ3 (Kaibuchi et al., 1983, Shattil and Brass, 1987).

After the initial wave of platelet activation, platelets release their granular contents as described in Section 1.3. The mechanism of platelet granule release is dependent on SNARE proteins – soluble NSF (an ATPase) attachment protein receptors (Blair and Flaumenhaft, 2009). SNAREs are membrane associated proteins situated on platelet granules and the plasma membrane. The close interaction of the granule SNARE and membrane SNARE generates energy leading to membrane fusion and exocytosis of contents.

1.2.2 Shape change and spreading

As mentioned previously in Section 1.1.1, resting platelets are discoid in shape due to their actin and microtubule cytoskeleton. Both structures are polarised, meaning they dismantle from one end and grow in another. This is responsible for inducing platelet shape change.

Upon activation, the platelet initially turns spherical. This change in shape from discoid to spherical is due to the dismantling of actin components to form filamentous actin structures. In fact, in resting platelets 60% of actin is not in the filamentous form and there is a large pool that can form rapid filament growth upon activation (Hartwig and DeSisto, 1991).

During early adhesion and spreading on fibrinogen and laminin, the filamentous actin (F actin) can also form nodules within the platelet. These are dense F actin regions that contain proteins such as Src family kinases and Wiskott-Aldrich syndrome protein (WASP) (Calaminus et al., 2008, Poulter et al., 2015). The dynamic actin structures grow at the polarised end to form spiky protrusions – filopodia. The platelet then flattens, with branched actin filaments formed called lamellipodia (Bearer, 1995). Granules and organelles then become central and the final morphology of the spread platelet resembles a fried egg. This increase in surface area may act to provide a larger area for secretion and therefore more receptors, including $\alpha\text{IIb}\beta\text{3}$ to get to the surface to bind fibrinogen (Moroi et al., 2020). Furthermore, a larger surface from spreading provides more membrane to interact with the coagulation cascade, with some steps of this cascade being membrane dependent (Wu, 2015).

1.2.3 Release of ADP as a secondary mediator

After initial activation, the release of ADP from dense granules can initiate a second wave of platelet activation in an autocrine and paracrine manner. This is due to ADP receptors,

P2Y1 and P2Y12 being present on the platelet surface. P2Y12 is more abundant, with P2Y1 only accounting for around 20 to 30% of total ADP binding sites (Savi et al., 1998).

P2Y1 and P2Y12 are G-protein coupled receptors (GPCRs) and upon ADP binding induces signalling resulting in calcium mobilisation and aggregation (Jin and Kunapuli, 1998). P2Y1 initiates ADP mediated shape change and platelet aggregation through G_q proteins initiating a transient rise in cytoplasmic Ca^{2+} (Jin et al., 1998). Whereas P2Y12 receptors couple to G_i proteins, resulting in the amplification and stabilisation of the aggregation response (Jin and Kunapuli, 1998) .

1.2.4 Thromboxane A2 production and release as a secondary mediator

Many agonists have been shown to induce Thromboxane A2 generation (TxA_2), including ADP (Jin et al., 2002) and collagen (Valles et al., 1991). TxA_2 is produced from phospholipids by a multistep pathway. Initially, phospholipids are hydrolysed to arachidonic acid via phospholipase A2. Then the cyclooxygenase enzyme 1 (COX-1) catalyses the production of prostaglandin H2, and finally thromboxane A2 is produced from thromboxane synthase (Hamberg et al., 1975). Similarly to ADP, the thromboxane A2 receptor $TP-\alpha$ is a GPCR. This receptor facilitates a secondary wave of activation through G_q protein mediated activation of $PLC\beta$ (Hirata et al., 1996).

1.2.5 Integrin shape change and fibrinogen binding

On circulating platelets, the integrin $\alpha IIb\beta 3$ is present in a 'closed' confirmation (Figure 1.2.6.1). Made up of the αIIb subunit and the $\beta 3$ subunit in a heterodimer, it is one of the most abundant proteins on the platelet surface with 60,000 – 80,000 copies (Burkhart et al., 2012). Resting αIIb is in a bent conformation, often likened to a knee joint. When the

'knee' is bent, the conformation of the integrin is closed and therefore has a low affinity to bind fibrinogen (Xiong et al., 2002).

Upon platelet activation through either primary or secondary mediators, intracellular signalling results in the calcium flux and activation of Protein Kinase C. This results in activation of Talin and other cytoskeletal proteins to unclip the intracellular domain. This results in transformation of the extracellular domain (extension of the 'knee') into a high affinity state for ligands. This is termed inside-out signalling. The open confirmation of the integrin has an increased affinity to bind to arginine-glycine-aspartic acid (RGD)-containing ligands, which include VWF, fibrin and the major ligand, fibrinogen (Springer et al., 2008). The binding of platelets to fibrinogen leads to crosslinked bridges between platelets, allowing the formation of aggregates and leading to platelet plug formation (Ma et al., 2007).

Due to its vital role in stability and growth of a thrombus, $\alpha\text{IIb}\beta\text{3}$ is also a therapeutic drug target. The clinically used antagonist integrin reversibly binds and inhibits the integrin by preventing the binding of its other agonists (O'Shea and Tchong, 2002).

1.2.6 Stable thrombus formation

After the initiation of the platelet plug via previously discussed common platelet activation events (Section 1.2.1- 1.2.5), a final step must follow to stabilise the platelet plug into a thrombus. This prevents the disaggregation of platelets. Attachment of fibrinogen to $\alpha\text{IIb}\beta\text{3}$ initiates outside in signalling, and results in cytoskeletal reorganisation. This leads to the clot retraction, and resulting in increased stability of the haemostatic plug (Payrastre et al., 2000) (Section 7, Figure 1.2.6.1).

Whilst platelet activation and plug formation is occurring, the coagulation cascade becomes active. This involves activation of coagulation factors ultimately leading to the stabilisation of the clot. Prothrombin is cleaved to thrombin, which can mediate the formation of soluble fibrinogen to long insoluble threads of fibrin. Thrombin is also a

powerful activator of platelets through the PAR1 receptor (Kim et al., 2009a). Fibrin forms a mesh like network on aggregated platelets, providing structural stability to the clot (Hoffman and Monroe, 2001, Monroe and Hoffman, 2006).

Resting platelet

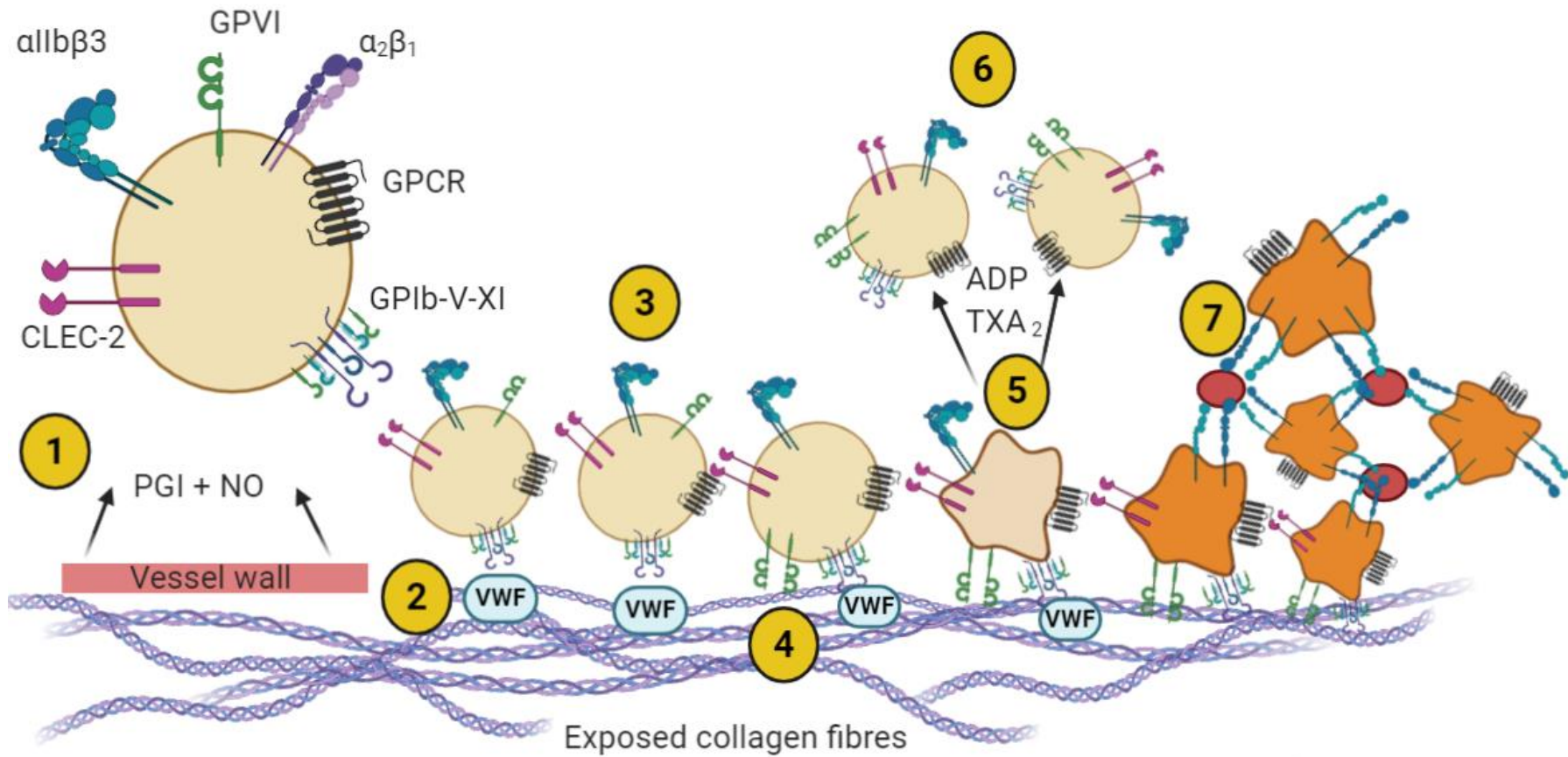


Figure 1.2.1 Schematic of haemostasis in response to vascular injury

(1) Platelets, with the receptors shown on their surface, in circulation are maintained in a quiescent state by the released of NO and PGI₂ from intact endothelial cells. (2) Injury to blood vessel exposes VWF and collagen present in the sub-endothelial matrix. At high shear rates, circulating platelets tether to the VWF through their GPIb-V-IX complex, which slows-down their movement. (3) This tethering facilitates platelet rolling along the sub-endothelium. (4) This reduced speed allows for GPVI to bind to collagen, which stimulates platelet signalling causing affinity upregulation of integrin αIIbβ3 and (5) secretion from α and dense granules. (6) Release of TxA₂ and ADP and activate more platelets in an autocrine and paracrine manner. (7) Activated integrin αIIbβ3 present on the platelet surface can now bind to fibrinogen (shown in red), which results in a platelet plug. The fibrinogen can then be converted to fibrin.

1.3 GPVI and FcR γ

After initial tethering of the platelet to the ECM, Glycoprotein VI, GPVI plays a major role in inducing platelet activation. GPVI is a receptor for collagen (Moroi et al., 1989), with around 9000 copies present upon the platelet surface (Burkhart et al., 2012). GPVI is constitutively associated with Fc receptor γ chain (FcR γ) (Gibbins et al., 1997). The FcR γ chain contains an immunoreceptor tyrosine-based activation motif (ITAM) - two YxxL/I sequences, with 7 amino acids between each of the two motifs (Reth, 1989).

The targeting of GPVI as an anti-thrombotic therapy is desirable due to its exclusive expression on the platelet-megakaryocyte lineage (Watkins et al., 2009, Senis et al., 2007).

People deficient in GPVI either through genetic mutations (Matus et al., 2013), or autoimmune antibodies against GPVI have mild bleeding disorders such as bruising (Moroi et al., 1989). Bruising is a well-tolerated side effect that can indicate altered hemostasis. After capillary damage, hemostasis may take longer to initiate and this causes more blood to flood to the area, causing bruising. This side effect is favoured as opposed to life threatening bleeds or gastrointestinal bleeding (often a cause of diarrhoea) which has been observed with some antiplatelet therapies (Mauri et al., 2014). Therefore, targeting GPVI and its signalling pathway may provide clinical benefit.

GPVI is a significant contributor to arterial thrombosis upon plaque rupture (Massberg et al., 2002). Studies using patients naturally deficient in GPVI or using function blocking anti GPVI antibodies have identified that GPVI is indispensable for the formation of stable aggregates on collagen (Moroi et al., 1996). Genetically modified mice to be deficient in GPVI (GPVI null) or FcR γ (FcR γ null) animals using targeted gene deletion also have a drastically reduced thrombus volume on collagen (Kato et al., 2003). Taken together, these show that GPVI has a role in the formation of stable aggregates under flow on collagen.

GPVI is cleaved by the Metalloproteinases of the a disintegrin and metalloproteinase (ADAM) family (Bergmeier et al., 2004, Gardiner et al., 2007, Bender et al., 2010). Using antibodies to induce cleavage of GPVI, and therefore decreasing its expression in mouse models, has also further provided evidence that GPVI deficiency is protective against a model of arterial thrombosis, induced by either ferric chloride or laser injury in the carotid arteries (Massberg et al., 2003). GPVI deficiency through this method has also been shown to be protective against a model of thromboembolism, where a bolus of collagen and epinephrine is injected into the mouse. In untreated mice, the percentage of mice that survived the procedure was very low. All the JAQ1 (anti GPVI antibody) treated mice survived. It was hypothesised that this could be due to diminished platelet counts as transient thrombocytopenia occurs when mice are injected with JAQ1. However, the procedures were performed after the platelet counts had returned to normal, but there was still no expression of GPVI on platelets when assessed by western blot (Nieswandt et al., 2001).

Mice deficient in GPVI via antibody depletion have a moderately increased bleeding time when compared to IgG treated mice. When compared against mice that have $\alpha\text{IIb}\beta\text{3}$ depletion (using the same method, but a different antibody), the bleeding time is shorter, suggesting that GPVI is a more desirable anti-platelet to protect against thrombosis but not greatly alter hemostasis (Nieswandt et al., 2001).

In contrast, a different group investigated the tail bleeding times of GPVI null mice. Compared to WT mice there is no significant difference in the bleeding time of these animals. Although, 3 of the 13 GPVI null mice subjected to the assay had a bleeding time of over 600 seconds, whereas no WT mice did (Kato et al., 2003). This suggests that in some individuals, GPVI is pivotal for hemostasis, whereas for others it is not. Another group has also published tail bleeding times to assess hemostasis with the GPVI null mice. There is no significant difference in the bleeding time when compared to WT controls, although it is increased by approximately 30 seconds. Whereas similarly to antibody depletion experiments, β3 null mice do have a prolonged bleeding time (Lockyer

et al., 2006). The sample size used for these experiments is much larger and therefore likely to be more reliable. Only the averages for each data were published and therefore it would have been interesting to identify if there were any outliers (bleeding times of over 600 seconds) as observed in the hands of Kato et al., 2003.

In humans, patients that have naturally developed anti-GPVI antibodies and therefore depleted GPVI surface levels do experience altered hemostasis such as easy bruising, epistaxis and gingival bleeding (Sugiyama et al., 1987, Arthur et al., 2007). This is consistent with patients naturally deficient in GPVI experiencing a mild bleeding diathesis (Moroi et al., 1989). Of note, these patients with autoimmune antibodies also have thrombocytopenia. This is because platelets that are coated with immunoglobulin G (IgG) are recognised and then phagocytosed by macrophages present within the spleen (Crow and Lazarus, 2003). The bleeding phenotype observed in these patients may be due to lack of platelets, as opposed to platelet function. Therefore, when developing antiplatelet therapies special care should be taken to ensure thrombocytopenia is not induced.

Nonetheless, GPVI is a desirable therapeutic target. There is development of a soluble GPVI-Fc fusion protein, Revacept (Ungerer et al., 2011), and downstream tyrosine kinase inhibitors such as Btk (Busygina et al., 2018) and Syk (Eeuwijk et al., 2016) to inhibit GPVI mediated signalling. Platelet activation by atherosclerotic plaque material is blocked by Revacept and is currently in Phase II clinical trials (Schüpke et al., 2019). This is a promising clinical target, as it does not seem to cause a bleeding phenotype, or thrombocytopenia which has been observed in patients with auto-antibodies against GPVI (Schüpke et al., 2019)

1.3.1 GPVI Ligands

Collagen is the main endogenous ligand for GPVI and plays the major role in facilitating platelet activation under shear stress. Upon vessel damage, collagen acts as an adhesive protein for platelets either directly through GPVI, $\alpha_2\beta_1$ or indirectly through GPIb-IX-V, as

well as an inducer of platelet aggregation. Collagen was identified as a mediator of thrombus formation as treatment of the sub-endothelium with collagenase, which denatures the collagen, prevents aggregation of platelets (Baumgartner and Haudenschild, 1972). Further cell line studies confirmed that collagen is a ligand for GPVI and that it promotes sustained signalling through this receptor (Tomlinson, et al 2007).

Integrin $\alpha_2\beta_1$ can also bind collagen. GPVI preferentially binds GPO amino acid sequences, whereas the integrin preferentially binds to GFOGER amino acid sequences (Jarvis et al., 2008). Using an $\alpha_2\beta_1$ function blocking antibody, the platelet response to collagen was altered. However the response to CRP-XL, a GPVI specific agonist consisting of GPO repeats, was not (Jarvis et al., 2002). The response to horm collagen (native type I fibrils from equine tendon and the collagen that was used in this study) was least affected by the function blocking antibody. Horm collagen was also confirmed to bind to GPVI, inducing activation and shape change, using FcR γ chain deficient mice (Jarvis et al., 2002). The lack of response to any GPVI agonist observed in FcR γ deficient mice is due the lack of expression of GPVI on the platelet surface, which is dependent on FcR γ chain expression *in vivo* (Nieswandt et al., 2000, Kato et al., 2003).

Fibrin is another endogenous ligand which causes similar tyrosine phosphorylation of the GPVI signalling cascade to collagen (Alshehri et al., 2015a) and can induce full spreading of murine platelets. Another independent group also identified that recombinant dimeric GPVI binds to fibrin, and further confirmed these results using GPVI deficient platelets as procoagulant activity (polymerisation of fibrinogen) was reduced (Mammadova-Bach et al., 2015). In those initial studies, neither group identified fibrinogen as being a ligand for GPVI using binding studies. Neither monomeric (shed from platelets) or recombinant dimeric GPVI became bound to fibrinogen (Alshehri et al., 2015a, Mammadova-Bach et al., 2015). Recently, it has been reported in human platelets that fibrinogen can bind and stimulate GPVI signalling as demonstrated using platelets deficient in GPVI not being able to spread on fibrinogen. Furthermore, platelets from mice expressing human GPVI fully spread whereas in contrast, WT mice do not (Mangin et al., 2018). Fibrinogen circulates

in plasma, which raised the question that if fibrinogen is a ligand for GPVI, why are platelets not constantly activated? However it has been theorised that binding of fibrinogen to monomeric GPVI would not induce the required clustering for activation, and therefore only when presented as a monolayer can it induce clustering and activation as evident in the work by Onseleer et al., 2017.

Recent work has come out opposing plasma fibrin as a GPVI ligand. Fibrin formed from recombinant fibrinogen looks drastically different to fibrin formed in plasma when assessed using super resolution microscopy. Fibrin formed in plasma has incorporated plasma proteins that cause large differences in the thickness of the fibrin strands and may be blocking GPVI binding and activation (Zhang et al., 2020)

GPVI does have exogenous ligands such as convulxin and collagen related peptide (CRP) respectively. Convulxin, a snake venom toxin, is able to induce platelet aggregation and adhesion (Francischetti et al., 1997, Jandrot-Perrus et al., 1997). It induces robust tyrosine phosphorylation in a cell line model (Tomlinson et al., 2007). CRP contains 10 repeats of Gly-Pro-Hyp, as this sequence is selectively bound by GPVI. It was found to induce potent platelet aggregation (Morton et al., 1995), however this only occurs after cross linking to induce a quaternary structure, mimicking collagen.

1.3.2 Structure

GPVI is approximately 62 kDa and belongs to the immunoglobulin superfamily. It has a total of 319 amino acids, with an additional N-Terminal 20 amino acids of signal sequence which is cleaved once GPVI reaches the membrane (Clemetson et al., 1999, Jandrot-Perrus et al., 2000). It is constitutively expressed with the Fc receptor γ chain (FcR γ) via a salt bridge between an Aspartic acid and an Arginine in the transmembrane domains of FcR γ and GPVI respectively (Berlenga et al., 2002). The FcR γ chain is a covalently linked homodimer, each chain containing an ITAM (Reth, 1989).

GPVI additionally contains a proline rich region where the Src family kinases Fyn and Lyn can bind via their SH3 domains (Ezumi et al., 1998, Suzuki-Inoue et al., 2002). It is hypothesised that some activated Lyn is constantly associated with the receptor (Schmaier et al., 2009). This 'primed and ready to go' complex enables fast initiation of signal transduction upon vessel injury; however it is unclear what prevents unwanted GPVI activation. It is suggested that the FcR γ chain may be dephosphorylated at a rate quicker than phosphorylation, and only upon GPVI activation is this overcome (Senis et al., 2014) and the level of receptor clustering plays a part.

On the surface of platelets, GPVI can be present as a monomer or a dimer (Miura et al., 2002). The monomeric form is predominant on resting platelets, with this structure having a lower avidity for binding collagen (Jung et al., 2012). On an activated platelet, the dimeric form is more prevalent and Horii et al., identified using molecular docking that the extracellular domains locate in a back to back dimeric structure which form the binding site for collagen (Horii et al., 2006). This study formed the basis for future work to identify that GPVI also expresses as a dimer upon the platelet surface in a resting state (Jung et al., 2009) and has a much higher affinity to binding collagen and CRP-XL (Jung et al., 2012).

Furthermore, it has been identified that GPVI can form oligomers on the platelet surface, with different GPVI agonists inducing a differing level of GPVI clustering (Poulter et al., 2017). This offers another mechanism of platelet regulation. The formation of oligomers may help to recruit signalling molecules required for GPVI signalling transduction.

The regulation of GPVI clustering is unknown. Tetraspanins are a family of transmembrane proteins which regulate lateral diffusion and clustering of proteins.

Tetraspanin Tspan9 is expressed on platelets, and knockouts of this have impaired GPVI function so it was believed that Tspan9 may play a part in modifying clustering of GPVI (Protsy et al., 2009). However, Tspan9 does not influence clustering when assessed using direct stochastic optical reconstruction microscopy (dSTORM) but does influence GPVI lateral diffusion when assessed using single particle tracking.

The clustering of GPVI is known to be Syk and Src family kinase independent. Using inhibitors at a concentration that inhibit phosphorylation and spreading, GPVI clusters were still able to be observed (Poulter et al., 2017).

Further regulation of GPVI signalling may be down to lipid rafts. One group found a significant amount of GPVI confined to lipid rafts in resting platelets (Wonerow et al., 2002). Whereas another independent group failed to identify any GPVI associated to lipid rafts in resting platelets, but large recruitment of GPVI to lipid rafts upon GPVI activation with convulxin (Locke et al., 2002). Recent proteomic analysis of lipid rafts from resting and GPVI stimulated platelets identified GPVI in lipid rafts in stimulated samples, and in basal samples but to a lesser extent (Izquierdo et al., 2019).

1.3.3 Signalling

Binding of Collagen or CRP-XL to GPVI initiates receptor clustering. This results in the phosphorylation of the ITAM within the FcR γ chain by Src family kinases Fyn and Lyn (Ezumi et al., 1998, Quek et al., 2000). This phosphorylated ITAM then recruits Syk via its dual SH2 domains (Chen et al., 1996). Syk is then phosphorylated by SFK's at position Y352 (Kurosaki et al., 1994), and is able to then undergo autophosphorylation at site Y525/6 (El-Hillal et al., 1997). The phosphorylation and activation of Syk enables phosphorylation of the adaptor protein Linker of Activated T Cells (LAT). Phosphorylated LAT, localised in lipid rafts (Wonerow et al., 2002) recruits Growth factor receptor-bound protein (Grb2), Grb2-related adapter protein downstream of Shc (Gads) and SH2 domain containing leukocyte protein of 76kDa (SLP-76) (Asazuma et al., 2000, Gross et al., 1999a, Hughes et al., 2008), forming the LAT signalosome. The LAT signalosome is essential in recruitment of phospholipase C γ 2 (PLC γ 2), with phosphotyrosine residues in LAT providing docking sites for PLC γ 2 via its SH2 domain (Watanabe et al., 2001).

In addition to tyrosine kinases, lipid kinases are also activated downstream of GPVI. Phosphoinositol 3 kinase (PI3K) is activated, which liberates PI(3,4,5)P₃ (PIP3) from

PI(4,5)P₂, (PIP₂) (Pasquet et al., 1999a). PIP₃ recruits Btk via its pleckstrin homology domain to lipid rafts present at the plasma membrane (Bolland et al., 1998, Várnai et al., 1999). Within the lipid rafts, Btk can be phosphorylated by SFK Lyn and Syk (Park et al., 1996, Rawlings et al., 1996). Additionally, both SFK's and Syk can also phosphorylate PLC γ 2 (Liao et al., 1993, Rodriguez et al., 2001), however it is believed the major kinase regulating PLC γ 2 phosphorylation is Btk (Quek et al., 1998). GPVI signalling can be visualised in Figure 1.3.1.

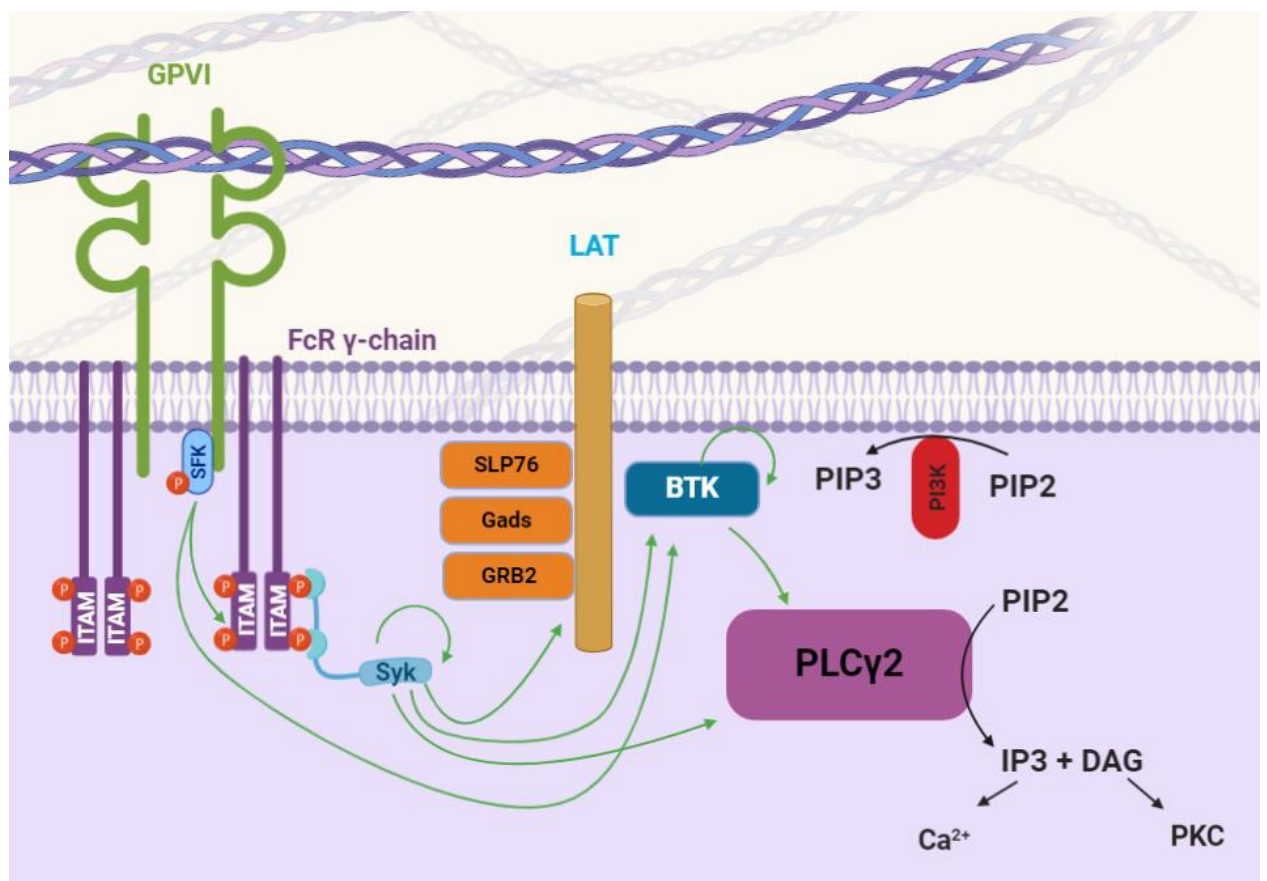


Figure 1.3.1 Platelet GPVI signalling

Collagen binds to GPVI and induces receptor clustering. This results in phosphorylation of the constitutively associated SFK's, which phosphorylate the dual YxxL motifs (ITAMS) in the FcR γ chain. This provides a site for Syk via its dual SH2 domains and Syk is

phosphorylated by SFK's. Syk is responsible for phosphorylating LAT, which recruits adaptor proteins SLP-76, Gads and Grb2. PI3K becomes active and is recruited to the signalosome. It catalyses the production of PIP3 from PIP2, which recruits Btk and PLC γ 2 where they can now interact with LAT in the signalosome. Btk is phosphorylated by SFK's or Syk, and together phosphorylated Syk and Btk mediate phosphorylation of PLC γ 2 resulting in PKC activation and calcium release. Kinases are shown in blue, adaptor proteins are shown in yellow and orange. Lipid metabolism shown with black arrows and tyrosine phosphorylation shown with green arrows.

1.3.4 Non haemostatic functions

Although its primary function is haemostasis, GPVI has been implicated in non-haemostatic functions such as the advancement of cancer metastasis. Galectin, a protein present on colon cancer cells, has been shown to bind GPVI (Dovizio et al., 2013). Furthermore, recent work by the Nieswandt group has identified that inhibiting GPVI using a function blocking Fab fragment, efficiently impairs platelet-tumour cell interaction and tumour metastasis (Mammadova-Bach et al., 2020).

Platelets are known to play a role in maintaining vascular integrity, as induced thrombocytopenic animals have endothelial thinning when analysed histologically. These animals also experience petechiae due to red blood vessel leakage via a more permeable endothelial layer (Hamberg et al., 1975, Kitchens and Weiss, 1975). This process is mediated by platelets and more specifically is maintained by platelet GPVI (Watson et al., 2010). The original hypothesis was that as laminin and collagen, GPVI agonists, are embedded in the endothelial layer and upon rupture, GPVI can bind and become active. The intracellular signalling results in α granule secretion, which promotes angiogenesis and lymphatic endothelial cell growth to repair the damaged endothelial layer (Kisucka et al., 2006).

The working hypothesis for GPVI being a key player in the maintenance of vascular integrity has been expanded. It is known that platelets can protect against haemorrhage during inflammation, as thrombocytopenic mice have augmented intra-alveolar bleeding during lung inflammation. This observed bleeding is not a result of thrombocytopenia, as a low platelet count does not cause haemorrhage unless there is inflammation present (Goerge et al., 2008). The proposed mechanism is that platelets act to seal the breach within the vessel wall after binding via GPVI to prevent inflammatory bleeding which was investigated using GPVI knockout platelets (Goerge et al., 2008, Gros et al., 2015). Of note, more severe inflammatory bleeding occurs in GPVI and CLEC-2 double knockout platelets as opposed to single GPVI knockouts, as CLEC-2 can provide some protection in this model which will be discussed later (Rayes et al., 2018).

Furthermore, it has been implicated that GPVI can play a protective role in another inflammatory condition – sepsis, induced by *Klebsiella pneumoniae*. Using a mouse model and antibody induced GPVI deficiency, bacterial load in the lungs and some distant organs was increased following infection with *K. pneumoniae* (Claushuis et al., 2018). GPVI activation promotes platelet leukocyte interactions, leading to enhanced phagocytosis of the bacteria. Interestingly, although GPVI has been shown to mediate platelet activation in response to *Staphylococcus aureus* (Hu et al., 2011), there are currently no reports that *K. pneumoniae* directly activates GPVI.

However, it is not clear whether GPVI can be protective in all methods of inducing sepsis. Using GPVI deficient mice in a cecal ligation and puncture model did not exacerbate clinical severity, whereas a receptor which has similar intracellular signalling as GPVI, CLEC-2, deficiency did (Rayes et al., 2017). The differences in bacteria and receptor depletion methods seem to influence the role of GPVI in sepsis.

1.4 ITAM signalling in other cells

ITAM's are not exclusive to platelets. ITAM's are commonly expressed within the hematopoietic lineage including B and T lymphocytes, macrophages and dendritic cells (Underhill and Goodridge, 2007). The B cell receptor (BCR) and T cell receptor (TCR) also signal through ITAM motifs.

The BCR signalling pathway is similar to GPVI signalling. BCR engagement induces phosphorylation of the ITAM by Src family kinases, creating docking sites for Syk via its SH2 domains (Rolli et al., 2002). PI3K is activated leading to recruitment of Btk via PIP3 (Saito et al., 2001). The formation of a signalosome is mediated by the adaptor protein B cell-linker molecule (BLNK) as opposed to LAT used for GPVI signalling, and Btk is able to be phosphorylated by Syk or Lyn (Rawlings et al., 1996, Park et al., 1996, Yang and Desiderio, 1997). Recruitment of proteins to the signalosome enables phosphorylation and activation of PLC γ 2, similarly to platelets.

The TCR signalling is divergent from BCR and platelet GPVI signalling due to differential expression of proteins; such as Zap-70 as opposed to Syk, lymphocyte-specific protein tyrosine kinase, (Lck) as opposed to Lyn, IL2-inducible T-cell kinase – Itk as opposed to Btk.

However, there are similarities. Upon TCR stimulation, Lck becomes active and phosphorylates the ITAMS present within the subunits of the receptor complex. This is comparable to how FcR γ chain is phosphorylated after GPVI stimulation. This leads to recruitment of Zap-70, which is then able to phosphorylate LAT and SLP-76 to mediate the formation of the LAT signalosome. Itk is recruited via the production of PIP3 from activated PI3K and interacts with SLP-76 and LAT via its SH2 and SH3 domains. Itk is then phosphorylated, and then is able to mediate activation of PLC γ 1 (Zhong et al., 2014).

1.5 CLEC-2

CLEC-2 is a 32 kDa type II transmembrane protein (Suzuki-Inoue et al., 2006) encoded for by the *CLEC1B* gene present on chromosome 12 (Navarro-Núñez et al., 2013).

CLEC-2 is referred to as a (hem)ITAM, due to it containing one YxxL motif within its intracellular domain as opposed to the dual YxxL motifs present in an ITAM receptor (Hughes et al., 2013).

There are 2016 ± 239 copies of CLEC-2 present on the platelet surface as analysed by flow cytometry (Gitz et al., 2014), consistent with the Burkhardt proteomic study which reported 3700 copies per platelet (Burkhardt et al., 2012). In contrast, mouse platelets express a considerably larger amount of CLEC-2, despite their smaller size, (approximately 20x more copies) (Dunster et al., 2020). The discrepancies in copy number may be related to function. CLEC-2 signalling may be more important in maintaining hemostasis for murine platelets, and this will be discussed in later Sections.

In contrast to GPVI, CLEC-2 expression is not limited to platelets and megakaryocytes (Jandrot-Perrus et al., 2000). CLEC-2 is expressed on liver sinusoidal endothelial cells (Chaipan et al., 2006), neutrophils and macrophages (Kerrigan et al., 2009).

1.5.1 Ligands

The first identified exogenous ligand, rhodocytin, was purified from *Calloselasma rhodostoma* (Shin and Morita, 1998). Before the identification of CLEC-2, rhodocytin was initially thought to interact with GPIIb α on the platelet surface (Suzuki-Inoue et al., 2001). It was also originally called aggrexin, and was also believed to interact with $\alpha_2\beta_1$, as aggrexin conjugated to sepharose was able to bind $\alpha_2\beta_1$ loaded liposomes (Suzuki-Inoue et al., 2001). Although this result is controversial as Eble et al., did not identify any binding between recombinant or WT $\alpha_2\beta_1$ which had been purified from platelets and immobilised rhodocytin. CLEC-2 was confirmed as the specific receptor that the snake venom

activates using knockout mouse models and function blocking antibody studies (Bergmeier et al., 2001).

Rhodocytin assembles as a tetramer composed of two α and two β chains (Shin and Morita, 1998). It induces tyrosine phosphorylation of CLEC-2 and many of the signalling molecules shared with the GPVI signal transduction pathway (Parguina et al., 2012).

Rhodocytin induces activation of CLEC-2 by inducing clustering of the receptor, causing platelet aggregation with a lag phase (Nagae et al., 2014, Watson and O'Callaghan, 2011).

Fucoidan has also been proposed as a ligand for CLEC-2. Indeed, fucoidan does induce platelet aggregation and granule release (Manne et al., 2013). Phosphorylation of Syk, LAT, SFK and PLC γ 2 is also observed, and is lost when treated with an SFK and Syk inhibitor, suggesting this agonist behaves similarly to a (hem)ITAM agonist. FcR γ chain knockout and CLEC-2 deficient mice were used to confirm that Fucoidan is an agonist for CLEC-2. Aggregation was lost at low fucoidan concentrations in the CLEC-2 knockout but maintained in the GPVI knockout (Manne et al., 2013). Further work using a higher concentration of fucoidan identified that CLEC-2 knockout mice can still undergo partial aggregation suggesting another receptor may also be partly responsible for mediating platelet activation. Indeed, using a double knockout model of GPVI and CLEC-2, no aggregation was observed in these mice even at high concentrations of fucoidan (Alshehri et al., 2015a). This demonstrates that Fucoidan can activate CLEC-2, but also partially activate other receptors.

More recently, a study has identified that fucoidan does not match the phosphorylation profile of rhodocytin, with key sites on Syk and PLC γ 2 not being phosphorylated.

Furthermore BAY 61-3606, a Syk inhibitor did not inhibit fucoidan mediated platelet aggregation (Kardeby et al., 2019). This is in contrast to previous studies which used the Syk inhibitors OXSI-2 and Go6976 which ablated the response to fucoidan (Manne et al., 2013). Both papers identifying Syk as the target of these inhibitors were from the same group (Bhavaraju et al., 2008, Getz et al., 2011). Indeed, Go-6976 was originally a protein

kinase C inhibitor and OXSI-2 is not deemed to be specific (Bhavaraju et al., 2008, Yaron et al., 2016). Therefore the inhibition observed with these 'Syk' inhibitors led the authors to believe that fucoidan was activating CLEC-2 signalling through Syk (Manne et al., 2013), when inhibition is likely to be due to off target effects.

The endogenous ligand, Podoplanin (also known as aggrus), is present throughout the body such as on lymphatic endothelial cells, cancer cells, brain cells, lung endothelial cells and kidney podocytes (Astarita et al., 2012). Podoplanin is not found circulating in the blood, and podoplanin has minimal expression in the subendothelium in the inferior vena cava vessel wall. However it is upregulated in the inflammatory condition deep vein thrombosis (DVT) (Payne et al., 2017).

Podoplanin is a glycoprotein, and upon glycosylation can bind CLEC-2. It binds to CLEC-2 in a similar way to rhodocytin (Nagae et al., 2014) and activates platelets leading to platelet aggregation (Suzuki-Inoue et al., 2007). Like rhodocytin, Podoplanin mediated aggregation also has a characteristic lag phase before inducing full aggregation *in vitro* (Chang et al., 2015, Christou et al., 2008). Platelet aggregation induced by cancer cells also has a characteristic lag phase and has been implicated in cancer metastasis (Kunita et al., 2007, Suzuki-Inoue et al., 2007).

It has been recently discovered that a product of intravascular haemolysis, hemin (the ferric, Fe³⁺ form of heme) is an agonist of CLEC-2. It induces aggregation, granule release and α IIb β 3 activation. Platelets could still aggregate when hFc-GPVI was preincubated with hemin, but not when hFc-CLEC-2, identifying that this was the true receptor (Bourne et al., 2020).

1.5.2 Structure

CLEC-2 has a cytoplasmic N-terminal domain, a single transmembrane region and extracellular C-terminal domain. Encompassed within the extracellular domain is a stalk region and a carbohydrate-like recognition domain for binding carbohydrates.

The cytoplasmic region of CLEC-2 consists of 31 amino acids. Within the cytoplasmic domain there is a single YxxL sequence – the hemITAM.

CLEC-2 is expressed on the surface as a homodimer (Figure 1.5.1), bringing two adjacent hemITAMs within close proximity (Watson et al., 2009). Like GPVI, clustering of CLEC-2 upon the surface determines the downstream signalling. Rhodocytin and podoplanin have two adjacent binding sites identified through crystallography (Hooley et al., 2008, Kato et al., 2008) and upon binding, it induces CLEC-2 clustering. Furthermore, evidence that the number of oligomerised CLEC-2 receptors increases upon activation with rhodocytin also supports this (Hughes et al., 2010b).

CLEC-2 undergoes glycosylation in the platelet. However, the reason for this is unknown. recombinant unglycosylated CLEC-2 expressed in bacteria was still able to bind to rhodocytin suggesting glycosylation does not modify the binding of CLEC-2 to its snake venom ligand (Watson et al., 2007).

1.5.3 Function in haemostasis

Mouse models have been used to assess the controversial role of CLEC-2 in hemostasis. May et al. developed CLEC-2 deficient platelets by consistent exposure of mice with an anti-CLEC-2 antibody. This initially induces transient thrombocytopenia, however then platelets are produced lacking CLEC-2. Under high and intermediate shear rates (1700 s^{-1} and 1000 s^{-1} respectively) CLEC-2 depleted platelets adhered to collagen but did not form a stable aggregate. Newly recruited platelets adhered but were released after a few seconds. This paper also identified that in CLEC-2 depleted mice there was an increase in tail bleeding time as a measurement of haemostasis. Furthermore, antibody treated CLEC-2 deficient platelets also had defective thrombus formation in a ferric chloride induced thrombus formation model as the time to occlude was significantly greater (May et al., 2009).

Initial work used a platelet specific CLEC-2 knockout mouse which was found to be embryonically / neonatally lethal (most pups die shortly after birth). This is due to cutaneous hemorrhage and failure of the blood lymphatics to separate (Suzuki-Inoue et al., 2010). To overcome this, and to be able to assess the function of CLEC-2 in mouse models of thrombosis and hemostasis, chimeric mice were utilised. WT mice were subjected to radiation to induce bone marrow failure. Fetal liver cells from the platelet specific CLEC-2 mouse were then injected into the tail to rescue the bone marrow failure mouse and change the phenotype. The mouse then produces CLEC-2 deficient platelets, which respond normally to other agonists but have abolished response to rhodocytin (Suzuki-Inoue et al., 2010). This study demonstrated that thrombus formation under collagen is impaired *in vitro*, along with *in vivo* arterial thrombosis when assessed in mesenteric capillaries in a laser injury model. However these mice do not have a significant increase in their tail bleeding times (Suzuki-Inoue et al., 2010).

Similarly, others report that CLEC-2 deficient mice do not have significantly different tail bleeding times using CLEC-2 chimeric mouse platelets (Hughes et al., 2010a). The methodologies are comparable to the work by Suzuki-Inoue and colleagues for the developing of platelets without CLEC-2. However, aggregation under flow was assessed at similar shear rates to May et al. and Suzuki-Inoue et al. In contrast to these two studies, the study by Hughes et al. identified that the platelets have normal aggregation on a concentration of collagen that is in between the two studies.

The method of using anti CLEC-2 antibodies to induce CLEC-2 depletion was also utilised and once again, tail bleeding time and thrombus formation was assessed. CLEC-2 depletion did not significantly increase tail bleeding times or have a significantly different thrombus size *in vivo* (Bender et al., 2013). The methodology of assessing the formation was similar as to previously published, using ferric chloride and mesenteric arterioles (Suzuki-Inoue et al., 2010, May et al., 2009). However, to analyse the data, Bender and colleagues considered the size of the vessel, whereas it is unclear if previous work did this. It would be expected that a larger vessel would cause a larger thrombus in WT mice,

so considering this biological variation of vessel size is important when investigating size of thrombi.

Lombard et. al., 2018 identified that human podoplanin can capture and activate human platelets under flow conditions, but not at physiological rates of shear. This alludes to a role for CLEC-2 in low shear and conditions at reduced flow. Indeed, CLEC-2 signalling is involved in deep vein thrombosis (DVT), which is a disease caused by a reduction and stasis of blood.

Deep vein thrombosis (DVT) is a thromboinflammatory disorder caused by the stagnation of blood which then becomes hypoxic. This then induces the release of inflammatory mediators; therefore, it is a thromboinflammatory condition. Using platelet inducible CLEC-2 knockout mice, it was demonstrated by Payne et al., that CLEC-2 exacerbates DVT as these mice do not form thrombi in a stenosis model compared to WT controls. Furthermore, CLEC-2 deficient platelets or podoplanin inhibition by an antibody showed reduced recruitment to the vessel wall showing that the CLEC-2 - podoplanin interaction is critical for DVT.

1.5.4 Signalling

Overall, hemITAM mediated signalling is similar to ITAM mediated signalling with many of the kinases being employed in both.

Similarly to GPVI signalling, upon either podoplanin (endogenous ligand) or rhodocytin (exogenous ligand) (Shin and Morita, 1998) stimulation, CLEC-2 dimers form oligomers (Hughes et al., 2010b). This recruits Syk to the hemITAMs where it is phosphorylated by Src family kinases (Mori et al., 2008), before it is able to undergo autophosphorylation similarly to ITAM signalling. Syk is essential in mediating CLEC-2 signal transduction (Severin et al., 2011, Spalton et al., 2009, Hughes et al., 2015) and when active, Syk is able to phosphorylate LAT, SLP-76, and SFK's can phosphorylate Btk. These proteins then work synergistically to enable phosphorylation of PLC γ 2, similarly to GPVI signalling.

Unlike GPVI signalling, it is known there is a requirement for secondary mediators to induce sustained CLEC-2 signalling (Pollitt et al., 2010, Manne et al., 2015b). ADP and a thromboxane A₂ mimetic could not induce phosphorylation of CLEC-2 alone, whereas rhodocytin could. Using inhibitors that block TxA₂ production (indomethacin) and scavenge ADP (apyrase), Pollitt et al., demonstrated that CLEC-2 phosphorylation is indirectly mediated by secondary mediators as CLEC-2 phosphorylation is greatly reduced in the presence of these inhibitors.

Like the function of CLEC-2 in hemostasis, the location of the receptor is also controversial. In platelets, it was first described as being present in lipid rafts (Pollitt et al., 2010). Using Brij – 58 as a detergent which disrupts the membrane but preserves lipid rafts, it was identified that the amount of CLEC-2 present in lipid rafts increases upon stimulation with rhodocytin. Furthermore, the amount of tyrosine phosphorylated CLEC-2 (and therefore activated) was greatly increased in the presence of rhodocytin suggesting that CLEC-2 signals in lipid rafts.

However Manne et al., argued that CLEC-2 was not found in lipid rafts. Using the same disruptor of lipid rafts as Pollitt *et al.*, the same result of reduced platelet aggregation to rhodocytin was observed. It was hypothesised that the altered CLEC-2 signalling was due to the disruption required secondary mediators TxA₂ and ADP which signal through GPCR's (Pollitt et al., 2010, Hardy et al., 2004, Hirata et al., 1996). Using a synthetic analog of ADP, platelets did not aggregate in the presence of methyl- β -cyclodextrin (M β CD), a cholesterol lowering agent which disrupts lipid rafts. This shows the dependency of ADP signalling on lipid rafts and it was therefore reasoned that this lack of aggregation to rhodocytin was due to the lack of required ADP signalling (Manne et al., 2015b).

To verify this, aggregation experiments were performed in the presence of a synthetic analog of ADP, M β CD and stimulated with rhodocytin to show that the response is the same. The experiments yield the same results of weak aggregation in the presence or

absence of ADP and from this, it is wrongfully concluded that the lack of aggregation is due to the disruption of ADP mediated G protein signalling.

Manne and colleagues did not investigate if TxA₂ signalling was altered with lipid rafts disrupted. TxA₂ was previously identified as the majority requirement for CLEC-2 signalling (Pollitt et al., 2010) and therefore it would have been interesting to see these results.

In protein phosphorylation studies, Manne and colleagues omitted the use of αIIbβ₃ inhibitor integrilin and therefore had aggregating platelet conditions. It is known that granule release of fibrinogen occurs in response to CLEC-2 (May et al., 2009) and that the integrin could become active. Therefore, the observed phosphorylation of PLCγ₂ in the presence of a lipid raft disruptor may be due to phosphorylation after outside in signalling (Huang et al., 2019). Another alternative explanation for the observed phosphorylation is the time point used to assess phosphorylation. Cells were lysed at 60 seconds, and phosphorylation of both Syk and PLCγ₂ is observed. This is unusually short, as it is known that CLEC-2 signalling has a characteristic lag time (Kato et al., 2008, Suzuki-Inoue et al., 2007). Indeed in later work by the same group, there is no phosphorylation at 60 seconds (Badolia et al., 2017). Therefore, the observed phosphorylation in the absence of lipid rafts may have been due to platelet pre activation due to experimental methods.

A more recent study could also not confirm the exact localisation of CLEC-2 (Izquierdo et al., 2019). This work stated that CLEC-2 was not found in lipid rafts. However four donors were assessed, with one donor presenting with CLEC-2 in the lipid raft fraction (stated in the supplementary materials), so it is not clear where CLEC-2 is localised. Membrane proteins are notoriously difficult to identify in proteomic studies due to their length and hydrophobicity (Eichacker et al., 2004).

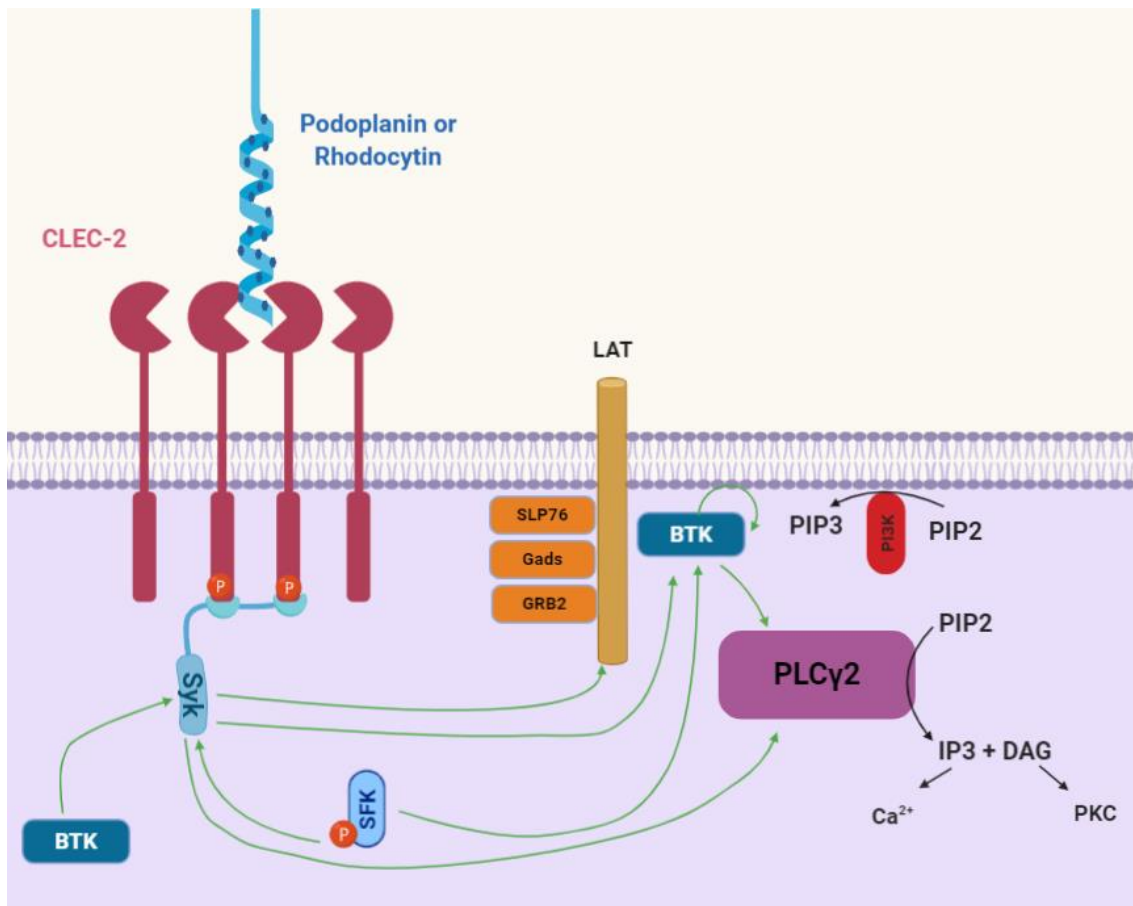


Figure 1.5.1 Platelet CLEC-2 signalling

Rhodocytin or podoplanin binds to CLEC-2 and induces receptor clustering. This provides dual YxxL motifs for Syk to bind to via its dual SH2 domains. Syk is then phosphorylated by SFK's. Syk is responsible for phosphorylating LAT, which recruits adaptor proteins SLP-76, Gads and Grb2. PI3K becomes active and is recruited to the signalosome. It catalyses the production of PIP3 from PIP2, which recruits Btk and PLCγ2 where they can now interact with LAT in the signalosome. Btk is phosphorylated by SFK's or Syk, and together phosphorylated Syk and Btk mediate phosphorylation of PLCγ2 resulting in PKC activation and calcium release. Btk is also proposed to be upstream of Syk by Manne et al. Kinases are shown in blue, adaptor proteins are shown in yellow and orange. Lipid metabolism shown with black arrows and tyrosine phosphorylation shown with green arrows.

1.5.5 Non-hemostatic roles of CLEC-2

1.5.5.1 Blood lymphatic development

There is a crucial role for the podoplanin/CLEC-2 axis in embryonic development. Global and platelet specific CLEC-2 knockout mice have blood lymphatic mixing and global KO's are not viable at birth (Finney et al., 2012, Hess et al., 2014). Furthermore, a mouse that cannot signal via CLEC-2 due to an amino acid point mutation within its hemITAM (Y7A) (Haining et al., 2017a), and mice deficient in key CLEC-2 signalling proteins such as Syk (Turner et al., 1995), SLP-76 (Clements et al., 1999) and PLC γ 2 (Ichise et al., 2009) also have a similar blood lymphatic mixing phenotype confirming that platelet CLEC-2 signalling plays a role.

Additionally, single knockouts of Btk or Tec have been reported to have normal blood lymphatic separation. However, the authors did not show WT controls for comparison making it difficult to confirm this result (Manne et al., 2015a). The authors of the same study also used double knockout mice, lacking both Btk and Tec, which did have severe blood lymphatic mixing (Manne et al., 2015a) which is consistent with other CLEC-2 or Syk deficient mice (Bertozzi et al., 2010). This suggests that Btk and Tec have a level of redundancy at that both must be absent for the phenotype to present itself.

1.5.5.2 Inflammation

Like GPVI, CLEC-2 plays a role in the prevention of haemorrhage induced by inflammation. HemITAM signalling plays a role in the thromboinflammatory disease, sepsis. Sepsis is a systemic inflammatory response which can result in multiple organ failure and death. In contrast to GPVI, in a cecal ligation and puncture model, CLEC-2 deletion via a platelet specific knockout increases measures of clinical severity such as organ damage (Rayes et al., 2017). This organ damage occurs due to the increased bacterial load caused by the inefficient recruitment and activation of macrophages (Rayes et al., 2017). CLEC-2 absence also accelerates lung function decline in a model of acute

respiratory distress syndrome (ARDS) (Lax et al., 2017). Taken together, these show a protective role for CLEC-2 in inflammatory conditions.

On the other hand it should be noted that CLEC-2 did not play a role in a sepsis model induced by *K. pneumonia*, and GPVI played the predominant protective role (Claushuis et al., 2018).

1.5.5.3 Cancer

Podoplanin is expressed on certain types of tumour cells including renal cell carcinoma and brain tumours (Shibahara et al., 2006). The interaction of platelet CLEC-2 and tumour podoplanin is believed to facilitate tumour metastasis, with increased podoplanin expression increasing malignancy. Blocking the podoplanin –platelet interaction using antibodies or depleting CLEC-2 reduces the metastasis of cancers. This implicates a role for the hemITAM bearing receptor in this process of cancer metastasis (Shirai et al., 2017).

1.6 Differences in ITAM and HemITAM mediated signalling

Although many of the components of (hem)ITAM mediated signalling are similar, there are some differences. These include the dependence of certain adaptors, actin polymerisation, and the requirement of lipid kinases.

Aside from the obvious difference of GPVI containing two YxxL motifs, and CLEC-2 only one, there are also differences in the kinases that mediate the phosphorylation of these motifs. Downstream of GPVI, the phosphorylation of the ITAM is mediated by SFK's (Ezumi et al., 1998, Quek et al., 2000, Suzuki-Inoue et al., 2002). The phosphorylated ITAMs then recruit Syk. Whereas downstream of CLEC-2, it is mediated by Syk as demonstrated with the Syk inhibitor R406, or absence of Syk, inhibits CLEC-2 mediated phosphorylation (Spalton et al., 2009, Severin et al., 2011).

One difference between GPVI and CLEC-2 mediated signalling is the requirement for actin polymerisation. Downstream of GPVI, aggregation is not blocked with high concentrations of an actin polymerisation inhibitor cytochalasin D. Whereas downstream of CLEC-2, aggregation was inhibited. Furthermore, phosphorylation of Syk and PLC γ 2 are inhibited in the presence of Cytochalasin D downstream of rhodocytin whereas they phosphorylation events are unaltered downstream of GPVI (Pollitt et al., 2010).

The absolute requirement of certain adaptor proteins differs between the two pathways. SLP-76 is an absolute requirement for GPVI mediated signalling as SLP-76 knockout platelets do not respond to convulxin (Judd et al., 2002, Sebzda et al., 2006). This lack of aggregation is not rescued in the presence of high concentrations of agonist. Whereas aggregation can be induced in SLP-76 KO platelets with high concentrations of rhodocytin, suggesting that there is a difference in the need for SLP-76 between the different pathways (Suzuki-Inoue et al., 2006). This has further been confirmed using Jurkat cells and a luciferase reporter assay. Jurkat T cells lacking SLP-76 could mediate

CLEC-2 signalling but not GPVI signalling (Fuller et al., 2007). This corroborates that although the SLP-76 plays a role in both pathways, the absolute requirement is different.

The necessity of PI3K activation is dissimilar downstream of GPVI and CLEC-2. PI3K is a lipid phosphatase that becomes active after GPVI (Laguerre et al., 1999) and CLEC-2 (Manne et al., 2015a) activation. It can also become active after outside-in signalling via $\alpha\text{IIb}\beta\text{3}$ (Battram et al., 2017). PI3K is recruited to the LAT signalosome via SH2 domains in its regulatory subunit, p85, and this allows its activation (Gibbins et al., 1998). It is then able to catalyse PIP2 into PIP3, which can recruit other proteins via PH domains.

Downstream of GPVI, PI3K activation is preferred as calcium flux is reduced in the presence of a range of PI3K inhibitors, but it is not abolished (Gilio et al., 2009).

Furthermore, this has been demonstrated in aggregation also, where in the presence of pan PI3K inhibitors wortmanin and LY294002, GPVI mediated aggregation to convulxin is largely reduced. However, in response to rhodocytin, aggregation is abolished (Manne et al., 2015a). This further shows a difference between GPVI and CLEC-2 signalling.

The requirement for secondary mediators in signal transduction is also different between the two receptors. CLEC-2 has an absolute requirement for secondary mediators ADP and TxA_2 (Pollitt et al., 2010, Badolia et al., 2017, Izquierdo et al., 2020). Whereas whole cell tyrosine phosphorylation induced by convulxin is normal in the presence of ADP antagonists and inhibitors of TxA_2 production (Atkinson et al., 2003b), demonstrating that GPVI does not depend on secondary mediators.

The final difference between the GPVI and CLEC-2 signalling cascades is that it is proposed by Manne et al. that Syk is downstream of Btk in CLEC-2 stimulated platelets. This is novel compared to how it is typically thought of in GPVI signalling. The Kunapali group propose that as a Syk inhibitor did not affect Btk translocation to lipid rafts and that Syk phosphorylation is inhibited at a concentration that Btk phosphorylation is inhibited, that Btk is upstream of Syk. This highlights another potential difference between the GPVI and CLEC-2 pathways, as it is known that in GPVI signalling, Btk phosphorylation is below Syk (Quek et al., 1998).

1.7 Tec family kinases

1.7.1 General

Tec family kinases are a family of non-receptor tyrosine kinases expressed in a range of hematopoietic cells. They are one of the largest family of cytoplasmic tyrosine kinases, alongside SFKs (Akinleye et al., 2013). Named after the first identified member, Tec, there are 4 other kinases present within the family – Btk, Itk, Bmx and Txk. The proteins have a similar protein structure as Figure 1.7.1 illustrates. Two tec family kinases have been identified in platelets, Btk and Tec, with them playing roles in (hem)ITAM signalling (Manne et al., 2015a, Quek et al., 1998).

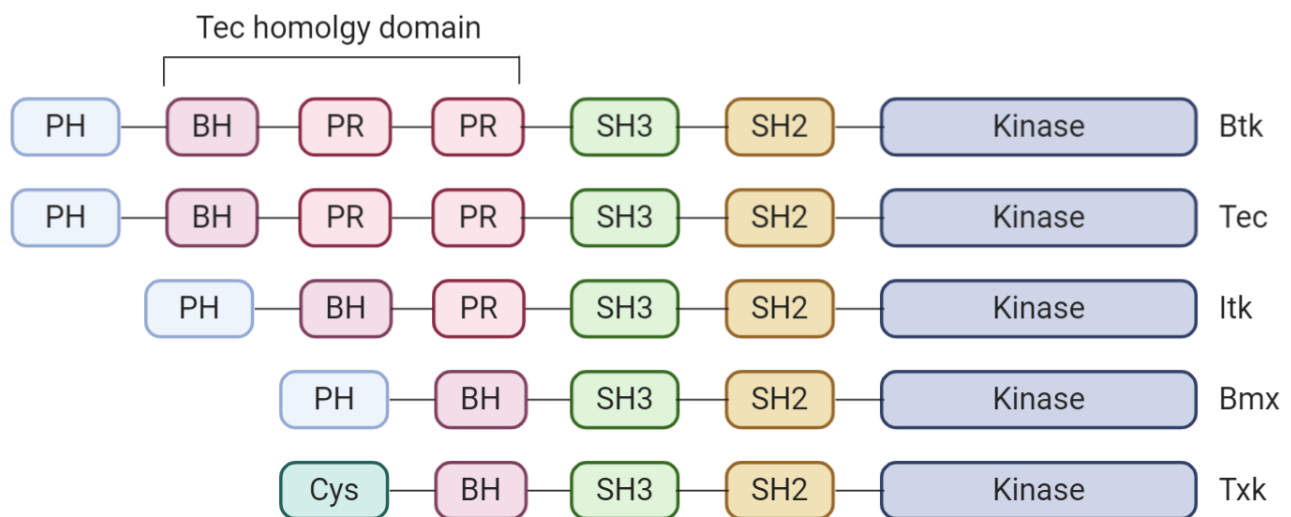


Figure 1.7.1 Tec family kinase structure

The TFK's are made up of a pleckstrin homology (PH) domain which can bind phosphatidylinositol lipids, a Tec homology domain which contains the Btk motif and two proline rich regions, an Src Homology 3 (SH3) domain which binds proline rich regions, a Src Homology 2 (SH2) domain which binds phosphotyrosines and finally a kinase domain.

1.7.2 Bruton's Tyrosine Kinase (Btk)

Bruton's tyrosine kinase (Btk), discovered by Ogdon Bruton in 1952, is a 659 amino acid protein with its structure and key phosphorylation sites highlighted in Figure 1.7.2. Under resting conditions, Btk is unphosphorylated, unable to induce phosphorylation and is localised to the cytoplasm (Figure 1.7.3, lower left) (Mohamed et al., 2000).

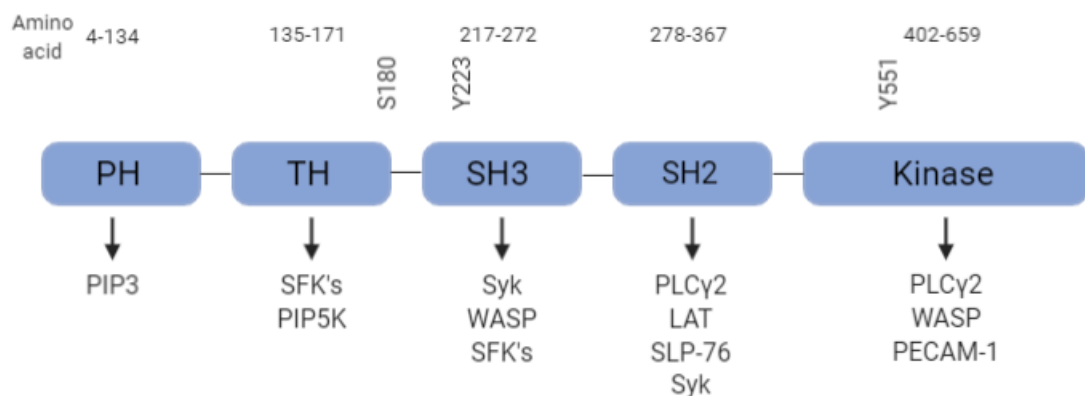


Figure 1.7.2 Domain structure of Btk

Btk is 659 amino acids long and contains a PH, TH, SH3, SH2 and a kinase domain with key protein interactions denoted below and phosphorylation sites listed above.

The N-terminal PH domain is required for translocation of Btk to the cell membrane upon production of PIP3 via PI3K (Várnai et al., 1999, Salim et al., 1996). Btk is one of the most abundant proteins that is bound to PIP3 when the PIP3 signalosome was investigated in platelets (Durrant et al., 2017). PH domains have the ability to bind any phospholipids, but the Btk PH domain preferentially binds to PIP3 (Salim et al., 1996). The PH domain of Btk has been shown to be required for initiating calcium flux in B cells (Takata and Kurosaki, 1996).

Adjacent to the PH domain is the TH domain. Figure 1.7.1 shows that this domain contains the zinc finger Btk motif (BH on Figure 1.7.1) and proline rich regions (PRRs). The PRRs of Btk have been shown to interact with Phosphatidylinositol-4-phosphate 5-kinase (PIP5K) (Saito et al., 2003). PIP5K is responsible for the catalysis of PtdIns[4]P (PIP) into PtdIns[4,5]P₂ (PIP2). Furthermore, the TH domain has been shown to provide the protein with stability (Vihinen et al., 1994a).

Neighbouring the TH domain is the SH3 domain, which is known to bind proline rich regions. The Btk-SH3 domain can bind to the proline rich region within its own TH domain *in vitro* (Patel et al., 1997). This self-folding provides a possible regulatory mechanism of Btk. Additionally, the SH3 domain can bind to PI3K (Saito et al., 2001) and work as a scaffold protein to ensure a complete loop of phosphatidyl lipid signalling as shown in Figure 1.7.3.

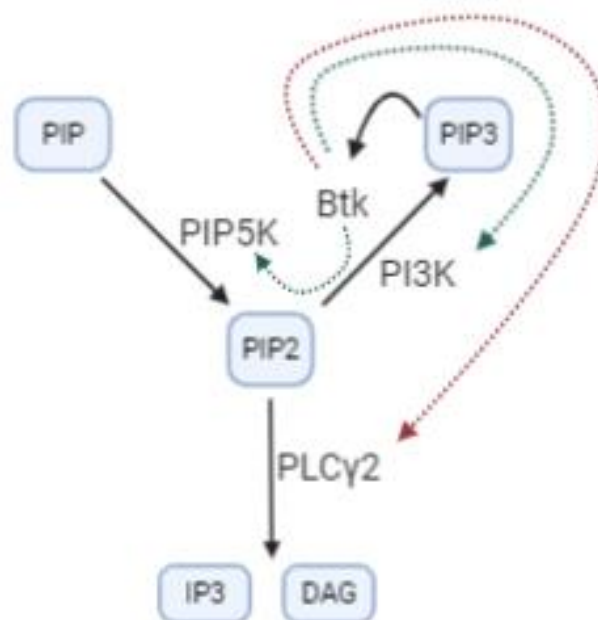


Figure 1.7.3 The interaction of Btk and phosphatidyl lipid signalling

The interactions of Btk and phosphatidyl lipid signalling. Btk can interact with PIP5K through its PRR in the Tec homology domain (interactions shown with green arrows). Btk

can interact with PIP3 via interactions in its PH domain. Interaction of Btk and PI3K is through the Btk SH3 domain. Btk can mediate phosphorylation of PLC γ 2. Lipid conversions are shown in Black and tyrosine phosphorylation is shown with red arrows.

SH2 domains bind to phosphotyrosine residues. It has been proposed that Btk can dock with many of the LAT signalosome proteins (Figure 1.7.2). Upon recruitment to the LAT signalosome, Btk can be trans-phosphorylated on site Y551 in the activation loop of the kinase domain (Wahl et al., 1997). This transphosphorylation is mediated by SFK's (Park et al., 1996, Rawlings et al., 1996, Dormann et al., 2001). Btk then undergoes phosphorylation at Y223 within the SH3 domain, rendering the kinase fully catalytically active. It is believed that this phosphorylation is mediated by self-phosphorylation (autophosphorylation) (Wahl et al., 1997), however it is unclear whether this phosphorylation could be mediated by another Btk molecule (Mohamed et al., 1999). Indeed, The PH of one Btk and the TH domain of another Btk have been shown to interact in a crystal structure forming the Saraste dimer (Hyvönen and Saraste, 1997). Recent work from two independent groups have provided strong evidence for PIP3 mediated Btk dimerization and phosphorylation at Y223 being mediated by another molecule of Btk (Chung et al., 2019, Wang et al., 2019b). This is illustrated in Figure 1.7.4.

Function altering point mutations and domain deletion studies have shown that the SH2 domain is essential for B cell signalling and calcium flux , however is not known if the same mechanisms play a role in Btk function in platelets (Fluckiger et al., 1998, Scharenberg et al., 1998, Takata and Kurosaki, 1996).

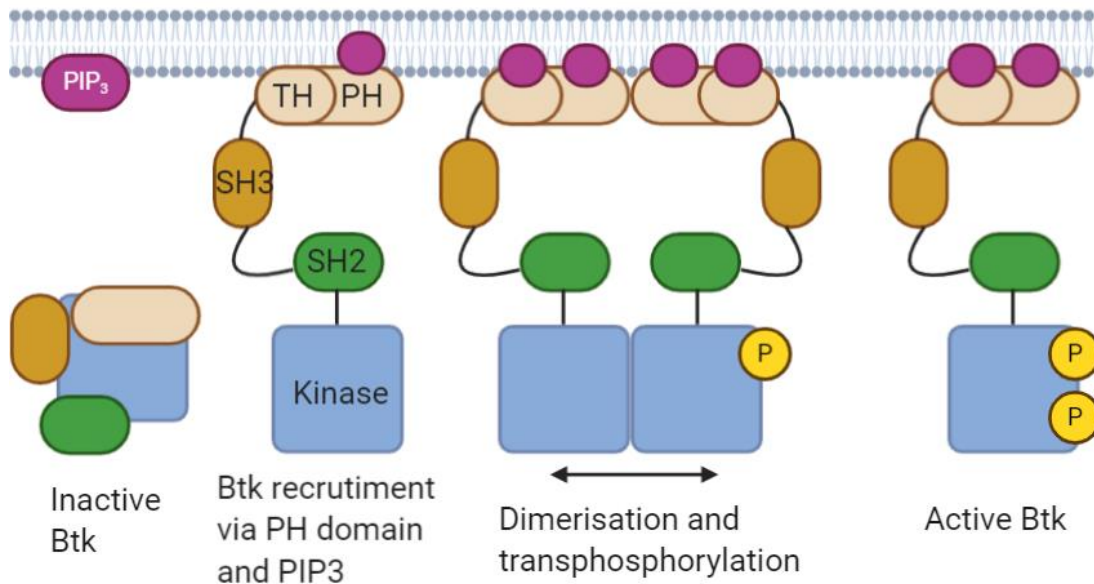


Figure 1.7.4 Saratase dimer formation

Btk is present in a closed inactive conformation (lower left). The production of PIP₃ (shown in purple) recruits Btk via its PH domain, where it forms an open shape and Btk can be transphosphorylated via SFK's (pY551). The PH-TH domains can undergo dimerization, bringing two kinase domains in close contact with one another promoting transphosphorylation (pY223). This results in an active form of Btk with phosphorylation at pY223 and pY551.

A domain that has been shown in some studies to be essential is the tyrosine kinase domain (Tomlinson et al., 2001). The kinase domain of Btk is comprised of approximately 250 residues (Vihinen et al., 1994b). Key amino acid residues within the kinase domain include K430. This conserved lysine is the adenosine triphosphate (ATP) binding residue. Kinase inactive mutants have an amino acid with a different charge meaning the triphosphate cannot bind (Mao et al., 2001).

Whether true Btk kinase activity is required to mediate signalling is controversial. It is known that Btk does have catalytic activity *in vitro* kinase assays and cell experiments. It has been shown that Btk can phosphorylate certain sites on PLC γ 2 in B cells, but in the absence of Btk there is some residual phosphorylation (Kim et al., 2004). Furthermore,

using the chicken B cell line DT40 deficient in Btk, phosphorylation of PLC γ 2 was reduced but not abolished. However, there is reduced IP $_3$ production and calcium flux (Takata and Kurosaki, 1996). In platelets, Btk has been shown to phosphorylate PLC γ 2 (partially) (Quek et al., 1998), Platelet endothelial cell adhesion molecule-1 (PECAM-1) (Tourdot et al., 2013) and suspected to phosphorylate β 3 (Bye et al., 2017). This suggests that Btk does require its kinase activity.

Phosphorylation of PLC γ 2 occurs on 4 sites – Y753, Y759, Y1197 and Y1217 (Watanabe et al., 2001). Y753 and Y759 are in the SH2-SH3 domain of PLC γ 2 whereas Y1197 and Y1217 fall within the C terminal region. Mutational studies of PLC γ 2 in DT40 cells proposed that tyrosine phosphorylation of PLC γ 2 in the SH2-SH3 region downstream of the BCR is partially required for activation; and these sites are mainly phosphorylated by Btk. However Syk can play a role in phosphorylating PLC γ 2 (Rowley et al., 1995, Rodriguez et al., 2001, Hashimoto et al., 1999a). Whereas the tyrosine phosphorylation in the C terminal (Y1197 and Y1217) is explicitly mediated by Btk (Watanabe et al., 2001).

Another study has confirmed that Btk predominantly phosphorylates Y753 and Y759 in PLC γ 2 in B cells, and these sites are required for activation (Humphries et al., 2004). Kim *et al*, also identified that phosphorylation of the SH2-SH3 region is required in B cells, and that this region is also phosphorylated in Ramos cells, Jurkats and Platelets (Kim et al., 2004). Furthermore, there is no phosphorylation of Y1217 downstream of convulxin stimulated platelets, and that pY1217 is also largely independent of Btk.

On the other hand, it has been proposed that kinase activity of Btk is not required. A recombinant oestrogen receptor bound version of Btk has been shown to mediate signalling with an inactive kinase (Tomlinson et al., 2001). Middendorp et al., 2003, also showed that a kinase inactive version of Btk is not required during B cell development to mediate PLC γ 2 phosphorylation and calcium flux. Furthermore, there was a peak of calcium flux, albeit greatly reduced compared to wild type, in a kinase dead version of Btk downstream of the BCR (Takata and Kurosaki, 1996). This suggests that a kinase

inactive mutant can partially mediate PLC γ 2 activation, and that therefore Btk could be possibly acting as a scaffold protein.

A requirement for the kinase function of Btk has been demonstrated with its interaction with Wiskott Aldrich Syndrome protein (WASP) in B cells (Guinamard et al., 1998). The interaction occurs through the Btk SH3 domain (Guinamard et al., 1998, Kinnon et al., 1997). In platelets, WASP is phosphorylated after GPVI stimulation (Oda et al., 2000, Oda et al., 1998) and this is blocked in the presence of wortmannin, a PI3K inhibitor. As production of PIP3 via PI3K is known to recruit Btk, it was hypothesised that this inhibition observed with wortmannin is due to the lack of Btk translocation. A study using Btk deficient (when assessed by western blot) X linked agammaglobulinemia (XLA) patients identified that phosphorylation of WASP is predominantly not mediated by Btk (Gross et al., 1999b, Oda et al., 2000). These patients do express Tec and it was proposed that this is mediating the phosphorylation of WASP as TFKs can have redundant roles (Atkinson et al., 2003a), however no other kinases were investigated in this study.

Negative regulation of Btk is controlled by Protein Kinase C. Serine 180 within the Tec homology domain (Figure 1.7.2) is phosphorylated and this initiates translocation away from the plasma membrane (Kang et al., 2001). Further evidence for this mechanism is provided from B cells deficient in PKC β which have prolonged and enhanced Btk tyrosine phosphorylation due to its close contact with tyrosine kinases (Leitges et al., 1996).

1.7.3 Clinical relevance of Btk mutations

The *Btk* gene is on the X chromosome, and gene mutations result in either total or partial deficiency and/or activity of Btk. This condition is called X-Linked Agammaglobulinemia (XLA). XLA is usually diagnosed during childhood as the affected children (most commonly males) manifest with reoccurring infections. Btk protein mutations / absence results in disrupted B cell signalling. This causes a reduction of mature B lymphocytes.

Less serum immunoglobulins are produced and consequentially, frequent infections occur. Therefore immunoglobulin transfusion is used as a treatment (Conley, 1985).

Sequence analysis of *Btk* is used to identify if a patient has XLA. These mutations have been uploaded to the Btkbase – a mutation database containing the sequence variants (Vihinen et al., 1996, Väliäho et al., 2006). Over half of the pathogenic variants are premature stop codons and frameshift variants resulting in improper processing of Btk mRNA. This results in patients not expressing Btk when detected by western blotting or flow cytometry (Hashimoto et al., 1999b, Gaspar et al., 1998).

Some patients express a 'leaky' phenotype, where the condition is not as severe, with some mature B lymphocytes circulating (Jones et al., 1996, Hashimoto et al., 1999b). Some 'leaky' patients have a mutation in the kinase domain causing reduced catalytic activity, therefore explaining the less severe phenotype (Gaspar et al., 2000). Further leaky patients have been identified, in which the mutations are not in the kinase domain. These patients have normal levels of Btk and Btk catalytic activity, but still have frequent albeit less severe infections. This suggests kinase function plays a large but not total role in the disease and other functioning Btk domains are required to prevent XLA.

Interestingly, XLA patients do not report bleeding as a side effect, even though the role of Btk in platelets has been shown (Quek et al., 1998). Cardiovascular side effects in these patients, such as hypertension are believed to be related to the use of intravenous immunoglobulin (Späth et al., 2015).

1.7.4 Tec

Tec is another member of the Tec family kinases present in platelets, albeit at a much lower copy number than Btk (1,300 copies of Tec, 11,100 copies of Btk) (Burkhart et al., 2012). It shares a similar structure to Btk (Figure 1.7.1) (Mohamed et al., 1999).

Tec has also been shown to directly phosphorylate PLC γ 2 *in vitro* (Zwolanek et al., 2014, Humphries et al., 2004) but there is less extensive research on whether the kinase activity of Tec is required to mediate signalling in cell-based assays. Furthermore, the phosphorylation sites in PLC γ 2 mediated by Tec are Y753 and Y759 which are the same as Btk (Humphries et al., 2004).

It is known that Tec is able to partially mediate GPVI signal transduction. Btk-deficient platelets undergo shape change in response to CRP-XL, and aggregate to collagen. However they are less responsive and require a higher concentration of agonist to induce aggregation. Furthermore, in Btk-deficient platelets, PLC γ 2 phosphorylation is not totally lost downstream of CRP-XL or collagen, alluding that Tec or other kinases such as Syk also have the ability to phosphorylate PLC γ 2 (Quek et al., 1998, Atkinson et al., 2003a). Additionally, using single knockouts of either Btk or Tec, or double knockouts (platelet specific) suggests that Tec is able to compensate for Btk in this pathway and others, such as Tec being able to phosphorylate WASP in the absence of Btk (Oda et al., 2000).

In contrast, downstream of CLEC-2, Tec is not believed to compensate in this pathway. The platelets of XLA patients do not aggregate even to maximal concentrations of rhodocytin (Nicolson et al., 2020). If Tec could compensate for Btk in CLEC-2 pathway, there would be some aggregation to this response.

Furthermore, after using inhibitors of Btk, the work by Chen et al., 2018, proposed that biochemical activity of Tec, measured in a range of *in vitro* kinase assays, did not correlate with platelet aggregation downstream of GPVI. The inhibition of Btk in the kinase assays strongly correlated with the potency of the Btk inhibitors in platelet aggregation (Chen et al., 2018). This suggests that Tec does not play a predominant role in mediating signalling downstream of either GPVI or CLEC-2.

1.8 Btk inhibitors

As Btk plays a role in mediating B cell receptor signalling, it is used as a therapeutic target in a B cell malignancy, chronic lymphocytic leukaemia, CLL. Chromosomal alterations in tumour suppressor genes or proteins that cause apoptosis, but not *Btk*, result in an increased number of small, mature appearing lymphocytes in the blood, bone marrow and lymph (Scarfò et al., 2016).

The B cell receptor signalling pathway is amplified in CLL and therefore inhibiting Btk is clinically beneficial. Ibrutinib, a first generation Btk inhibitor and acalabrutinib, a second-generation inhibitor are both used clinically to treat CLL as seen in Figure 1.8.1.

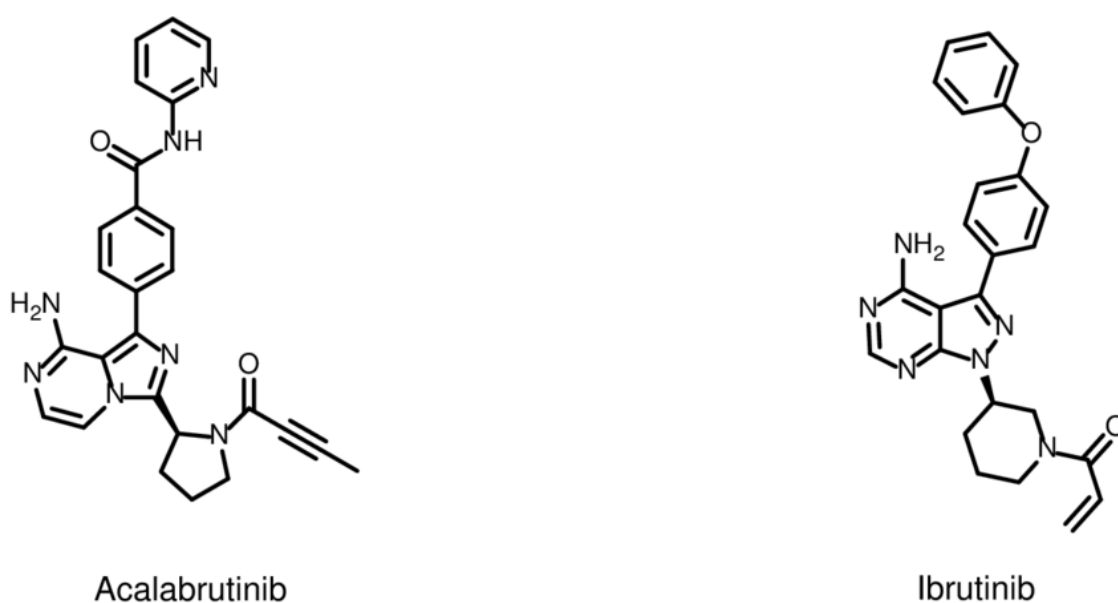


Figure 1.8.1 Structure of acalabrutinib and ibrutinib adapted from Byrd et al., 2016.

1.8.1 Ibrutinib

Ibrutinib (trade name Imbruvica, developed by Pharmacyclics) is a first generation Btk inhibitor that is used to treat CLL. It binds irreversibly to the Cys481 within the active site of Btk (Pan et al., 2007, Honigberg et al., 2010). After 4 hours, greater than 95% of Btk was occupied by ibrutinib in patients with B cell malignancies after oral administration at

most evaluated levels. Level of drug binding to Btk was determined using a fluorescently tagged derivative of ibrutinib (Honigberg et al., 2010). This occupancy level is maintained for over 24 hours (Byrd et al., 2013), showing its irreversible binding.

A number of studies have shown efficacy with ibrutinib by improving symptoms of CLL and it was approved for treatment of this disease in the UK in 2017 (Scheers et al., 2015, Byrd et al., 2013, Honigberg et al., 2010, Burger et al., 2015). Indeed, it is a very potent inhibitor of Btk, with IC_{50} values typically falling within the sub-nanomolar range in *in vitro* kinase assays (Pan et al., 2007, Liclican et al., 2020, Honigberg et al., 2010). Analysis of its potency in cell-based assays showed that for Btk pY223 and PLC γ 2 phosphorylation downstream of the BCR, IC_{50} s were still within the nM range (11 nM and 29 nM) respectively (Honigberg et al., 2010) showing that ibrutinib is a potent inhibitor of Btk.

Ibrutinib therapy has also been reported to cause undesirable side effects including headaches, diarrhoea, atrial fibrillation and more dangerously, bleeding. 61% of patients receiving ibrutinib in one clinical trial experienced altered haemostasis and displayed a bleeding side effect (Byrd et al., 2015). The majority of these adverse bleeding side effects were grade 1 (48%) which is the formation of petechiae and contusions. However, 7% of patients did have grade 3 bleeding events, which require transfusions and furthermore, 1 patient had a catastrophic bleed resulting in death. Although this occurred approximately 1 month after ibrutinib discontinuation and may have been related to the progression of the disease. These haematological side effects can occur even with a normal platelet count (Lipsky et al., 2015, Shatzel, 2017).

The side effects of ibrutinib are believed to be due to the non-specificity of the drug. In addition to Btk, other kinases are also inhibited by ibrutinib *in vitro* recombinant kinase assays, including Src ($IC_{50} = 19\text{nM} \pm 1$), Tec ($IC_{50} = 7.0\text{nM} \pm 2.5$), Fyn ($IC_{50} = 29\text{nM} \pm 0$) (Byrd et al., 2016). However different *in vitro* kinase assays can yield different results, with a recent paper reporting more potent inhibition of Tec (IC_{50} for Tec was 3.2nM) (Liclican et al., 2020). Furthermore, using *in vitro* kinases to assess the potency of an inhibitor may

not always be accurate as the kinase concentration and substrate can differ between groups and can therefore explain the differences observed.

In platelets, ibrutinib has been characterised downstream of GPVI (Bye et al., 2017, Bye et al., 2015, Nicolson et al., 2018, Levade et al., 2014, Series et al., 2019) and downstream of CLEC-2 (Manne et al., 2015a, Nicolson et al., 2020) where it has been shown to disrupt platelet function and will be discussed in chapter 3.

1.8.2 Acalabrutinib

Acalabrutinib (trade name Calquence, developed by Acerta Pharma) is a second generation Btk inhibitor, and is reported to be more selective than ibrutinib (Barf et al., 2017, Byrd et al., 2016, Patel et al., 2016). Similarly to ibrutinib, it is used for the treatment of CLL. The mechanism of action of acalabrutinib is the same as ibrutinib, with the drug binding to Cys481 within the binding loop of the active site, preventing ATP binding. This covalent binding is mediated by acalabrutinib's unique reactive butynamide group. This butynamide group causes lower electrophilicity when compared to ibrutinib's acrylamide group to bind to Cys481 and therefore may explain why acalabrutinib is more selective than ibrutinib (Barf et al., 2017, Patel et al., 2016).

Like ibrutinib, acalabrutinib has anti-cancer effects in murine models of CLL and treatment is associated with a significant increase in survival (Herman et al., 2015). The effectiveness of this drug in the treatment of CLL has also been shown in patients *in vivo* and is licenced for use (Byrd et al., 2016, Isaac and Mato, 2020).

In addition, acalabrutinib has also been proposed to cause similar side effects such as headaches and diarrhoea and albeit less frequently, atrial fibrillation (Isaac and Mato, 2020, Barf et al., 2017). Furthermore, acalabrutinib has been associated with a lower risk of bleeding than ibrutinib. Grade 3 bleeding events (gross blood loss, requiring transfusions) occurred in 8% of ibrutinib patients, whereas it was reported in 3% of patients taking acalabrutinib (Byrd et al., 2015, Furman et al., 2019). However, there are

no published results of clinical trials comparing the effectiveness of ibrutinib vs acalabrutinib in patients at treating CLL and their side effects (Isaac and Mato, 2020).

In vitro kinase assays have been used to assess the potency and selectivity of acalabrutinib over ibrutinib. Acalabrutinib is slightly less potent than ibrutinib for inhibiting Btk ($IC_{50} = 5.1nM \pm 1$ for acalabrutinib, $IC_{50} = 1.5nM \pm 0.2$ for ibrutinib) whereas it is also less potent at inhibiting Tec ($IC_{50} = 93nM \pm 35$) and Src ($IC_{50} = >1000nM$) (Byrd et al., 2016). Others also confirmed that acalabrutinib was less potent at inhibiting Btk than ibrutinib. Acalabrutinib's IC_{50} 's for Btk being between 2.5-3nM (with ibrutinib being approximately 5x more potent) (Covey et al., 2015, Liclican et al., 2020). Nevertheless, acalabrutinib is less potent at inhibiting Tec and Src *in vitro* compared to ibrutinib (Barf et al., 2017, Covey et al., 2015). This increased selectivity for Btk (although lesser potency) and sparing of other kinases is an advantage of acalabrutinib over ibrutinib.

Like ibrutinib, acalabrutinib has been utilised to study the role of Btk downstream of GPVI (Busygina et al., 2018, Bye et al., 2015, Dobie et al., 2019, Nicolson et al., 2018, Bye et al., 2017) and to a lesser extent CLEC-2 (Dobie et al., 2019, Nicolson et al., 2020). This will be discussed in more detail in chapter 3.

1.8.3 Btk inhibitors in non-ITAM mediated signalling events and experiments under flow

After patients taking ibrutinib for CLL were shown to have bleeding as a side effect, investigations into the role of this kinase inhibitor on platelet function were conducted. It was initially thought these bleeding side effects could be related to CLL. Some CLL patients have a lower platelet count, and the bleeding risk in thrombocytopenic individuals is increased already, independently of CLL. However, the association of reduced platelet aggregation to ristocetin and bleeding whilst taking ibrutinib is still significant regardless of platelet count (Kazianka et al., 2017). This highlighted the inhibition of platelet function is

responsible for the bleeding of ibrutinib patients and not the drop in platelet count, or the leukaemia itself.

Indeed, ibrutinib does inhibit platelet function and these effects are not limited to ITAM mediated signalling pathways. Platelet rolling along VWF is preserved in the presence of ibrutinib whereas firm adhesion is reduced (Levade et al., 2014). This effect is dependent on GPIb as using a function blocking antibody to GPIb blocked the adhesion, consistent with Btk can play a role downstream of GPIb (Liu et al., 2006). This is also mirrored in patients taking ibrutinib having a reduced platelet surface area coverage on VWF.

Although interestingly some donors did not have a reduced platelet surface area after 15 days of treatment (Levade et al., 2014). Another platelet receptor that can be inhibited in the presence of ibrutinib is $\alpha\text{IIb}\beta\text{3}$. This integrin is crucial for aggregation and clot retraction functionality as in Section 1.2.6. Therefore, it is unsurprising that ibrutinib has been demonstrated to inhibit clot retraction (Bye et al., 2015, Dobie et al., 2019).

Ibrutinib analogs have also been used to investigate the role of Btk in thrombus formation on collagen using shear flow conditions. The ibrutinib analog used in the study is a structurally similar variant of ibrutinib, that binds to Cys481 of Btk, with a similar IC_{50} value and selectivity profile as its parent drug. At a shear rate of $2,200\text{s}^{-1}$, which is the shear rate of stenosed arteries, the percent coverage was significantly decreased in the presence of the ibrutinib analog (Rigg et al., 2016). Whereas other work has shown that the surface coverage is not significantly different showing platelets adhere normally, however, the stability of the thrombus is significantly weaker in the presence of ibrutinib (Bye et al., 2015).

A study from an independent group used reconstituted blood to corroborate the finding that ibrutinib does not alter thrombus surface area, however, the stability of the thrombus was not shown (Nicolson et al., 2018). Recent work has also shown that ibrutinib also significantly inhibits thrombus formation *in vitro* on collagen, whereas other Btk inhibitors such as acalabrutinib or zanubrutinib do not (Bye et al., 2017, Dobie et al., 2019).

More physiologically relevant work using atherosclerotic plaque material extracted from human donors via endarterectomy as an agonist has recently been assessed. Plaque material contains morphologically different type I and type III fibres and induces platelet aggregation via GPVI but not the other collagen receptor $\alpha_2\beta_1$ (Jamal et al., 2015). Multiple electrode aggregometry was initially assessed to identify if Btk inhibition could modulate the response to plaque material. When stimulated with homogenised plaque, aggregation was abolished by treatment of whole blood with ibrutinib and acalabrutinib (Busygina et al., 2018). However, the response was spared when stimulated with type 1 collagen.

At high shear, ibrutinib treatment (0.5 μ M) inhibited the platelet aggregate formation on plaque homogenate, but not collagen. This was also observed at low shear and with acalabrutinib. When samples treated with either ibrutinib (0.5 μ M) or acalabrutinib (1 μ M) were flowed over plaque homogenate at a shear rate of 600/s, there was a significant reduction compared to vehicle control. However, the response on type 1 collagen was not inhibited in the presence of ibrutinib or acalabrutinib. This sparing of aggregation on collagen was found to be $\alpha_2\beta_1$ independent. Treatment with an $\alpha_2\beta_1$ -blocking antibody 6F1, but not ibrutinib, blocked platelet adhesion to soluble type I. This demonstrates that $\alpha_2\beta_1$ is required for aggregation on collagenous surfaces under arterial flow, but ibrutinib does not alter its downstream signalling.

The authors propose that that the use of plaque tissue and the use of native type I collagen represent the pathological process of atherothrombosis and the physiological process of hemostasis, respectively.

1.8.4 The platelet function of patients taking ibrutinib and acalabrutinib.

All the research discussed so far used inhibitors exogenously added to healthy donor platelets. Studies have also examined the platelet function of patients taking these drugs

in the clinic as an anti-CLL therapy. Peak *in vivo* plasma concentrations of ibrutinib and acalabrutinib have been estimated at approximately 300nM and 1.7µM, respectively (Byrd et al., 2016, Advani et al., 2013). Platelet inhibition is typically seen at concentrations greater than this in *ex vivo* studies, however *ex vivo* and *in vitro* studies do not consider drug accumulation, metabolism, or plasma binding.

Maximal platelet aggregation from patients taking ibrutinib was also assessed in response to collagen (3.3µg/mL). On ibrutinib therapy, not every patient has bleeding side effects. Using PRP, maximal aggregation was significantly inhibited in patients that do experience bleeding, along with platelet adhesion to VWF. This caused the authors to define the two groups and assess them differently. In patients experiencing bleeding, at day 15 of 60 maximal platelet aggregation and surface coverage on VWF under flow was almost abolished, whereas U44619 and ADP mediated aggregation was normal. Whereas non bleeders do not have a significant inhibition of aggregation to any agonist or adhesion of VWF (Levade et al., 2014).

Following on from the work of Levade et al., 2014, Kamel et al., also investigated platelet aggregation. This work showed that aggregation to both low and high doses of ADP were normal in patients taking ibrutinib, along with U46619 which induces platelet activation via the thromboxane A2 receptor. Before taking ibrutinib, patients have a high percent aggregation to low (2µg/ml) and high (10µg/mL) concentrations of collagen. Whilst taking the drug, the percentage aggregation drops by approximately half in response to high concentrations of collagen and by 75% to low concentrations of collagen (Kamel et al., 2015) demonstrating that ibrutinib is a potent inhibitor of platelet aggregation.

Thrombus formation under flow was also assessed in patients treated with ibrutinib and acalabrutinib. The thrombus volume positively correlated with the platelet count of these patients treated with acalabrutinib. There was no significant correlation between thrombus volume and platelet count in ibrutinib patients further confirming *in vitro* experiments that ibrutinib causes unstable thrombi (Bye et al., 2015, Bye et al., 2017). Recent work has also confirmed this result that patients taking ibrutinib form unstable thrombi when

compared to healthy controls, whereas another second generation inhibitor, zanubrutinib, does not (Dobie et al., 2019).

In the study by Busygina et al., patients on ibrutinib therapy had similar platelet counts to controls, and when multiple electrode aggregometry was assessed, aggregation was inhibited when stimulated with collagen or atherosclerotic plaque material consistent with their *in vitro* blood studies. When assessed under flow, ibrutinib patients had significantly decreased platelet coverage on plaque homogenate and tissue over a range of time points. On collagen, inhibition of thrombus formation was initially observed, however it was rescued and was not found to be significantly different at the end of the assay (Busygina et al., 2018).

Ibrutinib inhibits thrombus formation when stimulated with atherosclerotic plaque, but it is not different from controls on response to collagen. From this, the authors hypothesise that thrombus formation in pathological settings (activation via plaque material), but not in normal haemostasis (activation via collagen), Btk inhibitors can be utilised as an anti-platelet therapy (Busygina et al., 2018, Bye and Gibbins, 2018).

Little has been published regarding patients taking Btk inhibitors downstream of CLEC-2. Recent work by collaborators has shown that patients taking both ibrutinib and acalabrutinib do not aggregate in response to rhodocytin over a range of concentrations of agonist. Unlike CRP-XL as an agonist, where there has been shown to have a difference in the platelet response between patients on ibrutinib or acalabrutinib (Nicolson et al., 2018), there is no difference in between the responses downstream of CLEC-2 (Nicolson et al., 2020).

1.9 Aims and Hypothesis.

1.9.1 Differences in ITAM and hemITAM signalling

As discussed in Section 1.6, there are some differences in the GPVI and CLEC-2 signalling pathways. These include differences in the requirements of secondary mediators, actin polymerisation and the requirement of PI3K activity. These are all dispensable for GPVI signalling, but essential for CLEC-2 signalling. However, the scaffold protein SLP-76 is required for GPVI, but not for CLEC-2, highlighting another novel difference between the pathways.

One of the key differences is the position of Btk in the signalling cascades. It has been suggested that Btk is upstream of Syk in the CLEC-2 signalling pathway. This contrasts with GPVI signalling, where Btk is below Syk. Considering this difference it is not unreasonable to hypothesise that Btk may have a differential role downstream of GPVI compared to CLEC-2.

1.9.2 Btk kinase activity in B cells

Whether Btk behaves as an explicit kinase downstream of the BCR is debatable. Canonically it has been thought that Btk acts as a kinase downstream of the B cell receptor where it induces phosphorylation of PLC γ 2 (Takata and Kurosaki, 1996, Watanabe et al., 2001, Humphries et al., 2004). The development of kinase inhibitors that are clinically successful in treating BCR mediated diseases also contributes to the notion that Btk acts as a kinase downstream of the BCR (Pal Singh et al., 2018).

However, it has been shown that Btk may not act as an explicit kinase, as a kinase dead version of Btk can reconstitute BCR signalling (Tomlinson et al., 2001). Recently, non-catalytic variants of Btk have been shown to mediate PLC γ 2 activation (Wist et al., 2020). Furthermore, expression of non-catalytically active Btk causes a less severe phenotype of

XLA (Gaspar et al., 2000). This suggests that Btk can partially mediate BCR signalling in the absence of a functional kinase domain.

Recently, a study has proposed dual roles for Btk, as a scaffold and a kinase in the formation of the antigen- triggered immune synapse. Btk scaffolding is important for the initiation of the formation of an immune synapse, whereas kinase activity controls the accumulation of the antigen within the cell (Roman-Garcia et al., 2018). This shows that within the same cell, Btk can mediate signalling through a catalytic or scaffolding role.

1.9.3 Localisation of proteins

Although studies have identified a role for Btk downstream of (hem)ITAM signalling, there has been no systematic studies investigating the localisation of Btk in relation to key signalling molecules. Studies using biochemical techniques of membrane fractions have identified that Btk translocates to the membrane after stimulation with convulxin and rhodocytin (Manne et al., 2015a). The localisation of GPVI and CLEC-2 on the surface has been studied using microscopy (Dunster et al., 2020, Pollitt et al., 2014, Poulter et al., 2017), but has not yet been shown to interact with Btk.

It has been proposed that Btk undergoes clustering in order to become catalytically active (Chung et al., 2019, Wang et al., 2019b, Hyvönen and Saraste, 1997). However, there is no quantitative evidence showing that Btk undergoes clustering using microscopy.

1.9.4 Aims and hypothesis

While there are common mechanisms shared between GPVI and CLEC-2 mediated signalling there are differences. Btk is a kinase present in B cells, however, its kinase activity is not always required to mediate signalling. Patients taking a second generation Btk inhibitor do not experience bleeding as a side effect, suggesting that Btk may be playing a scaffolding or redundant role in platelets. Furthermore, localisation of Btk and key hemITAM signaling molecules, which has not been extensively studied in platelets may help to elucidate if Btk plays a differential role downstream of GPVI and CLEC-2.

The aims of this thesis are to:

- Identify if there is a differential role of Btk downstream of GPVI and CLEC-2.
- Investigate the role of the Btk kinase domain downstream of GPVI and CLEC-2
- To determine if Btk can act as a scaffold protein independently of its kinase domain
- To identify the localisation and clustering of Btk in relation to key signalling molecules in platelets.

Hypothesis

In platelets Btk plays a differential role downstream of GPVI and CLEC-2 by mediating signalling as a kinase or as a scaffold protein.

2 Materials and methods

2.1 Materials and Methods

2.1.1 Agonists and inhibitors

Collagen-related peptide (CRP-XL) was obtained from Professor Richard Farndale (University of Cambridge, Cambridge, UK). Type 1 Collagen was purchased from Nycomed (Munich, Germany). Rhodocytin was a kind gift from Dr Johannes Able (University of Münster, Münster, Germany). Fucoidan and ADP were purchased from Sigma Aldrich (Poole, UK). Ibrutinib and acalabrutinib were obtained from Medchem express (Sollentuna, Sweden). LY294002 was from Selleckchem (Houston, USA).

2.1.2 Antibodies

The antibodies used in this study are listed in Tables 2.1.1 and 2.1.2

Table 2.1.1 The primary antibodies used in this study

| Antibody | Species | Application | Dilution / Concentration | Source |
|---|---------|----------------|--------------------------|----------------------------------|
| FITC conjugated polyclonal antihuman fibrinogen | Rabbit | Flow cytometry | 1:100 | Dako (Glostrup, Denmark) |
| PE/Cy5 antihuman CD62P monoclonal antibody | Mouse | Flow cytometry | 1:100 | BD Biosciences (New Jersey, USA) |

| | | | | |
|---------------------------|--------|--|---------------------------------|---|
| pY223 Btk | Rabbit | Western blotting | 1:500 | Abcam (Cambridge, United Kingdom) |
| pY551 Btk | Rabbit | Western blotting | 1:500 | Abcam |
| pY200 LAT | Rabbit | Western blotting | 1:500 | Abcam |
| pY525 Syk | Rabbit | Western blotting | 1:500 | Cell Signalling Technology (London, United Kingdom) |
| pY759 PLC γ 2 | Rabbit | Western blotting | 1:500 | Cell Signalling Technology |
| pY416/8 Syk | Rabbit | Western blotting | 1:500 | Cell Signalling Technology |
| Phosphotyrosine (4G10) | Mouse | Western blotting, immunofluorescence | 1:1000 5 μ g/mL | Millipore (Massachusetts, USA) |
| GPVI (1G5) | Mouse | Western blotting Immunofluorescence Flow cytometry | (4 μ g/mL) 10 μ g/mL | Biocytex (Marseille, France) |
| PLC γ 2 (Q-20) | Rabbit | Western blotting Immunofluorescence | 1:1000 1 in 150 | Santa Cruz (Dallas, Texas) |
| Btk (E-9) | Mouse | Western blotting | 1:1000 | Santa Cruz |
| Btk (C-20) | Goat | Immunofluorescence | 1:150 | Santa Cruz |
| Syk (N-19) | Rabbit | Immunofluorescence | 1 μ g/mL | Santa Cruz |
| LAT (FL-233) | Rabbit | Immunofluorescence | 1:150 | Santa Cruz |
| CLEC-2 (AYP1) | Mouse | Immunofluorescence | 5 μ g/mL | Dr Alice Pollitt |

| | | | | |
|---------------|--------|--|--------------------|---|
| | | Immunoprecipitation Flow cytometry | 2µg/IP 10µg/mL | |
| CLEC-2 (AYP2) | Mouse | Western blotting | 2µg/mL | Dr Alice Pollitt |
| Btk (BL7) | Rabbit | Western blotting Immunofluorescence | 1:1000 1 in 150 | Dr Mike Tomlinson, University of Birmingham |
| Tec (BL17) | Rabbit | Western blotting | 1:1000 | Dr Mike Tomlinson |
| Tec (BL19) | Rabbit | Western blotting | 1:1000 | Dr Mike Tomlinson |
| Tubulin | Mouse | Western blotting | 1:2000 | ProteinTech (Illinois, USA) |
| Actin | Mouse | Western blotting | 1:2000 | Santa Cruz |

Table 2.1.2 Secondary antibodies used in this study

| Antibody | Species | Use | Concentration | Purchased from |
|---|---------|-----------------------------------|-----------------|------------------------------|
| Alexa Fluor 647 conjugated donkey anti-rabbit | Donkey | Western Blotting TIRF STORM | 1:4000 1:500 | Invitrogen (California, USA) |
| Alexa Fluor 488 conjugated goat anti-mouse | Goat | Western blotting TIRF | 1:4000 1:500 | Invitrogen |
| Alexa Fluor 555 conjugated donkey anti-mouse | Donkey | STORM | 1:500 | Invitrogen |
| Alexa Fluor 647 conjugated donkey anti-goat | Donkey | Western blotting STORM | 1:4000 1:500 | Invitrogen |
| Alexa Fluor 555 donkey anti-goat | Donkey | STORM | 1:500 | Invitrogen |

2.1.3 Other reagents

The Btk deficient DT40 cells, and plasmid constructs were a kind gift from Dr Mike Tomlinson (University of Birmingham, UK). FastDigest Bpil restriction enzyme and T4 DNA Ligase were obtained from ThermoFisher (Massachusetts, USA). EcoRI-HF, NotI-HF, BamHI-HF and T4 Polynucleotide kinase were from New England Biolabs (Massachusetts, USA). Phenol:Chloroform:Isoamyl Alcohol (24:24:1) was from ThermoFisher (Massachusetts, USA). Sybrsafe was purchased from Invitrogen (Massachusetts, USA). Fura-2-AM was from ThermoFisher (Massachusetts, USA).

Unless stated, all other reagents were of chemical grade and purchased from Sigma Aldrich (Poole, UK).

2.2 Methods

2.2.1 Human Washed Platelet Preparation

50 mL of blood was drawn from drug free, consenting individuals using methodology approved by the University of Reading research ethics committee, into a syringe containing 5mL sodium citrate (4% w/v). 7.5 mL warmed Acid Citrate Dextrose, (ACD -85 mM sodium citrate, 71mM citric acid and 110mM glucose) was added and centrifuged at 102g for 20 minutes to obtain platelet-rich plasma (PRP). The PRP was decanted and 10 μ L prostacyclin (PGI₂ 125 μ g/mL, solubilised in ethanol) was added and platelets pelleted by centrifugation at 1413g for 10 minutes. The pellet resuspended in 25mL of warmed Tyrode's buffer (30°C) (134mM NaCl, 2.9mM KCl, 0.34mM Na₂HPO₄, 12mM NaHCO₃, 20mM HEPES, 1mM MgCl₂ and 5mM glucose; pH 7.3) and 3mL of ACD. The platelet count was determined using a Sysmex counter (Sysmex, UK), 10 μ L PGI₂ was added and then following centrifugation at 1413g for 10 minutes, the platelet pellet was re-suspended to the appropriate cell density using Tyrode's buffer. Platelets were rested for 30 minutes to recover.

For ADP sensitive platelets, PRP was obtained from whole blood by centrifugation at 102g for 20 minutes after addition of ACD. The PRP was then decanted and the platelet count was obtained. Centrifugation at 350g for 20 minutes pelleted the platelets. The platelet poor plasma was then removed gently, and the platelet pellet was resuspended to 4x10⁸ cells/mL in warmed Tyrode's buffer. Platelets were used immediately.

2.2.2 Light transmission aggregometry

245 μ L of washed platelets at (4x10⁸ cells/mL) were added to a siliconized glass cuvette and incubated for 5 minutes with vehicle (0.1% (v/v) DMSO final) or 2.5 μ L ibrutinib or Acalabrutinib (10 μ M – 0.01 μ M final) and then 2.5 μ L of CRP-XL (1 μ g/mL final) or rhodocytin (10-300nM final) was added and light transmission monitored for 5 minutes for

CRP-XL or 7 minutes for rhodocytin at 37°C with constant stirring (1200rpm) using an aggregometer (Helena biosciences, Gateshead UK).

2.2.3 Western blot platelet sample production

222.5µL Platelets (4×10^8 cells/mL) were incubated with indomethacin (10µM), apyrase (2U/mL) and integrilin (9µM) to induce non aggregating conditions for GPVI mediated signalling and integrilin (9µM) for CLEC-2 mediated signalling. Platelets were incubated with 2.5µL acalabrutinib (0.01 -10µM), ibrutinib (0.01-10µM) or vehicle control (0.1% (v/v) DMSO final) before addition of 25µL of agonists (1µg/mL CRP-XL, 100nM or 300nM rhodocytin final) under stirring conditions. GPVI stimulated samples were allowed to stir for 180 seconds at 37°C before lysis with 6X sample buffer (12% (w/v) Sodium Dodecyl Sulphate (SDS), 30% (v/v) glycerol, 0.15M Tris-HCl (pH 6.8), 0.001% (w/v) Brilliant Blue R, 30% (v/v) b-mercaptoethanol), whereas CLEC-2 stimulated samples were allowed to stir for 5 minutes before lysis with 6X sample buffer. Samples were heated at 95°C for 5 minutes before freezing until SDS-PAGE.

2.2.4 Immunoprecipitation

445µL Washed platelets (8×10^8 cells/mL) under non-aggregating conditions were preincubated and stimulated with agonist as above. Platelets were preincubated with 5µl of the stated inhibitors or vehicle control for 5 minutes before stimulation with 50µl 300nM Rhodocytin for 3 minutes before lysis with an equal volume of 2x NP40 lysis buffer (100mM Tris, 300mM NaCl, 0.2% (w/v) SDS, 1% (w/v) Sodium deoxycholate, 1% (v/v) NP40) containing the protease inhibitors leupeptin (10µg/mL), AEBSF (200µg/mL), aprotinin (10µg/mL), Pepstatin (1µg/mL) and the phosphatase inhibitor sodium orthovanadate (5µM). Lysates were clarified by centrifugation at 15,000g for 10 minutes at 4°C before preclearing with 30µL protein A Sepharose beads for rabbit antibodies, or protein G for mouse antibodies for 30 minutes at 4°C. Lysates were incubated with

primary antibodies (concentrations stated within text), for 1 hour at 4°C before 25µL bead volume was added. Samples were incubated overnight at 4°C, before supernatant was removed. Beads were washed 1x in NP40 lysis buffer and then 3x in TBST (Tris buffered saline with Tween 20: 20mM Tris, 140mM NaCl, 0.1% Tween, pH 7.6) before elution into 35µL of 2X Sample buffer. Samples were boiled at 95°C for 5 minutes before storage or SDS-PAGE immunoblotting.

2.2.5 SDS-PAGE and Immunoblotting

Proteins were separated by SDS-PAGE (Laemmli, 1970), using 10% SDS-PAGE Gels which were submerged in 1X Tris/Glycine/SDS buffer (25mM Tris, 192mM glycine, 0.1% (w/v) SDS, pH 8.3) within a Mini-PROTEAN tetra vertical electrophoresis cell (Bio-Rad, CA, USA). Electrophoresis was run at a constant voltage of 120V.

Following protein separation, gels were removed from their plates. 2 pieces extra thick filter paper were soaked in Towbin transfer buffer (25 mM Tris, 192 mM glycine, 20% (v/v) methanol, pH 8.3). A Section of polyvinylidene difluoride (PVDF) membrane was soaked in methanol and then in Towbin transfer buffer. Semi-dry western blotting was performed using a Trans-blot Turbo blotter semi-dry transfer cell (Bio-Rad, CA, USA). Proteins were transferred from the gel to the PVDF membrane for 40 minutes at 15V. PVDF membranes were then transferred into a 5% (w/v) solution of bovine serum albumin (BSA) dissolved in TBST (Tris buffered saline with Tween 20; 20mM Tris, 140mM NaCl, 0.1% (v/v) Tween, pH 7.6) to block the membrane for 1 hour at room temperature. Primary antibodies were diluted to a concentration as stated in Table 2.1.1 in a 5% (w/v) solution of BSA dissolved in TBST and membranes were incubated with these solutions overnight at 4°C on a rotator. Primary antibody solutions were removed from the PVDF membranes the next day and membranes were washed 3x for 10 minutes with TBS-T.

Secondary antibodies (as stated in Table 2.1.2) were added 1:4000 to a 2.5% BSA (dissolved in TBS-T) solution, which was then added to PVDF membranes and incubated

in the dark at room temperature for 1 hour. PVDF membranes were washed 3x for 10 minutes with TBS-T. PVDF membranes were scanned using a Typhoon Trio fluorescence imager (Amersham Biosciences, Buckinghamshire, UK) and analysed. Band intensity was analysed using Imagequant software.

2.2.6 Calcium Flux

Methods were adapted from Bye et al., 2018. Whole blood was centrifuged to prepare PRP as described previously in Section 2.2.1. FURA 2-AM was added to PRP to a final concentration of 2 μ M. Platelets were incubated for 1 hour at 37°C for 1 hour with gentle inversions. Platelets were then pelleted and resuspended to 4x10⁸ cells/mL. 160 μ L of Fura-2 loaded platelets were incubated with inhibitors or vehicle for 5 mins at 37°C prior to addition of 40 μ L 5X concentration agonists (1 μ g/mL CRP or 300nM or 100nM rhodocytin final). Calcium fluorescence measurements with excitation at 340 and 380 nm and emission at 510 nm were recorded over a period of 5 minutes. The 340/380 ratio was plotted and the difference in the peak, area under the curve and time to peak of calcium was assessed.

2.2.7 Flow cytometry

In a flat-bottomed 96 well plate, 5 μ L of ADP insensitive washed platelets (4x10⁸ cells/mL) were incubated with 5 μ L 10X drug or vehicle control, 0.5 μ L anti-P-selectin and 0.5 μ L anti-fibrinogen antibody (stated in Table 2.1.1) for 5 minutes before the addition of 5 μ L 10X agonist, with a total reaction volume of 50 μ L made up with Tyrodes. The plate was incubated for 20 minutes in the dark before fixation with 150 μ L 0.2% formyl saline. Flow cytometric analysis was performed using a BD Accuri C6 flow cytometer (BD Biosciences, Oxford, UK) and data was collected from 10,000 events gated on platelets using side scatter (SSC) and forward scatter (FSC) measuring cell granularity and cell size, respectively. Analysis was performed using BD Accuri C6 plus software.

2.2.8 Platelet spreading microscopy

Coverslips were coated with 300 μ L 100nM rhodocytin, 10 μ g/mL collagen or 200 μ g/mL fucoidan overnight at 4°C. Coverslips were washed 3x with PBS before being blocked with 5mg/mL heat denatured protease free bovine serum albumin in PBS for 45 minutes at room temperature. The wells were then washed 3x PBS to remove any excess blocking reagent. Washed platelets (2×10^7 cells/mL) were incubated with stated concentrations of inhibitor or vehicle control (0.1% DMSO (v/v)) prior for 5 minutes at room temperature. In experiments using LY294002, platelets were preincubated with LY294002 or vehicle control (0.1% ethanol (v/v)) for 5 minutes before the addition of acalabrutinib (1 μ M or 0.1 μ M) or vehicle control (0.1% DMSO (v/v)). Platelets were allowed to spread for 45 minutes at 37°C. Wells were washed 3x with PBS before platelets were fixed with 10% Formalin for 10 minutes at room temperature. Slides were mounted using Hydramount before Differential Interference Contrast (DIC) imaging on a Nikon Eclipse Ti2 100x lens. Platelet spreading analysis was performed using ImageJ cell counter plugin to assess the number of platelets in the field of view. Surface area of each individual platelet was also calculated by manually tracing the platelets and using the measure function on ImageJ.

2.2.9 Cells and plasmids

The DT40 chicken lymphoma cell line and the cell line rendered deficient in Btk (Takata and Kurosaki, 1996) was cultured in RPMI 1640 medium supplemented with 10% (v/v) Fetal bovine serum, 1% (v/v) chicken serum, 100 U/mL penicillin, 100 μ g/mL streptomycin, 20 mM glutamine and 50 μ M 2 β -mercaptoethanol. GPVI, FcR γ and NFAT-luciferase containing plasmids have been described previously (Tomlinson et al., 2007). The wild type (WT) and kinase dead (KD) K430E Btk plasmids have been previously described (Tomlinson et al., 2001). The mutations R307K and W124F have been described previously (Li et al., 1995).

Plasmids were dissolved in water and DH5 α *Escherichia coli* were transformed.

Competent cells were incubated with 1 μ L circular DNA for 30 minutes on ice. Cells were heat shocked at 37°C for 30 seconds and replaced on ice for 2 minutes to allow cells to recover. Cells were added to Luria broth (LB) and incubated at 37°C for 1 hour at 250 rpm. 50 μ L of cells were then spread on agar plates containing 100 μ g/mL ampicillin, or 50 μ g/mL kanamycin, depending on the selection cassette. Plates were incubated at 37°C overnight. Antibiotic resistant colonies were picked and used to inoculate 200 mL Luria Broth supplemented with antibiotic (100 μ g/mL ampicillin, or 50 μ g/mL kanamycin) and shaken overnight at 250 rpm at 37°C to induce bacterial growth.

Cultures were maxi prepped the following day using a GenElute maxiprep kit according to manufacturer's instructions. The resulting yield was salt ethanol precipitated using sodium acetate (3M C₂H₃NaO₂ pH 5.2) and 100% ethanol to precipitate the DNA. DNA was pelleted at 16,000g for 30 minutes at 4°C. The supernatant was discarded, and the pellet was washed in 70% ethanol. After pelleting, removal of all ethanol and air drying, the DNA pellet was resuspended in ultrapure ddH₂O to achieve a concentration of 1 μ g/mL.

2.2.10 Transfections and luciferase assay

Cells were transfected in a volume of 0.4 mL of serum free RPMI using a Gene Pulser II Electroporator (Bio-Rad) set at 350 V and 500 μ F. Cells were transfected with 2 μ g of both GPVI and Fc γ or 10 μ g of CLEC-2, and 7.5 μ g of NFAT-luciferase plasmids and where stated, either 5 μ g WT or KD Btk plasmids or empty vector control. Twenty hours after transfection, live cells were counted by Trypan blue exclusion and diluted to 2x10⁶ live cells/mL. Cells (50 μ L) were stimulated with 50 μ L Horm collagen (10 μ g/mL final concentration) for GPVI or rhodocytin (50 nM final) for 6 hours. As a positive control, cells were also treated with phorbol 12-myristate 13-acetate, PMA (50 ng/mL) plus ionomycin (1 μ M). In experiments involving ibrutinib and acalabrutinib, cells were stimulated with collagen (10 μ g/mL final) or rhodocytin (50 nM final) in the presence of ibrutinib (0.5-10 μ M),

acalabrutinib (0.5-10 μ M) or vehicle (0.1% (v/v) DMSO final) for 6 hours in the absence of serum as these drugs have a high degree of plasma binding (Levade et al., 2014). Cells were then lysed with 11 μ L of lysis buffer (10% (v/v) Triton X-100, 200 mM NaPO₄ (pH 7.8), and 4 mM dithiothreitol) and added to an equal volume of assay buffer (200 mM NaPO₄, 20 mM MgCl₂ and 10 mM ATP). Luciferase activity was measured using a NOVOstar plate reader (BMGLabtech) following the addition of 50 μ L of 1 mM D-luciferin. Luciferase assay values were recorded in triplicate and averaged for each experiment.

2.2.11 Flow cytometry of DT40 cells

To confirm receptor expression, following transfection 450 μ L cells (2x10⁶ live cells/ mL) were pelleted and washed in FACS buffer (0.5% BSA/PBS) before resuspension in 10 μ g/mL 1G5 or AYP1 for GPVI and CLEC-2 transfected cells, respectively. Cells were washed 3 times with phosphate buffered saline and resuspended in Alexa Fluor 488-conjugated goat anti-mouse antibody before washing. Cells were resuspended and stained with propidium iodide to enable gating of live cells before flow cytometry analysis using a BD Accuri C6 flow cytometer.

2.2.12 DT40 Lysates and microscopy

DT40 cells were washed 2x with 1x PBS. Cells were pelleted and resuspended in 1X RIPA buffer (25mM Tris-HCl pH 7.6, 150mM NaCl, 0.1% (w/v) SDS, 1% (w/v) Sodium deoxycholate, 1% (v/v) Triton) with protease and phosphatase inhibitors as previously described to 1x10⁷ live cells/mL. Cells were lysed for at least 30 minutes on ice before the insoluble fraction of cytoskeletal components was removed by centrifugation at 16,000g for 10 minutes. The supernatant was removed and 6X sample buffer was added before western blotting as previously described in Section 2.2.5.

Methods were adapted from (Tomlinson et al., 2004b). Coverslips were coated with Poly-L-Lysine (0.01% (w/v)) before 1x washes in PBS and being allowed to dry. WT and Btk

KO DT40's were washed 3x with 1x PBS. 1×10^6 cells were allowed to adhere to the coated coverslips at 37°C for 1 hour, before non-adhered cells were removed. Cells were fixed using 10% Formalin for 15 minutes before permeabilisation with 0.1% (v/v) Triton for 7.5 minutes. Cells were blocked for 45 minutes at room temperature with heat denatured 5 mg/mL BSA/PBS. Cells in individual wells were stained with primary antibodies against Btk (rabbit, BL7, 1 in 150), PLC γ 2 (rabbit, Q- 20,1 in 150) or a rabbit IgG control (1 in 150) for 45 minutes at room temperature. Following 3x washes in PBS cells were stained with Alexa fluor 488 conjugated goat anti rabbit secondary antibody (1 in 500; 4 μ g/ml) for 45 minutes at room temperature before 3x washes in PBS and 1x wash in ultrapure water. Cells were mounted using mounting medium containing DAPI (4',6-diamidino-2-phenylindole). Slides were imaged on a Nikon A1R fluorescence confocal microscope using the 60x lens.

2.2.13 Creation of DT40 CRISPR Btk knockout.

sgRNAs were designed using the online tool Deskgen (Hough et al., 2016). The first exon of *Gallus gallus* (chicken) Btk was selected in the software and the guide RNA sequences with the least off target effects were chosen. Additional bases were added (5'CACCG, 3'CAA) for overhangs to ensure ligation into vector backbone after digestion with Bpil. An additional guanine (G) was added to the start of the nucleotide guide as the U6 promoter used to express the sgRNA prefers this nucleotide base to initiate the transcript.

Methods were adapted from Ran et al 2013.

1 μ g pSp-Cas9-2A-BB-Puro was digested with fast digest Bpil overnight at 37°C. The digested plasmid was run on a 1% agarose gel stained with 1x Sybrsafe for approximately 1 hour at 120 volts. Linearised plasmid was excised from the gel and gel extracted using a GenElute gel extraction kit (Sigma Aldrich, UK) and eluted into 30 μ L ddH₂O.

Forward and reverse oligos were ordered per each guide sequence as in Table 2.2.1 and resuspended to 100 μ M. The oligonucleotides were annealed and phosphorylated using a

thermocycler as conditions shown in Figure 2.2.1 and the components listed in Table 2.2.2. The annealed and phosphorylated oligonucleotides were diluted 1:200 before ligation into digested pSp-Cas9-2A-BB-Puro.

Table 2.2.1 The primers used in this study

| Primer name | Use | Sequence / Sequences |
|------------------------------|----------------------------|---|
| SN1 | Sequence W124F | 5' GAGGAGTCTAGTGAAATGGAA |
| SN2 | Sequence WW251/2LL | 5' AGGTCGTGGCCCTTTATGATT |
| SN3 | Sequence R307K | 5' GTGATCCGCCATTACGTT |
| SN7 | Sequence K430E | 5' CTACGGCAGCTGGGAGATCGA |
| U6 forward | CRISPR Cas9 Guide | 5' GAGGGCCTATTTCCCATGATTCC |
| SHN01 | Btk KO CRISPR | 5' CACCGACGAGTATGACTTTGAGCGT |
| SHN02 | guide pair 1 | 5' AAACACGCTCAAAGTCATACTCGTC |
| SHN03 | Btk KO CRISPR | 5' CACCGCGAGTATGACTTTGAGCGTG |
| SHN04 | guide pair 2 | 5' AAACACGCTCAAAGTCATACTCGTC |
| SHN05 | Btk KO CRISPR | 5' CACCGTACGAGTATGACTTTGAGCG |
| SHN06 | guide pair 3 | 5' AAACACGCTCAAAGTCATACTCGTC |
| SHN-W124F1 SHN-W124F2 | W124F CRISPR guide | 5' CACCGCAGAGGAGCTGCGCAAACGC 5' AAACGCGTTTGCGCAGCTCCTCTGC |
| SHN-WW251LL1 SHN-WW251LL2 | WW249/50LL CRISPR guide | 5' CACCGTGGAGGAAAGCCACCTGCCT 5' AAACAGGCAGGTGGCTTTCCTCCAC |

| | | |
|------------------------------------|------------------------------------|---|
| SHN-R307K1 SHN-R307K2 | R307K CRISPR guide | 5' CACCGAGATTCTACCAGCAAGACA 5' AAACGTCTTGCTGGTAGAATCTC |
| SHN-K430E1 SHN-K430E2 | K430E CRISPR guide | 5' CACCGGAGGGATCCATGTCAG 5' AAACCTGACATGGATCCCTCC |
| R307K.Seq.FwD R307K.Seq.Rev | Assessing R307K knockin and PCR | 5' GTCACTTCCTCACAAATACCCC 5' ATACAACGTAATGGCGGATCAT |

Table 2.2.2 Component mixture for oligonucleotide phosphorylation and annealing

| Component | Volume (μ L) |
|---|-------------------|
| 10x Buffer A | 2 |
| ATP (10mM) | 2 |
| Guide oligo top strand (100 μ M) | 1 |
| Guide oligo bottom strand (100 μ M) | 1 |
| T4 polynucleotide kinase | 1 |
| Ultrapure water | Up to 20 μ L |

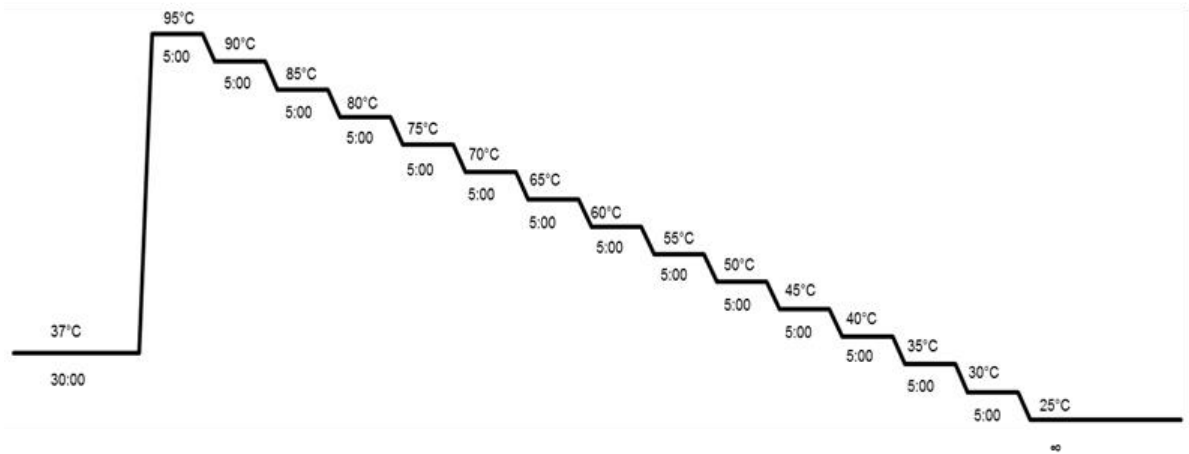


Figure 2.2.1 Thermocycling conditions used to phosphorylate and anneal single oligonucleotides

Ligations were performed using 100ng of digested plasmid, 1µL of diluted oligos, 2X ligation buffer and 0.5µL T4 DNA Ligase made up to a total volume of 20µL with water. Ligation reactions occurred at 4°C overnight.

DH5α *Escherichia coli* chemically competent cells were transformed using the ligation mixture. Competent cells were incubated with 5µL ligation mixture for 30 minutes on ice. Cells were heat shocked at 37°C for 30 seconds and replaced on ice for 2 minutes to allow cells to recover. Cells were added to Luria broth (LB, 1% tryptone, 0.5% yeast extract) and incubated for 1 hour as previously described in Section 2.2.9. 50µL Mixture was then spread on LB agar (LB and 1.5% w/v bacterial agar) containing 100µg/mL ampicillin and incubated at 37°C overnight.

Single colonies from each plate were picked aseptically and used to inoculate 5mL LB broth supplemented with 100µg/mL ampicillin and incubated overnight as previously described in Section 2.2.9. Glycerol stocks were made with 250µL of culture and 250µL glycerol to act as a cyropreservative. The remaining culture was processed using Gen Elute Miniprep kit (Sigma, Poole UK) and eluted into ultrapure 50µL H₂O. DNA concentration was measured using a Nanodrop before sequencing with the U6 forward primer (5'-3' GAGGGCCTATTTCCCATGATTCC) from Eurofins Genomics (Ebersberg, Germany).

After verification of ligation of the guide RNA into pSp-Cas9-2A-BB-Puro, 200mL LB supplemented with ampicillin as previously described was inoculated with glycerol stocks made previously (as described in the above paragraph). Cultures were then processed using a GenElute maxiprep kit (Sigma, Poole UK) and salt ethanol precipitated as described in Section 2.2.9.

WT DT40 cells were transfected using the previous method with the following adaptations based on (Abu-Bonsrah et al., 2016) – 30µg of guide containing plasmid and the electroporation conditions were modified to 300V and 900µF. Cells were left for 20 hours post transfection before stable selection. Serial dilution of cells was performed in the presence of 2µg/mL puromycin to isolate single-cell colonies. Cells were left for 7-10 days to ensure stable selection before colonies were expanded into 24 well plates and then into 6 well plates. Lysates were made as in Section 2.2.12 and western blotted as in Section 2.2.5 to confirm deletion of the protein.

2.2.14 Creation of DT40 CRISPR Btk knockins

Chicken (*Gallus gallus*, NP_989564.2), Mouse (*Mus musculus*, CH466598.2), Human Btk (*Homo sapiens*, Q06187.3), Zebrafish (*Danio rerio*, XP_697087.5) and beaver (*Castor canadensis*, JAV44149.1) were aligned using T-coffee (Notredame et al., 2000).

Sequences were presented with ESPrit 3 (Robert and Gouet, 2014) to identify if key sites in Btk were exactly homologous or conserved.

Guides were selected based on distance to mutation with the closest possible guides with the least amount of off target effects selected using Deskgen software and cloned into the pSpCas9-2A-BB-Puro plasmid as previously described (Section 2.2.13). Deskgen software (Hough et al., 2016) was also utilised to generate the donor sequence with the changed DNA codon to introduce a point mutation. Manual silent mutations were added into the donor sequence to remove the PAM site or mutate where the original guide would bind to prevent recutting. A further silent mutation of introducing or removing a restriction

enzyme site was introduced to allow for screening of mutants by restriction digestion. Donor sequences (Table 2.2.3) were ordered from Eurofins genomics in the pEX-A128 and dissolved in ddH₂O before transformation of *E. coli*.

Initial experiments were performed with 15µg of guide DNA plasmid and 15µg of donor DNA plasmid at 300V and 900µF. Further experiments utilised 15µg of guide DNA plasmid and 15µg of linearized donor DNA plasmid. The donor plasmid was linearized using EcoRI-HF overnight at 37°C (20 units of enzyme per 1µg of DNA in a 50µL reaction). A sample was run on a 1% (w/v) agarose gel to ensure plasmid linearization compared to linearized DNA control. Linearized donor DNA was purified using Phenol chloroform extraction. One volume of Phenol:Chloroform:Isoamyl Alcohol (24:24:1) was added to the sample and shaken by hand for 20 seconds. The solution was centrifuged at room temperature for 5 minutes at 16,000g. The upper aqueous phase was removed, and salt ethanol precipitated as previously described in Section 2.2.9.

Table 2.2.3 Donor sequences used in CRISPR-Cas9 Btk KI experiments

| Mutation | Donor sequence |
|------------|--|
| W124F | TCTGCGCTGGCTGCTTCGGGTGGCTGCAAGCCTCTGCTCTCCTATT CCCCTCTATGAGCCATGGCCCGGCGCTGAGCACGTTGTCTATAGG TGGTGTACGATGAGGGGCCCTCTACGTCTTCTCCCCGACAGAGG AGCTGCGCAAACGCTTCATCCATCAGCTGAAGAGTGGTGAGTTTTG GGGCACCCAGCTGCGCGTGC GGCGTGA CT CAGAGCATTGGGTTTC CGGGGGCTCGCTGCCTCGTGGTTACGATATCCCATATCTGCGGAA GAGAGAGCTCTATCAGAAAGTGCTCCCA |
| WW249/50LL | ATGAAGCCCCTGCCCCCTGAGCCAGCCCCCAGTGCAGCAGGTGAA ATGAAGAAGGTGGTGGCCCTGTACA ACTATGTGCCAATGAATGTGC AGGACCTGCAGCTTCAGAAGGGTGAGGAGTACCTCATCCTGGAGG AAAGCCACCTGCCTTTGTTGAAAGCACGAGACAAAAATGGGTAAGA ACTCCCCGCTATCCATGGCATT CACCCTGCAGCCGTGTCCTATCTC AGCATTGCTCCTGGGGCAGCCTCAGGGACCCACACCTGACACTGG GGAATCCCAGCTGGTCTCAGACTCTCA |
| R307K | CAGGACTCCTTTCATTCACTGCAGCCTCTCCAGTCATGCTGTGATT GTCCCTCTTGCTGTTATGGTCACTTCCTCACA AATACCCCTCCTAT CTCCTCCTTTTATTTTTTTCTTTTTAGGGTAAGGAAGGGGGCTTCATT GTTAAGGATTCTACCAGCAAGACAGGTAAATACACTGTTTCTGTTTA TGCCAAGTCCGCTGTGTAAGTGGATCTAAGAATAGCTTGTTGCTAT CTCAGAGCACCCCTCCAGGCACCTCTCACTCTCTGCTTGCCCTTCC CAAGCTGCTGACCCCATGC |
| K430E | GGCACCTGCACCCTCATCACACTCACACTCTCTGTCTAGGGTCGT GGGAGATTGACCCGAAGGACCTGACCTTCCTGAAGGAACTGGGGA CAGGGCAGTTTGGCGTAGTGAAGTACGGGAAATGGAGAGGCCAAT ACAACGTTGCCATCGAAATGATCAGGGAGGGATCTATGTCAGAAGA CGAGTTTATTGATGAAGCCAAAGTCATGATGTAAGTGGTGAGCAGC CCCCAGGTCAGTGCAGCATATATCTTGTCAGAATACCTGCACTCCC AGATGGTTTGGAGGGACAGCATCAGG |

2.2.15 DT40 DNA extraction and Touchdown PCR

2.2.15.1 DNA extraction

1mL of cells were pelleted and washed 1x in PBS and pelleted before being resuspended in 100µL DT40 lysis buffer (200 mM NaCl, 20 mM EDTA, 40 mM Tris-HCl, pH 8.0, 0.5% SDS, 0.5% 2-ME). 4µL of proteinase K was added (20µg/mL) and samples were digested overnight at 55°C. DNA was precipitated by the addition of 70µL of 5M NaCl and samples were shaken for 15 seconds before incubation on ice for 15 minutes. Samples were centrifuged at 12,000g for 30 minutes at 4°C and the supernatant removed. 250µL of 100% ethanol was added to the supernatant and samples were spun for 2 minutes at 4°C at 12,000g. The supernatant was removed and the DNA precipitate was washed with 500µL of 70% ethanol before further centrifugation at 12,000g for 1 minute at 4°C. Supernatant was removed and samples were allowed to air dry for 5 minutes before resuspension in 15µL of ddH₂O.

2.2.15.2 Touchdown PCR

Extracted DNA was amplified using REDTaq (Sigma Aldrich, Poole UK). Reaction mixture contained 5 µl 10× REDTaq PCR Reaction Buffer, 1µL DNTPs (final concentration 200µM for each DNTP). 2.5 µl of both forward and reverse primers (10 µM), 10 ng template DNA, 2.5µL of REDTaq DNA polymerase and ddH₂O to a final volume of 50 µl. Reaction conditions were 94°C 1 minute, then cycles of 94°C 1 minute for denaturing, 65°C for 2 minutes for annealing, 72°C for 3 minutes for extension with the annealing temperature dropping by 1°C each cycle to a final annealing temperature of 55°C. 20 cycles of 94°C 1 minute, then cycles of 94°C 1 minute, 55°C for 2 minutes and 72°C for 3 minutes then followed. PCR mixture was resolved via agarose gel electrophoresis, resulting fragments excised and purified using GenElute™ Gel Extraction Kit (Sigma-Aldrich) before sequencing.

2.2.16 Total internal reflection fluorescence microscopy (TIRFM) and Stochastic optical reconstruction microscopy (STORM)

sample preparation

Ibidi μ -slide wells were coated with 20 μ g/mL collagen overnight at 4°C, washed with PBS then blocked with 5mg/mL heat denatured protease-free bovine serum albumin in PBS (BSA/PBS) for 45 minutes at room temperature. The wells were washed 3 times with PBS before 200 μ L of washed platelets (2×10^7 cells/mL) were added and left to incubate for 45 minutes at 37°C. Non adhered platelets were aspirated and the wells washed 3 times in PBS before cells were fixed with 200 μ L 10% Formalin for 10 minutes followed by 3 washes in PBS. Cells were then permeabilised with 200 μ L 0.1% (v/v) Triton X-100 for 5 minutes before being washed 3 times in PBS before being blocked with BSA/PBS as described previously before being incubated with primary antibodies. Primary antibodies used for staining can be found in Table 2.1.1. Platelets were stained with primary antibody for 45 minutes at room temperature then washed 3 times in PBS followed by incubation with appropriate secondary antibodies (1 in 500) for 45 minutes then finally washed 3x in PBS before being imaged in PBS using a Nikon TIRF system mounted on a Nikon Eclipse Ti inverted microscope, with a Nikon 100x NA 1.49 TIRF objective.

2.2.17 TIRFM image analysis

Microscopy analysis was performed using ImageJ. Btk spot analysis was performed by thresholding the image to 1% to remove background and select for Btk spots. Particles were counted using the ImageJ tool 'Analyse Particles'. Particles between 0.1-10 microns and 0-1 circularity were included in the count. Colocalisation analysis was performed by thresholding the image and then using the JACoP plugin (Bolte and Cordelieres, 2006).

2.2.18 STORM imaging

Samples were imaged on a Nikon N-STORM system in dSTORM mode which is characterized by a Ti-E stand with Perfect Focus, using a 100x 1.49 NA TIRF objective.

To allow fluorophore blinking, samples were imaged in a PBS based buffer consisting of enzyme solution (catalase 1 µg/ml, Tris (2-carboxyethyl) phosphine hydrochloride 4 mM, glycerol 50%, KCl 25 mM, pH 7.5 Tris-HCl 20 mM, glucose oxidase 50 µg/ml), glucose solution (glucose 100 mg/mL, glycerin 10%) and reducing agent solution (100 mM MEA) (Metcalf et al., 2013).

For dual colour STORM imaging (Alexa647 and Alexa555) the N-STORM emission cube was used. Images were obtained with continuous activation. The 405 (for 647) and 488 (for 555) laser power was then increased by 5% every 30 seconds until maximum activation of 50% laser power during imaging to reactivate the fluorophores from the dark state. 20,000 frames per colour were captured using Nikon NIS Elements v4.5 software, and reconstructed using the Nikon STORM analysis module 3.2, applying the drift correction and the Gaussian rendering. 4 separate fields of view (FOV) from 3 independent experiments were imaged. Individual fluorescent blinking events were identified and were filtered on photon count and only those with a count >400 was selected for further cluster analysis.

2.2.19 STORM analysis

Nikon localisation co-ordinates were exported as a text file, and then separated into two colours and converted to a text file format using 'ChriSTORM' plug-in for ImageJ (Leterrier et al., 2015).

2.2.19.1 LAMA

Localisation microscopy analyser (LAMA) software (Malkusch and Heilemann, 2016) was used to assess cluster formation. Hierarchical cluster analysis was performed with

clustering analysis based on Density-based spatial clustering of applications with noise (DBSCAN). A cluster was defined as 10 points within a given observation radius (25nm, 50nm, 75nm and 100nm).

2.2.19.2 Plot profile

To assess the localisations of GPVI and Btk along a collagen fibre, Nikon NIS Elements analysis software was used to perform plot profile analysis. A line was drawn along the collagen fibre and the fluorescence profile for each channel was generated. This was converted into arbitrary units due to differing lengths with varying staining fluorescence intensities of each fibre. The arbitrary units are 1 for Btk being present, 2 for GPVI being present and 3 for both being present at that individual locus. The percentage of localisations on the collagen fibre was assessed and analysed using GraphPad Prism.

For images without collagen fibres, a random cross Section was drawn across the image over a range of platelets to generate the plot profile before it was analysed using excel and prism.

2.2.19.3 ClusDoC: Cluster detection with degree of colocalization

ClusDoc software (Pageon et al., 2016) was utilised to analyse colocalisation of clusters. At least 3 random regions of interest were selected for each field of view. Coordinate based colocalisation (CBC) is first used to assess the colocalisation of molecules of 'A' with 'B' and molecules of 'B' with 'A' within a defined diameter of 50 nm. ClusDoC utilises DBSCAN algorithms to analyse clusters. A cluster was defined as at least 10 points within 50nm radius. The cluster contours are defined and overlaid on the CBC maps and analysed. Colocalised clusters are defined as clusters with a CBC value above ≥ 0.4 .

2.2.20 Statistical analysis

Data was analysed and where appropriate normalised to the vehicle control. GraphPad Prism 7 was used to perform statistical analysis by 1-way ANOVA with Dunnett's or Tukey's multiple comparison post-test, 2-way ANOVA with Dunnett's or Tukey's multiple comparisons test or a two-way T Test. The level of significance of p values is as follows, * $p \leq 0.05$, ** $p \leq 0.01$, *** $p \leq 0.001$. Data presented are mean +/- standard error of the mean, unless stated. IC₅₀ values are shown with 95% confidence intervals

3 *Btk inhibitors inhibit CLEC-2 mediated platelet functions more severely than GPVI mediated function.*

3.1 Introduction

3.1.1 Btk deficient platelet function downstream of GPVI and CLEC-2

The initial study that proposed a role for Btk downstream of GPVI was performed by Quek et al., 1998. Btk deficient XLA patients were compared to healthy donors and did not aggregate in response to CRP-XL at two doses (1µg/mL and 5µg/mL) and, although reduced, PLCγ2 phosphorylation was still present when assessed using western blotting. This can also be observed in Btk deficient mouse platelets as they do not aggregate to low concentrations of CRP-XL (1µg/mL and 3µg/mL) (Atkinson et al., 2003a). Human Btk deficient platelets did aggregate in response to collagen, albeit to a lesser extent. There was also calcium flux in response to this agonist, but not to CRP-XL.

As PLCγ2 phosphorylation was not totally lost in these patients, it was hypothesised that Tec may be playing a compensatory role in mediating the phosphorylation (Atkinson et al., 2003a). A murine model of individual Btk and Tec knockouts, and a double knockout was used to investigate this hypothesis. When stimulated with collagen, PLCγ2 phosphorylation was only reduced in the double knockout platelets. This is mirrored in aggregation experiments where individual Tec family kinase (TFK) knockouts have normal aggregation, whereas it is reduced in the double knockout (Atkinson et al., 2003a).

When CRP-XL was used to ligate GPVI, high concentrations (10µg/mL) induced full aggregation in Tec knockouts, weak aggregation in Btk knockouts and no aggregation in double knockouts. Once again, this was mirrored in phosphorylation experiments with PLCγ2 phosphorylation being reduced in Btk deficient but not Tec deficient platelets. In double knockouts the levels of PLCγ2 phosphorylation were almost abolished at a high concentration of CRP-XL. This suggests Tec can compensate but not totally rescue the

platelet response in the absence of Btk, and only at high concentrations of agonist. At lower concentrations of agonist, Tec cannot play a compensatory role as aggregation is blocked in the absence of Btk for both human and mouse platelets (Quek et al., 1998, Atkinson et al., 2003a).

It was initially believed that downstream of CLEC-2, Tec could also play a compensatory role. CLEC-2 deficient embryos have a blood lymphatic mixing (Finney et al., 2012, Suzuki-Inoue et al., 2010, Pollitt et al., 2014). Double knockout mice deficient in Btk and Tec display blood lymphatic mixing showing the role for Btk and/or Tec downstream of CLEC-2. Whereas single knockouts of either TFK result in a normal phenotype *in vivo*, suggesting redundancy between the two kinases, (Manne et al., 2015a). However, it is not clear which KO is presented in the paper and therefore difficult to ascertain which kinase plays the predominant role.

3.1.2 Btk inhibitors downstream of GPVI

The effect of ibrutinib on platelet aggregation induced by GPVI agonists has been characterised by numerous groups. Using intermediate and low concentrations of collagen as an agonist, ibrutinib can inhibit platelet aggregation in washed platelets (Alberelli et al., 2018, Bye et al., 2015). There are some discrepancies in the literature as to what concentration of ibrutinib is required to cause total inhibition of platelet aggregation to collagen. Differences between concentrations may be due to differing platelet preparations, agonist concentrations and the methods of assessing aggregation. In the work of Bye et al., aggregation was abolished at 1 μ M in response to 1 μ g/mL collagen in washed platelets. The same concentration of ibrutinib (1 μ M) can also cause inhibition at higher concentrations of collagen (Alberelli et al., 2018, Levade et al., 2014).

It has been shown that low concentrations of ibrutinib can be overcome by high concentrations of agonist, as using 10x the concentration of collagen required 10x the concentration of ibrutinib to inhibit the response (Lee et al., 2017). This may be due to the

redundancies in protein signalling or an increased amount of receptor clustering. For example, an increased amount of GPVI receptor clustering may populate the local environment with FcR γ chain associated SFK's and Syk (Gibbins et al., 1996, Poole et al., 1997). These kinases may be playing the predominant role in mediating aggregation compared to Btk.

Similarly, to collagen, aggregation was inhibited in the presence of 1 μ M ibrutinib downstream of 1 μ g/mL CRP-XL. Spreading and adherence to CRP-XL was also greatly inhibited compared to vehicle control in the presence of 1 μ M ibrutinib. Whereas in contrast, only the spreading was inhibited on collagen, not the adherence (Bye et al., 2015). Ibrutinib has also been shown to inhibit exogenous GPVI ligands such as convulxin mediated platelet aggregation (Manne et al., 2015a), in addition to CRP-XL mediated aggregation.

Although ibrutinib has been studied in platelet aggregation, far less work has been published with acalabrutinib. Acalabrutinib is a more selective Btk inhibitor and does not inhibit Tec and other kinases including SFK at the same potency that ibrutinib does (Barf et al., 2017, Byrd et al., 2016, Herman et al., 2015). Therefore, it would be expected there would be less severe inhibition of platelet aggregation due to off target effects seen with ibrutinib. Indeed, at 2 μ M, a clinically relevant dose, the level of inhibition of aggregation with 3.3 μ g/mL of collagen was not as severe as ibrutinib. However, higher concentrations of acalabrutinib were able to fully inhibit aggregation (Series et al., 2019). When a higher concentration of agonist is used, (100 or 75 μ g/mL), 0.6 μ M acalabrutinib did not appear to inhibit aggregation as severely, however no statistical analysis directly comparing to vehicle control was used (Chen et al., 2018).

3.1.3 Btk inhibitors downstream of CLEC-2

Compared to GPVI, the use of inhibitors to investigate the role of Btk downstream of CLEC-2 has been less extensively researched (Manne et al., 2015a, Lee et al., 2017,

Nicolson et al., 2020). The first initial study was performed by the Kunapali group using ibrutinib. It was proposed by this group that Btk is positioned upstream of Syk after CLEC-2 stimulation as Syk phosphorylation is lost in the presence of ibrutinib (Manne et al., 2015a). This is in contrast to the proposed canonical model of hemITAM signalling which suggests that Syk precedes Btk (Fuller et al., 2007, Hughes et al., 2010b, Pollitt et al., 2014).

Within the work by Manne et al, low concentrations of ibrutinib (10nM) ablated the CLEC-2 mediated response to 10nM rhodocytin in mouse platelets. This concentration (10nM ibrutinib) was also inhibitory to human platelets, at a range of concentrations of rhodocytin. Phosphorylation events using 300nM or 100nM rhodocytin and 10nM ibrutinib showed an inhibition of the Syk active site pY525 and PLC γ 2 active site pY759, however the phosphorylation of Btk was not shown.

In the study by Manne et al., aggregation was blocked 10nM. However, the authors did not show total cell phosphorylation, or investigate the Btk transphosphorylation site, pY551. Therefore, it is unknown whether Btk was initially phosphorylated by SFK's which is required for it to be active (Wahl et al., 1997, Park et al., 1996). If the transphosphorylation site of Btk was shown, it would provide more convincing evidence that Syk lies downstream of Btk in CLEC-2 signalling.

An alternative interpretation of the results by Manne et al., may be explained by the requirement of secondary feedback to reinforce CLEC-2 signalling. Indeed, Manne et al., show that at the concentration of ibrutinib (10nM) and rhodocytin (30nM), ATP secretion is totally abolished. This would suggest that the release of ADP and production of TxA₂ is also inhibited under these conditions. It is known that the phosphorylation and reinforcement of CLEC-2 requires secondary messengers. The platelet preparation used by Manne et al would have prevented production of the secondary messenger TxA₂ due to the use of aspirin in the preparation (Koessler et al., 2016). Positive feedback and Syk activation are required to initiate CLEC-2 phosphorylation (Pollitt et al., 2010, Hughes et al., 2015) and therefore signalling, so the absence of positive feedback may explain the

80

absence of Syk phosphorylation. Of note, the authors did also not show Src pY416, a marker of active Src, which is responsible for phosphorylating Syk, which in turn phosphorylates CLEC-2 (Hughes et al., 2015). Therefore, it is difficult to conclude if Btk lies upstream of Syk in the CLEC-2 stimulated pathway.

A different study required 5 μ M of ibrutinib to block CLEC-2 mediated aggregation in mouse platelets, which is 50-fold higher than the concentration used by Manne et al., (Lee et al., 2017). The agonist used was podoplanin-Fc at 2 μ g/mL, and low concentrations of ibrutinib (0.5 μ M) did not cause inhibition of platelet aggregation. However, it is difficult to compare these results due to the different agonists and differences between mouse and humans.

3.2 Aims and hypothesis

There are few studies on the role of Btk downstream of hemITAM signalling, aside from one study suggesting that it is upstream of Syk (Manne et al., 2015a). There is more literature published describing a role of Btk downstream of ITAM signalling, however there are some inconsistencies across studies, summarised below:

- 1) Patients that have XLA and are deficient in Btk do not respond to CRP-XL but do respond to collagen (Quek et al., 1998). They do not experience bleeding side effects, likely to the compensation of Tec, but also other platelet stimulatory pathways (Atkinson et al., 2003a).
- 2) Patients taking ibrutinib, a Btk inhibitor, experience bleeding as a side effect (Covey et al., 2015, Lipsky et al., 2015).
- 3) Patients taking acalabrutinib, a second generation Btk inhibitor, are thought to experience less bleeding side effects.

Taken together, it is not clear whether Btk's catalytic activity is required to mediate GPVI signalling as no bleeding side effects are observed in XLA patients, or patients taking a more specific Btk inhibitor, acalabrutinib.

The impact of ibrutinib on platelet aggregation suggests off target effects on platelet function. This is unlikely to be mediated through Btk, as acalabrutinib does not seem to replicate these effects, with acalabrutinib patients tending to not experience bleeding side effects.

Downstream of CLEC-2, there are also unanswered questions in regard to Btk and its role within the signalling pathway (Manne et al., 2015a, Fuller et al., 2007, Hughes et al., 2010b, Pollitt et al., 2014).

The work published by Manne et al., uses ibrutinib, which can inhibit SFK phosphorylation (Patel et al., 2016). SFK inhibition would inhibit the release of secondary mediators and subsequently CLEC-2 phosphorylation (Severin et al., 2011). Therefore, a more selective

Btk inhibitor, acalabrutinib, will be used to investigate the role of Btk downstream of CLEC-2.

Aims

- To identify if acalabrutinib causes platelet inhibition in a similar manner to ibrutinib
- To characterise the effect of acalabrutinib downstream of GPVI and CLEC-2 using platelet aggregation, granule secretion and protein phosphorylation and to investigate where Btk lies in the CLEC-2 signalling cascade
- To investigate if rhodocytin can support platelet spreading and if it can, to investigate if acalabrutinib can inhibit platelet adhesion and spreading to rhodocytin and to compare this with collagen

Hypothesis

Inhibition of Btk will inhibit CLEC-2 mediated platelet responses to a greater effect than GPVI mediated signalling.

3.3 Results

3.3.1 Establishing conditions to assess CLEC-2 signalling in washed platelets

Rhodocytin is a purified snake venom toxin, and within the literature it has been used at a range of concentrations from 3-300nM (Suzuki-Inoue et al., 2001, Bergmeier et al., 2001, Suzuki-Inoue et al., 2006, Suzuki-Inoue et al., 2007) . Furthermore, responsiveness to low concentrations of rhodocytin varies from donor to donor. Therefore, washed platelet aggregation was performed to assess an appropriate concentration of rhodocytin to use for reproducible responses during this study.

Washed platelets (4×10^8 cells/mL) were stimulated with 10-300nM rhodocytin for 7 minutes. 300nM and 100nM induced maximal aggregation ($90.1\% \pm 4.5$ and $89.7\% \pm 7.0$ respectively) with there being a short lag/delay with 100nM of rhodocytin. 30nM of rhodocytin caused weak aggregation in some donors but not in others whereas 10nM did not induce aggregation. Therefore, 100nM and 300nM of rhodocytin were chosen as appropriate concentrations to reproducibly investigate CLEC-2 mediated platelet activation (Figure 3.3.1.B).

To assess an appropriate time point for CLEC-2 signalling studies, washed platelets (4×10^8 cells/mL) were stimulated with 300nM rhodocytin for the stated time points in the presence of $9 \mu\text{M}$ concentration integrin. Samples were separated using SDS-PAGE before western blotting to assess total tyrosine phosphorylation using 4G10 antibody. As Figure 3.3.1.C shows, 0 and 30 seconds have minimal tyrosine phosphorylation, which increases at 60 seconds and is maintained up until 5 minutes where levels peak. Therefore, stimulation for 5 minutes was used to investigate signalling downstream of CLEC-2.

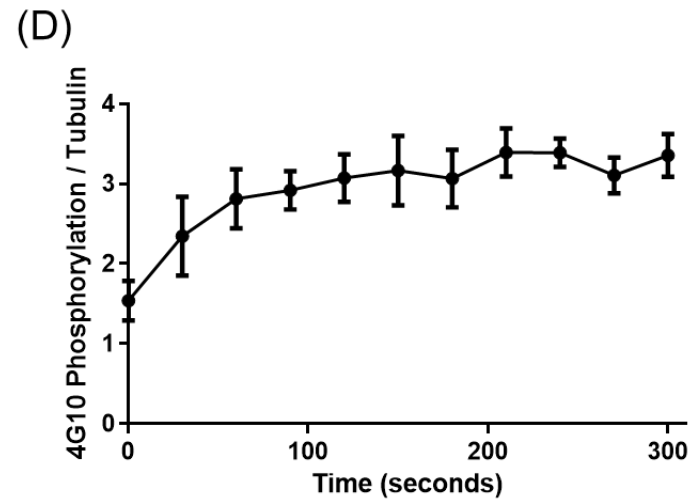
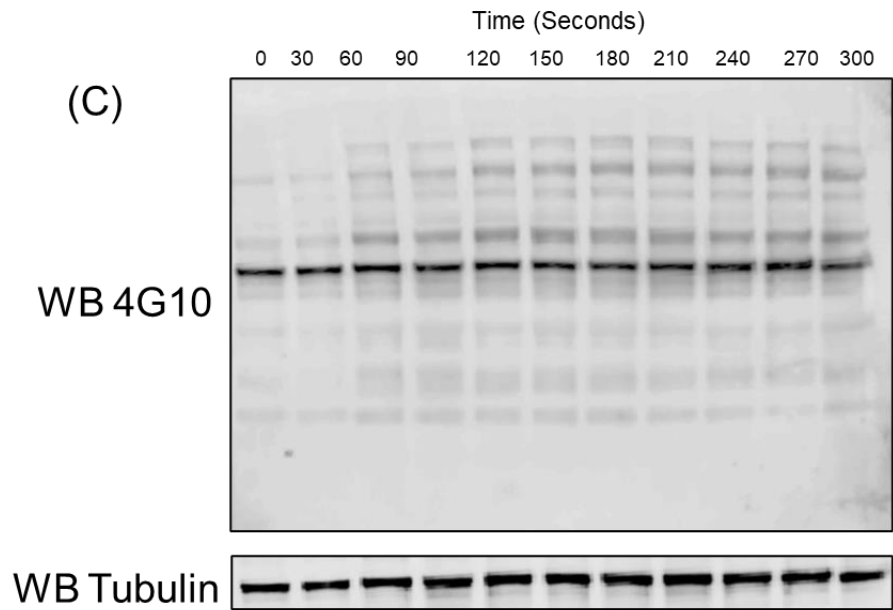
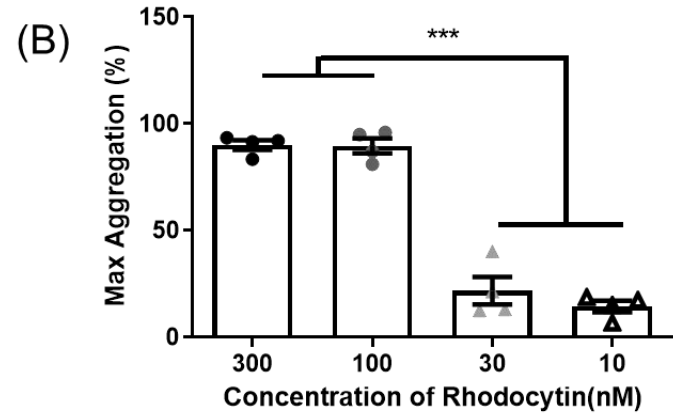
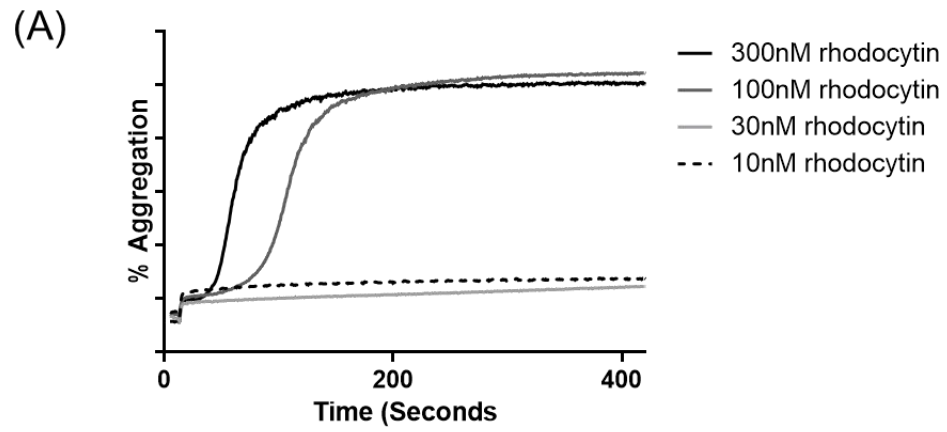


Figure 3.3.1 Washed platelets respond to rhodocytin at high concentrations and 300 seconds is an appropriate time point to assess downstream CLEC-2 phosphorylation.

(A, B) Washed platelets were stimulated with rhodocytin (10-300nM) for 7 minutes using light transmission aggregometry. (A) shows the representative trace and (B) shows the % aggregation values from three independent experiments. statistical significance was calculated using a one-way ANOVA against vehicle control with a Tukey's post-test. Graph represents mean \pm SEM. Significance was taken at *** $p \leq 0.001$. (C) washed platelets in the presence of integrilin (9 μ M) were stimulated with 100nM rhodocytin for the indicated times. Blots were probed with anti-phosphotyrosine antibody and tubulin antibody as a loading control. (D) Densitometry analysis was performed using ImageQuant. Graph represents mean \pm SEM, n=4.

3.3.2 Ibrutinib inhibits (hem)ITAM mediated washed platelet responses more severely than acalabrutinib, with hemITAM responses more severely inhibited

Previous studies suggest that Btk is essential for GPVI and CLEC-2 mediated aggregation and granule secretion. Patients deficient in Btk do not aggregate in response to CRP-XL (Quek et al., 1998) and a low dose of ibrutinib (10nM) blocked platelet aggregation to a low concentration of rhodocytin (30nM) (Manne et al., 2015a). Some work using Btk inhibitors has been published investigating the role of Btk in platelet aggregation (Rigg et al., 2016, Kamel et al., 2015, Levade et al., 2014, Lee et al., 2017), further suggesting that Btk may be mediating the platelet response.

Platelet α granule secretion is a common marker of platelet activation (Chen et al., 2000, Blair and Flaumenhaft, 2009). These granules contain molecules that contribute to platelet regulation and thrombus formation via an auto and paracrine mechanism. P selectin (CD62P) is a transmembrane receptor that is present within α granules and is exposed on the surface of platelets during the release of granule contents (Koedam et al., 1992). Measuring the exposure of P-Selectin from platelets using flow cytometry indirectly measures the α granule secretion of the platelet.

The activation of the integrin α IIb β 3 from its closed to open state is a critical process in platelet signalling. Inside-out signalling is the term for when the platelet becomes activated, transmits signals through the cell resulting in the opening of the integrin to its active state. Its ligand, fibrinogen, is then able to bind to the open conformation and cause outside-in signalling leading to platelet aggregate formation (Woods et al., 1986, Springer et al., 2008). The extent of fibrinogen binding to activated platelets was measured using flow cytometry, which provides an indirect estimation of the extent of integrin α IIb β 3 molecules present in the activated state on the platelet surface. This measure, together with α granule secretion show another readout of platelet activation.

Therefore, as ibrutinib has been shown to inhibit aggregation (Levade et al., 2014, Lee et al., 2017), these responses were also investigated, using acalabrutinib.

For aggregation, washed platelets (4×10^8 cells/mL) were incubated with a range of concentrations of acalabrutinib, ibrutinib or vehicle control for 5 minutes before stimulation with $1 \mu\text{g/mL}$ CRP-XL for 5 minutes or 100 nM rhodocytin for 7 minutes. 100 nM rhodocytin was selected as opposed to 30 nM used in the work by the Kunapali group as 30 nM did not elicit a strong response in washed platelets in this study (Figure 3.3.1). Consistent with other studies 5 minutes was selected as the appropriate time for drug preincubation (Bye et al., 2015, Nicolson et al., 2018).

For granule release and $\alpha\text{IIb}\beta_3$ activation, flow cytometric analysis was performed. ADP insensitive washed platelets (4×10^8 cells/mL) were incubated with ibrutinib, acalabrutinib or vehicle control, anti-P-Selectin Cy5/PE conjugated antibody and FITC conjugated anti-fibrinogen antibody for 5 minutes before the addition of agonist ($1 \mu\text{g/mL}$ CRP-XL or 100 nM rhodocytin). Platelets were incubated for 20 minutes in the dark and then fixed with 0.2% formyl saline prior to assessment using a BD Accuri C6 flow cytometer (BD Biosciences, Oxford, UK). Data was collected from 10,000 events gated on platelets using side scatter (SSC) and forward scatter (FSC), measures of cell granularity and cell size, respectively.

Downstream of CRP-XL, only $10 \mu\text{M}$ acalabrutinib inhibited aggregation and granule release (Figures 3.3.2 B and G), ($p \leq 0.001$). $\alpha\text{IIb}\beta_3$ activation was also inhibited at 10 and $3 \mu\text{M}$ acalabrutinib downstream of GPVI ($p \leq 0.001$ and $p \leq 0.05$). At lower concentrations of acalabrutinib (1 - $0.1 \mu\text{M}$), responses to aggregation, granule secretion and $\alpha\text{IIb}\beta_3$ activation were comparable to vehicle treated samples.

1 - $0.1 \mu\text{M}$ ibrutinib caused a significant reduction in platelet aggregation, with all values below 20% aggregation. Lower concentrations of ibrutinib did not inhibit aggregation in response to CRP-XL. This is also observed in granule secretion and $\alpha\text{IIb}\beta_3$ activation

downstream of GPVI, with 1 μ M ibrutinib inhibiting the response ($p \leq 0.01$) (Figures 3.3.2.F and I).

Figures 3.3.2.E, H and K compares the differences between the two drugs for the responses in aggregation, granule release and α IIb β 3 activation to CRP-XL. Ibrutinib is more potent at inhibiting aggregation, granule release and α IIb β 3 activation than acalabrutinib. This is reflected in the IC₅₀ values, with the shift of the curve to the left for ibrutinib.

At high concentrations of acalabrutinib (10 and 3 μ M), the aggregatory response to 100nM rhodocytin was ablated (Figures 3.3.3.A, B) ($p \leq 0.001$), as was granule release and α IIb β 3 activation ($p \leq 0.01$) (Figure 3.3.3.G and J).

1 μ M acalabrutinib significantly inhibited aggregation to rhodocytin on average to 30% (± 14) ($p \leq 0.001$), however, one donor had an almost normal response compared to the other donors which is reflected in the large error bars. 1 μ M acalabrutinib did not inhibit granule release downstream of CLEC-2 but did inhibit α IIb β 3 activation ($p \leq 0.05$). This shows responses are variable between donors at certain concentrations of inhibitor, which was also observed downstream of GPVI.

Only the two lowest concentrations of ibrutinib tested (0.01 μ M and 0.03 μ M), did not cause inhibition of aggregation downstream of CLEC-2. 1, 0.3 and 0.1 μ M all caused a significant reduction in aggregation as Figures 3.3.3.C and 3.3.3.D show. Inhibition of aggregation responses were similar to granule release and α IIb β 3, as 0.3 μ M also significantly reduced the response ($p \leq 0.05$).

When comparing between the two drugs, there is a significant difference in the platelet aggregation at 0.3 μ M ($p \leq 0.001$), 0.1 μ M ($p \leq 0.01$) and 0.03 μ M ($p \leq 0.05$), with ibrutinib being more inhibitory in CLEC-2 mediated responses.. The IC₅₀ for acalabrutinib is 0.69 μ M (95% confidence interval, 0.36 to 1.13), and 0.02 μ M (0.01 to

0.04) for ibrutinib. This demonstrates that ibrutinib is more potent at inhibiting CLEC-2 mediated aggregation.

The more potent inhibition of platelet responses downstream of CLEC-2 (as measured by smaller IC_{50} values with both ibrutinib and acalabrutinib) compared to GPVI suggests that Btk inhibition is more detrimental to CLEC-2 mediated signalling than GPVI mediated signalling.

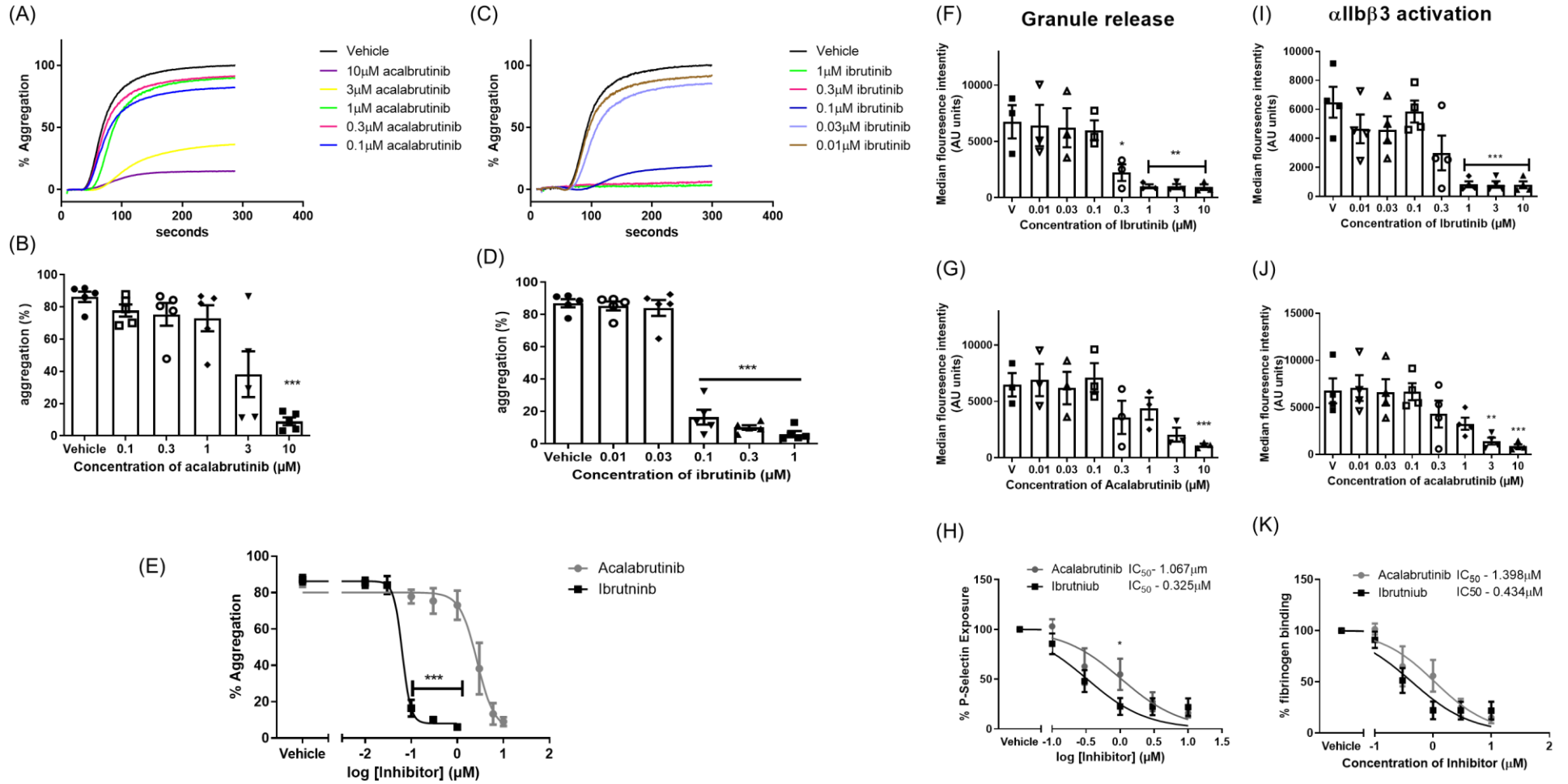


Figure 3.3.2 only high concentrations of Btk inhibitors inhibit GPVI washed platelets and Ibrutinib inhibits mediated α granule release and $\text{all}\beta\text{3}$ activation more than acalabrutinib mediated granule release

(A-E) Washed platelets were incubated with (A,B) acalabrutinib (10-0.1 μ M), (C,D) ibrutinib (10-0.1 μ M) or vehicle control (0.1% DMSO (v/v)) for 5 minutes before stimulation with 1 μ g/mL CRP in light transmission aggregometry. (A, C) shows representative traces, and (B,D) shows the quantified values. (E) shows the % aggregation of both inhibitors. Graphs represent mean \pm SEM, n=5. Statistical significance was calculated using a one-way ANOVA against vehicle control with a Dunnett's post-test. *p \leq 0.05, **p \leq 0.01, ***p \leq 0.001. (H-J) Washed platelets (4x10⁸ cells/mL) were incubated with (F,H) ibrutinib, (G,I) acalabrutinib or vehicle control (DMSO, 0.1% (v/v)) for 5 minutes, after which PE/Cy5 anti-human CD62P antibody and FITC-conjugated anti-fibrinogen were added to the sample prior to stimulation. Samples were stimulated with CRP-XL (1 μ g/mL) for 20 minutes before flow cytometric analysis. The Median fluorescence intensity was plotted against inhibitor concentration and analysed using one-way ANOVA with Dunnett's post-test, ***p \leq 0.001, **p \leq 0.01 and *p \leq 0.05. Graphs represent mean \pm SEM, n=4. The values were normalised to vehicle control being 100% and the (H, J) IC₅₀'s calculated.

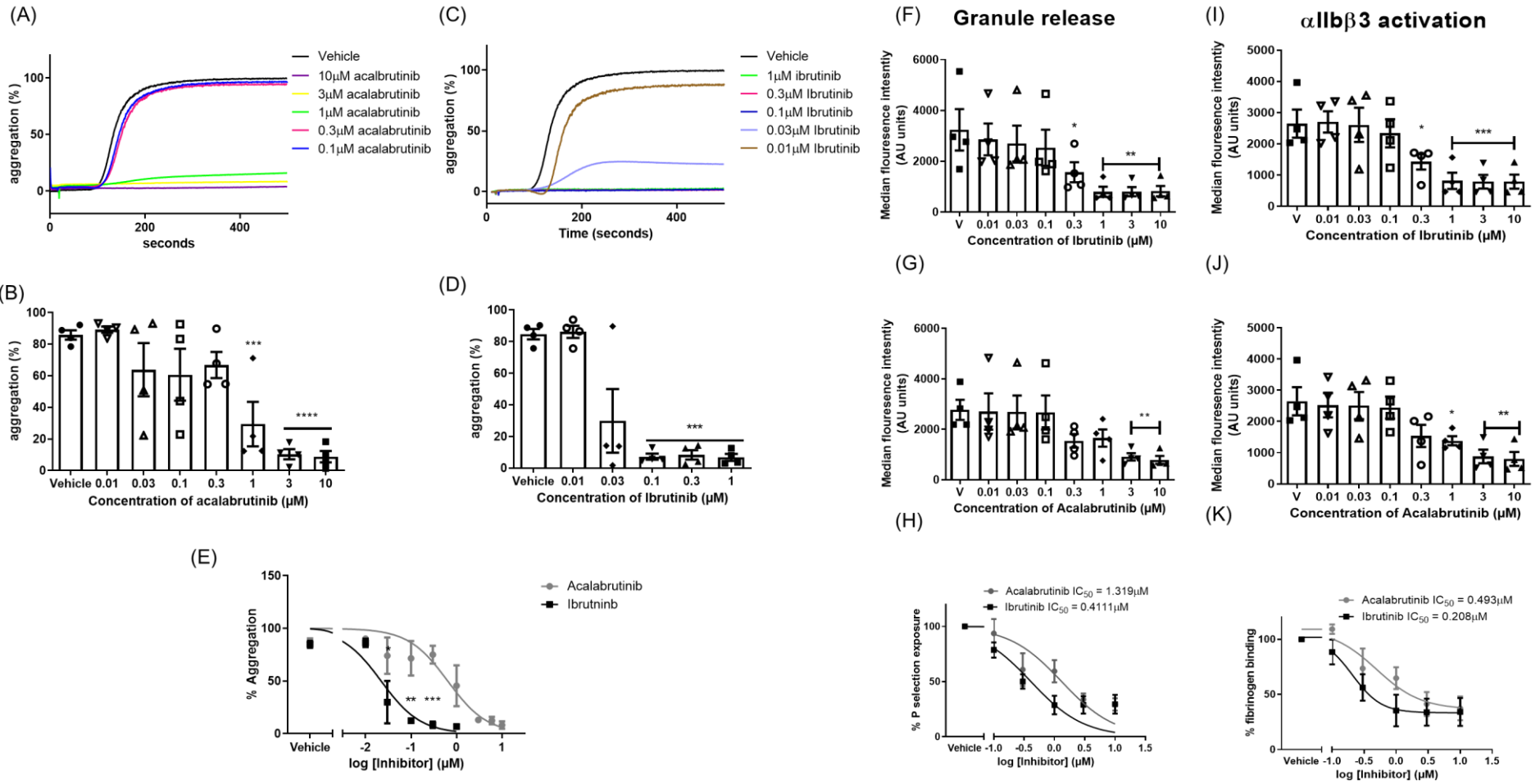


Figure 3.3.3 ibrutinib and acalabrutinib dose dependently inhibit CLEC-2 mediated platelet functions however ibrutinib is more potent.

(A-E) Washed platelets were incubated with (A,B) acalabrutinib (10-0.1 μ M), (C,D) ibrutinib (10-0.1 μ M) or vehicle control (0.1% DMSO (v/v)) for 5 minutes before stimulation with 100nM rhodocytin in light transmission aggregometry. (A, C) shows a representative trace, and (B,D) shows the quantified values. (E) shows the % aggregation of both inhibitors. Graphs represent mean \pm SEM, n=5. Statistical significance was calculated using a one-way ANOVA against vehicle control with a Dunnett's post-test. *p \leq 0.05, **p \leq 0.01, ***p \leq 0.001. (H-J) Washed platelets (4x10⁸ cells/mL) were incubated with (F,H) ibrutinib, (G,I) acalabrutinib or vehicle control (DMSO, 0.1% v/v) for 5 minutes, after which PE/Cy5 anti-human CD62P antibody and FITC-conjugated anti-fibrinogen were added to the sample prior to stimulation. Samples were stimulated with rhodocytin (100nM) for 20 minutes before flow cytometric analysis. The Median fluorescence intensity was plotted against inhibitor concentration and analysed using one-way ANOVA with Dunnett's post-test, ***p \leq 0.001, **p \leq 0.01 and *p \leq 0.05. Graphs represent mean \pm SEM, n \geq 3. The values were normalised to vehicle control being 100% and the (H, J) IC₅₀'s calculated.

3.3.3 Platelets can aggregate at concentrations despite loss of the autophosphorylation site downstream of GPVI

Granule secretion and aggregation are only inhibited by high concentrations of acalabrutinib (10 μ M) downstream of GPVI (Figure 3.3.2 B, G and J). The IC₅₀ of acalabrutinib calculated in *in vitro* kinase assays using recombinant Btk are often within the nanomolar range (Licican et al., 2020, Wu et al., 2016). Previous studies in platelets and B cells using acalabrutinib have shown inhibition of Btk autophosphorylation at site pY223 at concentrations lower than 10 μ M (Series et al., 2019, Herman et al., 2015). Consequently, it is not unreasonable to believe that Btk catalytic activity would be inhibited at concentrations where aggregation is normal. Therefore, protein phosphorylation studies were used to identify when there was inhibition of Btk autophosphorylation and how this inhibition related to aggregation and granule secretion.

To examine the effect of acalabrutinib on GPVI-mediated protein phosphorylation, acalabrutinib treated washed human platelets were lysed after stimulation with CRP-XL (1 μ g/mL) and lysates probed with phosphospecific antibodies. The time point used to assess phosphorylation was 180 seconds to be consistent with previous literature (Quek et al., 1998, Bye et al., 2017, Bye et al., 2015, Nicolson et al., 2018).

Experiments were performed under non aggregating conditions with integrilin to block α IIb β 3 activation and in the presence of apyrase and indomethacin to identify the GPVI signalling response without any input of secondary mediators.

Aggregation results from previously described (Figure 3.3.2) were overlaid for comparison. Total cell phosphorylation was assessed using anti-phosphotyrosine antibody 4G10. No striking differences were revealed in the total cell phosphorylation profile in the presence of acalabrutinib when compared to control lysates (Figure 3.3.4.A, upper panel). The phosphorylation of Src pY416 was not altered in the

presence of acalabrutinib (Figure 3.3.3.4.B). Syk pY525 phosphorylation was also unaltered when platelets were treated with acalabrutinib (Figure 3.3.3.4.B).

Unsurprisingly, as the kinases mediate the phosphorylation of Btk were not inhibited, Btk pY551 was also not altered in the presence of acalabrutinib, Figure 3.3.3.4.B.

The autophosphorylation site of Btk, pY223, was inhibited in the presence of acalabrutinib, with the IC_{50} value being calculated to 0.66 μ M (0.48 to 6.04). 10 μ M, 3 μ M and 1 μ M, all had significantly inhibited levels of phosphorylation at this site compared to the vehicle control ($p \leq 0.05$). Indeed, phosphorylation is greatly reduced, in some donors at 1 μ M whereas aggregation is normal and not inhibited. Similarly, acalabrutinib inhibits phosphorylation of PLC γ 2 pY759, with the IC_{50} value being 1.37 μ M, (0.69 to 2.74) with 1 μ M, 3 μ M, and 10 μ M acalabrutinib causing inhibition compared to vehicle control (Figure 3.3.4.B), $p \leq 0.05$.

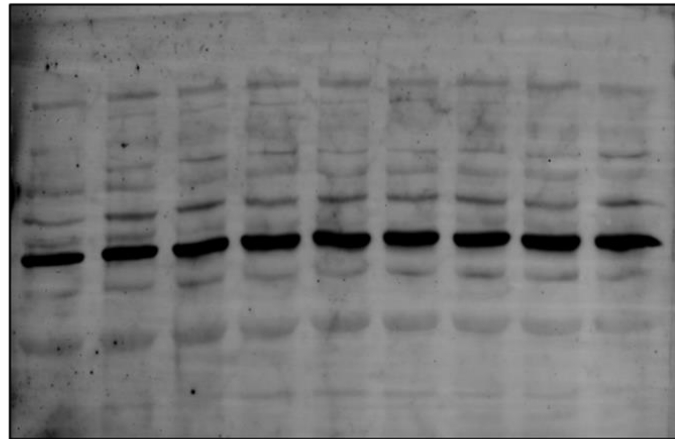
The phosphorylation of Btk Y223 does not significantly correlate with aggregation, ($p=0.104$). Whereas there is a positive correlation between Btk pY223 phosphorylation and PLC γ 2 pY759 phosphorylation, $r=0.765$ ($P=0.027$) suggesting some dependency on one another. However, correlation is not necessarily causative. There is also a significant correlation between PLC γ 2 and aggregation as $P=0.023$, $r=0.856$.

Taken together, these results suggest that in washed platelets stimulated with CRP-XL, Btk phosphorylation is not required to mediate aggregation.

(A)

| | | | | | | | | | |
|--------------------|---|---|------|------|-----|-----|---|---|----|
| CRP (1µg/mL) | - | + | + | + | + | + | + | + | + |
| Acalabrutinib (µM) | - | - | 0.01 | 0.03 | 0.1 | 0.3 | 1 | 3 | 10 |

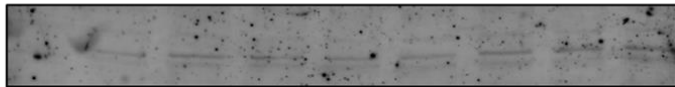
Pan pY



Src pY416



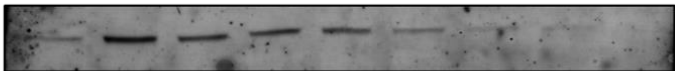
Syk pY525



Btk pY551



Btk pY223



PLCγ2 pY759



Total Syk



(B)

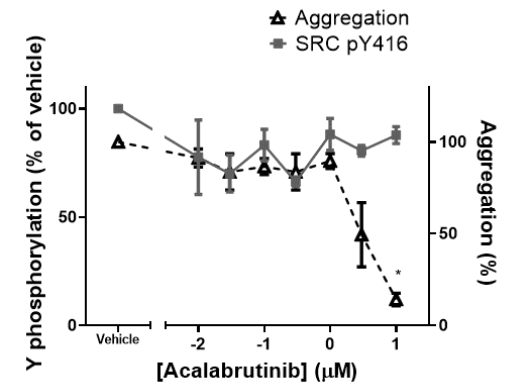
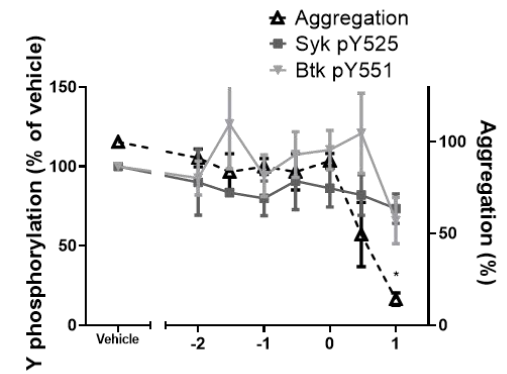
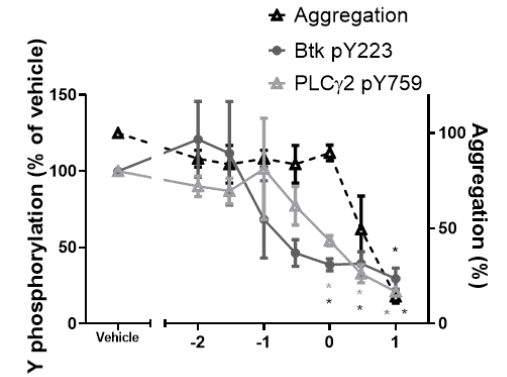


Figure 3.3.4 Platelets can still aggregate downstream of GPVI when Btk and PLC γ 2 phosphorylation is lost

(A) ADP insensitive washed platelets at (4×10^8 cells/mL) in the presence of integrilin ($9 \mu\text{M}$), apyrase (2units/mL) and indomethacin ($10 \mu\text{M}$) were incubated with acalabrutinib or vehicle (DMSO 0.1% (v/v)) for 5 minutes prior to stimulation with $1 \mu\text{g/mL}$ CRP-XL. Platelets were then lysed with 6X reducing sample buffer 180 seconds after addition of agonist. Whole cell lysates were then separated by SDS-PAGE and Western blots probed for whole cell phosphorylation or kinase specific phosphorylation with the stated antibodies. (A) Representative blot from 3 independent experiments. (B) Quantification of mean tyrosine phosphorylation levels \pm SEM of 3 independent experiments. Statistical significance was calculated using two-way ANOVA with Dunnett's post-test, with * in the colour of phosphorylation site / aggregation stated on the graph. * $p \leq 0.05$.

3.3.4 CLEC-2 phosphorylation is only reduced in ADP sensitive washed platelets at high concentrations of ibrutinib, but not acalabrutinib.

It is known that CLEC-2 phosphorylation is required to mediate signalling (Severin et al., 2011). The signalling components downstream of CLEC-2 and GPVI are strikingly similar, therefore it was hypothesised that a more severe effect of inhibition downstream of CLEC-2 may be related to inhibition of receptor phosphorylation. Furthermore, it is believed by Manne et al., that Btk lies upstream of Syk. Phosphorylation of CLEC-2 requires Syk and secondary feedback (Hughes et al., 2015, Pollitt et al., 2010). If CLEC-2 phosphorylation was lost in the presence of acalabrutinib which inhibits Btk, it would provide evidence in favour of the hypothesis proposed by this group (Manne et al., 2015a).

ADP sensitive and washed platelets were prepared to 8×10^8 cells/mL before preincubation with $1 \mu\text{M}$ and $0.1 \mu\text{M}$ ibrutinib, acalabrutinib or vehicle control for 5 minutes before stimulation with 300 nM of rhodocytin for 5 minutes. Cells were lysed with an equal volume of 2X NP40 lysis buffer with protease inhibitors before being subjected to immunoprecipitation with the anti-CLEC-2 antibody AYP1. After immunoprecipitation, samples were resolved using SDS-PAGE and Western blotted for tyrosine phosphorylation and CLEC-2. (Figure 3.3.5 A and B). Phosphorylation of CLEC-2 in vehicle treated platelets is significantly increased compared to resting platelets in both ADP sensitive and insensitive washed platelets ($p \leq 0.01$), showing that CLEC-2 is phosphorylated in agonist stimulated samples (Severin et al., 2011, Pollitt et al., 2010, Mori et al., 2008), Figure 3.3.5.C. When drug treated samples were compared to their vehicle treated samples, only $1 \mu\text{M}$ ibrutinib treatment of ADP sensitive washed platelets had a significant reduction in CLEC-2 phosphorylation.

This inhibition observed in only one condition suggests that CLEC-2 phosphorylation is unlikely to be directly mediated by Btk. This suggests that the more severe inhibitory phenotype of Btk inhibitors downstream of CLEC-2 is likely to be mediated by intracellular kinase signalling not because of receptor phosphorylation. As Syk is the tyrosine kinase responsible for CLEC-2 phosphorylation, it also provides evidence that Btk is downstream of Syk in the CLEC-2 signalling cascade.

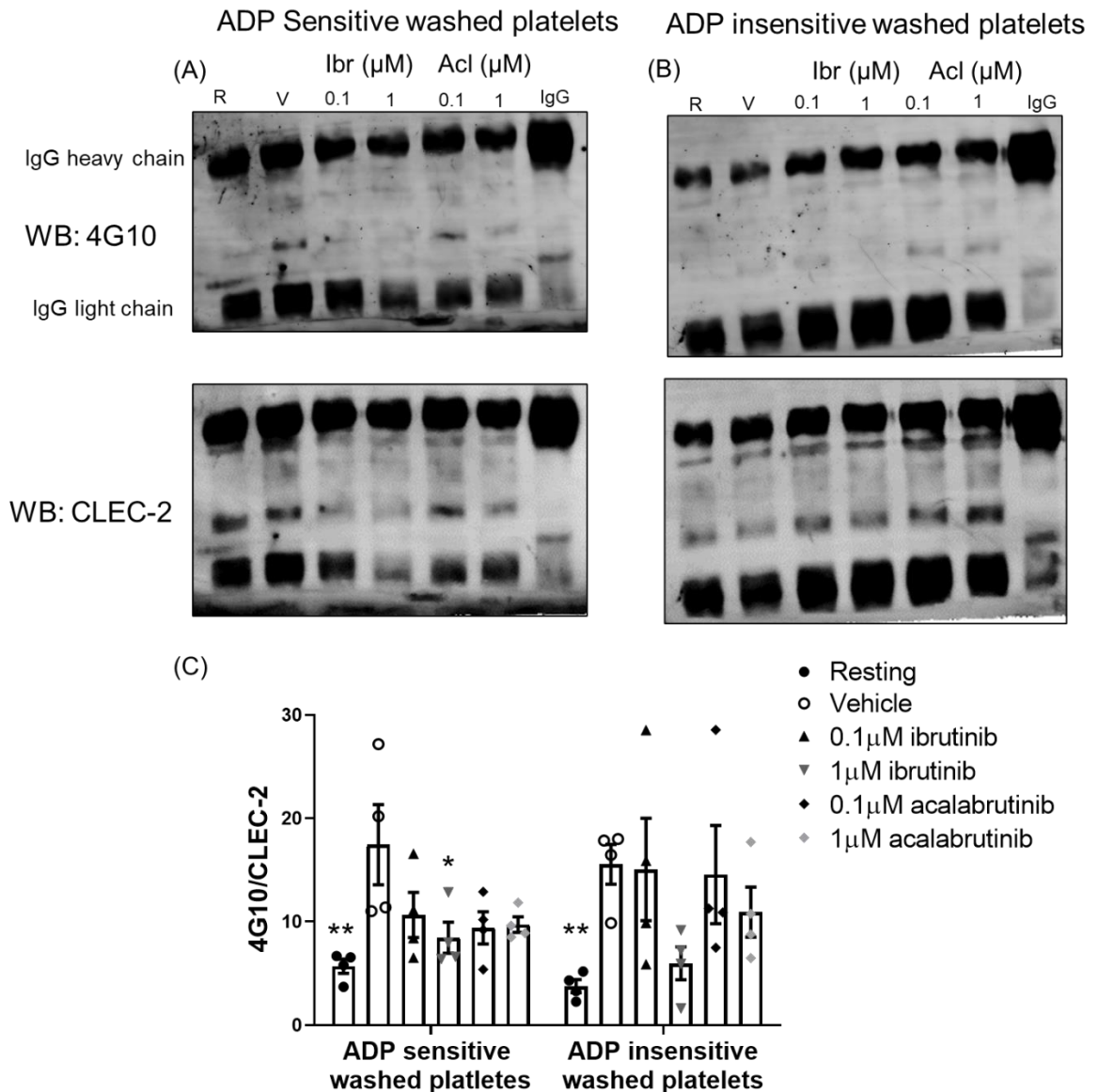


Figure 3.3.5 CLEC-2 phosphorylation is reduced in ADP sensitive washed platelets treated with ibrutinib but not acalabrutinib.

(A) ADP sensitive or (B) ADP insensitive washed platelets (8×10^8 cells/mL) were preincubated with integrilin ($9 \mu\text{M}$) and ibrutinib (0.1, $1 \mu\text{M}$) or acalabrutinib (0.1 or $1 \mu\text{M}$) or vehicle control (0.1% DMSO (v/v)) for 5 minutes. Samples were stimulated for 5 minutes with 300 nM rhodocytin under stirring conditions. Reactions were lysed using 2x NP40 lysis buffer with protease inhibitors. CLEC-2 was immunoprecipitated using anti-Clec-2 antibody AYP1 ($2 \mu\text{g/mL}$). Samples were eluted into 2X sample buffer before SDS PAGE and western blotting. Membranes were incubated with anti-phosphotyrosine antibody 4G10 and then incubated with Alexa Fluor 488 conjugated

goat anti-mouse. Gels were imaged, then stripped and reprobed for total CLEC-2 using the anti-CLEC-2 antibody AYP2. (C) quantification was assessed using ImageQuant, graph represents mean \pm SEM, n=4. Statistical testing was performed using a two-way ANOVA with Dunnett's multiple comparison, *p \leq 0.05, **p \leq 0.01.

3.3.5 Btk phosphorylation is inhibited downstream of CLEC-2 in washed platelets

CLEC-2 mediated aggregation is more severely inhibited by Btk inhibition compared to GPVI mediated aggregation. This effect is not mediated by a lack of CLEC-2 phosphorylation and must be related to Btk or off target tyrosine kinase inhibition. However, it is not likely due to Syk or Src inhibition as this would reduce phosphorylation of CLEC-2 (Severin et al., 2011, Pollitt et al., 2010, Hughes et al., 2015) . Therefore, protein phosphorylation downstream of rhodocytin stimulated platelets was investigated, (Figure 3.3.6).

Washed platelets were incubated with acalabrutinib (10-0.01 μ M) for 5 minutes and then stimulated with 300nM or 100nM rhodocytin for five minutes in the presence of integrilin. Unlike experiments investigating GPVI signalling, these experiments were not performed in the presence of apyrase and indomethacin, as there is a requirement for secondary mediators to reinforce CLEC-2 signalling (Badolia et al., 2017, Izquierdo et al., 2020, Pollitt et al., 2010).

In 300nM rhodocytin stimulated samples, there was a small reduction in total cell tyrosine phosphorylation in samples treated with acalabrutinib when compared to the vehicle control, (Figure 3.3.6.A, upper panel). Aggregation was inhibited at 10 μ M and 3 μ M acalabrutinib when compared to vehicle control. Src pY416 was reduced to 52% (\pm 8) of the vehicle control in the presence of 10 μ M acalabrutinib ($p \leq 0.001$). 3 μ M and 1 μ M acalabrutinib also caused a significant inhibition of Src pY416 ($p \leq 0.01$ and $p \leq 0.05$) when compared to vehicle control, (Figure 3.3.6.B).

On the other hand, Syk pY525 was not inhibited by acalabrutinib in either 300nM or 100nM rhodocytin stimulated platelets. The Syk pY525 is still present in concentrations of acalabrutinib when Btk pY223 is lost (Figure 3.3.6 B upper and middle panels). This

suggests that Btk is downstream of Syk in the CLEC-2 signalling cascade, in contrast to the work of Manne et al.

Btk pY551 is inhibited at the highest concentration of acalabrutinib (10 μ M, $p \leq 0.05$), which is likely as Src pY416, is reduced. Src pY416 is a marker of SFK activity and a mediator of Btk phosphorylation at pY551.

Btk pY223 was inhibited by acalabrutinib downstream of both concentrations of rhodocytin, with the IC₅₀ being 0.88 μ M (0.44 to 1.42) for 300nM rhodocytin. 0.3 μ M acalabrutinib and higher caused inhibition of Btk pY223 phosphorylation ($p \leq 0.05$).

The phosphorylation of PLC γ 2 Y759 was also inhibited by acalabrutinib downstream of CLEC-2, with the IC₅₀ being 1.06 μ M (0.56 to 2.03). 10 μ M, 3 μ M and 1 μ M acalabrutinib caused significant decreases in this pY759 compared to vehicle control.

Btk pY223 and PLC γ 2 pY759 phosphorylation correlate to each other ($r=0.928$, $p \leq 0.001$), suggesting these may be dependent on each other, Figure 3.3.6.B. However, PLC γ 2 pY759 correlates with aggregation ($r = 0.762$, $p=0.028$), whereas Btk pY223 does not ($r=0.691$, $p=0.058$). This suggests that the aggregation downstream of CLEC-2 at 300nM rhodocytin is not critically dependent on Btk phosphorylation, even though Btk's substrate, pY759 on PLC γ 2 is.

Similarly, to 300nM of rhodocytin 10 μ M, 3 μ M and 1 μ M acalabrutinib all significantly inhibit aggregation when washed platelets are stimulated with 100nM rhodocytin.

Phosphorylation of Btk pY223 is also significantly inhibited compared to vehicle control at these concentrations of acalabrutinib ($p \leq 0.01$ and $p \leq 0.001$), Figure 3.3.7.B. The data of aggregation and levels of Btk pY223 similarly overlap to each other, with aggregation being rescued at concentrations where Btk phosphorylation is also present (3.3.7.B).

Acalabrutinib is more selective for Btk in *in vitro* kinase assays, with ibrutinib having inhibitory effects on SFK's (Byrd et al., 2016). Therefore, the phosphorylation profile of

platelets treated with ibrutinib was also assessed downstream of CLEC-2. Samples were prepared as previously described except ibrutinib was used in place of acalabrutinib.

As Figure 3.3.7 D-F demonstrates, ibrutinib more potently inhibits SFK's over a range of concentrations when compared to acalabrutinib ($p \leq 0.01$). Furthermore, ibrutinib inhibits phosphorylation of Syk pY525 to a greater extent when compared to acalabrutinib, which is consistent with the results of the Kunapali group where Syk phosphorylation is lost in the presence of ibrutinib. This allowed the authors to form the hypothesis of Btk to be upstream of Syk in the CLEC-2 signalling cascade. However, when a more specific Btk inhibitor, acalabrutinib is used, Syk phosphorylation is present when Btk phosphorylation is lost suggesting that Btk is downstream of Syk in the CLEC-2 signalling cascade.

(A)

| | | | | | | | | | |
|---------------------------------|---|---|------|------|-----|-----|---|---|----|
| Rho (300nM) | - | + | + | + | + | + | + | + | + |
| Acalabrutinib (μM) | - | - | 0.01 | 0.03 | 0.1 | 0.3 | 1 | 3 | 10 |

Pan pY

Src pY416

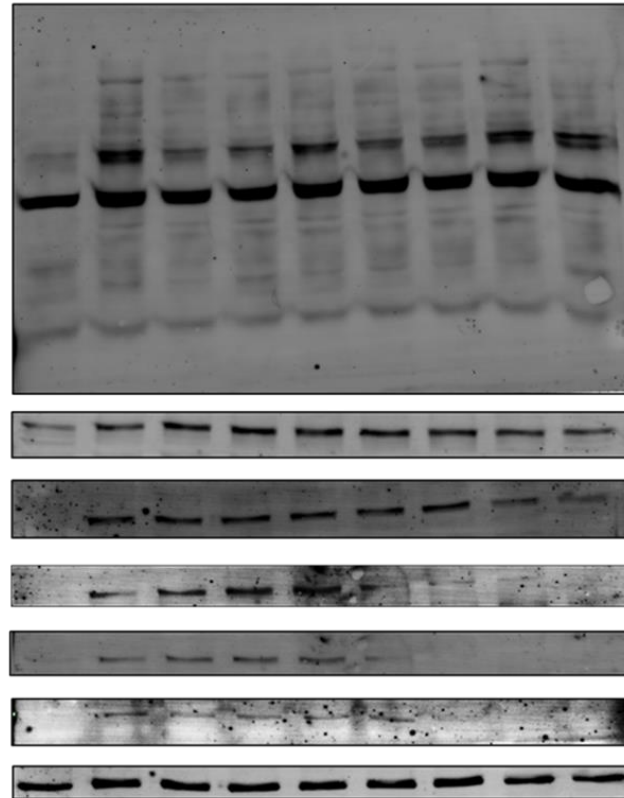
Syk pY525

Btk pY551

Btk pY223

PLC γ 2 pY759

Total Syk



(B)

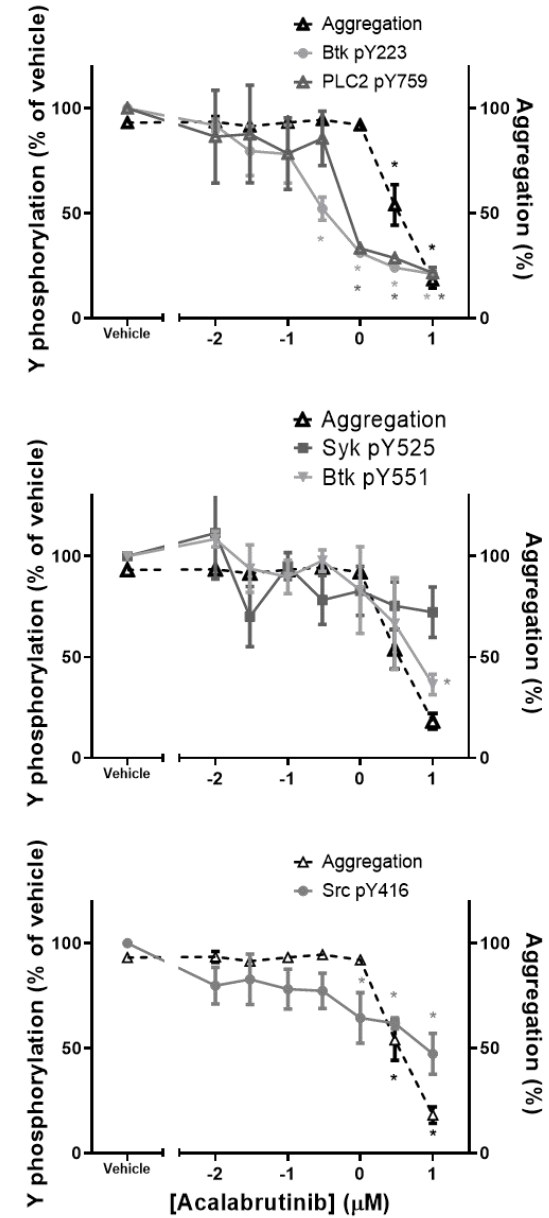


Figure 3.3.6 CLEC-2 mediated aggregation can occur where Btk phosphorylation is lost

(A) washed platelets at 4×10^8 cells/mL in the presence of 9 μ M integrilin were incubated with acalabrutinib or vehicle (DMSO 0.1% (v/v)) for 5 minutes prior to stimulation with 300nM rhodocytin. Platelets were then lysed with 6X reducing sample buffer 5 minutes after addition of agonist. Whole cell lysates were then separated by SDS-PAGE and western blots were probed for whole cell phosphorylation or kinase specific phosphorylation sites. (A) Representative blot from 4 independent experiments. (B) Mean tyrosine phosphorylation levels \pm SEM, n=4. Statistical testing was performed using a two-way ANOVA with Dunnett's multiple comparison test, with * in the colour of phosphorylation site / aggregation stated on the graph. Significance was taken at $*p \leq 0.05$.

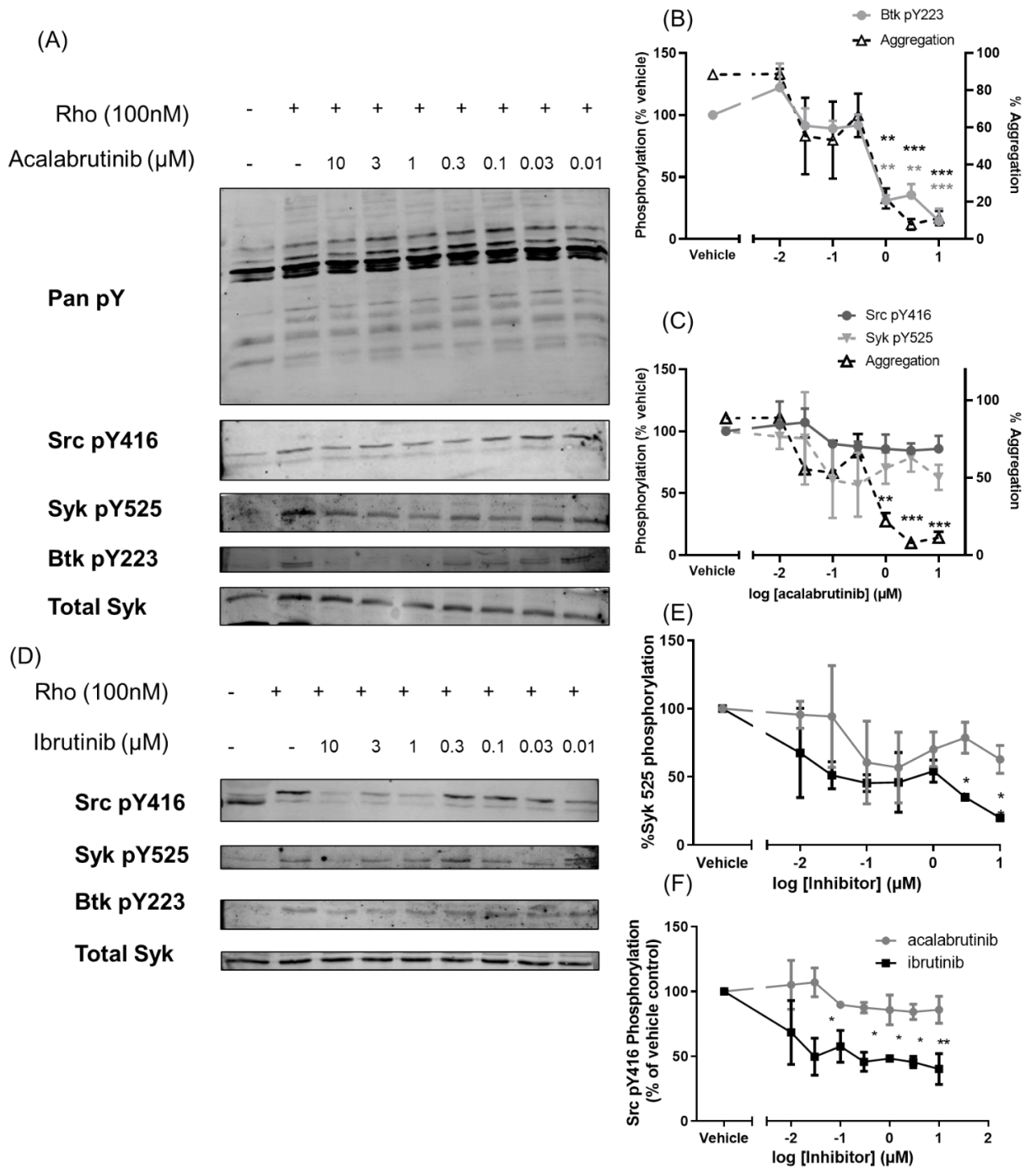


Figure 3.3.7 Platelets cannot aggregate downstream of 100nM CLEC-2 when Btk phosphorylation is lost and there is a differential pattern of phosphorylation downstream of ibrutinib compared to acalabrutinib

(A,D) washed platelets at 4×10^8 cells/mL in the presence of 9 μM integrilin were incubated with (A) acalabrutinib (0.1-10 μM), (D) ibrutinib (0.1 μM to 10 μM) or vehicle control (DMSO 0.1% (v/v)) for 5 minutes prior to stimulation with 100nM rhodocytin. Platelets were then lysed with 6X reducing sample buffer 5 minutes after addition of

agonist. Whole cell lysates were then separated by SDS-PAGE and western blots were probed for whole cell phosphorylation or kinase specific phosphorylation sites. (A) Representative blot from 3 independent acalabrutinib experiments. (B, C) Mean tyrosine phosphorylation levels \pm SEM, n=3. Statistical testing was performed using a two-way ANOVA with Dunnett's multiple comparison test, with * in the colour of phosphorylation site / aggregation stated on the graph. Significance was taken at *p \leq 0.05, ** p \leq 0.01 and *** p \leq 0.001. (D) Representative blot from 3 independent ibrutinib experiments. (D, F) Mean tyrosine phosphorylation levels \pm SEM of 3 independent experiments, significance was calculated using two-way ANOVA with Dunnett's multiple comparisons test. *p \leq 0.01 and **p \leq 0.05

3.3.6 ADP Sensitive platelets are less severely inhibited by acalabrutinib downstream of GPVI and CLEC-2.

Standard washed platelet experiments with rhodocytin show a stronger level of inhibition with acalabrutinib compared to CRP-XL (Figures 3.3.2 A, B and 3.3.3 A,B). It was hypothesised that as the platelets were ADP insensitive, less signalling was occurring due to reduced responses of secondary messengers and therefore resulting in a reduction in aggregation. Human platelet CLEC-2 signalling and activation is dependent on secondary mediators (Izquierdo et al., 2020, Badolia et al., 2017, Pollitt et al., 2010) and therefore it would be expected that if Btk was playing a similar role downstream of both CLEC-2 and GPVI the levels of inhibition in platelet aggregation would be the same in the presence of secondary mediators.

The fast centrifugation of platelets during washing steps has been shown to desensitise the ADP receptors, with washed platelets having reduced responsiveness to ADP. The surface levels of the purinergic receptors paradoxically increase but the overall platelet response (as measured by aggregation) decreases, suggesting that they have reduced functional activity (Koessler et al., 2016). To prevent ADP desensitisation, platelets can be washed at a lower speed of centrifugation, which does not require the use of PGI₂. This allows the platelets to be used immediately reducing ADP receptor desensitisation, which occurs if platelets are stored without apyrase (Koessler et al., 2016). To firstly investigate the degree of how responsive platelets are to ADP, light transmission aggregometry was used. PRP, washed platelets prepared by the ADP sensitive method, and washed platelets centrifuged once with PGI₂ and twice with PGI₂ were stimulated with 0.1- 10µM ADP for 5 minutes and aggregation was compared, Figure 3.3.8.A-D.

As Figure 3.3.8 E shows, at all concentrations of ADP tested, no significant differences in the aggregation can be observed between the methods of preparation. However,

Figure 3.3.8.F, shows there is a shift in the EC₅₀ curves between the preparations of platelets in the response to ADP. For 2 washes, the EC₅₀ was 45µM, 1 wash was 0.08µM, ADP sensitive washed platelets 0.08µM and for PRP 0.04µM showing a large difference between the standard preparation of washed platelets (2 washes) compared to the other preparation methods. This shows that platelets respond differently to the secondary mediator ADP, which is required for CLEC-2 signalling, depending on how they were prepared. Therefore, a preparation using slower spins of platelets was used to maintain secondary mediator feedback.

To investigate if ADP sensitivity plays a role in the response to aggregation, ADP sensitive platelets (4×10^8 cells/mL) were incubated with acalabrutinib (10-0.01µM) for 5 minutes before stimulation with 1µg/mL CRP-XL for 5 minutes, or rhodocytin (100nM) for 7 minutes.

When platelets are stimulated with CRP-XL, there is no significant inhibition of aggregation at any concentration of acalabrutinib tested. Similar results were observed for CLEC-2 stimulated platelets. However, in contrast to GPVI stimulated platelets, 10µM acalabrutinib caused a significant reduction in rhodocytin induced aggregation compared to vehicle control (*p ≤ 0.05), Figure 3.3.8.J.

This shows that ADP sensitive platelets are less severely inhibited by acalabrutinib compared to washed platelets. The level of inhibition is more severe downstream of CLEC-2 when compared to GPVI, as inhibition was only observed with high concentrations of acalabrutinib downstream of CLEC-2.

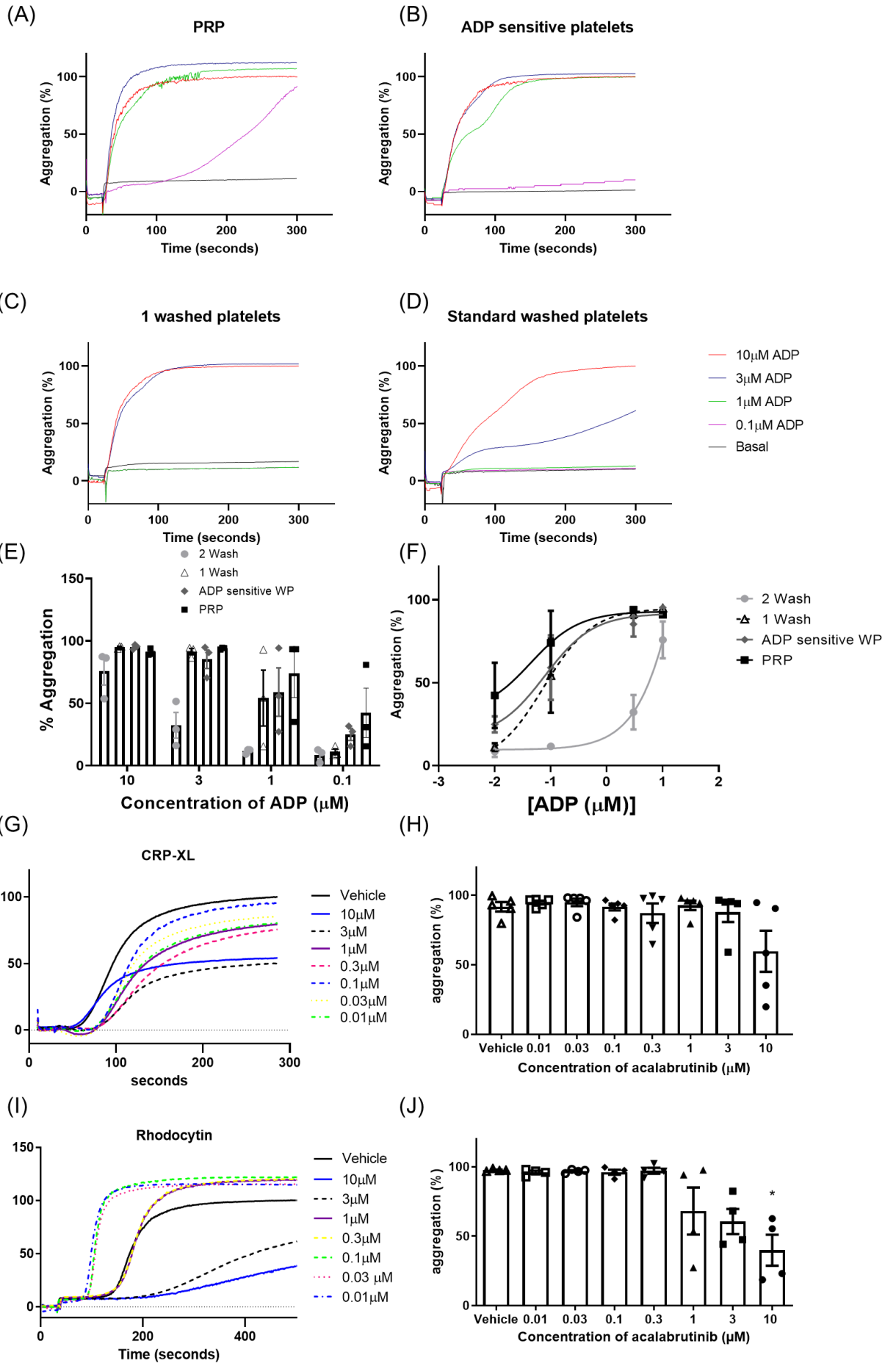


Figure 3.3.8 Platelet preparation effects their response to ADP and ADP sensitive platelets are less susceptible to Btk inhibition by acalabrutinib

(A) PRP, (B) ADP sensitive washed platelets, (C) PRP span 1x with PGI₂ at 1413g to obtain 1 washed platelet and (D) standard washed platelets were stimulated using 10-0.1µM ADP or PBS (basal). Platelets were allowed to aggregate under constant stirring at 1200rpm for 5 minutes. (E) Statistical significance was calculated using a two-way ANOVA against each method of platelet preparation at a single concentration of ADP with a Tukey's post-test with none found. (F) percentage aggregation was plotted to allow EC₅₀ values to be calculated. Graphs represents mean ± SEM, n=3. ADP sensitive washed platelets (4x10⁸ cells/mL) were incubated with (G-J) acalabrutinib or Vehicle (0.1% (v/v) DMSO) for five minutes before being stimulated with GPVI agonist (G,H) CRP-XL (1µg/mL) for 5 minutes or (I, J,) CLEC-2 agonist rhodocytin (100nM) for 7 minutes in light transmission aggregometry. (G, I) are representative traces and (H, J) are quantified values, n≥4. Statistical significance was calculated using a one-way ANOVA against vehicle control with a Dunnett's post-test. Graph represents mean ± SEM, n=4. Significance was taken at *p ≤ 0.05.

3.3.7 ADP sensitive platelets are less susceptible to inhibition by acalabrutinib downstream of GPVI.

Less severe inhibition of aggregation is seen in ADP sensitive platelets (Figure 3.3.8.H). Residual plasma proteins may remain more in the samples prepared by this method, which can potentially bind to acalabrutinib. However, they are also more responsive to secondary mediators. To investigate if this less acute effect observed is due to plasma binding, phosphorylation downstream of GPVI was assessed.

Experiments were performed in the presence of apyrase and indomethacin to allow for comparison with the experiments in Figure 3.3.4. This will help to deduce whether the less severe inhibition is related to plasma binding or secondary mediators. Therefore, if the effect is less strong, it may be due to the drug being plasma protein-bound, rather than the fact that the platelets are ADP sensitive.

Similarly, to washed platelets, total cell tyrosine phosphorylation remained unchanged in the presence of acalabrutinib downstream of GPVI in ADP sensitive platelets. The IC_{50} value for aggregation was $17\mu\text{M}$ (11.30 to 26.43), which is much higher than ADP insensitive washed platelets in Section 3.3.2.

Btk's transphosphorylation site (pY551), mediated by SFKs and required for its full activation, is not inhibited in the presence of acalabrutinib in ADP sensitive washed platelets, similarly to the observed phosphorylation in ADP insensitive washed platelets. pY551 remains present, even at high concentrations of inhibitor and this can be observed in the very high IC_{50} value - $46\mu\text{M}$. Src pY416 is also not significantly reduced and has an IC_{50} value of $8.83\mu\text{M}$ (4.014 to 23.26).

When compared to vehicle control, the inhibition of Btk pY223 is also inhibited in the presence of acalabrutinib at concentrations above $1\mu\text{M}$ ($p \leq 0.01$ and $p \leq 0.05$).

Furthermore, Btk pY223 is reduced with an IC_{50} value of $0.57\mu\text{M}$ (0.26 to $1.20\mu\text{M}$).

When compared to vehicle control, phosphorylation of PLC γ 2 pY759 is also reduced in the presence of acalabrutinib at concentrations of 1 μ M or greater ($p \leq 0.05$).

Btk pY223 and PLC γ 2 pY759 have a strong positive correlation ($r=0.894$, $p=0.03$) suggesting potential regulation with one another, however neither of the phosphorylation sites correlate with aggregation. This contrasts with ADP insensitive washed platelets, where PLC γ 2 pY759 activity correlates with aggregation.

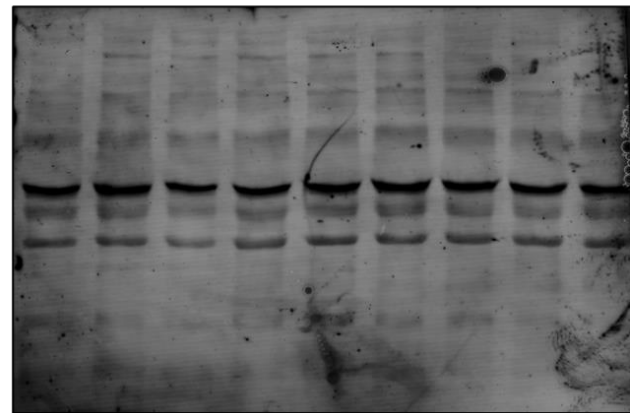
There are similar IC₅₀ values for both Btk pY223 in ADP sensitive and ADP insensitive washed platelets (Section 3.3.3), suggesting that the aggregation differences between platelet preparation in GPVI mediated aggregation is not related to Btk inhibition.

Although GPVI signalling is not dependent on secondary mediators downstream of GPVI ligation, it may help to reinforce the signalling (Atkinson et al., 2003b). Therefore, the more severe inhibition in washed platelets may be related to the lack of this.

ADP sensitive washed platelets

| | | | | | | | | | | |
|-----|--------------------|---|---|------|------|-----|-----|---|---|----|
| (A) | CRP (1µg/mL) | - | + | + | + | + | + | + | + | + |
| | Acalabrutinib (µM) | - | - | 0.01 | 0.03 | 0.1 | 0.3 | 1 | 3 | 10 |

Pan pY



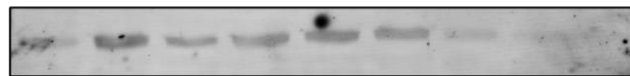
Src pY416



Btk pY551



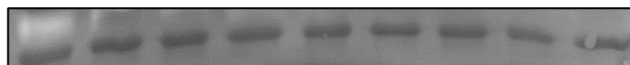
Btk pY223



PLCγ2 pY759



Total Syk



(B)

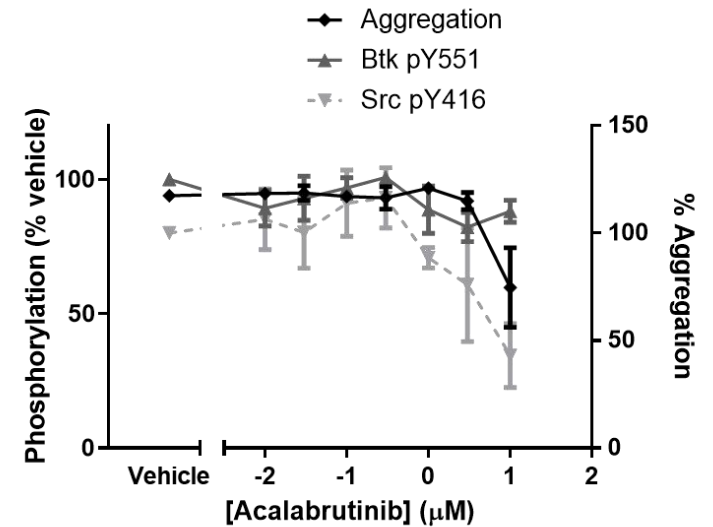
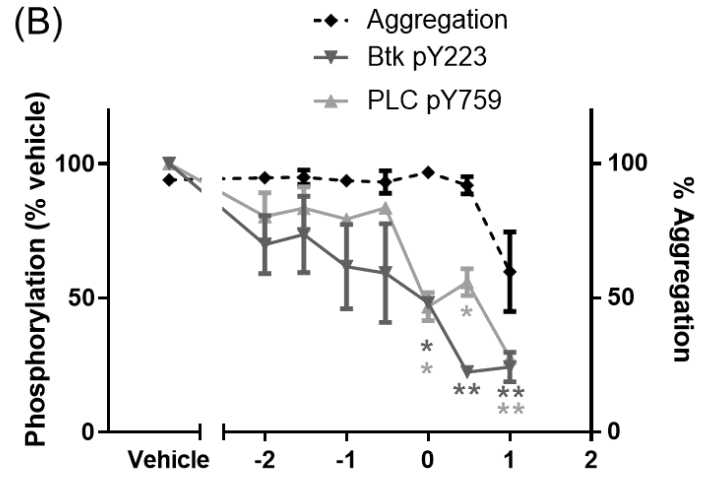


Figure 3.3.9 Platelets can still aggregate downstream of GPVI when Btk and PLC γ 2 phosphorylation is lost

(A) ADP sensitive washed platelets at (4×10^8 cells/mL) in the presence of integrilin ($9 \mu\text{M}$), apyrase (2units/mL) and indomethacin ($10 \mu\text{M}$) were incubated with acalabrutinib or vehicle control (DMSO 0.1% (v/v)) for 5 minutes prior to stimulation with $1 \mu\text{g/mL}$ CRP-XL. Platelets were then lysed with 6X reducing sample buffer 180 seconds after addition of agonist. Whole cell lysates were separated by SDS-PAGE and western blots were probed for whole cell tyrosine phosphorylation or kinase specific tyrosine phosphorylation. (A) Representative blot from 3 independent experiments. (B) Mean tyrosine phosphorylation levels \pm SEM, $n=3$. Statistical testing was performed using a two-way ANOVA with Dunnett's multiple comparison test, with * in the colour of phosphorylation site / aggregation stated on the graph. Significance was taken at $*p \leq 0.05$ and $** p \leq 0.01$.

3.3.8 Preparation of platelets depends on the degree on inhibition by ibrutinib and acalabrutinib to rhodocytin

Btk inhibitors are less inhibitory of rhodocytin induced platelet aggregation in ADP sensitive platelets when compared to washed platelets (Figures 3.3.6 and 3.3.8). It is known that ADP sensitive platelets can respond to ADP more than normal washed platelets, but there is also residual albumin and fibrinogen present in the samples (Cazenave et al., 2004). This may be binding the drug and preventing it from binding and therefore inhibiting Btk as Btk inhibitors are highly plasma bound (Scheers et al., 2015). To investigate if the reduced inhibition is mediated by the extra response to ADP or the amount of plasma protein present, different preparations of platelets were used to identify if the same concentration of drug can inhibit one preparation but not another due to the amount of drug binding.

Traditional twice washed platelets (two fast spins with PGI₂), once washed platelet (1 fast spin with PGI₂) and PRP were preincubated with ibrutinib (0.01-10µM) for 5 minutes before stimulation with 300nM rhodocytin for 7 minutes. Ibrutinib was used in these experiments as opposed to acalabrutinib for consistency with Nicolson et al., 2020. Figure 3.3.10 shows that there is a difference in the potency of inhibition depending on the preparation of platelets. At 10µM ibrutinib, all the platelet preparations were inhibited. PRP aggregated at any ibrutinib concentration lower than 10µM, whereas there are differences between the preparations at concentrations 3µM or lower. There was a statistically significant difference in aggregation between the preparations of platelets. The traditional 2 washed platelet did not undergo aggregation in the presence of 3µM or 1µM ibrutinib (aggregation of 16% ±2 and 13% ±2 respectively) when compared to 1 wash and compared to PRP (aggregation of 62%±18 and 94% ±1 for 1µM acalabrutinib for 1 wash and PRP respectively) ($p \leq 0.05$ and $p \leq 0.001$). IC₅₀ values were also calculated and as Figure 3.3.10.E shows, there is a clear shift to the left for 2 washed platelets showing more potent inhibition.

As there was no difference between one washed platelets and ADP sensitive platelets for the response to ibrutinib and overlapping EC₅₀ curves in response to ADP (Figure 3.3.10.E), only PRP, ADP sensitive platelets and washed platelets were used when the inhibitory effect of acalabrutinib on rhodocytin mediated effects. As Figure 3.3.11.D shows, there is a difference in response between preparations of platelets, with only washed platelets being inhibited in the presence of high concentrations of acalabrutinib.

These results show that there is a difference in the levels of inhibition of platelet aggregation depending on the platelet preparation. Taken together with the ADP sensitivity work, this effect is related to the response in ADP sensitivity due to the EC₅₀ curves being similar and is less likely to be related to the plasma binding.

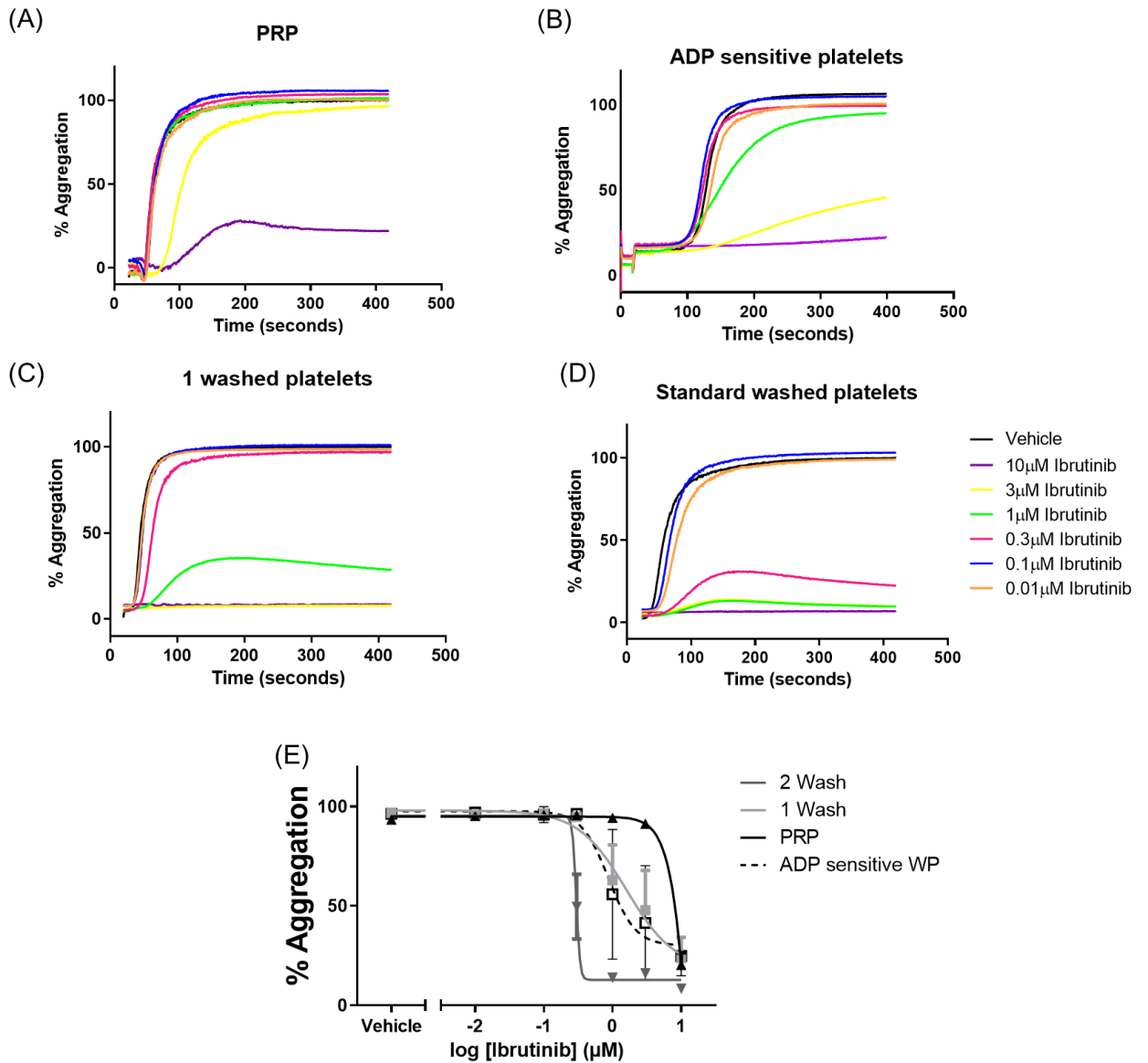


Figure 3.3.10 Platelet preparation effects their responses to rhodocytin in the presence of ibrutinib

(A) PRP, (B) ADP sensitive washed platelets or (C) ADP insensitive washed platelets with 1 spin or (D) ADP insensitive platelets with two spins (standard washed platelets) were incubated with doses of ibrutinib (0.01-10 μM) or vehicle control (0.1% DMSO v/v) for 5 minutes before stimulation with 300nM rhodocytin for 7 minutes and light transmission aggregometry was assessed for 5 mins at 1200rpm. (D) Values were plotted to calculate the IC₅₀ values. Graphs represent mean ± SEM, n=4.

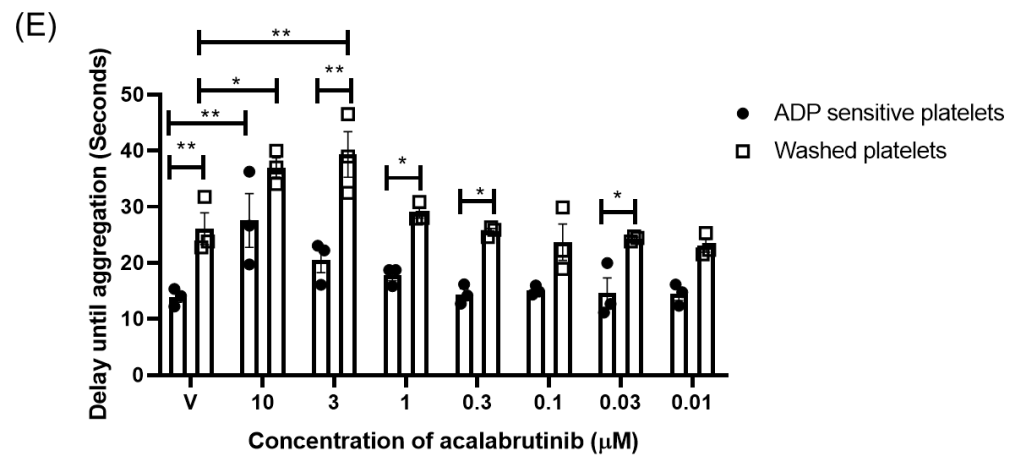
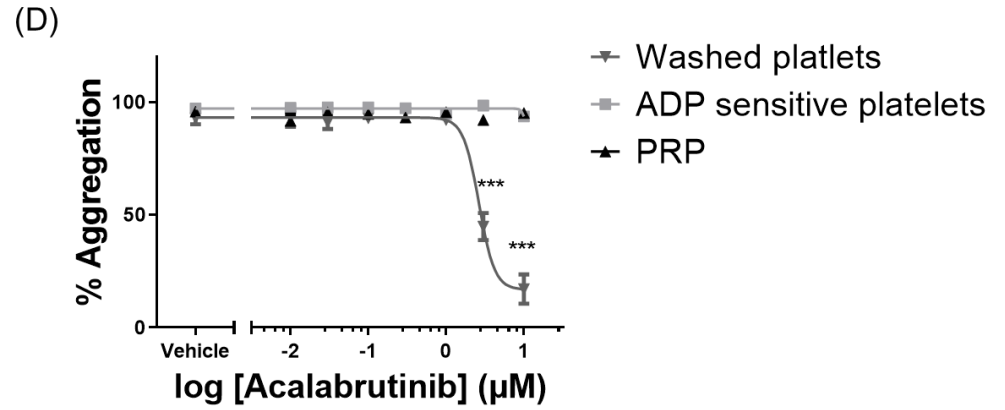
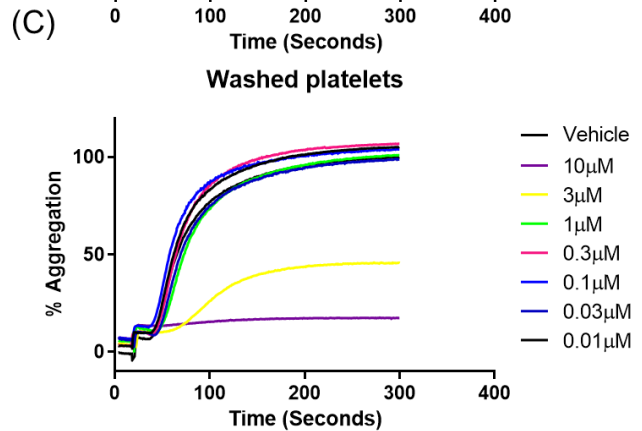
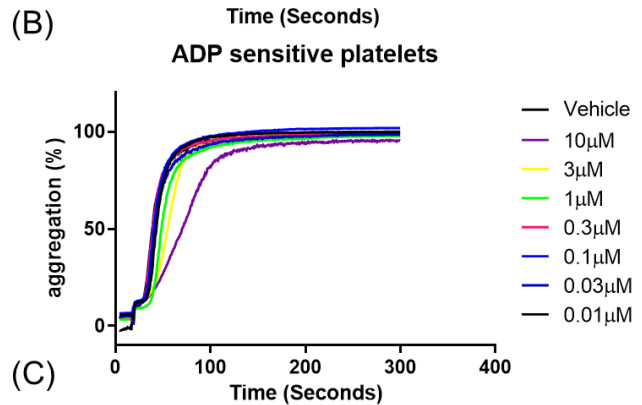
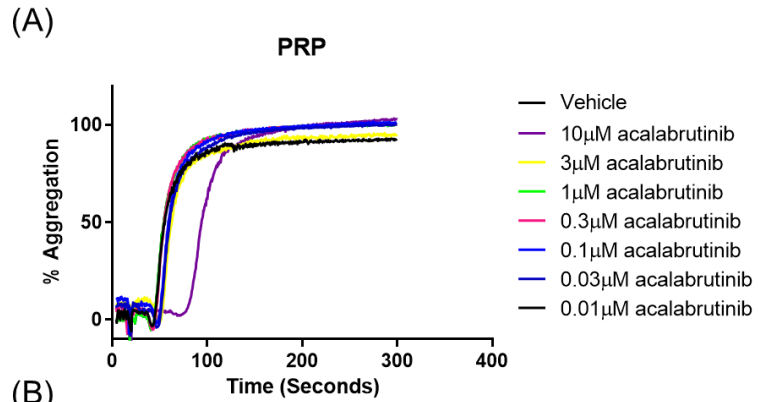


Figure 3.3.11 Platelet preparation affects the response of their aggregation to rhodocytin in the presence of acalabrutinib

(A) PRP, (B) ADP sensitive platelets or (C) washed platelets were incubated with doses of acalabrutinib (0.01-10 μ M) for 5 minutes before stimulation with 300nM rhodocytin for 5 minutes and light transmission aggregometry was assessed for 5 mins at 1200rpm (D), along with the (E) time taken to the initiation of aggregation following the addition of agonist. Statistical testing was performed using Two-way ANOVA using a Tukey's post-test. Significance was taken at * $p \leq 0.05$. ** $p \leq 0.01$, *** $p \leq 0.001$.

Graphs represent mean \pm SEM.

3.3.9 CLEC-2 mediated signalling of ADP sensitive platelets is not inhibited by acalabrutinib

As platelets that are more responsive to ADP are less inhibited by Btk inhibitors in aggregation (Figures 3.3.8 I, J and 3.3.11) signalling in these platelets was assessed to identify if Btk phosphorylation levels were similar as to ADP insensitive platelets. Due to the normal aggregation, it was hypothesised that Btk phosphorylation would be less inhibited.

Total cell tyrosine phosphorylation and aggregation are not inhibited in ADP sensitive CLEC-2 stimulated platelets samples, with aggregation not inhibited even at the highest concentrations of acalabrutinib (10 μ M) in contrast to ADP insensitive washed platelets (Figure 3.3.6). Furthermore, phosphorylation of Syk and LAT is not significantly inhibited when compared to vehicle control, Figure 3.3.12.B. Src pY416 is inhibited at 10 μ M acalabrutinib compared to vehicle control ($p \leq 0.05$). However, Btk pY551 phosphorylation is reduced to 71% \pm 7 of vehicle control when treated with 10 μ M acalabrutinib, but this is not statistically significant. As Btk pY551 and Syk phosphorylation is present when the amount of Btk pY223 is reduced, it further provides evidence that Btk is downstream of Syk in the CLEC-2 signalling cascade.

Downstream of rhodocytin induced signalling phosphorylation of Btk at pY223 is reduced to 26% \pm 4.6) of the vehicle control in the presence of 10 μ M acalabrutinib ($p \leq 0.01$), Figure 3.3.12.B upper panel. 3 μ M of acalabrutinib also leads to a reduction in pY223 phosphorylation ($p \leq 0.05$) and the IC₅₀ for 1.66 μ M (0.87 to 3.15) (Figure 3.3.12.B).

High concentrations of acalabrutinib also inhibit PLC γ 2 pY759 phosphorylation, with 10 μ M, 3 μ M and 1 μ M causing a significant reduction in phosphorylation when compared to vehicle control ($p \leq 0.01$). This is reflected in the IC₅₀, of 1.11 μ M (0.7 to 1.75), similar to, but smaller than the Btk pY223 IC₅₀.

Btk pY223 and PLC γ 2 pY759 strongly positively correlate, ($r= 0.890$, $p=0.003$), but neither of these correlate to rhodocytin induced aggregation. This could potentially suggest that high concentrations of rhodocytin may be inducing aggregation independently of Btk and PLC γ 2 phosphorylation. It is likely that this is mediated through secondary feedback mechanisms, as the platelets prepared through this method have a much stronger response to ADP (ADP Figure 3.3.8.) and drug treated samples have a delayed aggregation response compared to vehicle treated samples (3.3.11.E).

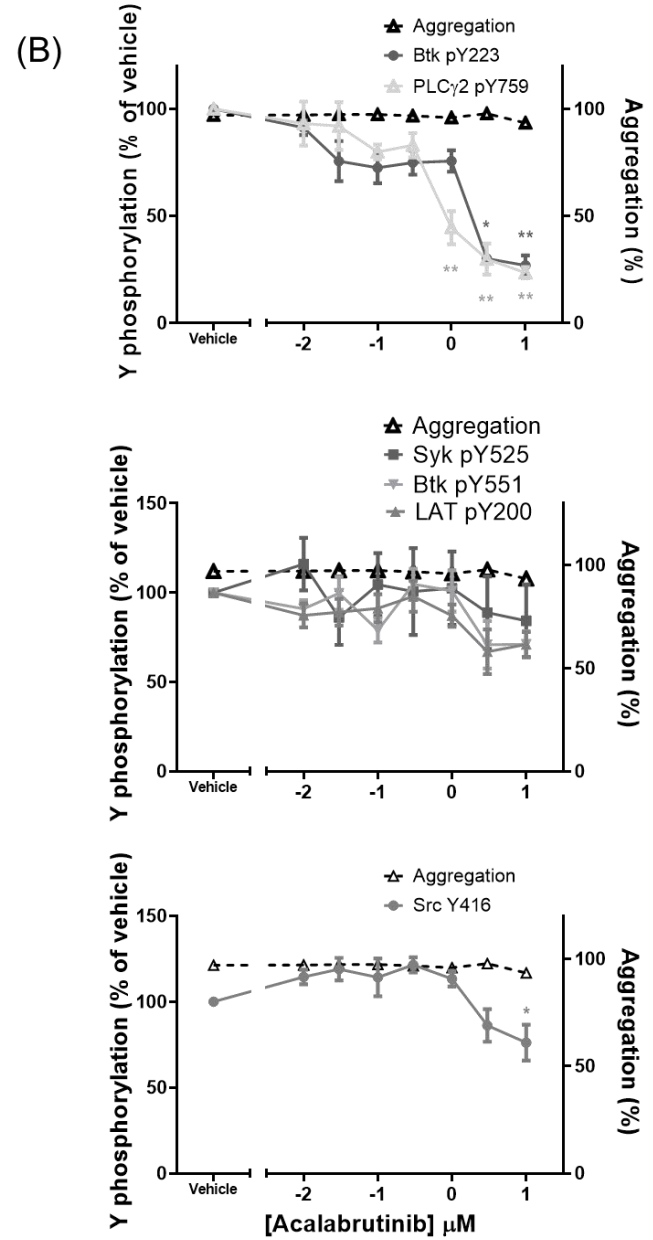
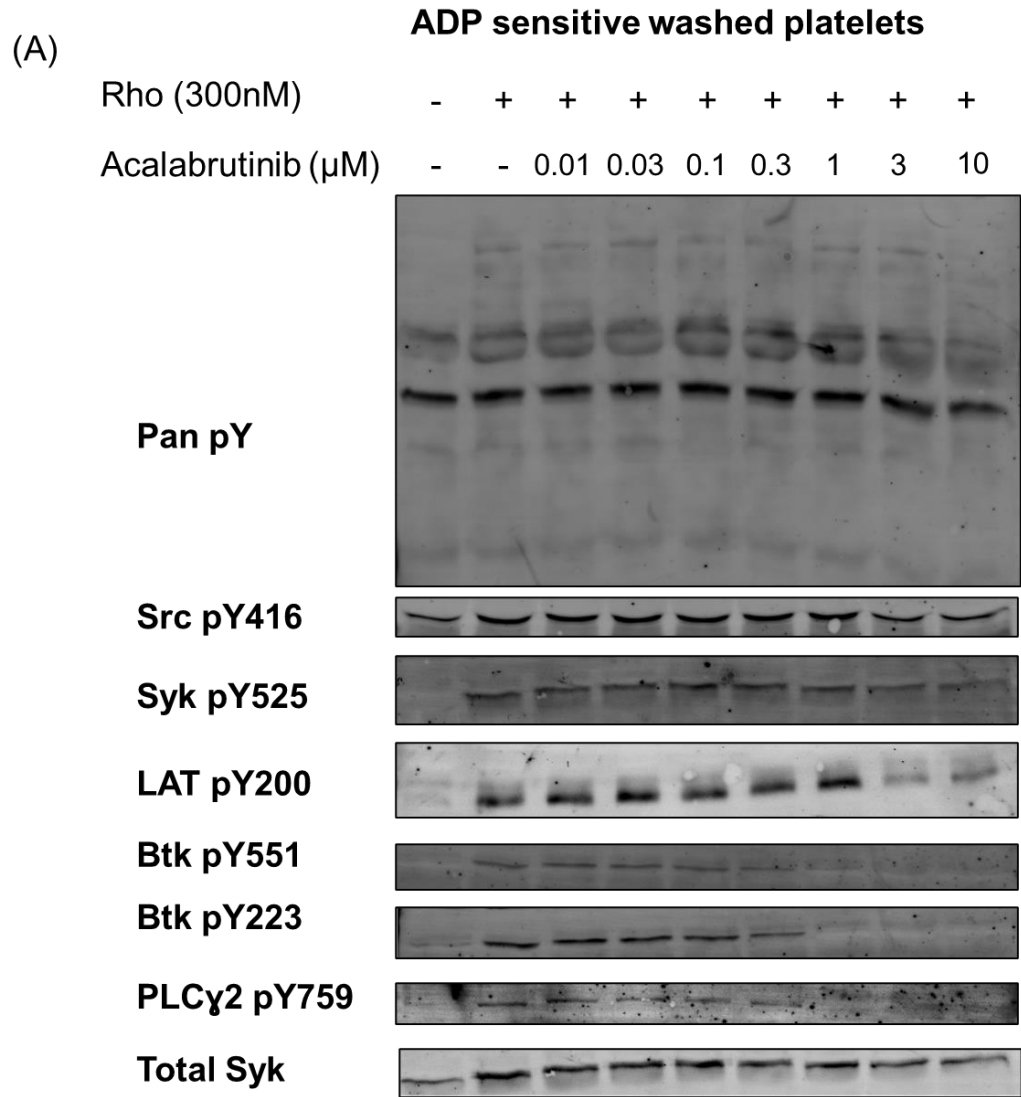


Figure 3.3.12 ADP sensitive washed platelets can aggregate to rhodocytin in the presence of acalabrutinib when Btk phosphorylation is lost

(A) ADP sensitive washed platelets at 4×10^8 cells/mL in the presence of integrilin $9 \mu\text{M}$ were incubated with acalabrutinib or vehicle (DMSO 0.1% (v/v)) for 5 minutes prior to stimulation with 300nM rhodocytin. Platelets were then lysed with 6X reducing sample buffer 5 minutes after addition of agonist. Whole cell lysates were then separated by SDS-PAGE and western blots probed for whole cell tyrosine phosphorylation or kinase specific phosphorylation sites. (A) Representative blots from 4 independent experiments. (B) Mean tyrosine phosphorylation levels \pm SEM, $n=4$. Statistical testing was performed using a two-way ANOVA with Dunnett's multiple comparison test, with * in the colour of phosphorylation site / aggregation stated on the graph. Significance was taken at $*p \leq 0.05$ and $** p \leq 0.01$.

3.3.10 Calcium flux downstream of GPVI is only inhibited at the highest concentration of acalabrutinib whereas acalabrutinib dose dependently inhibits calcium flux downstream of CLEC-2.

Calcium mobilisation is an essential step in platelet activation (Varga-Szabo et al., 2009). It has been previously shown that calcium mobilisation is inhibited by ibrutinib (Bye et al., 2015), but at the time of starting this study, no work investigating the role with acalabrutinib had been published. The inhibition of calcium flux observed with ibrutinib may be related to the inhibition of SFK's, as it is known that higher concentrations of ibrutinib inhibit SFK's (Figure 3.3.7.F and (Bye et al., 2015, Bye et al., 2017). Therefore, experiments using acalabrutinib, which has higher selectivity for Btk, were performed to investigate the role of the catalytic activity of Btk in these pathways.

PRP with ACD, was incubated with the Ca²⁺ sensitive dye Fura-2 AM. Platelets were then pelleted and resuspended to 4x10⁸ cells/mL. Platelets were incubated with acalabrutinib or vehicle control for 5 minutes before stimulation with 1µg/mL CRP, 300nM or 100nM rhodocytin and calcium flux was assessed using a FlexStation, Figures 3.3.13.A and 3.3.14 A, B.

When the area under the curve for 5 donors was calculated, vehicle treated samples (red dots) had a large increase in calcium flux downstream of GPVI as visible in Figure 3.3.13.A, B. 10µM acalabrutinib significantly reduced the area under the curve when compared to vehicle control (*p ≤ 0.05). The differences between the peak at 380/340 (the height of the peak – resting sample) ratio was also investigated. Using one-way ANOVA, only 10µM acalabrutinib caused a statistically significant reduction in the change of calcium flux compared to the vehicle control.

The dynamics of calcium flux may also be quantified. It has been previously shown that ibrutinib delays the onset of calcium flux but does not block platelet aggregation

(Nicolson et al., 2018). Therefore, the time to reach the maximum value of 380/340 was calculated for each concentration. If there was no peak due to a lack of calcium flux, the value was recorded as 300 seconds which was then end-point of the assay. The average time to peak for vehicle was 134 ± 9.8 seconds, which increased to 295 ± 84 seconds for $10 \mu\text{M}$ acalabrutinib treated samples, however this was not statistically significant ($p=0.0813$).

Downstream of CLEC-2, when the area under the curve was assessed, 300 nM rhodocytin caused a greater calcium flux than 100 nM rhodocytin in vehicle treated samples (Figure 3.3.14.D). When platelets were treated with $10 \mu\text{M}$ or $3 \mu\text{M}$ acalabrutinib, there is a significant inhibition in calcium flux when assessed by area under the curve ($p \leq 0.001$).

Similarly, when the change in peak was assessed, there was a difference between 100 nM and 300 nM rhodocytin, with 300 nM inducing a larger peak change ($p \leq 0.05$). When comparing vehicle treated samples to drug treated samples, independent of their concentration of agonist, there was a significant inhibition in the amount of calcium that fluxes at $10 \mu\text{M}$, $3 \mu\text{M}$ and $1 \mu\text{M}$ acalabrutinib ($p \leq 0.001$ and $p \leq 0.01$), Figure 3.3.14.C .

The time to peak was also inhibited for $10 \mu\text{M}$ and $3 \mu\text{M}$ acalabrutinib independent of their concentration of rhodocytin, Figure 3.3.14.E. This shows that $10 \mu\text{M}$ and $3 \mu\text{M}$ acalabrutinib ablate calcium flux in response to rhodocytin. $1 \mu\text{M}$ has an inhibited response.

The IC_{50} values for calcium flux in the presence of acalabrutinib downstream of CRP-XL and both concentrations of rhodocytin are similar. The value for CRP-XL is $1.48 \mu\text{M}$, and $1.35 \mu\text{M}$ and $1.51 \mu\text{M}$ for 300 nM and 100 nM rhodocytin, respectively. These values are similar, suggesting that the inhibition of calcium flux is similar across agonists.

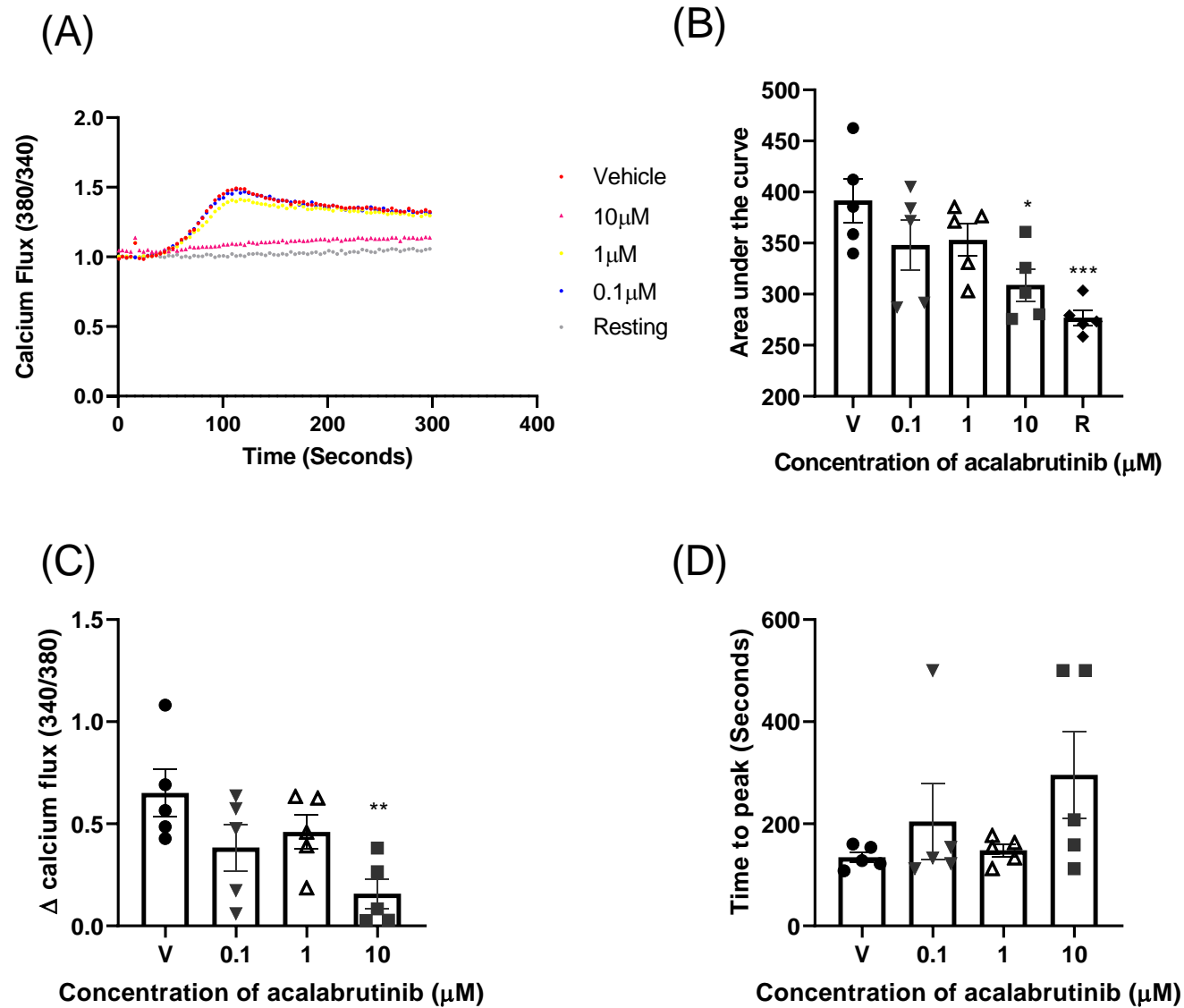


Figure 3.3.13 High concentration of acalabrutinib inhibits GPVI mediated calcium flux

ADP sensitive washed platelets at 4×10^8 cells/mL were incubated with the calcium sensitive dye Fura-2 AM and then with acalabrutinib or vehicle (DMSO 0.1% (v/v)) for 5 minutes. Platelets were then stimulated with $1 \mu\text{g/mL}$ CRP-XL and calcium flux assessed in a FlexStation. (A) representative trace of calcium flux from 5 independent experiments. (B) the area under the curves of each representative trace was calculated, along with the difference in peak height flux (C) and the time taken to reach the peak (D). Graph displays mean \pm SEM (n=5). Statistical significance was calculated using one-way ANOVA with Dunnett's multiple comparisons test and significance was taken at $*p \leq 0.05$, $**p \leq 0.01$, $***p \leq 0.001$

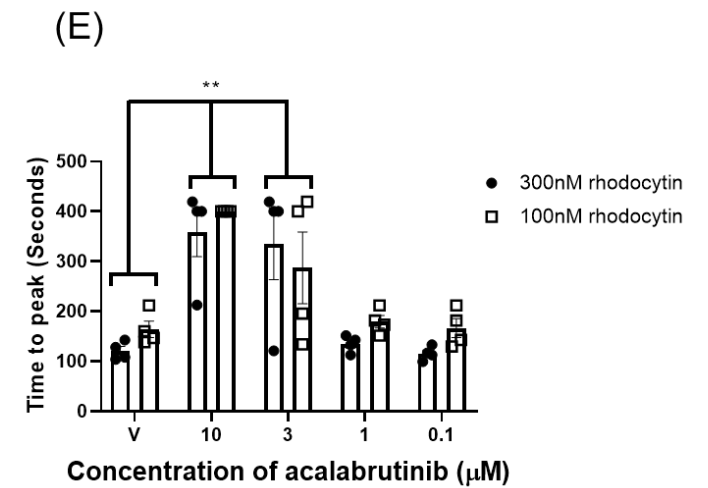
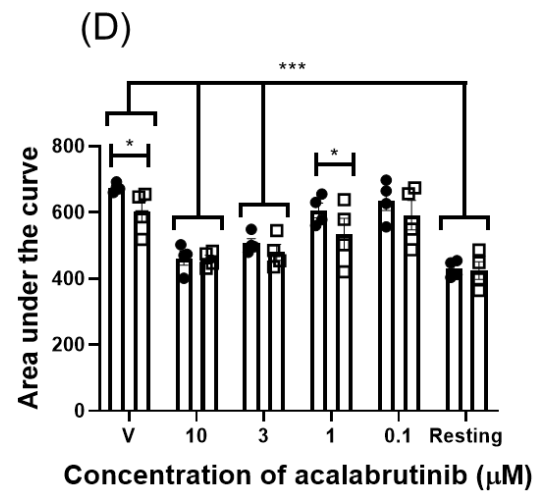
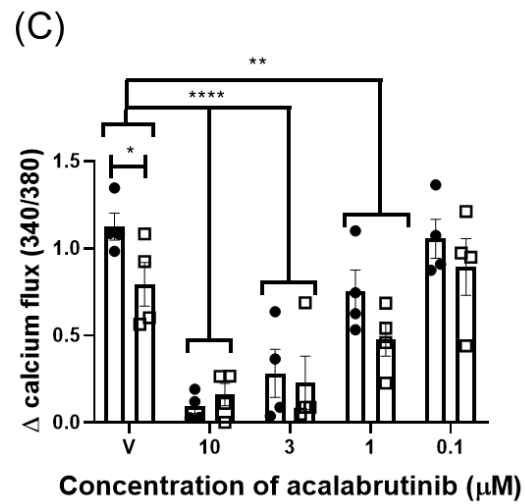
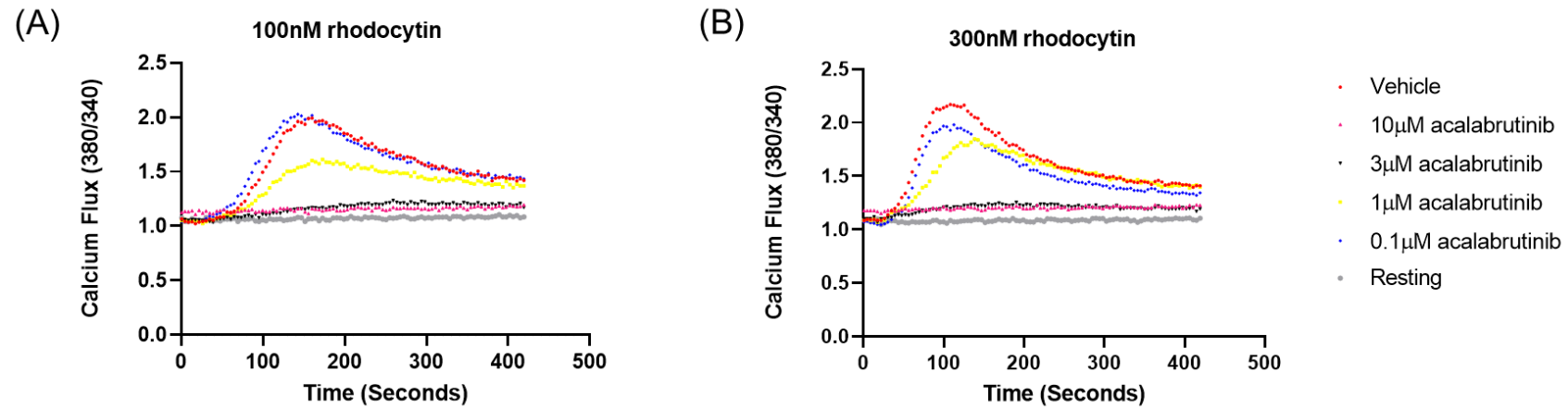


Figure 3.3.14 High concentrations of acalabrutinib inhibit CLEC-2 mediated calcium flux

ADP sensitive washed platelets at 4×10^8 cells/mL were incubated with the calcium sensitive dye Fura-2 AM followed by acalabrutinib or vehicle (DMSO (0.1% (v/v))) for 5 minutes. Platelets were then stimulated with 100nM or 300nM rhodocytin and calcium flux assessed using a FlexStation. (A) representative trace of calcium flux stimulated with 100nM rhodocytin from 4 independent experiments. (B) representative trace of calcium flux stimulated with 300nM rhodocytin from 4 independent experiments. (C) The difference in peak height flux, (D) The area under the curves of each trace was calculated, and the time taken to reach the peak. Graphs display mean \pm SEM, n=4. Statistical significance was calculated using two-way ANOVA with Dunnett's multiple comparisons test and significance was taken at *p \leq 0.05, **p \leq 0.01, and ****p \leq 0.001.

3.3.11 Platelets do not spread on fucoidan but spread weakly on rhodocytin.

Fucoidan has been proposed as a CLEC-2 agonist (Manne et al., 2013, Martynov et al., 2020, Buitrago et al., 2013). No previous work has been done identifying whether platelets can spread on fucoidan or the more well-established CLEC-2 ligand, rhodocytin. Bye et al., have previously studied the effect of ibrutinib on platelet spreading on collagen and CRP-XL. To determine if Btk played a role in platelet spread on CLEC-2 ligands it was first determined whether rhodocytin or fucoidan could support platelet spreading as there was a lack of CLEC-2 mediated spreading in the literature.

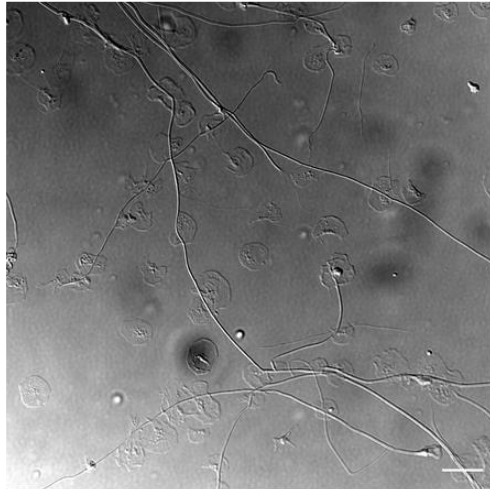
Washed platelets were allowed to spread on fucoidan (200 μ g/mL), rhodocytin (100nM) or collagen (10 μ g/mL) coated coverslips for 45 minutes before fixation. Slides were mounted using Hydromount before imaging on a Nikon TiE2 microscope using differential phase contrast with a 100x objective. Analysis was performed using ImageJ to count the number of adhered platelets and spread surface area.

As Figure 3.3.15.E shows, there are statistically fewer adhered platelets on fucoidan compared to collagen ($p \leq 0.05$). Although there is a trend for fewer platelets adhered on rhodocytin, this was not significant. The surface area of platelets spread on rhodocytin is also reduced, but this is not statistically significant when compared to collagen. As shown in Figure 3.3.15.F, platelets adhered to rhodocytin have an average surface area of $13.7\mu\text{m}^2 \pm 4$, whereas platelets spread more on collagen (with an average surface area of $43\mu\text{m}^2 \pm 6$). The platelets adhered to fucoidan do not undergo spreading and have a significantly smaller surface area compared to collagen ($p \leq 0.05$).

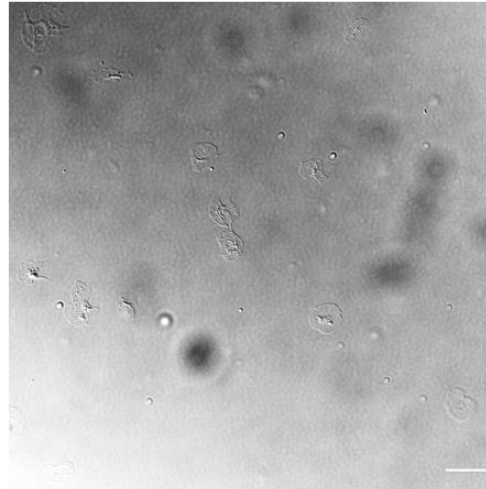
These results show for the first time that platelets spread on rhodocytin, and directly contradict the results of Martynov et al. showing that platelets spread on fucoidan.

Therefore, to investigate the role of Btk in CLEC-2 mediated spreading experiments, rhodocytin was used.

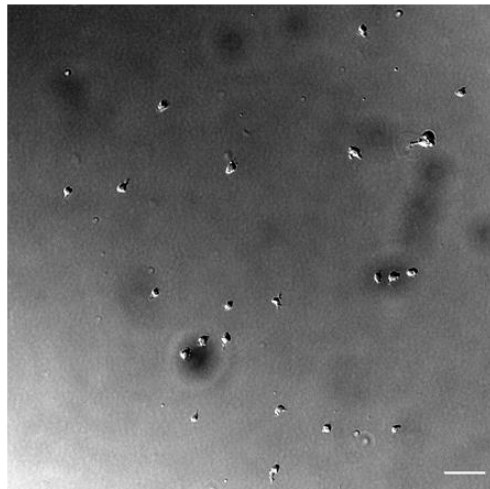
(A) Collagen



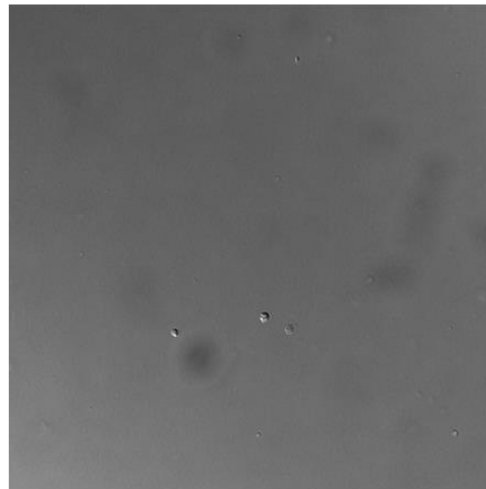
(B) Rhodocytin



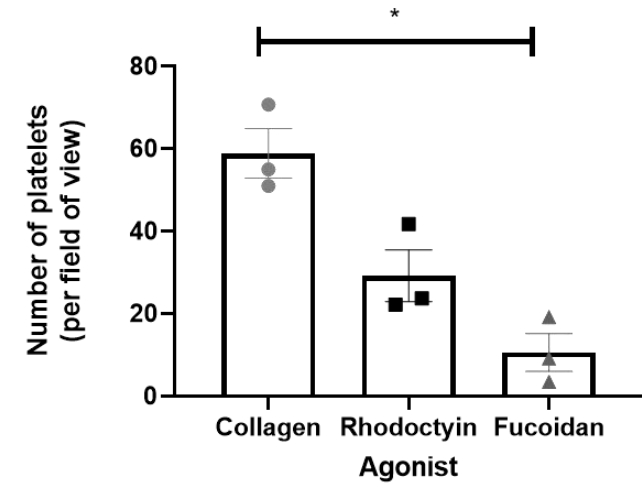
(C) Fucoidan



(D) BSA



(E)



(F)

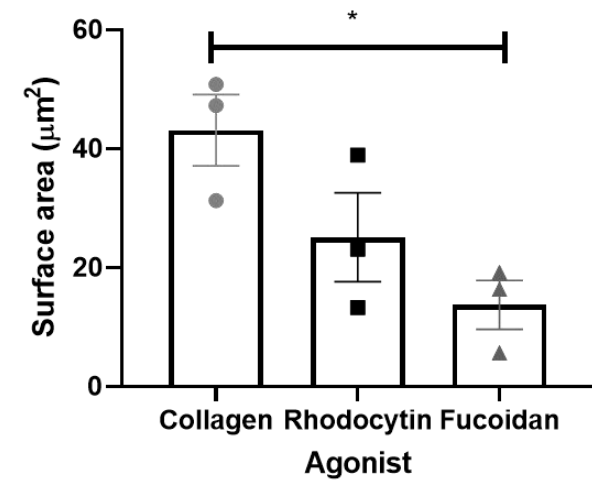


Figure 3.3.15 Platelets spread on collagen and rhodocytin but not fucoidan

Washed platelets were spread on (A) collagen (10 μ g/mL), (B) rhodocytin (100nM), (C) Fucoidan (200 μ g/mL) or (D) BSA (5mg/mL) coated coverslips for 45 minutes and then fixed. Slides were mounted using Hydromount before imaging on a Nikon TiE2 microscope with a 100x objective. Scale bar = 10 μ m. Analysis was performed using ImageJ to (E) count the number of platelets and to (F) determine surface area. Statistical testing was performed using one-way ANOVA using Tukeys post-test. Significance was taken at *p \leq 0.05. Graphs represent mean \pm SEM, n=3.

3.3.12 Platelet spreading on collagen or rhodocytin is not inhibited by acalabrutinib.

Previous work has shown that ibrutinib inhibits platelet spreading, but not adhesion to collagen (Bye et al., 2015). Acalabrutinib was used to investigate if this observation was related to ibrutinib's known off target effects or mediated by Btk. Furthermore, as it was determined that platelets could partially spread on rhodocytin, acalabrutinib was used to determine whether Btk inhibition can inhibit adhesion and spreading on this agonist. Previous work suggests that Btk activity is required downstream of CLEC-2 at submaximal concentrations of rhodocytin, and it would be expected that fewer platelets would adhere and/or fully spread on 100nM rhodocytin in the presence of acalabrutinib.

Washed platelets (2×10^7 cells/mL) were incubated with acalabrutinib (0.1-10 μ M) for 5 minutes before spreading on collagen (10 μ g/mL) or rhodocytin (100nM) for 45 minutes. Cells were then fixed and mounted before imaging on a Tie2 microscope using differential phase contrast. ImageJ was used to analyse the surface area and to count the number of platelets per field of view.

Preincubating the platelets with acalabrutinib did not inhibit the number of platelets adhered to either agonist compared to their vehicle controls (Figure 3.3.16.C).

Although 10 μ M acalabrutinib reduced the average surface area of platelets spreading on rhodocytin ($14.9 \mu\text{m}^2 \pm 2.5$ for 10 μ M acalabrutinib, compared to $25.1 \mu\text{m}^2 \pm 7.5$ for the vehicle control) it was not found to be statistically significant. Acalabrutinib did not inhibit the spreading on collagen, with all concentrations of acalabrutinib and vehicle having an average surface area within $7 \mu\text{m}^2$ of each other. Surprisingly, this suggests that acalabrutinib does not inhibit GPVI or CLEC-2 adherence or spreading.

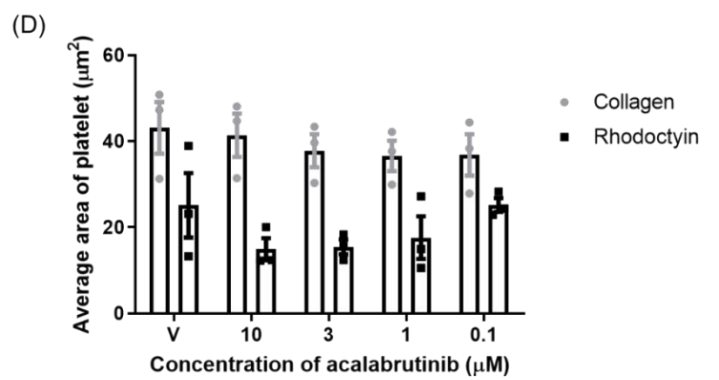
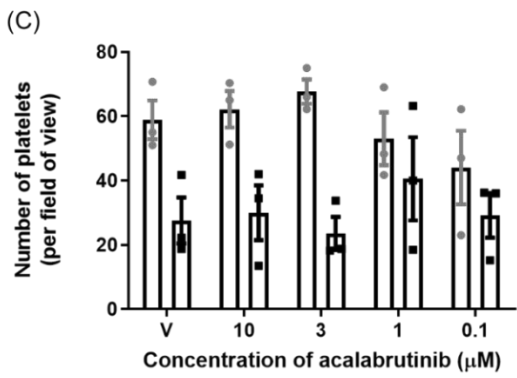
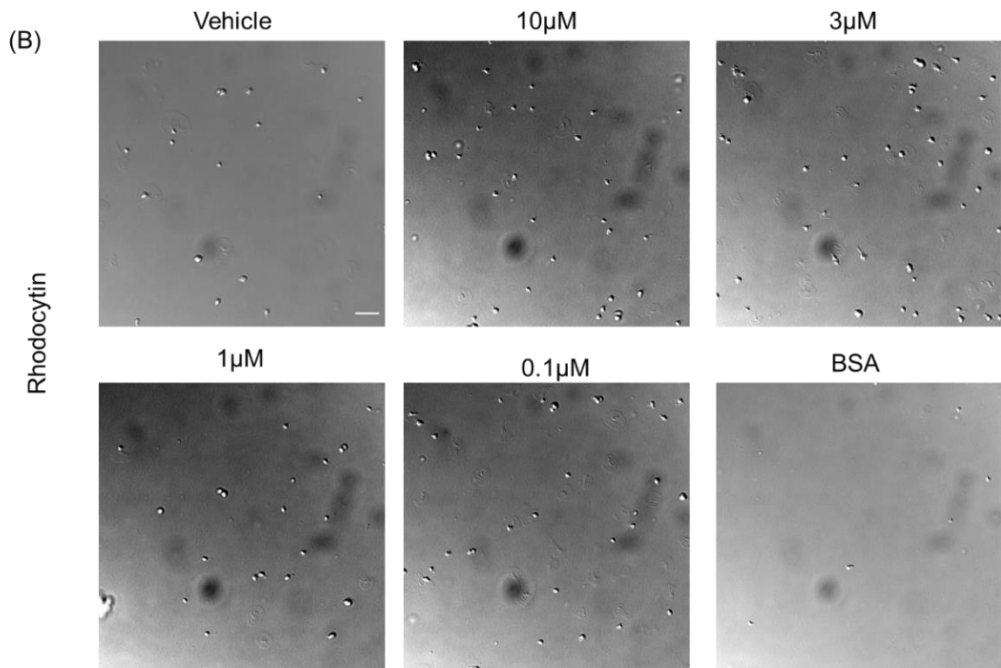
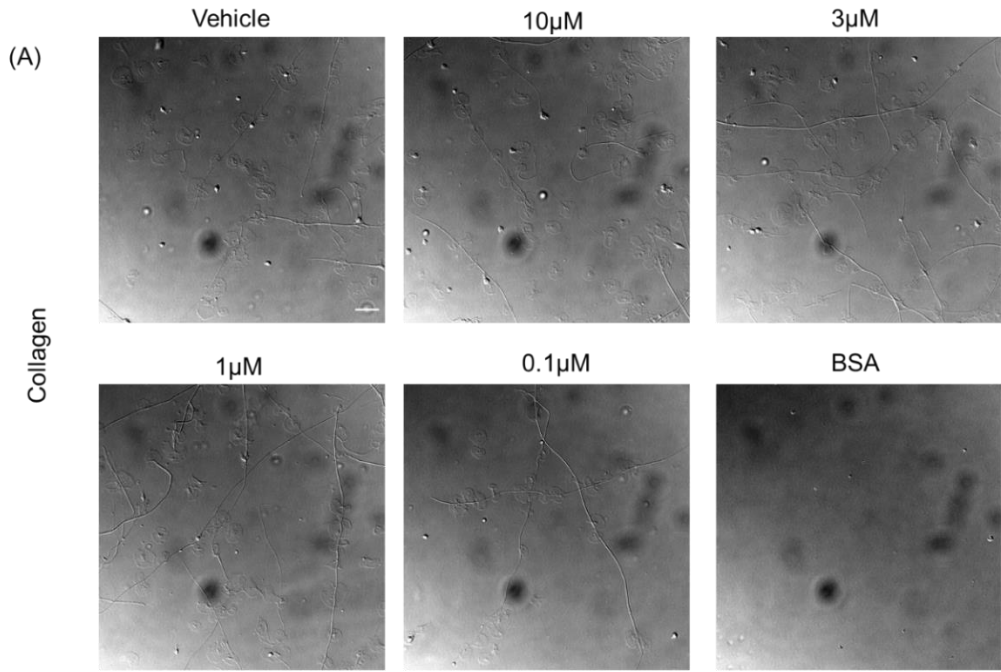


Figure 3.3.16 Platelet spreading is not inhibited in the presence of acalabrutinib on collagen or rhodocytin

Washed platelets were preincubated with acalabrutinib (0.1-10 μ M) or vehicle control for 5 minutes. Platelets were spread on (A) collagen (10 μ g/mL) or (B) rhodocytin (100nM) or BSA (5mg/mL) coated coverslips for 45 minutes and fixed. Slides were mounted using Hydromount before imaging on a Nikon TiE2 microscope with a 100x objective. Scale bar = 10 μ m. Analysis was performed using ImageJ to (E) count the number of platelets and to determine the (F) spread surface area. Statistical testing was performed using Two-way ANOVA using Dunnett's post-test. Significance was taken at *p \leq 0.05. **p \leq 0.01. Graphs represent mean \pm SEM, n=3.

3.3.13 PI3K inhibition reduces platelet adhesion and spreading on collagen

As adherence and spreading of platelets is not inhibited with 1 μ M acalabrutinib, a concentration that causes an inhibition of Btk phosphorylation, Btk is potentially playing a scaffolding role. To investigate if the potential scaffolding role of Btk is related to its recruitment via PIP3, experiments were performed using a PI3K inhibitor and acalabrutinib in combination. This was to investigate if there is any further inhibition observed when Btk is not recruited to the signalosome compared to when Btk kinase activity is blocked.

When treated with either concentration of acalabrutinib (1 μ M or 0.1 μ M), the number of platelets adhered to collagen is not significantly different from vehicle treated samples, Figure 3.3.17.B. Additionally, when treated with either concentration of LY294002, there is no significant inhibition in the number of adhered platelets when compared to the vehicle control. The addition of LY294002 at either concentration to either 1 μ M or 0.1 μ M acalabrutinib samples does not cause any further inhibition in the number of platelets adhered in the field of view.

100 μ M LY294002 caused a reduction of surface area to $18.5 \mu\text{m}^2 \pm 1.5$ which was significantly smaller than vehicle treated samples. The surface area of platelets treated with 1 μ M acalabrutinib is $43.7 \mu\text{m}^2 \pm 3.1$. When the platelets are also treated with 100 μ M LY294002 in addition to 1 μ M acalabrutinib, the surface area is significantly reduced to $13.7 \pm 1.1 \mu\text{m}^2$, ($p \leq 0.05$). This is also observed in 0.1 μ M acalabrutinib treated samples, with 100 μ M LY294002 and 0.1 μ M acalabrutinib causing an average platelet surface area of $14.5 \mu\text{m}^2 \pm 3.1$ ($p \leq 0.001$).

This suggests that there is no further effect of Btk inhibition on platelet spreading due to kinase inhibition, and that the lack of spreading observed in these experiments is mediated by PI3K inhibition.

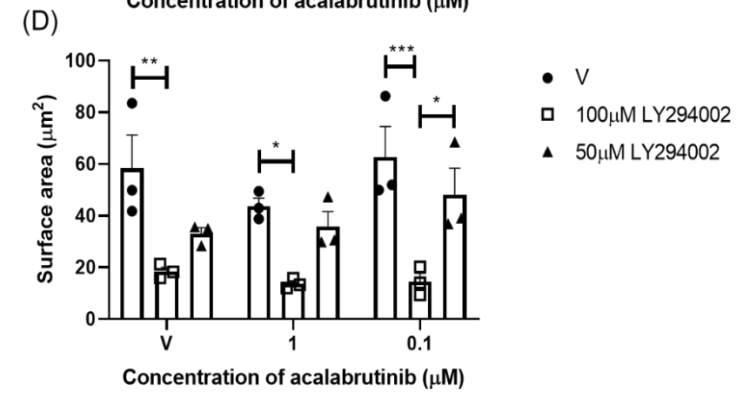
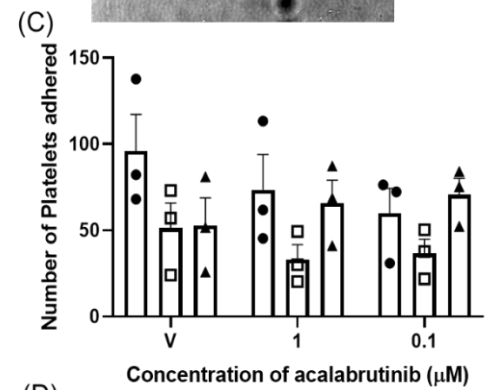
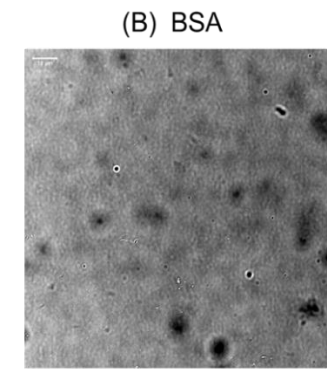
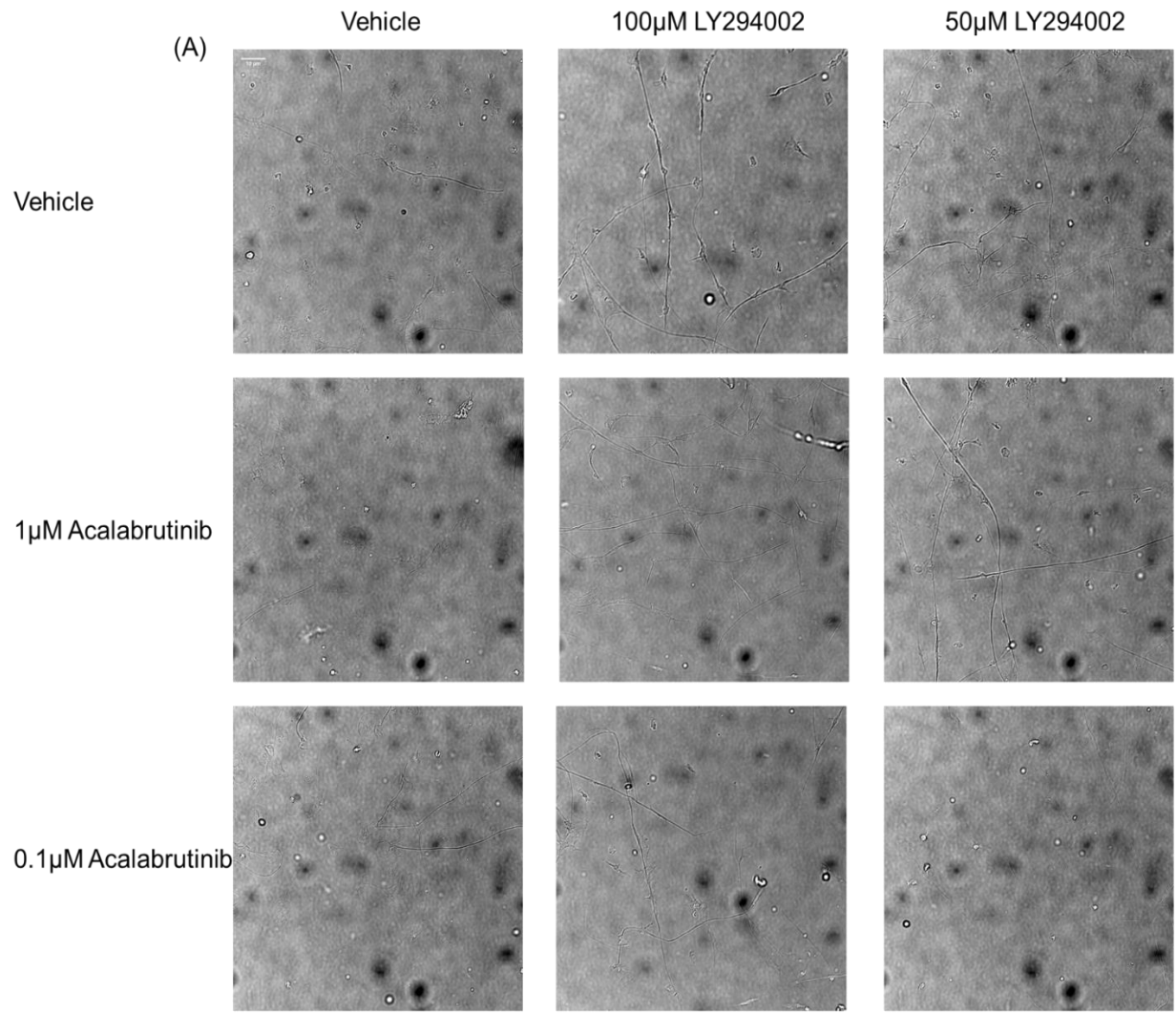


Figure 3.3.17 Addition of acalabrutinib does not further inhibit spreading with a PI3K inhibitor

Washed platelets were preincubated with acalabrutinib (1 or 0.1 μ M), 100 μ M or 50 μ M LY294002 or vehicle control (DMSO 0.1% (v/v)) individually or in combination for 5 minutes. (A) Platelets were spread on collagen (10 μ g/mL) or (B) BSA (5mg/mL) coated coverslips for 45 minutes before fixation. Slides were mounted using Hydromount before imaging on a Nikon TiE2 microscope with a 100x objective. Scale bar = 10 μ m. Analysis was performed using ImageJ to (B) count the number of adhered platelets and (C) to determine the surface area. Statistical testing was performed using Two-way ANOVA using Tukeys post-test. Significance was taken at * $p \leq 0.05$. ** $p \leq 0.01$, *** $p \leq 0.001$. Graphs represent mean \pm SEM, n=3.

Table 3.3.1 Calculated IC₅₀ values in this study

| Platelet preparation | Agonist | 100nM Rhodocytin | | 300nM Rhodocytin | | 1µg/mL CRP-XL | |
|---------------------------|--------------------|-----------------------|-------------------------|-----------------------|-------------------------|-----------------------|-------------------------|
| | Experiment | IC ₅₀ (µM) | 95% Confidence interval | IC ₅₀ (µM) | 95% Confidence interval | IC ₅₀ (µM) | 95% Confidence interval |
| ADP insensitive platelets | Aggregation | 0.21 | 0.07 to 0.53 | 3.54 | 2.87 to 4.36 | 2.99 | 1.85 to 4.85 |
| ADP insensitive platelets | Fibrinogen binding | 0.49 | 0.18 to 1.34 | | | 1.40 | 0.83 to 2.37 |
| ADP insensitive platelets | P selectin | 0.55 | 0.11 to 2.85 | | | 1.41 | 0.81 to 2.46 |
| ADP insensitive platelets | Btk pY223 | 1.02 | 0.55 to 1.94 | 0.87 | 0.47 to 1.63 | 1.83 | 0.44 to 7.54 |
| ADP insensitive platelets | PLCY pY759 | | | 1.12 | 0.53 to 2.34 | 1.41 | 0.67 to 2.97 |
| ADP insensitive platelets | Src pY416 | 39.93 | 15.86 to 1564 | 16.88 | 2.94 to 96.99 | Uncalculatable | |
| ADP insensitive platelets | Syk pY525 | 10.38 | 2.05 to 190.6 | Uncalculatable | | Uncalculatable | |
| ADP insensitive platelets | Btk pY551 | | | 13.76 | 2.21 to 85.58 | Uncalculatable | |

| | | | | | | | |
|-------------------------|-------------|------|----------------|----------------|----------------|-------|----------------|
| ADP sensitive platelets | Aggregation | 4.57 | 2.88 to 7.4105 | Uncalculatable | | 15.47 | 9.87 to 26.44 |
| ADP sensitive platelets | Btk pY223 | | | 1.66 | 0.87 to 3.150 | 0.57 | 0.19 to 1.65 |
| ADP sensitive platelets | PLCY pY759 | | | 1.11 | 0.69 to 1.751 | 0.28 | 1.01 to 3.55 |
| ADP sensitive platelets | Src pY416 | | | 20.83 | 3.26 to 133.2 | 8.83 | 4.01 to 23.26 |
| ADP sensitive platelets | Syk pY525 | | | 58.50 | 0.01 to 425988 | | |
| ADP sensitive platelets | Btk pY551 | | | | | 46.32 | 22.99 to 194.8 |

3.4 Discussion

Using Btk inhibitors in a range of platelet functional assays the following aims were addressed

3.4.1 Aim - To identify if acalabrutinib causes platelet inhibition to a similar manner to ibrutinib

3.4.1.1 Ibrutinib inhibits both GPVI and CLEC-2 aggregation, granule release and fibrinogen binding more potently than acalabrutinib and CLEC-2 responses are more severely inhibited

Downstream of GPVI, Figure 3.3.2 show that ibrutinib is more inhibitory than acalabrutinib. At 1µg/mL CRP-XL, only 10µM acalabrutinib caused inhibition of aggregation in washed platelets, whereas ibrutinib caused inhibition with concentrations as low as 0.1µM (Figures 3.3.2 B and D) consistent with previously published work (Dobie et al., 2019, Chen et al., 2018). The IC₅₀ values are 2.7µM (1.7 to 4.26) for acalabrutinib and 0.06µM (0.05 to 0.09) for ibrutinib which agree with the IC₅₀ values of Bye et al. However, larger IC₅₀ values for ibrutinib and acalabrutinib downstream of CRP-XL were obtained when investigated by the Watson group (ibrutinib- 1.19µM, (0.73 to 1.95) and acalabrutinib 21.25µM (12.27 to 37.11) (Nicolson et al., 2018), but this is likely due to the higher concentrations of agonist used (10µg/mL of CRP-XL compared to 1µg/mL CRP-XL). Nonetheless, this shows that ibrutinib is more potent at inhibiting platelet aggregation than acalabrutinib downstream of GPVI.

Similar results can be observed downstream of CLEC-2. There is a shift to the left of ibrutinib's IC₅₀ curve compared to acalabrutinib's (Figure 3.3.3 E, H, K), showing increased potency of ibrutinib. These values are in accordance with Nicolson et. al., 2020, and in direct contrast to the results on Manne et al, where 10nM ibrutinib abolished aggregation downstream of rhodocytin. Whereas in this study, 10nM ibrutinib does not

alter aggregation. Manne et al used 30nM of rhodocytin as an agonist which did not elicit a response in Figures 3.3.1.A and B.

For both agonists, there is a significant difference in the amount of aggregation at 1 μ M ($p \leq 0.01$), with ibrutinib being more inhibitory (Figures 3.3.2B and 3.3.3.B). Indeed, at this concentration Src pY416 is not inhibited with acalabrutinib downstream of GPVI (Figures 3.3.4.B). Downstream of CLEC-2 Src pY416 is inhibited at 1 μ M acalabrutinib, but not abolished, and levels are still approximately 50% (3.3.6.B lower panel). Furthermore, ibrutinib is more potent at inhibiting SFKs than acalabrutinib (Figure 3.3.7 D and F). This has also been confirmed in the literature (Bye et al., 2017).

This suggests that aside from Btk and SFK inhibition, there are other kinases being inhibited by ibrutinib. Btk deficient XLA patients do experience inhibition of aggregation when treated with 70nM ibrutinib. This concentration concentrations thought to be inhibitory for Btk only (Tec and Src phosphorylation is unaltered in healthy donors at 70nM ibrutinib) (Nicolson et al., 2018). This suggests that ibrutinib has other unknown targets that are mediating platelet inhibition. Because of the unknown off target effect of ibrutinib, acalabrutinib was used to further investigate the role of the Btk kinase in platelet responses to GPVI and CLEC-2 mediated signalling pathways.

In line with this study, ibrutinib has been shown in the literature to inhibit α granule secretion downstream of GPVI. P-selectin exposure, a marker of platelet activation, is also greatly inhibited by 1 μ M of ibrutinib in response to 1 μ g/mL CRP-XL (Bye et al., 2015). This has also been confirmed by another independent group, with 1 μ M ibrutinib inhibiting P-selectin exposure downstream of 0.25 μ g/mL of CRP-XL (Dobie et al., 2019). More recent work by Bye and colleagues has shown that acalabrutinib does not inhibit P-selectin exposure as severely as ibrutinib downstream of CRP-XL (Bye et al., 2017). These findings are consistent with the findings of this study (Figure 3.3.2F-H).

Fibrinogen binding downstream of 1 μ g/mL CRP-XL stimulated platelets is also significantly inhibited in the work by Bye *et al.*, which is also consistent with the results in

this study (Figure 3.3.2.I). Also consistent with this study is that ibrutinib also inhibited fibrinogen binding more severely than acalabrutinib downstream of CRP (Bye et al., 2017), Figure 3.3.3.I-K.

Recent research has demonstrated that ibrutinib can cause shedding of $\alpha\text{IIb}\beta\text{3}$ in the absence of agonist *in vitro* and *in vivo* via ADAM17. It is believed this increased activity of ADAM17 is caused by off target effects as using a more selective, but still irreversible, Btk inhibitor Zanubrutinib did not modulate receptor levels (Dobie et al., 2019). This may be a potential reason for why there is a stronger inhibition of ibrutinib on fibrinogen binding compared to acalabrutinib. However as acalabrutinib was not used in the work by Dobie et al., it cannot be confirmed.

The study by Dobie et al., also investigated granule secretion downstream of CLEC-2 in the presence of ibrutinib, however not for acalabrutinib. Concentrations of 0.5 μM and higher of ibrutinib prevented the release of α and dense granules when stimulated with 0.7 $\mu\text{g/mL}$ (23nM) rhodocytin. This is consistent with the results where concentrations greater than 0.3 μM ibrutinib inhibit P-selectin exposure downstream of 100nM rhodocytin (Figure 3.3.3.F). An alternative Btk inhibitor, zanubrutinib, did not cause inhibition dense or α granule secretion at low concentrations. However, it did as the concentration increased, similarly to ibrutinib (Dobie et al., 2019).

This group also investigate the activation of integrin $\alpha\text{IIb}\beta\text{3}$ downstream of rhodocytin. In contrast to this study, they assessed the active confirmation of the integrin using the PAC-1 antibody which binds to active confirmation of $\alpha\text{IIb}\beta\text{3}$ (Joo et al., 2015). The opening of the integrin was inhibited using ibrutinib, similarly to our study (3.3.3.I). Zanubrutinib was still inhibitory at inhibiting PAC-1 binding when stimulated with 23nM rhodocytin, but to a lesser extent than ibrutinib (Dobie et al., 2019). The concentrations of inhibitor used in these experiments is not stated so it is difficult to compare to the results obtained in Figure 3.3.3.I-J.

3.4.1.2 The phosphorylation of CLEC-2 is inhibited in the presence of ibrutinib but not acalabrutinib

As there was a more severe effect of Btk inhibition on CLEC-2 mediated aggregation than GPVI mediated aggregation, it was investigated that the receptor itself was reduced in its phosphorylation which would prevent signalling. The SFK's and Syk are responsible for the phosphorylation of CLEC-2 (Severin et al., 2011, Lorenz et al., 2015). Btk inhibition using acalabrutinib did weakly inhibit the phosphorylation of SFKs downstream of CLEC-2 (Figure 3.3.6). However, 1 μ M ibrutinib has been proposed to inhibit SFK's activity more potently (Figure 3.3.7.F) and published in literature (Bye et al., 2015, Nicolson et al., 2020) which may explain why 1 μ M ibrutinib causes a reduction in CLEC-2 phosphorylation whereas acalabrutinib does not. Interestingly however, this inhibition of phosphorylation is only in the ADP sensitive samples. This potentially may be due to the inhibition of the reinforced signalling by secondary mediators, that human CLEC-2 is dependent on, leading to a greater inhibitory effect.

3.4.2 Aim - To characterise the effect of acalabrutinib downstream of GPVI and CLEC-2 using platelet aggregation, granule secretion and protein phosphorylation and to investigate where Btk lies in the CLEC-2 signalling cascade

3.4.2.1 Dose dependent inhibition of platelet responses of acalabrutinib downstream of GPVI

High concentrations of acalabrutinib is inhibitory on aspects of platelet function mediated via GPVI. These include inhibition of aggregation (Figure 3.3.2 A and B), granule secretion (Figure 3.3.2.G) and calcium mobilisation (Figure 3.3.13). However, there is no inhibition in these responses at 1 μ M acalabrutinib, which is shown to have lost phosphorylation of Btk at pY223, a site that shows Btk is catalytically active (Figure 3.3.4

and 3.3.9). Only 10 μ M acalabrutinib inhibited aggregation and calcium release (Figures 3.3.2 A, B and 3.3.13B,C) which is consistent with two other studies (Bye et al., 2017, Nicolson et al., 2018).

Calcium mobilisation was lost at 10 μ M acalabrutinib, along with aggregation, Btk and PLC γ 2 phosphorylation. However, at 1 μ M acalabrutinib, calcium mobilisation was not inhibited despite inhibition of both Btk pY223 and PLC γ 2 pY759 in ADP sensitive and ADP insensitive washed platelets (Figures 3.3.4 and 3.3.9). This suggests that catalytic activity of Btk and PLC γ 2 phosphorylation at pY759 are not involved in calcium mobilisation.

PLC γ 2 has multiple phosphorylation sites, Y753, Y759, Y1197 and Y1217 (Kim et al., 2004, Rodriguez et al., 2001). It is possible, that phosphorylation of another / multiple other sites, or an unknown mechanism such as serine phosphorylation is responsible for mediating calcium mobilisation downstream of GPVI. Mutagenesis studies mutating all four sites (Y753, Y759, Y1197 and Y1217) did not result in abolished calcium mobilisation in DT40 cells, suggesting an alternative mechanism of activation (Watanabe et al., 2001). Another PLC γ 2 phosphorylation site, pY1217, which Btk has been proposed to phosphorylate *in vitro* (Watanabe et al., 2001), however it was not identified as phosphorylated in convulxin stimulated platelets (Kim et al., 2004). Western blotting was performed with this antibody; however it did not yield any results even in vehicle stimulated samples. Nonetheless, this suggests Btk catalytic activity at PLC γ pY759 is not required downstream of GPVI mediated responses. Although calcium flux was measured as an output of PLC γ 2 activity, a more direct measure of PLC γ 2 could be assessed to confirm these results. Measurement of IP₃ or DAG could be performed to further ascertain this result.

If Btk catalytic activity is not required downstream of GPVI, why is aggregation inhibited at 10 μ M? Calcium mobilisation is inhibited at 10 μ M acalabrutinib and this is likely the reason for inhibition of aggregation in both ADP sensitive and ADP insensitive platelets. Indeed, it is not likely related to other kinases such as SFK and Syk as Btk's pY551 site is still

present (suggesting it is transphosphorylated), and Syk pY525 and SFK pY416 are not significantly decreased at 10 μ M.

A potential reason for this is Btk's interaction with β_3 (Soriani et al., 2006, Crosby and Poole, 2002). Indeed, the measure of the activated integrin in flow cytometry was inhibited at 10 μ M and 3 μ M acalabrutinib which matches the aggregation inhibition profile in washed platelets (Figure 3.3.2). It has been shown that acalabrutinib at these concentrations can inhibit pY773 β_3 phosphorylation and that may be preventing full activation of the integrin. This would prevent a stable platelet aggregate forming (Bye et al., 2017).

3.4.2.2 Dose dependent inhibition of platelet responses of acalabrutinib

downstream of CLEC-2 and elucidating where Btk lies downstream of CLEC-2

When platelets are stimulated with 100nM rhodocytin, acalabrutinib dose dependently inhibits the aggregation of ADP insensitive platelets, with 10 μ M, 3 μ M and 1 μ M causing inhibition of aggregation, calcium flux and α granule secretion. Btk pY223 phosphorylation is also inhibited across these concentrations. A strong positive correlation for Btk pY223 phosphorylation and aggregation is observed. This suggests, but cannot totally confirm, that Btk pY223 is important for platelet aggregation at 100nM rhodocytin in ADP insensitive washed platelets.

In 300nM rhodocytin stimulated ADP insensitive washed platelets, 0.3 μ M or greater of acalabrutinib caused inhibition of Btk pY223, whereas in ADP sensitive platelets 1 μ M acalabrutinib did not cause inhibition of Btk pY223. However, 10 μ M and 3 μ M acalabrutinib caused significant inhibition of pY223 (Figure 3.3.12). Despite loss of pY223 platelets still underwent aggregation. Surprisingly, Src pY416, which is thought to be important for CLEC-2 mediated signalling was also inhibited under these conditions. It is likely that enough SFK catalytic activity is present to mediate aggregation in these samples, particularly as the Src pY416 site is reduced, but not totally abolished.

The aggregation observed in ADP sensitive platelets at concentrations when Btk phosphorylation is lost may also be related to secondary feedback mechanisms. It is known that platelets prepared this way are more sensitive to ADP as there is a shift to the left in the EC₅₀ curve when compared to washed platelets prepared by two fast spins (Figure 3.3.8 E, F). As a high concentration of rhodocytin was used in Figure 3.3.12, it could be reasoned that aggregation was mainly related to ADP and TxA₂ being released and acting in an autocrine manner (Pollitt et al., 2010). Experiments using 100nM rhodocytin show that there is inhibition of aggregation at concentrations of acalabrutinib where phosphorylation Btk pY223 is blocked. It is likely that there is less ADP / TxA₂ released when platelets are stimulated with 100nM rhodocytin (as seen in the differing levels of calcium flux between 300nM and 100nM rhodocytin, Figure 3.3.14), and therefore the inhibition of aggregation is due to this.

However, at high concentrations of rhodocytin, both ADP insensitive and ADP sensitive platelets still aggregate despite loss of Btk pY223 and PLC γ 2 pY759 in the presence of acalabrutinib. Aggregation occurs, despite the calcium mobilisation being blocked when assessed using the peak change during calcium flux. The differences in how these experimental assays are performed may be a reason why there is a discrepancy between aggregation and calcium mobilisation. The calcium assay is performed in a plate, whereas aggregation and the phosphorylation studies are performed under stirring conditions. This may impact the responsiveness to rhodocytin and therefore may explain the discrepancy.

Furthermore, aggregation is generally viewed as an all or nothing assay. If platelets start to aggregate, it is rare that they will disaggregate. However, disaggregation of platelets can be observed when platelets are stimulated with weak agonists such as ADP (Wadowski et al., 2017), but has not been observed in rhodocytin stimulated platelets. High concentrations of rhodocytin (300nM) may induce such strong receptor clustering of CLEC-2 it may cause an increased recruitment of SFK and Syk to the signalosome (Martyanov et al., 2020, Pollitt et al., 2014, Watson and O'Callaghan, 2011). This may bypass the need for Btk catalytic activity in inducing phosphorylation of PLC γ 2. In CLL

patients, resistance to ibrutinib has been observed, which are attributed to mutations in PLC γ 2. This suggests that downstream of the BCR there may be a Btk independent pathway of signalling at high agonist concentrations (Liu et al., 2015).

Btk pY223 is more inhibited in ADP insensitive platelets than ADP sensitive platelets as shown by a smaller IC₅₀ value for ADP insensitive platelets (1.74 μ M (0.02 to 0.46) for ADP sensitive and 0.4 μ M (0.24 to 0.65) for ADP insensitive).

As ADP insensitive platelets are less potently inhibited it was hypothesised that this could be due to acalabrutinib becoming plasma bound (Scheers et al., 2015). Indeed, all the calculated IC₅₀ values of phosphorylation sites are larger in ADP sensitive platelets, suggesting less potency of the drug (Figures 3.3.9, 3.3.12 and Table 3.3.1).

Experiments adding in BSA at relevant physiological concentrations to platelets prepared by two washes may help to deduce if the less severe inhibition is related to residual plasma proteins or the lesser response to ADP. However, it is likely that lesser potency of acalabrutinib in ADP sensitive platelets is not mediated through the drug binding mechanism. The IC₅₀ values for Btk pY223 downstream of GPVI are comparable between ADP sensitive and insensitive preparations (Figures 3.3.4 and 3.3.9). Therefore, it is likely to be related to the requirement of secondary feedback to reinforce CLEC-2 mediated signalling.

Indeed, the observed aggregation at 10 μ M acalabrutinib in ADP sensitive CLEC-2 stimulated platelets do have a significantly increased lag time to aggregate compared to vehicle treated samples. The delay in aggregation may be due to the time taken to produce and release TxA₂ and ADP to activate the platelet and re-enforce the CLEC-2 signalling. To verify these results, dense granule release of ATP using chronolume could be performed at the same time as aggregation to investigate the kinetics of dense granule release in the presence of inhibitor.

It was proposed by the Kunapali group that Btk is upstream of Syk as Syk phosphorylation is lost in the presence of ibrutinib. We show here, using acalabrutinib,

that Syk is above Btk in the CLEC-2 signalling cascade. Firstly, the phosphorylation of CLEC-2 is mediated by Syk (Hughes et al., 2010b, Severin et al., 2011) and CLEC-2 phosphorylation is maintained despite the inhibition of Btk (Figure 3.3.5)

Other experiments, using western blotting further confirms that Syk is upstream of Btk. Specifically, that the phosphorylation of Syk pY525 (Syk activatory site) is present at concentrations of acalabrutinib where Btk pY223 (catalytic activity site) is lost. This provides evidence that Btk is not phosphorylating Syk. Further evidence is provided by the loss of the Btk transphosphorylation site, pY551. This is reduced at concentrations where Syk pY525 phosphorylation is normal, further providing evidence that in the CLEC-2 signalling cascade, Btk is downstream of Syk (Figures 3.3.6, 3.3.7 and 3.3.12).

3.4.3 Aim - To investigate if rhodocytin can support platelet spreading and if it can, to investigate if acalabrutinib can inhibit platelet adhesion and spreading to rhodocytin and to compare this with collagen

3.4.3.1 Acalabrutinib does not inhibit GPVI or CLEC-2 mediated spreading or adhesion.

Platelet spreading in the presence of a Btk inhibitor has been investigated in this study. Currently, no published studies have investigated the effects of acalabrutinib on platelet spreading, whereas ibrutinib has been studied. Bye et al., investigated the role of Btk during spreading and adhesion of platelets to CRP-XL and collagen using ibrutinib. Overall adhesion to collagen was not inhibited, whereas spreading was, as demonstrated by a decrease in the formation of lamellipodia. Lamellipodia formation was also inhibited on CRP-XL, but unlike collagen, platelet adhesion was also inhibited. This may be due to the compensatory role of $\alpha_2\beta_1$ mediating the spreading on collagen as opposed to CRP-XL (Jarvis et al., 2002).

There has been no literature published investigating the ability of platelets to spread on rhodocytin. Experiments using podoplanin have been performed to show that platelets do adhere and spread via the CLEC-2 receptor (Pollitt et al., 2014). We show for the first time, that when compared to collagen, platelets adhere to rhodocytin. One experiment has been published with CLEC-2 and PEAR-1 receptor agonist fucoidan, where the platelets show very weak spreading (Martyanov et al., 2020), consistent with the results found in this study.

Interestingly, when compared to their vehicle control, downstream of both GPVI and CLEC-2 there is no difference in the number of platelets adhered or their average area in the presence of acalabrutinib. However, in the average surface area of the platelets, there is not a significant difference in the vehicle treated samples between rhodocytin and collagen mediated spreading, but there is in drug treated samples (10 μ M, 3 μ M and 1 μ M

154

acalabrutinib). Platelets spread on a CLEC-2 agonist are more severely inhibited in their spreading than a GPVI agonist, suggesting that Btk's catalytic activity may be more important downstream of CLEC-2 as opposed to GPVI.

In contrast, spreading and adhesion to collagen is not inhibited when treated with concentrations of acalabrutinib that block Btk phosphorylation. There are two potential reasons for this. It may be that $\alpha_2\beta_1$ may play a role in spreading on collagen when GPVI signalling is blocked (Gibbins, 2004, Jarvis et al., 2002, Jandrot-Perrus et al., 1997). However, using beads and a collagen sequence that specifically targets $\alpha_2\beta_1$, it has been proposed that Btk is also essential downstream of this integrin (Lima et al., 2018). The other potential reason that platelets may adhere and spread normally on collagen may be due to the presence of Tec. In Btk knockout mice, platelet spreading on collagen is normal, likely due to the redundancy of Tec (Atkinson et al., 2003a). However, at 10 μ M acalabrutinib, Tec would also likely be inhibited (Nicolson et al., 2018) when spreading is not inhibited in this study, and in published literature (Bye et al., 2017).

Taken together, this suggests that Btk and Tec may not play a significant role in mediating adhesion and spreading on collagen. Indeed, double knockouts of Tec and Btk have reduced but not total loss of spreading on collagen, and appear to adhere in a similar manner, however this is not quantified in the study (Atkinson et al., 2003a).

3.4.3.2 The potential mechanism of Btk playing a dual scaffolding role

It has been proposed in B cells that Btk can act as a scaffold through its interaction with PIP3, PIP5K and PLC γ 2 (Saito et al., 2003, Pasquet et al., 2000, Scharenberg et al., 1998). To investigate a potential mechanism for Btk's possible scaffolding behaviour, experiments using the PI3K inhibitor LY294002 were performed. The aim being to prevent Btk recruitment to the membrane by preventing the production of PIP3 and inhibiting the kinase activity of Btk using acalabrutinib.

It has been previously shown that platelets treated with 50 μ M LY294002 had normal PLC γ 2 phosphorylation downstream of CRP-XL (Pasquet et al., 1999a), suggesting that recruitment of Btk may not be involved in the regulation of PLC γ 2 phosphorylation. Of note, the phosphorylation is measured using immunoprecipitation and probed for total phosphotyrosine. Therefore it is possible that other sites compensate for Btk and it would have been interesting if Btk specific phosphosites had been assessed. Nonetheless, this suggests Btk independent activation of PLC γ 2.

When samples were treated with both the PI3K and Btk inhibitors, no additional inhibition of spreading was seen when compared to LY294002 alone (Figure 3.3.17.C, D). This suggests that Btk recruitment is more important than catalytic activity. However, the concentration of PI3K inhibitor was likely also impacting the normal platelet response, as this would likely inhibit Akt which is required for spreading (Kim et al., 2009b). Although it has been used at this concentration (50 μ M) in the literature, with platelets aggregating to high concentrations of CRP-XL (Pasquet et al., 1999a). Experiments should be repeated with lower concentrations of LY294002 to modulate the recruitment of Btk without inhibiting the platelet spreading.

An alternative approach to these experiments could be to use an inhibitor of Phosphatase and Tensin homolog (PTEN). This phosphatase is responsible for the removal of PIP3, and therefore it would increase Btk recruitment. Experiments could be performed with an inhibitor of PTEN, such as bpV(phen) (Pulido, 2018), in addition to acalabrutinib, to ensure Btk was present but catalytically inactive, to assess the potential scaffolding role of Btk (Myers et al., 1997).

3.5 Conclusions

Platelets can still aggregate and spread at concentrations where Btk phosphorylation is lost downstream of GPVI – this suggests a scaffolding role for Btk downstream of GPVI. At an intermediate concentration of rhodocytin, Btk cannot play a scaffolding role as

phosphorylation and platelet responses are inhibited when Btk phosphorylation is lost. However, at high concentrations of rhodocytin, Btk is not involved in the aggregation of these platelets, as aggregation occurs when phosphorylation of Btk is lost. This suggests other kinases and secondary feedback may play a role or a further potential scaffolding role downstream of CLEC-2.

We show for the first time that platelets adhere too, and spread on the CLEC-2 ligand rhodocytin, and spreading is not inhibited by Btk inhibition. Spreading on GPVI agonist collagen is also not inhibited by acalabrutinib and potentially suggests a redundant role of Btk in mediating both GPVI and CLEC-2 mediated spreading.

4 The use of the DT40 B cell line to investigate which functional Btk domains are required to convey GPVI and CLEC-2 signalling

4.1 Introduction

As platelets do not contain a nucleus, genetic modification of DNA is not possible using platelets directly. There is an emerging field of genetic manipulation of induced pluripotent stem (iPS) cells to make modified *in vitro* platelets (Moreau et al., 2016). However, currently platelet research is largely dependent on the genetic manipulation of animals. Animal work is slow due to time needed for the breeding of animals, cost ineffective and sometimes the genetic changes are not viable. For example, a mouse model with a double knockout of Btk and Tec is not viable beyond birth. This is due to the failure of the separation of the blood lymphatics and believed to be due to the disruption of the CLEC-2 podoplanin signalling axis (Manne et al., 2015a).

Therefore, research using model cell lines, genetic manipulation of DNA and the expression of mutant proteins using gene editing has been utilised to further unpick the role of proteins downstream of ITAM and hemITAM signalling.

4.1.1 DT40 cells

The DT40 cell line is a chicken (*Gallus gallus domesticus*) B cell line derived from Avian Leukosis Virus induced bursal lymphoma (Winding et al 2001). DT40 cells are used as a model cell line to investigate signalling pathways as they are easy to genetically manipulate. This is due to the increased ratio of targeted to random integration after transfection. The Kurosaki group were pioneers of genetic manipulation of this cell line, creating cell lines deficient in Syk, Lyn (Takata et al., 1994), PLC γ 2 (Takata et al., 1995) and Btk (Takata and Kurosaki, 1996) via homologous recombination. These cell lines have been vital in distinguishing the exact role of these proteins in ITAM mediated BCR signalling, and later for understanding the role of these proteins in platelet receptor signalling.

DT40 cells do not endogenously express either of the platelet ITAM containing FcR γ chain GPVI complex or the hemITAM containing CLEC-2 receptor (Fuller et al., 2007, Tomlinson et al., 2007). DT40 cells also endogenously express the signalling machinery needed for platelet (hem)ITAM receptor signalling, including Syk, Lyn and exclusively express the PLC γ 2 isoform (Takata et al., 1995). The ease of receptor transfection into this cell line allows the BCR signalling proteins to be exploited to study platelet (hem)ITAM signalling.

GPVI expression at the DT40 cell surface is only achieved when GPVI is co-transfected with FcR γ (Tomlinson et al., 2007, Mori et al., 2008). This is consistent with the FcR γ chain knockout mouse model which also has no GPVI detected at the surface of platelets using flow cytometry (Nieswandt et al., 2000).

Fuller and colleagues used DT40 cells to analyse the CLEC-2 signalling pathway. The Nuclear factor of T cells (NFAT) and luciferase reporter assay, which is a measure of cell signalling, was used to identify that these cells do not express endogenous CLEC-2. Furthermore, this study identified that hemITAM signalling requires Syk and its dual SH2 domains, Btk, PLC γ 2 and phosphorylation of CLEC-2 to mediate signalling, whereas a Lyn knockout cell potentiated the response to rhodocytin (Fuller et al., 2007). A potential reason for this is that Lyn could be involved in terminating hemITAM signalling, as it is known to be involved in negatively regulating ITAM signalling in platelets (Quek et al., 2000). This is due to Lyn's role in phosphorylating immunotyrosine-based inhibitory motifs (ITIMs) such as Platelet–endothelial cell adhesion molecule-1 (PECAM-1) (Ming et al., 2011, Tourdot et al., 2013). If no Lyn is present, once the response is initiated, it cannot be terminated, explaining the signal potentiation.

4.1.2 The study of signalling pathways using the NFAT Luciferase assay

The Nuclear factor of activated T cells (NFAT)-luciferase reporter assay is a sensitive assay to measure signalling induced within a cell. A reporter construct containing NFAT

which locates to the cytoplasm in a phosphorylated state, three copies of NFAT-activator protein-1 (AP-1) from the interleukin-2 gene promoter and a luciferase enzyme is transfected into the cell (Clipstone and Crabtree, 1992). The appropriate agonist binds to its respective receptor to induce intracellular signalling causing an increase in cellular calcium. This increase in subcellular calcium causes activation of the serine-threonine phosphatase calcineurin, which can dephosphorylate NFAT. This allows exposure of NFAT's nuclear localisation signal and thus allowing translocation to the nucleus (May et al., 2009). Additionally, AP-1 is phosphorylated by RAS/mitogen-activated protein kinase (MAPK), allowing nuclear translocation after activation of protein kinase C via PLC γ 2. This occurs simultaneously with the phosphatase activity of calcineurin (Fuller et al., 2007).

Experiments are always performed with a positive control to verify successful transcription of the NFAT and AP-1 proteins. Post transfection, cells are treated with phorbol 12-myristate 13-acetate (PMA) and ionomycin. These bypass the need for agonist binding and cell signalling by activating PKC and causing calcium flux, respectively. This allows nuclear translocation of the NFAT and AP-1 proteins.

Following the translocation of NFAT and AP-1 proteins to the nucleus, luciferase can then be translated and transcribed (Figure 4.1.1.A), as the luciferase gene transcription is controlled by the NFAT and AP-1 proteins. The luciferase enzyme is then able to catalyse luciferin to produce luminescence in the presence of ATP (Figure 4.1.1.B). More cell signalling results in an increased amount of luciferase transcribed, and this corresponds to the amount of light produced.

The use of the NFAT-luciferase assay is more favourable than measuring calcium flux due to the increased sensitivity of the assay. To maintain NFAT protein dephosphorylation, sustained calcineurin activation is required, and this is achieved with low continuous Ca²⁺ elevations (Dolmetsch et al., 1997). Sometimes, this low but sustained calcium flux is unmeasurable using fluorimetry or microscopy, and therefore the NFAT-luciferase assay is used (Tomlinson et al., 2007).

The NFAT luciferase assay has been utilised in cell signalling to elucidate both agonists, required proteins and protein domains involved in platelet signalling for both GPVI and CLEC-2 signalling (Mori et al., 2008, Tomlinson et al., 2007, Alshehri et al., 2015b, Hughes et al., 2013).

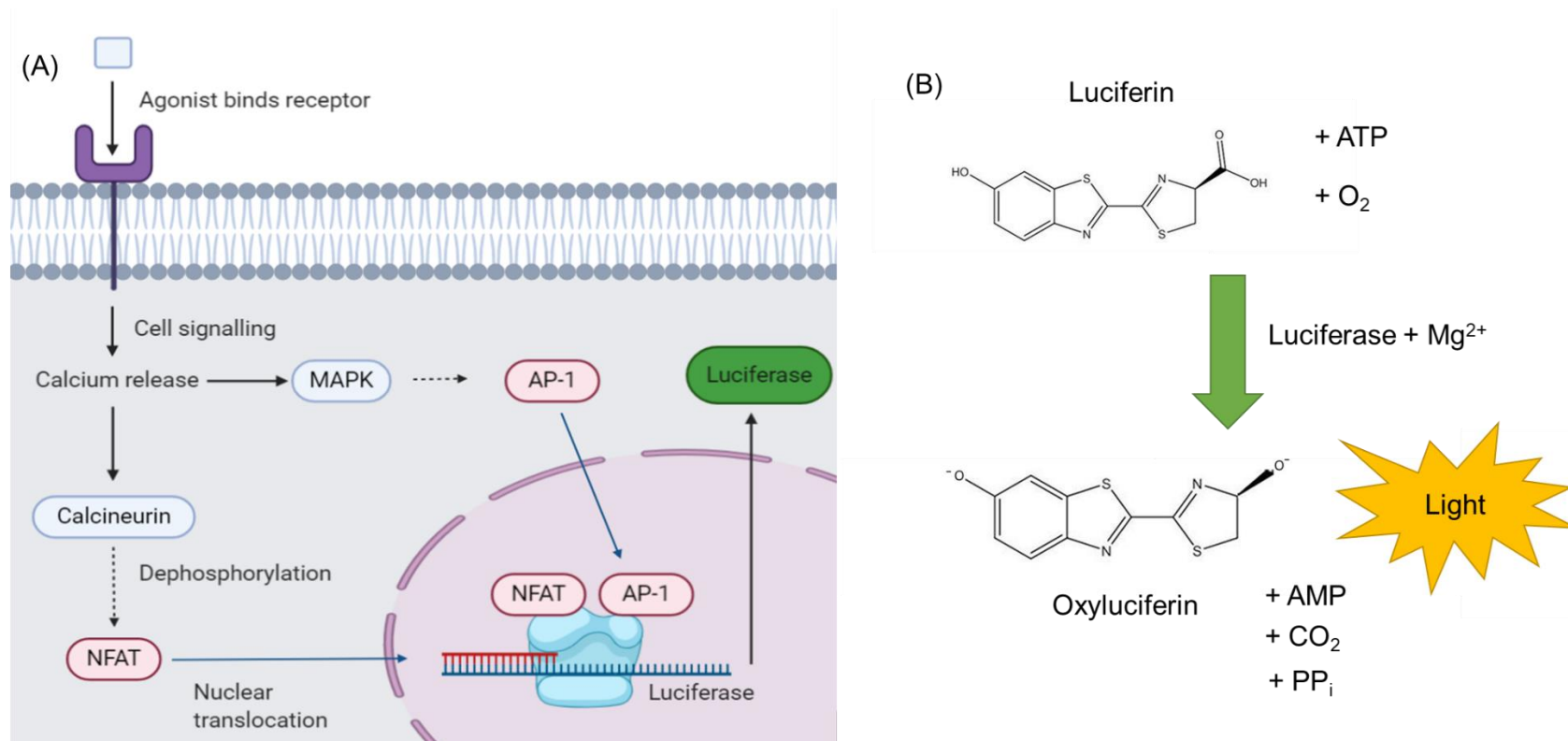


Figure 4.1.1 NFAT-Luciferase reporter assay

(A) Agonist binds to the receptor to initiate cell signalling through tyrosine kinases. This results in calcium release which activates the serine/threonine phosphatase Calcineurin. This dephosphorylates NFAT proteins present in the cytoplasm exposing their nuclear localisation signal and they translocate to the nucleus. Concurrently, nuclear localisation signals on AP-1 proteins are also exposed through MAPK

signalling after the rise in calcium. NFAT and AP-1 proteins then bind to promoters initiating transcription of the luciferase protein. (B) Luciferin in the presence of ATP, O₂, Mg²⁺ and Luciferase is catalysed to Oxyluciferin and light, which is measured.

4.1.3 CRISPR-Cas9

Clustered regularly interspaced short palindromic repeats (CRISPR) – Cas9 technology utilises a microbial adaptive immune system to result in genome editing of the host cell. This system, originally present in prokaryotes, results in the cleavage of pathogen DNA and therefore pathogen death. This protects the bacteria from infection with viruses and plasmids. However, it has been exploited and developed to gene edit eukaryotes.

The CRISPR-Cas9 system from *Streptococcus pyogenes* (SpCas9) has been widely utilised and consists of a Cas9 endonuclease and an oligonucleotide guide RNA which has been cloned into the same plasmid (see Figure 4.1.2). The guide sequence is 20-24 nucleotides that guides the Cas9 to the target cut site and must be upstream of the protospacer adjacent motif (PAM). The PAM site is required in order for activation of the Cas9 protein. Now in its active state with the guide RNA bound, Cas9 will only cut if there is sufficient homology between the guide and the target sequence. DNA is nicked by the SpCas9 ~3-4 nucleotides upstream of the PAM sequence, where a double strand break is introduced. The cell can then repair the DNA by 2 methods; non homologous end joining (NHEJ) or homology directed repair (HDR) (Jinek et al., 2012, Ran et al., 2013, Shalem et al., 2014).

Non-homologous end joining occurs after a double strand break and is the favoured method of DNA repair by cells (Mao et al., 2008). After the break, broken ends (typically with overhangs) are directly ligated without a homologous template. This is orchestrated by a variety of intracellular factors including ligases. Nucleotide bases are often added or deleted; however these bases are not always correct, due to its error prone nature. This often results in knockout or inactivation of the target protein, usually by the introduction of a frameshift (Lino et al., 2018). NHEJ usually destroys the PAM site due to the proximity of the cleavage preventing further re-edits. NHEJ is employed often to create 'knockout' protein cells.

Homology directed repair (HDR) is the alternative approach cells can take to repair their DNA after the induced double strand break. It is considered the more accurate mechanism of repair. It requires a donor template of the sequence to be repaired. The steps are shown in Figure 4.1.2. Briefly, a DSB is introduced and the repair template with homology arms lines up to near the area where the DSB is. The template is used to repair the double strand break by homology directed repair, integrating the template (which contains the desired mutations) into the DNA (Lino et al., 2018).

HDR is far more complex than NHEJ. Firstly, the site of mutagenesis is limited by the presence of a PAM site. PAM sites are required for the DNA editing to take place, and the PAM site should be within 10 base pairs of the cut to increase the chances of HDR. This can often be restrictive if there are less PAM sites present within the sequence.

Furthermore, the Cas9 will continue to cut the integrated DNA if there is still a PAM site present within the DNA after the HDR.

Nevertheless, CRISPR-Cas9 has been employed experimentally to create knockouts (Shalem et al., 2014, Abu-Bonsrah et al., 2016), point mutation knock-ins (Zhang et al., 2016) and introduced fluorescent tags to proteins (Khan et al., 2017). Therefore, it is a valuable and widely applicable experimental tool. Utilising CRISPR to create knock-ins is beneficial as it results in protein expression which is present under normal cellular control and regulation. Therefore, the expressed levels of protein are typically that of the endogenous protein, and experimental artefacts due to over expression levels can be disregarded. Any change in the expression of protein induced by the CRISPR-Cas9 editing is biologically relevant.

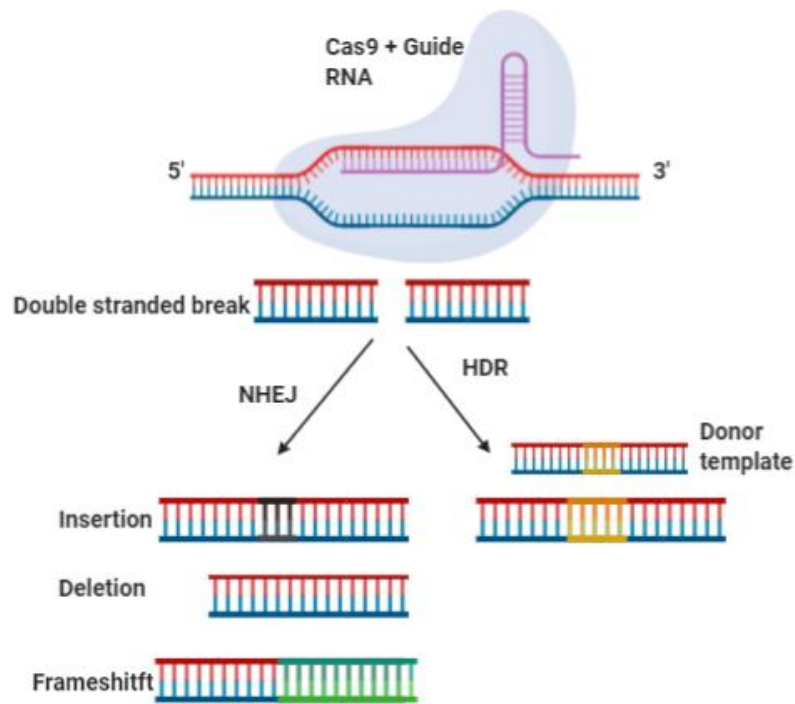


Figure 4.1.2 Mechanisms of DNA repair using CRISPR-Cas9 gene editing

The guide RNA targets the Cas9 to the appropriate site where it induces a double strand break. The cell can then repair the DNA damage via non homologous end joining (NHEJ) where base insertions or deletions can lead to a frameshift in the DNA. Alternatively, a donor template with homologous arms and mutations (shown in yellow) can be used. The cell can repair the DNA via homology directed repair, introducing specific mutations into the DNA.

4.1.4 Domains of Btk required for signalling

There is conflicting literature in B cells as to which Btk domains are required to mediate signalling. These are summarised in Table 4.1.1. Furthermore, this research is limited to signalling downstream of the B cell receptor, with limited literature on the role of Btk domains in platelet (hem)ITAM receptor signalling using these models, or with any work directly in platelets.

Table 4.1.1 Describes the Btk domain functions and evidence that they are or not required to mediate signalling

| Domain and interaction | Evidence that the domain and/or domain function is required | Evidence that the domain and/or domain function is not required |
|--|--|---|
| <p>PH and TH – PIP3, produced by PI3K.</p> | <p>Function altering point mutated Btk (R28C) did not undergo calcium flux in B cells in an overexpression model (Takata and Kurosaki, 1996).</p> <p>W124G point mutation reduces Btk signalling in a NIH 3T3 cell line (Li et al 1995).</p> <p>Btk activation dependent on PIP3 density at membrane (Chung et al., 2019) and PI3K inhibitors block Btk recruitment to the membrane fraction when platelets are stimulated with rhodocytin (Manne et al., 2015a)</p> <p>Multiple mutations in this domain have been identified as the cause of severe XLA in patients (Hyvönen and Saraste, 1997).</p> | <p>PLCγ2 phosphorylation is not reduced in the presence of a PI3K inhibitor in Ramos cells, although Btk may not be the kinase responsible for PLCγ2 phosphorylation in these cells (Kim et al., 2004).</p> |

| | | |
|-----------------------------------|---|--|
| <p>SH3 – proline rich regions</p> | <p>Numerous identified mutations in this domain resulting in XLA (Väliäho et al., 2006).</p> | <p>SH3 function of Tec is not required to mediate signalling in Jurkat cells when investigated using a functional altering point mutations (WW215/216LL) (Tomlinson et al., 2004b).</p> <p>SH3 domain is not required for signalling in a constitutively active Btk PH domain mutant (Li et al., 1995)</p> |
| <p>SH2 - phosphotyrosine</p> | <p>B cell signalling and flux blocked in function altering point mutation (R307K) and domain deletions (Fluckiger et al., 1998, Scharenberg et al., 1998).</p> <p>Several mutations in this domain have been identified as causative of XLA (Väliäho et al., 2006).</p> | <p>Downstream phosphorylation of PLCγ2 is reduced but not abolished in B cells in function altering point mutation (R307G) (Takata and Kurosaki, 1996).</p> <p>Not required for oncogenic activity to transform colonies in NIH 3T3 cells in a PH activating Btk mutant (Li et al., 1995)</p> |

| | | |
|--|---|---|
| <p>Kinase (SH1) – catalytic activity</p> | <p>Btk can be responsible for tyrosine phosphorylation of PLCγ2 (Watanabe et al., 2001).</p> <p>Kinase inhibitors ibrutinib and acalabrutinib that inhibit B cell signalling and are clinically successful for treatment of B cell malignancies (Patel et al., 2016, Isaac and Mato, 2020).</p> <p>Mutations in this domain lead to XLA, however it can be a less severe phenotype (Gaspar et al., 2000).</p> | <p>Kinase inactive mutant (K430R) - Not required in B cell development (Middendorp et al., 2003)</p> <p>A kinase inactive mutant (K430E) can mediate signalling downstream of the oestrogen receptor in B cells (Tomlinson et al., 2001).</p> <p>There was a peak of calcium flux, albeit greatly reduced compared to wild type, in a kinase dead version of Btk downstream of the BCR (Takata and Kurosaki, 1996).</p> |
|--|---|---|

The above table shows that there is conflicting information within the literature about what Btk domain functions are required to mediate signalling. It is suggested by multiple reports that the PH domain is absolutely required in both platelets and B cells (Manne et al., 2015, Pasquet et al., 2000), with little literature opposing this.

It is contentious if the SH3 domain is required, as there have been multiple reports where this is not required to mediate BCR signalling. Whereas there are fewer reports verifying it is essential (Table 4.1.1). The function altering SH2 domain mutations at R307 in some reports abolish signalling (Fluckiger et al., 1998). Whereas in other reports, the PLC γ 2 phosphorylation is reduced but not abolished (Takata and Kurosaki, 1996). Both the SH3 and SH2 domain functions would be difficult to block in platelets, as proline rich regions are endogenously expressed in proteins, and inhibiting tyrosine phosphorylation is likely to inhibit total platelet signalling (Watson et al., 2005).

Whether the kinase function of Btk is required is controversial. There are some reports that kinase activity is required in one setting, but not in another, and this may even be in the same cell depending on the method of cell activation such as the role of Btk at the immune synapse (Roman-Garcia et al., 2018). Btk inhibitors have been used in platelets to inhibit kinase function with differing results depending on the publishing group, with some platelets undergoing full aggregation at Btk inhibiting concentrations, whereas others do not (Series et al., 2019, Levade et al., 2014, Nicolson et al., 2018, Bye et al., 2015). In chapter 3, it was shown that Btk may be acting as a scaffold protein, and therefore, the role of the Btk kinase domain is still elusive downstream of GPVI and CLEC-2.

4.2 Aims of this chapter

While the functional domains of Btk have been explored downstream of the BCR using the overexpression of proteins, little work has investigated the role of these domains downstream of GPVI and CLEC-2.

As the DT40 cell line has been shown to be a valuable tool in investigating (hem)ITAM signalling, DT40 cells were utilised as a model to achieve the following aims:

Aims

- To elucidate which domains of Btk are required to mediate NFAT-Luciferase signalling downstream of GPVI and CLEC-2 using an overexpression model
- To genetically modify Btk using CRISPR-Cas9 to generate mutants to verify overexpression experimental models.

Hypothesis

Btk will require PH and SH2 but not SH3 domain function to mediate signalling downstream of GPVI and CLEC-2. It may require a functional kinase domain downstream of hemITAM but not ITAM signalling.

4.3 Results

4.3.1 WT DT40 cells express Btk and PLC γ 2 whereas Btk

Knockout cells only express PLC γ 2.

To ensure that the batch of DT40's was consistent with the literature, western blotting for the presence of key ITAM and hemITAM signalling proteins was assessed. DT40 cells (1×10^7 cells/mL) were sampled periodically over two weeks before being washed in PBS and lysed in 1X RIPA buffer with protease inhibitors. Cells were lysed for a minimum of 30 minutes before the appropriate volume of sample buffer was added before SDS-PAGE and western blotting.

Consistent with previous work and proteomic studies, we found that WT DT40s express PLC γ 2 and Btk, and do not express GPVI, CLEC-2 or Tec (Rees et al., 2015).

Furthermore, Btk KO cells (Dr Mike Tomlinson, University of Birmingham, UK) do not express Btk, and the level of PLC γ 2 is normal compared to WT cells (Figure 4.3.1). We did not see any evidence of Tec expression in WT DT40s nor a compensatory upregulation of Tec expression in the Btk KOs. Platelets were used as a positive control as known to express PLC γ 2, Tec and Btk (Burkhart et al., 2012).

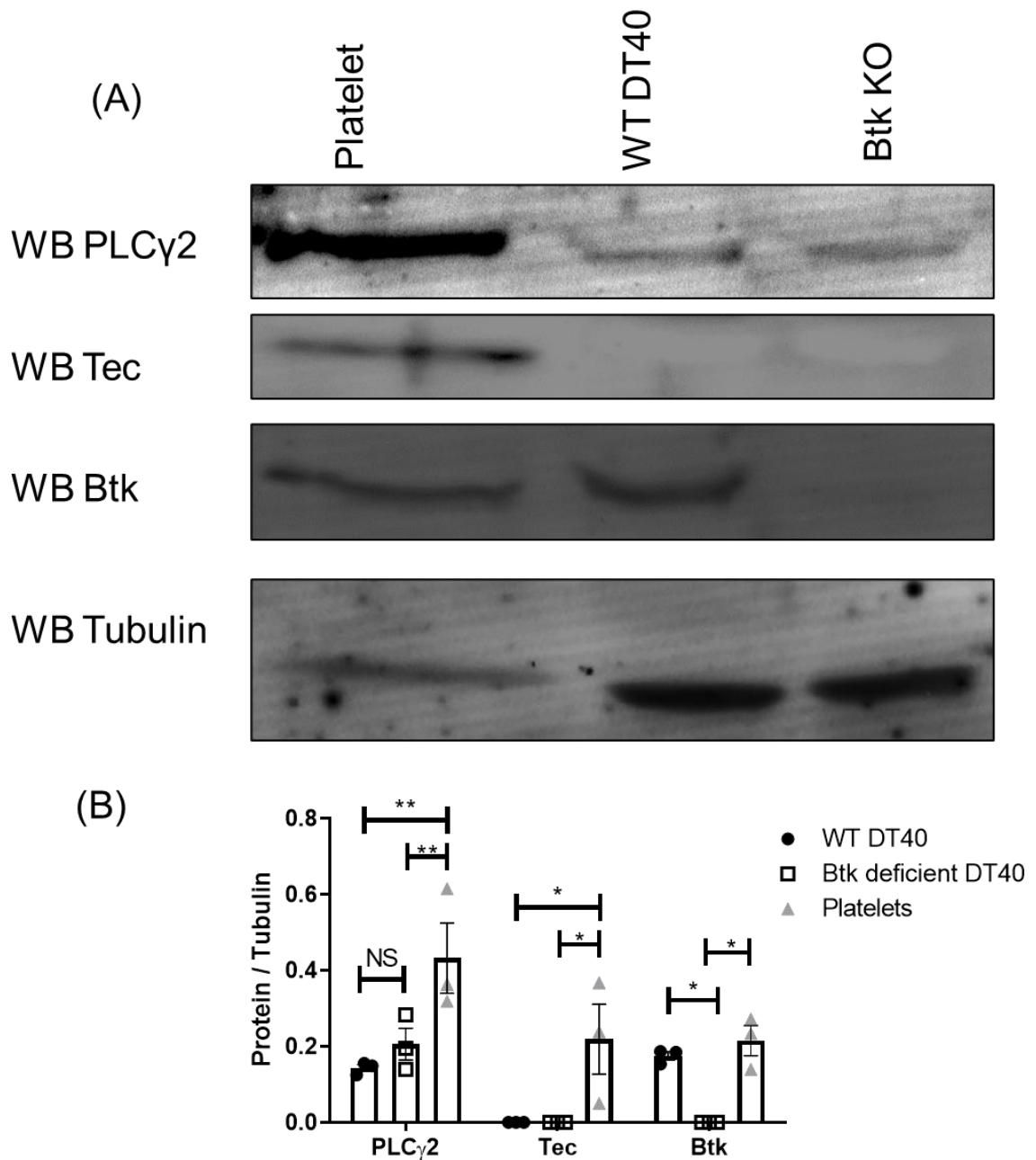


Figure 4.3.1 WT DT40's express Btk and PLC γ 2

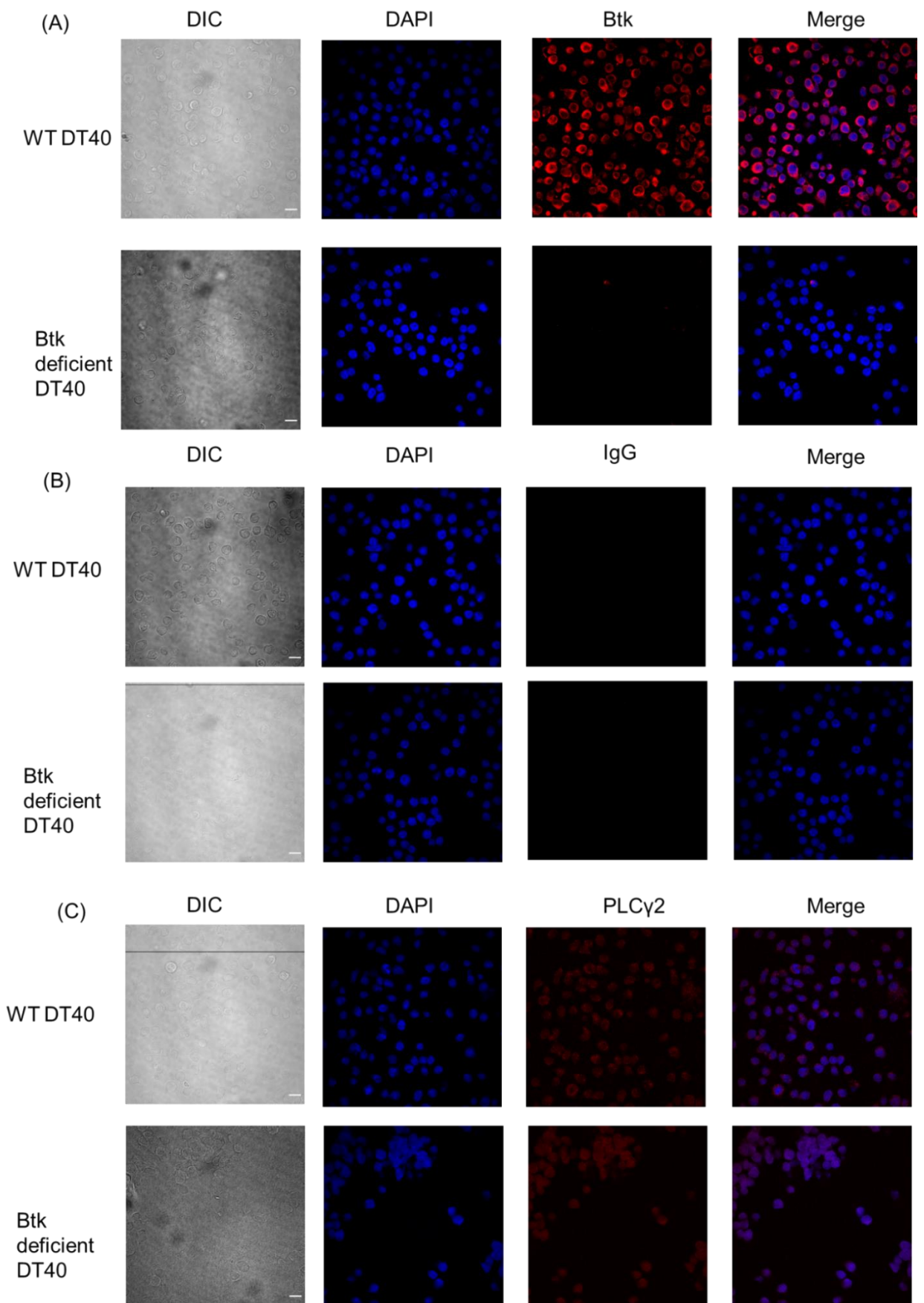
(A) Platelets, WT DT40's and Btk KO DT40's were lysed using 1X RIPA before subjected to SDS-PAGE with western blotting to blot for PLC γ 2, Tec, Btk. Tubulin was using as a loading control. (B) Quantification was performed using Imagequant. Statistical significance was calculated using a two-way ANOVA with a Tukey's post-test. Graph represents mean \pm SEM, n=3. Significance was taken at *p \leq 0.05, **p \leq 0.01.

4.3.2 WT DT40 cells express Btk and PLC γ 2 when assessed using microscopy, whereas Btk deficient cells only express PLC γ 2.

After verifying that the antibody is suitable to assess the levels of Btk in western blotting, its use in immunofluorescence was then tested. Another anti-Btk antibody in raised in a different host for future microscopy experiments was also assessed.

To investigate the specificity of the antibodies, of Btk and PLC γ 2, WT and Btk KO cells were adhered to poly-L-lysine-coated glass before fixation, permeabilisation and immunostaining with an anti-Btk antibody, an anti-PLC γ 2 antibody or IgG control. Samples were imaged using a Nikon A1R fluorescence confocal microscope.

In line with the previous reports, Btk KO cells do not express Btk and this further provides verification of the antibody used in later chapters for microscopy as being specific to Btk as no signal can be seen in these cells. Figure 4.3.2.A shows that WT DT40 cells express abundant amounts of Btk and Btk appears to localise to the perimeter in the cell. This observation is consistent as to what is observed in the work by Tomlinson and colleagues. Furthermore, consistent with the western blotting, both WT and Btk deficient DT40s express PLC γ 2 when analysed using microscopy, albeit to a lesser extent than Btk. This may be due to poor performance of the antibody or due to reduced expression of PLC γ 2 in these cells.



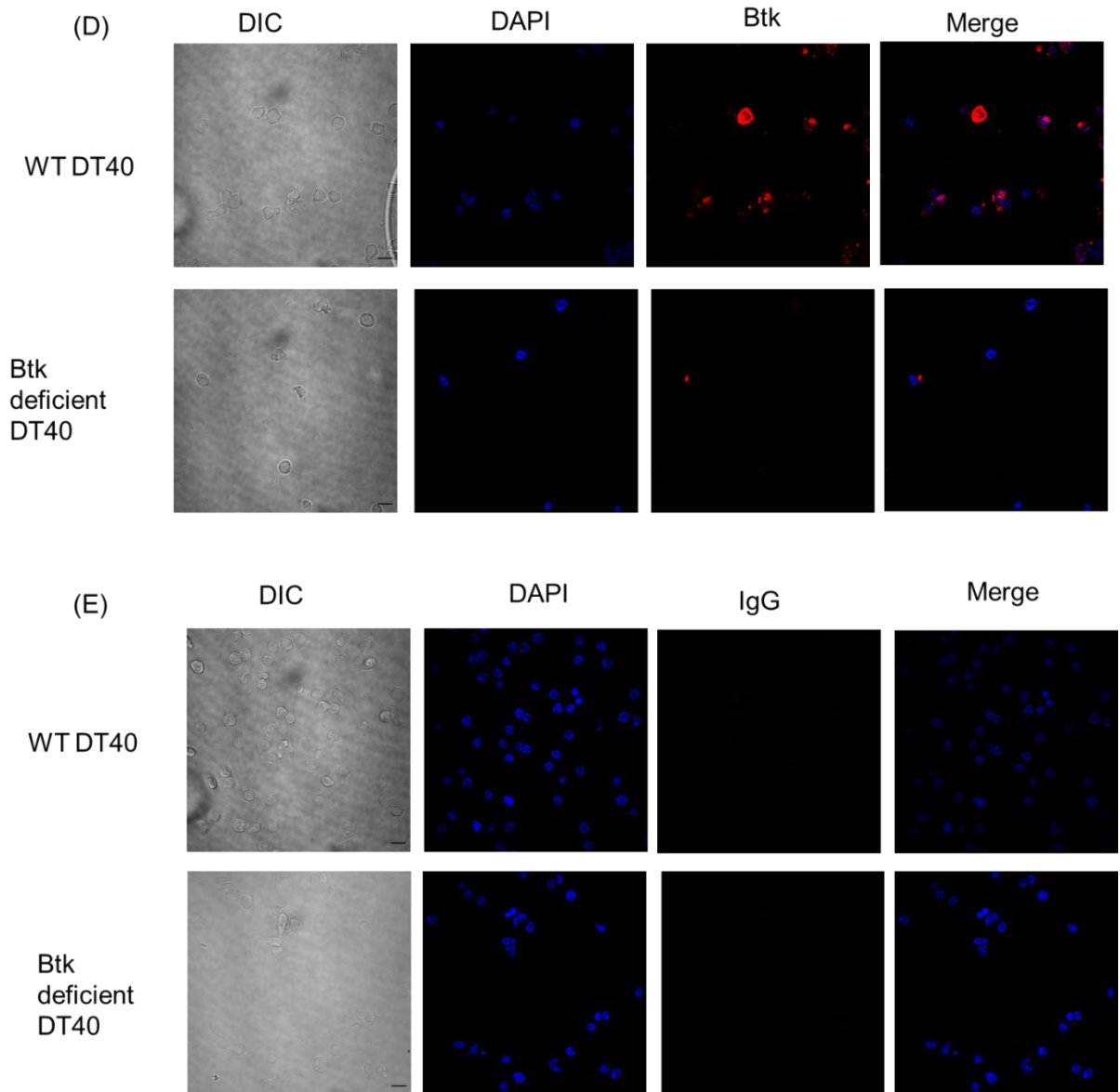


Figure 4.3.2 WT DT40's express Btk and PLCy2

WT DT40's and Btk KO DT40's were allowed to adhere to poly-L-Lysine before being fixed and permeabilised. Cells were stained with (A) rabbit anti-Btk, (B) rabbit IgG control, (C) rabbit anti-PLCy2, (D) goat anti-Btk or (E) Goat IgG. Samples were stained with secondary antibody Alexa Fluor 647 conjugated donkey anti-rabbit or Alexa Fluor 647 conjugated Donkey anti goat and imaged on Nikon A1R fluorescence confocal microscope.

4.3.3 Btk does not require a functional kinase domain to signal downstream of GPVI.

As mentioned above, B cell receptor signalling does not appear to require the kinase function of Btk in some experiments (Table 4.1.1). We performed similar experiments to identify whether the kinase function was required for GPVI or CLEC-2 signalling.

Kinase dead (KD) Btk has a point mutation at position 430, the ATP binding site (Vihinen et al., 1994b) which leads to a change from a lysine to a glutamic acid (Mahajan et al., 1995) – K430E. The change from a basic side chain amino acid to an acidic amino acid prevents ATP binding and this renders the kinase catalytically inactive (Mahajan et al., 1995, Tomlinson et al., 2001).

WT and mutant Btk sequences were created previously and supplied in the pApuroll plasmid by Dr Mike Tomlinson. Samples were maxi prepped and WT and mutant Btk sequences were verified using Sanger sequencing (Eurofins genomics). The change in amino acid at site K430 to E can be visualised in Figure 4.3.3. Primers used for sequencing are listed in Table 4.3.1.

Btk-deficient DT40 cells were transfected with WT or KD Btk, NFAT-luciferase and the appropriate receptors or empty vector controls. Cells were incubated for 6 hours in the presence or absence of collagen (10µg/mL), followed by lysis and an assay for luminescence (Figure 4.3.4). Btk-deficient cells transfected with GPVI, FcRγ chain and NFAT-luciferase plasmids did not induce signalling when stimulated with collagen (data not shown). Cells were also stimulated with PMA and Ionomycin for 6 hours to verify transfection of the NFAT-luciferase construct (data not shown).

Cells deficient in GPVI but transfected with WT Btk were unresponsive to collagen. Compared to the basal controls, a clear increase in signalling can be seen following collagen stimulation in the presence of WT Btk. KD Btk also allows signalling by GPVI, at a level statistically similar to WT Btk. This suggests the kinase function of Btk may not be required.

The level of WT and KD Btk expressed in the Btk deficient cells was analysed by SDS PAGE followed by western blotting. Both the WT and KD Btk were expressed at equal levels when the same amount of plasmid DNA was transfected into the cells (Figure 4.3.4.B). Flow cytometry was also performed to assess the levels of GPVI on the surface to verify any differences in level of signalling was not related to receptor expression level. 20 hours post transfection, cells were washed and stained with anti-GPVI antibody, 1G5 before washing and then secondary staining with Alexa Fluor 488 goat anti-mouse antibody. Figure 4.3.4.C shows that there is no significant difference between the levels of the receptor between the two Btk constructs and therefore differing levels of signalling are related to the kinase function of Btk.

Table 4.3.1 Primers used to sequence Btk plasmids with point mutations in this chapter

| DNA | Forward sequencing primer |
|-----------|----------------------------|
| K430E | AAGCACCTGTTTCAG CACCATC |
| W124F | GAGGAGTCTAGTGA AATGGAA |
| R307K | ATGTATGAGTGGTAT TCC |
| WW251/2LL | AGGTCGTGGCCCTT TATGATT |

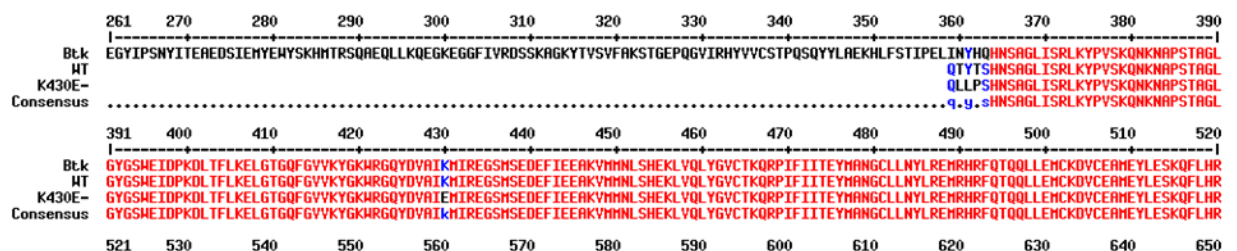


Figure 4.3.3 K430E plasmid has the mutation

K430E Plasmid was sequenced using primers listed in Table 4.3.1 using Sanger sequencing (Eurofins tubeseq sequencing service). The appropriate mutation was 179

confirmed by translating DNA into protein using EMBI EMBOSS Transeq (Rice et al., 2000), and using Mutlialign (Corpet, 1988) to check the mutation is the correct position for K430E.

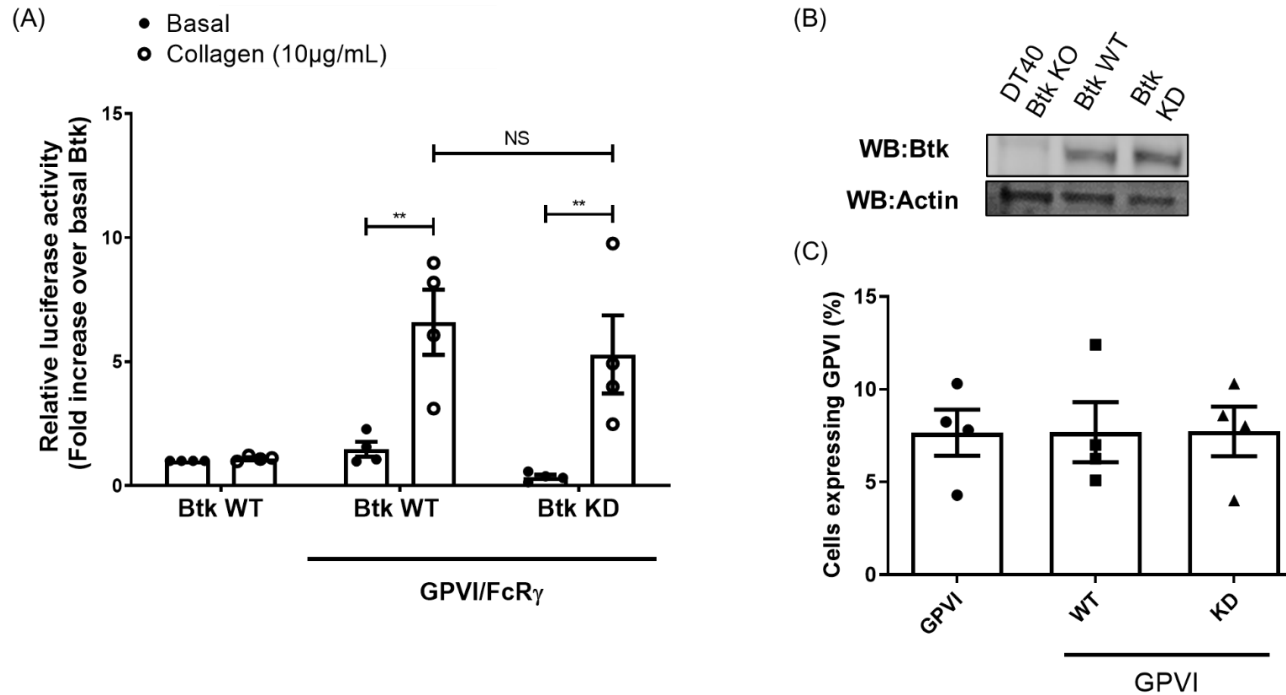


Figure 4.3.4 Kinase dead Btk is sufficient for GPVI signaling

(A) Btk deficient DT40 cells were transfected with GPVI, its binding partner FcR γ and NFAT-luciferase plasmids. These cells were also transfected with either wild type (WT) or kinase dead (KD) Btk. Transfected cells were then stimulated with the GPVI agonist collagen (10 µg/mL). Luciferase activity was compared using Two-way ANOVA with a Dunnett's multiple comparisons post-test. **p ≤ 0.01. Graph represents mean ± SEM, n=4. (B) Representative western blot showing equal Btk expression in WT and KD transfected cells. (C) Post transfection as described in (A) Cells were washed and stained with 1G5 anti-GPVI antibody (10µg/mL) followed by secondary staining with goat anti-mouse Alexa Fluor 488 (1/500) and washing antibody to assess receptor levels post transfection using flow cytometry.

4.3.4 Btk requires a functional kinase domain to signal downstream of CLEC-2

As shown in Figure 4.3.4, a functional kinase domain is not required to mediate signalling downstream of GPVI/FcR γ , an ITAM containing receptor. To investigate if an active Btk kinase domain is required for platelet hemITAM signalling the same experiment was carried out using CLEC-2.

Btk deficient DT40 cells were transfected with the WT or KD Btk, NFAT-luciferase plasmids and the CLEC-2 plasmid or empty vector controls as previously described. Cells were stimulated for 6 hours in the presence of basal medium or rhodocytin (50nM) before lysis and luminescence assayed (Figure 4.3.5.A). Btk deficient cells transfected with receptor and NFAT-luciferase alone did not induce signalling when stimulated with rhodocytin (data not shown), consistent with the work of Fuller et al., 2007. Flow cytometry was used to confirm equal expression of CLEC-2 and western blotting was used to show equal expression of WT and KD Btk constructs. Cells were also stimulated with PMA and Ionomycin for 6 hours to verify transfection of the NFAT-luciferase construct (data not shown).

Cells deficient in Btk or which do not express CLEC-2 were unresponsive to rhodocytin. WT Btk allows signalling downstream of CLEC-2 (Figure 4.3.5.A) when compared to basal controls (transfected receptor and WT Btk, but no stimulation with agonist), with relative luciferase activity being significantly increased for the rhodocytin treated cells (** $p \leq 0.001$). Kinase dead Btk does not induce signalling downstream of CLEC-2 when compared to basal treated cells. When compared to WT Btk + CLEC-2 and stimulated with rhodocytin there is a statistically significant reduction in the amount of signalling (** $p \leq 0.001$). This shows that in a cell line model, CLEC-2 signalling requires a functional Btk kinase domain.

The level of Btk expressed in the cells post transfection was assessed by cell lysis, SDS PAGE and western blotting. Both the WT and KD Btk were expressed at equal levels

when the same amount of WT and KD plasmid DNA was transfected in (Figure 4.3.5.B). Flow cytometry was also performed to assess the levels of CLEC-2 receptor. Post transfection, cells were washed and stained with anti-CLEC-2 antibody, AYP1 before washing and then secondary staining with anti-mouse Alexa Fluor 488 antibody. Figure 4.3.5.C shows that there is no significant difference between the levels of the receptor between the two Btk constructs and therefore differing levels of signalling are related to the kinase function of Btk.

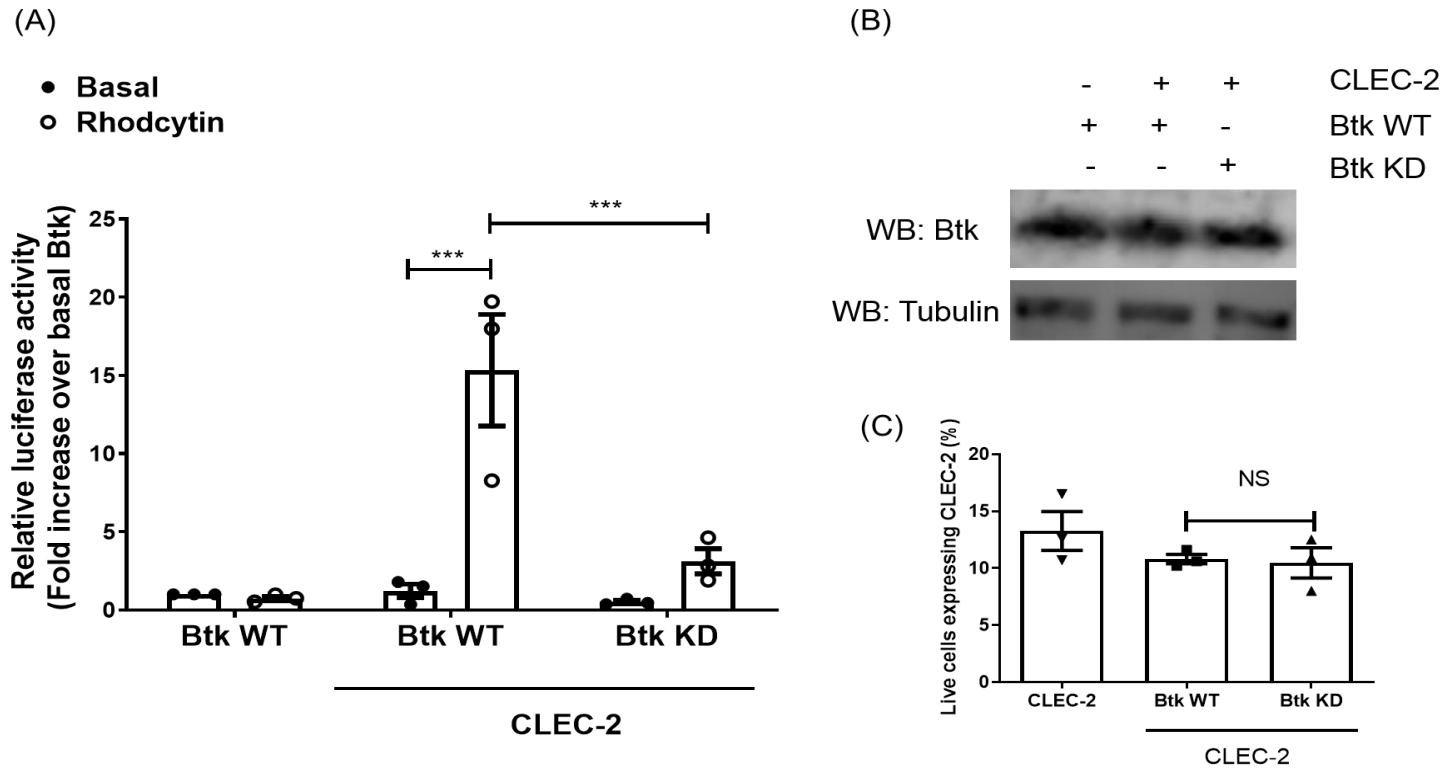


Figure 4.3.5 The kinase domain of Btk is required for CLEC-2 signalling

(A) Btk deficient DT40 cells were transfected with CLEC-2 and NFAT-luciferase plasmids and either wild type (WT) or kinase dead (KD) Btk. Transfected cells were then stimulated with the CLEC-2 agonist rhodocytin (50nM). (A) Luciferase activity was compared using Two-way ANOVA with a Dunnett's multiple comparisons post-test. *** $p \leq 0.001$. Results shown are mean \pm SEM, $n=3$. (B) Representative western blot

showing equal Btk expression in WT and KD transfected cells. (C) Cells were stained were washed and stained in AYP1 (10 μ g/mL) anti-CLEC-2 antibody and anti-mouse Alexa Fluor 488 secondary antibody to assess receptor levels post transfection.

4.3.5 Ibrutinib and acalabrutinib do not inhibit GPVI mediated signalling.

Ibrutinib and acalabrutinib are inhibitors of the kinase domain of Btk (Byrd et al., 2016, Byrd et al., 2013). We hypothesise that ibrutinib and acalabrutinib will render WT Btk kinase dead, verifying previous results (Figure 4.3.4). As cells with Btk KD already have no kinase function, if any further inhibition of signalling is observed in these cells, it may suggest alternative kinases are also being targeted by the drug; DT40s also express other potential ibrutinib targets, namely Fyn, Lyn and Syk (Watanabe et al., 2001, Takata et al., 1995, Takata and Kurosaki, 1996).

Btk deficient DT40 cells were transfected with WT Btk or KD Btk, as well as GPVI/FcR γ and NFAT luciferase plasmids as described in Section 4.3.3. Ibrutinib and acalabrutinib were incubated with the cells and collagen agonist for 6 hours. Unlike the experiments above, serum free media was used to ensure that the drugs do not become protein bound (Scheers et al., 2015).

High concentrations of ibrutinib (10 μ M) significantly inhibited signalling downstream of GPVI with both WT and KD Btk (** $p \leq 0.01$). Similar reductions in relative luciferase activity were observed in kinase dead Btk transfected cells compared with vehicle treated cells, with ibrutinib treated values similar to basal responses (Figure 4.3.6.A). There was no difference in the signalling when the lower concentrations of ibrutinib were compared to vehicle for both the WT and KD versions of Btk. When unstimulated cells containing WT Btk were compared to lower concentrations of ibrutinib and collagen, 5 μ M and 0.5 μ M ibrutinib treated cells did elicit signalling when stimulated with collagen (* $p \leq 0.05$ and ** $p \leq 0.01$). This provides further evidence that Btk can signal independently of its kinase function downstream of GPVI. The inhibition seen with high concentrations of ibrutinib is likely mediated through off target effects on SFK's (chapter 3) (Bye et al., 2017, Patel et al., 2016, Series et al., 2019).

In contrast to ibrutinib, acalabrutinib did not significantly inhibit NFAT signalling downstream of GPVI in WT and KD transfected cells even at high concentrations (Figure 4.3.6.B). WT Btk transfected cells stimulated with collagen in the presence of 10 μ M and 5 μ M or vehicle control acalabrutinib signalled approximately twice more than basal samples (* $p \leq 0.05$), further providing evidence that Btk can signal independently of its kinase function. In the kinase dead Btk transfected cells, vehicle treated cells had a greater relative luciferase activity compared to basal (** $p \leq 0.01$), as previously seen (Figure 4.3.3).

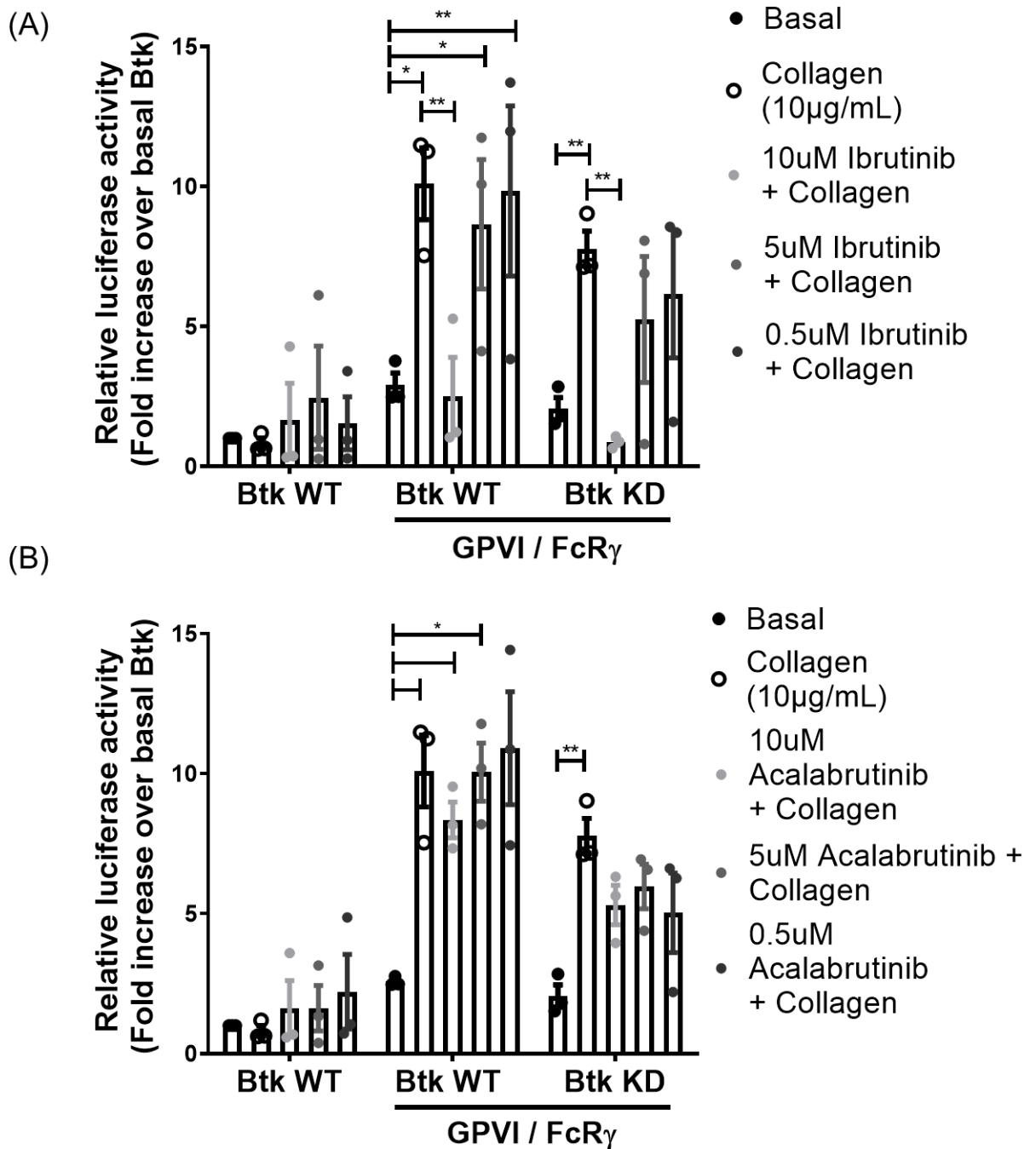


Figure 4.3.6 A high concentration of ibrutinib inhibits GPVI signalling whereas acalabrutinib does not in a cell line model

(A) Btk deficient DT40 cells were transfected with GPVI, its binding partner FcR γ and NFAT-luciferase plasmids. These cells were also transfected with either wild type (WT) or kinase dead (KD) Btk. Transfected cells were then stimulated with the GPVI agonist collagen (10 μ g/mL) in the presence of ibrutinib, acalabrutinib (10 μ M- 0.5 μ M), or vehicle control (0.1% (v/v) DMSO) for 6 hours. Luciferase activity was compared using two-way

ANOVA with a Tukey's post-test. Results shown are mean \pm SEM of 3 independent experiments.

4.3.6 Ibrutinib and acalabrutinib inhibit signalling downstream of CLEC-2

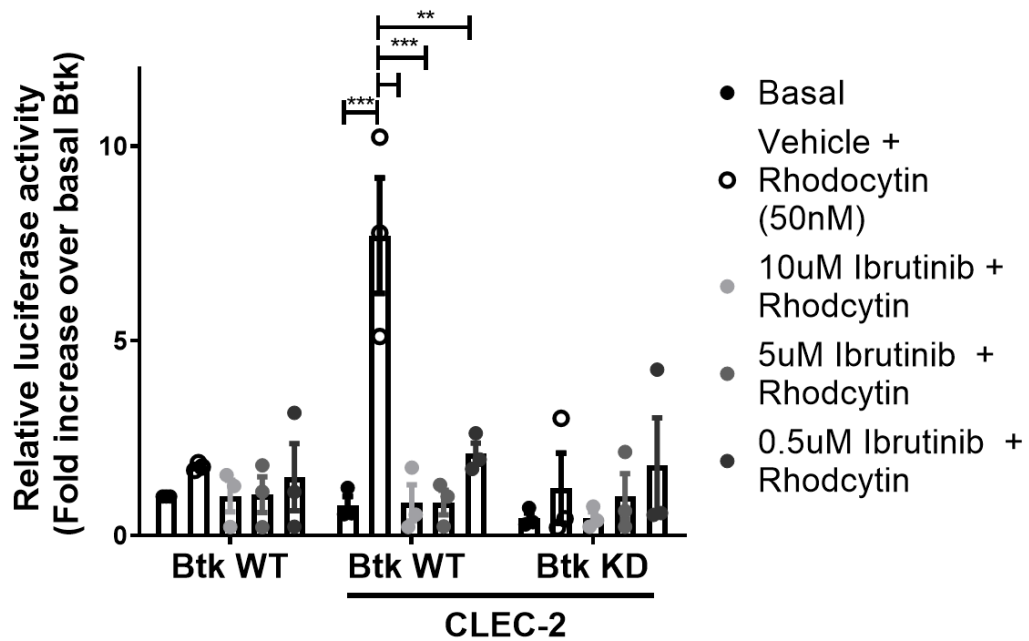
Previous experiments using a kinase dead version of Btk suggested that catalytic activity is required to mediate signalling downstream of CLEC-2 (Figure 4.3.4). Ibrutinib and acalabrutinib were used to inhibit catalytic activity of Btk to verify these previously obtained results were not an artefact of an overexpression model.

Experiments were performed as described above, but with CLEC-2 (replacing GPVI/FcR γ) or empty vector was transfected into the cells. Cells were treated the same as Section 4.3.5 except for the stimulation was performed with 50nM rhodocytin as opposed to collagen.

Downstream of CLEC-2, WT signalling was significantly increased when compared to basal controls, as expected. When treated with either Btk inhibitor, WT signalling was significantly reduced compared to vehicle control for both ibrutinib (10-0.5 μ M) ($p \leq 0.001$ and $p \leq 0.01$) (Figure 5C) and acalabrutinib (10 – 5 μ M) ($p \leq 0.01$) (Figure 4.3.7). The lowest concentration of acalabrutinib did not significantly inhibit signalling in WT cells.

There were no significant changes downstream of CLEC-2 for kinase dead Btk as vehicle treated cells do not signal when compared to basal treatment (Figure 4.3.7). This further verifies that Btk cannot induce signalling downstream of CLEC-2 without a functional kinase domain.

(A)



(B)

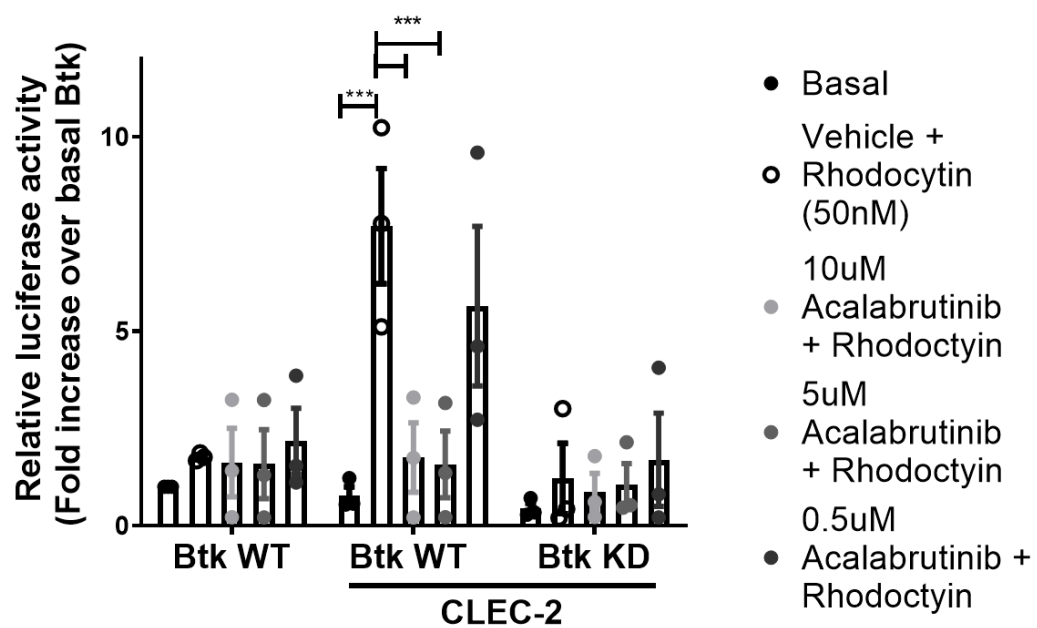


Figure 4.3.7 Ibrutinib and acalabrutinib inhibit CLEC-2 signalling in a cell line model

Cells were transfected as above and stimulated with the CLEC-2 agonist rhodocytin (50nM) in the presence of ibrutinib, acalabrutinib (10µM- 0.5µM), or vehicle control (0.1% (v/v) DMSO) for 6 hours. Luciferase activity was compared using two-way ANOVA with a Tukey's post-test. Results shown are mean ± SEM of 3 independent experiments.

4.3.7 The PH, SH3 and SH2 domain of Btk are required to mediate signalling downstream of GPVI.

As a functional kinase domain of Btk is not required to mediate signalling downstream of GPVI, experiments were performed to identify which other functional Btk domains are needed. It has been identified Tec needs both the PH and SH2 domain function to mediate signalling, but signalling could occur in a non-functional SH3 mutant (Tomlinson et al., 2004b). Therefore, it was hypothesised that like Tec, Btk requires its SH2 and PH domain activity to mediate signalling, but not its SH3 domain.

Each domain was rendered non-functional using a point mutation. The phenylalanine substitution of a tryptophan at position 124 (W124F) induces a non-functional PH domain, which is no longer able to bind inositol phosphates (Figure 4.3.8.A). There is a double tryptophan residue within the SH3 domain that when switched to leucine (WW251/2LL) renders this domain inactive (Figure 4.3.8.B). This domain is no longer able to bind proline rich regions. At site 307, there is an arginine in WT Btk SH2 domain. To render the SH2 domain non-functional, and therefore unable to bind phosphotyrosines, a mutation from arginine to lysine is introduced (R307K) (Takata and Kurosaki, 1996), (Figure 4.3.8.C). These Btk mutations were provided in a plasmid from Dr Mike Tomlinson, and sequencing was performed using the primers listed in Table 4.3.1.

Cells transfected with WT Btk, signal downstream of GPVI as shown above, when compared to basal treated cells. Cells that were transfected with any of the other domain mutants failed to signal downstream of GPVI when compared to basal (Figure 4.3.9.A). Furthermore, there was a significant inhibition of signalling compared to WT collagen treated cells ($p \leq 0.001$).

To verify that the lack of signalling was not down to differences in the level of protein expression, cells were lysed and protein expression was assessed by western blotting. Levels of the PH* and the SH3* mutant are similar. The SH2* mutant does not express as well as the others (Figure 4.3.9.B).

Taken together, these results suggest that to mediate signalling downstream of GPVI, aside from the kinase domain, all the other domains of Btk are required.

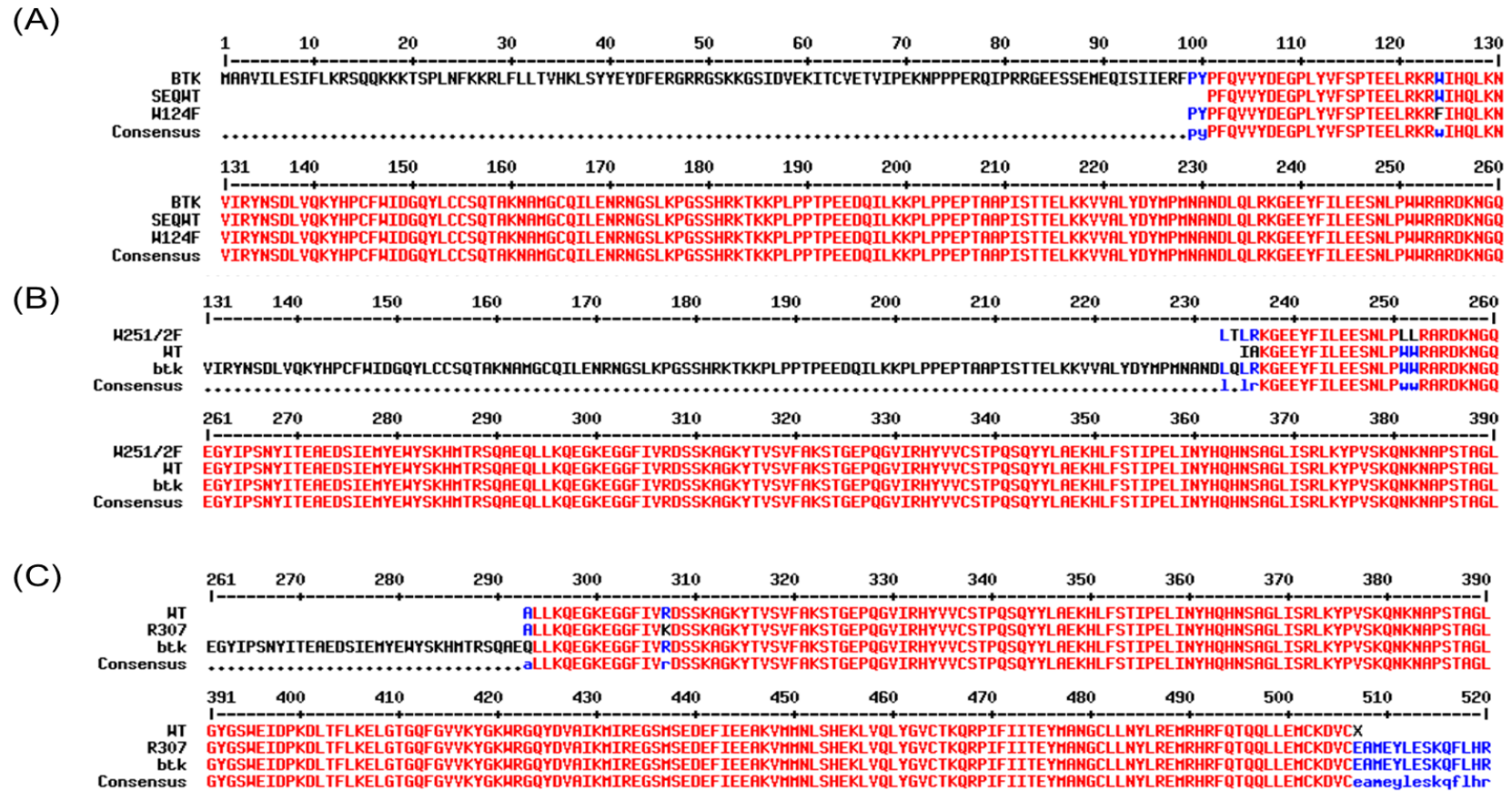


Figure 4.3.8 PH, SH3 and SH2 domain mutant plasmids have the mutation expected

(A) W124F, (B) WW251/2LL and (C) R307k plasmids were sequenced using primers listed in Table what using Sanger sequencing (Eurofins tubeseq sequencing service). The appropriate mutation was confirmed by translating DNA into protein using EMBI EMBOSS Transeq (Rice et al., 2000), and using Mutlialign (Corpet, 1988).

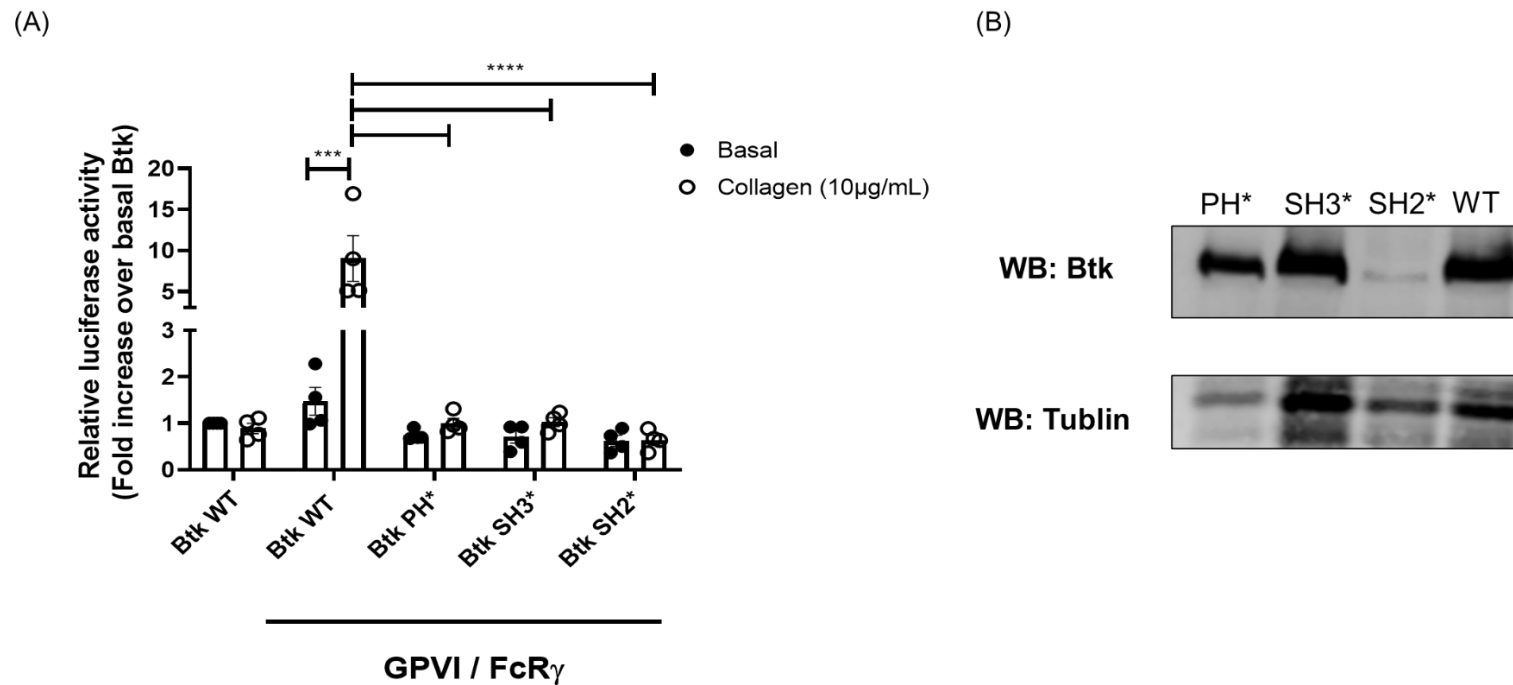


Figure 4.3.9 The PH, SH3 and SH2 domains of Btk are required to mediate GPVI signalling

(A) Btk deficient DT40 cells were transfected with GPVI, FcR γ chain and NFAT-luciferase plasmids. These cells were also transfected with either wild type (WT), PH (PH*), SH3 (SH3*) or SH2 (SH2*) domain inactivating mutants. Btk transfected cells were then stimulated with the GPVI agonist collagen (10 μ g/mL). Luciferase activity was compared using Two-way ANOVA with a Dunnett's multiple comparisons post-test.

, * $p \leq 0.001$. Results shown are mean \pm SEM, n=4. (B) Representative western blot showing reduced expression of the SH2 domain mutant of Btk.

4.3.8 The PH, SH3 and SH2 domain of Btk are required to mediate signalling downstream of CLEC-2.

As WT and KD Btk downstream of GPVI could mediate signalling, and all other functional domains were required (Figure 4.3.4 and Figure 4.3.9), this was also investigated downstream of CLEC-2. The kinase domain is absolutely required to mediate signalling, and therefore it was hypothesised that not all other functional domains may be required.

Experiments were performed as previously described except for CLEC-2 being transfected as opposed to GPVI and its binding partner FcR γ chain. As seen previously, WT Btk in the absence of receptor did not induce signalling. When CLEC-2 is co-transfected with WT Btk, there is a large increase of signalling compared to basal ($p \leq 0.001$). As seen with GPVI, none of the non-functional domain mutants induced signalling when compared to its own basal value. Furthermore, there is a significant decrease in the amount of signalling observed between the WT and different domain mutants when transfected in with CLEC-2 and stimulated with rhodocytin. This suggests that the PH, SH3 and SH2 domains are required to mediate CLEC-2 signalling (Figure 4.3.10).

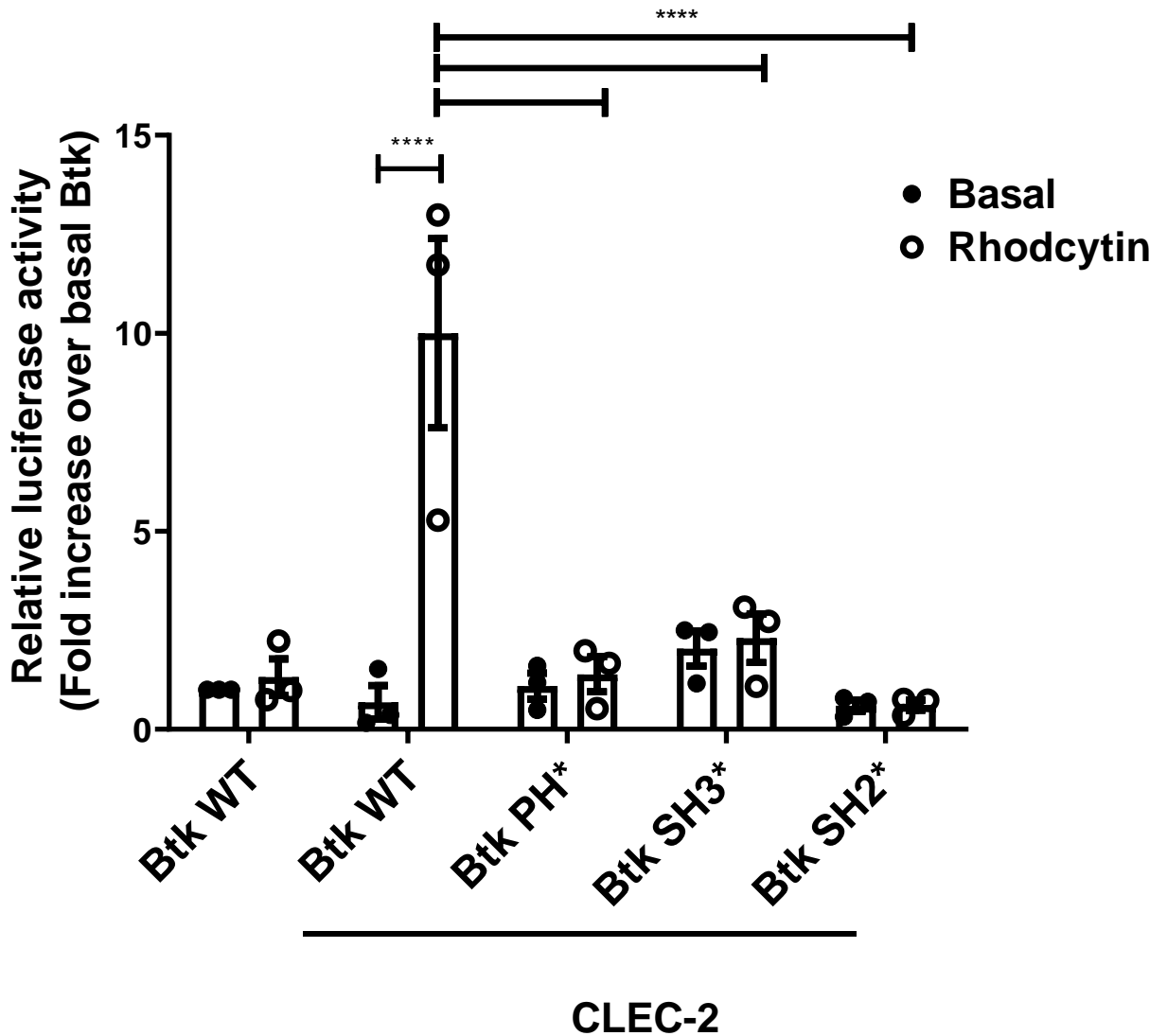


Figure 4.3.10 The PH, SH3 and SH2 domains of Btk are required to mediate CLEC-2
 (A) Btk deficient DT40 cells were transfected with CLEC-2 and NFAT-luciferase plasmids. These cells were also transfected with either wild type (WT) or PH (PH*), SH3 (SH3*) or SH2 (SH2*) domain inactivating mutants. Btk transfected cells were then stimulated with the CLEC-2 agonist rhodocytin (50 nM). Luciferase activity was compared using Two-way ANOVA with a Dunnett's multiple comparisons post-test. **** $p \leq 0.001$. Results shown are mean \pm SEM of three independent experiments.

4.3.9 Generation of a Btk deficient DT40 cell line using CRISPR-Cas9 gene editing

As the previous cell line work involved the overexpression of Btk in Btk deficient DT40 cells, CRISPR-Cas9 genome editing was used to ensure the signalling observed is not due to overexpression of the protein. It also eliminated the requirement of a KO cell line and transfection of Btk back into the cells. Although DT40's have been genetically modified using homologous recombination to create knockout cell lines (Takata and Kurosaki, 1996, Takata et al., 1995, Kurosaki et al., 1994, Takata et al., 1994), there is limited published research using CRISPR-Cas9 technology with DT40 cells (Abu-Bonsrah et al., 2016, Wang et al., 2019a, Costello et al., 2019). Prior to the use of CRISPR-Cas9 to introduce point mutations into Btk, CRISPR-Cas9 was used to generate a Btk KO as a proof of concept and validate the Btk KO generated by Takata and Kurosaki (Takata and Kurosaki, 1996).

Figure 4.3.11.A shows the design of the knockout guide RNA's. Deskgen software was used to select a target (Hough et al., 2016). Targets were selected based on the lowest off-target effects, which is calculated using the Hsu algorithm (Hsu et al., 2013). If guides had an equal off-target effects, the guide with the increased activity was selected. Activity is defined as how likely the Cas9 nuclease is to induce double strand breaks when paired with the guide (Doench et al., 2016). As multiple transcripts were listed for Btk – exon 3 was the first exon to have a consensus sequence, therefore guides were targeted there. For knockouts, guides are selected for early exons as the double stranded break (DSB) will be repaired by (non-homologous end joining) NHEJ causing an indel (insertion–deletion mutations). This will result in a frameshift leading to a premature stop codon. Most likely, this will lead to no protein being translated, however if the protein is still able to be translated it will likely be non-functional and very short as the sequence is stopped prematurely.

Guides are purchased as single stranded oligonucleotides termed SHN01, SHN02 up to SHN06 and were targeted to exon 3 and designed by adding compatible BpiI overhangs (5'CACCG, 3'CAAA) as displayed in Figure 4.3.11. The guides are annealed together and phosphorylated using T4 polynucleotide kinase using the thermocycling conditions shown in 4.3.11.B

Once annealed together the guide oligos are cloned in the host plasmid pspCas9(BB)-2A-Puro (Ran et al., 2013) (Figure 4.3.11.C), which was digested overnight using BpiI before running on 1% agarose gel to confirm that the vector has been linearised (Figure 4.3.11.D) before gel extraction. The host plasmid also contains antibiotic resistance for cells (puromycin) and *E. coli* (ampicillin) and the Cas9 protein (shown in purple in the plasmid).

Guide RNA's and host plasmid were annealed overnight before transformation into DH5 α *E. coli*. Positive colonies were selected and sequenced using the U6 forward primer to ensure the guide RNA's had been inserted as shown in Figure 4.3.12. These plasmids were termed SHN0102 and SHN0304. Guides were designed for SHN0506 but after sequence verification of multiple colonies, the guide was not present and therefore this plasmid was no longer used.

According to the previous study where DT40 cells were genome engineered using CRISPR-Cas9 (Abu-Bonsrah et al., 2016), 30 μ g of each respective SHN plasmid was transfected into WT DT40 cells. Also, in line with the previous study, conditions for transfection were slightly different than the overexpression experiments due to the large amount of DNA being transfected – conditions were 300kV, 900 μ F.

Cells were stably selected using puromycin, where cells with the integrated plasmid gained exhibiting resistance to this ribosome-inhibiting antibiotic, were expanded from single colonies. Initial selection was performed in 96-well plates with complete media supplemented with 2 μ g/mL puromycin, for approximately 1-2 weeks. If a single colony

was present, cells were expanded slowly (from a 24 well plate to a 6 well plate over approximately 2 weeks) until they could be sampled for protein expression.

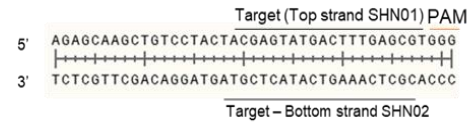
Lysates were made as previously described and samples were subjected to SDS-PAGE and western blotting for Btk. As Figure 4.3.13.A shows, guides SHN0102 and SHN0304 resulted in a knockout of Btk.

To verify the knockout behaved similarly to previous knockouts, the NFAT-luciferase assay was employed. SHN0102 clone 16 was transfected with 5 μ g of WT Btk or empty vector control, along with NFAT and the GPVI/FcR γ constructs as previously described. Cells transfected with GPVI and FcR γ chain and empty vector control did not signal downstream of GPVI, consistent with previous KO results (Section 4.3.3). When the cells are transfected with WT Btk in addition to GPVI and FcR γ , signalling does occur downstream of GPVI (4.3.13.B). This suggests that the cells were not damaged during the protein knockout process as it is known that CRISPR-Cas9 guides can have off target effects (Doench et al., 2016, Ran et al., 2013).

(A) *Gallus gallus* - Btk 202 locus



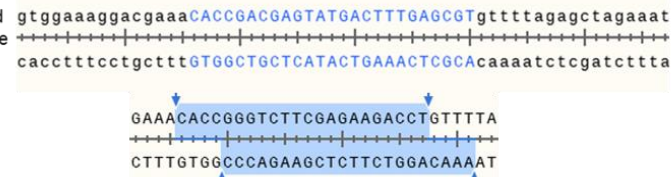
Target with least off target effects selected from Exon 1.



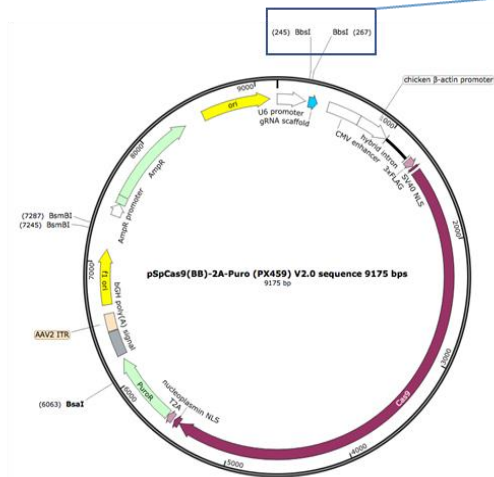
Bpil overhangs added to enable ligation into digested PspCas9-Puro.



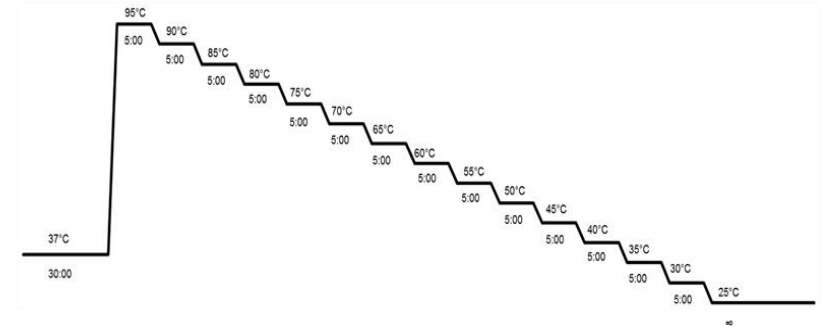
Single oligos are annealed and phosphorylated together before ligation into PspCas9-Puro.



(C)



(B)



(D)

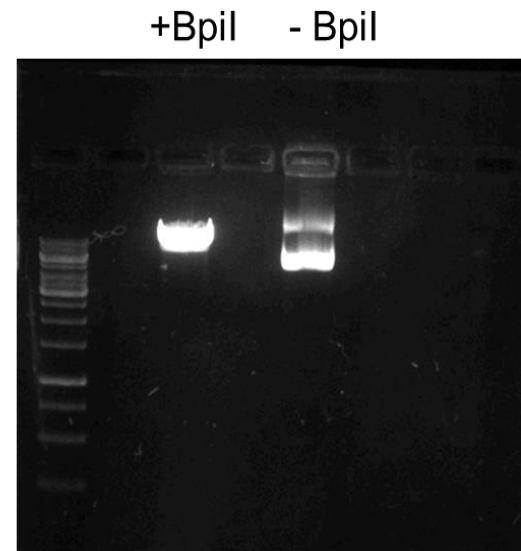


Figure 4.3.11 The CRISPR-Cas9 design strategy to create a Btk knockout

Guides used to create a Btk knockout cell line were selected using Deskgen (Hough et al., 2016), and guides with the least off target effects were selected. (A) The first common exon across all variants was targeted to have the shortest chance of target effects despite their activity. BpiL overhangs were manually added to the oligos to ligate into the plasmid as shown in (C). (B) Oligos were annealed and phosphorylated using the thermocycling conditions, using T4 Polynucleotide Kinase (PNK). (C) pSp-Cas9(BB) plasmid has the BpiL site highlighted as to where the restriction enzyme will cut. (D) 1µg of plasmid shown in was digested with Bpil overnight at 37°C before running on a 1% agarose gel to confirm complete linearization.

(A)

| Guide | Forward oligonucleotide | PAM | Exon | Activity | Off Target |
|-------|----------------------------|-----|------|----------|------------|
| SHN01 | 5'ACGAGTATGACT TTGAGCGT | GGG | 3 | 61 | 98 |
| SHN03 | 5'CGAGTATGACTT TGAGCGTG | GGG | 3 | 61 | 98 |
| SHN05 | 5'TACGAGTATGAC TTTGAGCG | TGG | 3 | 58 | 96 |



Figure 4.3.12 The cloning of the selected guides into the plasmid and verification by sequencing that the insert is present.

The guides were selected based on their least off target effects, with all off target effects being above 80. Guides were cloned into psp-Cas9 as described above before being confirmed with sequencing. The results confirm the guide is present in the plasmid.

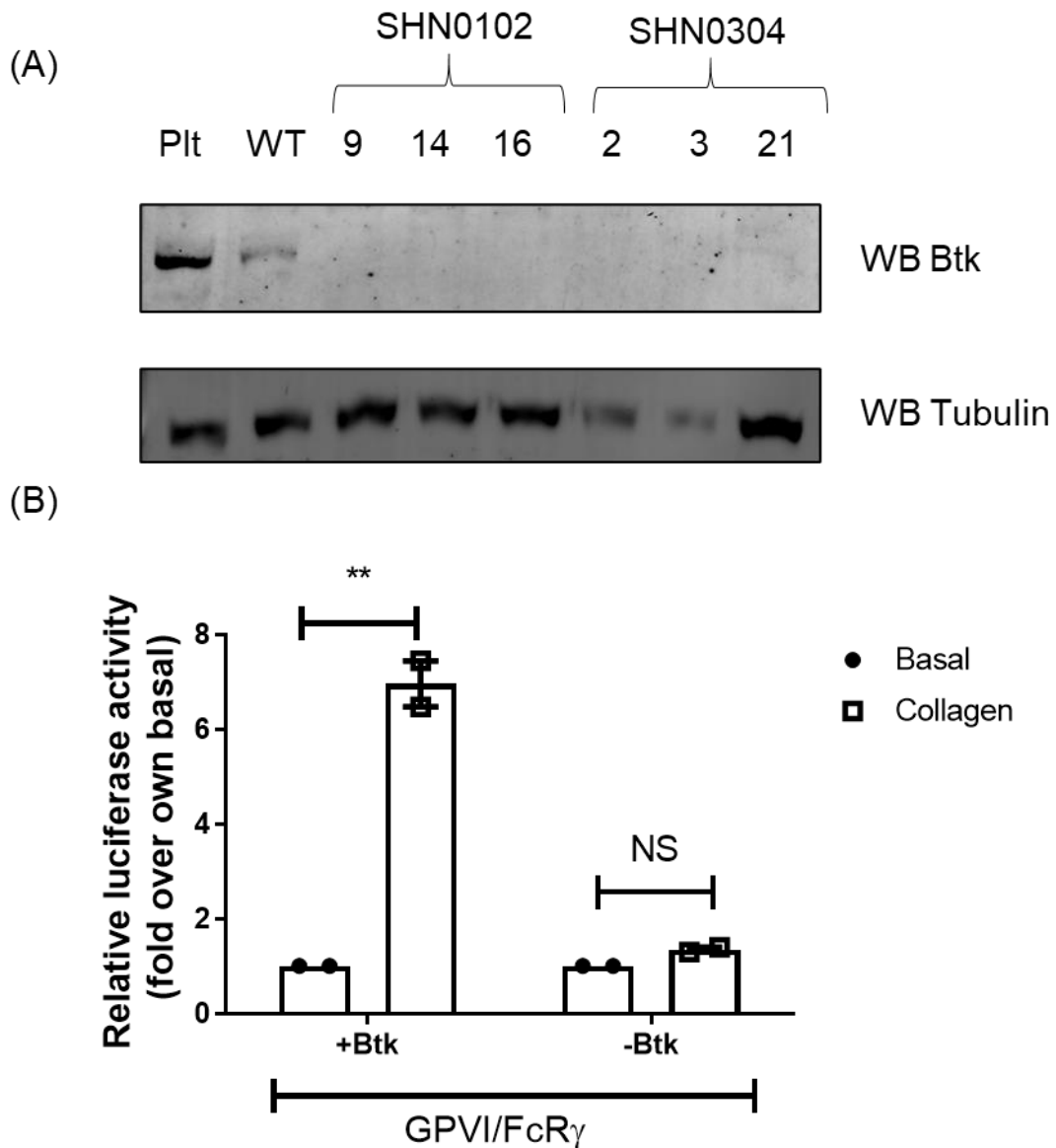


Figure 4.3.13 CRISPR-Cas9 can be utilised to generate Btk knockouts in DT40 cells and these knockouts behave as other Btk KO's.

(A) Stable cell mutants were lysed using 1x RIPA buffer and protease inhibitors before being subjected to western blotting. SHN0102 and SHN0304 guides produced knockout mutants when assessed for Btk. (B) SHN0102 clone number 16 was transfected with 5 μ g of WT Btk or empty vector control, along with NFAT and the GPVI/FcR γ constructs as previous. Cells were then stimulated with the GPVI agonist collagen (10 μ g/mL) or PMA and Ionomycin for 6 hours. Luciferase activity was compared using Two-way ANOVA with a Dunnett's multiple comparisons post-test. **p \leq 0.01. Results shown are mean \pm SEM of two independent experiments.

4.3.10 *Btk* gene is evolutionary conserved and sites for function altering CRISPR-Cas9 knockin mutations are present in Chicken *Btk*.

Previous experiments performed in this study and in the literature use overexpression of protein to investigate the role of Btk's domains in cell signalling. Overexpression of protein can change the mechanism of cell signalling orchestrated by that protein for a variety of reasons (Moriya, 2015). Overexpression of a protein may alter normal protein:protein interactions therefore it may not be able to interact with its proposed partner. Using CRISPR-Cas9 gene editing involves the introduction of mutations into the protein without intentionally changing the expression levels. The protein expression remains under the control of the endogenous promoter. However, some changes to expression level may still be possible due to protein instability. This may result in a lower expression, but the protein is not being continually expressed as it would be in an expression plasmid.

To induce function altering point mutations in each of Btk's domains using CRISPR-Cas9 knockins, sequences from multiple species were aligned. This was to confirm that the function altering mutations previously used in Sections 4.3.3 to 4.3.8 (W124F, WW251/2LL, R307K, and K430E) are also present in chicken Btk. This allowed for the appropriate sites to be selected for designing of guide RNAs.

Btk protein sequences from a range of species were aligned using T-coffee (Notredame et al., 2000) and presented with ESPrit 3 (Robert and Gouet, 2014) to assess similarity between the sequences (Figure 4.3.14). Simple Module Architecture Research Tool (SMART) software was utilised to identify the location of each Btk domain (Letunic et al., 2015).

Btk is largely conserved across the species, with some minor differences between chicken (*Gallus gallus*) and Zebrafish (*Danio rerio*), such as a large area missing within the pleckstrin homology domain of Zebrafish. The key regulatory Btk tyrosine phosphorylation sites, Y223 and Y551 are shown inside a black box, highlighting their

conservation. Another key site in Btk is C481, which is highlighted by an arrow. This is where Btk inhibitors such as ibrutinib and acalabrutinib bind, and once again this is evolutionary conserved (Covey et al., 2015). Interestingly, although this site is conserved, patients can become resistant to these drugs due to mutation of this C suggesting that although it is important due to it being conserved, alternative amino acids can be substituted at this site (Johnson et al., 2016, Woyach et al., 2017, Wist et al., 2020).

The sites of Btk function altering mutations previously used in above experiments (W124F, WW251/2LL, R307K and K430E) were generally found to also be conserved across species. WW251/2 is conserved in chicken, it is at WW249/250, due to slight length differences in the sequence between human, mouse, and chicken Btk.

Nonetheless, the sites were conserved across human, mice and chickens, therefore these sites were used as targets for CRISPR-Cas9 genome editing knock-ins.

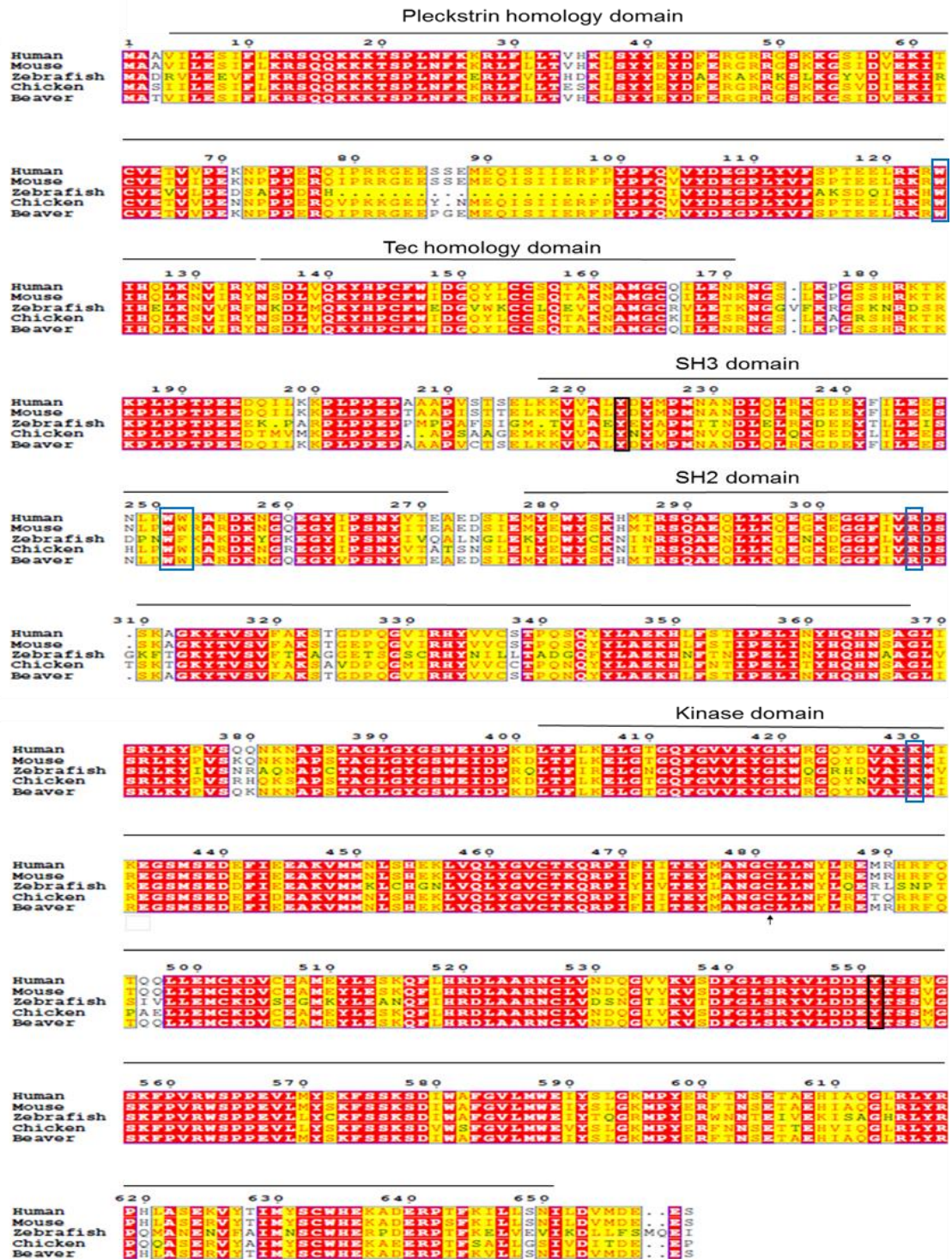


Figure 4.3.14 *Btk* is evolutionary conserved and CRISPR-Cas9 target sites are present in chicken *Btk*

Btk sequence alignment was analysed with T-Coffee and presented with ESPrit 3.

Domains were identified using SMART. Red areas are strict areas of common identity, areas in yellow are similarity of amino acids across groups. Blue boxes represent sites of

mutagenesis and black boxes are Btk phosphorylation sites. The arrow represents where ibrutinib and acalabrutinib bind to Btk.

4.3.11 Design of CRISPR-Cas9 donor sequence for function altering knockin mutations in Chicken *Btk*

After identifying the conserved targets of W124F, WW249/50LL, R307K and K430E through sequence alignment, guide RNA's and donor sequences as the repair template for homologous recombination for knock-ins were designed.

Deskgen software was used to generate the donor sequence with the changed DNA codons to cause a protein point mutation, such as changing from TGG (W) to TTC (F) (Table 4.3.2). A silent mutation was manually introduced to the donor sequence within the PAM site to destroy it. A silent mutation is when the nucleotide sequence of the DNA is altered but the amino acid sequence is not changed due to the redundancy of the triplet code. If the PAM site within the donor sequence is not mutated, the Cas9 protein will keep cutting the DNA resulting in a knockout. If the PAM site cannot be changed, the guide sequence can also be modified to prevent continuous cutting of the DNA. Furthermore, a silent mutation which created or destroyed a restriction enzyme site was introduced into the donor sequence. This was designed to enable a rapid method of screening mutants after DNA extraction and PCR amplification.

Guides were picked as close to the point mutation as possible, as the greater the distance between the DNA cut to the position of the mutation leads to a reduction in efficiency.

Guides were prepared as previously described (Section 4.3.9) and donor sequences were ordered from eurofins genomics and sequence verified. DH5 α *E. coli* were transformed with 1 μ L of donor sequence plasmid and subsequent colonies were maxi prepped.

A restriction enzyme digest was performed to verify that the plasmids contained the 300bp donor sequences prior to transfection. Digests were performed overnight with KpnI and BamHI-HF. Figure 4.3.15 shows that there is an insert of 300bp.

Table 4.3.2 Donor sequences for Btk CRISPR-Cas9 knockins

| Mutation | Guide, notes and Enzyme | Original donor sequence. | Mutated donor sequence. |
|-----------------------------------|--|---|--|
| W124F TGG->TTC | <u>GCAGAGGAGCTGCGCAAACGC</u> PAM is mutation site. BamHI can no longer cut and underlined section due to introduced mutation. | TCTGCGCTGGCTGCTTCGGGTGGCTGCAAGC CTCTGCTCTCCTATTCCCCTCTATGAGCCATG GCCCGGCGCTGAGCACGTTGTCTATAGGTGG TGTAACGATAGAGGGCCCTCTACGCTTCTCC CCGACAGAGGAGCTGCGCAAACGC <u>TGG</u> ATCC ATCAGCTGAAGAGTGGTGAAGTTTGGGGCAC CCAGCTGCGCGTGCGGCTGACTCAGAGCAT TGGTTTCCGGGGCTCGCTGCCTCGTGTT ACGATATCCATATCTGCGGAAGAGAGAGCTC TATCAGAAAGTGCTCCCA | TCTGCGCTGGCTGCTTCGGGTGGCTGCAA GCCTGTGCTCTCCTATTCCCCTCTATGAGCC ATGGCCCGGCGCTGAGCACGTTGTCTATAG GTGGTGTACGATAGAGGGCCCTCTACGTC TTCTCCCGACAGAGGAGCTGCGCAAACGC <u>C</u> <u>TTC</u> ATCCATCAGCTGAAGAGTGGTGAAGTTT TGGGGCACCCAGCTGCGCGTGCGGCTGTA CTCAGAGCATTGGTTTCCGGGGGCTCGCT GCCTCGTGTACGATATCCATATCTGCGG AAGAGAGAGCTCTATCAGAAAGTGCTCCCA |
| WW249/50LL TGGTGG -> TTGTTG | <u>TGGAGGAAAGCCACCTGCCT</u> PAM is mutation site. BsmAI can cut by changing TGA to AGA at underlined area. | ATGAAGCCCCTGCCCTGAGCCAGCCCCA GTGCAGCAGGTGAAATGAAGAAGTGGTGGC CCTGTACAATATGTGCCAATGAATGTCAGG ACCTGCAGTTCAGAAGGGTGAGGAGTACCT CATCTGAGGAAAGCCACCTGCCT <u>TGGTGG</u> AAAGCAGCTGACAAAAATGGGTAAGAACTCCC CGGTATCCATGGCATTACCCCTGCAGCCGTG CCTATCTCAGCATTGCTCCTGGGGCAGCCTCA GGGACCCACACCTGACACTGGGGAATCCCAG CTGTTCTCAGACTCTCA | ATGAAGCCCCTGCCCTGAGCCAGCCCCA CAGTGCAGCAGGTGAAATGAAGAAGTGGT GGCCCTGTACAATATGTGCCAATGAATGTC CAGGACCTGCAGTTCAGAAGGGTGAGGAA GTACCTCATCTGAGGAAAGCCACCTGCCT <u>TTC</u> <u>TTC</u> AAAGCAGCAGGACAAAAATGGGTTAA GAACCTCCCGCTATCCATGGCATTACCCCT GCAGCCGTGCTCCTATCTCAGCATTGCTCCT GGGGCAGCCTCAGGGACCCACACCTGACA CTGGGAATCCAGCTGTTCTCAGACTCTC A |
| R307K CGA->AAG | <u>GAGATTCTACCAGCAAGACA</u> PAM is 10BP away from mutation BsmAI can no longer cut at underlined area. | CAGGACTCCTTTCATTCACTGCAGCCTCTCCA GTATGCTGTGATTGTCCTCTTGCTGTAT GGTCACTTCTCACAAATACCCCTCCTATCTC CTCCTTTATTTTTTTCTTTTAGGGTAAGGAA GGGGGCTTCATTGTT <u>CGA</u> GATTCTACCAGCAA <u>GACA</u> GGGAAATACACTGCTCTGTTTATGCCA AGTCCGCTGTGAAGTGGATCTAAGAATAGCT TGTTGCTATCTCAGAGCACCCCTCCAGGCACC TCTACTCTGCTTGCCTTCCCAAGCTGCT GACCCCATGC | CAGGACTCCTTTCATTCACTGCAGCCTCTC CAGTCACTGTGATTGTCCTCTTGCTGTAT TATGGTCACTTCTCACAAATACCCCTCCTAT CTCCTCTTTTATTTTTTTCTTTTAGGGTAA GGAAAGGGGGCTTCATTGTT <u>AA</u> GATTCTAC <u>CAGCAAGACA</u> GGTAAATACACTGTTTCTGTT TATGCCAAGTCCGCTGTGAAGTGGATCTAA GAATAGCTTGTGCTATCTCAGAGCACCCCT CCAGGCACCTCACTCTGCTTGCCTT CCCAAGCTGCTGACCCCATGC |
| K430E AAG -> GAA | <u>GGAGGGATCCATGTCAG</u> PAM 5bp away –Changing of the TCC to TCT (underlined) within the guide ensures the PAM site did not need to be changed as the guide covers where the point mutation is. BamHI should have cut but changing the PAM prevents cutting. PAM site is on the bottom strand. | GGCACCTGCACCCTCATCACACTCACACTCTC TGTCTAGGGTCTGGGAGATTGACCCGAAG GACCTGACCTTCTGAAGGAAGTGGGGACAG GGCAGTTTGGCGTAGTGAAGTACGGGAAATG GAGAGGCCAATACAACGTTGCCATC <u>AA</u> GATGA TCAG <u>GGAGGGATCCATGTCAG</u> AAAGACGAGTT TATTGATGAAGCCAAAGTCATGATGTAAGTGGT GAGCAGCCCCAGGTGAGTGCAGCATATATCT TGTGAGAAATACCTGCACCTCCAGATGTTTGG AGGGACAGCATCAGG | GGCACCTGCACCCTCATCACACTCACACTCTC TCTGTCTAGGGTCTGGGAGATTGACCCG AAGGACCTGACCTTCTGAAGGAAGTGGGG ACAGGGCAGTTTGGCGTAGTGAAGTACGGG AAATGAGAGGGCCAATACAACGTTGCCATC <u>GA</u> ATGATCAGGGAGGGATCTATGTCAGAA <u>G</u> ACGAGTTTATTGATGAAGCCAAAGTCATGA TGTAAGTGGTGAAGCAGCCCCAGGTGAGT CAGCATATCTTGTGAGAAATACCTGCACCT CCAGATGTTTGGAGGGACAGCATCAGG |

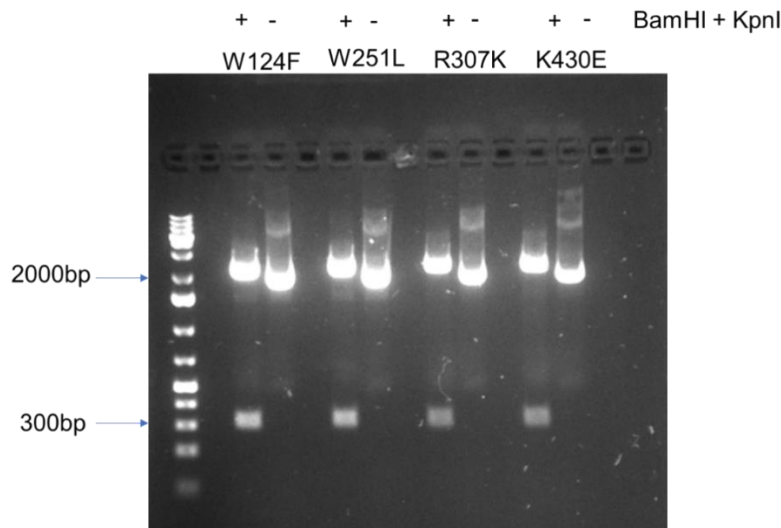


Figure 4.3.15 Donor plasmids contain the designed 300bp insert

Plasmid DNA was digested overnight at 37°C with BamHI and KpnI before being run on a 1% agarose gel stained with Sybrsafe. Images were taken on transilluminator (Syngene, Cambridge UK).

4.3.12 CRISPR-Cas9 did not induce function altering knock-ins in the Btk PH, SH3 pr kinase domain.

For the initial knock-in experiments, DT40 cells were transfected with 15µg guide RNA plasmid, and 15µg of circular donor plasmid. All the stable cell colonies resulted in a Btk protein knockout. This is likely due to the transfection with a circularised donor plasmid which may fail to integrate into the cell as efficiently (Liu et al., 2018). The next approach was to linearize the donor plasmid in order to increase the efficiency of homology directed repair (Ran et al., 2013), as circular plasmids may be broken at random points within the plasmid in order to become integrated (Song and Stieger, 2017). This random breaking of plasmid may be in the area of the donor sequence and therefore disrupt the HDR.

Donor plasmid was linearized with EcoRI-HF. DT40 cells were transfected with 15µg guide and 15µg linearized donor sequence. Subsequent plating out and stable clone selection was as previously described (Section 4.3.9).

As Table 4.3.3 demonstrates, K430E and WW251/2LL knock-in experiments did not yield any stable cell colonies. The R307K KI strategy produced 11 potential mutant clones. Additionally, the PH domain mutation, W124F did also produce 3 potential mutant clones. Western blotting was performed to identify the presence of Btk before further analysis. These samples were analysed alongside a WT DT40 lysate, a platelet lysate and a Btk KO DT40 lysate to act as positive and negative controls, respectively.

Figure 4.3.16 A+B shows that R307K KI strategy produced Btk knockouts with no Btk protein expression visible using western blotting in 9/11 cell lines (Figure A, B and data not shown). Only 3 stable cell line mutants were obtained in the time frame for W124F mutants with protein expression being undetectable by western blot (Figure 4.3.17.A). Mutants R307K 1D and 1H expressed full length Btk but to a lesser extent compared to WT cells. These clonal cell lines were taken forward and used in the NFAT luciferase assay to assess if they can mediate signalling and sequenced to verify the mutation.

Table 4.3.3 The number of viable cell colonies post stable selection

| Guide | Number of stable cell colonies post transfection with linearised DNA | Number of cell colonies that had Btk expressed when assessed by Western Blot. |
|-----------|--|---|
| W124F | 3 | 0 |
| WW251/2LL | 0 | 0 |
| R307K | 11 | 2 |
| K430E | 0 | 0 |

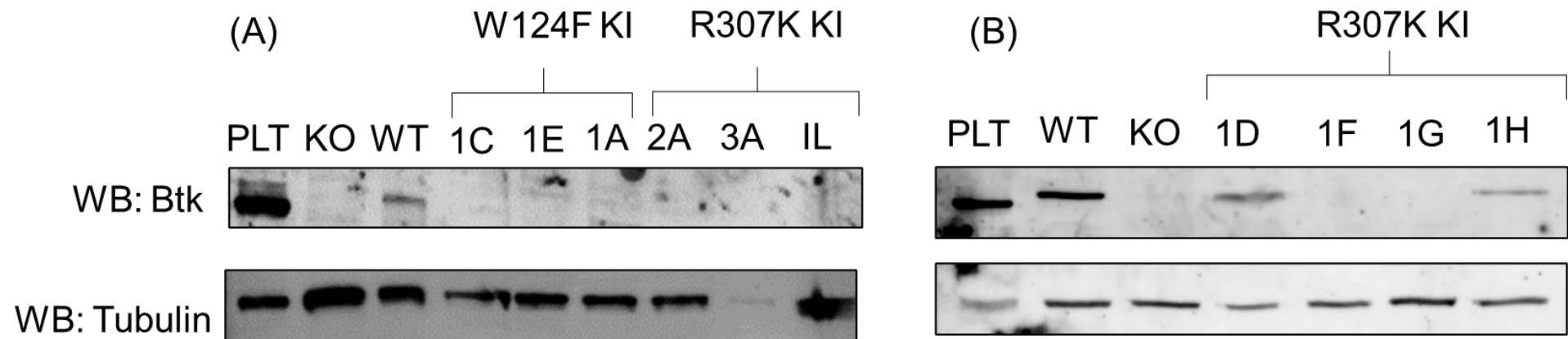


Figure 4.3.16 Expression of Btk post transfection with CRISPR-CAS9 R307K plasmids

Lysates from single cell colonies were made by washing cells 1x in PBS before lysis in 1x RIPA buffer of a cell count of 1×10^7 cells. Cells were lysed for over 30 minutes before 6X SB was added and lysates boiled for 5 minutes before subjection to SDS-PAGE and western blotting with anti-Btk

antibody. Anti-Tubulin antibody was used as a loading control. Lysates of colonies of cells that were transfected with plasmids to induce knockins of (A) W124F or (A,B) R307K.

4.3.13 An amino acid deletion in the SH2 domain renders Btk unable to signal downstream of GPVI.

The intended CRISPR-Cas9 mutation was to substitute the amino acid arginine at position 307 to a lysine as described above. DNA was extracted from WT cells, and mutants 1D and 1H cells using alkaline lysis (Kambe, 2014, Laird et al., 1991).

Touchdown PCR was performed to amplify the mutated region of interest using primers (R307KFWD, 5' GTCACCTCCTCACAAATACCCC and R307KREV 5'

ATACAACGTAATGGCGGATCAT) and DNA electrophoresis was performed to confirm the band was at the correct size (286bp). After the PCR band was extracted using a gen elute gel extraction kit, the DNA was sequenced using the R307K FWD primer.

Sequencing was performed by Eurofins genomics.

The DNA sequencing results are presented in Figure 4.3.17.B, with the guide (labelled as guide) and the ordered donor (labelled as donor) sequence shown. The Black AAG in the donor sequence was the intended mutation, however, it was not present in the D or H cellular DNA. In D, 6 DNA bases were missing, and in H, 3 DNA bases were missing. The T in the donor Section was also the mutation of the PAM site which would have been a silent mutation, however that was also not integrated into the mutants' DNA.

When the resulting DNA is transcribed into amino acids, D is missing a serine and lysine, whereas in H, only the lysine is missing at sites homologous to human S310 and K311 respectively (Figure 4.3.17.C). As there is more published literature on the role of human Btk than Chicken Btk, the homologous sites in humans was first investigated in Btkbase (Väliäho et al., 2006, Vihinen et al., 1996). There were no published mutations within Btkbase for these domains (Väliäho et al., 2006, Vihinen et al., 1996).

Experiments were performed to identify whether if the SH2 domain mutations would cause a reduction or loss of signalling downstream of GPVI. NFAT-luciferase experiments were performed as previously described. Briefly, WT, D or H mutant cell lines were transfected with GPVI, FcR γ chain and NFAT or empty vector controls. As shown in

Figure 4.3.17.D, only WT DT40 cells transfected with GPVI and FcR γ chain were able to signal ($p \leq 0.001$) compared to its basal control. No signalling was observed in either of the R307 mutants compared to its own basal value. R307 mutant H did have a slight increase in signalling in the presence of receptor and collagen, (2.04 ± 0.9) however, this was not found to be statistically significant.

To verify the lack of signalling in the R307 mutants 1D and 1H cells was not due to differences in the surface expression levels of GPVI, flow cytometry analysis was used as previously described, (Section 4.3.3). All transfected cells displayed similar levels of GPVI at the cell surface, Figure 4.3.17.E. This demonstrates that the lack of signalling in the mutants is not related to lack of GPVI receptor.

To verify the process of CRISPR-Cas9 gene editing did not have any off-target effects and therefore explain the lack of observed signalling, experiments were performed by reconstituting Btk back into the cell. This would be expected to rescue the signalling downstream of GPVI.

H mutant cells and WT cells were transfected with GPVI and FcR γ and NFAT plasmids and 5 μ g of Btk or empty vector control. 5 μ g was selected as it was the amount previously utilised in the knockout experiments and it is known that this should induce a signal downstream of GPVI (Section 4.3.3). The NFAT luciferase assay was performed as previously described.

WT cells transfected with FcR γ and GPVI signal well when stimulated with collagen, with the empty vector not reducing this signalling. Also like previous experiments, H did not signal when stimulated with collagen, despite receptor being transfected in. In mutant cells that were also transfected with Btk, signaling was restored in the presence of collagen ($p \leq 0.05$) (4.3.17.F). Furthermore, this level of signalling was not significantly different to the amount of WT signalling observed. Increased expression of Btk was confirmed using western blotting to verify that Btk had been transfected back in (Figure 4.3.17.G).

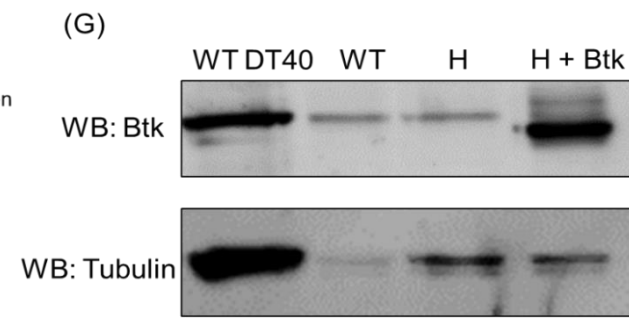
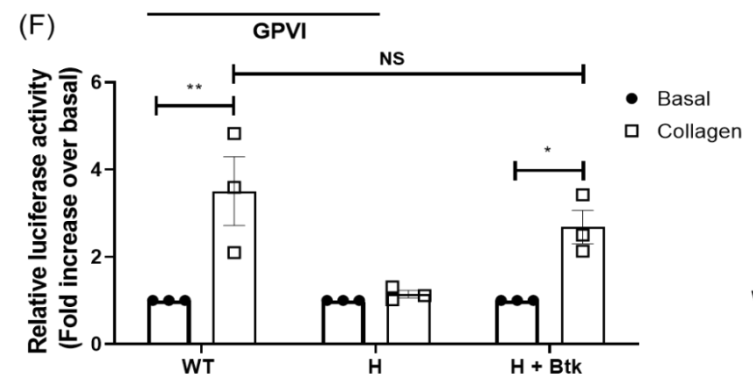
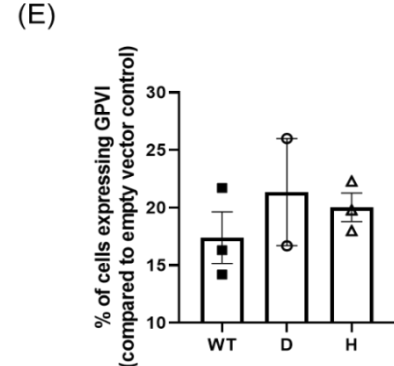
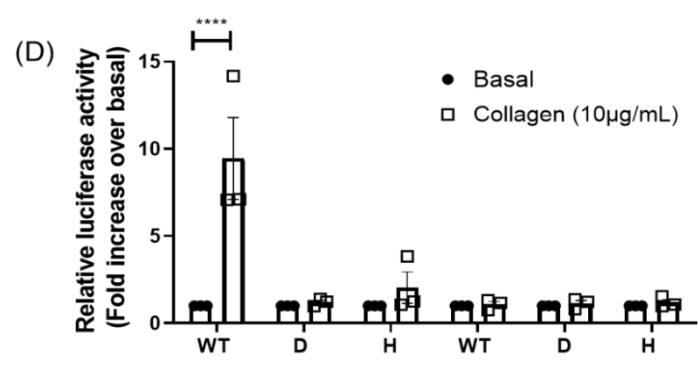
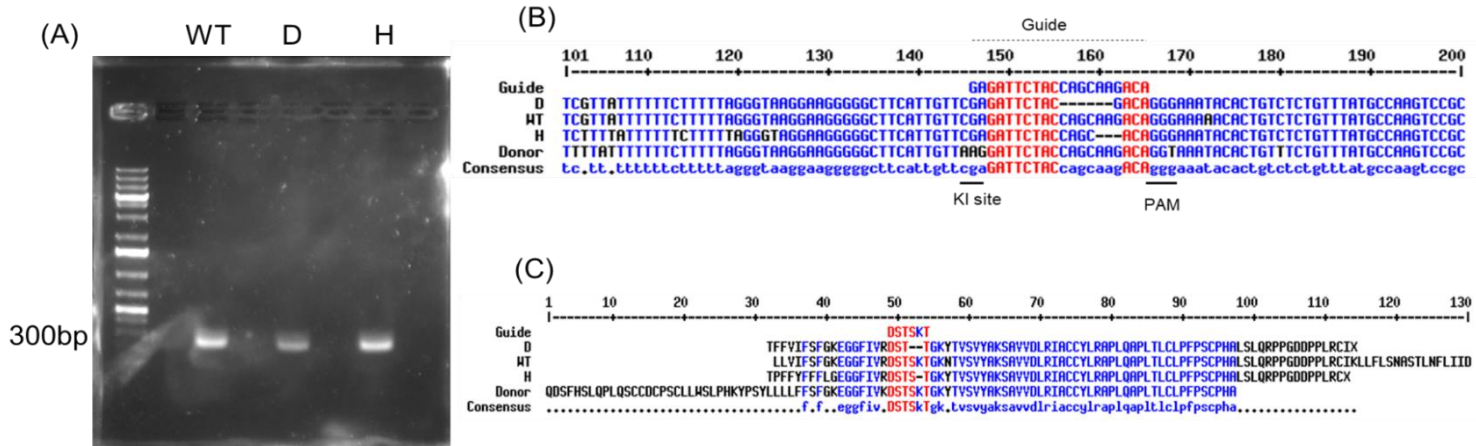


Figure 4.3.17 R307K KI strategy resulted in two amino acid deletions that render Btk inactive downstream of GPVI

(A) WT, D and H DNA was extracted using alkaline lysis and then touchdown PCR was performed using primers R307KFWD, 5' GTCACCTTCCTCACAAATACCCC and R307KREV 5' ATACAACGTAATGGCGGATCAT and resulting PCR was subjected to DNA electrophoresis. (B) Sequencing results of the PCR bands with the guide, D, H WT, and donor sequence of DNA present with the KI site, guide and PAM site labelled. (C) The transcribed protein sequence showing the absence of one or two amino acids in H or D, respectively. (D) SH2 domain CRISPR-Cas9 mutants (D, and H) were transfected with GPVI, FcR γ chain and NFAT-luciferase plasmids. Transfected cells were then stimulated with the GPVI agonist collagen (10 μ g/mL) or complete media (basal). Luciferase activity was compared using Two-way ANOVA with a Dunnett's multiple comparisons post-test. ****p \leq 0.001. Results shown are mean \pm SEM, n=3. (E) Surface GPVI levels were determined by staining transfected cells with 1G5 anti-GPVI antibody followed by secondary staining with Goat anti-mouse Alexa fluor 488. (F) WT cells and SH2 domain CRISPR-Cas9 mutant H were transfected with GPVI, FcR γ chain and NFAT-luciferase plasmids. Mutants H were also transfected with WT Btk (5 μ g) or empty vector control. Transfected cells were then stimulated with the GPVI agonist collagen (10 μ g/mL), complete media (basal) or PMA (50ng/mL) plus ionomycin (1 μ M). Luciferase activity was compared using Two-way ANOVA with a Dunnett's multiple comparisons post-test. ****p \leq 0.001. Results shown are mean \pm SEM, n=3. (G) Western blot of the cells post transfection to show increased expression of Btk after transfection of WT Btk into H cells.

4.4 Discussion

Using a cell line model for platelet signalling, the following aims were attempted to be addressed in this chapter.

4.4.1 Aim -To elucidate which domains of Btk are required to mediate NFAT-Luciferase signalling downstream of GPVI and CLEC-2 using an overexpression model

4.4.1.1 DT40'S as a model for platelet signalling

DT40 cells are a useful model to investigate platelet signalling. They are cost-effective and easy to culture, with growth being rapid therefore experiments can be performed at a sensible speed. Furthermore, unlike platelets they contain a nucleus, so they are genetically tractable. Despite being a B-cell line, they have strong similarities to platelets; they are suspension cells that can undergo spreading (Weber et al., 2008) and contain many of the proteins that are required in (hem)ITAM signalling (Kurosaki et al., 1994, Takata and Kurosaki, 1996, Takata et al., 1994).

There is some controversy whether DT40 cells express Tec. Tec is present in B cells and in some human B cell lines, but not all. In one paper, Tec is believed to be expressed in DT40 cells (Tomlinson et al., 2004b), whereas in another paper by the same authors Tec is not believed to be expressed in these cells (Tomlinson et al., 1999). Furthermore, evidence has emerged that in some leukemic cell lines (not DT40s) expression of Btk and Tec are inversely correlated with each other (de Bruijn et al., 2017).

The DT40 genome is published, however the genomic data is presented as scaffolds as opposed to whole genes. When Btk is searched, it is found as a scaffold with only one result and an E value of 0 which suggests it is present. Tec however similarly has a low E value but has some similar but not exact matches in the proteome. This may be due to the similarity of SH2 domains across different proteins. However, from the genomic data of this cell line it is also not clear that Tec is present in these cells.

In this research, Tec was undetectable in WT or Btk deficient DT40 cells using western blotting (Figure 4.3.1). This suggests that Tec is not expressed in the absence of Btk in these cells. Although these cells do not contain Tec like platelets (Figure 4.3.1), it does provide evidence that the signalling observed in later experiments is likely directly related to Btk and not compensation of Tec.

4.4.1.2 The use of the NFAT luciferase assay to measure intracellular signalling downstream of GPVI and CLEC-2

The NFAT- luciferase-reporter assay is a highly sensitive assay used to measure signalling when calcium flux may not be measurable following PLC γ 2 activation in DT40 cells (Tomlinson et al., 2007, Takata and Kurosaki, 1996, Tomlinson et al., 2001). The assay is a quantitative and relatively high throughput assay (i.e. 96-well plate format) after the cells have been transfected, allowing for multiple conditions to be tested at once, such as the treatment with ibrutinib and acalabrutinib observed in Figures 4.3.6 and 4.3.7.

Other positives to the assay are that unlike fluorescence-based assays, there is a low background level, due to the presence or absence of light. Furthermore, the chemistry of the experiment (ATP + H₂O -> Light) is relatively robust (Stecha et al., 2015). Failure of experiments tends to be at the transfection level such as the failure of receptor to be expressed on the surface of the cells, as opposed to the chemistry level. However, the use of the internal control, stimulation with PMA and ionomycin, which causes PKC activation and calcium flux, produces a large amount of light because of increased cell signalling when the cells are lysed. This ensures that the NFAT plasmid was successfully integrated into the cell, and low signalling values are not related to this and are related to the proteins mitigating the response.

Although useful, the NFAT-luciferase assay does miss some interesting mechanics of signalling. The assay is an endpoint assay, over a long period of time when compared to platelet signalling. It is known that the location of Btk changes upon cell activation, but the

speed and dynamics are unknown (Bobe et al., 2001, Kang et al., 2001, Várnai et al., 1999). As protein kinetics can have a valuable input to elucidating responses and roles, it would have been interesting to observe these experiments over a shorter time frame. The long-time frame is required to ensure proper transcription and translation of the luciferase plasmid before the cell assay is stopped by placing the assay plate at -80°C. An experiment with a shorter time frame, such as directly measuring Ca²⁺ flux may help to elucidate if the signalling can bypass Btk, for example, if PLCγ2 is independently recruited not via Btk. Although this is unlikely, as there is no signalling in the Btk deficient cells and receptor alone (Figure 4.3.11), so this suggests that signalling downstream of the hemITAM in this model requires Btk.

4.4.1.3 What domains of Btk are needed to mediate signalling?

In the Btk KO DT40 model of (hem)ITAM signalling, Btk is required. No NFAT-luciferase signalling is observed downstream of GPVI and CLEC-2 in its absence. This result is further confirmed by the CRISPR-Cas9 induced Btk KO's in Figure 4.3.11. Furthermore, reconstitution of WT Btk back into these cells restores the signalling between basal and collagen when the receptor is present. This suggests that Btk is required to mediate GPVI and CLEC-2 signalling in this cell line model.

The pioneering structural biology work by the Andreotti group, discovered how Btk becomes active at the membrane. The structure of Btk is in a folded compact formation, and the SH2 domain has an acidic latch keeping the kinase domain in its inactive confirmation (Agnew and Jura, 2017, Joseph et al., 2017). The PH-TH domain module also contributes to this inactive and closed structure, and in this formation, the PH-TH domains are blocking the catalytic active site.

Upon the production of phospholipids, where the PH-TH domains are recruited, the PH-TH modules can spontaneously dimerize – so the PH-TH modules of one molecule of Btk binds to another PH-TH of another Btk molecule, and the PIP3 makes it more stable. This then enables the phosphorylation of one Btk molecule to another, to render it catalytically active (Chung et al., 2019).

For this mechanism of action to occur, a functional SH2, PH-TH and kinase domain are required, which is consistent with the results obtained in this study for CLEC-2. The SH3 domain is required to keep the inactive conformation but to a lesser extent, but it does suggest all domains of Btk are required to become active. Therefore, function altering point mutations in each Btk domain in an overexpression model were used to investigate this.

4.4.1.4 The PH domain of Btk is required to mediate signalling downstream of GPVI and CLEC-2

Trp124 is conserved across PH domains of Tec family kinases (Smith et al., 2001) and is required for the interaction of the G β γ trimeric G proteins and phospholipids (Tsukada et al., 1994). The change of a tryptophan to phenylalanine renders this domain non-functional (Li et al., 1995). Although both amino acids are aromatic, tryptophan has more polarbilisility than phenylalanine and can therefore bind other amino acids better.

The recruitment of Btk to the signalosome is mediated by the PH domain of Btk in B cells (Fluckiger et al., 1998, Hyvönen and Saraste, 1997, Saito et al., 2001). Unsurprisingly, the results obtained in this study support this hypothesis as there is a lack of signalling observed in a function altering PH domain mutant.

Indeed, there has been little work published suggesting that Btk signalling is independent of its PH domain in B cells, supported by numerous studies which show that the PH domain of Btk is essential (Li et al., 1995, Tsukada et al., 1994).

The PH domain of Btk in mast cells and B cells can also interact with PKC (Johannes et al., 1999). A lack of NFAT signalling observed in these experiments (Sections 4.3.7 and 4.3.8) may be related to this. Downstream of PKC signalling is MAPK signalling, which results in the activation of the AP-1 proteins which are required for NFAT signalling. In fact, Phorbol 12-myristate 13-acetate is used as a positive control to directly activate PKC for signalling (Clipstone and Crabtree, 1992, Dolmetsch et al., 1997). There may be a

required interaction for Btk and PKC via its PH domain to mediate signalling in the NFAT luciferase model, and in the mutant, this is abolished. This may also contribute to the lack of signalling observed in Figures 4.3.8 and 4.3.9.

PH domain function has also been investigated indirectly in platelets and megakaryocytes. PIP3, produced by PI3K, is responsible for recruitment of Btk via its PH domain (Pasquet et al., 1999a, Laffargue et al., 1999, Bolland et al., 1998, Durrant et al., 2017). It has been shown that Btk recruitment to the membrane fraction is dependent on PIP3 production, as using PI3K inhibitors prevents translocation to the membrane fraction in GPVI (convulxin as an agonist) and CLEC-2 (rhodocytin as an agonist) stimulated platelets (Manne et al., 2015a). By preventing the interaction between PIP3 and Btk, which results in reduced or abolished aggregation, it shows an indirect role for the PH domain downstream of GPVI and CLEC-2. These results in platelets that the PH domain is required validate the Btk overexpression model and strengthen the results that a functional PH domain is required for (hem)ITAM signal transduction.

4.4.1.5 The SH3 domain of Btk is required to mediate signalling downstream of GPVI and CLEC-2.

The double mutation of aromatic amino acid tryptophan to leucine at site 251/2 renders the SH3 domain of Btk non-functional. Tryptophan is an aromatic amino acid, whereas leucine is an aliphatic amino acid (Hashimoto et al., 1999a). This change from aromatic to aliphatic alters the binding capacity of Btk's SH3 domain to proline rich regions.

A functional Btk SH3 domain is required to mediate signalling downstream of both CLEC-2 and GPVI (Figures 4.3.8 and 4.3.9). SH3 domains are responsible for mediating binding to proline rich regions, and it is believed that this is how Btk interacts with Lyn which is responsible for phosphorylation of Btk (Wahl et al., 1997). Btk needs to be phosphorylated to be catalytically active to mediate CLEC-2 signalling, therefore a functional SH3 domain is required (Figure 4.3.5). However, catalytically active Btk is not required to mediate

signalling downstream of GPVI (Figure 4.3.4). Therefore, it would not have been unreasonable to hypothesise that signalling would have been observed in the SH3 mutant downstream of GPVI, as it can act as a scaffold protein.

In contrast to the results obtained here, work by Tomlinson and colleagues involving the related family member, Tec, identified that a functional SH3 domain of Tec is not required to mediate NFAT luciferase signalling downstream of the TCR (Tomlinson et al., 2004b). There was signalling observed in Jurkat cells transfected with a SH3 domain inactive version of Tec and stimulated with an anti-TCR antibody. This is in direct contrast to this work, as the SH3 domain mutant of Btk did not induce signalling downstream of hemITAM receptors (Figures 4.3.8 and 4.3.9). There are discrepancies between the experiments. Firstly, although Btk and Tec are within the same family of kinases, they can play different roles within the same cell. In mature B cells, Btk is thought to mediate PLC γ 2 activation, whereas Tec is responsible for mediating Akt phosphorylation (de Bruijn et al., 2017), showing that the kinases can play different roles. Furthermore, the cell type used was different, as Jurkat cells were used as opposed to DT40's and finally, the receptor used was different. As shown in Sections 4.3.3 – 4.3.6, the kinase domain is not required downstream of GPVI, whereas it is downstream of CLEC-2, so there may be differences downstream of the TCR also.

The SH3 domain of Btk has also been proposed to be dispensable for PLC γ 2 phosphorylation in fibroblasts when cotransfected with Lyn. Deletion of this domain did not drastically alter the phosphorylation levels of PLC γ 2 in these cells when compared to WT Btk. This suggests that PLC γ 2 phosphorylation in fibroblasts is independent of the SH3 domain (Fluckiger et al., 1998). This is consistent with work using Tec by Tomlinson et al., but this finding is not consistent with the results obtained in this study. This may be related to the different cell models used.

However, there is evidence that this domain may be essential *in vivo*, as fewer mutations within the SH3 domain have been identified in XLA patients (Väliäho et al., 2006, Vihinen et al., 1996). There are more mutations within the other domains. This suggests that the

domain cannot tolerate mutations as well and it may be essential for normal B cell function. Further evidence is provided for this as this Section of Btk is highly conserved across species (Figure 4.3.14).

On the other hand, the reduced number of reported mutations within the SH3 domain could suggest that *in vivo* the domain does not participate in B cell signalling. If the SH3 domain is not involved in regulation of signalling in B cells, there would be antibodies produced, and therefore there would be no symptoms of the disease. Typically XLA is diagnosed upon presentation of frequent infections, and therefore if signalling is regulated as normal, there would be no infections (Mohamed et al., 1999, Pal Singh et al., 2018, Väliäho et al., 2006).

4.4.1.6 The SH2 domain of Btk is required to mediate signalling downstream of GPVI and CLEC-2

The SH2 mutation of arginine to lysine at position 307 causes loss of function of the SH2 domain of Btk (Li et al., 1995). This is due to the change in a positive polar side chain from arginine, to the negative polar side chain of lysine. The overall secondary structure is not changed by this mutation, however the function of binding to phosphotyrosines is lost (Mattsson et al., 2000).

As Figures 4.3.9 and 4.3.10 demonstrate, the Btk SH2 domain is required downstream of CLEC-2 and GPVI. However, this mutant does not express as well as the other two Btk mutants (Figure 4.3.9.B). This is consistent with data that this mutation of Btk does not express well in NIH 3T3 cells (Li et al., 1995). Mutations and deletions of the SH2 domain observed in XLA patients also affects Btk protein stability *in vivo* (Saffran et al., 1994).

These results were further confirmed using endogenous of Btk as the SH2 mutation was introduced using CRISPR-Cas9 gene editing. Like the over-expression model, the SH2 domain mutant expressed at a lower level compared to the endogenous WT protein

(Figure 4.3.9.B) and could not mediate signalling downstream of ITAM despite the presence of GPVI at the cell surface when assessed by flow cytometry.

It is unsurprising that this domain is required, as the SH2 domain of Btk has been proposed to interact with phosphotyrosine residues on BLNK (homologous to LAT in platelets) (Hashimoto et al., 1999a), and therefore for signalling to occur, it makes sense that the functional SH2 domain is required. A functional SH2 domain has also been shown to be required for PLC γ 2 phosphorylation in fibroblasts as there is a reduction in total PLC γ 2 phosphorylation after transfection with R307K Btk and Lyn when compared to WT Btk (Fluckiger et al., 1998), however it is not totally reduced to basal levels. This is consistent with the work of Takata and Kurosaki, 1996, as phosphorylation of PLC γ 2 is reduced but not abolished in B cells in this function altering point mutation (Takata and Kurosaki, 1996). This suggests that this domain plays a large but not total role in mediating PLC γ 2 phosphorylation as some residual phosphorylation remains.

4.4.1.7 The kinase function of Btk is required to mediate signalling downstream of CLEC-2 but not GPVI

Kinase dead (KD) Btk has a point mutation at 430 from a lysine to glutamic acid (Mahajan et al., 1995), which is the ATP binding site (Vihinen et al., 1994a). The change from a basic side chain amino acid to an acidic amino acid prevents ATP binding. This renders the kinase inactive (Vihinen et al., 1994a, Tomlinson et al., 2001, Fluckiger et al., 1998).

Btk does not require kinase function to induce calcium signalling downstream of GPVI in a cell line model (Figure 4.3.4). This observation is consistent with what has already been observed in B cells downstream of the B cell receptor (Tomlinson et al., 2001, Middendorp et al., 2003). Furthermore, there has been published data suggesting that PLC γ 2 does not require phosphorylation at a known Btk phosphorylation site, Y1217, to induce lipase activity (Kim et al., 2004). The finding that the Btk kinase domain is

dispensable for GPVI signalling was confirmed when the assay was performed in the presence of ibrutinib and acalabrutinib (Figure 4.3.6).

In the presence of ibrutinib, a less specific Btk inhibitor, only 10 μ M inhibited the NFAT luciferase signalling downstream of GPVI in WT and KD transfected cells ($p \leq 0.01$). NFAT signalling was not significantly different from vehicle treated cells at lower concentrations of ibrutinib. Acababrutinib did not inhibit signalling (Figure 4.3.6). The inhibition of signalling seen in cells treated with high concentrations of ibrutinib but not acalabrutinib is likely due to the selectivity of the inhibitors. Ibrutinib is known to have off target effects and can inhibit Src family kinases (Figure 3.3.7.F (Bye et al., 2017, Patel et al., 2016)), which are required for mediating signalling in GPVI/FcR γ chain transfected DT40 cell line (Mori et al., 2008).

In contrast, downstream of the hemITAM containing receptor CLEC-2, there is a requirement for a functional Btk kinase domain in a cell line model as shown in Figure 4.3.5. The use of ibrutinib and acalabrutinib in the assay also verifies this result (Figure 4.3.7). Previous work has also demonstrated that Btk requires its kinase function to mediate calcium signalling in Ramos cells downstream of the BCR (Fluckiger et al., 1998), and that Btk can phosphorylate PLC γ 2 *in vitro* (Watanabe et al., 2001). Therefore, CLEC-2 signalling requiring catalytic activity of Btk is not surprising.

4.4.2 Aim - To genetically modify Btk using CRISPR-Cas9 to generate mutants to verify overexpression experimental models.

4.4.2.1 CRISPR-Cas9 did not induce knock-ins for all the designed guides and donor sequences

For CRISPR-Cas9 KI experiments that had no colonies (K430E and WW251/2LL), new guides should be designed. No colonies were obtained which was unusual, as if

homologous directed repair does not occur, it is likely that NHEJ would occur, resulting in a protein knockout. It is likely that there was a failure of cutting by Cas9. This can occur if the Cas9 enzyme binds but does not release. The release of Cas9 initiates the DNA double strand break. Therefore failure of dissociation of Cas9 would not induce a DSB for the cell to initiate repair (Knight et al., 2015)

For the two guides that did yield colonies, with most cells being knockouts, there are multiple reasons to explain this. The efficiency of HDR in cells is very low, around 20% (Abu-Bonsrah et al., 2016), therefore it was not unexpected for protein KO to be induced in the majority of cases.

A method to try and rectify the failure of these experiments would be to optimise the donor template. The donor template used in these experiments had equal homology arms (150bp either side of the mutation). Literature has suggested that unequal homologous arms may be beneficial and favoured by the cell to introduce HDR (Richardson et al., 2016). The length of the homologous arms could also be changed, and as only one or two bases were being changed so altering the homology arm length may have improved efficiency (Liu et al., 2018)

Efficiency can be improved by linearizing the donor plasmid. The donor template was previously transfected in as a linearised and circular plasmid. To further improve efficiency, an alternate type of donor could be used. For example, some work has used single stranded oligonucleotides as the donor template for CRISPR with success (Jacobi et al., 2017). These could be commercially made, but they could also be PCR generated as dsDNA templates. However the latter has been suggested by Jacobi et al that these may be toxic (Jacobi et al., 2017).

4.4.2.2 CRISPR-Cas9 KI experiments resulted in amino acid deletions in the SH2 domain of Btk, which renders it inactive

After transfection and stable selection, two clones were obtained from CRISPR-Cas9 gene editing. The mutation was within the SH2 domain. The expression of Btk in these

cells was slightly lower than WT cells when the same number of cells were loaded (Figures 4.3.16 and 4.3.17). This is consistent as to what is observed in the overexpression model NFAT experiments (Figure 4.3.9) and as to what has been published (Li et al., 1995).

The deletion of either 3 or 6 bases (in mutants H and D respectively) suggests failure of HDR and by chance bases are deleted. Typically, deletion of bases via NHEJ results in a frameshift rendering the sequenced mismatched and therefore unstable (Ran et al., 2013). Whereas in mutants D and H, exactly the number of bases that fall with the triplet code have been deleted during the process of NHEJ, causing the deletion of two amino acids. Further proof that the mutants did not undergo HDR was that the silent mutation within the PAM site was not integrated into the DNA (Figure 4.3.17.B).

The two amino acids that have been deleted are Serine 310 and Lysine 311, near the start of the SH2 domain. S310 and K311 have not been identified as mutations in Btkbase (Väliäho et al., 2006). The S that is deleted (S310) is conserved in Src family kinases when aligned. It corresponds to S158 for Lyn, S178 for Fyn and S180 for Src. It has been proposed that mutation S178 in Fyn can contribute to rendering the SH2 domain inactive, but there were also other amino acid substitutions used to inactivate the SH2 domain in leukocytes (Bernardini et al., 2005).

Experiments performed to assess the function of the mutation in the SH2 domain was similar to those observed in the over-expression model, which suggests that function of the SH2 domain is lost (Figures 4.3.9.A and 4.3.17.D). This is consistent with previous literature in that Btk requires its SH2 domain to mediate a large proportion of the phosphorylation of PLC γ 2 in B cells, as in a function altering point mutation phosphorylation is reduced but not abolished (Takata and Kurosaki, 1996).

Of note, each one of the domains of Btk aside from the kinase domain, inhibits the signalling downstream of GPVI so it cannot be said for certain that this mutation has caused specific SH2 inactivity (Figure 4.3.17). The mutation may have caused an

irregular structure of Btk and it may be unable to unfold to become active in its correct confirmation (Chung et al., 2019, Wang et al., 2019b). Misfolded protein is typically degraded (Hanna et al., 2019) and therefore this may be related to the reduced expression of Btk in these mutants. To verify misfolded protein, modelling software such as Irtfold (McGuffin et al., 2019) could be used to compare the protein structures.

4.5 Conclusions

In a knockout and over expression DT40 cell line model of platelet signalling, all Btk domains are needed to reconstitute CLEC-2 mediated signalling. Whereas downstream of GPVI, Btk requires a functional PH, SH3 and SH2 domain whereas it can mediate signalling independently of its kinase activity. The ability of a kinase dead mutant Btk to reconstitute signalling downstream of GPVI suggest that Btk can act as a scaffold protein downstream of GPVI signalling, whereas it cannot downstream of CLEC-2. This highlights a novel difference between GPVI and CLEC-2 mediated signalling in the DT40 cell line model.

5 Total internal reflection fluorescence microscopy to identify the localisation of Btk in relation to GPVI, LAT and CLEC-2.

5.1 Introduction

5.1.1 The location of Btk in platelets and B cells.

Previous work using microscopy to study the location of Btk in platelets is limited. Most of the work to investigate localisation and protein-protein interactions is performed biochemically using immunoprecipitation and membrane fractionation. As platelets do not have a nucleus, they cannot be genetically transformed. Therefore, microscopy to investigate the localisation of proteins is limited to fixed samples and reliant on fluorescently labelled antibodies. Furthermore, microscopy requires specialist equipment and training when compared to immunoprecipitation and this may explain why there is less extensive research on Btk in platelets using microscopy.

Btk has been shown to biochemically interact with some proteins and lipids in platelets including; PIP3 which is involved in Btk recruitment (Battram et al., 2017), Lyn which is proposed to phosphorylate Btk (Quek et al., 1998), Protein Kinase C θ (Crosby and Poole, 2002) and LAT which orchestrates GPVI and CLEC-2 signalling by the formation of the signalosome (Pasquet et al., 1999b). However, no published studies have identified an interaction between Btk and GPVI or CLEC-2 using coimmunoprecipitation in platelets.

Furthermore, although co-immunoprecipitation have shown interactions biochemically, events are often difficult to identify due to the transient nature of some interactions or the disruption of weak interactions during the experimental process. Therefore, microscopy can evaluate where proteins are in relation to each other without the use of biochemical techniques and without the need for cell lysis.

While microscopy has not been used to investigate the localisation of Btk within platelets it has been used to investigate the localisation of several other proteins and signalling

events. GPVI has been shown to cluster on collagenous surfaces such as human collagen and CRP-XL (Poulter et al., 2017). Furthermore, GPVI and GPVI dimers have been shown to localise along collagen fibres (Poulter et al., 2017, Clark et al., 2019). Phosphotyrosine residues, stained with the phosphotyrosine specific antibody 4G10, were found to localise with some but not all GPVI molecules (Poulter et al., 2017) suggesting signalling primarily takes place along the collagen fibre. Enrichment of tyrosine phosphorylation has also been found in actin nodules using stochastic optical reconstruction microscopy (STORM). This suggests that nodules act as signalling hubs (Poulter et al., 2015). CLEC-2 has been identified to form clusters at the platelet surface using TIRFM when indirectly imaged using podoplanin clustering. However when investigated using STORM these clusters were found to be made up of smaller nanoclusters (Pollitt et al., 2014).

The localisation of Btk and its relationship to other proteins has been studied to a greater extent in B cells than in platelets. The hemITAM containing receptor Dectin1 has been shown to interact with Btk using coimmunoprecipitation in macrophages during infection with *Candida* yeast (Strijbis et al., 2013). Furthermore, this was mirrored using microscopy, where Btk was also found to colocalise with PIP3 and actin during infection and phagocytosis, but not with DAG (Strijbis et al., 2013).

Tec family kinases in B and T cells have been shown to form a punctate formation at the membrane in stimulated B and T cells (Woods et al., 2001, Tomlinson et al., 2004b, Kane and Watkins, 2005). This observed punctate formation may be due to Btk directly changing its location and undergoing protein clustering in order to become catalytically active (Gustafsson et al., 2012, Mohamed et al., 2000, Chung et al., 2019, Agnew and Jura, 2017). It also may be an indirect effect, as it is known that PIP3 can form clusters at the membrane and Btk is recruited via its PH domain to PIP3 (Wang and Richards, 2012).

5.1.2 Total internal reflection fluorescence microscopy

Total internal reflection fluorescence microscopy (TIRFM) is an advanced microscopy technique to illuminate within approximately 100nm of the coverslip. The idea of using reflection to visualise cells on the surface of glass was described in the 1950's (Ambrose, 1956), and then expanded by Axelrod in the 80's (Axelrod, 1981). The resolution, which is the distance of which the microscope can distinguish two separate molecules, is 200nm for TIRFM (Kudalkar et al., 2016).

The principle of TIRF is illustrated in Figure 5.1.1. Briefly, in standard fluorescent microscopy (on the left) light enters at a straight incident angle and illuminates the sample. In TIRFM, the incident light is directed at the sample at an angle. Most of this light is reflected away due to the coverslip, however a small portion is not. The non-reflected light forms an evanescent wave through the sample, illuminating approximately 100nm within the coverslip.

TIRF is able to work due to the different refractive indices of the sample (N_2) and the coverslip (N_1). N_2 (the sample contained in phosphate buffered saline) must have a lower refractive index than the N_1 (the glass coverslip). The Snells law equation (listed below) states there is bending of light (refraction) when changing between two different mediums that have different refractive indices.

The Snells law equation:

$$N_1 \times \sin\theta_1 = N_2 \times \sin\theta_2$$

Where N_1 = higher refractive index, N_2 = lower refractive index, θ_1 = angle of the incident beam in respect to the normal interface and θ_2 = the refracted beam angle within the lower index medium.

As the angle of θ_1 continues, so will the θ_2 which is the angle of refraction. When the θ_2 is $>90^\circ$, the critical angle (θ_c) is achieved (Figure 5.1.1). Any angle greater than the critical angle and no light will enter the sample – this is termed total internal reflection (Ambrose,

1956). An evanescent wave is generated at the point of total internal reflection and it exponentially decays whilst travelling through the sample. It excites fluorophores within this distance therefore visualizing close to the coverslip.

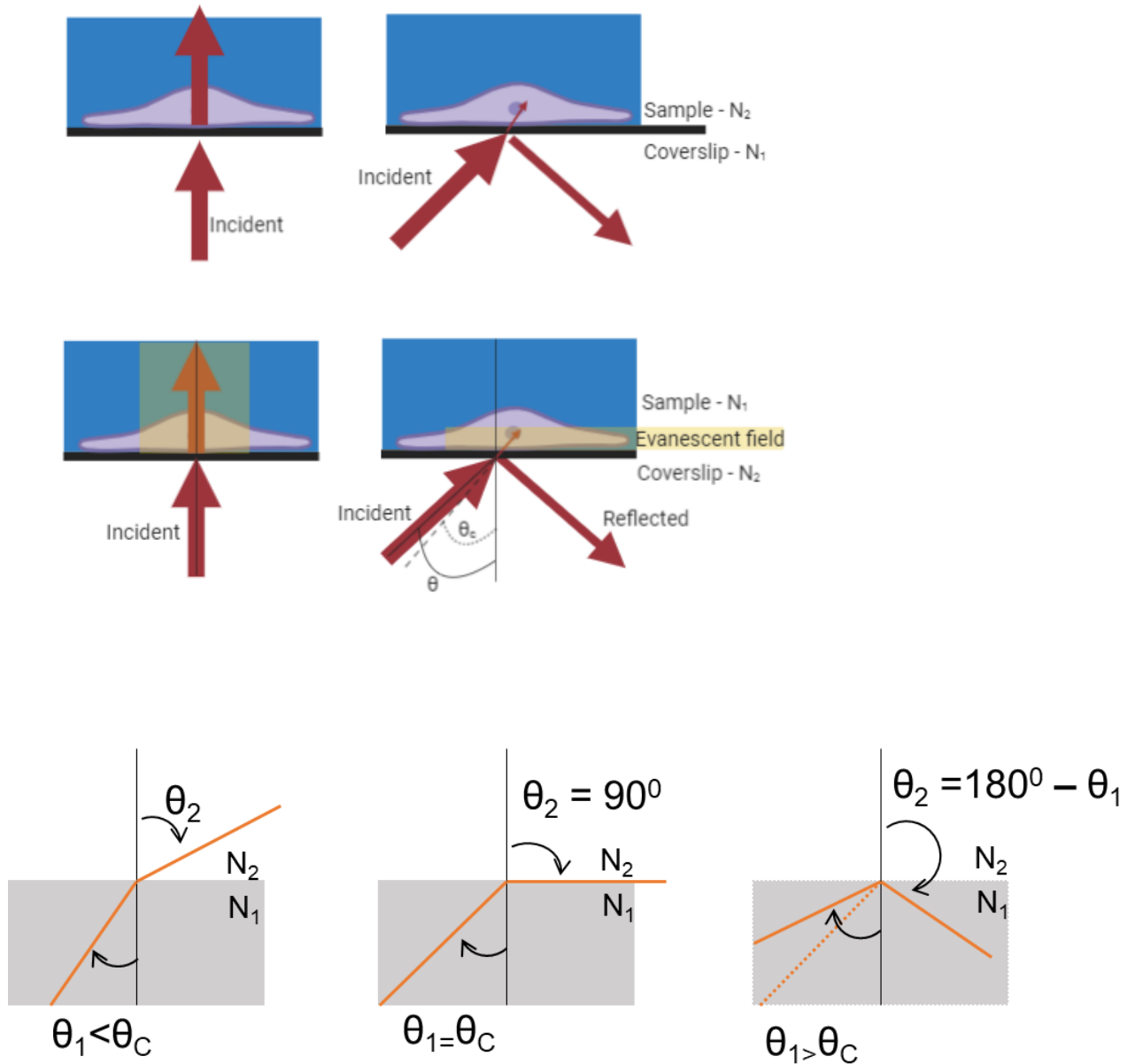


Figure 5.1.1 Principles of TIRFM

In conventional fluorescence microscopy, light enters vertically as seen on the left, with all of the depth of the sample being illuminated (lower left). In TIRFM the light enters at an angle (upper right). As the light is reflected away, an evanescent field is formed which refracts into the sample, illuminating within 100nm of the coverslip (lower right). The principles of Snells law are shown below.

TIRFM has been utilised to study a range of samples, including viruses, actin dynamics, cell substrate contact regions and intracellular signalling (Mattheyses et al., 2010). Within the platelet field, TIRFM has been utilised to identify platelet adherence to silica (Agnarsson et al., 2015), the cytoskeleton (Poulter et al., 2015) and receptor signalling and clustering (Pollitt et al., 2014, Poulter et al., 2017).

TIRFM is a relatively quick method of microscopy. It also a greater signal to noise ratio than confocal microscopy due to a small Section being illuminated and therefore reducing background fluorescence (Simon, 2009). As Btk localises to the membrane upon GPVI and CLEC-2 stimulation when assessed using membrane fractionation and western blotting (Manne et al., 2015a), it is suitable for imaging GPVI, CLEC-2 and the transmembrane protein LAT.

5.1.3 Colocalisation methods

Colocalisation is the spatial overlap of two or more proteins when analysed using fluorescent labels. Each of the fluorophores used must have a separate emission wavelength to identify if the targets are located close to each other. The analysis provides a numerical value to identify how molecules relate to each other in microscopy images (Bolte and Cordelieres, 2006, Malkusch et al., 2012, Malkusch and Heilemann, 2016, Pagoon et al., 2016). It can be calculated using a correlation-based method or a co-occurrence-based method.

Co-occurrence-based methods assess whether there is spatial overlap of two separate probes (Figure 5.1.2.A). Correlation based methods are when the probes overlay (as in co-occurrence), but also the number of probes increases in proportion to one another within the same structure (Figure 5.1.2.B). For example, as there is a higher proportion of red probes in a structure, the number of green probes also increases and they overlap.

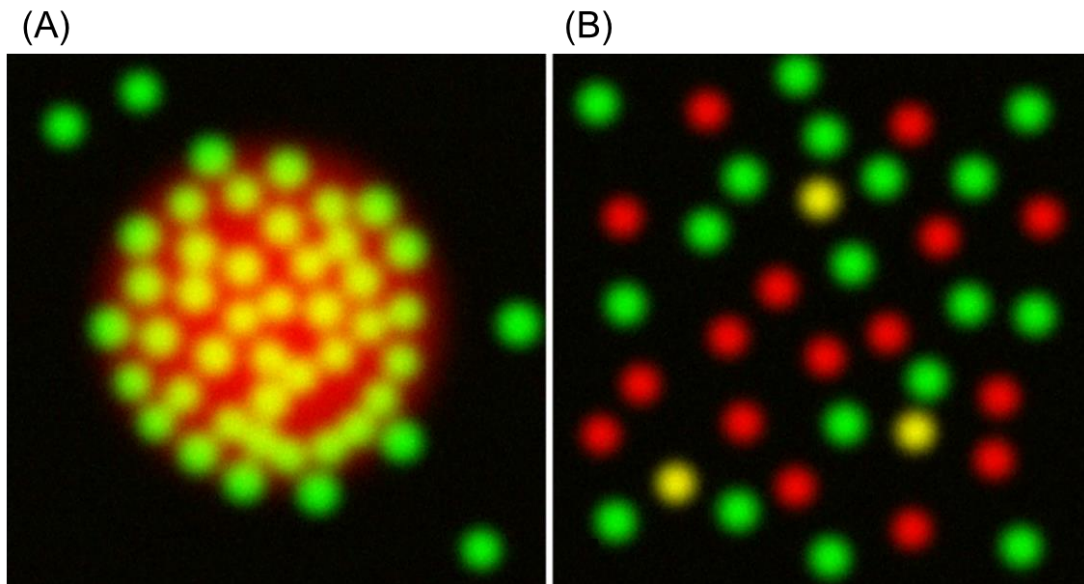


Figure 5.1.2 Co-occurrence and correlation based colocalisation analysis adapted from Aaron et al., 2018.

(A) The image shows an example of high co-occurrence of green with red, a lower co-occurrence of red with green but with low correlation as there is only one red molecule but numerous individual green molecules. (B) the image shown here displays a relatively low co-occurrence (only few yellow overlapping molecules) between the red and green channels. As there are a similar amount of green and red molecules the pixel intensities have a similar linear relationship, so there would be a high correlation value.

5.1.3.1 Pearson correlation coefficient

The original method of assessing colocalisation was developed by Pearson in 1896 (Dunn et al., 2011). Pearson correlation coefficient (PCC) is a statistical method of assessing colocalisation, measuring colocalisation as a correlation between the intensity of two imaged fluorophores. A range of values are produced between -1 to +1. PCC values of -1 are totally and inversely correlated images (as one probe increases, the other decreases in the same localisation), whereas values of +1 are totally correlated (both probes increase together). It is calculated by measuring the pixel by pixel covariance in the amount of signal of two images with the formula below:

$$PCC = \frac{\sum_i (M_i - \bar{M}) \times (G_i - \bar{G})}{\sqrt{\sum_i (M_i - \bar{M})^2 \times \sum_i (G_i - \bar{G})^2}}$$

Where M_i and G_i are the intensity of the magenta and green channels of pixel i and \bar{M} and \bar{G} refer to the mean intensity of the two respective channels across the image (Dunn et al., 2011). The technique expects co-occurrence to be linear. However, this may not always be the case due to protein copy number differences and the stoichiometry of protein-protein interactions.

PCC values between GPVI dimers and phosphotyrosine in the study of Poulter et al., on different GPVI activating ligands were below 0.3. They concluded from these values that some, but not all phosphotyrosine residues localise with GPVI due to the strong recruitment of GPVI at the collagen fibre (Poulter et al., 2017). A recent study has suggested values of equal to or greater than 0.4 are colocalised (Pallini et al., 2020). Therefore, a PPC of 0.4 was set as a threshold for determining if there is protein colocalization in this study.

5.1.3.2 Manders colocalisation coefficient

In contrast to PPC, Manders colocalisation coefficient (MCC) is based on co-occurrence rather than correlation. It was developed by Manders in response to hard to interpret negative PCC values. It assesses the fraction of one protein that colocalises with a second protein. The value of colocalisation is given between 0 (no co-occurrence) and 1 (total co-occurrence) and calculated using the following equations:

$$M_1 = \frac{\sum_i M_{i,colocal}}{\sum_i M_i} \text{ where } M_{i,colocal} = M_i, \text{ if } G_i > 0 \text{ and } M_{i,colocal} = 0 \text{ if } G_i = 0$$

$$M_2 = \frac{\sum_i G_{i,colocal}}{\sum_i G_i} \text{ where } G_{i,colocal} = G_i, \text{ if } M_i > 0 \text{ and } G_{i,colocal} = 0 \text{ if } M_i = 0$$

In contrast to PCC, MCC is independent of signal proportionality. It provides the fraction of fluorophore M with fluorophore G and the fraction of fluorophore G with M, which is excellent for assessing colocalisation without the need for a linear relationship which is

235

required for PCC. However, it is sensitive to background fluorescence and therefore images must be thresholded before processing (Bolte and Cordelieres, 2006, Dunn et al., 2011).

A value of equal to or greater than 0.4 suggest 40% of molecules of M are localised with molecule G. This value was selected as the value of colocalisation in this study (Pagoon et al., 2016, Luo et al., 2018).

5.2 Aims and Hypothesis

To our knowledge the spatial localisation of Btk has not been studied in platelets. In B and T cells, it is known that Tec family kinases localise in a punctate formation in stimulated cells and this is mediated by their PH domains (Woods et al., 2001, Tomlinson et al., 2004b, Kane and Watkins, 2005). Previous work has suggested that Btk may behave as a scaffolding protein downstream of the collagen receptor GPVI using platelet function assays, biochemical techniques, and a kinase dead mutant of Btk in a cell line reporter assay (chapters 3 and 4). Therefore, the localisation of Btk to areas of GPVI mediated signalling was investigated in the presence and absence of Btk Kinase inhibitors. If Btk acts as a scaffold it would be predicted that the localisation of Btk would not change in the presence of the inhibitors.

Compared to GPVI, at submaximal concentrations of rhodocytin, a functional kinase domain is required to mediate signalling as shown using western blotting and cell line reporter assays. Therefore, it would be expected that Btk would localise near the receptor due to its requirement. Additionally, Src and Syk are responsible for mediating CLEC-2 clustering and therefore likely to localise near the hemITAM receptor. Due to the interactions of Btk and Syk and SFKs (Bobe et al., 2001, Mahajan et al., 1995), and its requirement in this pathway, it is not unreasonable to believe that Btk may be located near CLEC-2 when spread on rhodocytin.

Hypothesis: As Btk acts as a protein scaffold, it will localise along collagen fibres with GPVI and other signalling proteins. This distribution will not change in the presence of Btk inhibitor. In comparison, Btk will localise to CLEC-2 when platelets are spread on rhodocytin, but due to the requirement of the kinase domain in mediating CLEC-2 signalling.

Aims of Chapter:

- To investigate the distribution of Btk in platelets
- To establish the localisation of Btk in relation to GPVI, LAT and CLEC-2 at the membrane using TIRFM
- To identify changes in Btk localisation in the presence of a Btk inhibitor.

5.3 Results

5.3.1 Btk and GPVI do not colocalise on collagen fibres using

TIRFM

Initial experiments were performed to identify whether Btk colocalises with GPVI. It is known that platelet GPVI localises along collagen fibres, with the majority of GPVI dimer staining restricted to the fibre (Poulter et al., 2017, Clark et al., 2019). It has also been shown that phosphotyrosine residues localise at the collagen fibre (Poulter et al., 2017). Although not assessed numerically for colocalisation, the distribution of phosphotyrosine and GPVI look strikingly similar, with localisations along the collagen fibre. As Btk is tyrosine phosphorylated downstream of GPVI, it was hypothesised that it will also localise with GPVI along collagen fibres. Pearson correlation coefficient (PCC) and Manders colocalisation coefficients (MCC) were used initially to assess colocalization of GPVI in relation to Btk.

Washed platelets were spread on collagen for 45 minutes before being fixed and permeabilised. Platelets were then stained with a rabbit anti-Btk antibody and a mouse anti-GPVI antibody. Platelets were then incubated with Alexa Fluor 647 conjugated donkey anti-rabbit and Alexa Fluor 488 conjugated goat anti-mouse secondary antibodies before washing and imaging. Samples were imaged using TIRFM and analysed using the ImageJ Just Another Colocalization Plugin (JACoP) (Bolte and Cordelieres, 2006, Schneider et al., 2012).

Btk forms a punctate pattern when platelets are spread on collagen. Some Btk puncta appear to be situated on the collagen fibre, however this is not evident throughout the image (Figure 5.3.1.A, magenta panel – Alexa fluor 647 staining). As previously reported in the work by Poulter and colleagues, staining of GPVI is mostly restricted to the collagen fibres (5.3.1.A, green panel, Alexa fluor 488 staining). When images are merged, areas of white suggest colocalization between Btk and GPVI. While some areas display clear colocalisation, other areas do not. To assess colocalisation PCC and MCC were used.

The PCC value between Btk and GPVI was 0.31 ± 0.01 . The MCC value for GPVI colocalising with Btk was 0.35 ± 0.02 and the value was 0.33 ± 0.02 for Btk localising with GPVI. All of these values are below the 0.4 threshold which suggests a lack of colocalization between Btk and GPVI (Bolte and Cordelieres, 2006, Dunn et al., 2011, Pagoon et al., 2016)

To confirm this result and to validate another antibody of Btk was used to assess for colocalisation between Btk and GPVI. In initial experiments, $100\mu\text{g/mL}$ of collagen was used which caused a high amount of fibres to be visualised in the DIC image (Figure 5.3.1.A). As experiments were investigating the localisation of proteins at the collagen fibre, the collagen concentration was reduced to reduce overcrowding of the fibres.

Experiments were performed as described previously with a goat anti-Btk antibody used in place of the rabbit anti-Btk antibody. As seen previously, GPVI (Green channel; secondary staining with Alexa fluor 555) localises along the collagen fibre seen imaged using DIC (Figure 5.3.1.C). As seen with the Rabbit anti-Btk antibody, Btk staining with the Goat anti-Btk antibody also forms a punctate pattern in the platelet (Figure 5.3.1.C, magenta panel; secondary staining with Alexa fluor 647). The merged image shows areas of white, suggesting colocalisation between GPVI and Btk. However, this is not uniform, suggesting colocalisation of some but not all of the Btk and GPVI molecules stained.

When assessing colocalisation, the values obtained for this antibody were similar to the rabbit anti-Btk antibody. Although the average value for PCC is 0.43 ± 0.1 , MCC for GPVI with Btk 0.44 ± 0.07 , and the MCC for Btk with GPVI 0.41 ± 0.07 is slightly increased compared to the rabbit Btk there is no significant difference when analysed by two-way ANOVA (Figure 5.3.1). These values are over 0.4 suggesting that Btk does weakly colocalise with GPVI although it is not confirmed across two antibodies and therefore it is not convincing that Btk and GPVI significantly colocalise. This may be due to reagent differences or the limitation of TIRFM.

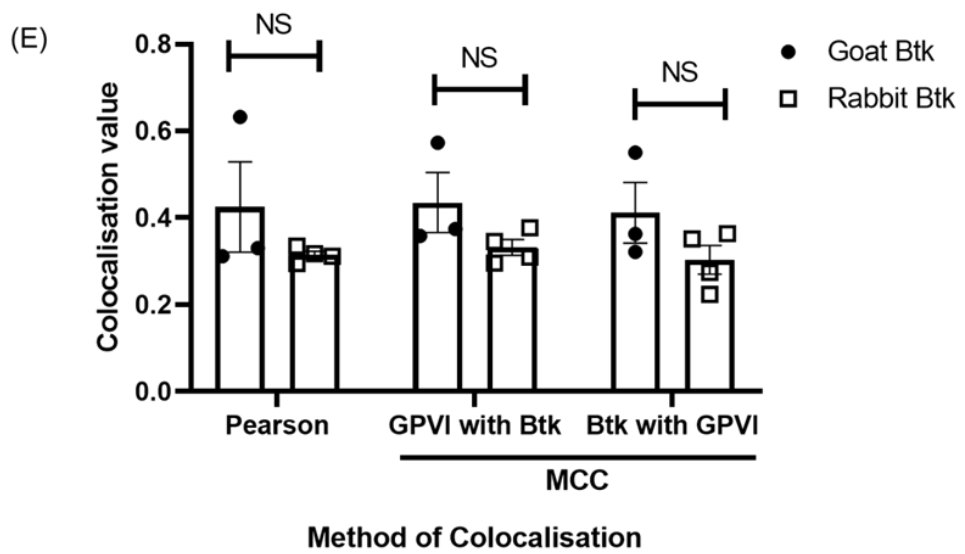
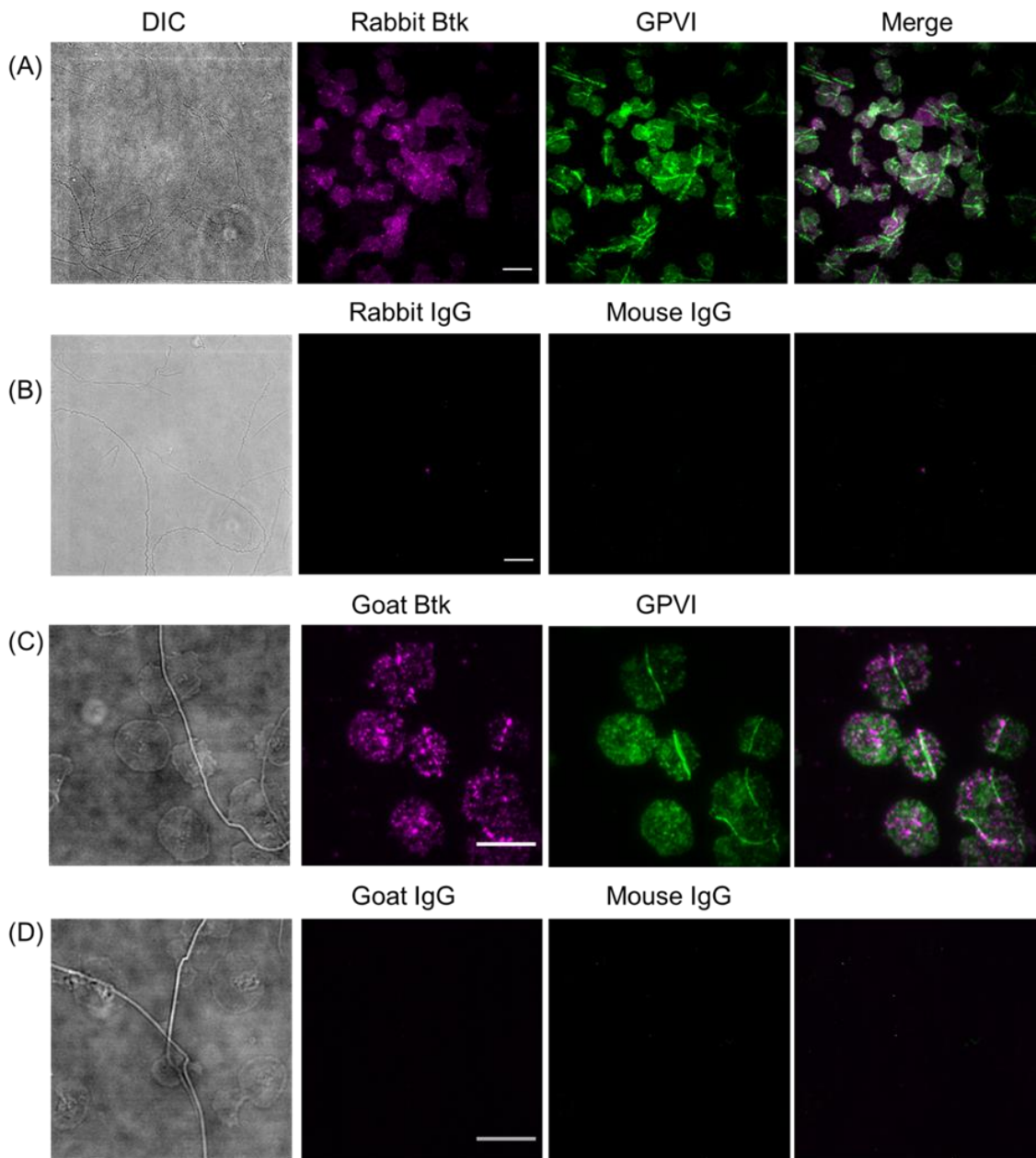


Figure 5.3.1 Btk and GPVI weakly colocalise

(A, B) Washed platelets 2×10^7 cells/mL were spread on collagen ($100 \mu\text{g/mL}$) for 45 minutes before fixation, permeabilization and staining with (A) rabbit anti-Btk and anti-GPVI antibodies or (B) IgG controls. Wells were then stained with Alexa Fluor 647 conjugated donkey anti-rabbit and Alexa Fluor 488 conjugated goat anti-mouse secondary antibodies. (C, D) Washed platelets (2×10^7 cells/mL) were spread on collagen ($10 \mu\text{g/mL}$) for 45 minutes before being stained with (C) goat anti-Btk and anti-GPVI antibodies or (D) IgG controls. Note – this lower concentration of collagen was used for all subsequent microscopy experiments as this allowed easier visualisation of individual collagen fibres. Samples were then with Alexa Fluor 555 conjugated donkey anti-mouse and Alexa Fluor 647 conjugated donkey anti-goat. Samples were imaged with Nikon TI-E 100x TIRf lens. Analysis was performed using JACoP in ImageJ to quantify colocalisation between (E) Btk and GPVI to identify if GPVI and Btk colocalise using PCC and MCC, $n \geq 3$, Data represents mean \pm SEM. Scale bar represents $10 \mu\text{m}$. Statistical testing was performed with Two-way ANOVA with Dunnett's multiple comparisons test, with no significance found.

5.3.2 Btk kinase inhibitors do not alter the localisation of Btk

The images taken above and colocalisation analysis suggested that Btk did not strongly colocalise with GPVI using TIRFM when platelets are spread on collagen. One catalytically active molecule of Btk has been suggested to phosphorylate of another molecule of Btk (Chung et al., 2019, Wang et al., 2019b). This regulatory mechanism could explain the punctate pattern observed in the Btk staining. Therefore, to investigate the role the Btk kinase domain has in the localisation and distribution of Btk, the kinase activity of Btk was inhibited using ibrutinib and acalabrutinib. The localisation of Btk in relation to GPVI was assessed. As previously shown in chapter 3 (Figure 3.3.4) the kinase activity of Btk, determined by the loss of the autophosphorylation site, is lost at 1 μ M acalabrutinib. 1 μ M ibrutinib was selected to identify if there are any differences between the two drugs independently of their kinase inhibition. Furthermore, 1 μ M ibrutinib was selected as it inhibits Btk but does not reduce spreading on collagen (Bye et al., 2015) so can be used to investigate the localisation of platelets without the artefact of less spreading.

Washed platelets were pre-treated with ibrutinib or acalabrutinib (1 μ M) or vehicle control (0.1% (v/v) DMSO) for 5 minutes before spreading on collagen. Cells were fixed and staining was performed as previously described (Section 5.3.1). Btk puncta analysis was performed by thresholding the image to remove background and select for Btk puncta. Particles were counted using the ImageJ tool, analyse particles. Particles between 0.1-10 microns and 0-1 circularity were included in the count. Colocalisation analysis was performed by thresholding the image and then using JACoP plug in (Bolte and Cordelieres, 2006).

To determine the contribution the Btk kinase domain has in the punctate appearance, the number of puncta were quantified in platelets treated with acalabrutinib, ibrutinib or vehicle. Btk kinase inhibition did not impact the number of Btk puncta. The average number of Btk spots per platelet which was 2 for each of the conditions (Figure 5.3.2.E).

There is no significant difference in the number of puncta between vehicle and drug

treated samples. Furthermore, the average size and mean intensity of the puncta is not significantly different when platelets are treated with inhibitor showing that there is no change in the morphology and brightness of the puncta in the presence of Btk kinase inhibitor.

There is no striking difference in the amount of colocalisation in the merged images between the treatment of drugs with some small areas of white being observed, however some areas are absent of white (Figure 5.3.2.A-C). No MCC or PCC values were over 0.4, suggesting that Btk and GPVI do not colocalise. Furthermore, there was no change in the amount of colocalisation when comparing vehicle and drug treated samples. This suggests that kinase function does not regulate the distribution of Btk or its localisation in relation to GPVI.

Taken together, these results suggest that Btk distribution and localisation in relation to GPVI is independent of its kinase domain.

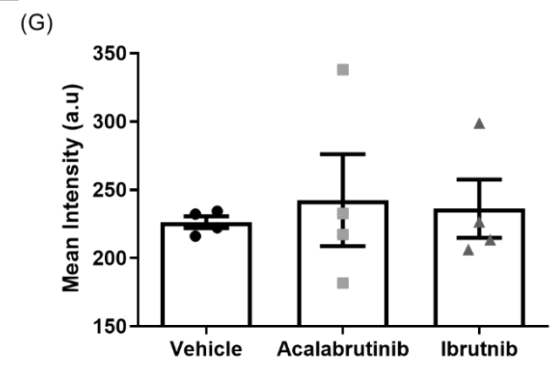
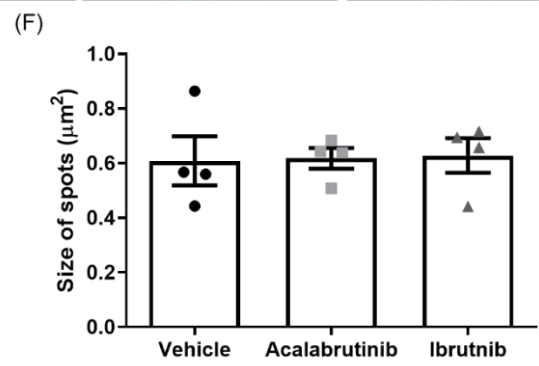
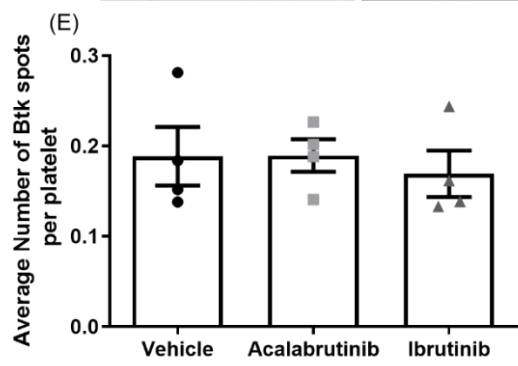
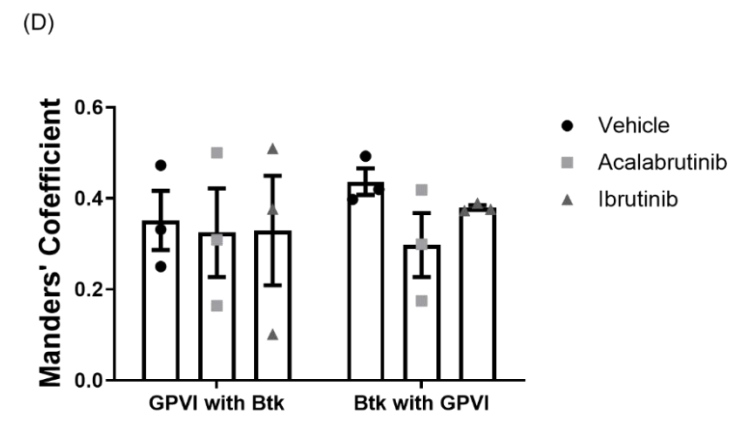
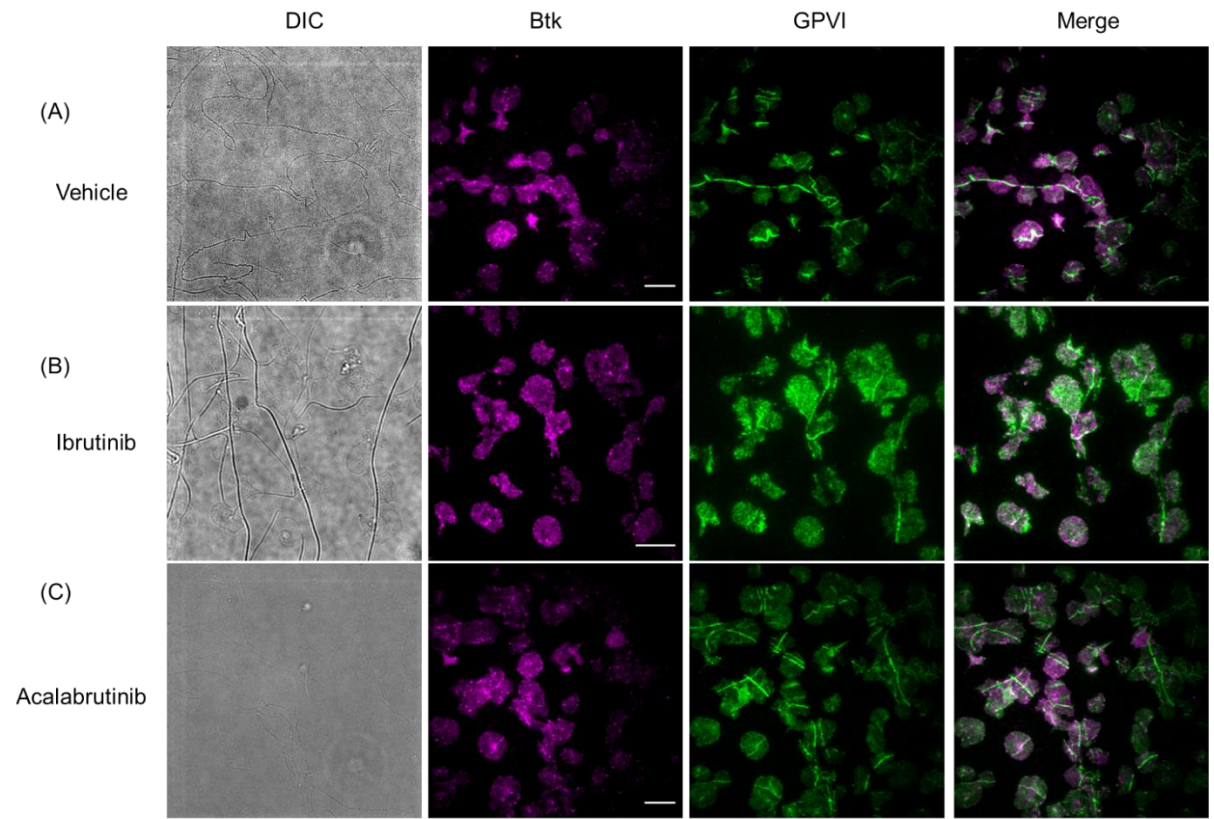


Figure 5.3.2 Inhibition of the Btk kinase domain does not alter the distribution and colocalisation of Btk using TIRFM

Washed platelets 2×10^7 were treated with (A) vehicle, (B) ibrutinib ($1 \mu\text{M}$), (C) acalabrutinib ($1 \mu\text{M}$) or vehicle for 5 minutes before spreading on $100 \mu\text{g/mL}$ collagen for 45 minutes before fixation, permeabilization and staining with anti-Btk and anti-GPVI antibodies and secondary stained with Alexa Fluor 647 conjugated donkey anti-rabbit and Alexa Fluor 488 conjugated goat anti-mouse secondary antibodies respectively. Samples were imaged with Nikon TI-E 100x TIRf lens. Analysis was performed using (D) JACoP in ImageJ to quantify colocalisation between Btk and GPVI. $N=3$, data represents mean \pm SEM. Statistical testing was performed with Two-way ANOVA with Dunnett's multiple comparisons test, with no significance found. Scale bar represents $10 \mu\text{m}$. Analysis to count the (E) number of spots per platelet, (F) the size of the spots in μm^2 , and (G) and mean intensity of the spots was performed using ImageJ analyse particles tool. Graphs represent mean \pm SEM. Statistical testing was performed with one-way ANOVA with Dunnett's post-test, with no significance found, $n=4$.

5.3.3 Btk and GPVI are distributed throughout the platelet when spread on CRP-XL, and do not colocalise when imaged in TIRFM

Btk did not directly colocalise with GPVI on collagen fibres. Strong GPVI localisation at the fibre is present (Figures 5.3.1 and 5.3.2), (Clark et al., 2019, Poulter et al., 2017). This may occlude Btk recruitment or be sterically preventing anti-Btk antibodies binding.

Furthermore, another potential reason for using CRP-XL is the potential for GPVI clustering to be different on CRP-XL compared to collagen (Poulter et al., 2017). Each molecule of CRP-XL has 30 binding sites for GPVI and can potentially change the way GPVI clusters, for example, potentially larger clusters, (Smethurst et al., 2007). As no certain colocalisation was observed on collagen (Figure 5.3.1), CRP-XL was used to assess whether there is colocalisation on this ligand.

CRP-XL is a non-fibrous ligand and has previously been used to assess spreading of platelets (Bye et al., 2015) and the localisation of GPVI (Poulter et al., 2017, Onselaer et al., 2020) and Syk (Dunster et al., 2020).

Washed platelets were spread on CRP-XL (1µg/mL) coated surfaces for 45 minutes before fixation and permeabilization. Platelets were then stained with a rabbit anti-Btk antibody and a mouse anti-GPVI antibody followed by secondary staining with Alexa Fluor 647 conjugated donkey anti-rabbit and Alexa Fluor 488 conjugated goat anti-mouse antibodies before washing and imaging. Samples were imaged using TIRFM and analysed using the ImageJ plugin JACoP (Bolte and Cordelieres, 2006).

Both the MCC and PCC values were approximately 0.25, and there was no significant difference between the methods of colocalisation (Figure 5.3.3.B). The amount of Btk that colocalised with GPVI was identical to the amount of GPVI that colocalised with Btk when assessed using the MCC (0.27 ± 0.09 or 0.27 ± 0.1 respectively). Neither of these values reach the threshold for ≥ 0.4 suggesting that Btk does not colocalise with GPVI in TIRFM.

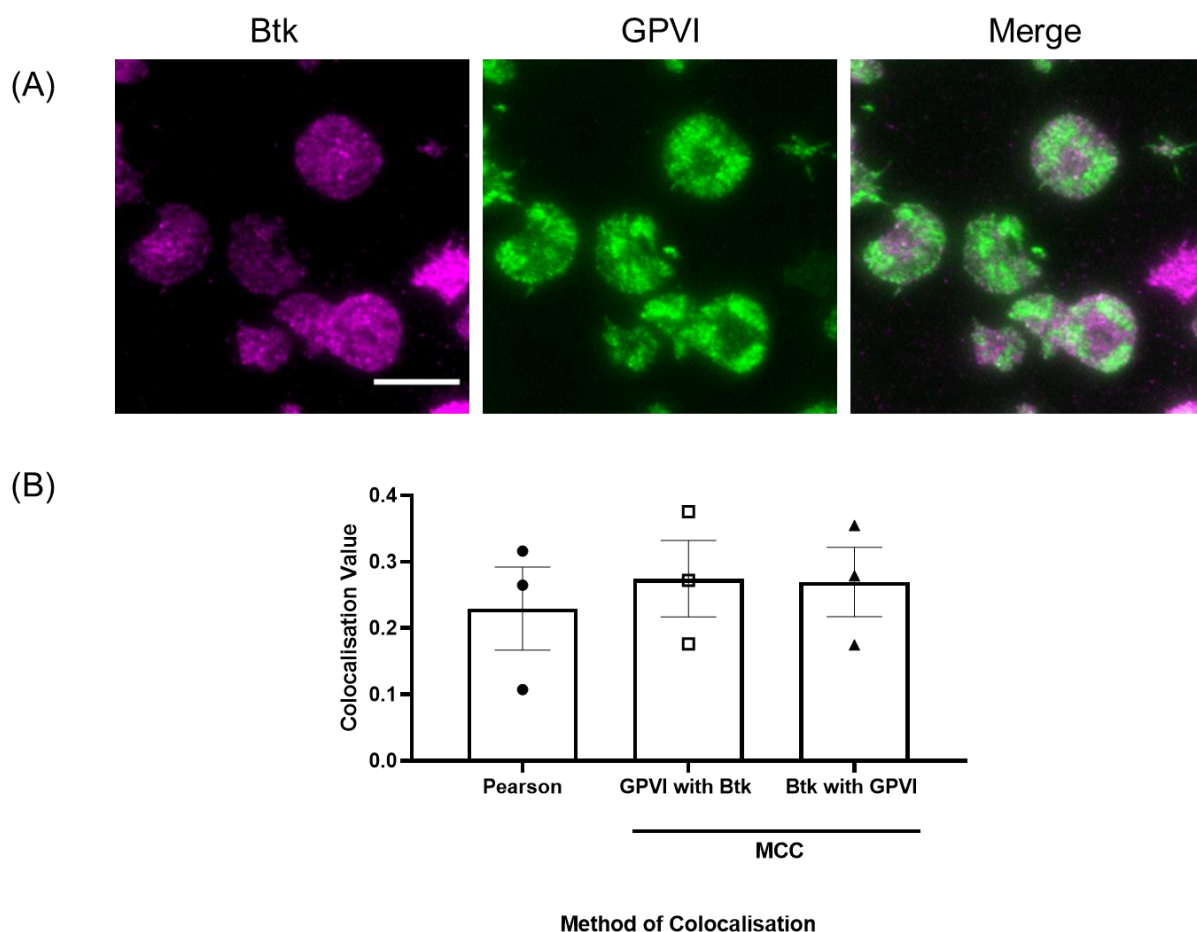


Figure 5.3.3 Btk and GPVI do not colocalise on CRP-XL

(A) Washed platelets were spread on CRP 1 μ g/mL for 45 minutes before being stained with anti-Btk (magenta panel, secondary antibody Alexa Fluor 647 conjugated donkey anti-rabbit), anti-GPVI (green panel, secondary antibody Alexa Fluor 488 conjugated goat anti-mouse). Samples were imaged in TIRFM. (B) ImageJ JACoP was used to assess colocalisation using Pearson correlation coefficient and manders co-localisation coefficient of the amount of GPVI that colocalises with Btk and the amount of Btk that colocalises with GPVI. n=3. Data presented mean \pm SEM. Statistical testing was performed using paired one-way ANOVA with Dunnett's multiple comparison test with no significance found. Scale bar represents 10 μ m.

5.3.4 Btk and phosphotyrosine residues do not colocalise in

TIRFM.

It is known that Btk is tyrosine phosphorylated downstream of GPVI (chapter 3, Figure 3.3.4 and (Atkinson et al., 2003a, Pasquet et al., 1999b, Quek et al., 1998). Therefore, it would be expected that Btk would localise with phosphotyrosine residues, stained for using the antibody 4G10. However, as there are more phosphotyrosine residues present than Btk molecules present, it is unlikely that there will be total colocalisation.

Washed platelets were spread as previously described on collagen and stained with anti-Btk and anti-phosphotyrosine (4G10) antibodies. Platelets were stained with Alexa Fluor 647 conjugated donkey anti-rabbit and Alexa Fluor 488 conjugated goat anti-mouse secondary antibodies before washing and imaging using TIRFM. Colocalisation between Btk and phosphotyrosine was analysed using JACoP (Bolte and Cordelieres, 2006). To investigate whether the lack of localisation observed previously on collagen was due to the limit of TIRF, images were taken in and out of TIRFM (epifluorescence microscopy where the whole sample is illuminated). A collagen fibre can be up to 67nm in diameter (Orgel et al., 2006). If the fibre does not lie directly flat on the coverslip, the platelet membrane interaction may be out of the illumination of the evanescent wave (100nm) in TIRFM.

Figures 5.3.4.B and C show that when compared to the DIC image, phosphotyrosines are enriched to the collagen fibre (pY - green panels), forming a similar pattern observed with GPVI (Figure 5.3.1). In agreement with earlier experiments, Btk does not directly localise to the fibre. When the images are merged, there is a small proportion of white, suggesting colocalisation between Btk and phosphotyrosines. A similar observation can be made when images are taken out of TIRF, however there appears to be some more white on the merged image.

In TIRF, there is no significant difference between the amount of Btk that localises with phosphotyrosine or the amount of phosphotyrosine residues localising with Btk with

values are approximately 0.2 using MCC. The PCC value was similar. Neither of these values are ≥ 0.4 suggesting Btk does not localise with 4G10 in TIRF.

This contrasts with the results out of TIRF, as all the colocalisation values are significantly larger compared to their TIRF counterparts ($***p \leq 0.001$). All values are approximately 0.4, suggesting more colocalisation of these two molecules occurs out of TIRF. This suggests that either Btk or phosphotyrosine residues are localised in a Z plane higher than the Z resolution of TIRF.

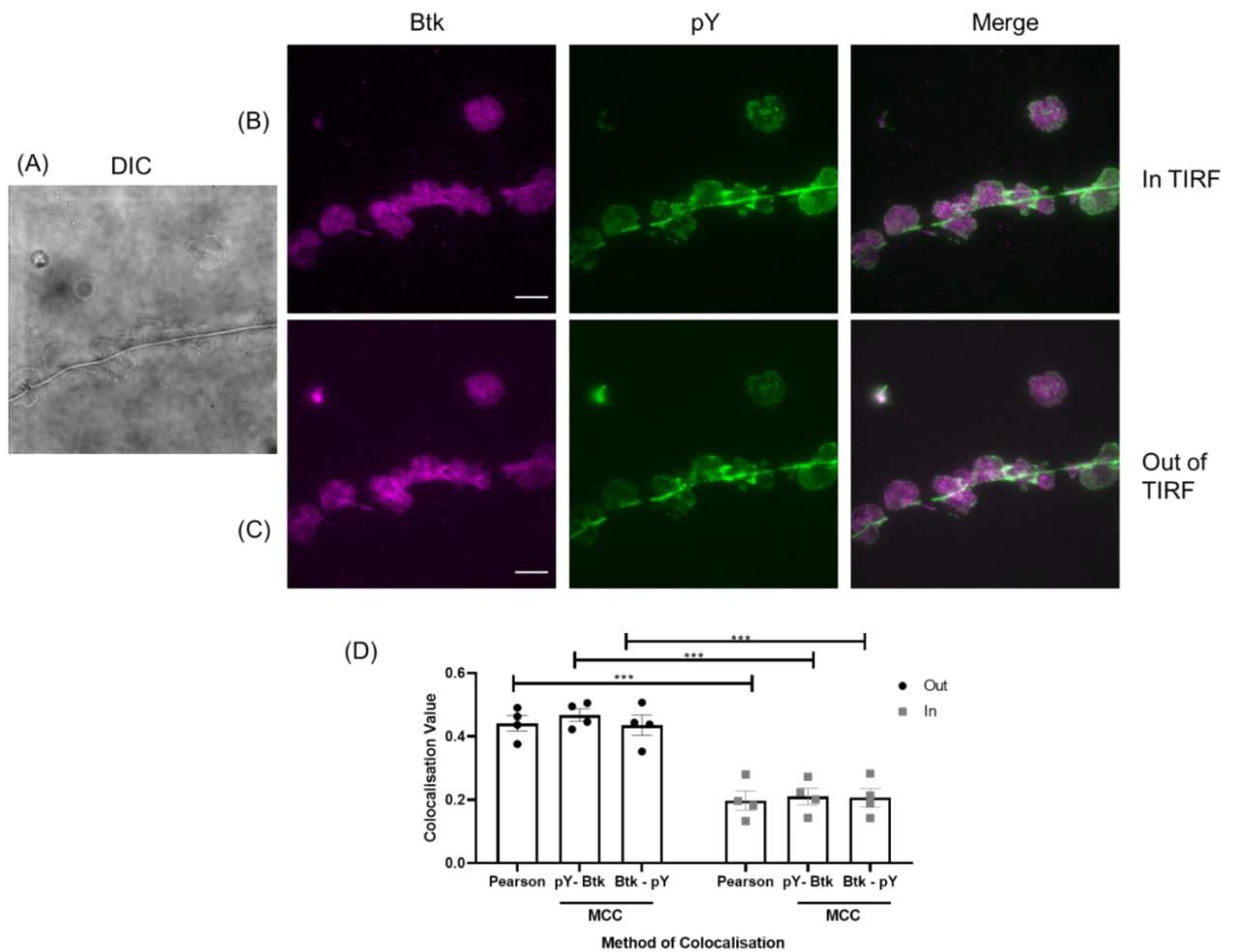


Figure 5.3.4 Btk and phosphotyrosines colocalise more out of TIRF than in TIRF

Washed platelets were spread on collagen 10µg/mL for 45 minutes before being stained with anti-Btk (magenta), anti-phosphotyrosine 4G10 (green) and secondary stained with Alexa Fluor 647 conjugated donkey anti-rabbit and Alexa Fluor 488 conjugated goat anti-mouse antibodies. Samples were imaged in (A) DIC, (B) in TIRF, or (C) out of TIRF. (D) ImageJ plugin JACoP was used to assess colocalisation using PCC and MCC coefficient of the amount of phosphotyrosines that colocalises with Btk and the amount of Btk that colocalises with phosphotyrosines n=4. Data presented mean ± SEM. Statistical testing was performed using paired 2-way ANOVA with Dunnett's multiple comparison test ***p ≤ 0.001. Scale bar represents 10µm.

5.3.5 Btk and LAT colocalise when spread on collagen and imaged in TIRFM

As Btk does not localise with GPVI in TIRFM it may be due to the fact Btk lies further downstream in the signalling cascade. LAT is a co-ordinator of GPVI signalling and many proteins are recruited to the signalosome (Hughes et al., 2008, Spalton et al., 2009, Pasquet et al., 1999b, Gibbins et al., 1998). Although Btk phosphorylation is not reduced in LAT deficient platelets (Pasquet et al., 1999b), it is hypothesised that Btk is recruited to the signalosome (Baba et al., 2001). Btk has been shown to co-immunoprecipitate with LAT in CRP-XL stimulated platelets (Pasquet et al., 1999b). Therefore, it is not unreasonable to hypothesise they will localise with each other spatially.

Btk and LAT localisation were assessed using TIRFM in platelets spread on collagen. As previously described, platelets were spread on 10µg/mL collagen for 45 minutes. Platelets were fixed, permeabilised and stained with anti-LAT and anti-Btk antibodies followed by secondary staining with Alexa Fluor 647 conjugated donkey anti-rabbit and Alexa Fluor 555 conjugated donkey anti-goat antibodies. Images were taken using TIRFM with colocalisation analysed in JACoP.

Btk, as shown previously, forms a punctate distribution. LAT is also distributed in a similar manner (Figure 5.3.5.A). The merged image shows a large proportion of white suggesting high levels of colocalisation between Btk and LAT when analysed using PCC and MCC. All average colocalisation values are greater than the 0.4 threshold, showing that there is some colocalisation between Btk and LAT, and values over 0.4 suggest that $\geq 40\%$ of molecules overlap with each other. There is no significant difference between the amount of Btk that colocalises with LAT and the amount of LAT that colocalises with Btk. It would be expected that more LAT would overlap with Btk than Btk with LAT as there are approximately half as many copies of LAT as there are Btk (Zeiler et al., 2014, Burkhart et al., 2012). However, this assumes all protein copies are localised in a way that would allow imaging, such as not being in tight complex or the epitope being blocked.

Nonetheless, Btk and LAT look to somewhat colocalise on collagen, as expected as it has been previously shown that they co-immunoprecipitate (Pasquet et al., 1999b).

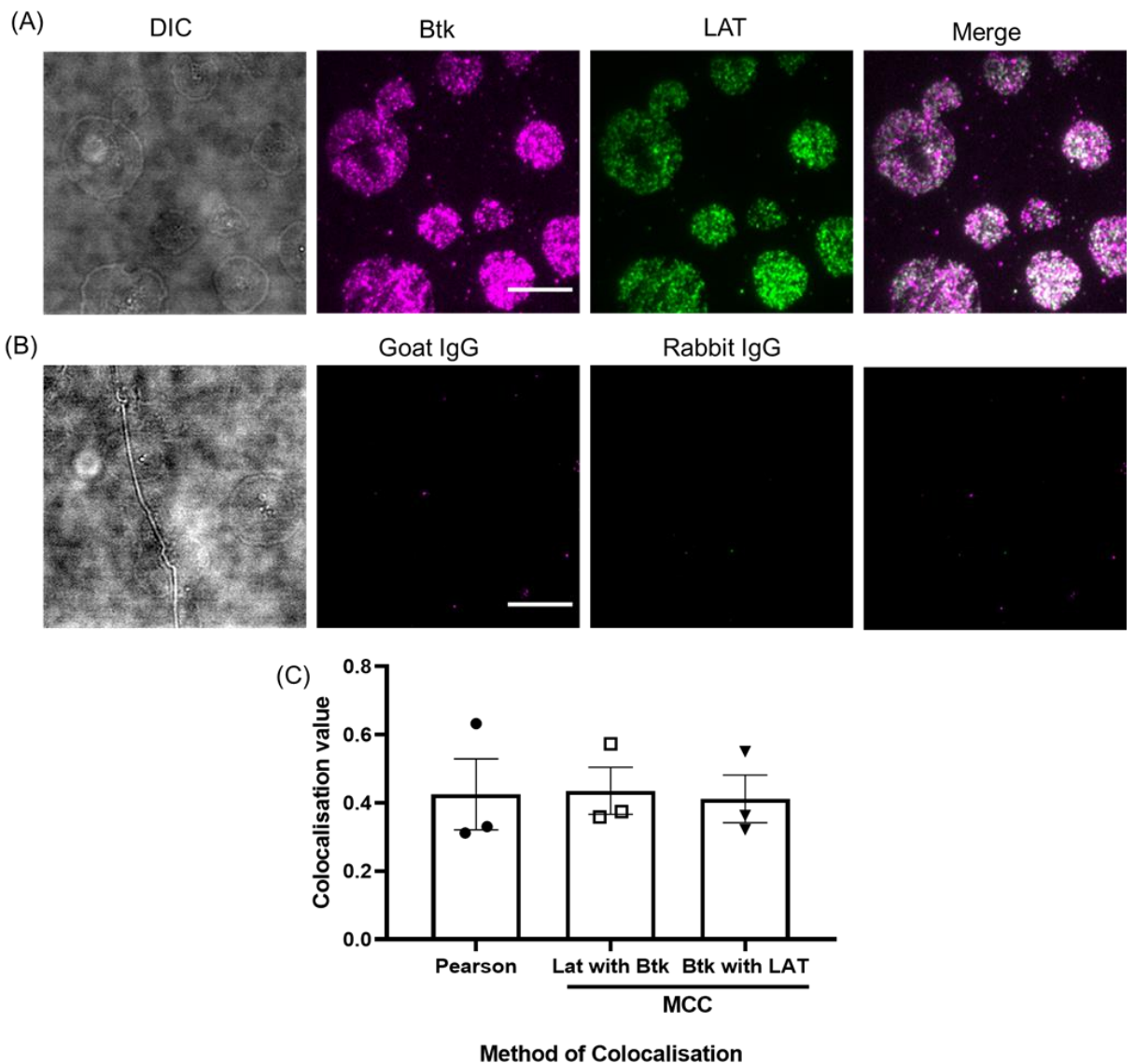


Figure 5.3.5 Btk and LAT colocalise in platelets when spread on collagen

Washed platelets were spread on collagen (10µg/mL) for 45 minutes before fixation and permeabilization. Platelets were stained with (A) anti-Btk (magenta) and anti-LAT (green) antibodies or (B) IgG controls and secondary stained using Alexa Fluor 555 conjugated donkey anti-goat and Alexa Fluor 647 conjugated donkey anti-rabbit. Images were taken in (A) TIRFM or DIC. Images were analysed using ImageJ JACoP to calculate the (C) PCC, and MCC to assess the visual colocalisation shown in the merged image. n=3, graph represents mean ± SEM. Scale bar represents 10µm.

5.3.6 Syk and GPVI colocalise when spread on collagen and imaged in TIRFM

Syk is known to precede Btk in the GPVI signalling cascade. It has been shown to directly interact with GPVI in GPVI pull down assays (Houck et al., 2019, Gibbins et al., 1997). Consequently, it was hypothesised that Syk would localise with GPVI. These experiments were performed as a positive control to further verify the lack of colocalisation between Btk and GPVI.

Washed platelets were spread on collagen for 45 minutes before being fixed and permeabilised as previously described. GPVI was stained using 1G5 as previous (Figure 5.3.1), and Syk was stained using N-19 as in Dunster et al., 2020. Samples were incubated with secondary antibodies Alexa Fluor 555 conjugated donkey anti-mouse and Alexa Fluor 647 conjugated donkey anti-rabbit. Images were taken using TIRFM.

Figure 5.3.6 confirms that Syk and GPVI colocalise when imaged using TIRFM. With colocalisation shown in white in the merged image, there is a clear area of colocalisation along the diagonal collagen fibre. When this was analysed using MCC after thresholding as described previously, the value for Syk with GPVI was 0.5 ± 0.03 and for GPVI with Syk was 0.47 ± 0.07 . This supports the observation that Syk and GPVI colocalise.

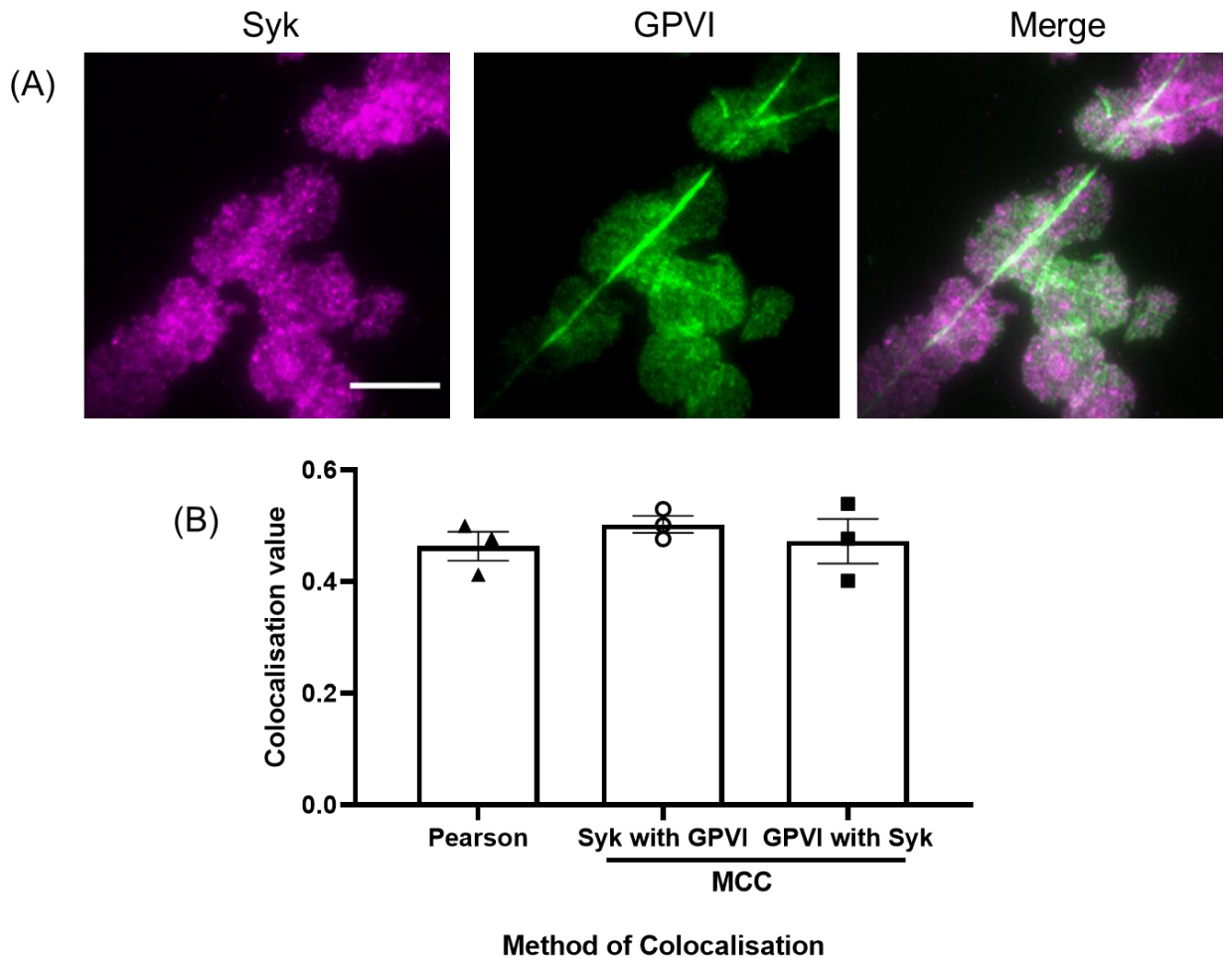


Figure 5.3.6 Syk and GPVI colocalise when platelets are spread on collagen

Washed platelets were spread on collagen for 45 minutes before being fixed, permeabilised and stained with (A) anti-Syk (magenta) and anti-GPVI (green) antibodies followed by secondary staining with Alexa Fluor 555 conjugated donkey anti-mouse and Alexa Fluor 647 conjugated donkey anti-rabbit antibodies. (B) ImageJ with JACoP plug in was used to assess colocalization between GPVI and Syk. n=3, graph represents mean \pm SEM. Scale bar represents 10 μ m.

5.3.7 Btk and CLEC-2 colocalise when imaged in TIRF and spread on rhodocytin

As shown in the previous chapter platelets spread weakly on rhodocytin (Figure 3.3.15). Experiments to investigate the localisation of Btk in relation to CLEC-2 were performed. It is known that CLEC-2 undergoes clustering which is mediated by Src and Syk family kinases in platelets (Pollitt et al., 2014). As Btk has been shown to interact with Syk and Src, it could be hypothesised that Btk may be localised near CLEC-2 (Oda et al., 2000, Wahl et al., 1997). Furthermore, as previous data suggests that there is a stronger requirement for Btk kinase function downstream of CLEC-2 than GPVI (chapter 3 and chapter 4), it is likely that Btk could be localising with CLEC-2 as opposed to GPVI.

Washed platelets were spread on rhodocytin (100nM) for 45 minutes before fixation. Samples were then stained with anti-Btk as previously described and anti-CLEC-2 (AYP1) or IgG controls followed by secondary staining with Alexa Fluor 647 conjugated donkey anti-rabbit and Alexa Fluor 555 conjugated donkey anti-mouse antibodies. Samples were then imaged using TIRFM.

Figure 5.3.7.A shows that Btk (magenta panel) forms a punctate distribution in a similar manner as seen previously when platelets are spread on GPVI ligands. CLEC-2 (green panel) is distributed over the platelet. When merged, there is areas of white, suggesting a large amount of colocalisation between Btk and CLEC-2.

A numerical value of colocalisation was calculated using ImageJ. Using MCC and PCC the mean colocalisation values were greater than 0.65 (Figure 5.3.7.C). This suggests a strong level of colocalization between Btk and CLEC-2.

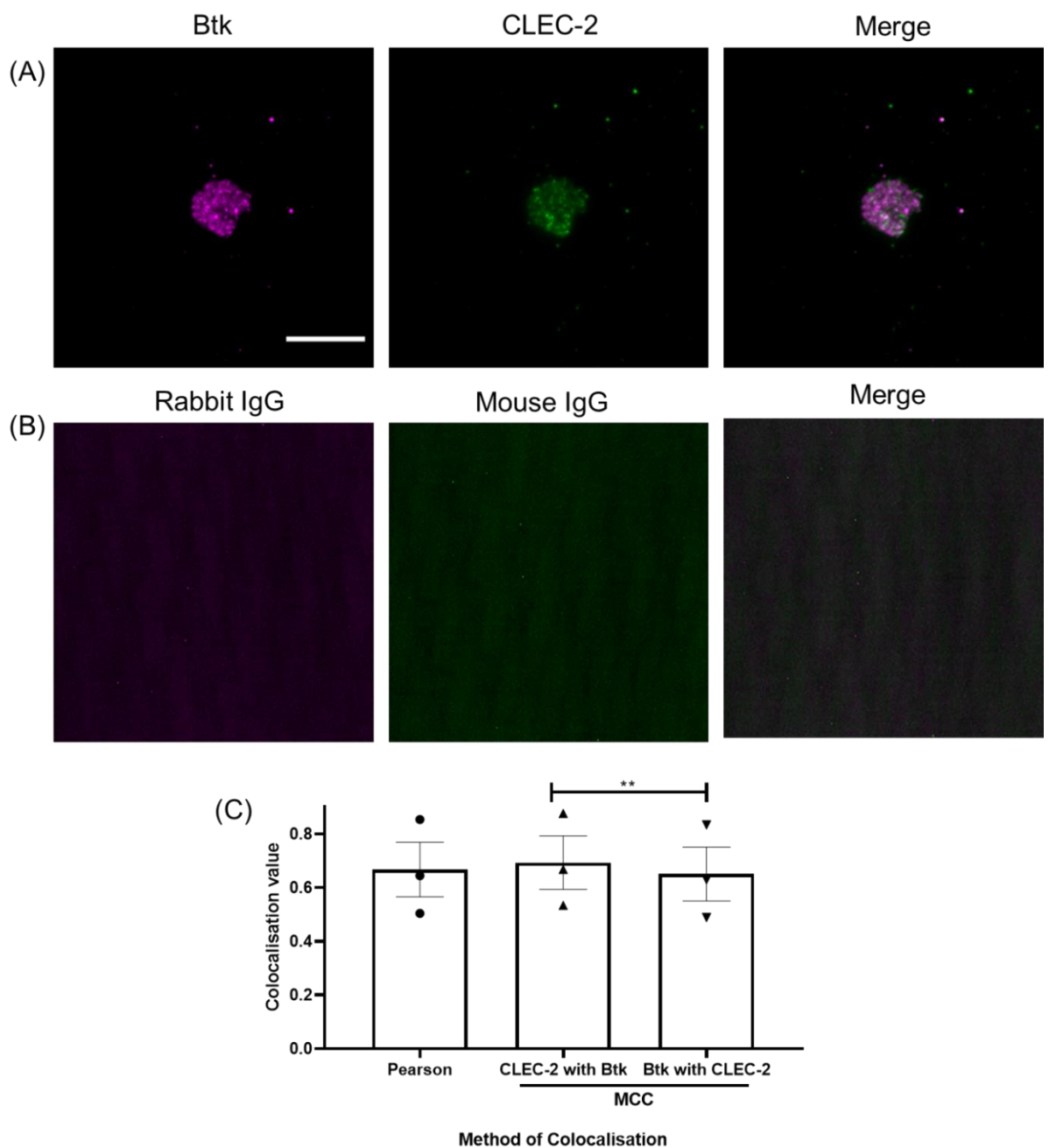


Figure 5.3.7 Btk and CLEC-2 colocalise when spread on rhodocytin

Washed platelets were spread on rhodocytin (100nM) for 45 minutes before being fixed, permeabilised and stained with (A) anti-Btk (magenta) and anti-CLEC-2 (green) or (B) IgG controls and then secondary stained with Alexa Fluor 647 conjugated donkey anti-rabbit and Alexa Fluor 555 conjugated donkey anti-mouse antibodies. Images were merged and (C) colocalization assessed using the ImageJ plugin JACoP n=3, Graph represents mean \pm SEM. Scale bar represents 10 μ m.

5.3.8 Btk and LAT colocalise when spread on CLEC-2 ligand rhodocytin and imaged in TIRFM

Btk and CLEC-2 look to colocalise more than Btk and GPVI. However in GPVI stimulated platelets, Btk looks more likely to localise with LAT. In T cells, the T cell receptor and LAT form distinct 'protein islands' which is where the proteins cluster and are separated by actin (Lillemeier et al., 2010). Therefore, it was investigated if Btk also localises with LAT when platelets spread on a CLEC-2 ligand to see if the protein islands theory is applicable to platelets. It was also to identify if Btk is recruited to the LAT signalosome and if it can be visualised microscopically.

As previously described, washed platelets were spread on rhodocytin for 45 minutes. Platelets were fixed, permeabilised and stained with anti-LAT and anti-Btk antibodies followed by secondary staining with secondary antibodies (Section 5.3.5). Images were taken using TIRFM. When the platelets were spread on rhodocytin, Btk was found to have a punctate distribution (Figure 5.3.8.A). LAT was seemingly localised all over the platelet as was observed previously in GPVI mediated spreading (Figure 5.3.5). The merged image does show a large proportion of white suggesting colocalisation.

Colocalisation was assessed using the ImageJ plugin JACoP. The mean PCC value is 0.54 ± 0.14 , suggesting colocalization of Btk and LAT. Using MCC there is no difference in the amount of Btk that colocalises with LAT, and the amount of LAT that overlaps with Btk, with both values being approximately 0.55, again, suggesting colocalisation between Btk and LAT.

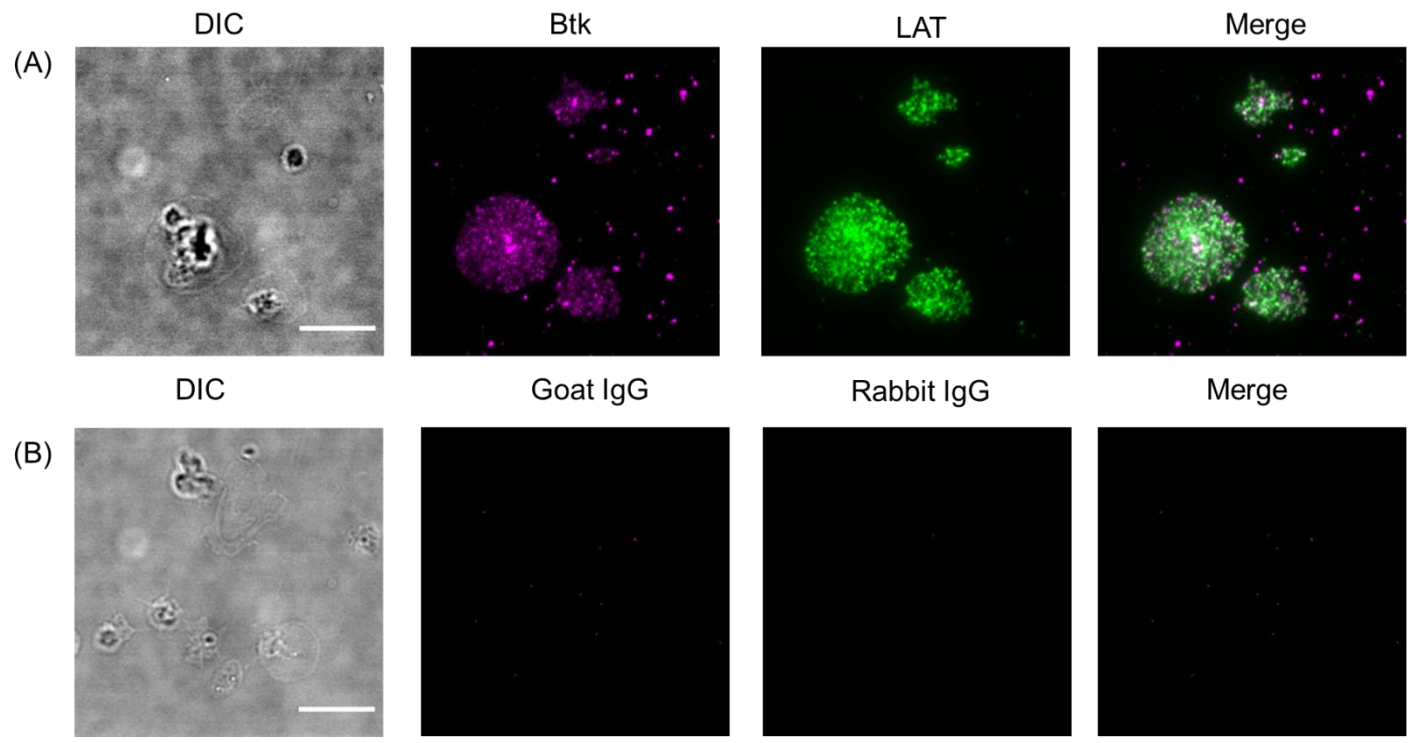


Figure 5.3.8 Btk and LAT colocalise when spread on rhodocytin

Washed platelets were spread on rhodocytin for 45 minutes before being fixed, permeabilised and stained with (A) anti-Btk (magenta) and anti-LAT (green), or (B) IgG controls and secondary stained with Alexa Fluor 647 conjugated donkey anti-rabbit and Alexa Fluor 555 donkey anti

goat antibodies. (C) Images were merged and (C) colocalization assessed using the ImageJ plugin JACoP n=3 Graph represents mean \pm SEM.
Scale bar represents 10 μ m.

5.4 Discussion

Using TIRFM the following aims were addressed

5.4.1 Aim - To investigate the distribution of Btk in platelets

5.4.1.1 Btk forms a punctate pattern when imaged in TIRFM

Btk forms a punctate pattern in spread platelets when imaged using TIRFM (Figures 5.3.1, 5.3.2, 5.3.5, 5.3.7). The punctate appearance also lines up with the collagen fibre in some instances as shown in Figure 5.3.1.C. In other cell types, punctate subcellular localisation patterns can arise from proteins localised to membrane bound organelles, such as apoptotic proteins accumulating in the mitochondria (Wolter et al., 1997), or from macromolecular complexes of sufficient size such as LAT protein islands seen in T cells (Lillemeier et al., 2010).

It is unlikely that Btk forms a punctate pattern in platelets due to localisation of membrane bound organelles, as there is no evidence to show that it is recruited to the mitochondria or is present in α or dense granules (Maynard et al., 2010, Maynard et al., 2007, Meyers et al., 1982). It is more likely that the observed formation of Btk puncta imaged in TIRFM is due to the formation of macromolecular complexes and protein clustering. To support this, Btk has been shown to form a punctate distribution in B cells which is similar to the pattern seen in platelets (Tomlinson et al., 2004b).

Btk's punctate formation may also be related to the localisation of PI3K and the production of PIP3 when platelets are activated downstream of GPVI and CLEC-2. PI3K is expressed at a relatively low level (2,100 copies) per human platelet, as opposed to Btk (11,100 copies) (Burkhart et al., 2012). The punctate pattern of Btk may be due to it localising with the few copies of this protein as it produces PIP3. Furthermore, PI3K and Btk have been shown to co-immunoprecipitate (Battram et al., 2017), suggesting there is an interaction, however it is unknown whether this is directly, or through PIP3. PI3K itself forms cytoplasmic punctate patterns in other cell types, namely NIH-3T3, A431 and MCF-7 cells (Gillham et al., 1999), and PIP3 has been shown to spontaneously cluster (Wang

261

et al., 2015). The punctate distribution of GFP-Tec is also dependent on the production of PIP3 in D10 mouse T cells (Kane and Watkins, 2005). An inhibitor of PI3K, to block the production of PIP3, caused a reduction in the density of the GFP-Tec clusters. Therefore, recruitment of Btk to areas of concentrated PIP3 via its PH domain may explain the punctate appearance of Btk in platelets using TIRFM.

A good direction to take this work and further investigate the puncta formation of Btk in platelets would be to verify the puncta formation is not related to the limited resolution of TIRFM. To do this, a more advanced microscopy technique such as STORM should be used. PI3K inhibitors could also be added to platelets whilst spreading to prevent PIP3 production, and this would help deduce if the punctate formation of Btk is PIP3 dependent.

5.4.2 Aim - To establish the localisation of Btk in relation to GPVI, LAT and CLEC-2 at the membrane using TIRFM

5.4.2.1 Distribution of Btk in platelets spread on GPVI ligands.

Btk does not colocalise with GPVI when platelets are spread on CRP-XL. Values for colocalisation were less than 0.4 which was the threshold value for colocalization set (Figure 5.3.3). In contrast, when spread on collagen, the data suggests that Btk and GPVI may localise, with one species of antibody giving colocalization values greater than 0.4. However, another species of antibody does not, but these values are not statistically significant from each other (Figure 5.3.1.E). The resolution limit of TIRFM may not allow for the localisation for Btk and GPVI to be fully confirmed.

However, there is a significant difference in the localisation of Btk and phosphotyrosine residues when imaged in and out of TIRF ($p \leq 0.01$). All the phosphotyrosine residues within the cell could be stained with 4G10 and therefore it may be that more of the phosphotyrosines are present out of the 100nm imaging area. It is known that proteins can move within the Z plane such as LAT in T cells (Griffié et al., 2017), and therefore

some of the phosphotyrosine residues may be above the TIRF illumination limit when the platelet was fixed. These residues may be the opposite cell membrane, which has continuously phosphorylated proteins present such as Lyn (Schmaier et al., 2009, Aquino et al., 2011). An alternative approach would be to use phosphospecific antibodies.

There appears to be some areas along the collagen fibre that Btk is localised where GPVI is not. This can be visualised in Figure 5.3.1.C. Proteins can be recruited, perform their role and then be in the process of returning to their normal location, such as Syk recruitment to the ITAM containing BCR and then subsequently leaving (Zhou et al., 2006). Therefore, the areas where Btk is absent may be where Btk has left the fibre after performing its role when the cells are fixed.

However, Btk may not localise with GPVI. A recent study using B cells has demonstrated that phosphorylated Btk (assessed using phosphospecific antibodies) does not strongly colocalise with the BCR when assessed using confocal microscopy, with PCC values below 0.4 (Jing et al., 2020). As Btk does not directly localise with the ITAM containing B cell receptor, this is consistent with the data presented in this chapter.

When spread on collagen, Btk and LAT show some colocalisation, with MCC and PCC values being greater than 0.4. A potential reason that Btk may colocalise with LAT as opposed to GPVI is the position Btk lies in the signalling pathway. It has been shown in T cells that LAT and the TCR form distinct 'protein islands' which are signalling complexes separated by actin (Lillemeier et al., 2010). While LAT has been shown to colocalise with the adaptor proteins SLP-76 and Grb2 in T cells using TIRFM (Zhang et al., 2018, Balagopalan et al., 2018), there have been no studies demonstrating that Tec family kinases and adaptor proteins (LAT and BLNK in T and B cells respectively) colocalise using microscopy. It is unknown whether protein islands form in platelets, but it may explain why Btk localises with LAT rather than GPVI.

5.4.2.2 Distribution of Btk in platelets spread on a CLEC-2 ligand

When spread on a CLEC-2 agonist, Btk and CLEC-2 have high colocalisation values when imaged in TIRFM (Figure 5.3.7). More CLEC-2 localises with Btk as opposed to Btk localising with CLEC-2 ($p \leq 0.01$). This may be related to differences in copy number as there are ~6 fold more copies of Btk present in platelets than copies of CLEC-2 (Burkhart et al., 2012, Dunster et al., 2020, Gitz et al., 2014).

Similarly high colocalisation values, when assessed by PCC and MCC, were observed for Btk with LAT when platelets were spread on rhodocytin. However, in the representative images, some platelets spread to a greater extent than others on rhodocytin. The higher values of colocalisation may be related to the degree of platelet spreading as molecules maybe densely localised in unspread platelets compared to spread platelets.

5.4.2.3 Possible reasons for the lack of colocalization between of Btk and other proteins in this study

Using two methods of assessing colocalisation, MCC and PCC, Btk did not strongly colocalise with GPVI, but did with CLEC-2 (Figures 5.3.1 and 5.3.7). In a recent study using biochemical methods, Btk was found to be absent from lipid rafts following platelet stimulation with both GPVI and CLEC-2 agonists. Therefore it unsurprising that it did not colocalise with GPVI which was found to be present in lipid rafts (Izquierdo et al., 2019). It is controversial whether CLEC-2 is present in lipid rafts, with reports of CLEC-2 being present (Pollitt et al., 2010), and absent from lipid rafts (Manne et al., 2015b). As Btk does not localise in lipid rafts (Izquierdo et al., 2019), it is not unreasonable that it is localising with CLEC-2 as it also may not be in lipid rafts. However, Btk does appear to localise with LAT, which is known to be present in lipid rafts (Locke et al., 2002, Bodin et al., 2003, Izquierdo et al., 2019), so this hypothesis may not be correct.

In order to test this hypothesis, experiments could be performed to gently disrupt lipid rafts, but this may impact spreading (Lier et al., 2005). Or, alternative experiments to stain

for Btk in conjunction with cholesterol may identify if Btk is localising to lipid rafts, where GPVI signalling is known to take place (Locke et al., 2002).

Another possible explanation for the lack of colocalisation of Btk and other proteins may be related due to the copy numbers. Perfect colocalisation (MCC score of 1) is very unlikely in studies between Btk, and phosphotyrosines due to the large variations of copy number within the platelet. There is not an exact number of phosphotyrosines present within a stimulated platelet, but it would be expected it to be significantly larger than the 11,100 copies of Btk (Burkhart et al., 2012). There are 9600 copies of GPVI and 4800 of LAT. As there are more copies of Btk, the ratios of these proteins are not 1:1, which may explain why there is a low level of colocalisation.

The use (or not) of phosphospecific antibodies may have also altered the results. In the recent pre-publication by Pallini et al 2020, a phosphospecific Syk antibody and a Syk antibody which binds regardless of phosphorylation (referred to as total-Syk) were used to investigate the localisation of Syk in relation to the collagen fibre. The total-Syk antibody labels the entire platelet in confocal microscopy, whereas the phosphospecific Syk antibody appears to localise along the collagen fibre. This is also mirrored when antibodies for phosphospecific LAT and total-LAT are used.

A further possible reason may be that the time point of 45 mins was too short. Indeed, Pallini et al demonstrated that while there is some phosphorylated LAT that colocalises with GPVI in confocal microscopy in this time frame, the level of colocalization is greatly increased after 3 hours of spreading (Pallini et al., 2020). This suggests that LAT is recruited to the fibre at a slower rate, or prolonged signalling may mediate the recruitment of different proteins. This may be happening to Btk.

As Btk has been to co-immunoprecipitate with LAT (Pasquet et al., 1999b), it is not unreasonable to believe that more Btk may be present at the fibre at a later time point. However, the biochemical studies are much shorter in time frame, so it may not be applicable to reason that Btk would be present at a later time point due to its interaction

with LAT in a short biochemical experiment. Nonetheless, experiments could be performed using a longer time point, or shorter time points such as stimulating in suspension, to investigate this further.

5.4.3 Aim - To identify changes in Btk localisation in the presence of a Btk inhibitor

The punctate distribution of Btk did not change in the presence of the Btk kinase inhibitors ibrutinib and acalabrutinib (Figure 5.3.2). In B cells and platelets, the recruitment of Btk is mediated by the PH domain of Btk and its interaction with the lipid PIP3 (Saito et al., 2001, Várnai et al., 1999, Salim et al., 1996, Durrant et al., 2017, Patel et al., 2019). This mechanism is not believed to be kinase dependent, therefore it is consistent with the results in this study that the localisation does not change in the presence of a Btk inhibitor.

Interestingly, when investigating the clustering of GFP-Tec in T cells using TIRFM, a Src inhibitor caused a greater inhibition of Tec clustering density when compared to a PI3K inhibitor. This suggests that catalytic activity of Tec is required for its clustering, as SFK's are responsible for the phosphorylation of Tec family kinases (Park et al., 1996, Wahl et al., 1997). However, SFKs are not just responsible for phosphorylation of TFK's, they also phosphorylate ZAP-70, which mediates the phosphorylation of LAT. The inhibition of SFK catalytic activity may prevent Tec clustering through a reduction in LAT signalosome tyrosine phosphorylation. Therefore Tec may not be recruited to the LAT signalosome via its SH2 domain interactions (Palacios and Weiss, 2004).

Although the platelets are pre-treated with ibrutinib and acalabrutinib it is difficult to know if the drug is bound to the platelets. There has been a study using a fluorescent version of ibrutinib to image tumour cells. The fluorescently labelled ibrutinib colocalised strongly with a fluorescently tagged Btk. It was less efficacious than unlabelled ibrutinib, as a higher concentration was required in order to cause Btk inhibition in a cell free assay than unlabelled ibrutinib (Turetsky et al., 2014, Kim et al., 2015). Nonetheless, the use of

fluorescently tagged ibrutinib would allow for the confirmation that the drug is entering the platelet and would enable for visualisation of Btk in a live cell without the use of antibodies.

5.5 Conclusion

Using TIRFM, Btk does not strongly colocalise with GPVI when platelets are spread on CRP-XL. There is a suggestion of weak colocalization of Btk and GPVI on collagen and Btk may localise to areas of the collagen fibre in areas that GPVI is not absent through an unknown mechanism. Btk and LAT look to colocalise more strongly than Btk and GPVI on collagen.

When spread on rhodocytin, Btk looks to localise with CLEC-2, LAT and phosphotyrosine residues but this may be an artefact due to the lack of full spreading in the platelets.

The resolution, which is the distance of which the microscope can distinguish two separate molecules, is limited at 200nm for TIRFM (Kudalkar et al., 2016). This may conceal true results of colocalisation. Therefore alternative methods to assess colocalisation should be used to confirm the results obtained. Stochastic optical reconstruction microscopy, has a greater optical resolution limit of approximately 20-50nm (Rust et al., 2006). This allows for more accurate distinguishing of molecules and was used in the next chapter to further investigate the localisation of Btk in relation to GPVI, LAT and CLEC-2. It also allows for the assessment of protein clustering which can act as a mechanism of protein regulation.

6 Investigating the localisation and clustering of Btk, GPVI, LAT and CLEC-2 using Stochastic optical reconstruction microscopy.

The distance of which two separate molecules can be distinguished is limited at 200nm for TIRFM (Kudalkar et al., 2016). This may have concealed or potentiated true results of colocalisation in chapter 5. Stochastic optical reconstruction microscopy (STORM) was used to further investigate the localisation of Btk in platelets. STORM allows for increased fluorophore localisation and therefore can be used to investigate colocalisation and protein clustering more accurately due to the higher resolution (Metcalf et al., 2013, Ovesný et al., 2014, Rust et al., 2006).

6.1 Introduction

6.1.1 Protein clustering as a mechanism of regulation

Protein clustering provides an extra layer of regulation upon signal activation. Large protein clusters are connected to enhanced signalling as it brings kinases closer to their targets, reducing the space that molecules need to move or diffuse too. This makes the signalling more efficient (Cebecauer et al., 2010). In platelets, clustering of GPVI and CLEC-2 is required for the initiation of signalling (Pollitt et al., 2014, Poulter et al., 2017). Clustering has also been demonstrated to play a role in signal termination, such as clustering of the TCR and the phosphatase CD45 has been implicated in terminating signalling in T cells (Varma et al., 2006)

GPVI clustering is determined by the ligand that the platelet is interacting with and is a level of regulation for GPVI mediated signalling and platelet activation (Poulter et al., 2017, Dunster et al., 2020). Although platelet spreading and adherence to a variety of GPVI ligands is reduced in the presence of a Syk or SFK inhibitor, clustering of GPVI is still present when assessed using TIRFM (Poulter et al., 2017). Therefore, the mechanism

which regulates GPVI clusters in unknown but appears to be Src and Syk kinase independent.

Losartan has been proposed to inhibit GPVI clustering. This molecule is an angiotensin II receptor antagonist, and it inhibits platelet aggregation to collagen and CRP-XL, but it is not a GPVI antagonist. FcR γ chain phosphorylation was inhibited in the presence of losartan in stimulated samples so it was hypothesised that the GPVI clustering was being inhibited. Indeed, using the proximity ligation assay Duolink, it was identified that losartan did inhibit GPVI clustering via an unknown mechanism (Jiang et al., 2015). Work from another group did corroborate that aggregation to collagen was inhibited. However, when GPVI clustering was assessed using STORM the cluster density (number of clusters per μm^2) and the cluster area were unaltered in the presence of losartan, suggesting that losartan did not alter GPVI clustering (Onselaer et al., 2020). Both studies used the same GPVI ligands and losartan concentrations, so the differences may be due to experimental methods.

The concept of receptor clustering providing a level of regulation is not limited to GPVI in platelets. CLEC-2 has also been demonstrated to undergo clustering following ligand engagement with Podoplanin (Watson et al., 2009, Pollitt et al., 2014). However, SFK's and Syk tyrosine kinases regulate the clustering of CLEC-2 (Pollitt et al., 2014).

Furthermore, if the receptor were to cluster, clustering of the intracellular tyrosine kinases responsible for mediating signalling would also be expected. This has been observed in B cells with Btk recruited to microclusters (0.5 to $1\mu\text{m}$ in size) and larger clusters (average surface area of $16\mu\text{m}^2$) during BCR signalling (Fleire et al., 2006). In addition to Btk, these clusters consist of other phosphorylated proteins including Syk, BLNK and PLC γ 2 (Weber et al., 2008). Disruption of clusters through a lack of protein recruitment can result in immunodeficiencies (Wang et al., 2014), highlighting the importance of protein clustering.

In B cells, Btk is not thought to be directly responsible for mediating the clustering of the BCR, however, it is indirectly involved. Btk deficient B cells have reduced actin

polymerisation when assessing the amount of free actin monomers (G actin) over time when stimulated (Sharma et al., 2009). This suggests that in B cells, Btk is involved in actin remodelling, which contributes towards the merging of BCR microclusters (Liu et al., 2011). Microclusters move towards the centre of the cell in *in vitro* 2D experiments. Actin decreases around individual BCR clusters and remodels around the outer edge of the central BCR cluster, resulting in centripetal movement of the cluster (Liu et al., 2016). The centripetal large BCR cluster is known as the immune synapse (IS), which forms at the interface between the antigen presenting cell and the B cell. Btk contributes to IS formation via shuttling and scaffolding other proteins but also by its catalytic activity (Roman-Garcia et al., 2018).

6.1.2 Microscopy techniques and analysis methods used in this study

6.1.2.1 Stochastic optical reconstruction microscopy

Stochastic optical reconstruction microscopy (STORM) is a single molecule localisation method of microscopy that yields quantitative and qualitative data (co-ordinates and an 'image'). First described by Rust et al., 2006, it is a technique that utilises individually tagged fluorescent molecules to generate an image. It has far superior imaging resolution compared to TIRFM, with a resolution of up to 20nm (Rust et al., 2006).

Direct STORM (DSTORM) is the most widely used form of STORM due to its relative simplicity compared to other types. Images can be used to generate a 3D image to investigate the axial location of molecules within a cell. Or images can be taken within TIRF to investigate proteins close to the plasma membrane. Images are taken in a fixed sample, identifying the location of proteins of interest using fluorescently labelled antibodies. High laser power in a redox buffer initiates the stochastic switching of fluorophores. This is often referred to as blinking. Immediately before imaging, the liquid present in the well is removed and replaced with chemicals and enzymes that stabilise the

blinking by regulating the photophysical properties of the fluorophores. The chemicals include reducing agents to induce the dark state and oxygen scavengers to ensure the fluorophore spends the correct amount of time in each state (Heilemann et al., 2008).

Figure 6.1.1.A shows the limits of conventional fluorescence microscopy, with different fluorophores overlapping. The advantage to STORM is that fluorophore molecules are individually turned on and off in a sequential stochastic fashion repeatedly during a user defined number of frames. During the reconstruction phase, algorithms within the software use the point spread function (Figure 6.1.1.B) to pinpoint the location of the fluorophore for each of the blinks. This generates a super-resolved reconstructed image (Figure 6.1.2) and the co-ordinates of the blinks as an output (Poulter et al., 2018).

STORM microscopy is a quantitative method of microscopy. The fluorophore co-ordinates enable analysis of data such as protein clustering and colocalisation with a greater resolution than traditional methods. STORM has been used in platelets to investigate the structure of actin nodules (Poulter et al., 2015) and the clustering of proteins such as GPVI, CLEC-2 and Syk (Pollitt et al., 2014, Poulter et al., 2017, Haining et al., 2017b, Clark et al., 2019, Dunster et al., 2020).

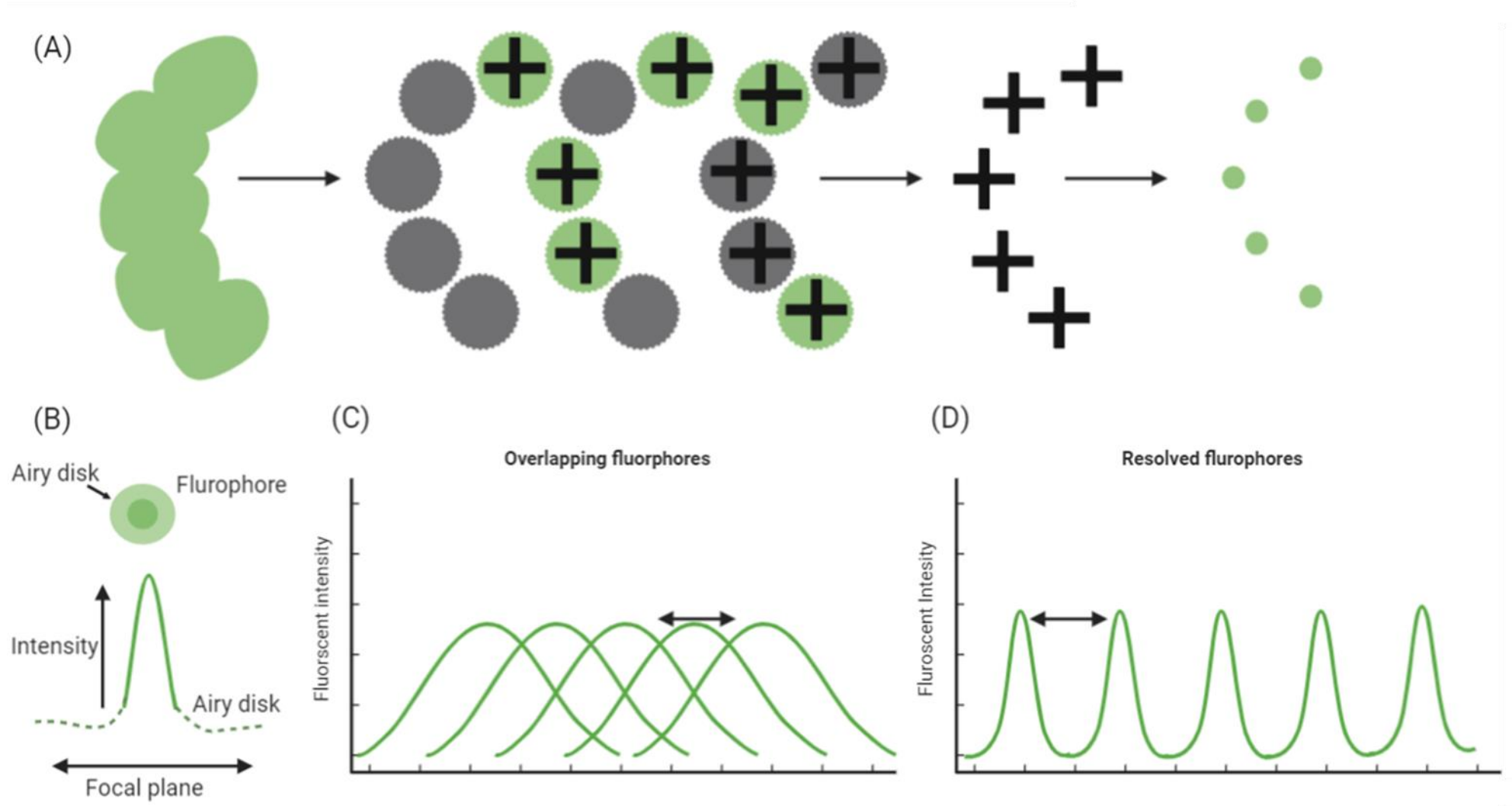


Figure 6.1.1 Principles of STORM

(A) Traditional conventional fluorescence microscopy cannot distinguish fluorophores closer than 200nm (far left). STORM involves the stochastic switching on (in green) and off (in grey) of fluorophores to create a reconstructed image with greater resolution. (B) Fluorophores emit light in an airy disk where there is a bright centre with (dark green) with decreasing intensity around it (airy disk). Below is the fluorescence profile representations of the refraction pattern which is the point spread function (B, dark crosses in A). The sequential blinking and STORM algorithm the centre of the point spread function of the fluorophore as shown by the crosses, which allows for distinct fluorophores to be viewed with a greater resolution. (C) in conventional microscopy (Figure A, first panel) the overlapping point spread functions does not distinguish between PSF (black arrow). Whereas in STORM generates a reconstructed image with (D) increased resolution as the PSFs can be separated.

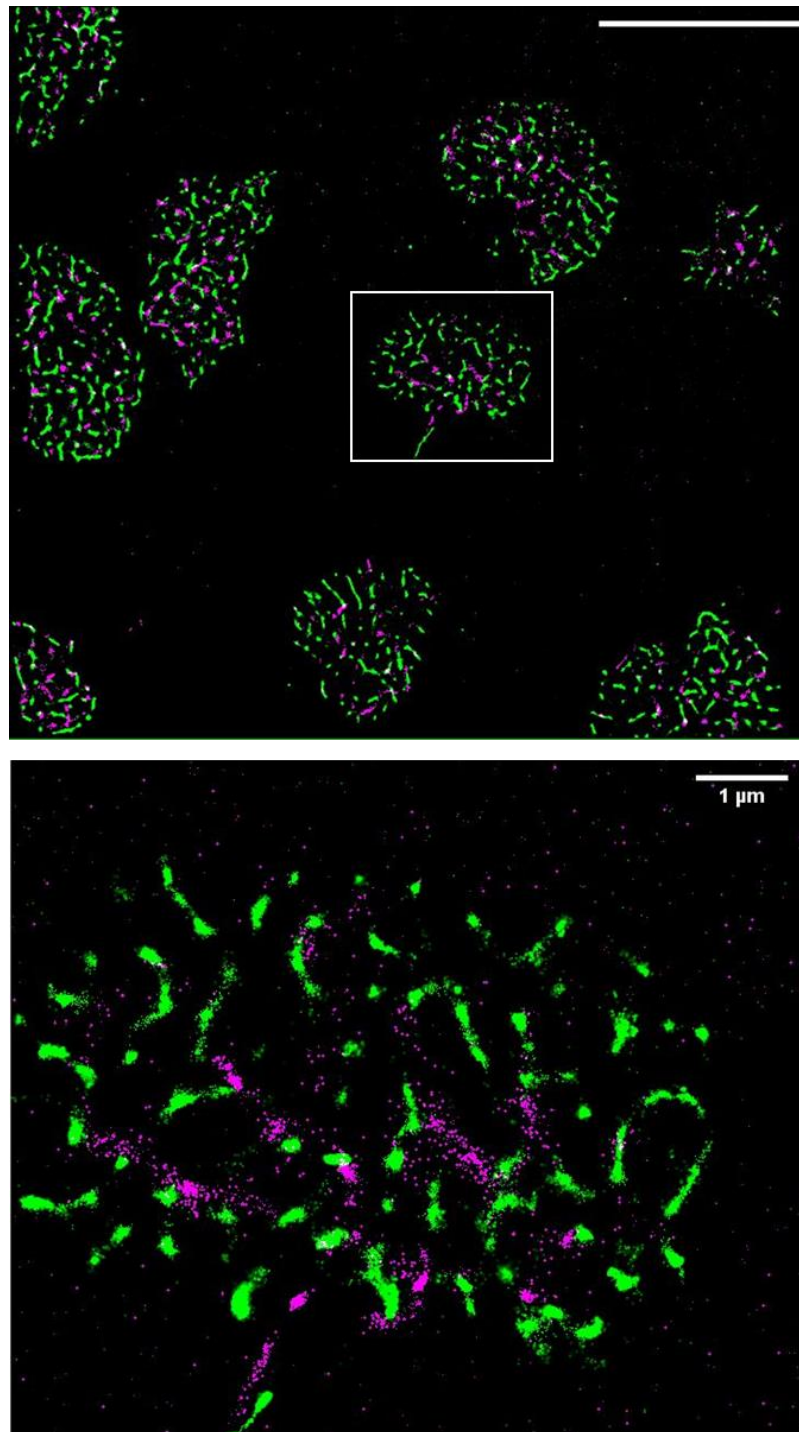


Figure 6.1.2 Reconstructed STORM image of platelets

A reconstructed STORM image with a zoomed in Section to show that the resolution allows for single molecule localisation and clustering. Each dot represents a blink Scale bar 10 μ m and 1 μ m.

6.1.3 Coordinate based colocalisation

Coordinate based Colocalisation (CBC) is a method to assess the amount of Colocalisation seen in super resolution co-ordinate files (Malkusch et al., 2012, Malkusch and Heilemann, 2016, Pagon et al., 2016). CBC is a measure of how molecule A is distributed throughout the cell in relation to molecule B within a certain defined radius, as shown in Figure 6.1.3. Each point is assigned a density gradient of the number of molecules of the opposite species are present. Once each molecule has a density gradient, the output values are ranked using Spearman's correlation coefficient. This gives each localisation a CBC value between -1 and +1. A CBC of -1 means that the localisations of the two molecules are segregated, a value of 0 is random distribution, and a value of +1 defines localisations that are totally colocalised. These localisations would be stacked upon each other if the images were overlaid. Values >0 is deemed to be more colocalised than would randomly occur, but 0.4 is defined as the threshold to identify colocalisation suggested Pagon and colleagues.

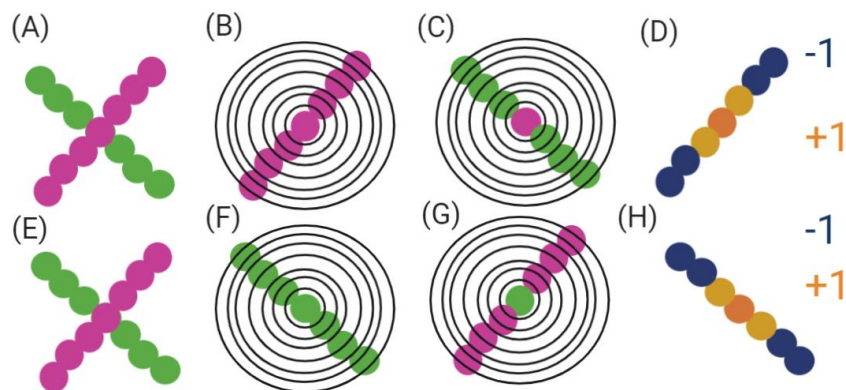


Figure 6.1.3 Principles of CBC analysis

(A), (E), are the single molecule localisations of two different molecules, represented as magenta and green dots. (B), (F), each localisation of either colour, the distribution of the neighbour localisations of the same species is calculated as the radius (black circles) increases in user defined increments, this creates the density gradient for each individual channel (C), (G), in the second step the density gradient (distribution of neighbour

localizations) from centre of the radius of the alternate colour is calculated. (D), (H), Each local density is tested for correlation using Spearman's correlation coefficient, with +1 values shown in orange being colocalised and blue values being anti colocalised. Each single molecule localisation of each different molecule is given an individual colocalisation value. Figure adapted from Malkusch et al., 2012.

6.1.4 Density based spatial clustering of applications with noise (DBSCAN)

DBSCAN is an algorithm that clusters data based on distance and a number of minimum points required to form a cluster. A schematic is shown in Figure 6.1.4. It is a propagative cluster method (the clusters are not set to a particular size). Localisations are connected to form a cluster if the number of neighbouring point (minimum points) is above the threshold within a particular radius (r). Both parameters are user defined. Localisations are recruited to the propagating cluster until the parameters are no longer fulfilled (Malkusch and Heilemann, 2016, Pagoon et al., 2016). DBSCAN also identifies noise localisations – molecules that do not cluster and are not on the propagative edge which is beneficial (Pagoon et al., 2016). DBSCAN is also advantageous as it can detect arbitrary shaped clusters, whereas other clustering methods such as Ripley's K function cannot.

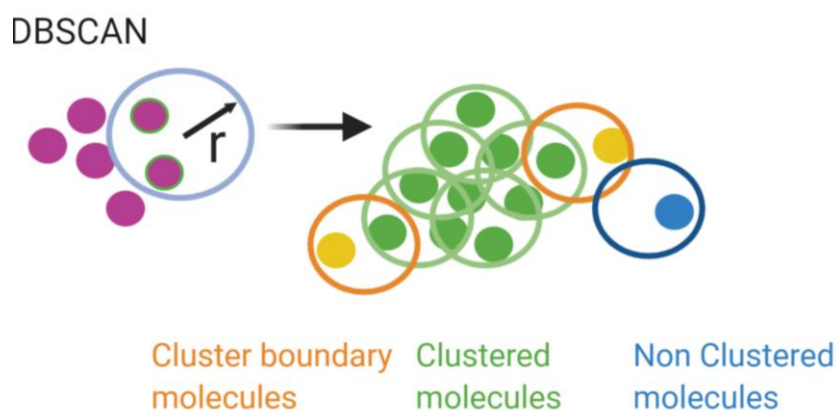


Figure 6.1.4 Schematic of DBSCAN

DBSCAN is a propagative cluster detection method where connectivity between localisations is established if the number of neighbouring localisations is above a certain threshold (e.g. 2 in the diagram) within a radius r (e.g. 20 nm). The connection is propagated if the parameters are fulfilled (green dots) and stops when the parameters are no longer fulfilled (yellow dots). This method can also identify any remaining isolated points or noise (blue dot).

6.1.5 Software used in this study

6.1.5.1 ChriSTORM

ChriSTORM is a series of ImageJ macros and scripts (Leterrier et al., 2015) that allow translation of Nikon N-STORM output files to be in the correct format to analyse data using ThunderSTORM (Ovesný et al., 2014). In addition, the scripts allow for the two colours to be separated into individual colours in order to be processed in LAMA (Malkusch and Heilemann, 2016).

6.1.5.2 LocAlisation Microscopy Analyser - LAMA

LAMA software, designed by Malkusch and Heilemann, 2016, is a freely available software that extracts quantitative information from single molecule data. The software concentrates on producing biologically relevant information such as clustering, CBC and localisation accuracy (Malkusch and Heilemann, 2016).

Clustering analysis is performed using DBSCAN (Section 6.1.4). In addition to DBSCAN, it implements a polygon-based morphology algorithm to provide information on the individual cluster size and number of localisations to cluster.

6.1.5.3 Cluster detection with a degree of colocalisation -ClusDoC

Published after LAMA, ClusDoC combines both cluster detection using DBSCAN and CBC to achieve more detailed analysis (Pageon et al., 2016). The software runs through MATLAB and allows data to be subclassified for a detailed analysis to give the number of clusters that are colocalised. The typical workflow is shown in Figure 6.1.5 below.

It is split into two Sections – the CBC analysis (Section 6.1.3 and shown in red in Figure 6.1.5), whilst simultaneously clustering the localisations using DBSCAN (shown in green, Figure 6.1.5). The ClusDoC module (shown in blue) compiles the previous Sections by amalgamating cluster detection information and CBC values to distinguish between colocalised clusters and non-clustered molecules.

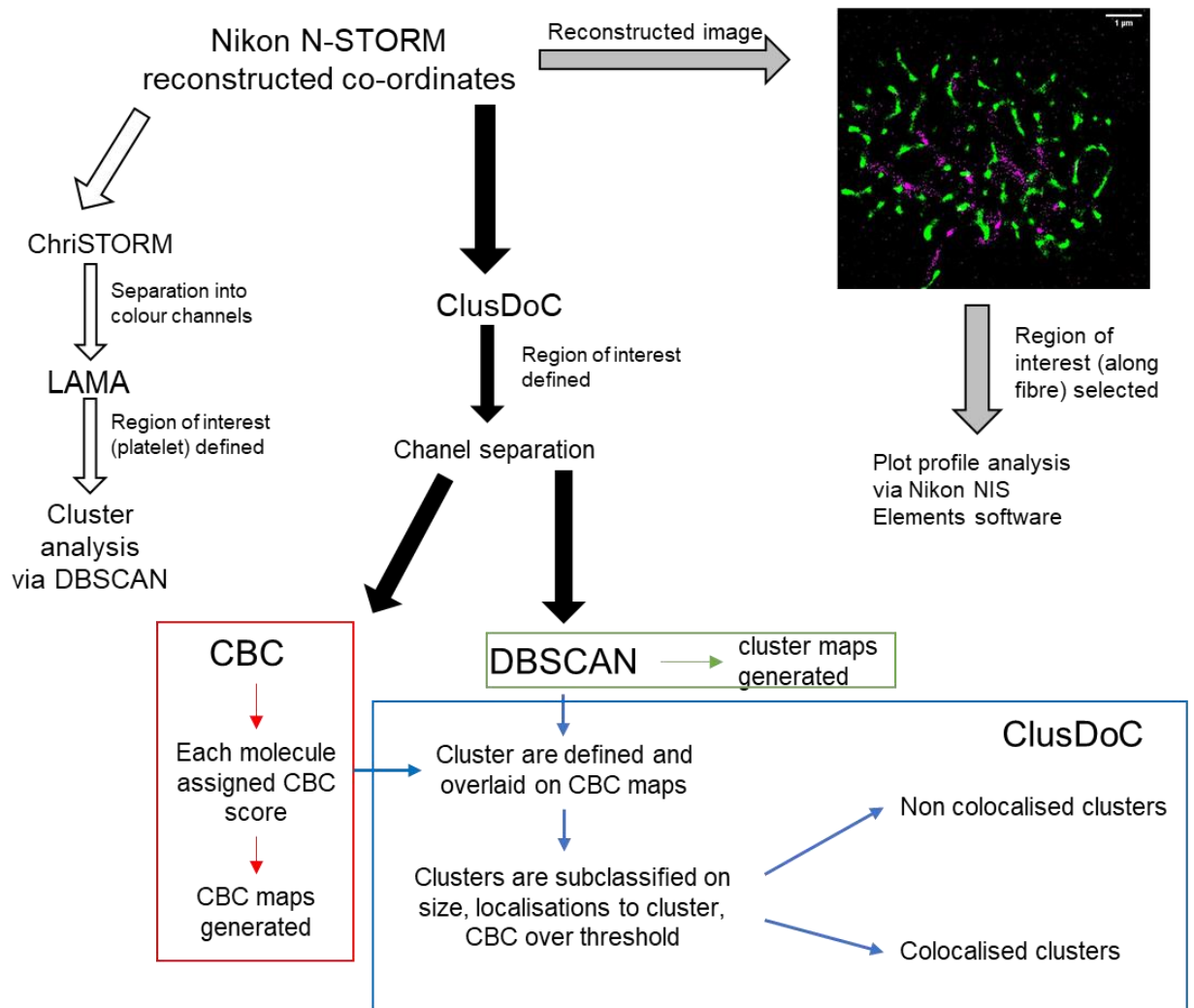


Figure 6.1.5 The analysis workflow taken in this study. ClusDoC workflow from Pagon et al., 2016

A Nikon reconstructed image is loaded into ChriSTORM and separated into two colour coordinates for LAMA. LAMA then uses DBSCAN analysis to provide clustering parameters of the two separate channels. ClusDoC was used to investigate co-clustering. The CBC values for each individual localisation in a user defined radius (visualised in red) are calculated. Meanwhile, clustering analysis is performed using DBSCAN to yield

information about clustering and cluster maps (green Section). The final Section compiles the data from the CBC and DBSCAN. The output is the amount of colocalised and non-colocalised clusters and their parameters. The reconstructed image from the co-ordinates was analysed in Nikon NIS elements using plot profile to assess for colocalization

6.2 Aims and Hypothesis

Little is known about the distribution and localisation of Btk in platelets. Previous experiments, using TIRFM, suggested that Btk may be weakly localised with GPVI and LAT. There is stronger evidence that Btk is localising with LAT and CLEC-2 when spread on rhodocytin. However, the resolution offered with TIRF cannot confirm these observations.

Irrespective of ligand, Btk forms a punctate distribution in platelets (chapter 5, Figure 5.3.1), similarly to the distribution observed in immune cells (Kane and Watkins, 2005, Tomlinson et al., 2004b). This alludes to the ability of Btk to cluster. Furthermore, using modelling studies, it is believed that Btk would undergo protein clustering due to the phosphorylation of one molecule of Btk by an already active molecule of Btk (Chung et al., 2019). Therefore, it is likely that Btk will undergo clustering when platelets are active. More clustering may be observed on rhodocytin due to the stronger requirement of Btk in CLEC-2 mediated signalling (chapter 3 and 4).

Hypothesis: Btk will cluster when platelets are spread on GPVI and CLEC-2 ligands. Btk will colocalise with LAT on both rhodocytin and collagen but is less likely to localise with GPVI. Btk will localise with CLEC-2.

Aims

- To investigate the clustering of Btk on collagen, CRP-XL and rhodocytin.

- To confirm if Btk recruitment is independent of its kinase function as suggested using TIRFM.
- Identify if clustering of GPVI is dependent on Btk kinase activity using acalabrutinib
- To verify the colocalisation results in chapter 5 using dSTORM, a greater resolution method of microscopy.

6.3 Results

6.3.1 Investigating protein clustering analysis using STORM and LAMA

GPVI and CLEC-2 are present on the surface of platelets as dimers, and form clusters following activation (Clark et al., 2019, Pallini et al., 2020, Poulter et al., 2017, Martyanov et al., 2020, Pollitt et al., 2014). Btk forms a punctate formation in platelets (chapter 5, Figures 5.3.1 onwards), alluding to cluster formation. Hence, the clustering of Btk and other proteins was investigated on GPVI and CLEC-2 ligands.

Cluster analysis was performed using LAMA software on reconstructed STORM coordinates. A cluster was defined as 10 points across a range of radii (25 to 100 nm) to investigate the degree of clustering, and to identify an appropriate cluster diameter. Each cluster is identified by a different colour in the representative image.

6.3.1.1 *Btk and GPVI cluster on collagen*

Btk has not been shown to cluster using dSTORM, whereas clustering of GPVI on collagen is required for signalling and has been described in the literature (Poulter et al., 2017, Dunster et al., 2020, Onselaer et al., 2020, Pallini et al., 2020, Clark et al., 2019). Initial experiments were performed to confirm that the clustering approaches applied in this study were consistent with the literature.

Washed platelets were spread on collagen (10µg/mL). Cells were fixed and stained with anti Btk and anti GPVI, before staining with secondary antibodies Alexa Fluor 555 conjugated donkey anti-mouse and Alexa Fluor 647 conjugated donkey anti-goat. Samples were imaged using a Nikon N-STORM system in blinking buffer to induce fluorophore blinking (Metcalf et al., 2013). 20,000 frames per fluorophore were captured and reconstructed using Nikon NIS-Elements STORM analysis module, applying drift correction and gaussian rendering. Individual fluorescent blinking events were filtered on photon count and only those with a count >400 were selected for further analysis.

Clustering analysis was performed using LAMA and DBSCAN, to obtain the clusters in the field of view and the cluster size (Malkusch and Heilemann, 2016). A cluster was defined as the minimum radius (25 to 100nm) and having a minimum of 10 points consistent with the work of Poulter and colleagues who selected 10 points within 50nm.

For Btk clusters, as the radius increases, both the cluster size and the number of localisations to a cluster positively correlate with each other ($p \leq 0.01$), Figure 6.3.1.C. For GPVI as the radii increases, the cluster size also increases ($p \leq 0.05$), whereas the number of localisations to a cluster does not (Figure 6.3.1.D). The number of clusters gets smaller as the radii increases, ($p \leq 0.01$). This may be a result of clusters merging to form larger clusters.

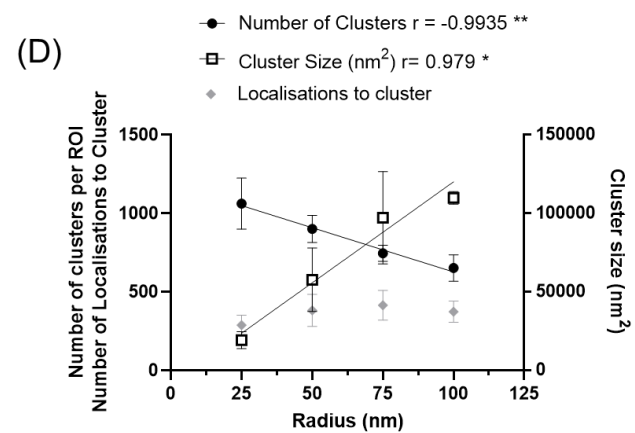
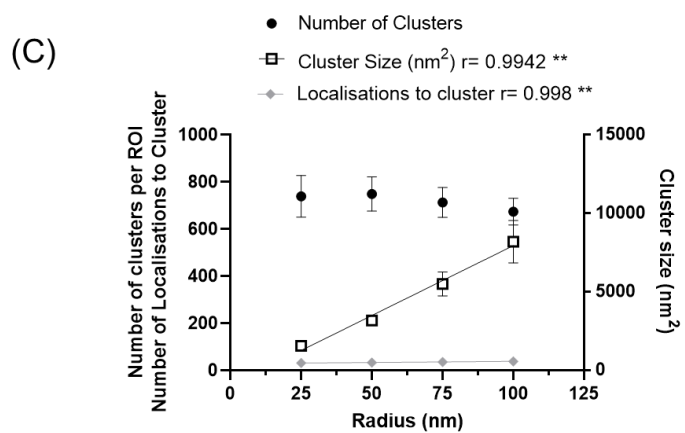
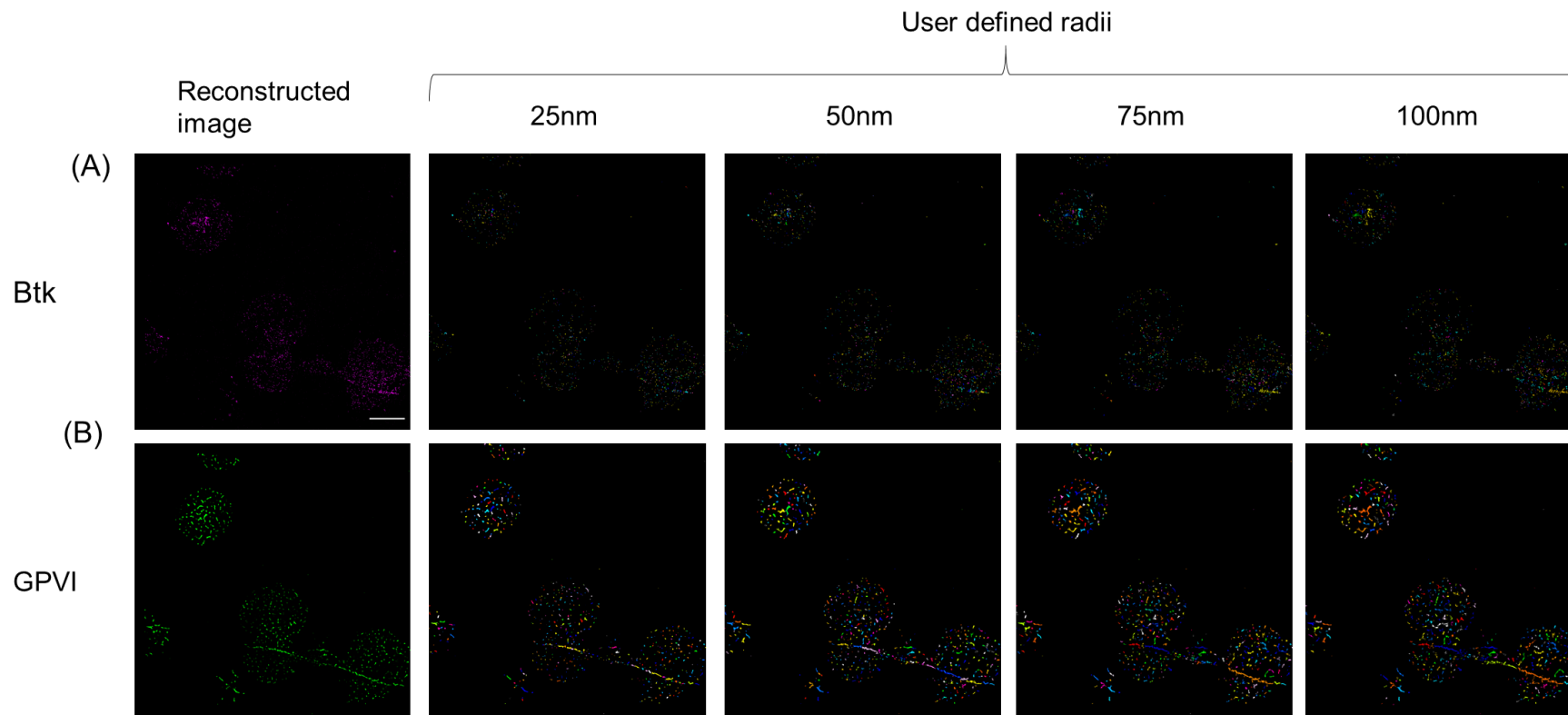


Figure 6.3.1 GPVI and Btk cluster on collagen

Washed platelets 2×10^7 cells /mL were spread on $10 \mu\text{g/mL}$ collagen for 45 minutes before fixation, permeabilization and staining with (A) Anti-Btk and (B) Anti-GPVI antibodies followed by secondary staining with Alexa Fluor 555 conjugated donkey anti-mouse and Alexa Fluor 647 conjugated donkey anti-goat . Samples were imaged using a Nikon N-STORM system in blinking buffer to induce fluorophore blinking. 20,000 frames were captured and reconstructed using Nikon NIS-Elements STORM analysis module, applying drift correction and gaussian rendering. 3 fields of view from 3 independent experiments were imaged. Individual fluorescent blinking events were filtered on photon count and only those with a count >400 were selected for further analysis. Cluster analysis was performed using DBSCSAN algorithm in LAMA software, with a cluster being defined as 10 localisations within 25nm, 50nm, 75nm and 100nm. Correlation analysis was performed using GraphPad Prism 8 with the significant R values of correlation being stated on the graph for (C) Btk clusters and (D) GPVI clusters. Graphs represents mean \pm SEM * $p \leq 0.05$, ** $p \leq 0.01$. Scale bar represents $5 \mu\text{m}$.

6.3.1.2 Btk and GPVI cluster on CRP-XL

After Btk was shown to cluster on collagen, similar experiments were performed with CRP-XL. This was to identify if Btk clustering is a result specific to the fibrous ligand of collagen, and to discount for any interplay of the integrin $\alpha_2\beta_1$. It is known that there is differences in the level clustering of GPVI on CRP-XL as opposed to collagen (Poulter et al., 2017), and it is not unreasonable to hypothesise that Btk clustering could be different.

Washed platelets were spread on CRP-XL (1 μ g/mL) for 45 minutes. Platelets were then fixed, permeabilised and stained with antibodies as previously described (Section 5.3.3). Samples were imaged and analysed as described in Section 6.3.1.1.

When the radii is increased, the number of Btk clusters and the size of the Btk clusters both strongly positively correlate as r values are both almost 1 (0.997 and 0.993 for number and size of clusters respectively, $p \leq 0.01$) (Figure 6.3.2.C).

For GPVI, as the parameter of the cluster radii increased, so did the cluster size ($r = 0.995$, $**p \leq 0.01$). This is consistent to as what has been observed in other experiments and is also is what is observed as to what happens on collagen. In contrast, as radii increases, the number of clusters is negatively correlated. The r value is -0.953, $p \leq 0.05$, suggesting strong negative correlation. The number of localisations per cluster strongly positively correlates, indicating these correlations are likely due to the larger radii incorporating smaller clusters into larger clusters as the set parameter increases.

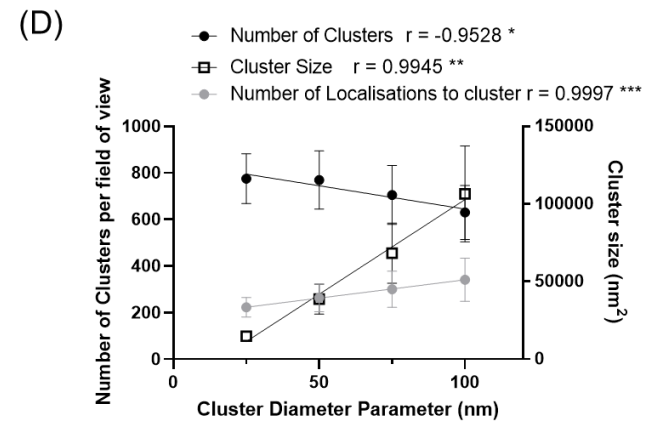
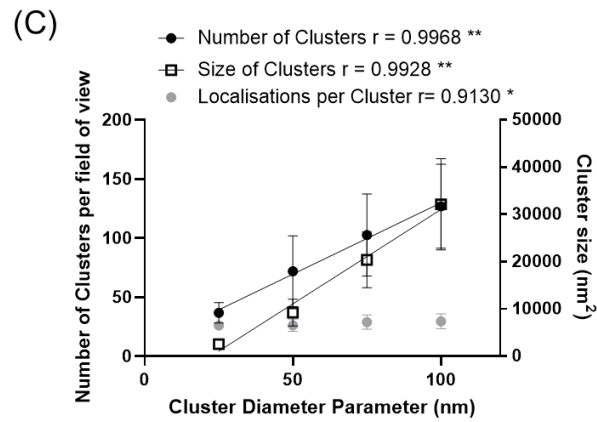
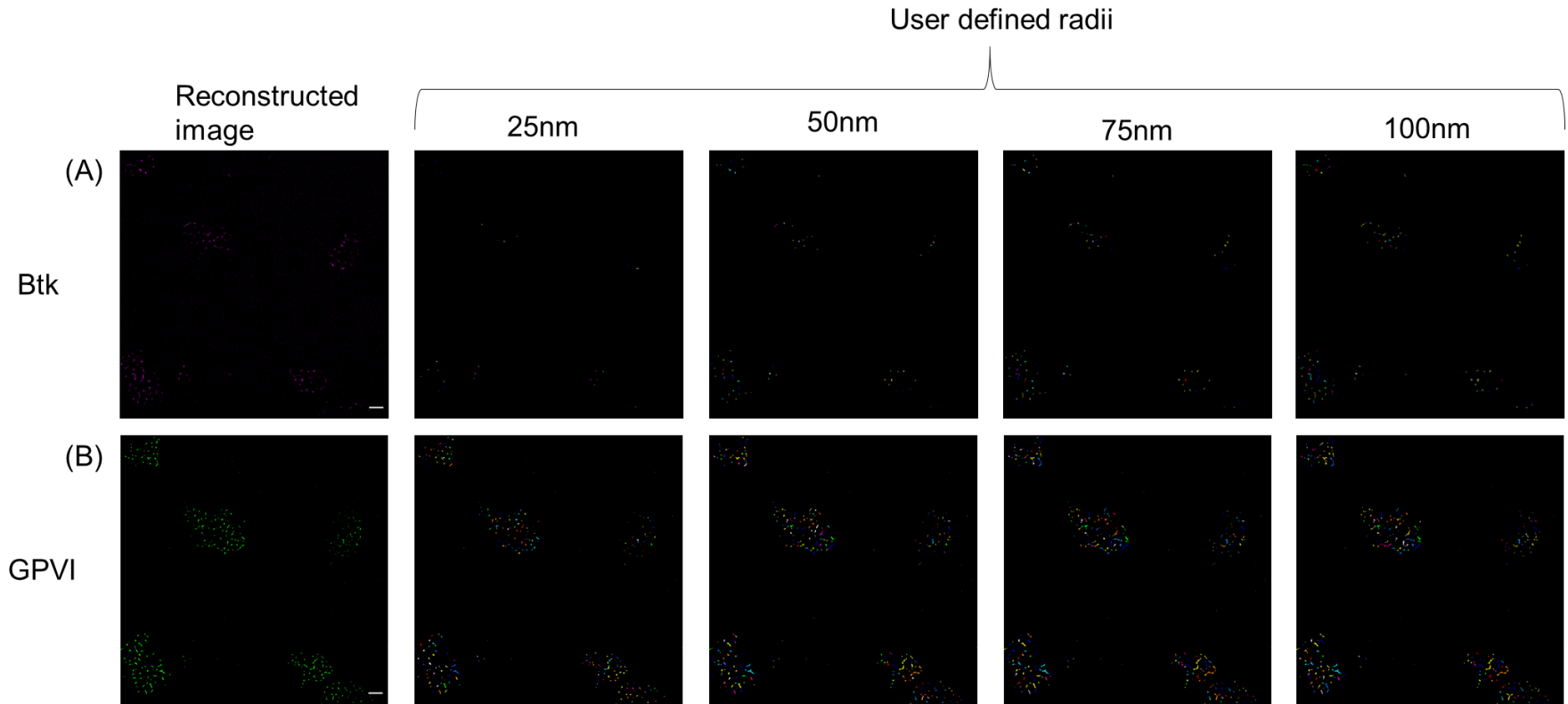


Figure 6.3.2 Btk and GPVI cluster on CRP-XL

Washed platelets 2×10^7 cells /mL were spread on $1 \mu\text{g/mL}$ CRP-XL for 45 minutes before fixation, permeabilization and staining with anti-Btk (magenta, A) and anti- GPVI (green, B) followed by secondary staining with Alexa Fluor 555 conjugated donkey anti-mouse and Alexa Fluor 647 conjugated donkey anti-goat. Samples were imaged using a Nikon N-STORM system in blinking buffer to induce fluorophore blinking. 20,000 frames were captured and reconstructed using Nikon NIS-Elements STORM analysis module applying drift correction and gaussian rendering. ≥ 3 fields of view from 3 independent experiments were imaged. Individual fluorescent blinking events were filtered on photon count and only those with a count >400 were selected for further analysis. Cluster analysis was performed using DBSCSAN algorithm in LAMA software, with a cluster being defined as 10 localisations within 25nm, 50nm, 75nm and 100nm. Correlation analysis was performed using GraphPad Prism 8 with the r value of correlation being stated on the graph for (C) Btk clusters and (D) GPVI clusters. Graphs represent mean \pm SEM. Scale bar $5 \mu\text{m}$.

6.3.1.3 Inhibition of Btk catalytic activity does not impact Btk clustering but does impact GPVI clustering

Initial TIRFM experiments suggested that the punctate distribution of Btk is not altered in the presence of the Btk inhibitor acalabrutinib (Section 5.3.2). However, as Btk has been proposed to cluster due to transphosphorylation (Chung et al., 2019), dSTORM was used to quantify Btk cluster parameters, to identify changes in the presence of acalabrutinib. This approach may identify changes in Btk cluster size and density which cannot be visualised with the resolution of TIRFM.

1 μ M blocks Btk's kinase activity as determined by a loss of autophosphorylation using biochemical assays (Chapter 3) and therefore this and a lower concentration were used to inhibit Btk kinase activity. Washed platelets were treated with either 1 μ M acalabrutinib, 0.1 μ M acalabrutinib or vehicle control before being spread on collagen (10 μ g/mL) for 45 minutes. Samples were fixed, permeabilised, stained and imaged as previously described (Section 6.3.1.1). Clustering analysis was performed using LAMA software, with a cluster being defined as 10 points within 50nm (Malkusch and Heilemann, 2016). These parameters were selected to be consistent with Poulter et al., 2017.

Compared to control treated platelets, the average number of Btk clusters does not change in the presence of acalabrutinib. However, 1 μ M of acalabrutinib treatment resulted in a significant decrease in the number of GPVI clusters (Figure 6.3.3.B). This effect was lost at 0.1 μ M of acalabrutinib. While there was a decrease in the number of GPVI clusters, there was an overall increase in the size of GPVI clusters, suggesting that clusters were merging.

In summary, the kinase activity of Btk is not required for Btk clustering as quantified using DSBCAN and cluster parameters of a minimum 10 points per 50nm but is involved in the regulation of GPVI cluster size.

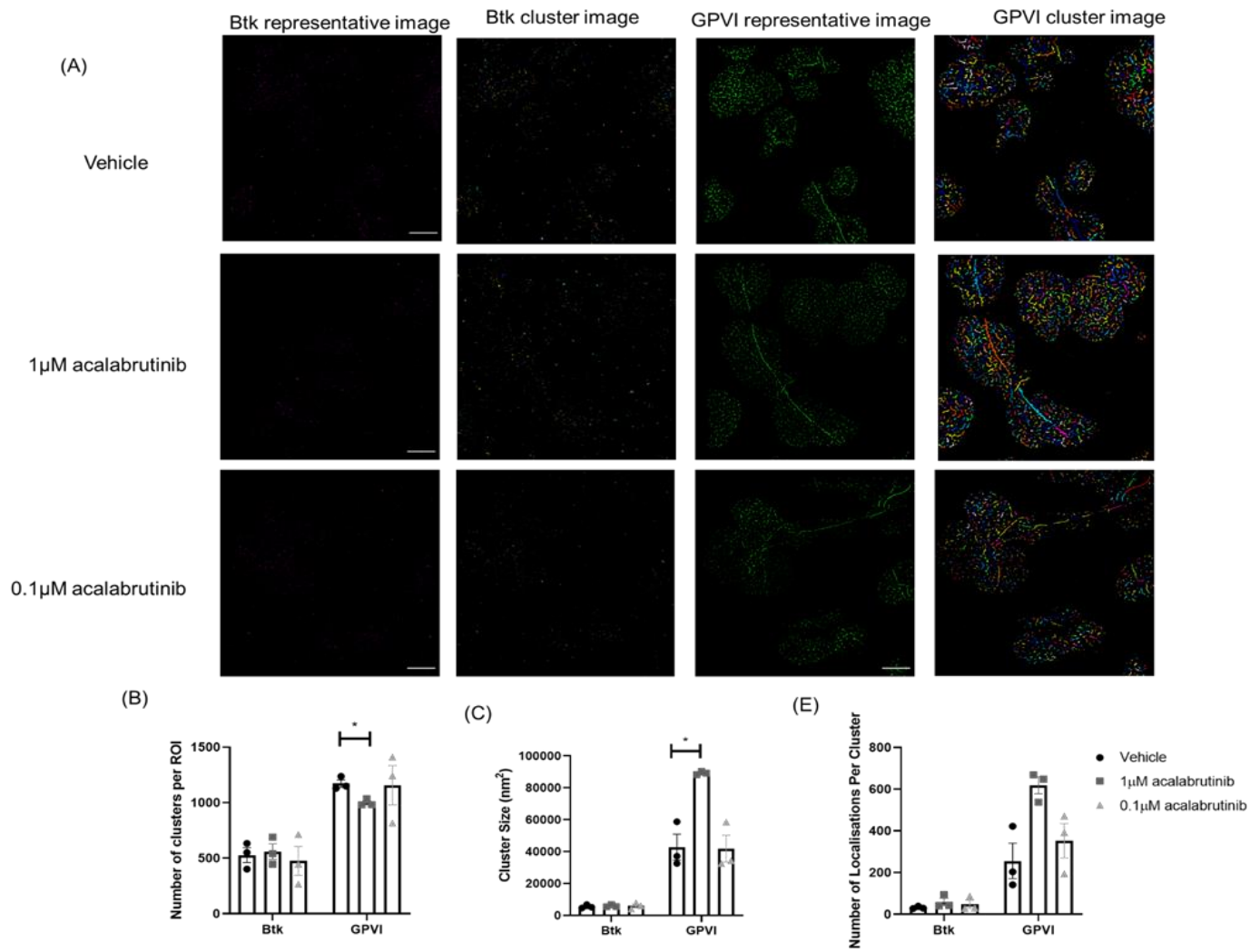


Figure 6.3.3 High concentrations of acalabrutinib inhibit the number of GPVI but not Btk clusters compared to vehicle control

(A) Washed platelets 2×10^7 cells/mL were treated acalabrutinib ($1 \mu\text{M}$ or $0.1 \mu\text{M}$) or vehicle (0.1% DMSO (v/v)) for 5 minutes before spreading on $10 \mu\text{g/mL}$ collagen for 45 minutes then fixed, permeabilised and stained with anti-Btk and anti-GPVI followed by secondary staining with Alexa Fluor 555 conjugated donkey anti-mouse and Alexa Fluor 647 conjugated donkey anti-goat before being imaged using a Nikon N-STORM system in blinking buffer to induce fluorophore blinking. 20,000 frames were captured and reconstructed using Nikon NIS-Elements STORM analysis module, applying drift correction and gaussian rendering. 3 fields of view from 3 independent experiments were imaged. Individual fluorescent blinking events were filtered on photon count and only those with a count >400 selected for further analysis. Cluster analysis was performed using DBSCAN algorithm in LAMA software, with a cluster being defined as 10 localisations within 50nm. (B) The number of clusters of Btk and GPVI were analysed along with the (C) cluster size and (D) number of localisations per cluster. Graphs represents mean \pm SEM. Statistical testing was performed using Two-way ANOVA with Dunnett's post-test. Scale bar represents $5 \mu\text{m}$.

6.3.1.4 Btk and LAT cluster on collagen

Experiments using TIRFM suggested weak colocalisation for Btk and LAT (Section 5.3.5). LAT has been shown to cluster in T cells (Lillemeier et al., 2010), and therefore it was investigated if it undergoes clustering when spread on collagen.

Washed platelets were spread on collagen (10 μ g/mL) for 45 minutes. Platelets were fixed, permeabilised and stained with anti-LAT and anti-Btk followed by secondary staining with Alexa Fluor 647 conjugated donkey anti rabbit and Alexa Fluor 555 conjugated donkey anti goat. Imaging and analysis was performed as previously described (Section 6.3.1.1).

When the radii cluster parameter is increased, the number of LAT clusters decreases, with the r value being -0.997 ($p \leq 0.01$), Figure 6.3.4.C. However, the size of the LAT clusters and the number of localisations per cluster both strongly positively correlate with r values being almost 1 almost 1 (0.989 and 0.958 for number of localisations to a cluster and size of clusters respectively). This is statistically significant ($p \leq 0.05$). This is likely due to the larger radii incorporating smaller clusters into larger clusters leading to a decrease in the overall number of clusters as the radius increases.

The increase in cluster radii leads to a decrease in the number of LAT clusters is also mirrored for Btk clusters ($r = -0.992$, $**p \leq 0.01$) (Figure 6.3.4.D). In contrast, as the radius increases, the size of the clusters strongly positively correlates with the cluster size with the r value being 0.998 ($***p \leq 0.001$). Furthermore, the number of localisations per cluster also increases with the increase in radii ($p \leq 0.05$).

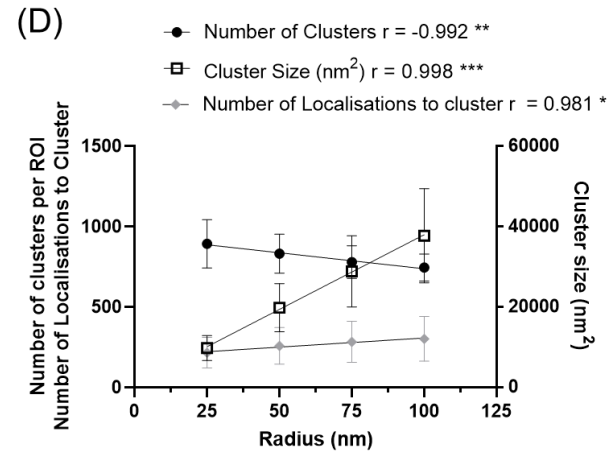
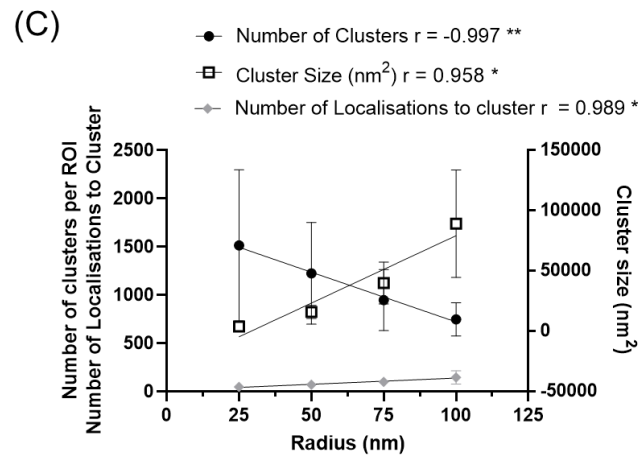
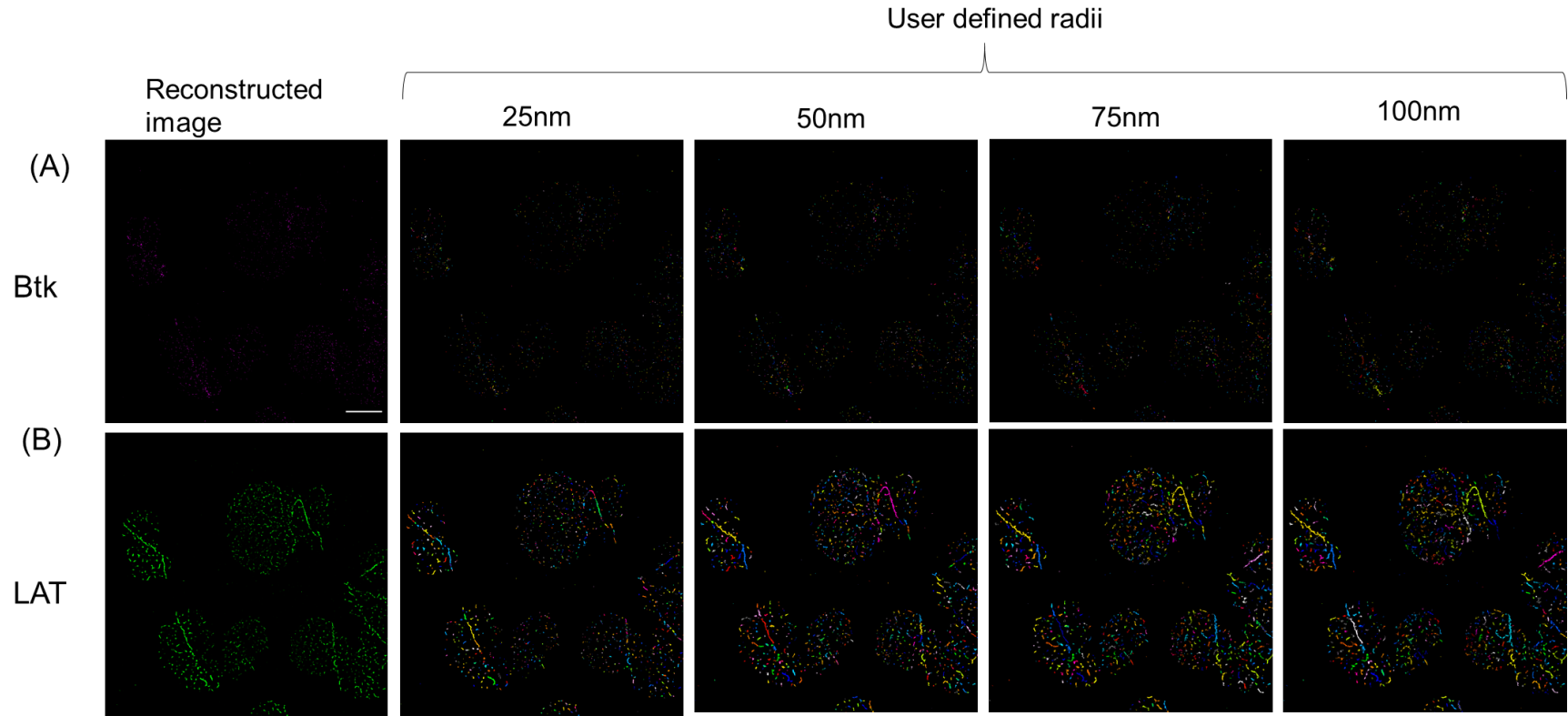


Figure 6.3.4 Btk and LAT cluster on collagen

Washed platelets were spread on collagen for 45 minutes before being fixed, permeabilised and stained with (A) anti-Btk (magenta), or (B) anti-LAT (green) and secondary stained with Alexa Fluor 647 conjugated donkey anti-rabbit and Alexa Fluor 555 donkey anti goat antibodies. Samples were imaged using a Nikon N-STORM system in blinking buffer to induce fluorophore blinking. 20,000 frames of each colour were captured and reconstructed using Nikon NIS-Elements STORM analysis module, applying drift correction and gaussian rendering. ≥ 3 separate fields of view from 3 independent experiments were imaged. Individual fluorescent blinking events were filtered on photon count and only those with a count >400 were selected for further analysis. Cluster analysis was performed using the DBSCSAN algorithm in LAMA software, with a cluster being defined as 10 localisations within 25nm, 50nm, 75nm and 100nm. Correlation analysis was performed using GraphPad Prism 8 with the r value of correlation being stated on the graph for (C) LAT clusters and (D) Btk clusters.

6.3.1.5 Btk and CLEC-2 cluster when platelets spread on rhodocytin

Btk is distributed as a punctate pattern on GPVI ligands. It was investigated to see if Btk formed a similar distribution when platelets were spread on a CLEC-2 ligand rhodocytin

Washed platelets were spread on 100nM rhodocytin for 45 minutes before fixation, permeabilization and staining with anti-Btk and anti-CLEC-2 followed by secondary staining with Alexa Fluor 647 conjugated donkey anti-rabbit and Alexa Fluor 555 conjugated donkey anti-mouse as in Section 5.3.7 Imaging and cluster analysis were performed as previously described (Section 6.3.1.1).

Similarly, as to when platelets spread on collagen, as the radius increases the number of Btk clusters decreases ($r = -0.995$, $p \leq 0.01$). Whereas, as the radius increases there is a positive correlation with cluster size and the number of localisations per cluster ($p \leq 0.05$, $r = 0.98$), Figure 6.3.5.C. This can be viewed in the representative image as when the cluster diameter is 25nm there are clusters that are close together that are different colours, whereas in the images with an increased in diameter such as 100nm, clusters are the same colour showing they have merged.

As the size of the radius increase, the number of CLEC-2 clusters also decreased, Figure 6.3.5.D. In contrast, the size of the CLEC-2 clusters and the number of localisations per cluster both strongly positively correlated with the increased radii size ($r > 0.95$ and $*p \leq 0.05$ for both size of clusters and the number of localisations per cluster).

Taken together, this suggests that Btk and CLEC-2 cluster in platelets spread on rhodocytin and that small clusters are localised near each other, that amalgamate with other clusters when a larger radius is selected for analysis.

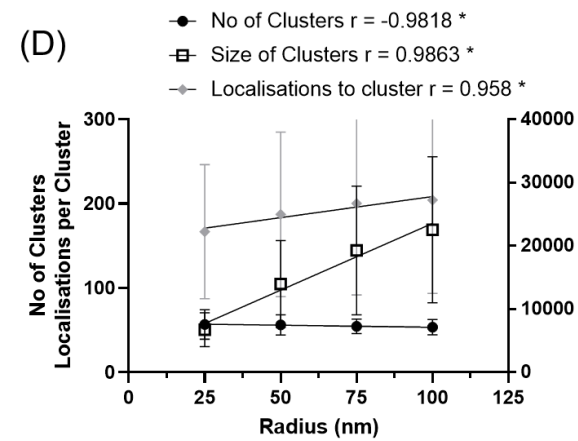
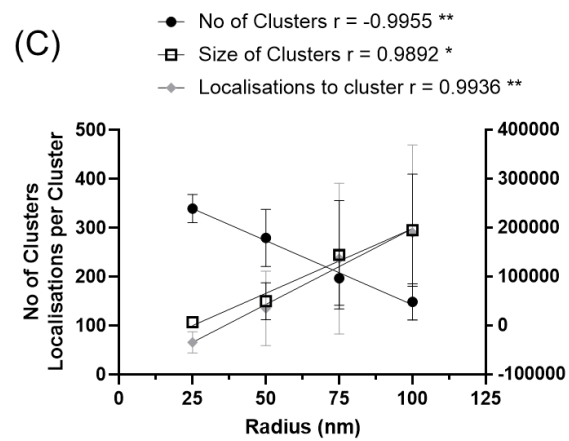
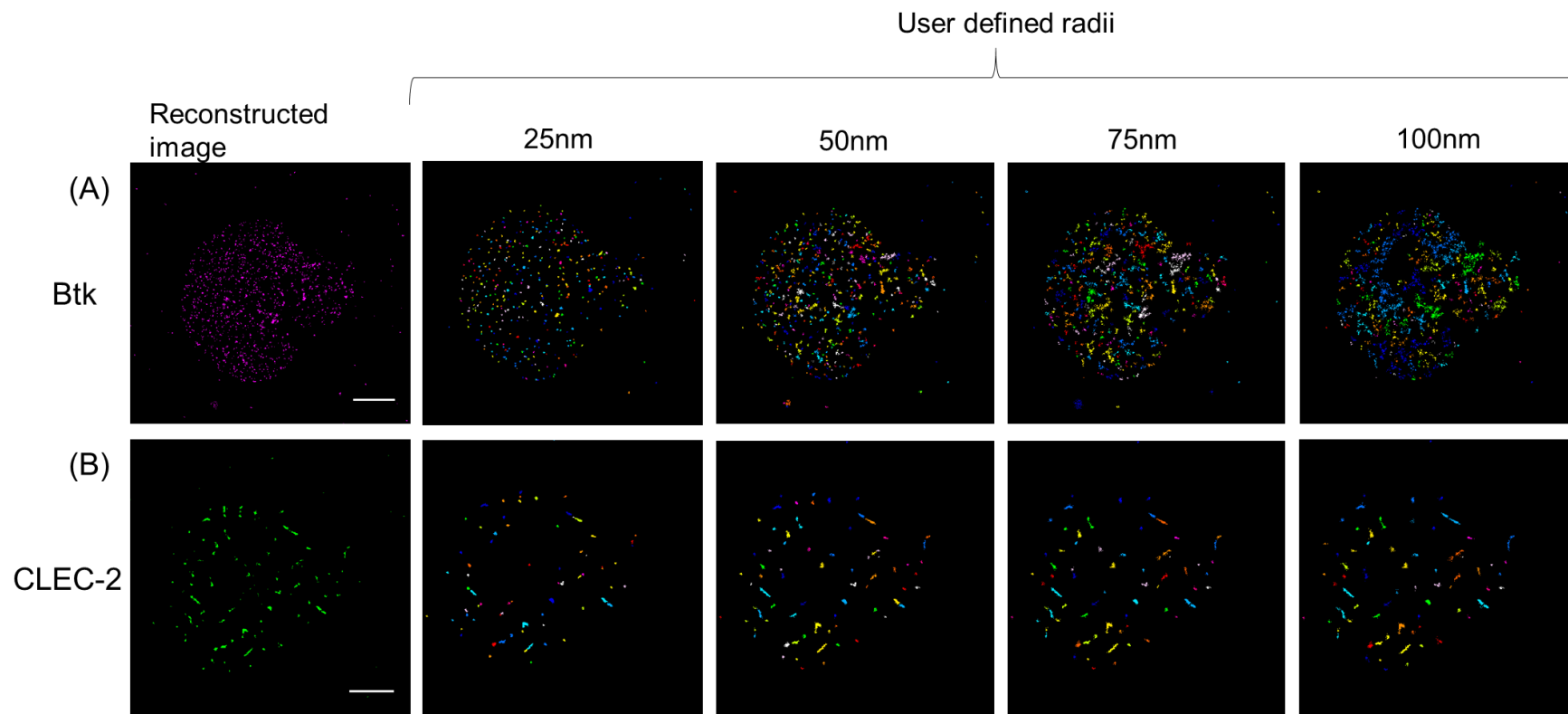


Figure 6.3.5 Btk and CLEC-2 cluster on rhodocytin

Washed platelets 2×10^7 cells /mL were spread on 100nM rhodocytin for 45 minutes before fixation, permeabilization and staining with anti-Btk (magenta, A) and anti-CLEC-2 (green, B) followed by secondary staining with Alexa Fluor 647 conjugated donkey anti-rabbit and Alexa Fluor 555 conjugated donkey anti-mouse. Samples were imaged using a Nikon N-STORM system in blinking buffer to induce fluorophore blinking. 20,000 frames of each colour were captured and reconstructed using Nikon NIS-Elements STORM analysis module, applying drift correction and gaussian rendering. ≥ 3 fields of view from 3 independent experiments were imaged. Individual fluorescent blinking events were filtered on photon count and only those with a count >400 were selected for further analysis. Cluster analysis was performed using the DBSCAN algorithm in LAMA software, with a cluster being defined as 10 localisations within 25nm, 50nm, 75nm and 100nm. Correlation analysis was performed using GraphPad Prism 8 with the R value of correlation being stated on the graph for (C) Btk clusters and (D) CLEC-2 clusters. Graph represents mean \pm SEM * $p \leq 0.05$, ** $p \leq 0.01$. Scale bar represents $1\mu\text{m}$.

6.3.1.6 Btk and LAT cluster when platelets spread on rhodocytin

Btk and LAT were shown to cluster on collagen, and therefore this was investigated downstream of CLEC-2, on rhodocytin. Washed platelets were spread on rhodocytin (100nM) for 45 minutes. Platelets were then fixed, permeabilised, stained, imaged, and analysed as in Section 6.3.1.4. The representative images in Figure 6.3.6 show that both LAT and Btk form a punctate pattern which can be observed in Figure 6.3.6.A and B.

As observed with platelets spread on collagen, the number of LAT clusters decreases as the defined radius of the cluster analysis increases, with a strong correlation ($r=-0.995$, $p \leq 0.01$), Figure 6.3.6.C. The cluster size, ($r=0.951$, $p \leq 0.05$), and the number of localisations per cluster also increases as the radius increases ($r=0.987$, $p \leq 0.05$). For Btk, as the radius increased, similarly to LAT, the number of clusters decreased with a strong negative correlation ($r=-0.99$, $p \leq 0.01$). The cluster size and number of localisations per cluster has a strong positive correlation, as the radii increases (both $r>0.99$, $p \leq 0.01$), Figure 6.3.6.D. This suggests that for both LAT and Btk, smaller clusters are being incorporated into larger clusters as the radius increases.

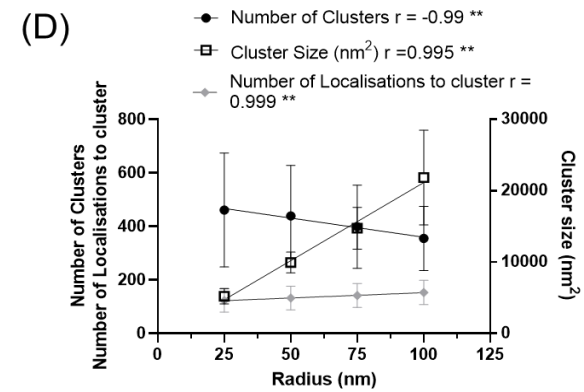
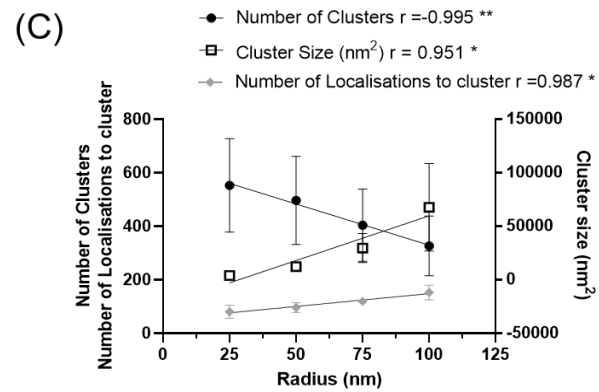
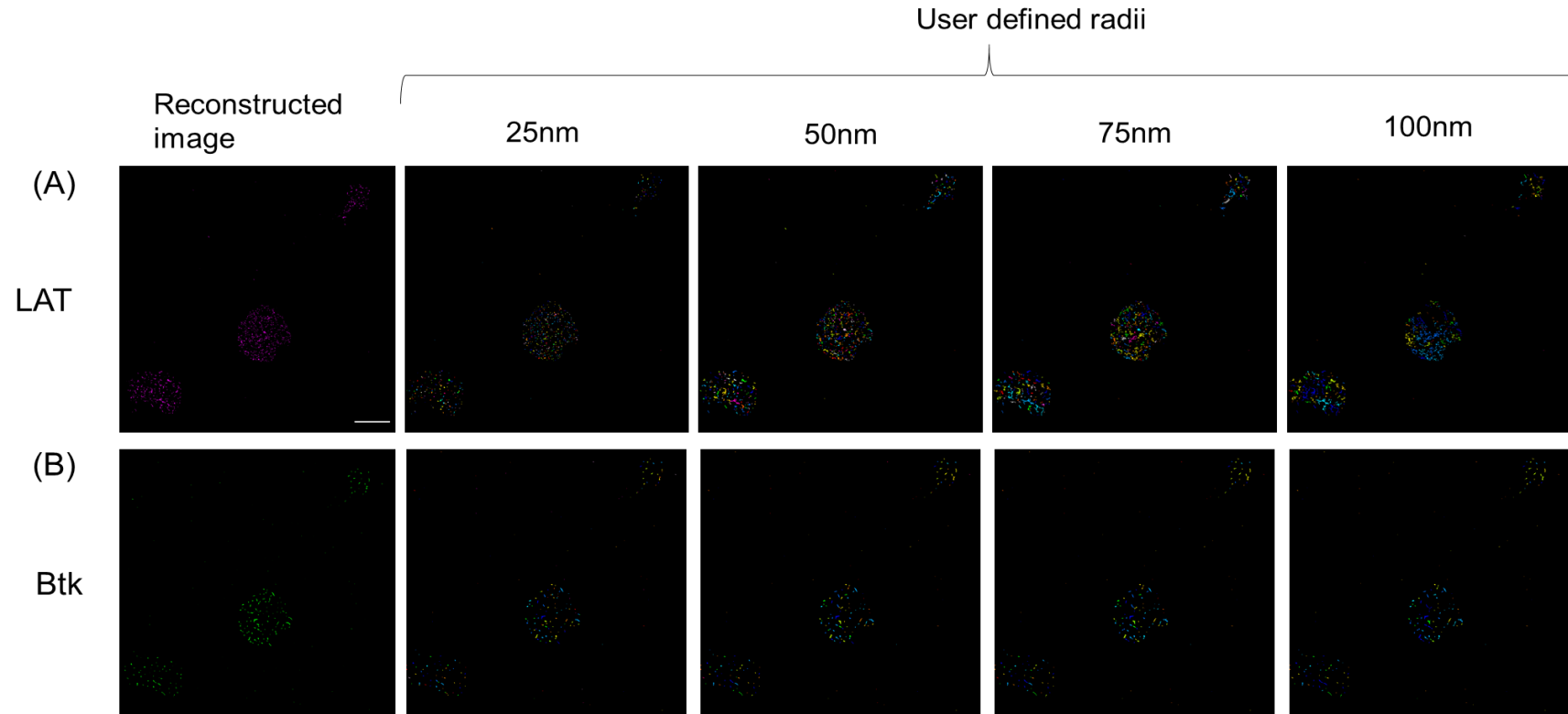


Figure 6.3.6 Btk and CLEC-2 cluster on rhodocytin

Washed platelets 2×10^7 cells /mL were spread on 100nM rhodocytin for 45 minutes before fixation, permeabilization and staining with anti-LAT (magenta, A) and anti-Btk (green, B) followed by secondary staining with Alexa Fluor 647 conjugated donkey anti-rabbit and Alexa Fluor 555 donkey anti goat antibodies. Samples were imaged using a Nikon N-STORM system in blinking buffer to induce fluorophore blinking. 20,000 frames of each colour were captured and reconstructed using NIS-Elements Nikon STORM analysis module, applying drift correction and gaussian rendering. ≥ 3 fields of view from 3 independent experiments were imaged. Individual fluorescent blinking events were filtered on photon count and only those with a count >400 were selected for further analysis. Cluster analysis was performed using the DBSCSAN algorithm in the LAMA software, with a cluster being defined as 10 localisations within 25nm, 50nm, 75nm and 100nm. Correlation analysis was performed using GraphPad Prism 8 with the R value of correlation being stated on the graph for LAT clusters (C) and Btk clusters (D). Graph represents mean \pm SEM *P \leq 0.05, **p \leq 0.01. Scale bar represents 5 μ m.

6.3.2 Colocalisation analysis using plot profile along a collagen fibre or line across a platelet

Plot profile analysis

Btk did not strongly localise with GPVI in TIRFM, however, it did look to form an inverse relationship along the fibre, with Btk puncta being present in areas where GPVI is absent (chapter 5, Figure 5.3.1). To assess the distribution of Btk and GPVI along the collagen fibre the plot profile function in Nikon NIS-Elements software was used. Plot profile displays the numerical output of the fluorescence converted into an arbitrary unit if fluorescence is present in either channel separately or together along a line within a reconstructed STORM images. To account for different length of collagen fibre these values were presented as a percentage of total localisations present at the fibre, excluding areas where no localisations were present. An example is shown in Figure 6.3.7.A, with nonfibrous ligands a line across the platelet was used, Figure 6.3.7.B.

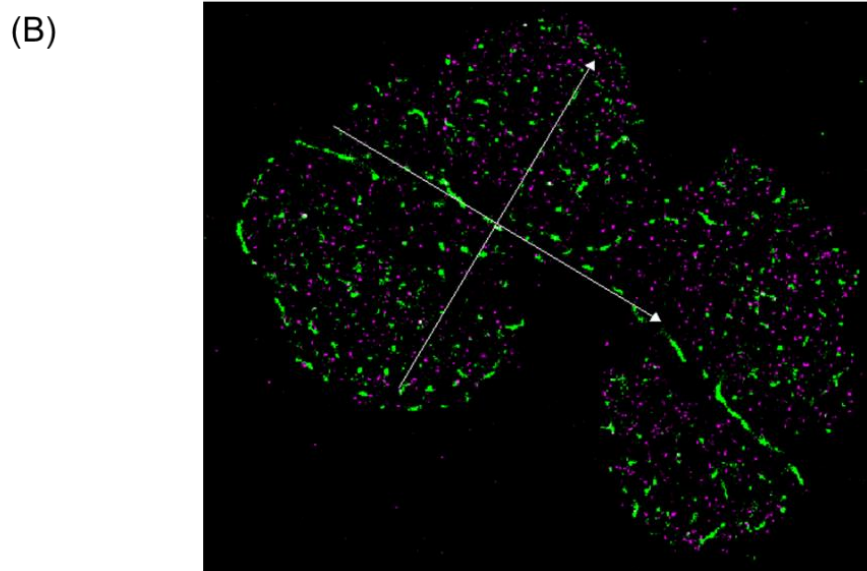
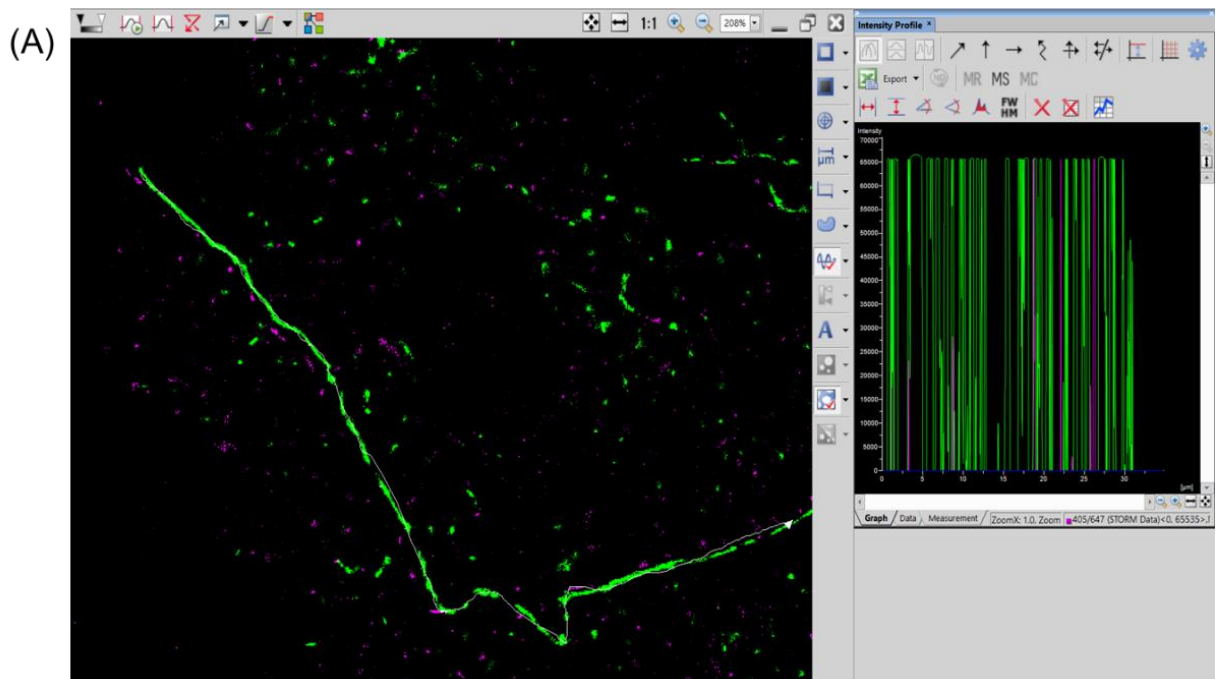


Figure 6.3.7 Plot profile analysis method

A reconstructed STORM image with Btk (magenta) and GPVI (green) staining of platelets spread on collagen is opened in Nikon NIS-Elements software. The DIC image is also opened (not shown) to confirm the location of the collagen fibre. The fluorescence profile of Btk and GPVI along the fibre is analysed by drawing along the fibre and a resulting graph is made (right hand panel of (A)). This is then analysed in excel to quantify the % localisations of the fibre to normalise for the differences in fibre length across samples.

(B) For nonfibrous ligands, a random cross Section through the platelet is taken.

6.3.2.1 Syk and GPVI colocalise to collagen fibres when evaluated using plot profile analysis

Published (Dunster et al., 2020, Pallini et al., 2020) and previous work suggests that Syk and GPVI colocalise when imaged using TIRFM (Chapter 5). The localisation of GPVI and Syk in relation to each other was investigated using STORM and analysed using plot profile analysis.

Samples were prepared as described in Section 5.3.6. Platelets were then imaged using STORM and reconstructed (Section 6.3.1.1). The plot profile along the collagen fibre was used to assess recruitment and colocalisation of GPVI and Syk to the fibre. As seen in previous TIRFM experiments GPVI and Syk strongly localise to collagen fibre (Section 5.3.6 and Figure 6.3.1.A). Syk is abundantly located but colocalisation with GPVI can be seen in the merged image, represented by white areas (Figure 6.3.8.A).

GPVI alone makes up most of the localisations on the fibre ($38.9\% \pm 2.3$). However, a large proportion of GPVI is colocalised with Syk ($32.2\% \pm 0.6$) Figure 6.3.8.B. Together this suggests that Syk and GPVI colocalise along the collagen fibre and provide validity of the analysis methods

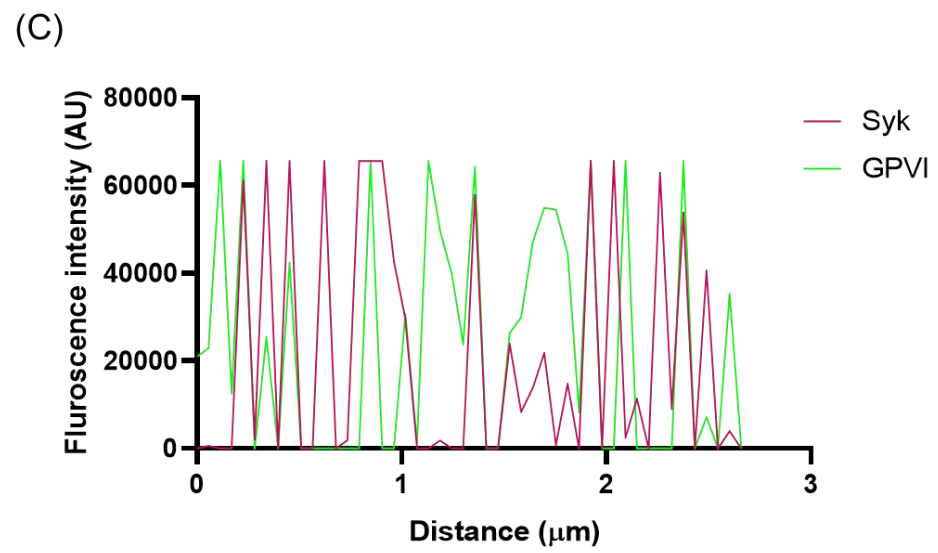
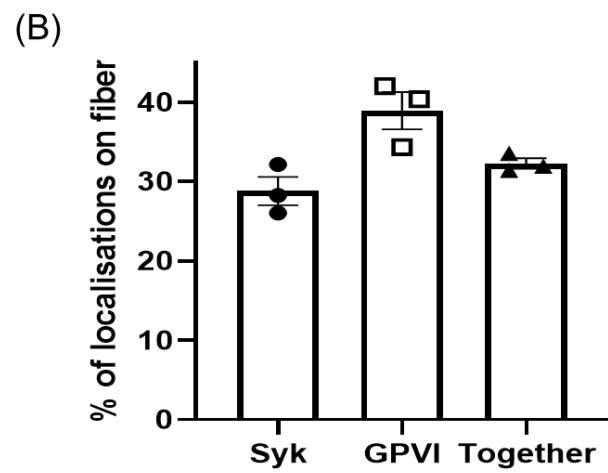
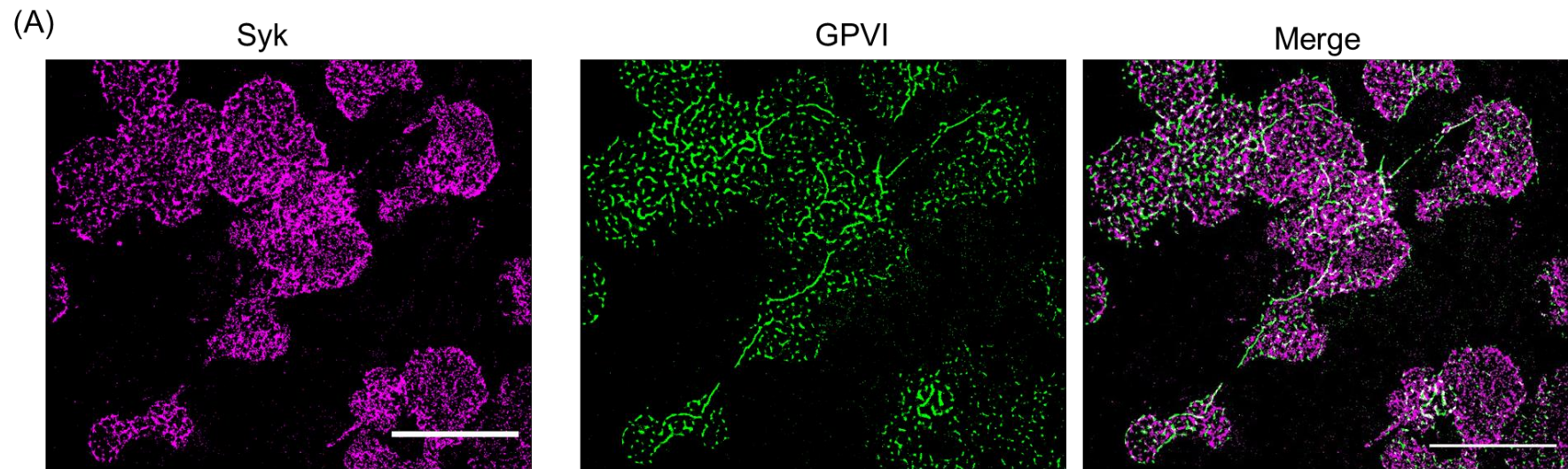


Figure 6.3.8 Syk and GPVI colocalise when spread on collagen and imaged in STORM

(A) Washed platelets were spread on collagen for 45 minutes before being fixed, permeabilised and stained with anti-Syk (magenta) and anti-GPVI (green). Samples were secondary stained with Alexa Fluor 647 donkey anti rabbit and Alexa Fluor 555 goat anti mouse and imaged using a Nikon N-STORM system in blinking buffer to induce fluorophore blinking. 20,000 frames were captured and reconstructed using Nikon STORM analysis module, applying drift correction and gaussian rendering. 3 separate fields of view from 3 independent experiments were imaged. Individual fluorescent blinking events were filtered on photon count and only those with a count >400 was selected for further analysis. Scale bar represents 10 μ m. Plot profile analysis was performed using Nikon NIS-Elements by selecting 3 random fibres to draw along. The resulting values were put into Excel to identify if there was fluorescent present in the Syk or GPVI channel or present in both at the same location. (B) The percentage of localisations was then calculated. Graph represents mean \pm SEM, n=3. Statistical testing was performed using one-way ANOVA with Tukey's multiple comparisons post-test. (C) A representative trace along part of a collagen fibre showing the fluorescence intensity before normalisation.

6.3.2.2 Btk and GPVI partly colocalise in STORM on collagen

Plot profile was used to investigate the localisations of Btk and GPVI at the collagen fibre. Samples were prepared, imaged, and reconstructed as in Section 6.3.1.1. Plot profile analysis was performed as explained above in Section 6.3.2.

The localisations along the fibre were predominantly made up of GPVI (Figure 6.3.9.E), with single GPVI localisations accounting for an average 65.8% (± 9.9) of localisations at the fibre. Btk localisations made up less than 10% of the localisations ($9.8\% \pm 5.1$), suggesting that Btk is only present in small amounts in the absence of GPVI. Interestingly, Btk is largely present colocalised with GPVI, with Btk and GPVI colocalising along approximately 25% of the fibre's length, as evident from Figure 6.3.9.C, where the slight resemblance of a fibre can be observed in magenta, Btk channel.

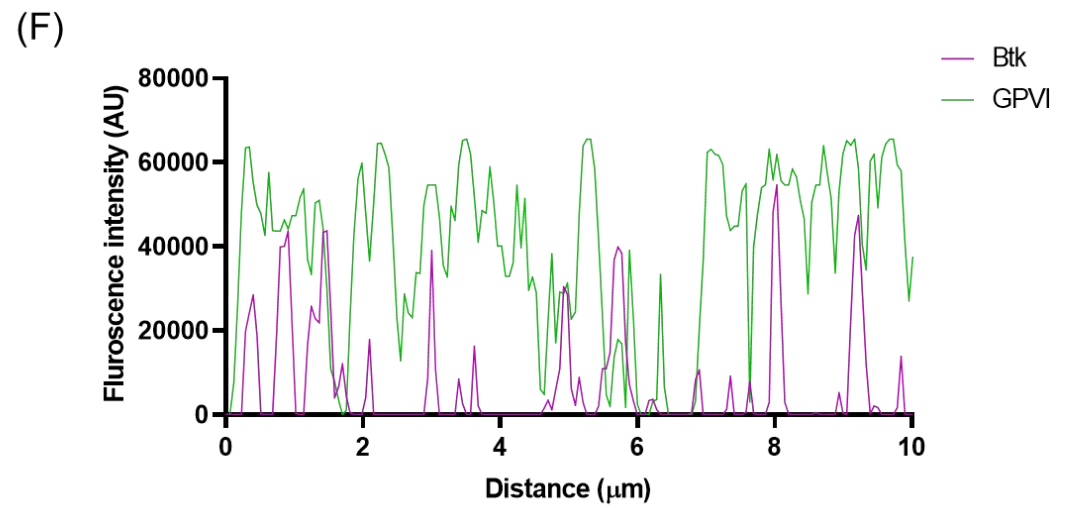
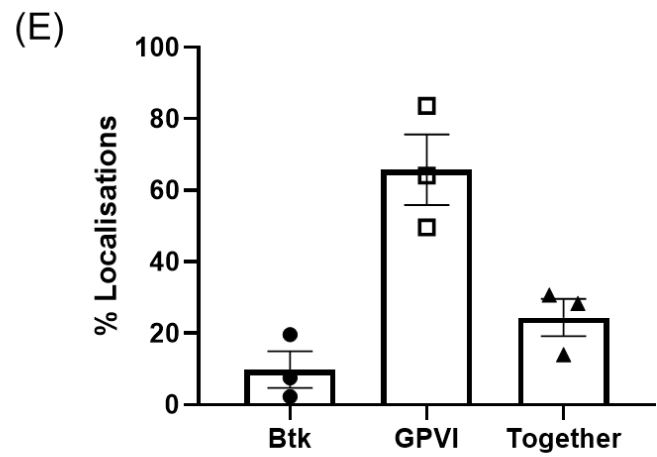
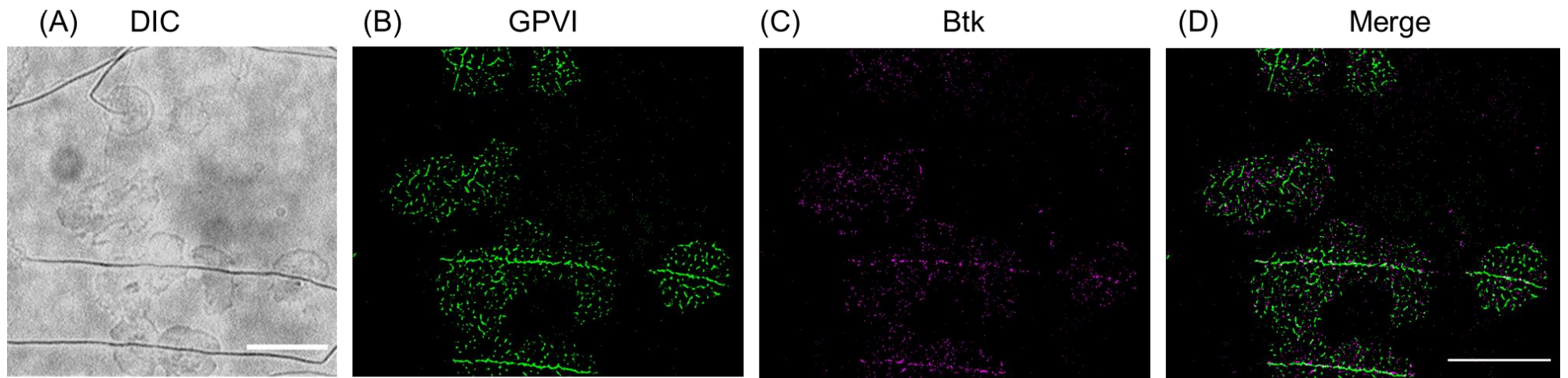


Figure.6.3.9 Btk and GPVI colocalise along collagen fibres when imaged using STORM

Washed platelets 2×10^7 cells /mL were spread on $10 \mu\text{g}/\text{mL}$ collagen for 45 minutes before fixation, permeabilization and staining with (B) anti-GPVI and (C) anti-Btk followed by secondary staining with Alexa Fluor 555 conjugated donkey anti-mouse and Alexa Fluor 647 conjugated donkey anti-goat . Samples were imaged using (A) DIC to visualise the collagen fibres or (B, C) using a Nikon N-STORM system in blinking buffer to induce fluorophore blinking. 20,000 frames were captured and reconstructed using Nikon NIS-Elements STORM analysis module, applying drift correction and gaussian rendering. 3 fields of view from 3 independent experiments were imaged. Individual fluorescent blinking events were filtered on photon count and only those with a count >400 were selected for further analysis. Scale bar represents $10 \mu\text{m}$. Plot profile analysis was performed using Nikon NIS-Elements and selecting 3 random collagen fibres per image identified using DIC (A) to draw along. The resulting values were put into excel to identify the presence of Btk, GPVI or both at each pixel along the fibre, converting the fluorescence into binary units (E) The % of localisations along the fibres were then calculated. (F) represents a Section of raw data before normalisation. Scale bar 10nm . Graph represents Mean \pm SEM. Statistical testing was performed using one-way ANOVA with Tukey's multiple comparisons post-test.

6.3.2.3 Btk kinase inhibition does not change the amount of Btk and GPVI recruited to the collagen fibre

As approximately 25% of the fibre's localisations has Btk and GPVI colocalised, it was investigated if the recruitment of Btk was dependent on its kinase activity. Therefore, the recruitment of Btk to the collagen fibres in the presence of acalabrutinib was assessed using STORM and analysed using the plot profile approach described above. This may provide further evidence for a scaffolding role for Btk.

1 μ M blocks Btk's kinase activity as determined by a loss of autophosphorylation using biochemical assays (Chapter 3). Therefore, 1 μ M and 0.1 μ M acalabrutinib were used to investigate the role of Btk kinase function in Btk recruitment to collagen fibres. Washed platelets were pre-treated with acalabrutinib before being spread on 10 μ g/mL collagen before fixation, permeabilization and staining as previously described (Section 6.3.1.3). Imaging and plot profile analysis was assessed as previously described.

GPVI lines up along the collagen fibre. Interestingly in the representative image of the 0.1 μ M acalabrutinib treated platelets, there appears to be a Section of Btk that looks to localise in a line near the fibre, but it does not overlap with GPVI in the merged image, Figure 6.3.10.C.

Drug treatment does not alter the proportion of Btk and GPVI colocalising together along the fibre. However, 0.1 μ M acalabrutinib increases the proportion of Btk present at the fibre ($p \leq 0.05$) and subsequently reduces the amount of GPVI present at the fibre ($p \leq 0.05$) when compared to the vehicle control. This shows that the fibre is made up of predominantly GPVI localizations, and Btk does not look to localise with GPVI but this does not change in the presence of Btk inhibitor. This further provides evidence for a scaffolding function of Btk.

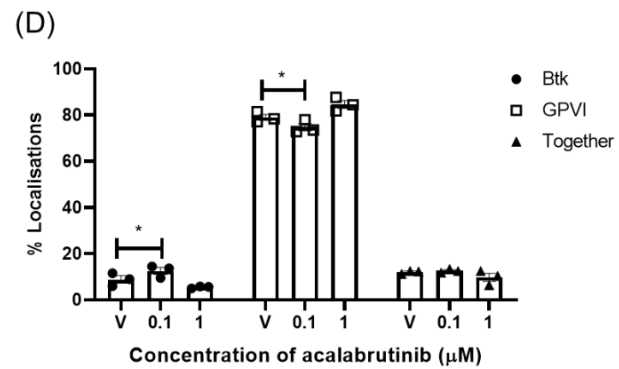
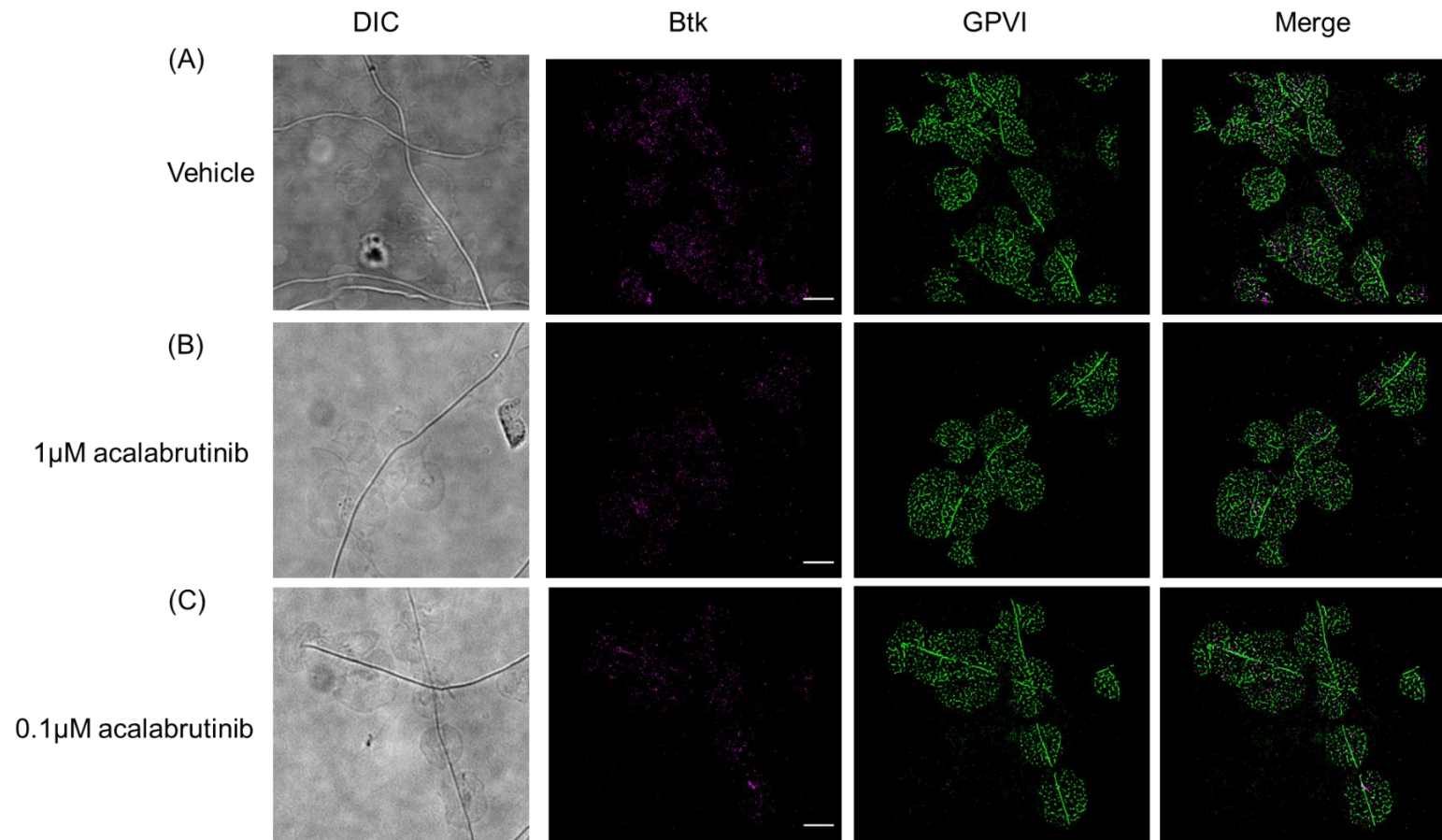


Figure 6.3.10 Treatment with Btk inhibitors can change the location of Btk and GPVI when analysed using the plot profile method.

Washed platelets were treated with (A) vehicle control, (B) 1 μ M acalabrutinib or (C) 0.1 μ M acalabrutinib and then spread on collagen for 45 minutes. Samples were fixed, permeabilised and stained with anti-Btk (magenta) and anti-GPVI (green) followed by secondary staining with Alexa Fluor 555 conjugated donkey anti-mouse and Alexa Fluor 647 conjugated donkey anti-goat before being imaged. Samples were imaged using DIC or the Nikon N-STORM system in blinking buffer to induce fluorophore blinking. 20,000 frames per fluorophore were captured and reconstructed using Nikon NIS-Elements STORM analysis module, applying drift correction and gaussian rendering. 3 fields of view from 3 independent experiments were imaged. Individual fluorescent blinking events were filtered on photon count and only those with a count >400 were selected for further analysis. Scale bar represents 5 μ m. Plot profile analysis was performed using Nikon NIS-Elements selecting 3 random collagen fibres per image identified in the DIC image to draw over. The resulting values were put into excel to identify if fluorescence was present in the Btk, GPVI or both channels. (D) The percentage of localisations was then calculated. Graph represents Mean \pm SEM. Statistical testing was performed using Two-way ANOVA with Dunnett's multiple comparisons post-test, * $p \leq 0.05$.

6.3.2.4 When assessed using plot profile analysis Btk and GPVI do not strongly colocalise in platelets spread of CRP-XL

The data presented above demonstrated that GPVI is strongly localised to collagen fibres and that a proportion of Btk colocalises with GPVI. To determine if GPVI and Btk colocalise on a non-fibrous GPVI ligand platelets were spread on CRP-XL and imaged using STORM and analysed using plot profile using a random cross-section through the middle of the platelet, an example is presented in Figure 6.3.7.B.

Using this approach approximately 10% of localisations among the plot profile contained both GPVI and Btk (Figure 6.3.11.D). GPVI and Btk are largely discretely present (approximately 60% and 30% respectively).

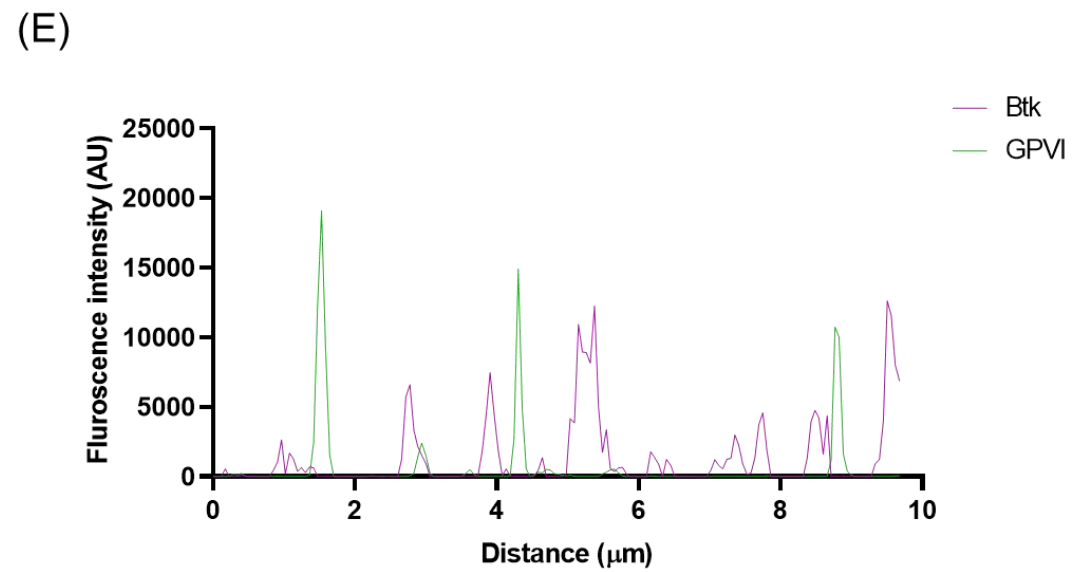
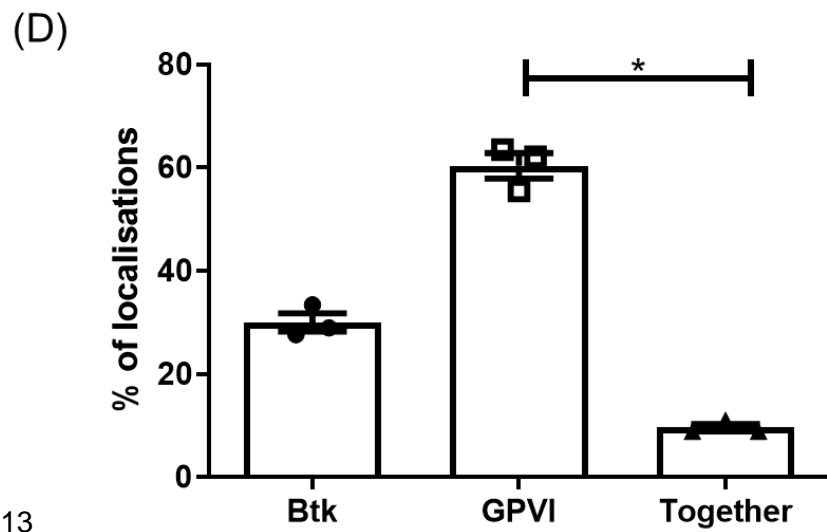
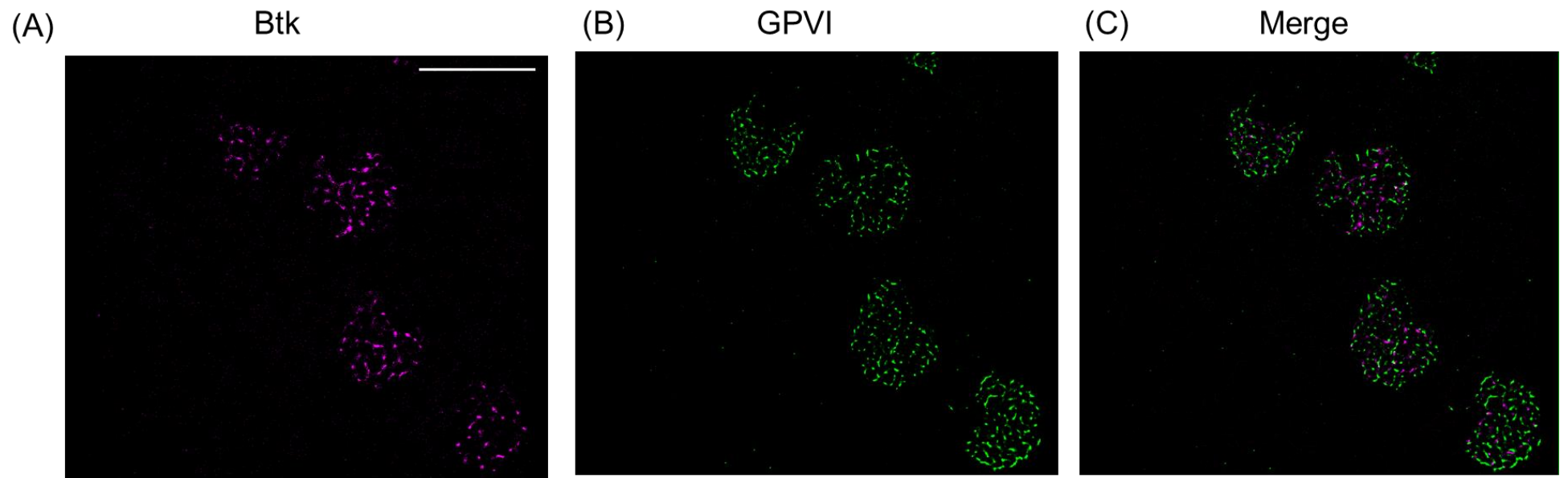


Figure 6.3.11 Plot profile assessment of Btk and GPVI colocalisation in platelets spread of CRP-XL

Washed platelets were spread on CRP for 45 minutes before being fixed, permeabilised and stained with (A) anti-Btk (magenta) and (B) anti-GPVI (green) followed by secondary staining with Alexa Fluor 647 conjugated donkey anti-rabbit and Alexa Fluor 488 conjugated goat anti-mouse. Samples were imaged using a Nikon N-STORM system in blinking buffer to induce fluorophore blinking. 20,000 frames were captured and reconstructed using Nikon NIS-Elements STORM analysis module, applying drift correction and gaussian rendering. 3 fields of view from 3 independent experiments were imaged. Individual fluorescent blinking events were filtered on photon count and only those with a count >400 were selected for further analysis. Scale bar represents 5µm. Plot profile analysis was performed using Nikon NIS-Elements and selecting 3 random cross Sections through the platelets (A). The resulting values were put into excel to identify pixels with fluorescence for Btk, GPVI or both. (E)The percentage of localisations was then calculated. Graph represents Mean ± SEM. Statistical testing was performed using one-way ANOVA with Tukey's multiple comparisons post-test, *p ≤ 0.05.

6.3.2.5 Btk and LAT partially colocalise at collagen fibres when assessed using plot profile analysis

Btk did not strongly colocalise with GPVI but it may interact with proteins further down the GPVI signalling pathway, for example LAT. Btk has been shown to co-immunoprecipitate with LAT (Pasquet et al., 1999b). Therefore, STORM experiments were utilised to investigate if Btk colocalises with LAT along collagen fibres.

Experiments were performed and analysed as previously described in Sections 6.3.1.4 and 6.3.2.

As Figure 6.3.12.B shows, Btk, looks to be recruited to the fibre in some parts of the image (Btk in magenta), but not wholly. When colocalisation at the fibre was assessed using plot profile analysis, the majority of Btk present was localising with LAT ($43.1\% \pm 5.4$, $p \leq 0.05$ comparing to Btk alone). A small proportion of the localisations were Btk alone ($15.9\% \pm 4.8$), but a large amount of LAT was seemingly present along the fibre alone ($41.1\% \pm 0.7$), which is greater than the proportion of Btk ($p \leq 0.05$). This suggests that Btk can partially be localised with LAT.

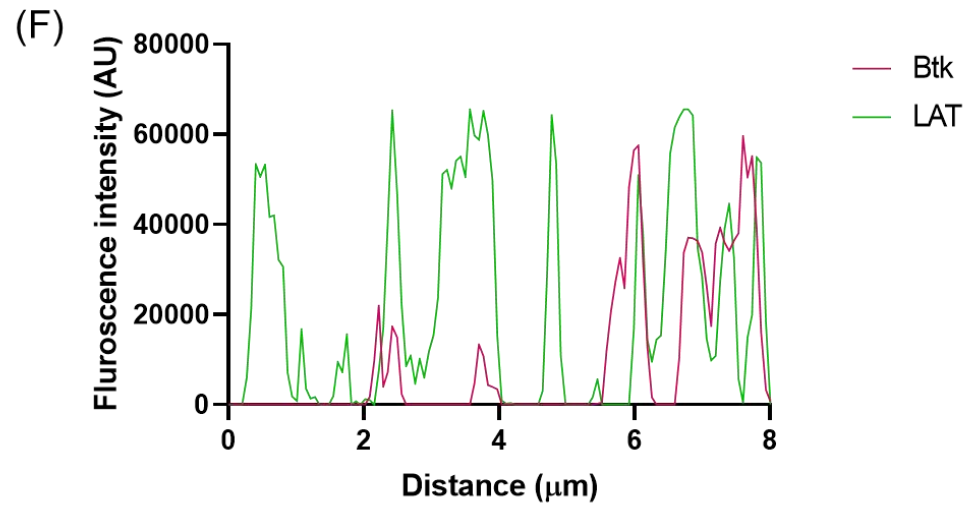
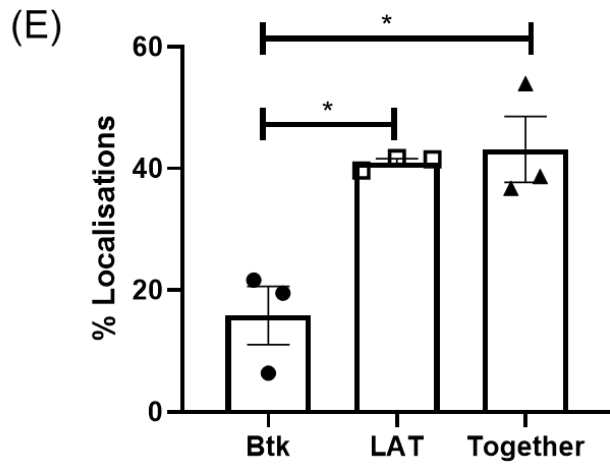
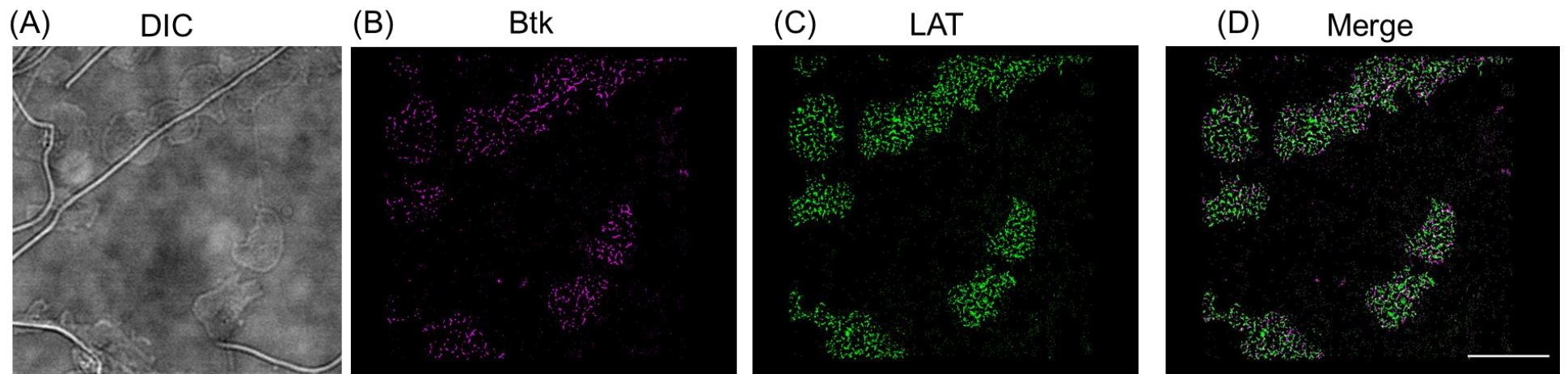


Figure 6.3.12 Btk can partially colocalise with LAT along collagen fibres when assessed using plot profile analysis

Washed platelets were spread on 10µg/mL collagen for 45 minutes before being fixed, permeabilised and stained with (B) anti-Btk (magenta), or (C) anti-LAT (green) and secondary stained with Alexa Fluor 647 conjugated donkey anti-rabbit and Alexa Fluor 555 donkey anti goat antibodies. Samples were imaged using a Nikon N-STORM system in blinking buffer to induce fluorophore blinking. 20,000 frames of each colour were captured and reconstructed using Nikon NIS-Elements STORM analysis module, applying drift correction and gaussian rendering. ≥3 fields of view from 3 independent experiments were imaged. Individual fluorescent blinking events were filtered on photon count and only those with a count >400 were selected for further analysis. Scale bar represents 10µm. Plot profile analysis was performed using Nikon NIS-Elements by selecting 3 random collagen fibres identified using the DIC image (A). The resulting values were put into Excel to identify if there was fluorescent present in the Btk or GPVI channel or present in both at the same location. (E) The percentage of localisations was then calculated. Graph represents Mean ± SEM, n=3. Statistical testing was performed using one-way ANOVA with Tukey's multiple comparisons post-test, *p ≤ 0.05. (F) shows a representative fluorescent intensity plot profile image.

6.3.2.6 Btk and CLEC-2 look to colocalise when spread on rhodocytin and examined using plot profile analysis

Syk and SFK regulate CLEC-2 clustering (Pollitt et al., 2014). As Btk is involved in CLEC-2 signalling (Chapter 3) and the relation of Btk to these tyrosine kinases (Li et al., 1997, Park et al., 1996, Wahl et al., 1997), it was hypothesized that Btk may influence clustering of CLEC-2 and may be localised near it. Therefore, the localisation of the two proteins was assessed in relation to each other using plot profile analysis.

Platelets were spread on rhodocytin (100nM) for 45 minutes before fixation, staining and imaging in STORM as previously described (Section 6.3.1.5).

As the panel on the right in Figure 6.3.13.A shows that Btk is seemingly localised all throughout the platelet as observed on other agonists. In addition, CLEC-2 is also generally distributed throughout the platelet. The merged image does show areas of white suggesting that some Btk is colocalised with CLEC-2 when platelets spread on rhodocytin.

The average percentage of localisations of Btk and CLEC-2 together was almost 40% (39.64 ± 1.4), which is approximately 10% more than Btk alone ($29.14\% \pm 4.9$). This suggests that a portion of Btk molecules in the platelet colocalise with CLEC-2 and vice versa. However, a high proportion of Btk does not localise with CLEC-2, and the proportion of Btk that localises with CLEC-2 is not significantly increased compared to the non-colocalised proportion. Therefore it is difficult to ascertain whether these values are random or biologically relevant as there is no statistical significance.

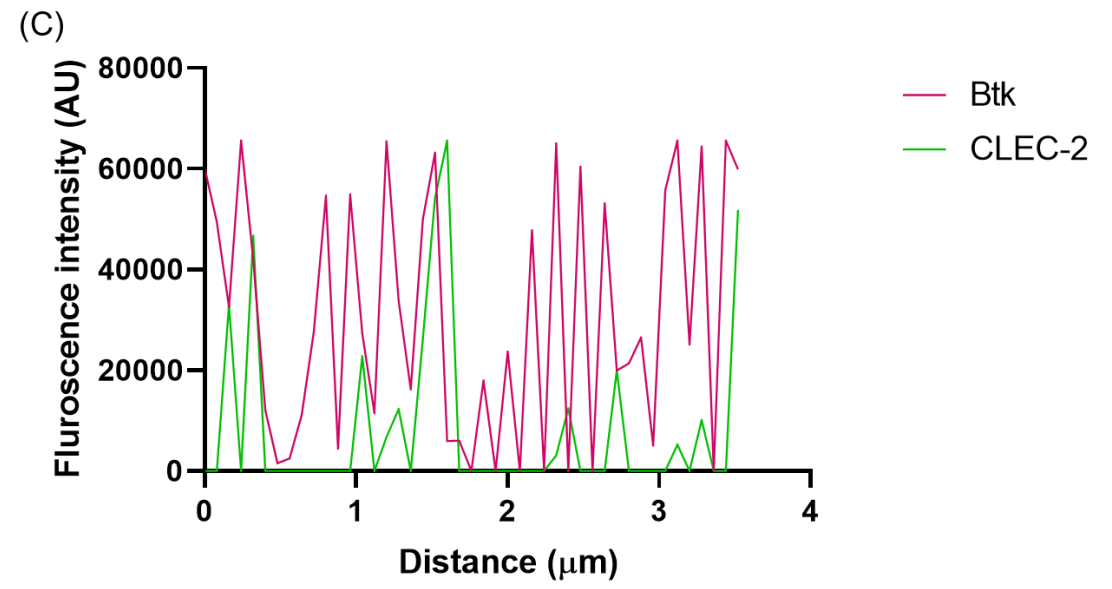
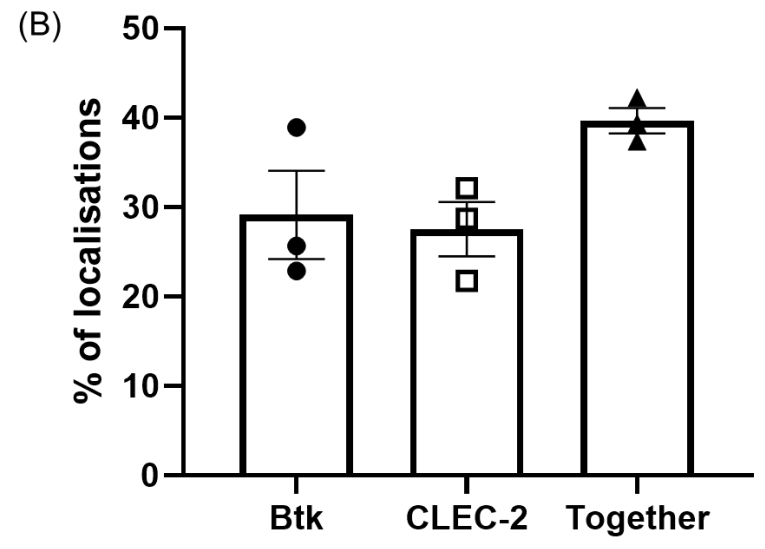
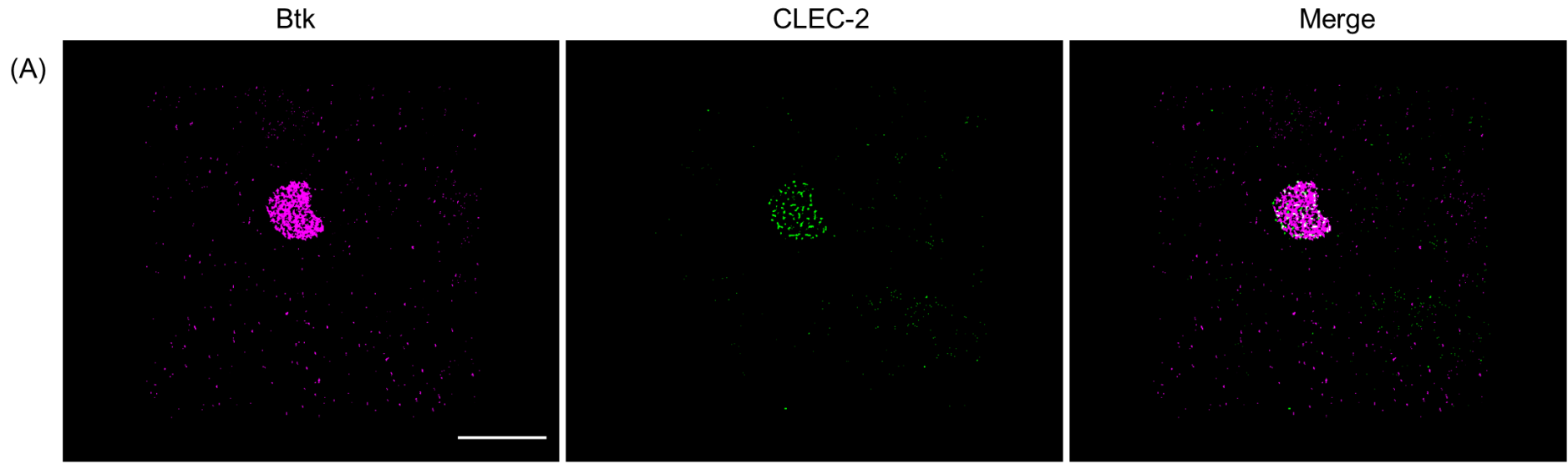


Figure 6.3.13 Btk and CLEC-2 localise together in spread platelets on rhodocytin when analysed using plot profile analysis

(A) Washed platelets 2×10^7 cells /mL were spread on 100nM rhodocytin for 45 minutes before fixation, permeabilization and staining with anti-Btk and anti-CLEC-2 before being imaged using a Nikon N-STORM system in blinking buffer to induce fluorophore blinking. 20,000 frames were captured and reconstructed using Nikon NIS-Elements STORM analysis module, applying drift correction and gaussian rendering. 3 fields of view from 3 independent experiments were imaged. Individual fluorescent blinking events were filtered on photon count and only those with a count >400 were selected for further analysis. Scale bar represents $10\mu\text{m}$. Plot profile analysis was performed using Nikon NIS-Elements by selecting 3 random cross Sections through the middle of the platelet. The resulting values were put into Excel to identify if there was fluorescence present in the Btk or CLEC-2 channel individually or together. (B) The percentage of localisations was then calculated. Graph represents mean \pm SEM, $n=3$. Statistical testing was performed using one-way ANOVA with Tukey's multiple comparisons post-test with no significance found. (C) shows a representative fluorescence intensity image of a random cross Section through the middle of the imaged platelet before normalisation.

6.3.2.7 Btk and LAT look to colocalise when spread on rhodocytin and examined using plot profile analysis

Initial work using TIRFM suggested that Btk and LAT colocalise when spread on rhodocytin. Therefore, plot profile was used to investigate if this colocalisation was maintained when imaged at a higher resolution using STORM.

Samples were prepared, imaged, and reconstructed as previously described in Section 6.3.1.5. Random cross Sections across the platelet were selected and the fluorescence intensity across the channels analysed (Figure 6.3.14.F).

When spread on rhodocytin and imaged using STORM, Btk and LAT do not look to directly colocalise as shown in the lack of white colour in the merged image (Figure 6.3.14.D). This is in direct contrast as to what was observed in TIRFM imaging.

Furthermore, when the proportion of localisations across a random cross Section were analysed, there appears to be an approximately equal amount of Btk and LAT in separate areas. There is significantly more Btk localising on its own, than with LAT ($p \leq 0.05$). This suggests that in STORM microscopy and assessment using plot profile analysis, Btk and LAT do not fully colocalise.

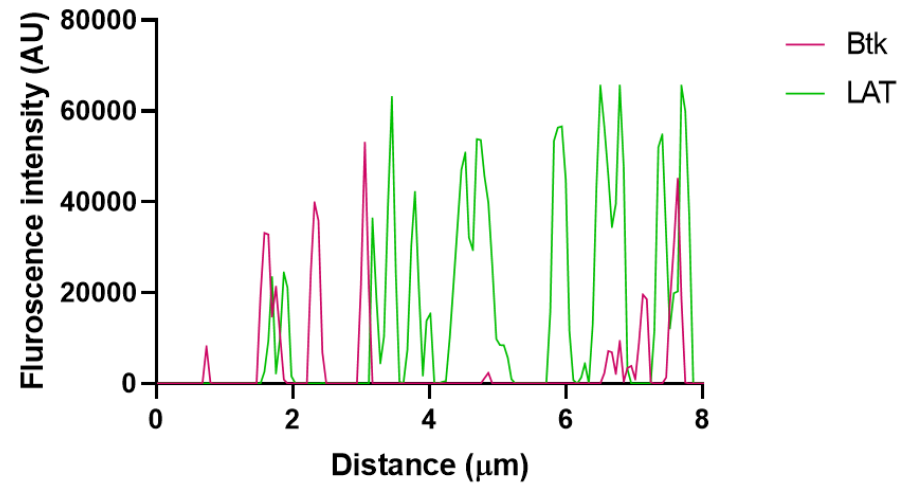
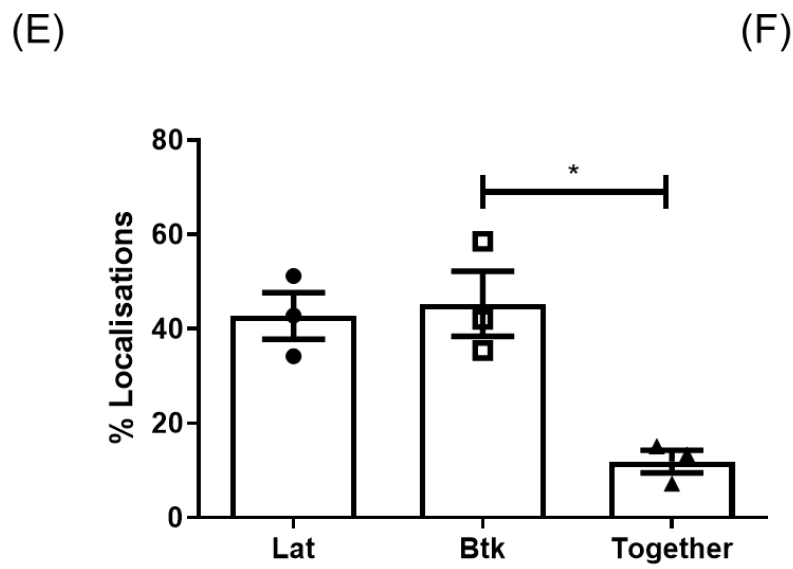
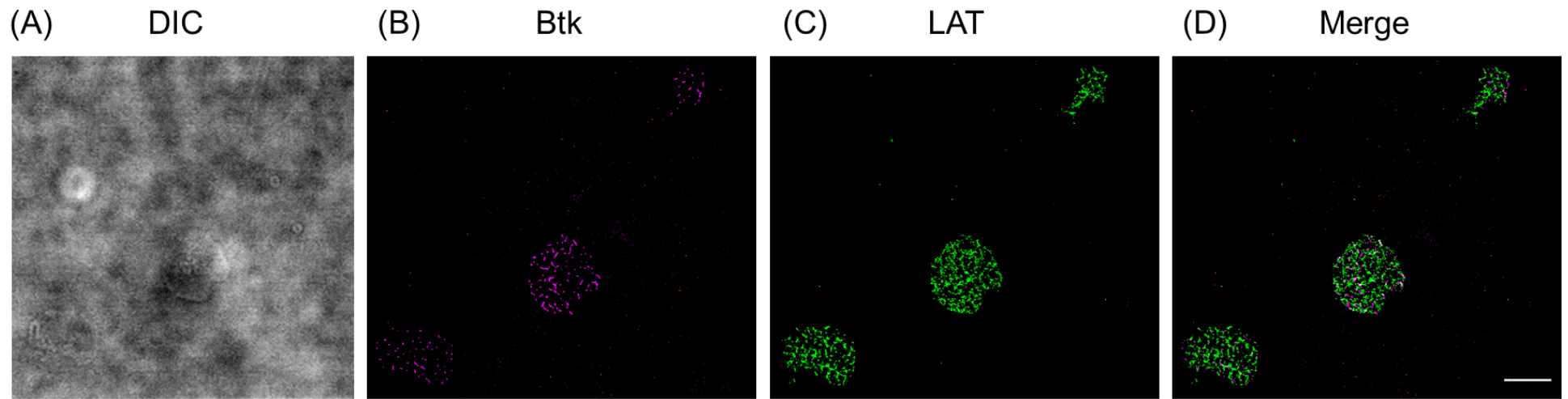


Figure 6.3.14 Btk and LAT do not look to colocalise when assessed using plot profile when spread on rhodocytin

(A-D) Washed platelets 2×10^7 cells /mL were spread on 100nM rhodocytin for 45 minutes before fixation, permeabilization and staining with (B) anti-Btk and (C) anti-LAT before being imaged using a Nikon N-STORM system in blinking buffer to induce fluorophore blinking. 20,000 frames were captured and reconstructed using Nikon NIS-Elements STORM analysis module, applying drift correction and gaussian rendering. 3 fields of view from 3 independent experiments were imaged. Individual fluorescent blinking events were filtered on photon count and only those with a count >400 were selected for further analysis (A). Scale bar represents $5\mu\text{m}$. Plot profile analysis was performed using Nikon NIS-E elements using 3 random cross Sections to analyse. The resulting values were put into Excel to identify if there was fluorescent present or absent in the Btk or LAT channel or present in both at the same location. (B) The percentage of all localisations was then calculated. Graph represents mean \pm SEM, $n=3$. Statistical testing was performed using one-way ANOVA with Tukey's multiple comparisons post-test with no significance found. (C) shows a representative fluorescence intensity image of a random cross Section through a platelet before normalisation.

6.3.3 Investigating the colocalisation of protein clusters

Previous Sections in this Chapter have investigated the clustering of proteins in platelets and the amount of colocalisation along a fibre or along a cross Section. The data above is analysed to determine if two molecules colocalise in a binary fashion. To analyse how clusters of molecules interact with each other ClusDoc software was utilised to investigate cluster colocalisation. (Pageon et al., 2016).

All samples were imaged and reconstructed as previously described in Sections 6.3.1. Co-ordinate files were loaded into ClusDoc which runs via MATLAB. Cluster parameters were set as a minimum of 10 points within a 50nm radius (epsilon) as described in Poulter et al. A CBC value of 0.4 or over was selected as a measurement of colocalisation according to recommendations from the literature (Pageon et al., 2016).

6.3.3.1 Clusters of GPVI colocalise with Btk more than clusters of Btk with GPVI

There is no significant difference in the number of clusters that are colocalised for Btk with GPVI when platelets are spread on collagen. However, there is a significant number of GPVI clusters that colocalise with Btk compared with GPVI without Btk, Figure 6.3.16.B ($p \leq 0.01$).

GPVI clusters are much larger than Btk clusters ($p \leq 0.05$). As DBSCAN analysis is propagative, the GPVI clusters are larger when associated with the collagen fibre. Indeed, the GPVI colocalised clusters are significantly less circular than their non-colocalised counterparts, suggesting colocalised clusters are along the fibre, Figure 6.3.16.E

Furthermore, there is a significant increase in the size of GPVI clusters that colocalise with Btk compared to GPVI clusters which do not colocalise ($p \leq 0.05$), Figure 6.3.16.D.

This is also reflected in the increased number of localisations per colocalised GPVI cluster ($p \leq 0.05$), Figure 6.3.16.E.

ROI
Btk - green
GPVI - red

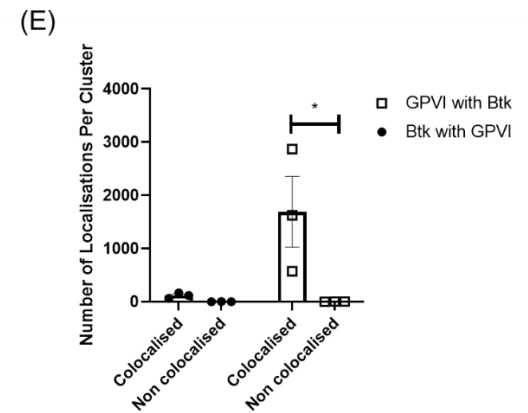
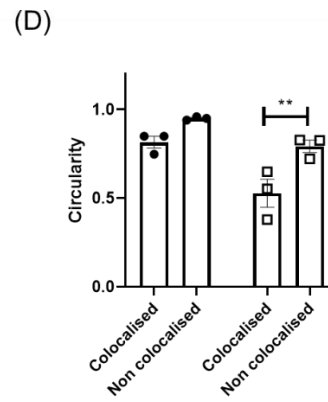
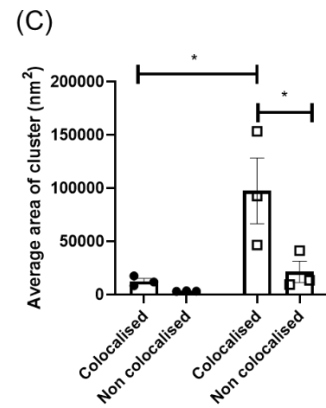
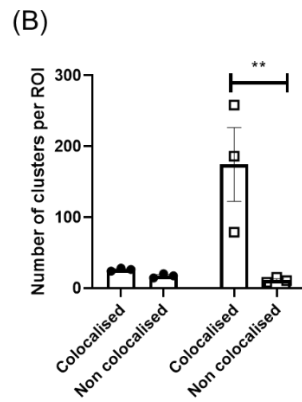
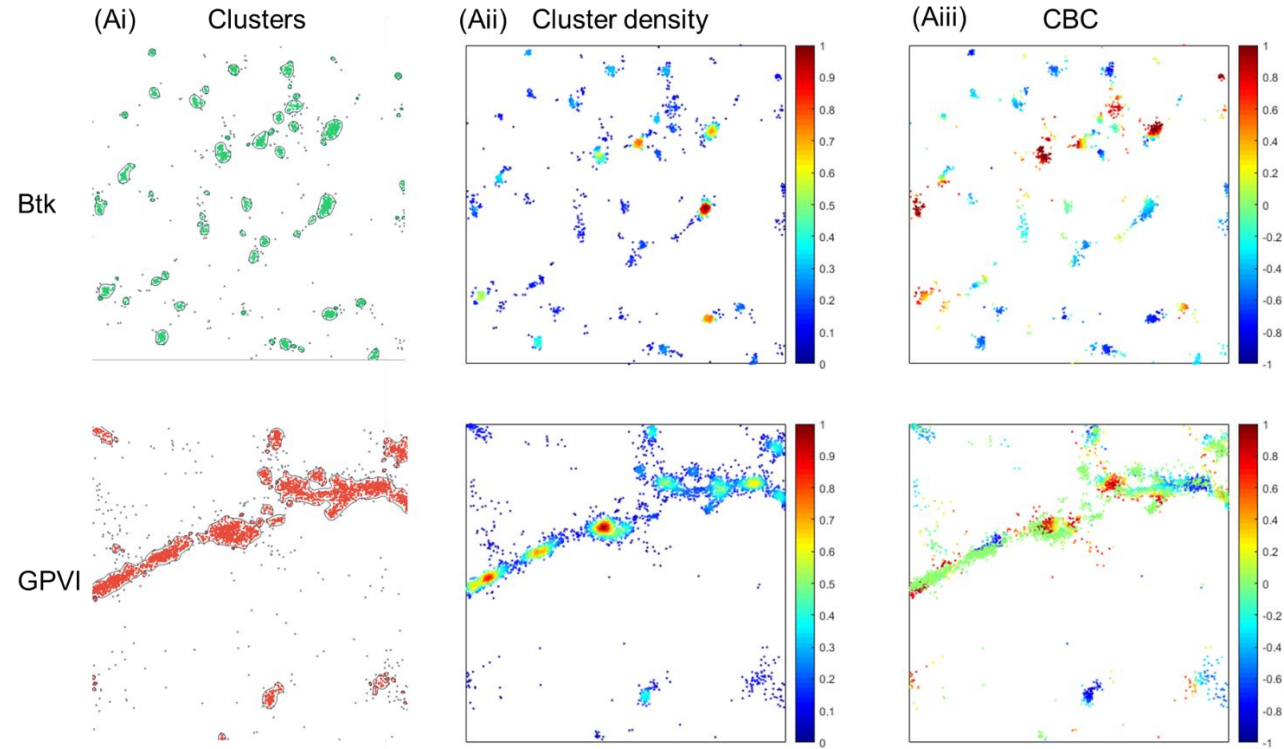
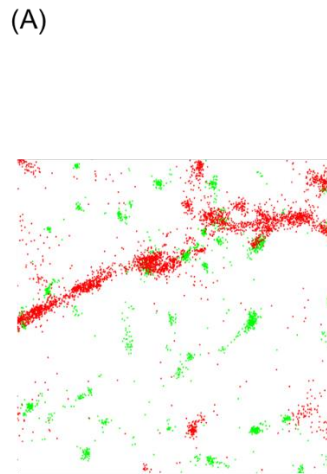


Figure 6.3.15 Cluster analysis of Btk and GPVI co-clusters

Washed platelets 2×10^7 cells /mL were spread on $10 \mu\text{g/mL}$ collagen for 45 minutes before fixation, permeabilization and staining with anti-Btk and anti-GPVI before being imaged. Samples were imaged using a Nikon N-STORM system in blinking buffer to induce fluorophore blinking. 20,000 frames were captured and reconstructed using Nikon NIS-Elements STORM analysis module, applying drift correction and gaussian rendering. 3 fields of view from 3 independent experiments were imaged. Individual fluorescent blinking events were filtered on photon count and only those with a count >400 were selected for further analysis using ClusDoC. (A) Representative ROI from a reconstructed image with Btk in green and GPVI in red, with clusters of GPVI and Btk identified (cluster defined as ≥ 10 localisations within 50nm) (i), the cluster density (ii) and the CBC plots (radius is also 50nm) (iii). Clusters with CBC values greater than 0.4 were analysed further and the (B) number of clusters (C) average area of a cluster, (D) circularity of a cluster and the $\bar{\epsilon}$ number of localisations per cluster were quantified. Graphs represent mean \pm SEM, $n=3$. Statistical testing was performed using two-way ANOVA with Dunnett's post-test, $*p \leq 0.05$.

6.3.3.2 Btk kinase inhibition does not inhibit the number of GPVI or Btk clusters, or their colocalisation relative to each other.

Using LAMA and DBSCAN in Section 6.3.1.3, it was identified that 1 μ M acalabrutinib increased the size of GPVI clusters. ClusDoC was used to quantify the relationship between Btk and GPVI in the presence of the Btk inhibitor acalabrutinib. If Btk clusters and GPVI clusters colocalise when its kinase activity is inhibited, it would suggest a potential negative regulation as a scaffold in downstream of GPVI clustering.

Compared to vehicle control, there is no significant difference in the number of clusters, the average area of a cluster, the circularity of a cluster or the number of localisations per cluster for drug treated platelets spread on collagen for GPVI clusters and Btk clusters which colocalise or not (Figure 6.3.17 Di-Hii). This suggests using this analysis that clustering of GPVI and Btk is not regulated by the catalytic activity of Btk in contrast to the results identified in Section 6.3.1.3.

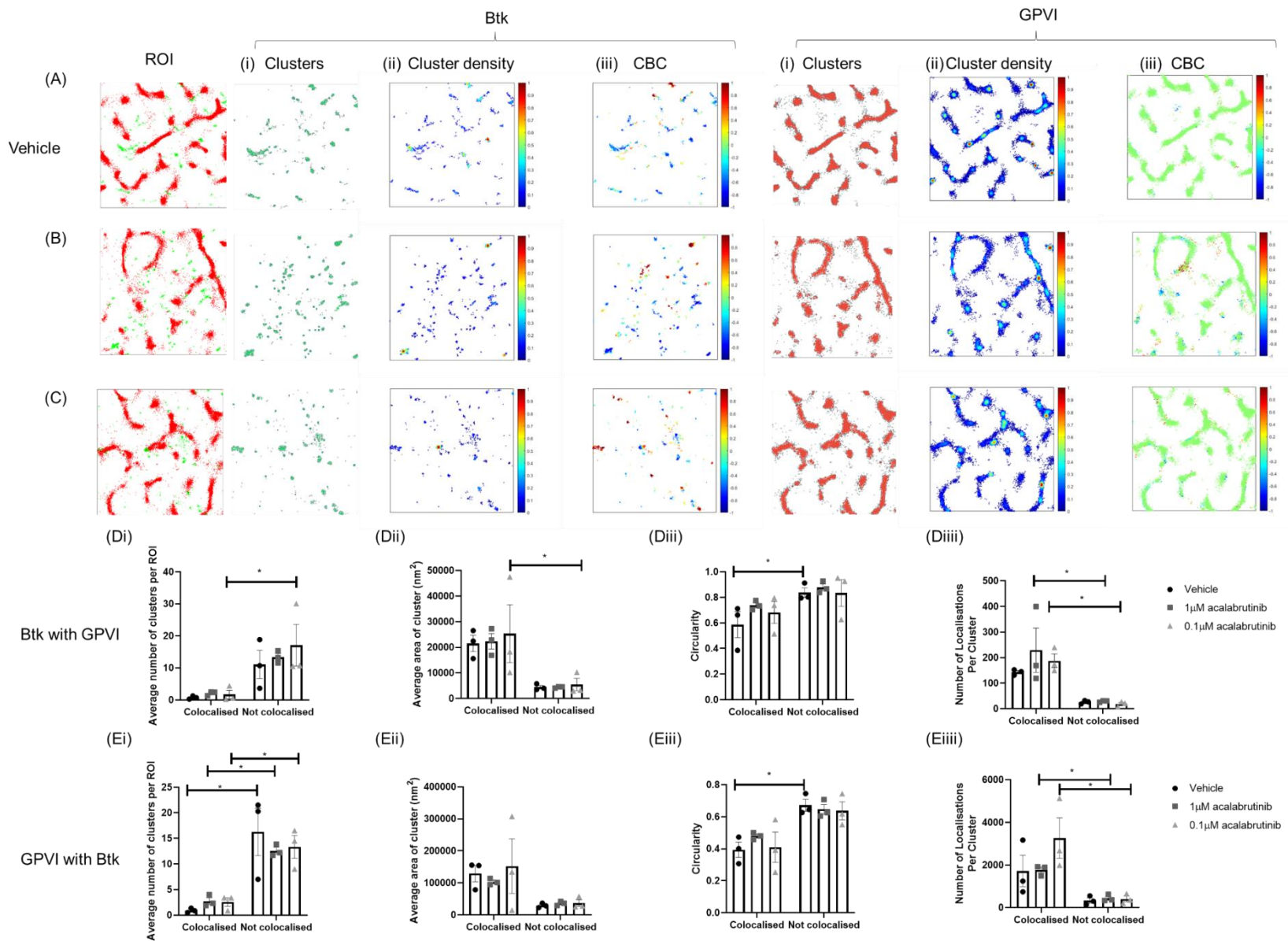


Figure 6.3.16 Acalabrutinib does not alter clustering of Btk and GPVI using ClusDoC

Washed platelets 2×10^7 cells /mL were pre-treated with $1 \mu\text{M}$, $0.1 \mu\text{M}$ acalabrutinib or vehicle control before being spread on $10 \mu\text{g/mL}$ collagen for 45 minutes before fixation, permeabilization and staining with anti-Btk and anti-GPVI before being imaged using a Nikon N-STORM system in blinking buffer to induce fluorophore blinking. 20,000 frames were captured and reconstructed using Nikon NIS-Element STORM analysis module, applying drift correction and gaussian rendering. 3 fields of view from 3 independent experiments were imaged. Individual fluorescent blinking events were filtered on photon count and only those with a count >400 were selected for further analysis using ClusDoC. Representative ROI from (A) vehicle (B) $1 \mu\text{M}$ acalabrutinib and (C) $0.1 \mu\text{M}$ acalabrutinib treated platelets; reconstructed image with Btk in green and GPVI in red, with clusters of GPVI and Btk identified (cluster defined as ≥ 10 localisations within 50nm) (i) the cluster density (ii) and the CBC plots (radius is also 50nm) (iii). Clusters with CBC values greater than 0.4 were analysed further and the number of clusters (D_i , E_i) average area of a cluster, (D_{ii} , E_{ii}) circularity of a cluster and the (D_{iii} , E_{iii}) number of localisations per cluster (D_{iiii} , E_{iiii}) for Btk (D_{i-iii}) and GPVI (E_{i-iiii}) were quantified. Graphs represent mean \pm SEM, $n=3$. Statistical testing was performed using two-way ANOVA with Dunnett's post-test, $*p \leq 0.05$.

6.3.3.3 *Btk and GPVI clusters do not colocalise on CRP-XL*

When platelets are spread on CRP-XL there are more clusters of GPVI than there are of Btk, with most of the GPVI clusters not associated with Btk ($p \leq 0.001$) (Figure 6.3.18.B). GPVI clusters that do not localise with Btk have more molecules per cluster than those which colocalise with Btk ($p \leq 0.05$), Figure 6.3.18.F.

Taken together this suggests, although there are less of them, the GPVI clusters that are colocalised with Btk are more compact. As the localisations per cluster increase, but the cluster area does not (Figure 6.3.18.C). More compact clusters may be a sign of increased activity due to more molecules being present.

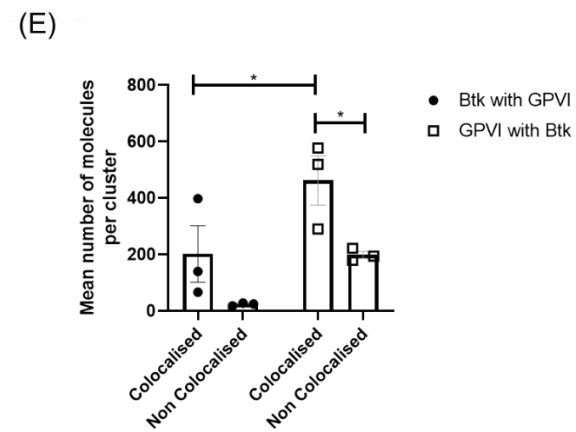
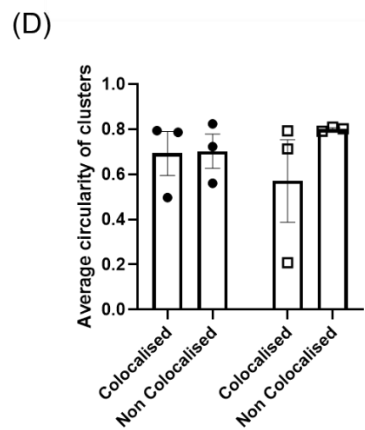
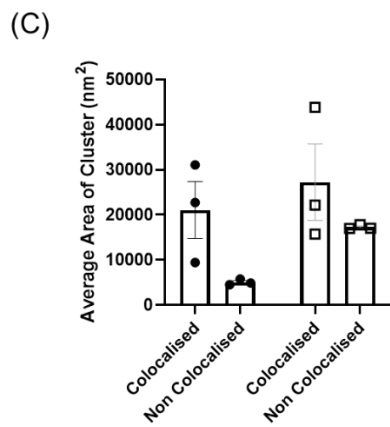
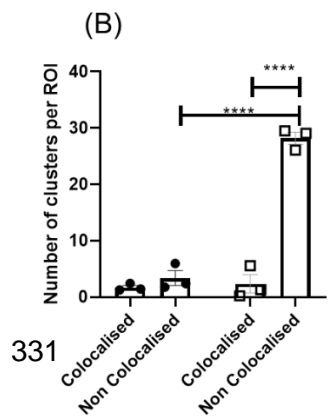
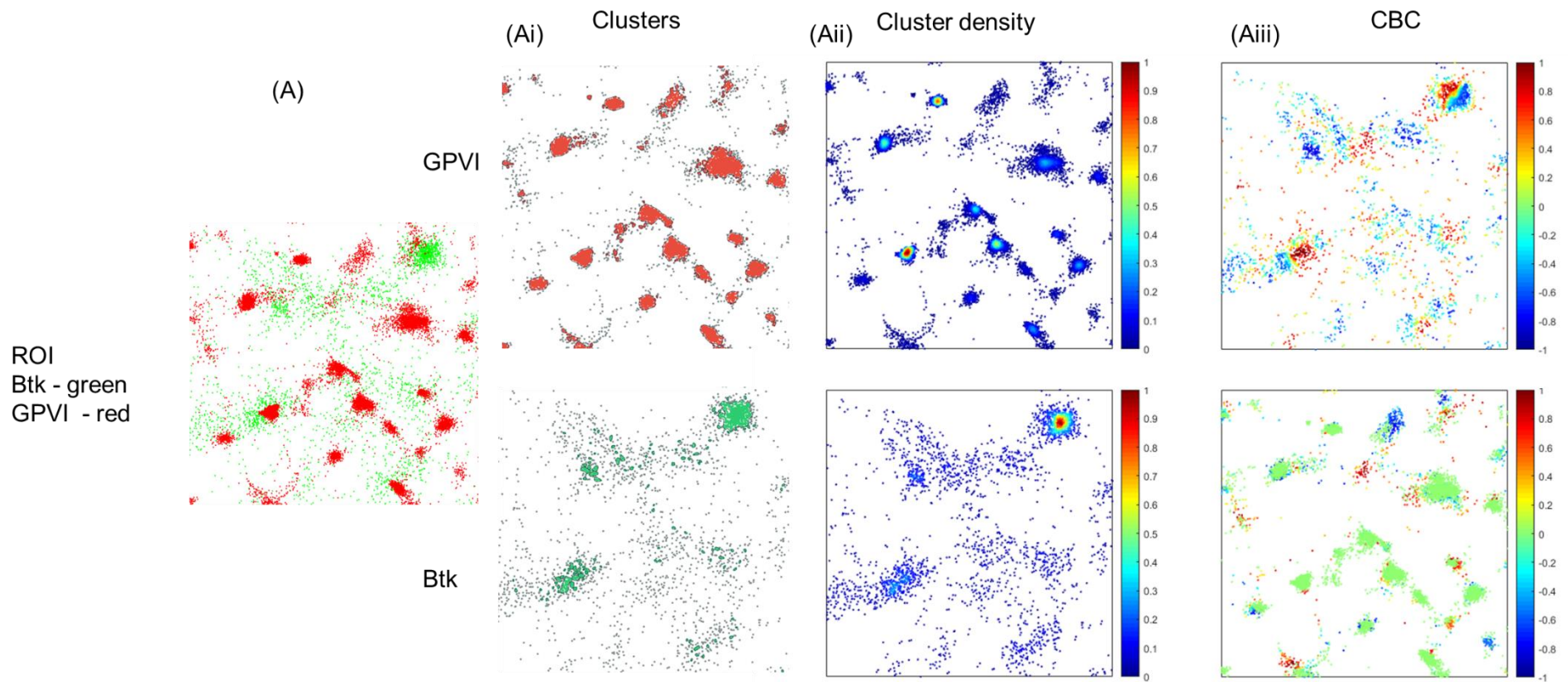


Figure 6.3.17 Btk and GPVI do not localise when platelets are spread on CRP-XL

Washed platelets 2×10^7 cells /mL were spread on $1 \mu\text{g/mL}$ CRP for 45 minutes before fixation, permeabilization and staining with anti-Btk and anti-GPVI before being imaged using a Nikon N-STORM system in blinking buffer to induce fluorophore blinking. 20,000 frames were captured and reconstructed using Nikon NIS-Elements STORM analysis module, applying drift correction and gaussian rendering. 3 fields of view from 3 independent experiments were imaged. Individual fluorescent blinking events were filtered on photon count and only those with a count >400 were selected for further analysis using ClusDoC. (A) Representative ROI from a reconstructed image with Btk in green and GPVI in red, with clusters of GPVI and Btk identified (cluster defined as ≥ 10 localisations within 50nm) (i) the cluster density (ii) and the CBC plots (radius is also 50nm) (iii). Clusters with CBC values greater than 0.4 were analysed further and the (B) number of clusters (C) average area of a cluster, (D) circularity of a cluster and the (E) number of localisations per cluster were quantified. Statistical testing was performed using two-way ANOVA with Dunnett's post-test, $*p \leq 0.05$, $****p \leq 0.001$. Graphs represent mean \pm SEM. $n=3$.

6.3.3.4 Btk preferentially localises with LAT when platelets spread on collagen.

Coclustering of Btk and LAT were investigated using ClusDoC. There is an equal number of LAT clusters that form with and without Btk, Figure 6.3.19.B. However, there are significantly more clusters of Btk that have LAT present (colocalised) compared with non-colocalised clusters, Figure 6.3.19.B, and these have significantly more localisations per cluster (Figure 6.3.19.E). Taken together, this suggests that Btk preferentially localises with LAT as there are more clusters of Btk that have LAT within them. These clusters of Btk with LAT have more localisations, suggesting more molecules present which may represent increased recruitment of Btk to signalling areas.

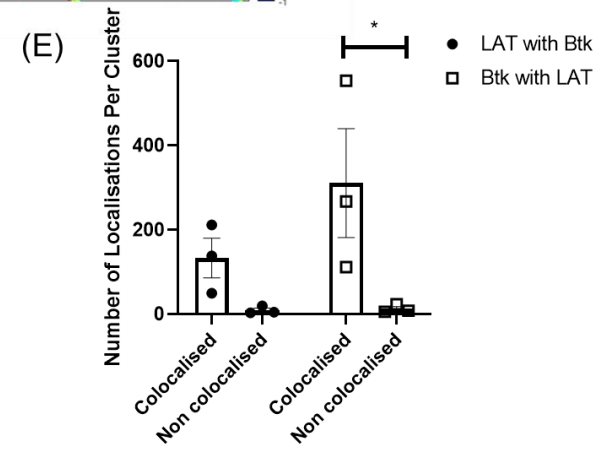
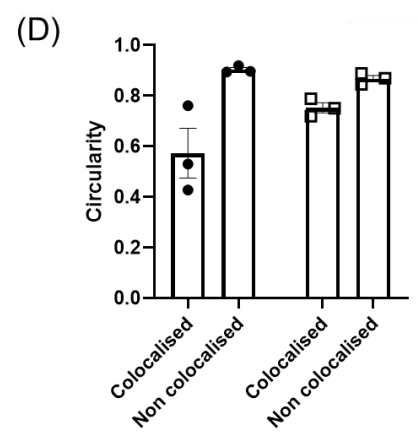
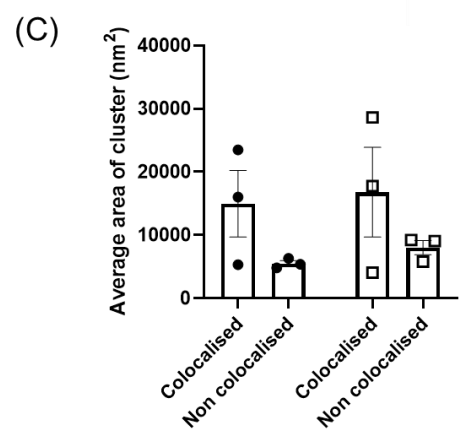
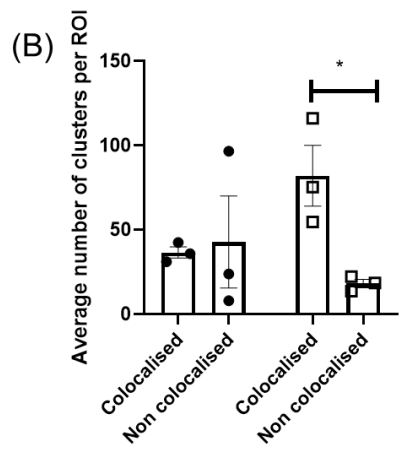
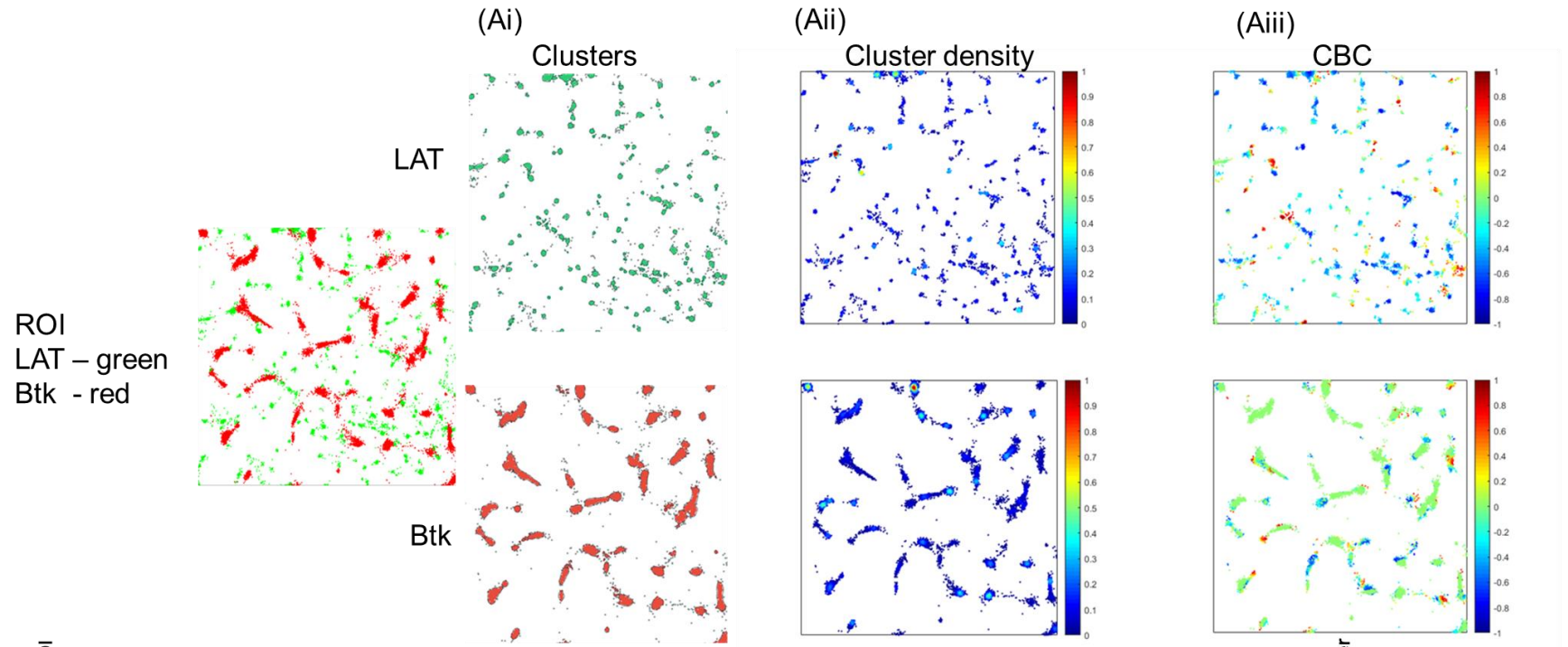


Figure 6.3.18 Btk preferentially colocalises with LAT

Washed platelets 2×10^7 cells/mL were spread on $10 \mu\text{g/mL}$ collagen for 45 minutes before fixation, permeabilization and staining with anti-Btk and anti-LAT before being imaged using a Nikon N-STORM system in blinking buffer to induce fluorophore blinking. 20,000 frames were captured and reconstructed using Nikon NIS-Elements STORM analysis module, applying drift correction and gaussian rendering. 3 fields of view from 3 independent experiments were imaged. Individual fluorescent blinking events were filtered on photon count and only those with a count >400 were selected for further analysis using ClusDoC. (A) Representative ROI from a reconstructed image with Btk in red and LAT in green, with clusters of LAT and Btk identified (cluster defined as ≥ 10 localisations within 50nm) (i) the cluster density (ii) and the CBC plots (radius is also 50nm) (iii). Clusters with CBC values greater than 0.4 were analysed further and the (B) number of clusters (C) average area of a cluster, (D) circularity of a cluster and the (E) number of localisations per cluster were quantified. Statistical testing was performed using two-way ANOVA with Dunnett's post-test, $*p \leq 0.05$. Graphs represent mean \pm SEM. $n=3$.

6.3.3.5 Btk and CLEC-2 do not colocalise when platelets spread on rhodocytin

Using TIRFM and MCC and plot profile, Btk looks to colocalise with CLEC-2 more than GPVI, it was investigated to identify if clusters of Btk and CLEC-2 colocalise together.

Most of the Btk clusters are not associated with CLEC-2. There is on average approximately 10x more clusters of Btk that do not seem to colocalise with CLEC-2 (74.59 ± 19.33 , ($p \leq 0.01$ when compared to colocalised Btk clusters. The Btk clusters that do colocalise with CLEC-2 are significantly larger than the clusters that do not. However, for CLEC-2 clusters, there is no difference in the average cluster area if they are colocalised with Btk or not, (Figure 6.3.20.C).

In addition to being larger, Btk clusters have more Btk localisations per cluster when they colocalises with CLEC-2. This is consistent with the observations that Btk colocalises with CLEC-2 when assessed using TIRFM.

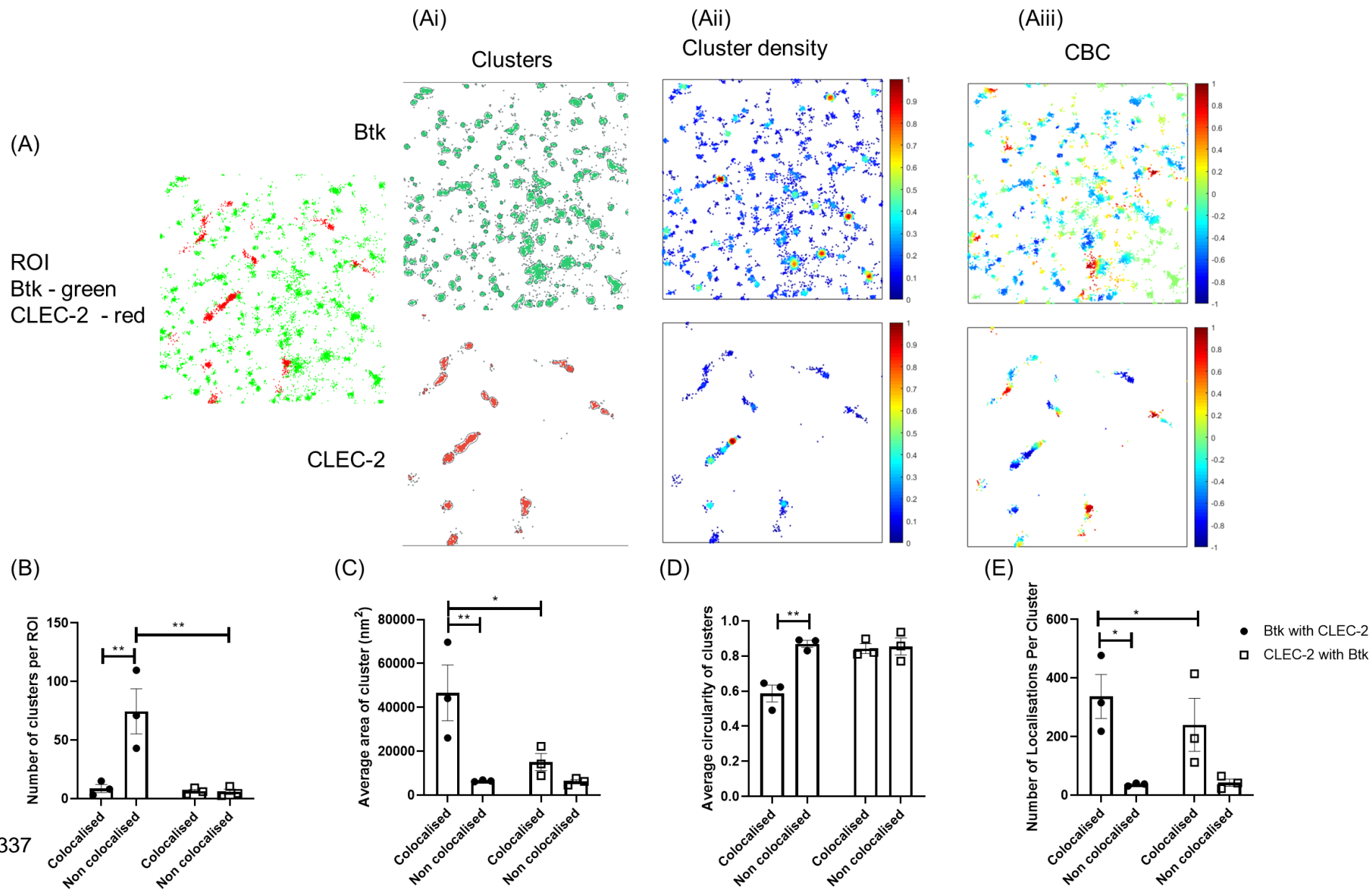


Figure 6.3.19 Btk and CLEC-2 do not strongly colocalise

Washed platelets 2×10^7 cells /mL were spread on 100nM rhodocytin for 45 minutes before fixation, permeabilization and staining with anti-Btk and anti-CLEC-2 before being imaged using a Nikon N-STORM system in blinking buffer to induce fluorophore blinking. 20,000 frames were captured and reconstructed using Nikon NIS-Elements STORM analysis module, applying drift correction and gaussian rendering. 3 fields of view from 3 independent experiments were imaged. Individual fluorescent blinking events were filtered on photon count and only those with a count >400 were selected for further analysis using ClusDoC. (A) Representative ROI from a reconstructed image with Btk in green and CLEC-2 in red, with clusters of CLEC-2 and Btk identified (cluster defined as ≥ 10 localisations within 50nm) (i) (, the cluster density (ii) and the CBC plots (radius is also 50nm) (iii). Clusters with CBC values greater than 0.4 were analysed further and the (B) number of clusters (C) average area of a cluster, (D) circularity of a cluster and (E) number of localisations per cluster were quantified. Statistical testing was performed using two-way ANOVA with Dunnett's post-test, $*p \leq 0.05$, $***p \leq 0.01$. Graphs represent mean \pm SEM. n=3.

6.3.3.6 Btk partially colocalised with LAT when platelets spread on rhodocytin

As Btk and LAT look to co-cluster when spread on collagen (Section 6.3.3.4), this was investigated on the CLEC-2 ligand, rhodocytin.

Significantly more clusters of LAT are identified without the presence of Btk ($p \leq 0.05$).

Whereas there was similar number of clusters of Btk localising with and without LAT (18 ± 3 and 19 ± 6 respectively), (Figure 6.3.21.B). Clusters of LAT that colocalise are approximately 5x larger than clusters that do not colocalise ($p \leq 0.05$). There is no significant difference in the size of the clusters of Btk colocalised with LAT compared to without LAT. However, the number of localisations detected per cluster is significantly greater for Btk clusters colocalised with LAT than Btk clusters without LAT ($p \leq 0.01$). This is also observed with LAT clusters (Figure 6.3.21.E), and LAT clusters which are significantly larger when colocalised with Btk than LAT clusters without Btk ($p \leq 0.05$), (Figure 6.3.21.C).

This suggests that colocalised clusters of LAT are larger, even though there are fewer of them. In contrast, Btk clusters that are colocalised are the same size but denser than non-colocalised clusters. This suggests stronger recruitment of Btk to LAT than LAT to Btk, consistent with literature that LAT recruits Btk (Hashimoto et al., 1999a).

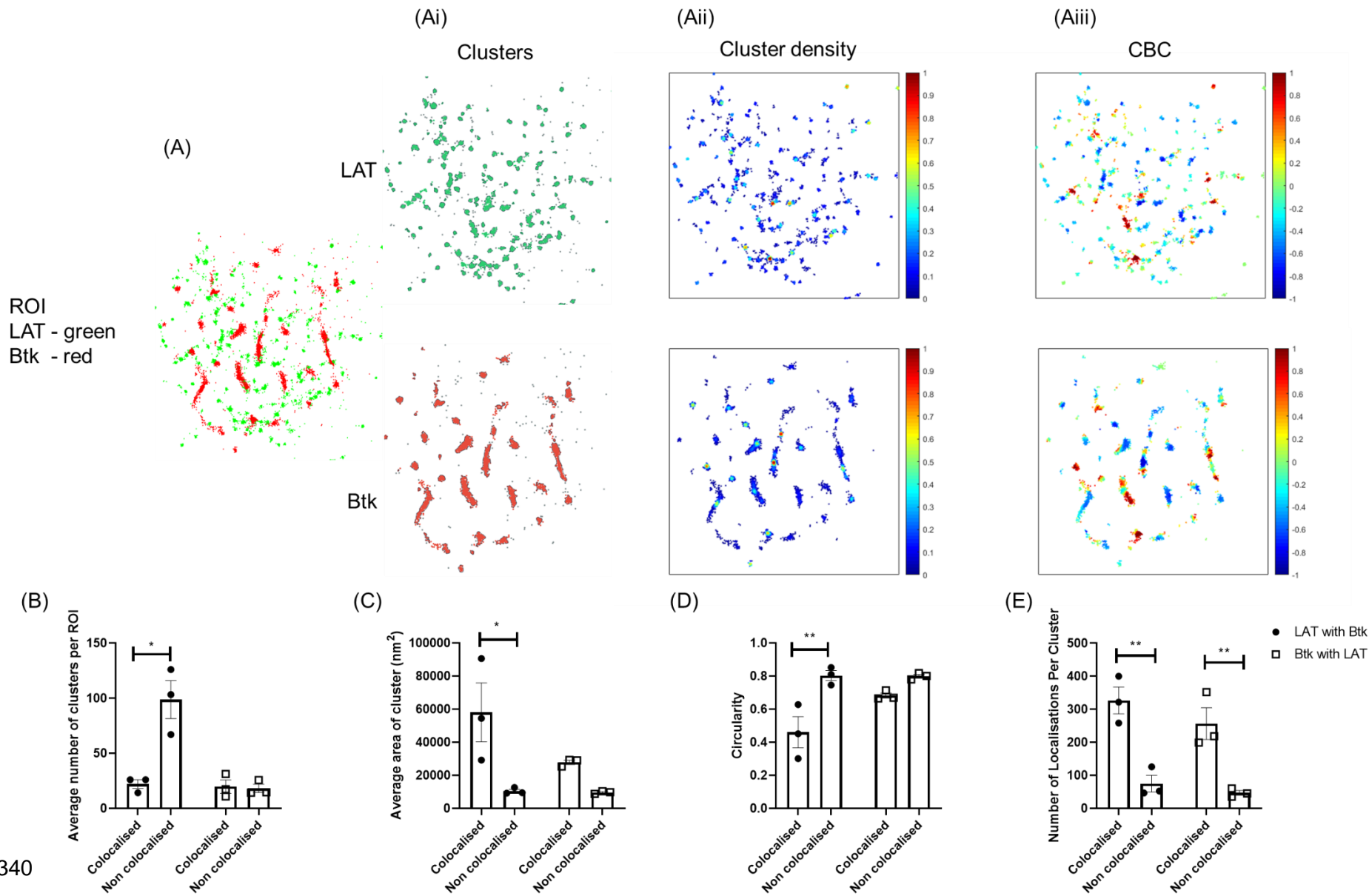


Figure 6.3.20 Btk partially colocalises with LAT when platelets are spread on rhodocytin

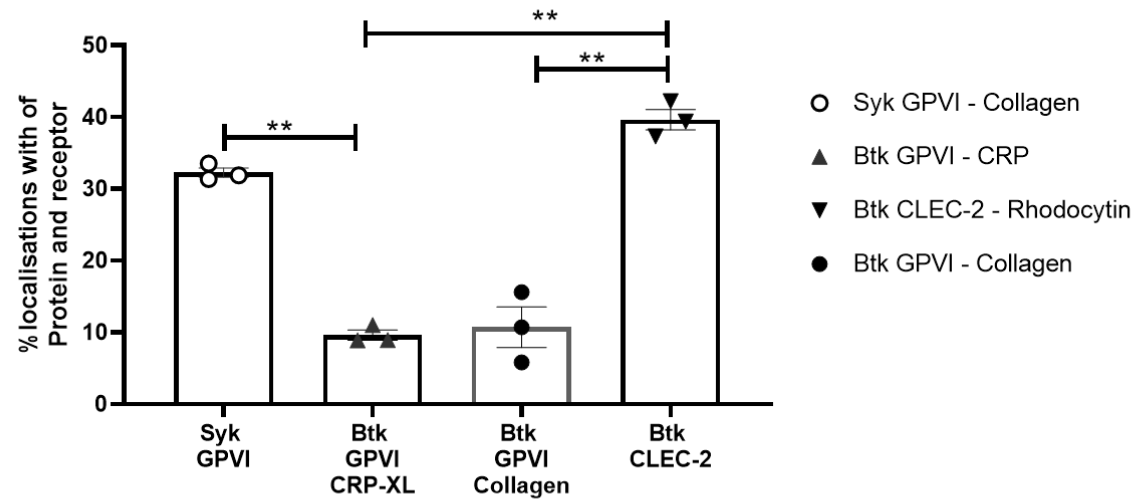
Washed platelets 2×10^7 cells /mL were spread on 100nM rhodocytin for 45 minutes before fixation, permeabilization and staining with anti-Btk and anti-LAT before being imaged using a Nikon N-STORM system in blinking buffer to induce fluorophore blinking. 20,000 frames were captured and reconstructed using Nikon NIA-Elements STORM analysis module, applying drift correction and gaussian rendering. 3 fields of view from 3 independent experiments were imaged. Individual fluorescent blinking events were filtered on photon count and only those with a count >400 were selected for further analysis using ClusDoC. (A) Representative ROI from a reconstructed image with Btk in red and LAT in green, with clusters of LAT and Btk identified (cluster defined as ≥ 10 localisations within 50nm) (i) (, the cluster density (ii) and the CBC plots (radius is also 50nm) (iii). Clusters with CBC values greater than 0.4 were analysed further and the (B) number of clusters (C) average area of a cluster, (D) circularity of a cluster and the (E) number of localisations per cluster were quantified. Statistical testing was performed using two-way ANOVA with Dunnett's post-test, $*p \leq 0.05$, $***p \leq 0.01$ Graphs represent mean \pm SEM. n=3.

6.3.4 Results summary

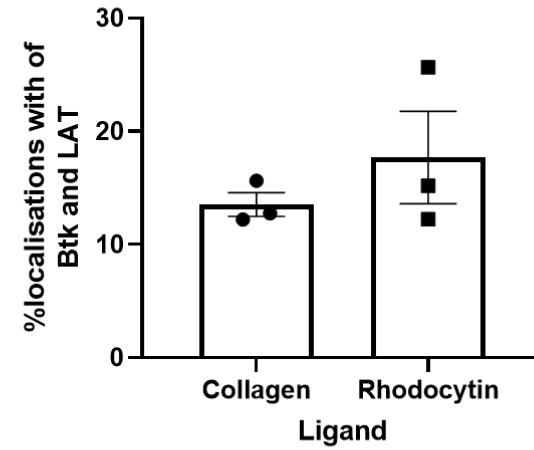
From the calculated plot profiles, the % localisations that appear together were taken and compared. As Figure 6.3.22.A shows, the percentage of localisations of Syk and GPVI together is significantly greater than the amount of Btk localising with GPVI spread on CRP-XL ($p \leq 0.01$), but not on collagen. This suggests that Btk localises nearer to GPVI on collagen than it does on CRP-XL. Btk and CLEC-2 significantly localise together more than Btk and GPVI, independently of if it spread on collagen or CRP (* $p \leq 0.05$, ** $p \leq 0.01$). This suggests that Btk localises more with CLEC-2 than GPVI. The localisations of Btk with LAT were compared across ligands, and there is no significant difference between collagen and rhodocytin. This suggests that Btk is localising with LAT on both ligands.

Heat maps to summarise the ClusDoC cluster output of Btk clusters colocalising with GPVI, LAT or CLEC-2 were calculated with red being areas of low. As Figure 6.3.22.C shows, Btk colocalises with LAT when spread on collagen the most.

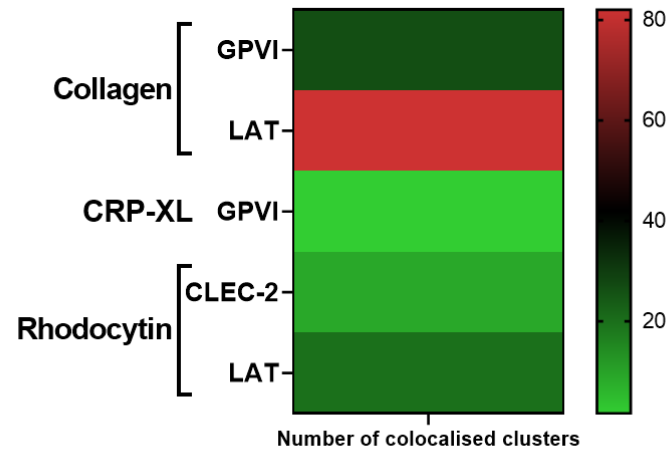
(A)



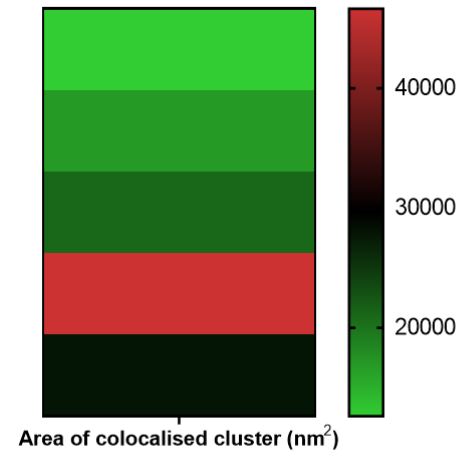
(B)



(C)



(D)



(E)

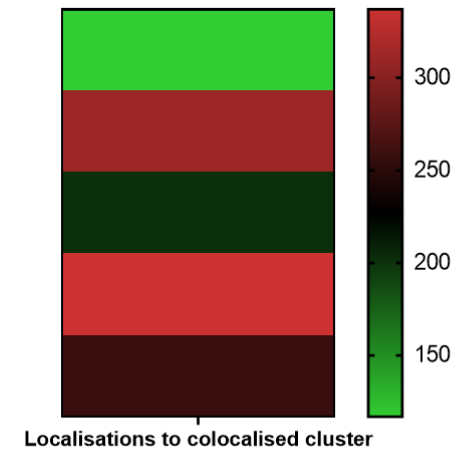


Figure 6.3.21 Btk and CLEC-2 colocalise more than Btk and GPVI and there is no difference in the localisation of Btk and LAT on either rhodocytin or collagen.

(A) The amount of localizations together was plotted into a graph from plot profile analysis and compared using one-way ANOVA with Tukey's multiple comparisons test with significance taken at $*p \leq 0.05$ and $**p \leq 0.01$. Graph represents mean \pm SEM, N=3. (B) plot profile analysis from Btk and LAT spread on collagen and rhodocytin were calculated. Statistical testing was performed using a two-way T – Test with no significance found. (C) the mean number of colocalised clusters, (D) the average area of a colocalised cluster and (E) the number of localisations to a colocalised cluster were plotted into heat maps for Btk colocalising with GPVI on collagen and CRP-XL, LAT on rhodocytin and collagen and CLEC-2. Areas of green indicate low numbers, with red being high values.

6.4 Discussion

6.4.1 Aim - Investigate the localisation of Btk in relation to GPVI, LAT and CLEC-2 and verify the colocalisation results in chapter 5

Btk and GPVI

Using plot profile analysis drawing along the collagen fibre, as expected, most of the localisations present were GPVI (Figure 6.3.9). Some Btk can be found with GPVI at the fibre, but more GPVI is present alone. However, there is a proportion (approximately 20%) where Btk and GPVI are localised together. This suggests that Btk is recruited to the collagen fibre to help mediate the signalling.

In some images, Btk looks adjacent to the collagen fibre. The diameter of a collagen fibre is anywhere between 30 to 300nm, so it is possible that Btk may be localised at the fibre, however, the parameters selected in ClusDoC do not allow for appropriate analysis (Orgel et al., 2006). Using ClusDoC, there are similar number of Btk clusters that colocalise with GPVI as without GPVI, whereas there is trend of more GPVI clusters colocalising with Btk.

When spread on CRP-XL, a smaller proportion of Btk and GPVI localise together when assessed using plot profile (around 10%), and when assessed using ClusDoc, indicated in a lighter shade of green in the heatmaps in Figure 6.3.22.C. When platelets are spread on collagen, there are significantly more clusters of Btk that localise with GPVI which is shown in the darker green in the heatmap (Figure 6.3.22.C). This suggests on a specific GPVI agonist that Btk does not localise as near to GPVI, as non an agonist for both GPVI and $\alpha_2\beta_1$.

Btk and CLEC-2

Using plot profile, Btk looks to localise with CLEC-2 across a random cross section of a platelet. However, colocalisation was assessed using ClusDoC, and significantly more Btk clusters form with no CLEC-2 present (Figure 6.3.20). This contrasts with the results obtained for plot profile (Figure 6.3.13). It is known that molecular partners with a common function do not always particularly congregate in clusters. This is observed in proteins involved in vesicle fusion, SNAP25 and Syntaxin 1. The clusters are located near each other, but are not arising in the same structure (Halemani et al., 2010). Therefore, this may explain why it looks that Btk and CLEC-2 colocalise using plot profile, but do not using ClusDoC.

Btk and LAT

There is no difference in localisation of Btk with LAT when spread on either GPVI agonist collagen or CLEC-2 agonist rhodocytin using plot profile (Figure 6.3.22.B). LAT is a key mediator in both pathways (Pasquet et al., 1999b, Suzuki-Inoue et al., 2006, Fuller et al., 2007). Btk also does not look to strongly localise with GPVI, but does LAT. The TCR and LAT have been shown to form into distinct 'protein islands' in T cells (Lillemeier et al., 2010), so Btk may not be localising with GPVI as it is at the LAT 'protein island'.

For Btk clusters which have LAT present, the sizes look similar (around 20,000nm²) on both ligands (Figure 6.3.19 and 6.3.21). However, for LAT clusters colocalising with Btk, the clusters are much larger on rhodocytin when compared to the colocalised clusters on collagen. It is possible that as Btk is localising near the larger clusters of LAT, it may also be near CLEC-2. Therefore, it may explain why Btk looks to localise more with CLEC-2 than GPVI in plot profile analysis.

The results showing that Btk localises with LAT in a spread platelet are unsurprising as Btk and LAT have been shown to interact biochemically when LAT is pulled down (Pasquet et al., 1999b). Interestingly, FcR γ chain is also pulled down when LAT is

immunoprecipitated, so therefore it is not unreasonable to believe that the limit of resolution of ClusDoc and plot profile may be missing the interaction between GPVI and Btk.

In Figure 6.3.19.Aiii, Btk and LAT look to form discrete protein complexes, however they seemingly have small contacts with each other which is demonstrated in areas of red. This fits with the hypothesis that protein complexes can form 'islands' and can likely interact with one another. Furthermore, protein clusters that are next to each other with some partial overlap can be observed in monocytes (Garcia-Parajo et al., 2014). Lymphocyte function-associated antigen-1 forms clusters approximately 70nm in diameter, and glycosylphosphatidylinositol-anchored proteins form clusters approximately 10nm in diameter. These protein clusters are situated next to one another and interact to form a nanoplatform to mediate signalling (Garcia-Parajo et al., 2014). The interaction is only at the perimeters of the clusters, not total cluster integration of the proteins. This may explain the observed partial colocalisation of Btk and LAT, where it looks like part of Btk clusters interact with LAT clusters but not total overlap.

6.4.2 Aim - To investigate the clustering of Btk on collagen, CRP-XL and rhodocytin.

In silico evidence has suggested that Btk undergoes clustering as one molecule of Btk is responsible for phosphorylating another molecule of Btk (Chung et al., 2019, Wang et al., 2019b). No work has been published investigating if Btk undergoes clustering in platelets.

Btk clustering on collagen

At a range of radii, a number of clusters are detected on collagen, which suggests that indeed, Btk is undergoing clustering (Figure 6.3.1). There are more clusters of Btk on collagen than there are on CRP-XL (Figure 6.3.2). This suggests there may be a potential difference in the regulation of Btk on collagen compared to CRP-XL.

Less clusters of Btk on CRP-XL suggests there may be more free molecules of Btk (not in a cluster) in the spread CRP-XL platelet. A potential reason for this is Btk clustering may be a mechanism of reserve. Clustering of multiple proteins into stable entities would avoid loss of components from functional complexes, so would likely result in a sustained signal (Lang and Rizzoli, 2010). Keeping Btk in a cluster may prevent Btk from interacting with other proteins such as SHIP1 (Pasquet et al., 2000, Tomlinson et al., 2004a, Chari et al., 2009). SHIP1 acts as a negative regulator on GPVI signalling, acting as a terminator (Chari et al., 2009). This may be more essential for collagen mediated activation compared to CRP-XL as it is known that collagen signalling is more sustained (Tomlinson et al., 2007).

There is also another collagen receptor, $\alpha 2\beta 1$. This binds the GFOGER sequence in collagen. There may be more clusters on collagen as opposed to CRP-XL due to Btk also undergoing clustering to help mediate signalling through this integrin. Experiments to investigate the localisation of $\alpha 2\beta 1$ in relation to Btk should be performed to investigate this.

Btk clustering on rhodocytin

Compared to collagen ligands, there are fewer clusters of Btk when spread on rhodocytin (Figures 6.3.5 and 6.3.6). However, the number of clusters is similar on CRP-XL. The number of Btk clusters significantly decreases as the set cluster radius increases, suggesting smaller clusters are being incorporated into larger clusters due to the propagative analysis of DBSCAN (Malkusch and Heilemann, 2016).

6.4.3 Aim – To confirm if Btk recruitment and clustering is independent of its kinase function downstream of GPVI.

The clustering of GPVI is a level of regulation for the signalling (Poulter et al., 2017, Dunster et al., 2020, Pallini et al., 2020). Therefore, it would be interesting to identify what is regulating the clustering of GPVI to potentially target therapeutics to this mechanism.

As Btk is indirectly involved in the regulation of the clustering of the ITAM containing BCR, it was hypothesized that Btk could potentially be involved in the regulation of the clustering of the ITAM containing FcR γ chain and GPVI. It is currently unknown what regulates the clustering of GPVI.

Both the TIRFM (chapter 5) and STORM experiments (Figures 6.3.3 and 6.3.10), show that the localisation of Btk does not drastically change when treated with a Btk kinase inhibitor. In B cells and platelets, the recruitment of Btk is mediated by its PH domain and PIP3 interaction (Saito et al., 2001, Várnai et al., 1999, Salim et al., 1996). This mechanism is not believed to be kinase dependent, therefore it is consistent with the results in this study.

In the plot profile experiments, interestingly, a lower concentration of acalabrutinib (0.1 μ M) increases the amount of Btk present at the fiber alone, and subsequently decreases the amount of GPVI present. This is unexpected, as 0.1 μ M acalabrutinib does not fully inhibit Btk phosphorylation. At lower concentrations of acalabrutinib, it was proposed by Bye et al., that there is increased SFK activity and the increased recruitment of Btk may be related to this. As SFK's are responsible for phosphorylating Btk, if their activity is increased at this low concentration of acalabrutinib, it is possible that more Btk is present, being phosphorylated by SFK's.

Although plot profile analysis may not be the best for assessing recruitment to the fibre. Indeed, the results are converted into binary values and represent the proportion of all the localisations, disregarding areas which do not have any localisations. Therefore, it is likely not accurate for assessing the recruitment in the presence of drugs, as this may alter the amount of Btk or GPVI molecules present. Other methods of analysis should be performed to fully confirm this result.

In the clustering experiments, 1 μ M acalabrutinib caused GPVI clusters to be significantly larger than vehicle treated samples ($p \leq 0.05$). It also caused a significant reduction in the number of clusters compared to vehicle control. The clusters are only larger in terms of

area and not the number of localisations per cluster as this was not significantly different. This shows that 1 μ M acalabrutinib causes a more diffuse GPVI cluster.

This more diffuse GPVI cluster caused by acalabrutinib is not related to Btk clustering. Consistent with TIRFM data of Btk puncta not changing, the clustering of Btk is not changed in the presence of acalabrutinib (Figure 6.3.3B-D)

This more diffuse GPVI cluster observed in 1 μ M acalabrutinib treated samples may be related to the expected number of GPVI localisations present. The cluster should also be larger with more molecules of GPVI present (measured as by the increase of localisations per GPVI cluster). Although there is a trend of increase in 1 μ M samples, it is not significantly increased compared to vehicle treated samples ($p = 0.08$).

A further reason may be due to the catalytic activity of Btk being involved in the regulation of GPVI clustering. Btk is implicated in being involved in the clustering of the BCR, as when the catalytic activity of Btk is inhibited, there is less BCR accumulation when assessed using fluorescence microscopy (Liu et al., 2011). This is due to Btk being responsible for regulation of WASP, which is involved in polymerisation of actin (Oda et al., 1998, Liu et al., 2011). It has been hypothesised that actin polymerisation may be playing a role in mediating the clustering of GPVI. Actin dynamic inhibitors inhibited GPVI dimer formation at high concentrations, however at lower threshold inhibitory concentrations, there is still the formation of dimers (Poulter et al., 2017). Further evidence supporting the hypothesis of actin mediated GPVI clustering is that Rac1 (small GTPase that is involved in regulating actin) is required for proper GPVI signalling (Pleines et al., 2009). Therefore, the increased GPVI clustering in the presence of acalabrutinib may be related to Btk's interaction with WASP.

6.5 Conclusion

Btk and GPVI do not colocalise when spread on CRP-XL. However, when spread on collagen, Btk and GPVI colocalise more. Btk and LAT do look to weakly colocalise when spread on collagen. More clusters of GPVI have Btk present within the cluster radius than molecules of Btk that have GPVI within the cluster radius when spread on collagen. Btk and CLEC-2 colocalise, and the clustering of Btk and CLEC-2 correlate to one another. Similarly, on rhodocytin, Btk and LAT look to colocalise and clustering may be regulated by one another.

7 General Discussion

7.1 Summary of results

This study uses the specific Btk inhibitor acalabrutinib, microscopy and a cell line model of CLEC-2 and GPVI signalling to investigate the role of Btk domains, with particular emphasis on the kinase domain, in GPVI and CLEC-2 mediated signalling.

At concentrations of acalabrutinib where Btk phosphorylation (1 μ M) is lost, GPVI mediated aggregation, granule secretion and α IIb β 3 activation is unaffected, suggesting that it functions as a scaffold rather than a kinase (Figures 3.3.2 and 3.3.4). At intermediate concentrations of rhodocytin, Btk does not play a scaffolding role downstream of CLEC-2 as phosphorylation and platelet responses are lost when Btk phosphorylation is reduced (Figures 3.3.3 and 3.3.7). Whereas at high concentrations of rhodocytin, Btk phosphorylation is lost, but aggregation is unaffected, suggesting Btk is playing a scaffolding role or it is not required for aggregation (Figure 3.3.6).

In contrast to the work of Manne et al., we show that Btk is downstream of Syk in the CLEC-2 signalling cascade. Phosphorylation of Syk pY525, an indicator of active Syk, is only reduced at concentrations where Btk transphosphorylation (initial phosphorylation site) pY551 is lost (Figure 3.3.6 and 3.3.7). Also in contrast to the work of the Kunapali group and Martyanov et al., we show that fucoidan cannot mediate CLEC-2 mediated spreading, however, we show for the first time that platelets adhere to and spread on the CLEC-2 ligand rhodocytin. This is surprisingly unaffected by Btk inhibition, although it may be explained by agonist being presented through a surface as opposed to in solution. Spreading on collagen is also unaffected by acalabrutinib and suggests a redundant role of Btk catalytic activity in platelet spreading on rhodocytin and collagen.

To further investigate whether the catalytic activity of Btk is required for GPVI or CLEC-2 mediated signalling, a cell line model was used. Downstream of CLEC-2, each functional domain of Btk was required to mediate signalling (Figures 4.3.5, 4.3.7 and 4.3.10).

Whereas downstream of GPVI, Btk requires functional PH, SH3 and SH2 domains, but

Btk can mediate signalling independently of its kinase domain (Figures 4.3.4, 4.3.6 and 4.3.9). This was shown using the over-expression of Btk mutants, with the additional use of CRISPR-Cas9 gene editing to generate a Btk SH2 domain mutant cell line to verify the requirement of the Btk SH2 domain (Figures 4.3.17 and 4.3.18).

As a potential role for Btk as a scaffold protein downstream of GPVI was identified, the localisation of Btk to areas of GPVI mediated signalling was investigated in the presence and absence of acalabrutinib. Using TIRFM, Btk does not strongly colocalise with GPVI when platelets are spread on CRP-XL (Figure 5.3.3). There is a suggestion of weak colocalization of Btk and GPVI on collagen and Btk may localise to areas of the collagen fibre in areas where GPVI is absent. The mechanism of this segregation is unknown (Figure 5.3.1). Btk and LAT appear to colocalise to a greater extent than Btk and GPVI on collagen (Figure 5.3.5).

The resolution is limited at 200nm for TIRFM (Kudalkar et al., 2016). This may overestimate the level of true colocalization and therefore STORM, which has a resolution of 20-50nm (Rust et al., 2006) was utilised to investigate the suspected protein-protein interactions.

Using STORM and quantified using plot profile and ClusDoC, Btk and GPVI do not colocalise when platelets spread on CRP-XL, consistent with the spreading data where Btk inhibition does not affect GPVI mediated spreading. However, when spread on collagen, Btk and GPVI colocalise to a greater extent (Figures 6.3.9 6.3.2.2 and 6.3.16). Btk and LAT colocalise when platelets spread on collagen showing an interaction between these proteins (Figure 6.3.12 and 6.3.19), which agrees with biochemical data previously published (Pasquet et al., 1999b). Btk inhibition increases the GPVI cluster size in platelets spread on collagen, suggesting a potential negative feedback role for Btk in GPVI clustering (Figure 6.3.3). This may be through Btk being unable to phosphorylate the negative regulator of platelet signalling, Platelet endothelial cell adhesion molecule-1, (PECAM-1) (Tourdot et al., 2013).

Compared to GPVI, at submaximal concentrations of rhodocytin, a functional Btk kinase domain is required to mediate signalling as shown using western blotting and cell line reporter assays. Therefore, it would be expected that it would localise near the receptor due to the requirement for its kinase domain. Indeed, when spread on rhodocytin, Btk appears to localise with CLEC-2 and LAT in TIRFM (Figures 5.3.7 and 5.3.8). This was confirmed using STORM (Figures 6.3.20, 6.3.21). However, platelets spread on rhodocytin are smaller, and the colocalisation may be an artefact due to a reduced surface area of the platelet.

7.1.1 What domains are important for Btk signalling?

7.1.1.1 The PH domain of Btk is required for GPVI and CLEC-2 signalling

PH domains bind to phospholipids. Btk's PH domain selectively binds to PIP3 rather than PIP2 (Salim et al., 1996). Using platelets, microscopy, and a cell line model this study show that the PH domain is required downstream of GPVI and CLEC-2 signalling.

The formation of puncta of Btk is observed using TIRFM (Figure 5.3.5 and 5.3.6), may be a result of PIP3 production which is known to form clusters at the membrane (Wang and Richards, 2012). Indeed, in other cell types the recruitment of other Tec family kinases has been shown to be dependent on their PH domain (Kane and Watkins, 2005, Qi et al., 2006). In future experiments, it would be interesting to label PIP3 in conjunction with Btk to identify if the puncta overlap in TIRFM and STORM.

In a study of the PIP3 signalosome, Btk is one of the most common binding partners of the phospholipid (Durrant et al., 2017). Therefore, it is not surprising that in a cell line model of GPVI and CLEC-2 signalling the PH domain is required (Figures 4.3.6 and 4.3.7). The PI3K inhibitor LY294002, to inhibit the formation for PIP3, was used to investigate PH requirement for GPVI mediated spreading (Figure 3.3.17). However at the concentration used platelet spreading was greatly inhibited; it has been published that aggregation is not affected at this concentration of LY294002 although the agonist

concentration used by the authors was also greater than in this study (Pasquet et al., 1999a).

However, it should be noted that downstream of PI3K is Akt (Protein kinase B), which has been shown to be required in mediating the platelet response downstream of GPVI and CLEC-2 in ADP dependent and independent signalling pathways (Kim et al., 2009b, Badolia et al., 2017). Therefore, the inhibition of spreading seen with a PI3K inhibitor may be related to this rather than an effect on Btk activation.

Therefore, future work to investigate spreading experiments in the presence of lower concentrations of LY294002 could be repeated, this would confirm the PH requirement of Btk in GPVI mediated signalling.

An alternative way to investigate the function of Btk PH domain without inhibiting PI3K would be to target PTEN. Inhibiting PI3K may inhibit Akt, and this may inhibit the spreading response. Furthermore, as the hypothesis is that Btk can behave as a scaffold protein, Btk would need to be present at the signalosome to mediate signalling. Inhibiting PI3K is likely to inhibit recruitment of Btk due to the lack of PIP3. Alternatively PTEN could be targeted. PTEN is responsible for conversion of PIP3 to PIP2 and it has been shown in the Jurkat T cell model that PTEN deficiency increases the amount of Itk present at the cell membrane (Shan et al., 2000). Therefore it can be hypothesised that inhibition of PTEN would result in increased Btk recruitment to the membrane, confirming the role of the Btk PH domain in GPVI and CLEC-2 mediated signalling.

7.1.1.2 The SH3 domain is required for GPVI and CLEC-2 signalling

SH3 domains bind to proline rich regions and are important for protein-protein interactions (Yang et al., 1995). In this work, we show a functional SH3 domain is required to mediate GPVI and CLEC-2 signalling. Interestingly, this result contrasts with literature investigating the Tec SH3 domain. In T cells, the SH3 domain of Tec is not required for TCR signal

transduction, with SH3 mutants of Tec able to mediate signalling (Tomlinson et al., 2004b).

The Btk SH3 domain is responsible for mediating the binding to BLNK (analogous to LAT) in B cells. Therefore, it is not unreasonable to hypothesise that the SH3 domain is mediating the interaction of LAT and Btk when spread on collagen and rhodocytin in Figures 5.3.5, 5.3.8 and 6.3.22. However, it would be difficult to investigate this further in platelets, therefore an *in silico* approach could be used. Indeed, using this approach, ankyrin repeat domain 54 (ANKRD54) has been proposed to preferentially select the Btk SH3 domain in an SH3 domain library (Gustafsson et al., 2017, Gustafsson et al., 2012). In B cells, ANKRD54 is involved in the nuclear translocation of Btk, and retention of Btk in the cytoplasm to mediate signalling. ANKRD5 has not been identified in platelets (Burkhart et al., 2012, Zeiler et al., 2014), but it shows potential mechanisms and functions of the SH3 domain.

An approach to confirm the requirement of the Btk domain roles, and to avoid overexpression artefacts would be to continue to use CRISPR-Cas9 gene editing to knockin domain inactivating mutations in to the DT40 model. However as these do not endogenously express the platelet receptors CLEC-2 and GPVI it would be interesting to move into a more physiologically relevant cell line. Candidates include iPS cells (Moreau et al., 2016). The KI of mutations into iPS cells has the potential to produce platelets expressing the domain mutations without the need to overexpress mutants. This would further help verify which domains of Btk are needed to mediate signalling.

7.1.1.3 SH2 domain function is required for GPVI and CLEC-2 signalling

Evidence that Btk requires a functional SH2 domain can be found in Chapter 4, along with further platelet evidence *in vitro*. In B cells, Btk has been shown to predominantly bind to BLNK via its SH2 domain following phosphorylation of BLNK by Syk (Hashimoto et al., 1999a). As phosphorylation of both LAT and Btk are blocked downstream of a Syk inhibitor (Nicolson et al., 2020), it suggests that Btk and LAT may interact via the SH2

domains of Btk, however an interaction between Btk and LAT was not detected using immunoprecipitation.

7.1.1.4 The kinase function of Btk downstream of GPVI is not required

Downstream of GPVI, this thesis provides evidence that Btk acts as a scaffold protein as signalling can occur independently of its kinase function. At 1 μ M acalabrutinib, downstream of 1 μ g/mL CRP-XL, aggregation, granule release and α IIb β 3 activation are all normal compared to vehicle controls (Figure 3.3.2), but Btk pY223 and PLC γ 2 pY759 are lost (Figure 3.3.4). As these sites are lost but responses are normal, it suggests that the phosphorylation of these sites are not required for activation, suggesting a scaffolding role for Btk.

Evidence that GPVI signalling is dependent on Btk, and that Btk is not a redundant protein in the GPVI signalling cascade can be found in Chapter 4. Btk deficient DT40 cells are unable to reconstitute signalling downstream of GPVI (Figure 4.3.13, (Tomlinson et al., 2007)). Platelets from Btk KO mice do not undergo aggregation in response to CRP-XL (1 μ g/mL) (de Porto et al., 2019), similar to how human XLA patients platelets do not undergo aggregation at this agonist concentration (Quek et al., 1998).

Chapter 4 also provides further evidence of a scaffolding role of Btk downstream of GPVI using a cell line model. A kinase dead Btk mutant was able to reconstitute signalling to a similar level as WT Btk in the DT40 cell model (Figure 4.3.4). This was also not blocked by high concentrations of acalabrutinib but, was in the presence of ibrutinib (Figure 4.3.6). The effect of ibrutinib was due to off-target effects on SFK's (Figure 3.3.7) and confirmed in the literature (Bye et al., 2017, Series et al., 2019, Nicolson et al., 2018).

Btk partially colocalises with GPVI (Figures 6.3.2.4 and 6.3.3.2), however its localisation does not change in the presence of the kinase inhibitor. This provides further evidence that its role in GPVI signalling is kinase independent. To further confirm this result, microscopy studies using fluorescently labelled ibrutinib could be performed (Turetsky et al., 2014, Kim et al., 2015). This would allow the Btk localisation to be followed in real

time in the presence of Btk kinase inhibition. If the fluorescently tagged ibrutinib was recruited to the fibre, it would provide further evidence that Btk can behave as a scaffold protein independently of its kinase domain.

However, there is a suggestion that kinase activity may play a role in the negative regulation of GPVI signalling in platelets. Inhibition of Btk results in increased GPVI clustering (Figure 6.3.3). Although no potentiation was seen in the responses of GPVI signalling in aggregation or granule secretion, a trend towards potentiation was observed with spreading experiments, as higher concentrations of acalabrutinib caused slightly but not significantly increased number of platelets to adhere per field of view (Figure 3.3.16). Potentiation can also be seen in the cell line model, where once again there was a trend of increased signalling in cells treated with acalabrutinib (Figure 4.3.6).

Potentiation of SFK phosphorylation was observed in the work of Bye et al., using ibrutinib, and it could be the role of SFK that is mediating this clustering. SFK activity is negatively regulated by phosphorylation by C terminal Src kinase, Csk. The domain structure of Csk (SH3-SH2-Kinase) is structurally similar to Btk (Filippakopoulos et al., 2009). Ibrutinib has an IC_{50} value of 2.3nM for Csk (compared to an IC_{50} of 0.5nM for Btk), showing that it is a potent inhibitor of Csk (Bose et al., 2016, Barf et al., 2017). A recent study has also shown that the common ibrutinib side effect of atrial fibrillation is mediated through inhibition of Csk (Xiao et al., 2020). Therefore, as ibrutinib and acalabrutinib are similar in their binding to Cys481, the increase in GPVI clustering in the presence of acalabrutinib may be related to this. However, acalabrutinib is less likely to inhibit Csk, as acalabrutinib has a greater selectivity for Btk (Herman et al., 2015). Furthermore, it is not thought GPVI clustering is dependent on SFK's (Poulter et al., 2017, Pallini et al., 2020) so this may suggest an alternative mechanism for increased GPVI clustering.

In addition to SFK Lyn, both Csk and Btk are found downstream of PECAM-1 (Tourdot et al., 2013). PECAM-1 is involved in the inhibition of GPVI signalling. It contains two immunoreceptor tyrosine-based inhibitory motifs, (ITIMs) and the C terminal ITIM is firstly

phosphorylated by Lyn (Tourdot et al., 2013). Then the subsequent N terminal ITIM is phosphorylated by either Btk or Csk when investigated using recombinant proteins. For Csk, the initial interaction is due to the Csk SH2 domain binding to the phosphorylated tyrosine in the C terminal ITIM, which then allows the Csk kinase domain to phosphorylate the N terminal ITIM. However, the interaction of Btk with the N terminal ITIM is not wholly dependent on its SH2 domain (Tourdot et al., 2013). It has been shown that PI3K can co-immunoprecipitate with PECAM-1 and the interaction between Btk's kinase domain and PECAM-1 may be mediated through Btk's PH domain mediated recruitment to PIP3 (Moraes et al., 2010). In acalabrutinib treated platelets, Btk may be recruited to PECAM-1, but unable to phosphorylate the ITIM. This may potentially explain why an increase in GPVI clustering was observed.

To confirm this, a further potential avenue is to investigate if Btk can colocalise with PECAM-1, and whether there is any change in the presence of acalabrutinib. It would be expected that Btk would be present in close proximity to the platelet inhibitory receptor, due to its proposed role in phosphorylating the N terminal ITIM of PECAM-1.

In this study it cannot be ruled out that Tec phosphorylation is not mediating the signalling downstream of GPVI. However, this seems unlikely, as the use of acalabrutinib instead of ibrutinib is far more selective for Btk, and does not cause as strong Tec inhibition (Byrd et al., 2016). Further publications also suggest that Tec phosphorylation is only partially inhibited at concentrations of acalabrutinib (0.5 μ M, and 2 μ M) where aggregation is normal downstream of GPVI (Figure 3.3.2) (Nicolson et al., 2018) or not inhibited at all (Bye et al., 2017). Additionally, the concentration of agonist (1 μ g/mL CRP-XL) used in these studies is unlikely to have triggered the compensatory role of Tec. Only agonist concentrations at least 10-fold higher than the amount used in this study (10 μ g/mL and 30 μ g/mL) induce aggregation in Btk-deficient platelets, demonstrating the compensatory role of Tec is only induced under high levels of GPVI ligation (Atkinson et al., 2003a).

Future work to investigate the hypothesis of Btk potentially having a scaffolding role could include the use of patients with XLA. The patients used in the study by Nicolson et al.

2018 and 2020 were all deficient in Btk, which help prove that Btk is needed to mediate signalling. Indeed, many patients that have XLA are deficient in Btk. However, there are a subset of patients who have a 'leaky' phenotype (Gaspar et al., 2000). This describes patients who express catalytically inactive Btk and have a less severe immunodeficiency than patients who are deficient in Btk. Investigating their platelet function through aggregation, calcium mobilisation and phosphorylation downstream of GPVI could further help deduce the role of Btk in this pathway and determine the role of the catalytic activity without the use of inhibitors having off target effects.

7.1.1.5 The kinase domain of Btk is required at low concentrations, but not at high concentrations of CLEC-2 ligation

It is unclear whether the kinase domain is required downstream of CLEC-2. At submaximal concentrations of rhodocytin (100nM, 50nM), it is known that downstream of CLEC-2, Btk kinase activity is required for aggregation (Figures 3.3.2, 3.3.7), calcium secretion (Figure 3.3.14) and mediation of the signalling in a cell line assay (Figure 4.3.5). In the cell line assay, only WT Btk can mediate CLEC-2 signalling (Figure 4.3.5). When both platelets and DT40's are treated with acalabrutinib, there is an inhibition of signalling, showing that at lower concentrations of rhodocytin (100nM and 50nM) concentrations of rhodocytin, Btk catalytic activity is required (Figures 3.3.7 and 4.3.7).

Similar to GPVI, the presence of Btk is required to mediate signalling. Btk deficient DT40 cells are unable to mediate CLEC-2 signalling (Chapter 4, (Fuller et al., 2007) and Btk deficient platelets do not aggregate in response to high concentrations of rhodocytin (Nicolson et al., 2020). This suggests that Btk expression is essential for CLEC-2 signalling.

However, at high concentrations of rhodocytin (300nM), platelet aggregation still occurs when Btk pY223 phosphorylation is lost due to acalabrutinib treatment, in both ADP insensitive and ADP sensitive platelets, as shown in Figures 3.3.6 and 3.3.12. There are

several reasons for this. The aggregation of ADP sensitive platelets observed with 300nM of rhodocytin suggests that the aggregation is mainly through secondary mediators. These platelets are prepared using a method that allows them to respond to ADP (Figure 3.3.9) and does not interrupt the COX-1 signalling pathway during the washing process, removing the potential loss of thromboxane release. Indeed, although there is no inhibition of aggregation at high concentrations of acalabrutinib, there is a delay compared to vehicle treated samples (Figure 3.3.7) suggesting that is due to the production and release of secondary mediators. To verify this, experiments assessing the release of ATP in conjunction with aggregation could be performed to elucidate the kinetics of aggregation.

At high concentrations of rhodocytin, aggregation still occurs despite the loss of Btk pY223 and PLC γ 2 pY759 phosphorylation. This suggests that at high concentrations of rhodocytin, this PLC γ 2 phosphorylation site is not essential for mediating aggregation downstream of CLEC-2. As the concentration of rhodocytin was high, it may have been inducing a high level of CLEC-2 clustering, and therefore bypassing Btk to mediate signalling. This can be observed for several other proteins when they are genetically deleted, examples include LAT, where PLC γ 2 phosphorylation is lost but the platelets are still able to aggregate to high concentrations of rhodocytin and CRP-XL (Hughes et al., 2008, Judd et al., 2002), and SLP-76 where aggregation is not required downstream of rhodocytin, suggesting that there is a SLP-76 independent pathway of CLEC-2 activation (Suzuki-Inoue et al., 2006). However, this is only at high concentrations of agonist *in vitro*, and is surprising as SLP-76 deficient platelets exhibit the blood lymphatic mixing phenotype, suggesting that podoplanin present on lymphatic endothelial cells is not enough to bypass this signalling (Clements et al., 1999). Of note, LAT and SLP76 are both scaffolding proteins, further supporting the concept that Btk has dual roles, that of a scaffold and a kinase.

An alternative hypothesis has been proposed in the work by Wist et. al., where catalytically inactive Btk (treated with acalabrutinib) can mediate BCR signalling. At higher

degrees of BCR activation, catalytically independent Btk functions come into effect such as scaffolding or shuttling between proteins (Wist et al., 2020). Due to this, acalabrutinib acquires the property of a partially effective inhibitor. When CLEC-2 is ligated using a high concentration of rhodocytin, and no inhibition is observed, it may be related to the increased scaffolding role of Btk, and therefore there is only partial effectiveness of acalabrutinib inhibiting the amount of Btk that is catalytically active. This may explain why inhibition is observed in ADP insensitive platelets, but not ADP sensitive platelets.

Moreover, Tec may be mediating CLEC-2 aggregation despite Btk inhibition at 300nM rhodocytin whereas it does not at lower concentrations of rhodocytin. This compensation at high concentrations is seen downstream of GPVI in mouse platelets where Tec can partially compensate for Btk; at high concentrations of CRP-XL (10µg/mL), Tec can compensate for Btk, whereas at lower concentrations (3µg/mL CRP-XL) it cannot (Atkinson et al., 2003a). Although this is unlikely, as at the concentrations of acalabrutinib where Btk phosphorylation is lost, it has been shown that Tec phosphorylation is also reduced in platelets (albeit downstream of GPVI) (Nicolson et al., 2018). However, due to the lack of phosphospecific antibodies for Tec, it is unknown whether the phosphorylation observed is the Src phosphorylation site, the autophosphorylation site or both.

Nonetheless, it suggests that Tec is not playing a compensatory role.

Future work using 'leaky' XLA patients could be performed to investigate the role of Btk kinase function downstream of CLEC-2, similarly to GPVI as described above.

Furthermore, it would be interesting to investigate if there is a lower risk of diseases specifically related to CLEC-2 signalling dysfunction in these patients. It would be expected that these patients would have a reduced risk of CLEC-2 mediated disease such as DVT due to the disruption of its signalling. Population studies using XLA patients (who take intravenous IgG for treatment) compared to patients who also take intravenous IgG could be investigated to further confirm or deny this is, and would control for the intravenous immunoglobulin which has been proposed to have side effects.

One of the side effects for patients taking intravenous IgG is an increased risk of hemolytic anaemia (Berard et al., 2012). Hemolytic anaemia causes an increased risk of thrombotic events (Ruggeri and Rodeghiero, 2016), which could be attributed partly from the free heme activating the CLEC-2 receptor on platelets (Bourne et al., 2020). XLA patients are likely to be protected from this risk as they do not contain Btk, which is essential for CLEC-2 signalling at concentrations of heme present in the blood as shown in the work by Bourne et al., using a Btk inhibitor. Indeed, XLA patients do not seem to be at an increased risk for thrombus formation (Chen et al., 2016).

7.1.2 The localisation of Btk, and differences between analysis methods

In summary, when platelets spread on the GPVI ligand Btk and GPVI appear to partially colocalise, however there is stronger evidence that Btk colocalises with LAT. The localisation of Btk and LAT is also observed when platelets spread on rhodocytin.

The results obtained from TIRFM and STORM imaging tend to be consistent with one another. For example, Btk appears to colocalise with LAT when spread on collagen, and this is mirrored in the plot profile experiments, where a large proportion of the localisations on the fibre are LAT and Btk together (Figures 5.3.5 and 6.3.12). This suggests that there is a stronger colocalisation of LAT and Btk when platelets spread on collagen that was unmasked using STORM.

The puncta distribution of Btk observed in TIRFM was not changed in the presence of acalabrutinib (Figure 5.3.2). This suggests that Btk is clustered independent of its kinase activity, however TIRFM does not accurately allow for the quantification of clusters.

Therefore, STORM was employed to quantify the distribution of Btk. In the presence of acalabrutinib when imaged in TIRFM or STORM, Btk clustering does not change showing consistency between the two methods of microscopy.

However, there are some differences in the results obtained in TIRFM and STORM.

When spread on rhodocytin, Btk and LAT weakly colocalise in TIRFM, but do not appear to directly localise together in plot profile experiments. This highlights that there are differences in the results obtained by the methods of microscopy.

Possible reasons to explain the observed differences is the resolution difference between STORM and TIRFM. The resolution, which is the distance of which the microscope can distinguish two separate molecules, is limited at 200nm for TIRFM (Kudalkar et al., 2016). However, for STORM, the optical resolution is higher at approximately 20-50nm (Rust et al., 2006). This allows for more accurate distinguishing of individual molecules, and therefore may explain why there is a difference in the results obtained with TIRFM and STORM.

Further differences observed between TIRF and STORM may also be explained due to the differing resolution limits and experimental parameters. A primary antibody and a secondary antibody (where the blink (a localisation) is identified), can be up to 30nm long which may exclude localisations if the cluster diameter is set too small. To combat this, clustering experiments were performed over a range of diameters (Section 6.3.1) (Ries et al., 2012). Experiments could be repeated with directly conjugated primary antibodies, nanobodies or aptamers to ensure the distance between the fluorophore and the protein of interest is smaller and would enable more accurate localisation precision (Opazo et al., 2012). Alternatively, a clustering method where high density regions are identified, Super Resolution Optical Fluctuation, (SOFI), could be employed to analyse the clusters. This algorithm provides quantitative molecular density analysis of protein distributions independent of any user defined parameters (Lukeš et al., 2017). Clustering using LAMA which works via DBSCAN has an arbitrary cut off of 100nm which may not be appropriate for assessing clusters that are larger, such as the clusters of GPVI along a collagen fibre. The output of SOFI is the size in area, number and diameter of a high-density region and therefore is comparable to clustering.

Aside from the limitations due to resolution, there are some other limitations in regarding microscopy. STORM is often used to assess protein clustering; however, it may not be the most accurate. The fluorescent tag on the protein that is imaged, not the protein itself (which could only be imaged using fluorescently tagged proteins, unable to do in platelets). So therefore, clusters may appear larger than they are, or may give false positives. In addition, it has been proposed that antibody induced clustering can occur in the membrane even after fixation, particularly if the proteins are GPI-anchored membrane bound (Tanaka et al., 2010). However, the membrane bound proteins in this study (GPVI, CLEC-2 and LAT) are not anchored via Glycosylphosphatidylinositol.

In a paper trying to identify whether Tetraspanins are involved in GPVI clustering, there was no significant difference in clustering using STORM, comparing wild type to knockout platelets, but there was an effect on lateral membrane diffusion suggesting a change in the movement of GPVI which could be only visualised in unfixed cells (Haining et al., 2017b). This suggests that the sample preparation and imaging in STORM may obscure some of the dynamic changes that occur during receptor clustering.

The use of an immobilised ligand to investigate protein clustering is also not representative of what may be happening *in vivo*. It has been shown that CLEC-2 undergoes clustering, which has been indirectly measured by assessing the clustering of podoplanin in a lipid bilayer model. Although CLEC-2 undergoes clustering, it is currently unclear whether that is mediated through podoplanin clustering or itself (Pollitt et al., 2014). Therefore, the experiments using a static ligand of rhodocytin to investigate CLEC-2 clustering may have not been physiologically relevant. In order to assess this in future experiments, a supported lipid bilayer model using podoplanin should be used to mimic a cell.

Although, platelet spreading on immobilised ligands is widely used to investigate signalling pathways, it may be a good model of *in vivo* platelet substrate interactions. It is believed that platelets can sense the mechanical properties of the ligand they are spreading on, however it is unclear how this relates to protein cluster formation. Collagen

365

which is tagged to polyacrylamide gels of various thickness induce varying levels of platelet spreading (Kee et al., 2015). On stiffer collagen-gel substrates platelets are more coagulant as demonstrated by the increase in surface area and phosphatidyl serine exposure. Stiffer vessels are likely atherosclerotic / diseased vessels, and the experiments used in this study use collagen or rhodocytin coated glass wells or coverslips (Chapters 3,5,6). Glass is a solid medium and may therefore be representative of what would occur in a diseased vessel.

Furthermore, signalling processes are dynamic and stoichiometry often plays a part. It has been shown that LAT is able to move within Z planes in a spreading T cell (Zhang et al., 2018, Balagopalan et al., 2018). The investigations in this study are at a fixed time point on a static ligand. It is known that interactions between signalling proteins can be transient, such as the nucleocytoplasmic shuttling of Btk in B cells (Mohamed et al., 2000), and transient recruitment of Syk to the BCR (Zhou et al., 2006). Activation of platelets in solution over a time course may help to deduce the dynamic protein-protein interaction events.

Furthermore, cell line studies could be used to investigate the clustering and localisation of Btk. The Yellow fluorescent protein (YFP)-based protein fragment complementation assay (PCA) technique for visualizing protein-protein interactions involves expressing a protein (Btk) tagged with YFP fragment 1 (first 158 amino acids of the protein) and expressing another plasmid of Btk tagged with YFP2 (latter half of the protein). Alone, these proteins would not be able to emit fluorescence. However, upon homo-oligomerisation of the proteins, the two fragments would be in close proximity and complement together resulting in a functional protein capable of fluorescence that could be measured (Nyfeler et al., 2005). It has been demonstrated that Itk undergoes protein clustering using this method (Qi et al., 2006), and it could be extended to other proteins in the signalling cascade such as LAT.

7.2 Is Btk a pseudokinase or a scaffold protein?

The definition of a classical scaffold protein is the absence of inherent catalytic activity required for signalling (Zeke et al., 2009). As Btk contains a functional kinase domain (Rawlings et al., 1996), it would be expected that Btk is unlikely to be a scaffold protein. However, there is the possibility that the kinase domain within Btk could be a pseudokinase downstream of GPVI and CLEC-2 at high agonist concentrations. A pseudokinase is an inactive enzyme in which catalytic activity cannot occur. Integrin linked kinase (ILK) and JAK2 (Saharinen et al., 2000) are pseudokinases in platelets. Pseudokinase domains have similar structures to catalytically active kinases so it is not unreasonable to hypothesise that Btk could be a pseudokinase. However when examined, the kinase domain of Btk and the pseudokinase domain of JAK2 share 41% of the same residues suggesting little similarity, when compared to the similarity of the kinase domains of Syk and Btk (Stothard, 2000). This result suggests that Btk is more similar to a classical kinase and it is unlikely that it is a pseudokinase. As Btk catalytic activity is required downstream of CLEC-2 at lower agonist concentrations, it suggests that it is unlikely that Btk is a pseudokinase. It is more likely that downstream of GPVI, Btk kinase function is not required. This is typical of an adaptor / scaffold protein and that Btk may be acting as one of these molecules.

Using bioinformatic prediction approaches Hu et al., predicted scaffold proteins from protein-protein interaction data and kinase-substrate relationships. Of all the scaffold proteins predicted, 18.9% contained a kinase domain. Interestingly, Btk and Tec were predicted to be a scaffold protein within the Syk-PLC γ 2 pathway (Hu et al., 2015). Although the study did verify some of their predicted scaffold proteins using *in vitro* experiments, Btk was not one selected.

Btk has also been predicted to be a scaffold protein in another study based on the criteria that there is interaction between the scaffold and two other partner proteins, and they are facilitated through two separate domains (Oh and Yi, 2016). Downstream of both GPVI and CLEC-2 in a cell line model, it was shown that each of the domains of Btk were

required to mediate the signalling, suggesting the interactions that the domains mediate are required. Btk has been shown to interact with PIP3 through its PH domain, (Salim et al., 1996), Phosphatidylinositol-4-phosphate 5- kinases (PIP5K) through its TH domain (Saito et al., 2001), PLC γ 2 through its kinase domain (Kim et al., 2004) and Syk through its SH3 domain (Morrogh et al., 1999) and therefore this may be why it has been predicted as a scaffold protein. Although, these predictions are only theoretical due to limited validation against the known 78 scaffold proteins.

Further *in silico* evidence for Btk being a scaffold protein is its size. Scaffold proteins tend to be larger, with Hu et al., (2015) predicting an optimal size of 670 residues. Btk is 659 amino acids (Rohrer et al., 1994), close to the predicted optimal size when compared to the median amino acid length of 375 (Brocchieri and Karlin, 2005). LAT however is much smaller than the optimal predicted size suggesting that this data modelling may need further validation.

Btk forms a punctate pattern when platelets are spread on collagen or rhodocytin (Figures 5.3.1 to 5.3.9). This observation is consistent with the punctate pattern of Tec (Tomlinson et al., 2004b) and Itk seen in Jurkat cells (Qi et al., 2006). Scaffold proteins often localise in a punctate pattern to increase the local concentration of signal components (Hu et al., 2015), which may explain Btk's punctate distribution. Furthermore, there is evidence in the literature that increased Itk clustering leads to a decrease in catalytic activity, as the kinase interacts with itself as opposed to its substrates, so the puncta formation of Btk provides further evidence that Btk may have a scaffolding role (Joseph and Andreotti, 2009). The lack of change in the number or distribution of the Btk puncta / clusters in the presence of a Btk inhibitor also contributes to this concept (Figures 5.3.2 and 6.3.3).

However, in contrast to the scaffolding hypothesis is the work of Chang et al. The authors propose that Btk clustering is required for catalytic activity and may explain the puncta and clusters observed in Chapters 5 and 6. Moreover, puncta can be observed when platelets spread on rhodocytin, where Btk pY223 phosphorylation and catalytic activity is required to mediate CLEC-2 signalling (Figure 3.3.7), providing evidence in favour of

368

Chang et al. This proposes an alternative argument suggesting that the punctate formation is linked to the catalytic activity of Btk rather than a scaffolding role.

Signalosome studies have identified the adaptor proteins ELMO1 and DAAP1 along with Btk as proteins that are most commonly bound to PIP3 in platelets (Patel et al., 2019, Durrant et al., 2017). Both ELMO and DAAP1 are all implicated in the negative regulation of GPVI, as platelets from mouse models deficient in these proteins have enhanced GPVI signalling (Patel et al., 2019, Durrant et al., 2017). This suggests that binding of proteins PIP3 and subsequent interactions may be involved in the regulation and termination of GPVI signalling. Of note, both ELMO1 and DAAP1 are scaffolding proteins, further providing evidence that Btk may also have a potential scaffold role.

Further evidence for the kinase/scaffolding role of Btk is the resistance to ibrutinib and acalabrutinib in B cell malignancies. Btk inhibitors which prevent Btk from being catalytically active can help control the disease by managing the excess BCR signalling (Akinleye et al., 2013, Burger et al., 2015), confirming the kinase role of Btk. Resistance can occur due to mutations in either Btk or PLC γ 2 which overcome the kinase inhibition to restore signalling (Woyach et al., 2017, Woyach et al., 2014). Although mutations may occur in some PLC γ 2 domains more than others, D993G has been identified as a prominent mutation in patients. This mutation is believed to promote the interaction of PLC γ 2 with the membrane, bringing it closer to phosphoinositol lipids (Liu et al., 2015) in order for conversion. As Btk would be catalytically inert, but able to recruit proteins its interaction with PLC γ 2 suggests a scaffolding role.

A similar increase in signalling due to increased recruitment to the membrane can be observed with SH2 domain-containing inositol 5-phosphatase (SHIP) deficient platelets. SHIP is responsible for the conversion of PIP3 into PIP2 (Damen et al., 2001), and therefore deficiency causes an increase in the membrane concentration of PIP3. SHIP is therefore an indirect negative regulator of Btk, as reducing PIP3 levels reduce the recruitment of the kinase to the membrane.

Indeed, SHIP deficient platelets have increased levels of PIP3 and Btk phosphorylation in basal samples. The calcium flux at basal levels are increased compared to WT mice, but the fold change in response to CRP-XL is similar between WT and SHIP deficient mice. In addition, the levels of the metabolite of DAG and IP₃, phosphatidic acid were unchanged between SHIP KO and WT platelets downstream of GPVI, suggesting that PLC γ 2 is not hyperactive. Finally, this was confirmed using total tyrosine phosphorylation of PLC γ 2, where it was found to be normal. If Btk was an exclusive kinase, it would also be expected that PLC γ 2 phosphorylation would be increased due to Btk phosphorylating its substrate.

Obtaining resistance to Btk inhibitors ibrutinib and acalabrutinib via PLC γ 2 mutation is rare compared to resistance via mutation of Btk (Lampson and Brown, 2018). The most common mutation to confer resistance is mutation of Btk Cys481 to a serine or arginine (Woyach et al., 2014, Ahn et al., 2017). The change in amino acid abolishes the thiol present on the kinase to which the inhibitor can no longer bind covalently, therefore allowing Btk to be more catalytically active than previously, suggesting that Btk still requires and favours (as more common than PLC γ 2 resistance) a catalytic role in B cell malignancies.

The potential mechanism for Btk's scaffolding role has been proposed in B cells and is related to its interaction with lipid kinases and is shown in Figure 7.2.1. Btk interacts with PIP3 through its PH domain (Bolland et al., 1998, Durrant et al., 2017, Pasquet et al., 2000). PIP3 can be converted to PIP2 via SHIP / PTEN (Pasquet et al., 2000, Myers et al., 1997). Btk can also interact with PIP5K, which is responsible for production of PIP2 from PIP3 (Saito et al., 2003). PLC γ 2 catalyses PIP2 into IP3 and DAG which result in calcium flux. As Btk brings PIP5K and therefore PIP2 to PLC γ 2, IP3 and DAG can be produced independently of phosphorylation (Saito et al., 2003)

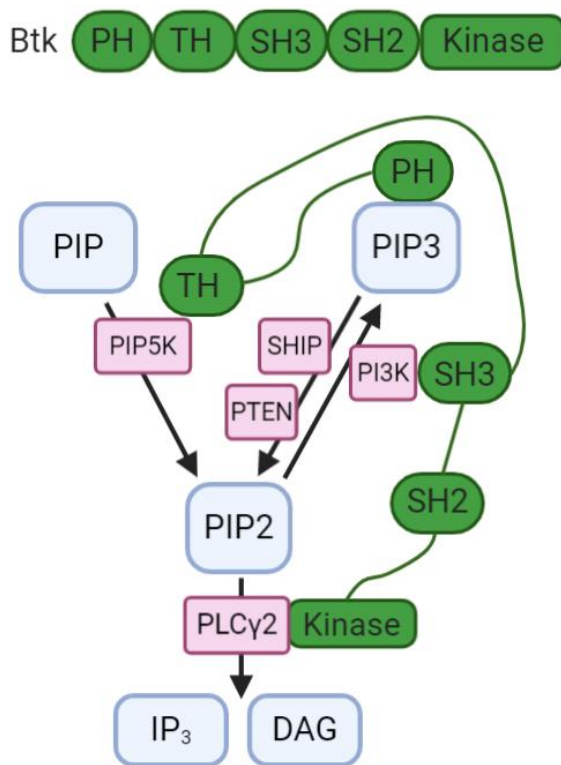


Figure 7.2.1 Btk's interaction with phospholipid metabolism

Btk and its domains are shown in green with the reference Btk at the top. Black arrows show phospholipid metabolism, with the enzymes responsible being shown in pink. PIP is catalysed to PIP₂ by PIP5K, which Btk can interact with via its proline rich regions in its TH domain. PIP₂ can be converted to IP₃ and DAG via PLC γ 2, which Btk can phosphorylate downstream of low concentrations of CLEC-2. PIP₂ can be converted to PIP₃ via PI3K, which Btk interacts with through its SH3 domain. PIP₃ recruits Btk via its PH domain. PIP₃ can be converted to PIP₂ via SHIP or PTEN, inhibition of both leads to an increase in Btk recruitment.

7.3 Use of Btk inhibition in COVID-19 treatment

Severe acute respiratory syndrome coronavirus 2 (SARS-COV-2) is the causative pathogen for the current coronavirus disease 2019 (COVID19) pandemic. The disease is caused by virus binding to the angiotensin converting enzyme 2 (ACE2) receptors on pulmonary epithelial cells, leading to viral pneumonia. A systemic inflammatory response follows this, leading to acute respiratory distress and multi organ failure. The systemic

inflammatory response is a cytokine storm, through excessive macrophage activation and release of interleukin-6. Patients with COVID19 have abnormal coagulation (increased prothrombin time) and abnormal thrombosis (Thachil et al., 2020). Both arterial and venous thrombosis are implicated in causing a more severe disease phenotype of COVID-19 as patients experience both myocardial infarctions and venous thrombosis, and therefore there is potential for Btk inhibition using acalabrutinib in order to cause a less severe disease.

Acalabrutinib is a clinically safe drug with less severe side effects already approved for treatment. The occupancy level and tolerable dosage (without dangerous side effects) is already known (Barf et al., 2017, Wu et al., 2016, Byrd et al., 2016). The repurposing of drugs is far quicker than the development of new drugs and therefore is useful to use during a pandemic.

COVID19 patients have altered coagulopathy, with increased thrombosis in the microvasculature of the lungs and other organs, reflected in increased D dimers (Goshua et al., 2020). These thrombi are likely a result of thromboinflammation, where inflammation triggers thrombus formation. Both GPVI and CLEC-2 have been implicated in thromboinflammatory conditions.

GPVI has been implicated in thromboinflammation in ischemia-reperfusion injuries in a stroke model. The reperfusion of blood induces an inflammatory response which leads to microthrombi and infarcts through platelet activation, T cells and neutrophils (Boulaftali et al., 2018). Inhibiting GPVI signalling using a competitive antagonist, Revacept reduces the damage caused by the platelets and these cells, suggesting that in certain models, GPVI is responsible for mediating thromboinflammation.

At high concentrations of rhodocytin, Btk signalling is not required for CLEC-2 mediated aggregation. However, this used the agonist rhodocytin, which is a snake venom and not present in the body. Rhodocytin likely induced a strong response which induces activation mainly through potentiation of secondary mediators. The endogenous ligands of CLEC-2

include podoplanin and heme. Rhodocytin induces a stronger aggregatory response than podoplanin (Suzuki-Inoue et al., 2007) but no studies comparing rhodocytin and heme have been published. As Btk inhibits more potently downstream of CLEC-2 at submaximal concentrations of rhodocytin, it is not unreasonable to believe that CLEC-2 mediated podoplanin signalling would be inhibited. It is beneficial to use acalabrutinib to inhibit podoplanin / heme induced CLEC-2 signalling, whilst likely sparing GPVI signalling. Although if the activation of CLEC-2 is very high, it may only have partial effectiveness.

CLEC-2 has also been demonstrated to play a role in thromboinflammation. After infection with salmonella, tissue macrophages upregulate podoplanin on the surface in response to inflammation. This activates CLEC-2, leading to hepatic thrombus formation (Hitchcock et al., 2015). CLEC-2 is also implicated in playing a role in venous thrombosis, as CLEC-2 KO mice are protected from venous thrombosis (Payne et al., 2017). Therefore inhibiting Btk, which is downstream of CLEC-2 may be beneficial in reducing the increased risk of VTE which COVID19 patients have (Chang et al., 2020, Al-Samkari et al., 2020).

In vivo work using ibrutinib in a mouse model of protection of venous thrombosis has shown a trend towards inhibition, but no significant reduction (Nicolson et al., 2020). It may be that the mice may not have full pharmacological blockage throughout the 48 hours required for the model, and that mouse CLEC-2 is not as critically dependent on Btk as human CLEC-2 signalling. Nonetheless, CLEC-2 does play a role in DVT, and as this is frequently seen in patients with COVID19, Btk is a potential therapeutic target.

A case study followed a CLL patient who was taking ibrutinib prior to COVID-19. Upon admittance to the hospital, the ibrutinib therapy stopped, however the disease progressed, with elevated D-Dimers. Ibrutinib therapy was resumed whilst the patient was extubated, and the levels of D-Dimer dropped. This suggests that inhibition of Btk with ibrutinib may have a protective effect in thromboinflammatory COVID-19 (Lin et al., 2020).

However, there is conflicting literature about whether CLEC-2 inhibition is suitable in all models of thromboinflammation. Absence of platelet CLEC-2 accelerates lung function

decline in a model of ARDS (Lax et al., 2017), and COVID19 involves damage of the lungs, so Btk inhibition downstream of CLEC-2 may further this lung damage. CLEC-2 deletion results in a more severe phenotype of organ failure during sepsis, which is another thromboinflammatory condition (Rayes et al., 2017). Therefore, inhibition of the CLEC-2 signalling cascade with acalabrutinib may not be wholly beneficial. Of note, these experiments were performed using CLEC-2 KO mice. This total lack of signalling may explain the phenotype, therefore a partial inhibition of the CLEC-2 signalling pathway may not result in as severe phenotype as a knockout.

Entry of virus is believed to occur via angiotensin converting enzyme 2 (ACE2) and there is controversy whether this is present on platelets. One group has proposed that viral particles and COVID19 spike proteins can potentiate platelet activation in response to collagen and thrombin and this is through direct interaction of the virus with ACE2 (Zhang et al., 2020). The downstream signalling after ACE2 engagement is through MAPK, and Btk is not believed to play a role downstream of this pathway (Zhang et al., 2020). Therefore, inhibition of Btk would not yield any differing outcomes of disease.

In contrast, it has been reported that ACE2 is not expressed in platelets, but viral entry can still occur (Manne et al., 2020). This group and others propose that there are alternate mechanisms for SARS-COV-2 to mediate entry into cells, and this may be through toll like receptors (Patra et al., 2020, Manne et al., 2020). Initially thought to only bind lipopolysaccharide and therefore bacteria, TLR4 has been shown to be activated by viral particles, such as dengue virus non-structural protein 1 (Olejnik et al., 2018, Modhiran et al., 2017).

TLR4 is present on platelets, macrophages and monocytes, where it is known that Btk contributes to mediating the signalling resulting in increased cytokine release (Gilbert et al., 2003). The cytokine storm produced by macrophages and monocytes contributes to lung damage (Krupa et al., 2014). It has been shown previously that silencing Btk using siRNA suppresses the production of IL-6, Tumour necrosis factor α , (TNF- α) and results in less interstitial lung damage from LPS mediated sepsis (Zhou et al., 2014).

TLR4 is present in platelets, and signalling can occur through Myeloid differentiation factor-88- (MyD88-) dependent and independent pathways (Vallance et al., 2017). TLR4 signalling through the MyD88- pathway results in production of TNF- α , contributing to the cytokine storm. In neutrophils, Btk has been seen to directly act with MyD88- (Krupa et al., 2013), and therefore it is not unreasonable to believe that Btk could be involved in the MyD88- signalling pathway in platelets. Inhibiting Btk in platelets could inhibit release of TNF- α , reducing the pro-inflammatory effects seen in COVID19 patients.

Furthermore, indirect evidence of platelet Btk being important downstream of TLR has been published. Platelet Btk is important for maintaining the lung integrity in *Streptococcus pneumoniae* induced pneumonia, but it is not required for host defence as the levels of colony forming units are similar in WT littermate controls. Platelets were less activated and as a result, there was an increase in the bleeding score and D-Dimers (de Porto et al., 2019). However, platelet GPVI is not responsible for mediating the response of *Streptococcus* induced pneumococcal pneumonia (Claushuis et al., 2018, de Porto et al., 2019), so Btk must be required in another pathway. It is not known whether platelet Btk and its role in maintaining lung integrity is mediated through CLEC-2 signalling as the C type lectin receptor Mincle on macrophages has the ability to bind to this bacterium (Rabes et al., 2015), but platelet CLEC-2 has not yet been studied. However, *Streptococcus pneumoniae* has been shown to induce platelet aggregation via TLR activation, leading to initiation of PI3K signalling (Keane et al., 2010). This would subsequently involve Btk recruitment. Taken together, this suggests that Btk may be downstream of TLR signalling in platelets.

However, these studies investigate the role of Btk and the aforementioned receptors downstream of bacteria, and not viruses using Btk deficient mice. The work in this thesis contributes the notion that Btk is required downstream of GPVI and CLEC-2, but catalytic activity is not, so the severe phenotype seen in the work of de Porto et al. may be related to a loss of a scaffolding role of Btk downstream of GPVI. Furthermore, as there is a difference in the platelet-host response between species of bacteria (de Porto et al., 2019,

Claushuis et al., 2018), it would be expected there would be differences between bacteria and virus. Therefore, although Btk inhibition may not be beneficial in response to bacteria, it could be in response to viral mediated inflammation.

There are only limited reports, but both GPVI and CLEC-2 have been shown to interact with viruses. GPVI is reported to interact with the hepatitis C virus, and CLEC-2 with human immunodeficiency virus although the clinical significance is unknown (Chaipan et al., 2006, Zahn et al., 2006). Therefore, it is not wholly unreasonable that COVID19 could bind to these (hem)ITAM containing receptors. However, neither of these studies investigate intracellular tyrosine kinase signalling, so it is unclear if these viruses are causing activation of the platelet, and therefore using a Btk inhibitor may not be clinically beneficial.

Furthermore, in a gene expression study, Btk gene expression is reduced in platelets from patients with COVID19. Reduced gene expression compared to healthy donors suggests that Btk is not essential in the platelet in promoting the inflammatory response (Manne et al., 2020). Furthermore, only 40% of CLL clinicians would continue patients on their current Btk inhibitor regime (Koffman et al., 2020). Further work with CLL patients identified that there were similar survival rates of COVID19 patients taking Btk inhibitors compared to patients who did not receive their Btk inhibitors (Mato et al., 2020). However, a large proportion of patients had their Btk inhibitor held when symptomatic for COVID19, suggesting that these survival rates may not be accurate.

Further reasons why Btk inhibition would be an undesirable target in COVID19 are the development of immunity to the virus and/or a vaccine. Btk is responsible for mediating B cell maturity, and therefore the production of IgG, as XLA patients in Btk have low serum IgG (Conley, 1985). Inhibition of Btk with acalabrutinib would likely prevent the production of antibodies needed to build immunity to the virus, leading patients taking acalabrutinib to be more susceptible to disease.

Finally, although it is not reported that there is an increased risk of haemorrhage for patients taking acalabrutinib, COVID19 patients do have an altered coagulopathy. One study identified that the percentage of COVID19 patients with venous thrombosis was similar to the number that experienced haemorrhage (Al-Samkari et al., 2020), including one fatal bleed. Therefore using a platelet inhibitor such as acalabrutinib may result in further bleeding side effects.

7.4 Conclusion

In this thesis, we show that the catalytic activity of Btk is not required downstream of GPVI mediated platelet responses and a cell line model of GPVI signalling (Figure 7.4.1, left panel). We also show that Btk catalytic activity is not required for its localisation or clustering, however we do show that it is involved in the regulation of GPVI clustering through an unknown mechanism. We also confirm published biochemical studies showing that Btk can interact with LAT, supporting its recruitment to the signalosome.

Whereas, downstream of CLEC-2, at submaximal concentrations of CLEC-2 agonist, Btk is a kinase as platelet responses are inhibited at concentrations where there is no evidence of Btk catalytic activity. This was also confirmed in a cell line model of CLEC-2 signalling. Similarly to GPVI signalling, Btk and LAT colocalise when platelets spread on a

CLEC-2 agonist, showing that this interaction is similar across (hem)ITAM signalling (Summarised in Figure 7.4.1 middle panel). At high concentrations of rhodocytin, Btk activity is not required as CLEC-2 mediated signalling and aggregation can occur when phosphorylation of Btk is lost (Figure 7.4.1 right panel). The dependency of CLEC-2 signalling on secondary mediators is likely playing a role.

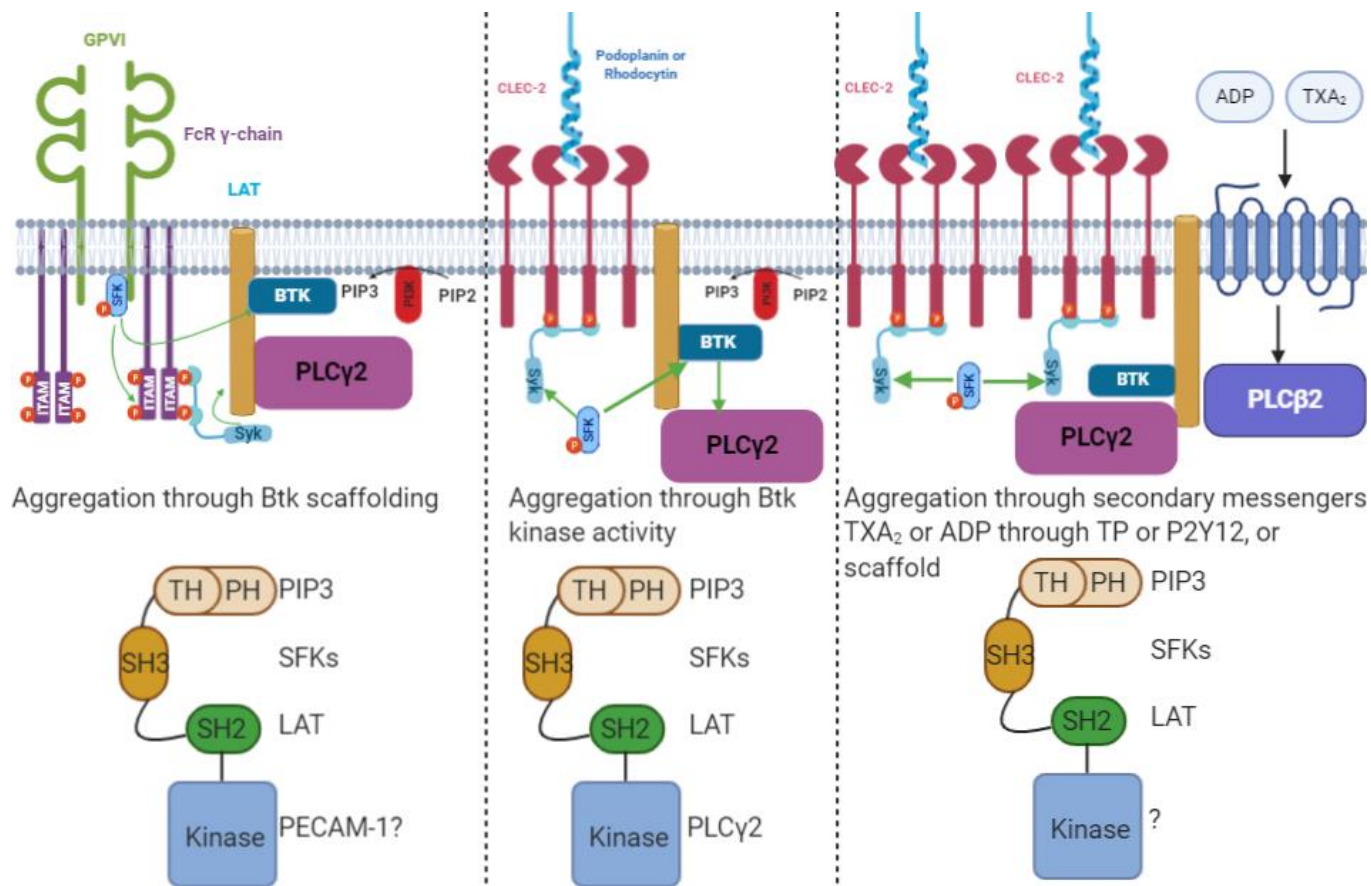


Figure 7.4.1 Overview of the role of Btk downstream of GPVI and CLEC-2

At concentrations of CRP-XL used in this study (left panel), Btk mediates GPVI signalling through a scaffolding role, and it localises with LAT.

At submaximal concentrations of rhodocytin (centre panel), Btk mediates CLEC-2 signalling through its kinase activity, as shown by the green

arrows (phosphorylation arrows are shown in green). Whereas at high concentrations (right panel), aggregation is independent on Btk and mediated through secondary mediators or scaffold function of Btk. Independent of agonist, Btk localises with LAT (shown in orange), and CLEC-2 more than it localises with GPVI.

8 References

- ABU-BONSRAH, K. D., ZHANG, D. & NEWGREEN, D. F. 2016. CRISPR/Cas9 Targets Chicken Embryonic Somatic Cells In Vitro and In Vivo and generates Phenotypic Abnormalities. *Sci Rep*, 6, 34524.
- ADVANI, R. H., BUGGY, J. J., SHARMAN, J. P., SMITH, S. M., BOYD, T. E., GRANT, B., KOLIBABA, K. S., FURMAN, R. R., RODRIGUEZ, S., CHANG, B. Y., SUKBUNTHERN, J., IZUMI, R., HAMDY, A., HEDRICK, E. & FOWLER, N. H. 2013. Bruton tyrosine kinase inhibitor ibrutinib (PCI-32765) has significant activity in patients with relapsed/refractory B-cell malignancies. *J Clin Oncol*, 31, 88-94.
- AGNARSSON, B., LUNDGREN, A., GUNNARSSON, A., RABE, M., KUNZE, A., MAPAR, M., SIMONSSON, L., BALLY, M., ZHDANOV, V. P. & HÖÖK, F. 2015. Evanescent Light-Scattering Microscopy for Label-Free Interfacial Imaging: From Single Sub-100 nm Vesicles to Live Cells. *ACS Nano*, 9, 11849-62.
- AGNEW, C. & JURA, N. 2017. Switching on BTK—One Domain at a Time. *Structure*, 25, 1469-1470.
- AHN, I. E., UNDERBAYEV, C., ALBITAR, A., HERMAN, S. E. M., TIAN, X., MARIC, I., ARTHUR, D. C., WAKE, L., PITTALUGA, S., YUAN, C. M., STETLER-STEVENSON, M., SOTO, S., VALDEZ, J., NIERMAN, P., LOTTER, J., XI, L., RAFFELD, M., FAROOQUI, M., ALBITAR, M. & WIESTNER, A. 2017. Clonal evolution leading to ibrutinib resistance in chronic lymphocytic leukemia. *Blood*, 129, 1469-1479.
- AKINLEYE, A., CHEN, Y., MUKHI, N., SONG, Y. & LIU, D. 2013. Ibrutinib and novel BTK inhibitors in clinical development. *Journal of hematology & oncology*, 6, 59-59.
- AL-SAMKARI, H., KARP LEAF, R. S., DZIK, W. H., CARLSON, J. C. T., FOGERTY, A. E., WAHEED, A., GOODARZI, K., BENDAPUDI, P. K., BORNIKOVA, L., GUPTA, S., LEAF, D. E., KUTER, D. J. & ROSOVSKY, R. P. 2020. COVID-19 and coagulation: bleeding and thrombotic manifestations of SARS-CoV-2 infection. *Blood*, 136, 489-500.
- ALBERELLI, M. A., INNOCENTI, I., AUTORE, F., LAURENTI, L. & DE CANDIA, E. 2018. Ibrutinib does not affect ristocetin-induced platelet aggregation evaluated by light transmission aggregometry in chronic lymphocytic leukemia patients. *Haematologica*, 103, e119-e122.
- ALSHEHRI, O. M., HUGHES, C. E., MONTAGUE, S., WATSON, S. K., FRAMPTON, J., BENDER, M. & WATSON, S. P. 2015a. Fibrin activates GPVI in human and mouse platelets. *Blood*, 126, 1601-1608.
- ALSHEHRI, O. M., MONTAGUE, S., WATSON, S., CARTER, P., SARKER, N., MANNE, B. K., MILLER, J. L., HERR, A. B., POLLITT, A. Y., O'CALLAGHAN, C. A., KUNAPULI, S., ARMAN, M., HUGHES, C. E. & WATSON, S. P. 2015b. Activation of glycoprotein VI (GPVI) and C-type lectin-like receptor-2 (CLEC-2) underlies platelet activation by diesel exhaust particles and other charged/hydrophobic ligands. *Biochem J*, 468, 459-73.
- AMBROSE, E. J. 1956. A Surface Contact Microscope for the study of Cell Movements. *Nature*, 178, 1194-1194.
- AQUINO, D., SCHÖNLE, A., GEISLER, C., MIDDENDORFF, C. V., WURM, C. A., OKAMURA, Y., LANG, T., HELL, S. W. & EGNER, A. 2011. Two-color nanoscopy of three-dimensional volumes by 4Pi detection of stochastically switched fluorophores. *Nature Methods*, 8, 353-359.
- ARTHUR, J. F., DUNKLEY, S. & ANDREWS, R. K. 2007. Platelet glycoprotein VI-related clinical defects. *British Journal of Haematology*, 139, 363-372.

- ASAZUMA, N., WILDE, J. I., BERLANGA, O., LEDUC, M., LEO, A., SCHWEIGHOFFER, E., TYBULEWICZ, V., BON, C., LIU, S. K., MCGLADE, C. J., SCHRAVEN, B. & WATSON, S. P. 2000. Interaction of linker for activation of T cells with multiple adapter proteins in platelets activated by the glycoprotein VI-selective ligand, convulxin. *J Biol Chem*, 275, 33427-34.
- ASTARITA, J. L., ACTON, S. E. & TURLEY, S. J. 2012. Podoplanin: emerging functions in development, the immune system, and cancer. *Frontiers in Immunology*, 3, 283.
- ATKINSON, B. T., ELLMEIER, W. & WATSON, S. P. 2003a. Tec regulates platelet activation by GPVI in the absence of Btk. *Blood*, 102, 3592-9.
- ATKINSON, B. T., JARVIS, G. E. & WATSON, S. P. 2003b. Activation of GPVI by collagen is regulated by alpha2beta1 and secondary mediators. *J Thromb Haemost*, 1, 1278-87.
- AXELROD, D. 1981. Cell-substrate contacts illuminated by total internal reflection fluorescence. *The Journal of cell biology*, 89, 141-145.
- BABA, Y., HASHIMOTO, S., MATSUSHITA, M., WATANABE, D., KISHIMOTO, T., KUROSAKI, T. & TSUKADA, S. 2001. BLNK mediates Syk-dependent Btk activation. *Proceedings of the National Academy of Sciences of the United States of America*, 98, 2582-2586.
- BADOLIA, R., INAMDAR, V., MANNE, B. K., DANGELMAIER, C., EBLE, J. A. & KUNAPULI, S. P. 2017. G(q) pathway regulates proximal C-type lectin-like receptor-2 (CLEC-2) signaling in platelets. *The Journal of biological chemistry*, 292, 14516-14531.
- BALAGOPALAN, L., YI, J., NGUYEN, T., MCINTIRE, K. M., HARNED, A. S., NARAYAN, K. & SAMELSON, L. E. 2018. Plasma membrane LAT activation precedes vesicular recruitment defining two phases of early T-cell activation. *Nature Communications*, 9, 2013.
- BARF, T., COVEY, T., IZUMI, R., VAN DE KAR, B., GULRAJANI, M., VAN LITH, B., VAN HOEK, M., DE ZWART, E., MITTAG, D., DEMONT, D., VERKAIK, S., KRANTZ, F., PEARSON, P. G., ULRICH, R. & KAPTEIN, A. 2017. Acalabrutinib (ACP-196): A Covalent Bruton Tyrosine Kinase Inhibitor with a Differentiated Selectivity and In Vivo Potency Profile. *Journal of Pharmacology and Experimental Therapeutics*, 363, 240-252.
- BATTRAM, A. M., DURRANT, T. N., AGBANI, E. O., HEESOM, K. J., PAUL, D. S., PIATT, R., POOLE, A. W., CULLEN, P. J., BERGMEIER, W., MOORE, S. F. & HERS, I. 2017. The Phosphatidylinositol 3,4,5-trisphosphate (PI(3,4,5)P3) Binder Rasa3 Regulates Phosphoinositide 3-kinase (PI3K)-dependent Integrin α IIb β 3 Outside-in Signaling. *The Journal of biological chemistry*, 292, 1691-1704.
- BAUMGARTNER, H. R. & HAUDENSCHILD, C. 1972. Adhesion of platelets to subendothelium. *Ann N Y Acad Sci*, 201, 22-36.
- BEARER, E. L. 1995. Cytoskeletal domains in the activated platelet. *Cell Motil Cytoskeleton*, 30, 50-66.
- BENDER, M., HOFMANN, S., STEGNER, D., CHALARIS, A., BÖSL, M., BRAUN, A., SCHELLER, J., ROSE-JOHN, S. & NIESWANDT, B. 2010. Differentially regulated GPVI ectodomain shedding by multiple platelet-expressed proteinases. *Blood*, 116, 3347-3355.
- BENDER, M., MAY, F., LORENZ, V., THIELMANN, I., HAGEDORN, I., FINNEY, B. A., VÖGTLE, T., REMER, K., BRAUN, A., BÖSL, M., WATSON, S. P. & NIESWANDT, B. 2013. Combined in vivo depletion of glycoprotein VI and C-type lectin-like receptor 2 severely compromises hemostasis and abrogates arterial thrombosis in mice. *Arteriosclerosis, thrombosis, and vascular biology*, 33, 926-934.

- BERARD, R., WHITTEMORE, B. & SCUCCIMARRI, R. 2012. Hemolytic anemia following intravenous immunoglobulin therapy in patients treated for Kawasaki disease: a report of 4 cases. *Pediatric rheumatology online journal*, 10, 10-10.
- BERGER, G., MASSE, J. M. & CRAMER, E. M. 1996. Alpha-granule membrane mirrors the platelet plasma membrane and contains the glycoproteins Ib, IX, and V. *Blood*, 87, 1385-95.
- BERGMEIER, W., BOUVARD, D., EBLE, J. A., MOKHTARI-NEJAD, R., SCHULTE, V., ZIRNGIBL, H., BRAKEBUSCH, C., FASSLER, R. & NIESWANDT, B. 2001. Rhodocytin (aggrexin) activates platelets lacking alpha(2)beta(1) integrin, glycoprotein VI, and the ligand-binding domain of glycoprotein Ibalpha. *J Biol Chem*, 276, 25121-6.
- BERGMEIER, W., RABIE, T., STREHL, A., PIFFATH, C. L., PROSTREDNA, M., WAGNER, D. D. & NIESWANDT, B. 2004. GPVI down-regulation in murine platelets through metalloproteinase-dependent shedding. *Thromb Haemost*, 91, 951-8.
- BERLANGA, O., TULASNE, D., BORI, T., SNELL, D. C., MIURA, Y., JUNG, S., MOROI, M., FRAMPTON, J. & WATSON, S. P. 2002. The Fc receptor gamma-chain is necessary and sufficient to initiate signalling through glycoprotein VI in transfected cells by the snake C-type lectin, convulxin. *Eur J Biochem*, 269, 2951-60.
- BERNARDINI, G., KIM, J. Y., GISMONDI, A., BUTCHER, E. C. & SANTONI, A. 2005. Chemoattractant induces LFA-1 associated PI 3K activity and cell migration that are dependent on Fyn signaling. *The FASEB Journal*, 19, 1305-1307.
- BERTOZZI, C. C., SCHMAIER, A. A., MERICKO, P., HESS, P. R., ZOU, Z., CHEN, M., CHEN, C.-Y., XU, B., LU, M.-M., ZHOU, D., SEBZDA, E., SANTORE, M. T., MERIANOS, D. J., STADTFELD, M., FLAKE, A. W., GRAF, T., SKODA, R., MALTZMAN, J. S., KORETZKY, G. A. & KAHN, M. L. 2010. Platelets regulate lymphatic vascular development through CLEC-2-SLP-76 signaling. *Blood*, 116, 661-670.
- BHAVARAJU, K., KIM, S., DANIEL, J. L. & KUNAPULI, S. P. 2008. Evaluation of [3-(1-methyl-1H-indol-3-yl-methylene)-2-oxo-2, 3-dihydro-1H-indole-5-sulfonamide] (OXSI-2), as a Syk-selective inhibitor in platelets. *Eur J Pharmacol*, 580, 285-90.
- BIRD, G. S., AZIZ, O., LIEVREMONT, J. P., WEDEL, B. J., TREBAK, M., VAZQUEZ, G. & PUTNEY, J. W., JR. 2004. Mechanisms of phospholipase C-regulated calcium entry. *Curr Mol Med*, 4, 291-301.
- BLAIR, P. & FLAUMENHAFT, R. 2009. Platelet alpha-granules: basic biology and clinical correlates. *Blood Rev*, 23, 177-89.
- BOBE, R., WILDE, J. I., MASCHBERGER, P., VENKATESWARLU, K., CULLEN, P. J., SIESS, W. & WATSON, S. P. 2001. Phosphatidylinositol 3-kinase-dependent translocation of phospholipase Cgamma2 in mouse megakaryocytes is independent of Bruton tyrosine kinase translocation. *Blood*, 97, 678-84.
- BODIN, S., TRONCHÈRE, H. & PAYRASTRE, B. 2003. Lipid rafts are critical membrane domains in blood platelet activation processes. *Biochimica et Biophysica Acta (BBA) - Biomembranes*, 1610, 247-257.
- BOLLAND, S., PEARSE, R. N., KUROSAKI, T. & RAVETCH, J. V. 1998. SHIP modulates immune receptor responses by regulating membrane association of Btk. *Immunity*, 8, 509-16.
- BOLTE, S. & CORDELIÈRES, F. P. 2006. A guided tour into subcellular colocalization analysis in light microscopy. *J Microsc*, 224, 213-32.
- BONNEFOY, A., ROMIJN, R. A., VANDERVOORT, P. A., I, V. A. N. R., VERMYLEN, J. & HOYLAERTS, M. F. 2006. von Willebrand factor A1 domain can adequately substitute for A3 domain in recruitment of flowing platelets to collagen. *J Thromb Haemost*, 4, 2151-61.

- BOSE, P., GANDHI, V. V. & KEATING, M. J. 2016. Pharmacokinetic and pharmacodynamic evaluation of ibrutinib for the treatment of chronic lymphocytic leukemia: rationale for lower doses. *Expert opinion on drug metabolism & toxicology*, 12, 1381-1392.
- BOULAFTALI, Y., MAWHIN, M.-A., JANDROT-PERRUS, M. & HO-TIN-NOÉ, B. 2018. Glycoprotein VI in securing vascular integrity in inflamed vessels. *Research and practice in thrombosis and haemostasis*, 2, 228-239.
- BOURNE, J. H., COLICCHIA, M., DI, Y., MARTIN, E., SLATER, A., ROUMENINA, L. T., DIMITROV, J. D., WATSON, S. P. & RAYES, J. 2020. Heme induces human and mouse platelet activation through C-type-lectin-like receptor-2. *Haematologica*, haematol.2020.246488.
- BROCCHIERI, L. & KARLIN, S. 2005. Protein length in eukaryotic and prokaryotic proteomes. *Nucleic Acids Research*, 33, 3390-3400.
- BUITRAGO, L., BHAVANASI, D., DANGELMAIER, C., MANNE, B. K., BADOLIA, R., BORGOGNONE, A., TSYGANKOV, A. Y., MCKENZIE, S. E. & KUNAPULI, S. P. 2013. Tyrosine phosphorylation on spleen tyrosine kinase (Syk) is differentially regulated in human and murine platelets by protein kinase C isoforms. *The Journal of biological chemistry*, 288, 29160-29169.
- BURGER, J. A., TEDESCHI, A., BARR, P. M., ROBAK, T., OWEN, C., GHIA, P., BAIREY, O., HILLMEN, P., BARTLETT, N. L., LI, J., SIMPSON, D., GROSICKI, S., DEVEREUX, S., MCCARTHY, H., COUTRE, S., QUACH, H., GAIDANO, G., MASLYAK, Z., STEVENS, D. A., JANSSENS, A., OFFNER, F., MAYER, J., O'DWYER, M., HELLMANN, A., SCHUH, A., SIDDIQI, T., POLLIACK, A., TAM, C. S., SURI, D., CHENG, M., CLOW, F., STYLES, L., JAMES, D. F. & KIPPS, T. J. 2015. Ibrutinib as Initial Therapy for Patients with Chronic Lymphocytic Leukemia. *N Engl J Med*, 373, 2425-37.
- BURKHART, J. M., VAUDEL, M., GAMBARYAN, S., RADAU, S., WALTER, U., MARTENS, L., GEIGER, J., SICKMANN, A. & ZAHEDI, R. P. 2012. The first comprehensive and quantitative analysis of human platelet protein composition allows the comparative analysis of structural and functional pathways. *Blood*, 120, e73-82.
- BUSYGINA, K., JAMASBI, J., SEILER, T., DECKMYN, H., WEBER, C., BRANDL, R., LORENZ, R. & SIESS, W. 2018. Oral Bruton tyrosine kinase inhibitors selectively block atherosclerotic plaque-triggered thrombus formation in humans. *Blood*, 131, 2605-2616.
- BYE, A. P. & GIBBINS, J. M. 2018. Move along, nothing to see here: Btk inhibitors stop platelets sticking to plaques. *J Thromb Haemost*.
- BYE, A. P., UNSWORTH, A. J., DESBOROUGH, M. J., HILDYARD, C. A. T., APPLEBY, N., BRUCE, D., KRIEK, N., NOCK, S. H., SAGE, T., HUGHES, C. E. & GIBBINS, J. M. 2017. Severe platelet dysfunction in NHL patients receiving ibrutinib is absent in patients receiving acalabrutinib. *Blood Advances*, 1, 2610-2623.
- BYE, A. P., UNSWORTH, A. J., VAIYAPURI, S., STAINER, A. R., FRY, M. J. & GIBBINS, J. M. 2015. Ibrutinib Inhibits Platelet Integrin α IIb β 3 Outside-In Signaling and Thrombus Stability But Not Adhesion to Collagen. *Arterioscler Thromb Vasc Biol*, 35, 2326-35.
- BYRD, J. C., FURMAN, R. R., COUTRE, S. E., BURGER, J. A., BLUM, K. A., COLEMAN, M., WIERDA, W. G., JONES, J. A., ZHAO, W., HEEREMA, N. A., JOHNSON, A. J., SHAW, Y., BILOTTI, E., ZHOU, C., JAMES, D. F. & O'BRIEN, S. 2015. Three-year follow-up of treatment-naïve and previously treated patients with CLL and SLL receiving single-agent ibrutinib. *Blood*, 125, 2497-506.
- BYRD, J. C., FURMAN, R. R., COUTRE, S. E., FLINN, I. W., BURGER, J. A., BLUM, K. A., GRANT, B., SHARMAN, J. P., COLEMAN, M., WIERDA, W. G., JONES, J. A., ZHAO, W., HEEREMA, N. A., JOHNSON, A. J., SUKBUNTHERNG, J.,

- CHANG, B. Y., CLOW, F., HEDRICK, E., BUGGY, J. J., JAMES, D. F. & O'BRIEN, S. 2013. Targeting BTK with ibrutinib in relapsed chronic lymphocytic leukemia. *N Engl J Med*, 369, 32-42.
- BYRD, J. C., HARRINGTON, B., O'BRIEN, S., JONES, J. A., SCHUH, A., DEVEREUX, S., CHAVES, J., WIERDA, W. G., AWAN, F. T., BROWN, J. R., HILLMEN, P., STEPHENS, D. M., GHIA, P., BARRIENTOS, J. C., PAGEL, J. M., WOYACH, J., JOHNSON, D., HUANG, J., WANG, X., LANNUTTI, B. J., COVEY, T., FARDIS, M., MCGREIVY, J., HAMDY, A., ROTHBAUM, W., IZUMI, R., DIACOVO, T. G., JOHNSON, A. J. & FURMAN, R. R. 2016. Acalabrutinib (ACP-196) in Relapsed Chronic Lymphocytic Leukemia. *The New England journal of medicine*, 374, 323-332.
- CALAMINUS, S. D., THOMAS, S., MCCARTY, O. J., MACHESKY, L. M. & WATSON, S. P. 2008. Identification of a novel, actin-rich structure, the actin nodule, in the early stages of platelet spreading. *J Thromb Haemost*, 6, 1944-52.
- CAZENAVE, J.-P., OHLMANN, P., CASSEL, D., ECKLY, A., HECHLER, B. & GACHET, C. 2004. Preparation of Washed Platelet Suspensions From Human and Rodent Blood. *Methods in molecular biology (Clifton, N.J.)*, 272, 13-28.
- CEBECAUER, M., SPITALER, M., SERGÉ, A. & MAGEE, A. I. 2010. Signalling complexes and clusters: functional advantages and methodological hurdles. *Journal of Cell Science*, 123, 309-320.
- CHAIPAN, C., SOILLEUX, E. J., SIMPSON, P., HOFMANN, H., GRAMBERG, T., MARZI, A., GEIER, M., STEWART, E. A., EISEMANN, J., STEINKASSERER, A., SUZUKI-INOUE, K., FULLER, G. L., PEARCE, A. C., WATSON, S. P., HOXIE, J. A., BARIBAUD, F. & POHLMANN, S. 2006. DC-SIGN and CLEC-2 mediate human immunodeficiency virus type 1 capture by platelets. *J Virol*, 80, 8951-60.
- CHANG, H., ROCKMAN, C. B., JACOBOWITZ, G. R., SPERANZA, G., JOHNSON, W. S., HOROWITZ, J. M., GARG, K., MALDONADO, T. S., SADEK, M. & BARFIELD, M. E. 2020. Deep Venous Thrombosis in Hospitalized Patients with Coronavirus Disease 2019. *Journal of Vascular Surgery. Venous and Lymphatic Disorders*.
- CHANG, Y.-W., HSIEH, P.-W., CHANG, Y.-T., LU, M.-H., HUANG, T.-F., CHONG, K.-Y., LIAO, H.-R., CHENG, J.-C. & TSENG, C.-P. 2015. Identification of a novel platelet antagonist that binds to CLEC-2 and suppresses podoplanin-induced platelet aggregation and cancer metastasis. *Oncotarget*, 6, 42733-42748.
- CHARI, R., KIM, S., MURUGAPPAN, S., SANJAY, A., DANIEL, J. L. & KUNAPULI, S. P. 2009. Lyn, PKC-delta, SHIP-1 interactions regulate GPVI-mediated platelet-dense granule secretion. *Blood*, 114, 3056-3063.
- CHEN, D., BERNSTEIN, A. M., LEMONS, P. P. & WHITEHEART, S. W. 2000. Molecular mechanisms of platelet exocytosis: role of SNAP-23 and syntaxin 2 in dense core granule release. *Blood*, 95, 921-9.
- CHEN, J., KINOSHITA, T., GURURAJA, T., SUKBUNTHERNG, J., JAMES, D., LU, D., WHANG, J., VERSELE, M. & CHANG, B. Y. 2018. The effect of Bruton's tyrosine kinase (BTK) inhibitors on collagen-induced platelet aggregation, BTK, and tyrosine kinase expressed in hepatocellular carcinoma (TEC). *European Journal of Haematology*, 101, 604-612.
- CHEN, T., REPETTO, B., CHIZZONITE, R., PULLAR, C., BURGHARDT, C., DHARM, E., ZHAO, Z., CARROLL, R., NUNES, P., BASU, M., DANHO, W., VISNICK, M., KOCHAN, J., WAUGH, D. & GILFILLAN, A. M. 1996. Interaction of phosphorylated FcepsilonR1gamma immunoglobulin receptor tyrosine activation motif-based peptides with dual and single SH2 domains of p72syk. Assessment of binding parameters and real time binding kinetics. *J Biol Chem*, 271, 25308-15.
- CHEN, X.-F., WANG, W.-F., ZHANG, Y.-D., ZHAO, W., WU, J. & CHEN, T.-X. 2016. Clinical characteristics and genetic profiles of 174 patients with X-linked

- agammaglobulinemia: Report from Shanghai, China (2000–2015). *Medicine*, 95, e4544.
- CHRISTOU, C. M., PEARCE, A. C., WATSON, A. A., MISTRY, A. R., POLLITT, A. Y., FENTON-MAY, A. E., JOHNSON, L. A., JACKSON, D. G., WATSON, S. P. & O'CALLAGHAN, C. A. 2008. Renal cells activate the platelet receptor CLEC-2 through podoplanin. *The Biochemical journal*, 411, 133-140.
- CHUNG, J. K., NOCKA, L. M., DECKER, A., WANG, Q., KADLECEK, T. A., WEISS, A., KURIYAN, J. & GROVES, J. T. 2019. Switch-like activation of Bruton's tyrosine kinase by membrane-mediated dimerization. *Proc Natl Acad Sci U S A*, 116, 10798-10803.
- CLARK, J. C., KAVANAGH, D. M., WATSON, S., PIKE, J. A., ANDREWS, R. K., GARDINER, E. E., POULTER, N. S., HILL, S. J. & WATSON, S. P. 2019. Adenosine and Forskolin Inhibit Platelet Aggregation by Collagen but not the Proximal Signalling Events. *Thromb Haemost*, 119, 1124-1137.
- CLAUSHUIS, T. A. M., DE VOS, A. F., NIESWANDT, B., BOON, L., ROELOFS, J. J. T. H., DE BOER, O. J., VAN 'T VEER, C. & VAN DER POLL, T. 2018. Platelet glycoprotein VI aids in local immunity during pneumonia-derived sepsis caused by gram-negative bacteria. *Blood*, 131, 864-876.
- CLEMENTS, J. L., LEE, J. R., GROSS, B., YANG, B., OLSON, J. D., SANDRA, A., WATSON, S. P., LENTZ, S. R. & KORETZKY, G. A. 1999. Fetal hemorrhage and platelet dysfunction in SLP-76-deficient mice. *Journal of Clinical Investigation*, 103, 19-25.
- CLEMETSON, J. M., POLGAR, J., MAGNENAT, E., WELLS, T. N. C. & CLEMETSON, K. J. 1999. The Platelet Collagen Receptor Glycoprotein VI Is a Member of the Immunoglobulin Superfamily Closely Related to Fc α R and the Natural Killer Receptors. *Journal of Biological Chemistry*, 274, 29019-29024.
- CLIPSTONE, N. A. & CRABTREE, G. R. 1992. Identification of calcineurin as a key signalling enzyme in T-lymphocyte activation. *Nature*, 357, 695-7.
- CONLEY, M. E. 1985. B cells in patients with X-linked agammaglobulinemia. *J Immunol*, 134, 3070-4.
- CORPET, F. 1988. Multiple sequence alignment with hierarchical clustering. *Nucleic Acids Res*, 16, 10881-90.
- COSTELLO, R., CANTILLO, J. F. & KENTER, A. L. 2019. Chicken MBD4 Regulates Immunoglobulin Diversification by Somatic Hypermutation. *Frontiers in immunology*, 10, 2540-2540.
- COVEY, T., BARF, T., GULRAJANI, M., KRANTZ, F., VAN LITH, B., BIBIKOVA, E., VAN DE KAR, B., DE ZWART, E., HAMDY, A., IZUMI, R. & KAPTEIN, A. 2015. Abstract 2596: ACP-196: a novel covalent Bruton's tyrosine kinase (Btk) inhibitor with improved selectivity and in vivo target coverage in chronic lymphocytic leukemia (CLL) patients. *Cancer Research*, 75, 2596-2596.
- CROSBY, D. & POOLE, A. W. 2002. Interaction of Bruton's tyrosine kinase and protein kinase C θ in platelets. Cross-talk between tyrosine and serine/threonine kinases. *J Biol Chem*, 277, 9958-65.
- DAMEN, J. E., WARE, M. D., KALESNIKOFF, J., HUGHES, M. R. & KRYSTAL, G. 2001. SHIP's C-terminus is essential for its hydrolysis of PIP3 and inhibition of mast cell degranulation. *Blood*, 97, 1343-51.
- DE BRUIJN, M. J. W., RIP, J., VAN DER PLOEG, E. K., VAN GREUNINGEN, L. W., TA, V. T. B., KIL, L. P., LANGERAK, A. W., RIMMELZWAAN, G. F., ELLMEIER, W., HENDRIKS, R. W. & CORNETH, O. B. J. 2017. Distinct and Overlapping Functions of TEC Kinase and BTK in B Cell Receptor Signaling. *The Journal of Immunology*, 198, 3058-3068.
- DE PORTO, A., CLAUSHUIS, T. A. M., VAN DER DONK, L. E. H., DE BEER, R., DE BOER, O. J., FLORQUIN, S., ROELOFS, J., HENDRIKS, R. W., VAN DER POLL, T., VAN'T VEER, C. & DE VOS, A. F. 2019. Platelet Btk is Required for

- Maintaining Lung Vascular Integrity during Murine Pneumococcal Pneumosepsis. *Thromb Haemost*, 119, 930-940.
- DOBIE, G., KURIRI, F. A., OMAR, M. M. A., ALANAZI, F., GAZWANI, A. M., TANG, C. P. S., SZE, D. M.-Y., HANDUNNETTI, S. M., TAM, C. & JACKSON, D. E. 2019. Ibrutinib, but not zanubrutinib, induces platelet receptor shedding of GPIb-IX-V complex and integrin $\alpha\text{IIb}\beta\text{3}$ in mice and humans. *Blood advances*, 3, 4298-4311.
- DOENCH, J. G., FUSI, N., SULLENDER, M., HEGDE, M., VAIMBERG, E. W., DONOVAN, K. F., SMITH, I., TOTHOVA, Z., WILEN, C., ORCHARD, R., VIRGIN, H. W., LISTGARTEN, J. & ROOT, D. E. 2016. Optimized sgRNA design to maximize activity and minimize off-target effects of CRISPR-Cas9. *Nat Biotechnol*, 34, 184-191.
- DOLMETSCH, R. E., LEWIS, R. S., GOODNOW, C. C. & HEALY, J. I. 1997. Differential activation of transcription factors induced by Ca^{2+} response amplitude and duration. *Nature*, 386, 855-8.
- DORMANN, D., CLEMETSON, J. M., NAVDAEV, A., KEHREL, B. E. & CLEMETSON, K. J. 2001. Alboaggregin A activates platelets by a mechanism involving glycoprotein VI as well as glycoprotein Ib. *Blood*, 97, 929-36.
- DOVIZIO, M., MAIER, T. J., ALBERTI, S., DI FRANCESCO, L., MARCANTONI, E., MUNCH, G., JOHN, C. M., SUESS, B., SGAMBATO, A., STEINHILBER, D. & PATRIGNANI, P. 2013. Pharmacological inhibition of platelet-tumor cell cross-talk prevents platelet-induced overexpression of cyclooxygenase-2 in HT29 human colon carcinoma cells. *Mol Pharmacol*, 84, 25-40.
- DUNN, K. W., KAMOCKA, M. M. & MCDONALD, J. H. 2011. A practical guide to evaluating colocalization in biological microscopy. *American journal of physiology. Cell physiology*, 300, C723-C742.
- DUNSTER, J. L., UNSWORTH, A. J., BYE, A. P., HAINING, E. J., SOWA, M. A., DI, Y., SAGE, T., PALLINI, C., PIKE, J. A., HARDY, A. T., NIESWANDT, B., GARCÍA, Á., WATSON, S. P., POULTER, N. S., GIBBINS, J. M. & POLLITT, A. Y. 2020. Interspecies differences in protein expression do not impact the spatiotemporal regulation of glycoprotein VI mediated activation. *Journal of thrombosis and haemostasis : JTH*, 18, 485-496.
- DURRANT, T. N., HUTCHINSON, J. L., HEESOM, K. J., ANDERSON, K. E., STEPHENS, L. R., HAWKINS, P. T., MARSHALL, A. J., MOORE, S. F. & HERS, I. 2017. In-depth PtdIns(3,4,5)P(3) signalosome analysis identifies DAPP1 as a negative regulator of GPVI-driven platelet function. *Blood advances*, 1, 918-932.
- EEUWIJK, J. M. M. V., STEGNER, D., LAMB, D. J., KRAFT, P., BECK, S., THIELMANN, I., KIEFER, F., WALZOG, B., STOLL, G. & NIESWANDT, B. 2016. The Novel Oral Syk Inhibitor, BI1002494, Protects Mice From Arterial Thrombosis and Thromboinflammatory Brain Infarction. *Arteriosclerosis, Thrombosis, and Vascular Biology*, 36, 1247-1253.
- EICHACKER, L. A., GRANVOGL, B., MIRUS, O., MÜLLER, B. C., MIESS, C. & SCHLEIFF, E. 2004. Hiding behind Hydrophobicity: TRANSMEMBRANE SEGMENTS IN MASS SPECTROMETRY. *Journal of Biological Chemistry*, 279, 50915-50922.
- EL-HILLAL, O., KUROSAKI, T., YAMAMURA, H., KINET, J. P. & SCHARENBERG, A. M. 1997. syk kinase activation by a src kinase-initiated activation loop phosphorylation chain reaction. *Proc Natl Acad Sci U S A*, 94, 1919-24.
- EZUMI, Y., SHINDOH, K., TSUJI, M. & TAKAYAMA, H. 1998. Physical and Functional Association of the Src Family Kinases Fyn and Lyn with the Collagen Receptor Glycoprotein VI-Fc Receptor γ Chain Complex on Human Platelets. *The Journal of Experimental Medicine*, 188, 267-276.
- FINNEY, B. A., SCHWEIGHOFFER, E., NAVARRO-NUNEZ, L., BENEZECH, C., BARONE, F., HUGHES, C. E., LANGAN, S. A., LOWE, K. L., POLLITT, A. Y.,

- MOURAO-SA, D., SHEARDOWN, S., NASH, G. B., SMITHERS, N., REIS E SOUSA, C., TYBULEWICZ, V. L. & WATSON, S. P. 2012. CLEC-2 and Syk in the megakaryocytic/platelet lineage are essential for development. *Blood*, 119, 1747-56.
- FLEIRE, S. J., GOLDMAN, J. P., CARRASCO, Y. R., WEBER, M., BRAY, D. & BATISTA, F. D. 2006. B cell ligand discrimination through a spreading and contraction response. *Science*, 312, 738-41.
- FLUCKIGER, A. C., LI, Z., KATO, R. M., WAHL, M. I., OCHS, H. D., LONGNECKER, R., KINET, J. P., WITTE, O. N., SCHARENBERG, A. M. & RAWLINGS, D. J. 1998. Btk/Tec kinases regulate sustained increases in intracellular Ca²⁺ following B-cell receptor activation. *The EMBO Journal*, 17, 1973-1985.
- FRANCISCHETTI, I. M., SALIOU, B., LEDUC, M., CARLINI, C. R., HATMI, M., RANDON, J., FAILI, A. & BON, C. 1997. Convulxin, a potent platelet-aggregating protein from *Crotalus durissus terrificus* venom, specifically binds to platelets. *Toxicon*, 35, 1217-28.
- FULLER, G. L., WILLIAMS, J. A., TOMLINSON, M. G., EBLE, J. A., HANNA, S. L., POHLMANN, S., SUZUKI-INOUE, K., OZAKI, Y., WATSON, S. P. & PEARCE, A. C. 2007. The C-type lectin receptors CLEC-2 and Dectin-1, but not DC-SIGN, signal via a novel YXXL-dependent signaling cascade. *J Biol Chem*, 282, 12397-409.
- FURMAN, R. R., WIERDA, W. G., SCHUH, A., DEVEREUX, S., CHAVES, J. M., BROWN, J. R., HILLMEN, P., MARTIN, P., AWAN, F. T., STEPHENS, D. M., GHIA, P., BARRIENTOS, J. C., PAGEL, J. M., WOYACH, J., BURKE, K., COVEY, T., GULRAJANI, M., HAMDY, A., IZUMI, R., FRIGAULT, M. M., PATEL, P., ROTHBAUM, W., WANG, M. H., O'BRIEN, S. M. & BYRD, J. C. 2019. Acalabrutinib Monotherapy in Patients with Relapsed/Refractory Chronic Lymphocytic Leukemia: 42-Month Follow-up of a Phase 2 Study. *Blood*, 134, 3039-3039.
- GARCIA-PARAJO, M. F., CAMBI, A., TORRENO-PINA, J. A., THOMPSON, N. & JACOBSON, K. 2014. Nanoclustering as a dominant feature of plasma membrane organization. *Journal of Cell Science*, 127, 4995-5005.
- GARDINER, E. E., KARUNAKARAN, D., SHEN, Y., ARTHUR, J. F., ANDREWS, R. K. & BERNDT, M. C. 2007. Controlled shedding of platelet glycoprotein (GP)VI and GPIb-IX-V by ADAM family metalloproteinases. *J Thromb Haemost*, 5, 1530-7.
- GASPAR, H. B., FERRANDO, M., CARAGOL, I., HERNANDEZ, M., BERTRAN, J. M., DE GRACIA, X., LESTER, T., KINNON, C., ASHTON, E. & ESPANOL, T. 2000. Kinase mutant Btk results in atypical X-linked agammaglobulinaemia phenotype. *Clinical and experimental immunology*, 120, 346-350.
- GASPAR, H. B., LESTER, T., LEVINSKY, R. J. & KINNON, C. 1998. Bruton's tyrosine kinase expression and activity in X-linked agammaglobulinaemia (XLA): the use of protein analysis as a diagnostic indicator of XLA. *Clin Exp Immunol*, 111, 334-8.
- GETZ, T. M., MAYANGLAMBAM, A., DANIEL, J. L. & KUNAPULI, S. P. 2011. Go6976 abrogates GPVI-mediated platelet functional responses in human platelets through inhibition of Syk. *Journal of thrombosis and haemostasis : JTH*, 9, 608-610.
- GIBBINS, J., ASSELIN, J., FARNDAL, R., BARNES, M., LAW, C. L. & WATSON, S. P. 1996. Tyrosine phosphorylation of the Fc receptor gamma-chain in collagen-stimulated platelets. *J Biol Chem*, 271, 18095-9.
- GIBBINS, J. M. 2004. Platelet adhesion signalling and the regulation of thrombus formation. *J Cell Sci*, 117, 3415-25.
- GIBBINS, J. M., BRIDDON, S., SHUTES, A., VAN VUGT, M. J., VAN DE WINKEL, J. G. J., SAITO, T. & WATSON, S. P. 1998. The p85 Subunit of Phosphatidylinositol 3-Kinase Associates with the Fc Receptor γ -Chain and

- Linker for Activator of T Cells (LAT) in Platelets Stimulated by Collagen and Convulxin. *Journal of Biological Chemistry*, 273, 34437-34443.
- GIBBINS, J. M., OKUMA, M., FARNDAL, R., BARNES, M. & WATSON, S. P. 1997. Glycoprotein VI is the collagen receptor in platelets which underlies tyrosine phosphorylation of the Fc receptor γ -chain. *FEBS Letters*, 413, 255-259.
- GILBERT, C., LEVASSEUR, S., DESAULNIERS, P., DUSSEAULT, A.-A., THIBAUT, N., BOURGOIN, S. G. & NACCACHE, P. H. 2003. Chemotactic Factor-Induced Recruitment and Activation of Tec Family Kinases in Human Neutrophils. II. Effects of LFM-A13, a Specific Btk Inhibitor. *The Journal of Immunology*, 170, 5235-5243.
- GILES, C. 1981. The Platelet Count and Mean Platelet Volume. *British Journal of Haematology*, 48, 31-37.
- GILIO, K., MUNNIX, I. C. A., MANGIN, P., COSEMANS, J. M. E. M., FEIJGE, M. A. H., VAN DER MEIJDEN, P. E. J., OLIESLAGERS, S., CHRZANOWSKA-WODNICKA, M. B., LILLIAN, R., SCHOENWAELDER, S., KOYASU, S., SAGE, S. O., JACKSON, S. P. & HEEMSKERK, J. W. M. 2009. Non-redundant roles of phosphoinositide 3-kinase isoforms alpha and beta in glycoprotein VI-induced platelet signaling and thrombus formation. *The Journal of biological chemistry*, 284, 33750-33762.
- GILLHAM, H., GOLDING, M. C., PEPPERKOK, R. & GULLICK, W. J. 1999. Intracellular movement of green fluorescent protein-tagged phosphatidylinositol 3-kinase in response to growth factor receptor signaling. *The Journal of cell biology*, 146, 869-880.
- GITZ, E., POLLITT, A. Y., GITZ-FRANCOIS, J. J., ALSHEHRI, O., MORI, J., MONTAGUE, S., NASH, G. B., DOUGLAS, M. R., GARDINER, E. E., ANDREWS, R. K., BUCKLEY, C. D., HARRISON, P. & WATSON, S. P. 2014. CLEC-2 expression is maintained on activated platelets and on platelet microparticles. *Blood*, 124, 2262-70.
- GOERGE, T., HO-TIN-NOE, B., CARBO, C., BENARAF, C., REMOLD-O'DONNELL, E., ZHAO, B. Q., CIFUNI, S. M. & WAGNER, D. D. 2008. Inflammation induces hemorrhage in thrombocytopenia. *Blood*, 111, 4958-64.
- GOSHUA, G., PINE, A. B., MEIZLISH, M. L., CHANG, C. H., ZHANG, H., BAHREL, P., BALUHA, A., BAR, N., BONA, R. D., BURNS, A. J., DELA CRUZ, C. S., DUMONT, A., HALENE, S., HWA, J., KOFF, J., MENNINGER, H., NEPARIDZE, N., PRICE, C., SINER, J. M., TORMEY, C., RINDER, H. M., CHUN, H. J. & LEE, A. I. 2020. Endotheliopathy in COVID-19-associated coagulopathy: evidence from a single-centre, cross-sectional study. *The Lancet Haematology*, 7, e575-e582.
- GRIFFIÉ, J., SHLOMOVICH, L., WILLIAMSON, D. J., SHANNON, M., AARON, J., KHUON, S., L BURN, G., BOELEN, L., PETERS, R., COPE, A. P., COHEN, E. A. K., RUBIN-DELANCHY, P. & OWEN, D. M. 2017. 3D Bayesian cluster analysis of super-resolution data reveals LAT recruitment to the T cell synapse. *Scientific reports*, 7, 4077-4077.
- GROS, A., SYVANNARATH, V., LAMRANI, L., OLLIVIER, V., LOYAU, S., GOERGE, T., NIESWANDT, B., JANDROT-PERRUS, M. & HO-TIN-NOÉ, B. 2015. Single platelets seal neutrophil-induced vascular breaches via GPVI during immune-complex-mediated inflammation in mice. *Blood*, 126, 1017-26.
- GROSS, B. S., LEE, J. R., CLEMENTS, J. L., TURNER, M., TYBULEWICZ, V. L., FINDELL, P. R., KORETZKY, G. A. & WATSON, S. P. 1999a. Tyrosine phosphorylation of SLP-76 is downstream of Syk following stimulation of the collagen receptor in platelets. *J Biol Chem*, 274, 5963-71.
- GROSS, B. S., WILDE, J. I., QUEK, L., CHAPEL, H., NELSON, D. L. & WATSON, S. P. 1999b. Regulation and Function of WASp in Platelets by the Collagen Receptor, Glycoprotein VI. *Blood*, 94, 4166-4176.

- GUINAMARD, R., ASPENSTRÖM, P., FOUGEREAU, M., CHAVRIER, P. & GUILLEMOT, J. C. 1998. Tyrosine phosphorylation of the Wiskott-Aldrich syndrome protein by Lyn and Btk is regulated by CDC42. *FEBS Lett*, 434, 431-6.
- GUSTAFSSON, M. O., HUSSAIN, A., MOHAMMAD, D. K., MOHAMED, A. J., NGUYEN, V., METALNIKOV, P., COLWILL, K., PAWSON, T., SMITH, C. I. & NORE, B. F. 2012. Regulation of nucleocytoplasmic shuttling of Bruton's tyrosine kinase (Btk) through a novel SH3-dependent interaction with ankyrin repeat domain 54 (ANKRD54). *Mol Cell Biol*, 32, 2440-53.
- GUSTAFSSON, M. O., MOHAMMAD, D. K., YLÖSMÄKI, E., CHOI, H., SHRESTHA, S., WANG, Q., NORE, B. F., SAKSELA, K. & SMITH, C. I. E. 2017. ANKRD54 preferentially selects Bruton's Tyrosine Kinase (BTK) from a Human Src-Homology 3 (SH3) domain library. *PLOS ONE*, 12, e0174909.
- HAINING, E. J., CHERPOKOVA, D., WOLF, K., BECKER, I. C., BECK, S., EBLE, J. A., STEGNER, D., WATSON, S. P. & NIESWANDT, B. 2017a. CLEC-2 contributes to hemostasis independently of classical hemITAM signaling in mice. *Blood*, 130, 2224-2228.
- HAINING, E. J., MATTHEWS, A. L., NOY, P. J., ROMANSKA, H. M., HARRIS, H. J., PIKE, J., MOROWSKI, M., GAVIN, R. L., YANG, J., MILHIET, P.-E., BERDITCHEVSKI, F., NIESWANDT, B., POULTER, N. S., WATSON, S. P. & TOMLINSON, M. G. 2017b. Tetraspanin Tspan9 regulates platelet collagen receptor GPVI lateral diffusion and activation. *Platelets*, 28, 629-642.
- HALEMANI, N. D., BETHANI, I., RIZZOLI, S. O. & LANG, T. 2010. Structure and dynamics of a two-helix SNARE complex in live cells. *Traffic*, 11, 394-404.
- HAMBERG, M., SVENSSON, J. & SAMUELSSON, B. 1975. Thromboxanes: a new group of biologically active compounds derived from prostaglandin endoperoxides. *Proceedings of the National Academy of Sciences of the United States of America*, 72, 2994-2998.
- HANNA, J., GUERRA-MORENO, A., ANG, J. & MICOOGULLARI, Y. 2019. Protein Degradation and the Pathologic Basis of Disease. *The American journal of pathology*, 189, 94-103.
- HARDY, A. R., JONES, M. L., MUNDELL, S. J. & POOLE, A. W. 2004. Reciprocal cross-talk between P2Y1 and P2Y12 receptors at the level of calcium signaling in human platelets. *Blood*, 104, 1745-52.
- HARTWIG, J. H. & DESISTO, M. 1991. The cytoskeleton of the resting human blood platelet: structure of the membrane skeleton and its attachment to actin filaments. *J Cell Biol*, 112, 407-25.
- HASHIMOTO, S., IWAMATSU, A., ISHIAI, M., OKAWA, K., YAMADORI, T., MATSUSHITA, M., BABA, Y., KISHIMOTO, T., KUROSAKI, T. & TSUKADA, S. 1999a. Identification of the SH2 domain binding protein of Bruton's tyrosine kinase as BLNK--functional significance of Btk-SH2 domain in B-cell antigen receptor-coupled calcium signaling. *Blood*, 94, 2357-64.
- HASHIMOTO, S., MIYAWAKI, T., FUTATANI, T., KANEGANE, H., USUI, K., NUKIWA, T., NAMIUCHI, S., MATSUSHITA, M., YAMADORI, T., SUEMURA, M., KISHIMOTO, T. & TSUKADA, S. 1999b. Atypical X-linked agammaglobulinemia diagnosed in three adults. *Intern Med*, 38, 722-5.
- HEILEMANN, M., VAN DE LINDE, S., SCHÜTTPELZ, M., KASPER, R., SEEFELDT, B., MUKHERJEE, A., TINNEFELD, P. & SAUER, M. 2008. Subdiffraction-resolution fluorescence imaging with conventional fluorescent probes. *Angew Chem Int Ed Engl*, 47, 6172-6.
- HERMAN, S. E. M., MONTRAVETA, A., NIEMANN, C. U., MORA-JENSEN, H., GULRAJANI, M., KRANTZ, F., HARRINGTON, B. K., COVEY, T., LANNUTTI, B. J., IZUMI, R., ULRICH, R. G., BYRD, J. C., WIESTNER, A., JOHNSON, A. J. & WOYACH, J. A. 2015. The Bruton Tyrosine Kinase (BTK) Inhibitor ACP-

- 196 Demonstrates Clinical Activity in Two Mouse Models of Chronic Lymphocytic Leukemia. *Blood*, 126, 2920-2920.
- HESS, P. R., RAWNSLEY, D. R., JAKUS, Z., YANG, Y., SWEET, D. T., FU, J., HERZOG, B., LU, M., NIESWANDT, B., OLIVER, G., MAKINEN, T., XIA, L. & KAHN, M. L. 2014. Platelets mediate lymphovenous hemostasis to maintain blood-lymphatic separation throughout life. *The Journal of Clinical Investigation*, 124, 273-284.
- HIRATA, T., USHIKUBI, F., KAKIZUKA, A., OKUMA, M. & NARUMIYA, S. 1996. Two thromboxane A2 receptor isoforms in human platelets. Opposite coupling to adenylyl cyclase with different sensitivity to Arg60 to Leu mutation. *J Clin Invest*, 97, 949-56.
- HITCHCOCK, J. R., COOK, C. N., BOBAT, S., ROSS, E. A., FLORES-LANGARICA, A., LOWE, K. L., KHAN, M., DOMINGUEZ-MEDINA, C. C., LAX, S., CARVALHO-GASPAR, M., HUBSCHER, S., RAINGER, G. E., COBBOLD, M., BUCKLEY, C. D., MITCHELL, T. J., MITCHELL, A., JONES, N. D., VAN ROOIJEN, N., KIRCHHOFER, D., HENDERSON, I. R., ADAMS, D. H., WATSON, S. P. & CUNNINGHAM, A. F. 2015. Inflammation drives thrombosis after Salmonella infection via CLEC-2 on platelets. *J Clin Invest*, 125, 4429-46.
- HOFFMAN, M. & MONROE, D. M., 3RD 2001. A cell-based model of hemostasis. *Thromb Haemost*, 85, 958-65.
- HONIGBERG, L. A., SMITH, A. M., SIRISAWAD, M., VERNER, E., LOURY, D., CHANG, B., LI, S., PAN, Z., THAMM, D. H., MILLER, R. A. & BUGGY, J. J. 2010. The Bruton tyrosine kinase inhibitor PCI-32765 blocks B-cell activation and is efficacious in models of autoimmune disease and B-cell malignancy. *Proc Natl Acad Sci U S A*, 107, 13075-80.
- HOOLEY, E., PAPAGRIGORIOU, E., NAVDAEV, A., PANDEY, A. V., CLEMETSON, J. M., CLEMETSON, K. J. & EMSLEY, J. 2008. The crystal structure of the platelet activator aggregin reveals a novel (alphabeta)₂ dimeric structure. *Biochemistry*, 47, 7831-7.
- HORII, K., KAHN, M. L. & HERR, A. B. 2006. Structural basis for platelet collagen responses by the immune-type receptor glycoprotein VI. *Blood*, 108, 936-42.
- HOUCK, K. L., YUAN, H., TIAN, Y., SOLOMON, M., CRAMER, D., LIU, K., ZHOU, Z., WU, X., ZHANG, J., OEHLER, V. & DONG, J.-F. 2019. Physical proximity and functional cooperation of glycoprotein 130 and glycoprotein VI in platelet membrane lipid rafts. *Journal of Thrombosis and Haemostasis*, 17, 1500-1510.
- HOUGH, S. H., AJETUNMOBI, A., BRODY, L., HUMPHRYES-KIRILOV, N. & PERELLO, E. 2016. Desktop Genetics. *Personalized medicine*, 13, 517-521.
- HSU, P. D., SCOTT, D. A., WEINSTEIN, J. A., RAN, F. A., KONERMANN, S., AGARWALA, V., LI, Y., FINE, E. J., WU, X., SHALEM, O., CRADICK, T. J., MARRAFFINI, L. A., BAO, G. & ZHANG, F. 2013. DNA targeting specificity of RNA-guided Cas9 nucleases. *Nature biotechnology*, 31, 827-832.
- HU, H., ARMSTRONG, P. C. J., KHALIL, E., CHEN, Y.-C., STRAUB, A., LI, M., SOOSAIRAJAH, J., HAGEMEYER, C. E., BASSLER, N., HUANG, D., AHRENS, I., KRIPPNER, G., GARDINER, E. & PETER, K. 2011. GPVI and GPIIb α mediate staphylococcal superantigen-like protein 5 (SSL5) induced platelet activation and direct toward glycans as potential inhibitors. *PloS one*, 6, e19190-e19190.
- HU, J., NEISWINGER, J., ZHANG, J., ZHU, H. & QIAN, J. 2015. Systematic Prediction of Scaffold Proteins Reveals New Design Principles in Scaffold-Mediated Signal Transduction. *PLoS Computational Biology*, 11, e1004508.
- HUANG, J., LI, X., SHI, X., ZHU, M., WANG, J., HUANG, S., HUANG, X., WANG, H., LI, L., DENG, H., ZHOU, Y., MAO, J., LONG, Z., MA, Z., YE, W., PAN, J., XI, X. & JIN, J. 2019. Platelet integrin α IIb β 3: signal transduction, regulation, and its therapeutic targeting. *Journal of Hematology & Oncology*, 12, 26.

- HUGHES, C. E., AUGER, J. M., MCGLADE, J., EBLE, J. A., PEARCE, A. C. & WATSON, S. P. 2008. Differential roles for the adapters Gads and LAT in platelet activation by GPVI and CLEC-2. *J Thromb Haemost*, 6, 2152-9.
- HUGHES, C. E., FINNEY, B. A., KOENTGEN, F., LOWE, K. L. & WATSON, S. P. 2015. The N-terminal SH2 domain of Syk is required for (hem)ITAM, but not integrin, signaling in mouse platelets. *Blood*, 125, 144-154.
- HUGHES, C. E., NAVARRO-NUNEZ, L., FINNEY, B. A., MOURAO-SA, D., POLLITT, A. Y. & WATSON, S. P. 2010a. CLEC-2 is not required for platelet aggregation at arteriolar shear. *J Thromb Haemost*, 8, 2328-32.
- HUGHES, C. E., POLLITT, A. Y., MORI, J., EBLE, J. A., TOMLINSON, M. G., HARTWIG, J. H., O'CALLAGHAN, C. A., FUTTERER, K. & WATSON, S. P. 2010b. CLEC-2 activates Syk through dimerization. *Blood*, 115, 2947-55.
- HUGHES, C. E., SINHA, U., PANDEY, A., EBLE, J. A., O'CALLAGHAN, C. A. & WATSON, S. P. 2013. Critical Role for an acidic amino acid region in platelet signaling by the HemITAM (hemi-immunoreceptor tyrosine-based activation motif) containing receptor CLEC-2 (C-type lectin receptor-2). *J Biol Chem*, 288, 5127-35.
- HUMPHRIES, L. A., DANGELMAIER, C., SOMMER, K., KIPP, K., KATO, R. M., GRIFFITH, N., BAKMAN, I., TURK, C. W., DANIEL, J. L. & RAWLINGS, D. J. 2004. Tec Kinases Mediate Sustained Calcium Influx via Site-specific Tyrosine Phosphorylation of the Phospholipase C γ Src Homology 2-Src Homology 3 Linker. *Journal of Biological Chemistry*, 279, 37651-37661.
- HYVÖNEN, M. & SARASTE, M. 1997. Structure of the PH domain and Btk motif from Bruton's tyrosine kinase: molecular explanations for X-linked agammaglobulinaemia. *The EMBO journal*, 16, 3396-3404.
- ICHISE, H., ICHISE, T., OHTANI, O. & YOSHIDA, N. 2009. Phospholipase C γ 2 is necessary for separation of blood and lymphatic vasculature in mice. *Development*, 136, 191-5.
- ISAAC, K. & MATO, A. R. 2020. Acalabrutinib and Its Therapeutic Potential in the Treatment of Chronic Lymphocytic Leukemia: A Short Review on Emerging Data. *Cancer management and research*, 12, 2079-2085.
- IZQUIERDO, I., BARRACHINA, M. N., HERMIDA-NOGUEIRA, L., CASAS, V., EBLE, J. A., CARRASCAL, M., ABIÁN, J. & GARCÍA, Á. 2019. Platelet membrane lipid rafts protein composition varies following GPVI and CLEC-2 receptors activation. *J Proteomics*, 195, 88-97.
- IZQUIERDO, I., BARRACHINA, M. N., HERMIDA-NOGUEIRA, L., CASAS, V., MORÁN, L. A., LACERENZA, S., PINTO-LLORENTE, R., EBLE, J. A., DE LOS RÍOS, V., DOMÍNGUEZ, E., LOZA, M. I., CASAL, J. I., CARRASCAL, M., ABIÁN, J. & GARCÍA, A. 2020. A Comprehensive Tyrosine Phosphoproteomic Analysis Reveals Novel Components of the Platelet CLEC-2 Signaling Cascade. *Thromb Haemost*, 120, 262-276.
- JACOBI, A. M., RETTIG, G. R., TURK, R., COLLINGWOOD, M. A., ZEINER, S. A., QUADROS, R. M., HARMS, D. W., BONTHUIS, P. J., GREGG, C., OHTSUKA, M., GURUMURTHY, C. B. & BEHLKE, M. A. 2017. Simplified CRISPR tools for efficient genome editing and streamlined protocols for their delivery into mammalian cells and mouse zygotes. *Methods*, 121-122, 16-28.
- JAMASBI, J., MEGENS, R. T., BIANCHINI, M., MUNCH, G., UNGERER, M., FAUSSNER, A., SHERMAN, S., WALKER, A., GOYAL, P., JUNG, S., BRANDL, R., WEBER, C., LORENZ, R., FARNDAL, R., ELIA, N. & SIESS, W. 2015. Differential Inhibition of Human Atherosclerotic Plaque-Induced Platelet Activation by Dimeric GPVI-Fc and Anti-GPVI Antibodies: Functional and Imaging Studies. *J Am Coll Cardiol*, 65, 2404-15.
- JANDROT-PERRUS, M., BUSFIELD, S., LAGRUE, A. H., XIONG, X., DEBILI, N., CHICKERING, T., LE COUEDIC, J. P., GOODEARL, A., DUSSAULT, B., FRASER, C., VAINCHENKER, W. & VILLEVAL, J. L. 2000. Cloning,

- characterization, and functional studies of human and mouse glycoprotein VI: a platelet-specific collagen receptor from the immunoglobulin superfamily. *Blood*, 96, 1798-807.
- JANDROT-PERRUS, M., LAGRUE, A. H., OKUMA, M. & BON, C. 1997. Adhesion and activation of human platelets induced by convulxin involve glycoprotein VI and integrin $\alpha 2\beta 1$. *J Biol Chem*, 272, 27035-41.
- JARVIS, G. E., ATKINSON, B. T., SNELL, D. C. & WATSON, S. P. 2002. Distinct roles of GPVI and integrin $\alpha(2)\beta(1)$ in platelet shape change and aggregation induced by different collagens. *Br J Pharmacol*, 137, 107-17.
- JARVIS, G. E., RAYNAL, N., LANGFORD, J. P., ONLEY, D. J., ANDREWS, A., SMETHURST, P. A. & FARNDAL, R. W. 2008. Identification of a major GpVI-binding locus in human type III collagen. *Blood*, 111, 4986-4996.
- JIANG, P., LOYAU, S., TCHITCHINADZE, M., ROPERS, J., JONDEAU, G. & JANDROT-PERRUS, M. 2015. Inhibition of Glycoprotein VI Clustering by Collagen as a Mechanism of Inhibiting Collagen-Induced Platelet Responses: The Example of Losartan. *PLoS one*, 10, e0128744-e0128744.
- JIN, J., DANIEL, J. L. & KUNAPULI, S. P. 1998. Molecular basis for ADP-induced platelet activation. II. The P2Y₁ receptor mediates ADP-induced intracellular calcium mobilization and shape change in platelets. *J Biol Chem*, 273, 2030-4.
- JIN, J. & KUNAPULI, S. P. 1998. Coactivation of two different G protein-coupled receptors is essential for ADP-induced platelet aggregation. *Proc Natl Acad Sci U S A*, 95, 8070-4.
- JIN, J., QUINTON, T. M., ZHANG, J., RITTENHOUSE, S. E. & KUNAPULI, S. P. 2002. Adenosine diphosphate (ADP)-induced thromboxane A₂ generation in human platelets requires coordinated signaling through integrin $\alpha IIb\beta 3$ and ADP receptors. *Blood*, 99, 193-198.
- JINEK, M., CHYLINSKI, K., FONFARA, I., HAUER, M., DOUDNA, J. A. & CHARPENTIER, E. 2012. A Programmable Dual-RNA-Guided DNA Endonuclease in Adaptive Bacterial Immunity. *Science*, 337, 816-821.
- JING, Y., DAI, X., YANG, L., KANG, D., JIANG, P., LI, N., CHENG, J., LI, J., MILLER, H., REN, B., GONG, Q., YIN, W., LIU, Z., MATTILA, P. K., NING, Q., SUN, J., YU, B. & LIU, C. 2020. STING couples with PI3K to regulate actin reorganization during BCR activation. *Science advances*, 6, eaax9455-eaax9455.
- JOHANNES, F.-J., HAUSSER, A., STORZ, P., TRUCKENMÜLLER, L., LINK, G., KAWAKAMI, T. & PFIZENMAIER, K. 1999. Bruton's tyrosine kinase (Btk) associates with protein kinase C μ . *FEBS Letters*, 461, 68-72.
- JOHNSON, A. R., KOHLI, P. B., KATEWA, A., GOGOL, E., BELMONT, L. D., CHOY, R., PENUEL, E., BURTON, L., EIGENBROT, C., YU, C., ORTWINE, D. F., BOWMAN, K., FRANKE, Y., TAM, C., ESTEVEZ, A., MORTARA, K., WU, J., LI, H., LIN, M., BERGERON, P., CRAWFORD, J. J. & YOUNG, W. B. 2016. Battling Btk Mutants With Noncovalent Inhibitors That Overcome Cys481 and Thr474 Mutations. *ACS Chem Biol*, 11, 2897-2907.
- JONES, A., BRADLEY, L., ALTERMAN, L., TARLOW, M., THOMPSON, R., KINNON, C. & MORGAN, G. 1996. X linked agammaglobulinaemia with a 'leaky' phenotype. *Arch Dis Child*, 74, 548-9.
- JOO, S.-J., CHOI, J.-H., KIM, S.-Y., KIM, K.-S., KIM, Y. R. & KANG, S. H. 2015. An Assay of Measuring Platelet Reactivity Using Monoclonal Antibody against Activated Platelet Glycoprotein IIb/IIIa in Patients Taking Clopidogrel. *Korean circulation journal*, 45, 378-385.
- JOSEPH, R. E. & ANDREOTTI, A. H. 2009. Conformational snapshots of Tec kinases during signaling. *Immunological reviews*, 228, 74-92.
- JOSEPH, R. E., WALES, T. E., FULTON, D. B., ENGEN, J. R. & ANDREOTTI, A. H. 2017. Achieving a Graded Immune Response: BTK Adopts a Range of

- Active/Inactive Conformations Dictated by Multiple Interdomain Contacts. *Structure*, 25, 1481-1494.e4.
- JUDD, B. A., MYUNG, P. S., OBERGFELL, A., MYERS, E. E., CHENG, A. M., WATSON, S. P., PEAR, W. S., ALLMAN, D., SHATTIL, S. J. & KORETZKY, G. A. 2002. Differential requirement for LAT and SLP-76 in GPVI versus T cell receptor signaling. *J Exp Med*, 195, 705-17.
- JUNG, S. M., MOROI, M., SOEJIMA, K., NAKAGAKI, T., MIURA, Y., BERNDT, M. C., GARDINER, E. E., HOWES, J.-M., PUGH, N., BIHAN, D., WATSON, S. P. & FARNDAL, R. W. 2012. Constitutive Dimerization of Glycoprotein VI (GPVI) in Resting Platelets Is Essential for Binding to Collagen and Activation in Flowing Blood. *The Journal of Biological Chemistry*, 287, 30000-30013.
- JUNG, S. M., TSUJI, K. & MOROI, M. 2009. Glycoprotein (GP) VI dimer as a major collagen-binding site of native platelets: direct evidence obtained with dimeric GPVI-specific Fabs. *J Thromb Haemost*, 7, 1347-55.
- KAIBUCHI, K., TAKAI, Y., SAWAMURA, M., HOSHIJIMA, M., FUJIKURA, T. & NISHIZUKA, Y. 1983. Synergistic functions of protein phosphorylation and calcium mobilization in platelet activation. *J Biol Chem*, 258, 6701-4.
- KAMBE, T. 2014. Chapter Five - Methods to Evaluate Zinc Transport into and out of the Secretory and Endosomal-Lysosomal Compartments in DT40 Cells. In: CONN, P. M. (ed.) *Methods in Enzymology*. Academic Press.
- KAMEL, S., HORTON, L., YSEBAERT, L., LEVADE, M., BURBURY, K., TAN, S., COLE-SINCLAIR, M., REYNOLDS, J., FILSHIE, R., SCHISCHKA, S., KHOT, A., SANDHU, S., KEATING, M. J., NANDURKAR, H. & TAM, C. S. 2015. Ibrutinib inhibits collagen-mediated but not ADP-mediated platelet aggregation. *Leukemia*, 29, 783-7.
- KANE, L. P. & WATKINS, S. C. 2005. Dynamic regulation of Tec kinase localization in membrane-proximal vesicles of a T cell clone revealed by total internal reflection fluorescence and confocal microscopy. *J Biol Chem*, 280, 21949-54.
- KANG, S. W., WAHL, M. I., CHU, J., KITAURA, J., KAWAKAMI, Y., KATO, R. M., TABUCHI, R., TARAKHOVSKY, A., KAWAKAMI, T., TURCK, C. W., WITTE, O. N. & RAWLINGS, D. J. 2001. PKC β modulates antigen receptor signaling via regulation of Btk membrane localization. *The EMBO Journal*, 20, 5692-5702.
- KARDEBY, C., FÄLKER, K., HAINING, E. J., CRIEL, M., LINDKVIST, M., BARROSO, R., PÅHLSSON, P., LJUNGBERG, L. U., TENGDÉLIUS, M., RAINGER, G. E., WATSON, S., EBLE, J. A., HOYLAERTS, M. F., EMSLEY, J., KONRADSSON, P., WATSON, S. P., SUN, Y. & GRENEGÅRD, M. 2019. Synthetic glycopolymers and natural fucoidans cause human platelet aggregation via PEAR1 and GPIb α . *Blood advances*, 3, 275-287.
- KATO, K., KANAJI, T., RUSSELL, S., KUNICKI, T. J., FURIHATA, K., KANAJI, S., MARCHESE, P., REININGER, A., RUGGERI, Z. M. & WARE, J. 2003. The contribution of glycoprotein VI to stable platelet adhesion and thrombus formation illustrated by targeted gene deletion. *Blood*, 102, 1701-1707.
- KATO, Y., KANEKO, M. K., KUNITA, A., ITO, H., KAMEYAMA, A., OGASAWARA, S., MATSUURA, N., HASEGAWA, Y., SUZUKI-INOUE, K., INOUE, O., OZAKI, Y. & NARIMATSU, H. 2008. Molecular analysis of the pathophysiological binding of the platelet aggregation-inducing factor podoplanin to the C-type lectin-like receptor CLEC-2. *Cancer Sci*, 99, 54-61.
- KAZIANKA, L., DRUCKER, C., SKRABS, C., THOMAS, W., MELCHARDT, T., STRUVE, S., BERGMANN, M., STABER, P. B., PORPACZY, E., EINBERGER, C., HEINZ, M., HAUSWIRTH, A., RADERER, M., PABINGER, I., THALHAMMER, R., EGGLE, A., WENDTNER, C. M., FOLLOWS, G., HOERMANN, G., QUEHENBERGER, P., JILMA, B. & JAEGER, U. 2017. Ristocetin-induced platelet aggregation for monitoring of bleeding tendency in CLL treated with ibrutinib. *Leukemia*, 31, 1117-1122.

- KEANE, C., TILLEY, D., CUNNINGHAM, A., SMOLENSKI, A., KADIOGLU, A., COX, D., JENKINSON, H. F. & KERRIGAN, S. W. 2010. Invasive Streptococcus pneumoniae trigger platelet activation via Toll-like receptor 2. *J Thromb Haemost*, 8, 2757-65.
- KEE, M. F., MYERS, D. R., SAKURAI, Y., LAM, W. A. & QIU, Y. 2015. Platelet Mechanosensing of Collagen Matrices. *PLOS ONE*, 10, e0126624.
- KERRIGAN, A. M., DENNEHY, K. M., MOURÃO-SÁ, D., FARO-TRINDADE, I., WILLMENT, J. A., TAYLOR, P. R., EBLE, J. A., SOUSA, C. R. E. & BROWN, G. D. 2009. CLEC-2 is a phagocytic activation receptor expressed on murine peripheral blood neutrophils. *Journal of immunology (Baltimore, Md. : 1950)*, 182, 4150-4157.
- KHAN, A. O., SIMMS, V. A., PIKE, J. A., THOMAS, S. G. & MORGAN, N. V. 2017. CRISPR-Cas9 Mediated Labelling Allows for Single Molecule Imaging and Resolution. *Scientific reports*, 7, 8450-8450.
- KIM, E., YANG, K. S., KOHLER, R. H., DUBACH, J. M., MIKULA, H. & WEISSLEDER, R. 2015. Optimized Near-IR Fluorescent Agents for in Vivo Imaging of Btk Expression. *Bioconjug Chem*, 26, 1513-8.
- KIM, S., CARRILLO, M., KULKARNI, V. & JAGADEESWARAN, P. 2009a. Evolution of primary hemostasis in early vertebrates. *PLoS One*, 4, e8403.
- KIM, S., MANGIN, P., DANGELMAIER, C., LILLIAN, R., JACKSON, S. P., DANIEL, J. L. & KUNAPULI, S. P. 2009b. Role of phosphoinositide 3-kinase beta in glycoprotein VI-mediated Akt activation in platelets. *The Journal of biological chemistry*, 284, 33763-33772.
- KIM, Y. J., SEKIYA, F., POULIN, B., BAE, Y. S. & RHEE, S. G. 2004. Mechanism of B-cell receptor-induced phosphorylation and activation of phospholipase C-gamma2. *Mol Cell Biol*, 24, 9986-99.
- KINNON, C., CORY, G. O., MACCARTHY-MORROGH, L., BANIN, S., GOUT, I., LOVERING, R. C. & BRICKELL, P. M. 1997. The identification of Bruton's tyrosine kinase and Wiskott-Aldrich syndrome protein associated proteins and signalling pathways. *Biochem Soc Trans*, 25, 648-50.
- KISUCKA, J., BUTTERFIELD, C. E., DUDA, D. G., EICHENBERGER, S. C., SAFFARIPOUR, S., WARE, J., RUGGERI, Z. M., JAIN, R. K., FOLKMAN, J. & WAGNER, D. D. 2006. Platelets and platelet adhesion support angiogenesis while preventing excessive hemorrhage. *Proc Natl Acad Sci U S A*, 103, 855-60.
- KITCHENS, C. S. & WEISS, L. 1975. Ultrastructural changes of endothelium associated with thrombocytopenia. *Blood*, 46, 567-78.
- KNIGHT, S. C., XIE, L., DENG, W., GUGLIELMI, B., WITKOWSKY, L. B., BOSANAC, L., ZHANG, E. T., EL BEHEIRY, M., MASSON, J. B., DAHAN, M., LIU, Z., DOUDNA, J. A. & TJIAN, R. 2015. Dynamics of CRISPR-Cas9 genome interrogation in living cells. *Science*, 350, 823-6.
- KOEDAM, J. A., CRAMER, E. M., BRIEND, E., FURIE, B., FURIE, B. C. & WAGNER, D. D. 1992. P-selectin, a granule membrane protein of platelets and endothelial cells, follows the regulated secretory pathway in AtT-20 cells. *The Journal of cell biology*, 116, 617-625.
- KOESSLER, J., HERMANN, S., WEBER, K., KOESSLER, A., KUHN, S., BOECK, M. & KOB SAR, A. 2016. Role of Purinergic Receptor Expression and Function for Reduced Responsiveness to Adenosine Diphosphate in Washed Human Platelets. *PLoS ONE*, 11, e0147370.
- KOFFMAN, B., MATO, A., BYRD, J. C., DANILOV, A., HEDRICK, B., UJJANI, C., ROEKER, L., STEPHENS, D. M., DAVIDS, M. S., PAGEL, J. M. & SHADMAN, M. 2020. Management of CLL patients early in the COVID-19 pandemic: An international survey of CLL experts. *American journal of hematology*, 95, E199-E203.

- KRUPA, A., FOL, M., RAHMAN, M., STOKES, K. Y., FLORENCE, J. M., LESKOV, I. L., KHORETONENKO, M. V., MATTHAY, M. A., LIU, K. D., CALFEE, C. S., TVINNEREIM, A., ROSENFELD, G. R. & KURDOWSKA, A. K. 2014. Silencing Bruton's tyrosine kinase in alveolar neutrophils protects mice from LPS/immune complex-induced acute lung injury. *American journal of physiology. Lung cellular and molecular physiology*, 307, L435-L448.
- KRUPA, A., FUDALA, R., FLORENCE, J. M., TUCKER, T., ALLEN, T. C., STANDIFORD, T. J., LUCHOWSKI, R., FOL, M., RAHMAN, M., GRYCZYNSKI, Z., GRYCZYNSKI, I. & KURDOWSKA, A. K. 2013. Bruton's tyrosine kinase mediates FcγRIIa/Toll-like receptor-4 receptor crosstalk in human neutrophils. *American journal of respiratory cell and molecular biology*, 48, 240-249.
- KUDALKAR, E. M., DAVIS, T. N. & ASBURY, C. L. 2016. Single-Molecule Total Internal Reflection Fluorescence Microscopy. *Cold Spring Harbor protocols*, 2016, pdb.top077800-pdb.top077800.
- KUNITA, A., KASHIMA, T. G., MORISHITA, Y., FUKAYAMA, M., KATO, Y., TSURUO, T. & FUJITA, N. 2007. The Platelet Aggregation-Inducing Factor Aggrus/Podoplanin Promotes Pulmonary Metastasis. *The American Journal of Pathology*, 170, 1337-1347.
- KUROSAKI, T., TAKATA, M., YAMANASHI, Y., INAZU, T., TANIGUCHI, T., YAMAMOTO, T. & YAMAMURA, H. 1994. Syk activation by the Src-family tyrosine kinase in the B cell receptor signaling. *J Exp Med*, 179, 1725-9.
- LAEMMLI, U. K. 1970. Cleavage of Structural Proteins during the Assembly of the Head of Bacteriophage T4. *Nature*, 227, 680-685.
- LAFFARGUE, M., RAGAB-THOMAS, J. M., RAGAB, A., TUECH, J., MISSY, K., MONNEREAU, L., BLANK, U., PLANTAVID, M., PAYRASTRE, B., RAYNAL, P. & CHAP, H. 1999. Phosphoinositide 3-kinase and integrin signalling are involved in activation of Bruton tyrosine kinase in thrombin-stimulated platelets. *FEBS Lett*, 443, 66-70.
- LAGRUE, A. H., FRANCISCHETTI, I. M., GUIMARÃES, J. A. & JANDROT-PERRUS, M. 1999. Phosphatidylinositol 3'-kinase and tyrosine-phosphatase activation positively modulate Convulxin-induced platelet activation. Comparison with collagen. *FEBS Lett*, 448, 95-100.
- LAIRD, P. W., ZIJDERVELD, A., LINDERS, K., RUDNICKI, M. A., JAENISCH, R. & BERNS, A. 1991. Simplified mammalian DNA isolation procedure. *Nucleic Acids Research*, 19, 4293-4293.
- LAMPSON, B. L. & BROWN, J. R. 2018. Are BTK and PLCG2 mutations necessary and sufficient for ibrutinib resistance in chronic lymphocytic leukemia? *Expert review of hematology*, 11, 185-194.
- LANG, T. & RIZZOLI, S. O. 2010. Membrane Protein Clusters at Nanoscale Resolution: More Than Pretty Pictures. *Physiology*, 25, 116-124.
- LAX, S., RAYES, J., WICHAIYO, S., HAINING, E. J., LOWE, K., GRYGIELSKA, B., LALOO, R., FLODBY, P., BOROK, Z., CRANDALL, E. D., THICKETT, D. R. & WATSON, S. P. 2017. Platelet CLEC-2 protects against lung injury via effects of its ligand podoplanin on inflammatory alveolar macrophages in the mouse. *Am J Physiol Lung Cell Mol Physiol*, 313, L1016-L1029.
- LEE, R. H., PIATT, R., CONLEY, P. B. & BERGMEIER, W. 2017. Effects of ibrutinib treatment on murine platelet function during inflammation and in primary hemostasis. *Haematologica*, 102, e89-e92.
- LEITGES, M., SCHMEDT, C., GUINAMARD, R., DAVOUST, J., SCHAAL, S., STABEL, S. & TARAKHOVSKY, A. 1996. Immunodeficiency in protein kinase cβ-deficient mice. *Science*, 273, 788-91.
- LETERRIER, C., POTIER, J., CAILLOL, G., DEBARNOT, C., RUEDA BORONI, F. & DARGENT, B. 2015. Nanoscale Architecture of the Axon Initial Segment Reveals an Organized and Robust Scaffold. *Cell Reports*, 13, 2781-2793.

- LETUNIC, I., DOERKS, T. & BORK, P. 2015. SMART: recent updates, new developments and status in 2015. *Nucleic Acids Res*, 43, D257-60.
- LEVADE, M., DAVID, E., GARCIA, C., LAURENT, P. A., CADOT, S., MICHALLET, A. S., BORDET, J. C., TAM, C., SIE, P., YSEBAERT, L. & PAYRASTRE, B. 2014. Ibrutinib treatment affects collagen and von Willebrand factor-dependent platelet functions. *Blood*, 124, 3991-5.
- LI, T., TSUKADA, S., SATTERTHWAITTE, A., HAVLIK, M. H., PARK, H., TAKATSU, K. & WITTE, O. N. 1995. Activation of Bruton's tyrosine kinase (BTK) by a point mutation in its pleckstrin homology (PH) domain. *Immunity*, 2, 451-60.
- LI, Z., WAHL, M. I., EGUINO, A., STEPHENS, L. R., HAWKINS, P. T. & WITTE, O. N. 1997. Phosphatidylinositol 3-kinase-gamma activates Bruton's tyrosine kinase in concert with Src family kinases. *Proc Natl Acad Sci U S A*, 94, 13820-5.
- LIAO, F., SHIN, H. S. & RHEE, S. G. 1993. In vitro tyrosine phosphorylation of PLC-gamma 1 and PLC-gamma 2 by src-family protein tyrosine kinases. *Biochem Biophys Res Commun*, 191, 1028-33.
- LICLICAN, A., SERAFINI, L., XING, W., CZERWIENIEC, G., STEINER, B., WANG, T., BRENDZA, K. M., LUTZ, J. D., KEEGAN, K. S., RAY, A. S., SCHULTZ, B. E., SAKOWICZ, R. & FENG, J. Y. 2020. Biochemical characterization of tirabrutinib and other irreversible inhibitors of Bruton's tyrosine kinase reveals differences in on - and off - target inhibition. *Biochim Biophys Acta Gen Subj*, 1864, 129531.
- LIER, M., LEE, F., FARNDALE, R., GORTER, G., VERHOEF, S., OHNO-IWASHITA, Y., AKKERMAN, J. W. & HEIJNEN, H. 2005. Adhesive surface determines raft composition in platelets adhered under flow. *Journal of thrombosis and haemostasis : JTH*, 3, 2514-25.
- LILLEMEIER, B. F., MÖRTELMAIER, M. A., FORSTNER, M. B., HUPPA, J. B., GROVES, J. T. & DAVIS, M. M. 2010. TCR and Lat are expressed on separate protein islands on T cell membranes and concatenate during activation. *Nat Immunol*, 11, 90-6.
- LIMA, A. M., WEGNER, S. V., MARTINS CAVACO, A. C., ESTEVÃO-COSTA, M. I., SANZ-SOLER, R., NILAND, S., NOSOV, G., KLINGAUF, J., SPATZ, J. P. & EBLE, J. A. 2018. The spatial molecular pattern of integrin recognition sites and their immobilization to colloidal nanobeads determine $\alpha 2\beta 1$ integrin-dependent platelet activation. *Biomaterials*, 167, 107-120.
- LIN, A. Y., CUTTICA, M. J., ISON, M. G. & GORDON, L. I. 2020. Ibrutinib for chronic lymphocytic leukemia in the setting of respiratory failure from severe COVID-19 infection: Case report and literature review. *EJHaem*.
- LINO, C. A., HARPER, J. C., CARNEY, J. P. & TIMLIN, J. A. 2018. Delivering CRISPR: a review of the challenges and approaches. *Drug delivery*, 25, 1234-1257.
- LIPSKY, A. H., FAROOQUI, M. Z. H., TIAN, X., MARTYR, S., CULLINANE, A. M., NGHIEM, K., SUN, C., VALDEZ, J., NIEMANN, C. U., HERMAN, S. E. M., SABA, N., SOTO, S., MARTI, G., UZEL, G., HOLLAND, S. M., LOZIER, J. N. & WIESTNER, A. 2015. Incidence and risk factors of bleeding-related adverse events in patients with chronic lymphocytic leukemia treated with ibrutinib. *Haematologica*, 100, 1571-1578.
- LIU, C., MILLER, H., HUI, K. L., GROOMAN, B., BOLLAND, S., UPADHYAYA, A. & SONG, W. 2011. A balance of Bruton's tyrosine kinase and SHIP activation regulates B cell receptor cluster formation by controlling actin remodeling. *J Immunol*, 187, 230-9.
- LIU, J., FITZGERALD, M. E., BERNDT, M. C., JACKSON, C. W. & GARTNER, T. K. 2006. Bruton tyrosine kinase is essential for botrocetin/VWF-induced signaling and GPIIb-dependent thrombus formation in vivo. *Blood*, 108, 2596-2603.

- LIU, M., REHMAN, S., TANG, X., GU, K., FAN, Q., CHEN, D. & MA, W. 2018. Methodologies for Improving HDR Efficiency. *Front Genet*, 9, 691.
- LIU, T.-M., WOYACH, J. A., ZHONG, Y., LOZANSKI, A., LOZANSKI, G., DONG, S., STRATTAN, E., LEHMAN, A., ZHANG, X., JONES, J. A., FLYNN, J., ANDRITSOS, L. A., MADDOCKS, K., JAGLOWSKI, S. M., BLUM, K. A., BYRD, J. C., DUBOVSKY, J. A. & JOHNSON, A. J. 2015. Hypermorphic mutation of phospholipase C, $\gamma 2$ acquired in ibrutinib-resistant CLL confers BTK independency upon B-cell receptor activation. *Blood*, 126, 61-68.
- LIU, W., WANG, H. & XU, C. 2016. Antigen Receptor Nanoclusters: Small Units with Big Functions. *Trends in Immunology*, 37, 680-689.
- LO, P. H., HUANG, Y. F., CHANG, C. C., YEH, C. C., CHANG, C. Y., CHERNG, Y. G., CHEN, T. L. & LIAO, C. C. 2016. Risk and mortality of gastrointestinal hemorrhage in patients with thrombocytopenia: Two nationwide retrospective cohort studies. *Eur J Intern Med*, 27, 86-90.
- LOCKE, D., CHEN, H., LIU, Y., LIU, C. & KAHN, M. L. 2002. Lipid rafts orchestrate signaling by the platelet receptor glycoprotein VI. *J Biol Chem*, 277, 18801-9.
- LOCKYER, S., OKUYAMA, K., BEGUM, S., LE, S., SUN, B., WATANABE, T., MATSUMOTO, Y., YOSHITAKE, M., KAMBAYASHI, J. & TANDON, N. N. 2006. GPVI-deficient mice lack collagen responses and are protected against experimentally induced pulmonary thromboembolism. *Thrombosis Research*, 118, 371-380.
- LORENZ, V., STEGNER, D., STRITT, S., VÖGTLE, T., KIEFER, F., WITKE, W., SCHYMEINSKY, J., WATSON, S. P., WALZOG, B. & NIESWANDT, B. 2015. Targeted downregulation of platelet CLEC-2 occurs through Syk-independent internalization. *Blood*, 125, 4069-4077.
- LUKEŠ, T., GLATZOVÁ, D., KVÍČALOVÁ, Z., LEVET, F., BENDA, A., LETSCHERT, S., SAUER, M., BRDIČKA, T., LASSER, T. & CEBECAUER, M. 2017. Quantifying protein densities on cell membranes using super-resolution optical fluctuation imaging. *Nature Communications*, 8, 1731.
- LUO, T., MITRA, S. & MCBRIDE, J. 2018. Ehrlichia chaffeensis TRP75 Interacts with Host Cell Targets Involved in Homeostasis, Cytoskeleton Organization, and Apoptosis Regulation To Promote Infection. *mSphere*, 3, e00147-18.
- MA, Y. Q., QIN, J. & PLOW, E. F. 2007. Platelet integrin $\alpha(\text{IIb})\beta(3)$: activation mechanisms. *J Thromb Haemost*, 5, 1345-52.
- MAHAJAN, S., FARGNOLI, J., BURKHARDT, A. L., KUT, S. A., SAOUAF, S. J. & BOLEN, J. B. 1995. Src family protein tyrosine kinases induce autoactivation of Bruton's tyrosine kinase. *Mol Cell Biol*, 15, 5304-11.
- MALKUSCH, S., ENDESFELDER, U., MONDRY, J., GELLERI, M., VERVEER, P. J. & HEILEMANN, M. 2012. Coordinate-based colocalization analysis of single-molecule localization microscopy data. *Histochem Cell Biol*, 137, 1-10.
- MALKUSCH, S. & HEILEMANN, M. 2016. Extracting quantitative information from single-molecule super-resolution imaging data with LAMA - LocAlization Microscopy Analyzer. *Sci Rep*, 6, 34486.
- MAMMADOVA-BACH, E., GIL-PULIDO, J., SARUKHANYAN, E., BURKARD, P., SHITYAKOV, S., SCHONHART, C., STEGNER, D., REMER, K., NURDEN, P., NURDEN, A. T., DANDEKAR, T., NEHEZ, L., DANK, M., BRAUN, A., MEZZANO, D., ABRAMS, S. I. & NIESWANDT, B. 2020. Platelet glycoprotein VI promotes metastasis through interaction with cancer cell-derived galectin-3. *Blood*, 135, 1146-1160.
- MAMMADOVA-BACH, E., OLLIVIER, V., LOYAU, S., SCHAFF, M., DUMONT, B., FAVIER, R., FREYBURGER, G., LATGER-CANNARD, V., NIESWANDT, B., GACHET, C., MANGIN, P. H. & JANDROT-PERRUS, M. 2015. Platelet glycoprotein VI binds to polymerized fibrin and promotes thrombin generation. *Blood*, 126, 683-91.

- MANGIN, P. H., ONSELAER, M. B., RECEVEUR, N., LE LAY, N., HARDY, A. T., WILSON, C., SANCHEZ, X., LOYAU, S., DUPUIS, A., BABAR, A. K., MILLER, J. L., PHILIPPOU, H., HUGHES, C. E., HERR, A. B., ARIENS, R. A., MEZZANO, D., JANDROT-PERRUS, M., GACHET, C. & WATSON, S. P. 2018. Immobilized fibrinogen activates human platelets through glycoprotein VI. *Haematologica*, 103, 898-907.
- MANNE, B. K., BADOLIA, R., DANGELMAIER, C., EBLE, J. A., ELLMEIER, W., KAHN, M. & KUNAPULI, S. P. 2015a. Distinct Pathways Regulate Syk Protein Activation Downstream of Immune Tyrosine Activation Motif (ITAM) and hemITAM Receptors in Platelets. *The Journal of Biological Chemistry*, 290, 11557-11568.
- MANNE, B. K., BADOLIA, R., DANGELMAIER, C. A. & KUNAPULI, S. P. 2015b. C-type lectin like-receptor 2 (CLEC-2) signals independently of lipid raft microdomains in platelets. *Biochemical pharmacology*, 93, 163-170.
- MANNE, B. K., DENORME, F., MIDDLETON, E. A., PORTIER, I., ROWLEY, J. W., STUBBEN, C., PETREY, A. C., TOLLEY, N. D., GUO, L., CODY, M., WEYRICH, A. S., YOST, C. C., RONDINA, M. T. & CAMPBELL, R. A. 2020. Platelet gene expression and function in patients with COVID-19. *Blood*, 136, 1317-1329.
- MANNE, B. K., GETZ, T. M., HUGHES, C. E., ALSHEHRI, O., DANGELMAIER, C., NAIK, U. P., WATSON, S. P. & KUNAPULI, S. P. 2013. Fucoidan is a novel platelet agonist for the C-type lectin-like receptor 2 (CLEC-2). *The Journal of biological chemistry*, 288, 7717-7726.
- MAO, C., ZHOU, M. & UCKUN, F. M. 2001. Crystal Structure of Bruton's Tyrosine Kinase Domain Suggests a Novel Pathway for Activation and Provides Insights into the Molecular Basis of X-linked Agammaglobulinemia. *Journal of Biological Chemistry*, 276, 41435-41443.
- MAO, Z., BOZZELLA, M., SELUANOV, A. & GORBUNOVA, V. 2008. DNA repair by nonhomologous end joining and homologous recombination during cell cycle in human cells. *Cell cycle (Georgetown, Tex.)*, 7, 2902-2906.
- MARTYANOV, A. A., BALABIN, F. A., DUNSTER, J. L., PANTELEEV, M. A., GIBBINS, J. M. & SVESHNIKOVA, A. N. 2020. Control of Platelet CLEC-2-Mediated Activation by Receptor Clustering and Tyrosine Kinase Signaling. *Biophysical Journal*, 118, 2641-2655.
- MASSBERG, S., BRAND, K., GRUNER, S., PAGE, S., MULLER, E., MULLER, I., BERGMEIER, W., RICHTER, T., LORENZ, M., KONRAD, I., NIESWANDT, B. & GAWAZ, M. 2002. A critical role of platelet adhesion in the initiation of atherosclerotic lesion formation. *J Exp Med*, 196, 887-96.
- MASSBERG, S., GAWAZ, M., GRÜNER, S., SCHULTE, V., KONRAD, I., ZOHLNHÖFER, D., HEINZMANN, U. & NIESWANDT, B. 2003. A crucial role of glycoprotein VI for platelet recruitment to the injured arterial wall in vivo. *The Journal of experimental medicine*, 197, 41-49.
- MATO, A. R., ROEKER, L. E., LAMANNA, N., ALLAN, J. N., LESLIE, L., PAGEL, J. M., PATEL, K., OSTERBORG, A., WOJENSKI, D., KAMDAR, M., HUNTINGTON, S. F., DAVIDS, M. S., BROWN, J. R., ANTIC, D., JACOBS, R., AHN, I. E., PU, J., ISAAC, K. M., BARR, P. M., UJJANI, C. S., GEYER, M. B., BERMAN, E., ZELENETZ, A. D., MALAKHOV, N., FURMAN, R. R., KOROPSAK, M., BAILEY, N., HANSON, L., PERINI, G. F., MA, S., RYAN, C. E., WIESTNER, A., PORTELL, C. A., SHADMAN, M., CHONG, E. A., BRANDER, D. M., SUNDARAM, S., SEDDON, A. N., SEYMOUR, E., PATEL, M., MARTINEZ-CALLE, N., MUNIR, T., WALEWSKA, R., BROOM, A., WALTER, H., EL-SHARKAWI, D., PARRY, H., WILSON, M. R., PATTEN, P. E. M., HERNÁNDEZ-RIVAS, J.-Á., MIRAS, F., FERNÁNDEZ ESCALADA, N., GHIONE, P., NABHAN, C., LEBOWITZ, S., BHAVSAR, E., LÓPEZ-JIMÉNEZ, J., NAYA, D., GARCIA-MARCO, J. A., SKÅNLAND, S. S., CORDOBA, R. &

- EYRE, T. A. 2020. Outcomes of COVID-19 in patients with CLL: a multicenter international experience. *Blood*, 136, 1134-1143.
- MATTHEYSES, A. L., SIMON, S. M. & RAPPOPORT, J. Z. 2010. Imaging with total internal reflection fluorescence microscopy for the cell biologist. *J Cell Sci*, 123, 3621-8.
- MATTSSON, P. T., LAPPALAINEN, I., BÄCKESJÖ, C.-M., BROCKMANN, E., LAURÉN, S., VIHINEN, M. & SMITH, C. I. E. 2000. Six X-Linked Agammaglobulinemia-Causing Missense Mutations in the Src Homology 2 Domain of Bruton's Tyrosine Kinase: Phosphotyrosine-Binding and Circular Dichroism Analysis. *The Journal of Immunology*, 164, 4170-4177.
- MATUS, V., VALENZUELA, G., SÁEZ, C. G., HIDALGO, P., LAGOS, M., ARANDA, E., PANES, O., PEREIRA, J., PILLOIS, X., NURDEN, A. T. & MEZZANO, D. 2013. An adenine insertion in exon 6 of human GP6 generates a truncated protein associated with a bleeding disorder in four Chilean families. *Journal of Thrombosis and Haemostasis*, 11, 1751-1759.
- MAURI, L., KEREIAKES, D. J., YEH, R. W., DRISCOLL-SHEMPP, P., CUTLIP, D. E., STEG, P. G., NORMAND, S.-L. T., BRAUNWALD, E., WIVIOTT, S. D., COHEN, D. J., HOLMES, D. R., KRUCOFF, M. W., HERMILLER, J., DAUERMAN, H. L., SIMON, D. I., KANDZARI, D. E., GARRATT, K. N., LEE, D. P., POW, T. K., LEE, P. V., RINALDI, M. J., MASSARO, J. M. & ON BEHALF OF THE DUAL ANTIPLATELET THERAPY STUDY, I. 2014. Twelve or 30 Months of Dual Antiplatelet Therapy After Drug-eluting Stents. *The New England journal of medicine*, 371, 2155-2166.
- MAY, F., HAGEDORN, I., PLEINES, I., BENDER, M., VOGTLE, T., EBLE, J., ELVERS, M. & NIESWANDT, B. 2009. CLEC-2 is an essential platelet-activating receptor in hemostasis and thrombosis. *Blood*, 114, 3464-72.
- MAYNARD, D. M., HEIJNEN, H. F., HORNE, M. K., WHITE, J. G. & GAHL, W. A. 2007. Proteomic analysis of platelet alpha-granules using mass spectrometry. *J Thromb Haemost*, 5, 1945-55.
- MAYNARD, D. M., HEIJNEN, H. F. G., GAHL, W. A. & GUNAY-AYGUN, M. 2010. The Alpha Granule Proteome: Novel Proteins in Normal and Ghost Granules in Gray Platelet Syndrome. *Journal of thrombosis and haemostasis : JTH*, 8, 1786-1796.
- MCGUFFIN, L. J., ADIYAMAN, R., MAGHRABI, A. H. A., SHUID, A. N., BRACKENRIDGE, D. A., NEALON, J. O. & PHILOMINA, L. S. 2019. IntFOLD: an integrated web resource for high performance protein structure and function prediction. *Nucleic Acids Research*, 47, W408-W413.
- METCALF, D. J., EDWARDS, R., KUMARSWAMI, N. & KNIGHT, A. E. 2013. Test samples for optimizing STORM super-resolution microscopy. *J Vis Exp*.
- MEYERS, K. M., HOLMSEN, H. & SEACHORD, C. L. 1982. Comparative study of platelet dense granule constituents. *Am J Physiol*, 243, R454-61.
- MIDDENDORP, S., DINGJAN, G. M., MAAS, A., DAHLENBORG, K. & HENDRIKS, R. W. 2003. Function of Bruton's tyrosine kinase during B cell development is partially independent of its catalytic activity. *J Immunol*, 171, 5988-96.
- MING, Z., HU, Y., XIANG, J., POLEWSKI, P., NEWMAN, P. J. & NEWMAN, D. K. 2011. Lyn and PECAM-1 function as interdependent inhibitors of platelet aggregation. *Blood*, 117, 3903-3906.
- MIURA, Y., TAKAHASHI, T., JUNG, S. M. & MOROI, M. 2002. Analysis of the interaction of platelet collagen receptor glycoprotein VI (GPVI) with collagen. A dimeric form of GPVI, but not the monomeric form, shows affinity to fibrous collagen. *J Biol Chem*, 277, 46197-204.
- MODHIRAN, N., WATTERSON, D., BLUMENTHAL, A., BAXTER, A. G., YOUNG, P. R. & STACEY, K. J. 2017. Dengue virus NS1 protein activates immune cells via TLR4 but not TLR2 or TLR6. *Immunol Cell Biol*, 95, 491-495.

- MOHAMED, NORE, CHRISTENSSON & SMITH 1999. Signalling of Bruton's Tyrosine Kinase, Btk. *Scandinavian Journal of Immunology*, 49, 113-118.
- MOHAMED, A. J., VARGAS, L., NORE, B. F., BACKESJO, C. M., CHRISTENSSON, B. & SMITH, C. I. 2000. Nucleocytoplasmic shuttling of Bruton's tyrosine kinase. *J Biol Chem*, 275, 40614-9.
- MONROE, D. M. & HOFFMAN, M. 2006. What does it take to make the perfect clot? *Arterioscler Thromb Vasc Biol*, 26, 41-8.
- MOREAU, T., EVANS, A. L., VASQUEZ, L., TIJSSEN, M. R., YAN, Y., TROTTER, M. W., HOWARD, D., COLZANI, M., ARUMUGAM, M., WU, W. H., DALBY, A., LAMPELA, R., BOUET, G., HOBBS, C. M., PASK, D. C., PAYNE, H., PONOMARYOV, T., BRILL, A., SORANZO, N., OUWEHAND, W. H., PEDERSEN, R. A. & GHEVAERT, C. 2016. Large-scale production of megakaryocytes from human pluripotent stem cells by chemically defined forward programming. *Nature communications*, 7, 11208-11208.
- MORI, J., PEARCE, A. C., SPALTON, J. C., GRYGIELSKA, B., EBLE, J. A., TOMLINSON, M. G., SENIS, Y. A. & WATSON, S. P. 2008. G6b-B Inhibits Constitutive and Agonist-induced Signaling by Glycoprotein VI and CLEC-2. *The Journal of Biological Chemistry*, 283, 35419-35427.
- MORIYA, H. 2015. Quantitative nature of overexpression experiments. *Molecular biology of the cell*, 26, 3932-3939.
- MOROI, M., FARNDAL, R. W. & JUNG, S. M. 2020. Activation-induced changes in platelet surface receptor expression and the contribution of the large-platelet subpopulation to activation. *Research and practice in thrombosis and haemostasis*, 4, 285-297.
- MOROI, M., JUNG, S., SHINMYOZU, K., TOMIYAMA, Y., ORDINAS, A. & DIAZ-RICART, M. 1996. Analysis of platelet adhesion to a collagen-coated surface under flow conditions: the involvement of glycoprotein VI in the platelet adhesion. *Blood*, 88, 2081-2092.
- MOROI, M., JUNG, S. M., OKUMA, M. & SHINMYOZU, K. 1989. A patient with platelets deficient in glycoprotein VI that lack both collagen-induced aggregation and adhesion. *Journal of Clinical Investigation*, 84, 1440-1445.
- MORROGH, L. M., HINSHELWOOD, S., COSTELLO, P., CORY, G. O. & KINNON, C. 1999. The SH3 domain of Bruton's tyrosine kinase displays altered ligand binding properties when auto-phosphorylated in vitro. *Eur J Immunol*, 29, 2269-79.
- MORTON, L. F., HARGREAVES, P. G., FARNDAL, R. W., YOUNG, R. D. & BARNES, M. J. 1995. Integrin alpha 2 beta 1-independent activation of platelets by simple collagen-like peptides: collagen tertiary (triple-helical) and quaternary (polymeric) structures are sufficient alone for alpha 2 beta 1-independent platelet reactivity. *Biochem J*, 306 (Pt 2), 337-44.
- MYERS, M. P., STOLAROV, J. P., ENG, C., LI, J., WANG, S. I., WIGLER, M. H., PARSONS, R. & TONKS, N. K. 1997. P-TEN, the tumor suppressor from human chromosome 10q23, is a dual-specificity phosphatase. *Proc Natl Acad Sci U S A*, 94, 9052-7.
- NAGAE, M., MORITA-MATSUMOTO, K., KATO, M., KANEKO, MIKA K., KATO, Y. & YAMAGUCHI, Y. 2014. A Platform of C-type Lectin-like Receptor CLEC-2 for Binding O-Glycosylated Podoplanin and Nonglycosylated Rhodocytin. *Structure*, 22, 1711-1721.
- NAVARRO-NÚÑEZ, L., LANGAN, S. A., NASH, G. B. & WATSON, S. P. 2013. The physiological and pathophysiological roles of platelet CLEC-2. *Thromb Haemost*, 109, 991-8.
- NICOLSON, P. L. R., HUGHES, C. E., WATSON, S., NOCK, S. H., HARDY, A. T., WATSON, C. N., MONTAGUE, S. J., MALCOR, J. D., THOMAS, M. R., POLLITT, A. Y., TOMLINSON, M. G., PRATT, G. & WATSON, S. P. 2018.

- Inhibition of Btk by Btk-specific concentrations of ibrutinib and acalabrutinib delays but does not block platelet aggregation to GPVI. *Haematologica*.
- NICOLSON, P. L. R., NOCK, S. H., HINDS, J., GARCIA-QUINTANILLA, L., SMITH, C. W., CAMPOS, J., BRILL, A., PIKE, J. A., KHAN, A. O., POULTER, N. S., KAVANAGH, D. M., WATSON, S., WATSON, C. N., CLIFFORD, H., HUISSOON, A. P., POLLITT, A. Y., EBLE, J. A., PRATT, G., WATSON, S. P. & HUGHES, C. E. 2020. Low dose Btk inhibitors selectively block platelet activation by CLEC-2. *Haematologica*.
- NIESWANDT, B., BERGMEIER, W., SCHULTE, V., RACKEBRANDT, K., GESSNER, J. E. & ZIRNGIBL, H. 2000. Expression and Function of the Mouse Collagen Receptor Glycoprotein VI Is Strictly Dependent on Its Association with the FcR γ Chain. *Journal of Biological Chemistry*, 275, 23998-24002.
- NIESWANDT, B., SCHULTE, V., BERGMEIER, W., MOKHTARI-NEJAD, R., RACKEBRANDT, K., CAZENAVE, J. P., OHLMANN, P., GACHET, C. & ZIRNGIBL, H. 2001. Long-term antithrombotic protection by in vivo depletion of platelet glycoprotein VI in mice. *The Journal of experimental medicine*, 193, 459-469.
- NOTREDAME, C., HIGGINS, D. G. & HERINGA, J. 2000. T-Coffee: A novel method for fast and accurate multiple sequence alignment. *J Mol Biol*, 302, 205-17.
- NYFELER, B., MICHNICK, S. W. & HAURI, H.-P. 2005. Capturing protein interactions in the secretory pathway of living cells. *Proceedings of the National Academy of Sciences of the United States of America*, 102, 6350-6355.
- O'ROURKE, F. A., HALENDA, S. P., ZAVOICO, G. B. & FEINSTEIN, M. B. 1985. Inositol 1,4,5-trisphosphate releases Ca²⁺ from a Ca²⁺-transporting membrane vesicle fraction derived from human platelets. *J Biol Chem*, 260, 956-62.
- O'SHEA, J. C. & TCHENG, J. E. 2002. Eptifibatid: a potent inhibitor of the platelet receptor integrin glycoprotein IIb/IIIa. *Expert Opin Pharmacother*, 3, 1199-210.
- ODA, A., IKEDA, Y., OCHS, H. D., DRUKER, B. J., OZAKI, K., HANDA, M., ARIGA, T., SAKIYAMA, Y., WITTE, O. N. & WAHL, M. I. 2000. Rapid tyrosine phosphorylation and activation of Bruton's tyrosine/Tec kinases in platelets induced by collagen binding or CD32 cross-linking. *Blood*, 95, 1663-1670.
- ODA, A., OCHS, H. D., DRUKER, B. J., OZAKI, K., WATANABE, C., HANDA, M., MIYAKAWA, Y. & IKEDA, Y. 1998. Collagen Induces Tyrosine Phosphorylation of Wiskott-Aldrich Syndrome Protein in Human Platelets. *Blood*, 92, 1852-1858.
- OH, K. & YI, G.-S. 2016. Prediction of scaffold proteins based on protein interaction and domain architectures. *BMC Bioinformatics*, 17, 220.
- OLEJNIK, J., HUME, A. J. & MÜHLBERGER, E. 2018. Toll-like receptor 4 in acute viral infection: Too much of a good thing. *PLoS pathogens*, 14, e1007390-e1007390.
- ONSELAER, M.-B., NAGY, M., PALLINI, C., PIKE, J. A., PERRELLA, G., QUINTANILLA, L. G., EBLE, J. A., POULTER, N. S., HEEMSKERK, J. W. M. & WATSON, S. P. 2020. Comparison of the GPVI inhibitors losartan and honokiol. *Platelets*, 31, 187-197.
- OPAZO, F., LEVY, M., BYROM, M., SCHÄFER, C., GEISLER, C., GROEMER, T. W., ELLINGTON, A. D. & RIZZOLI, S. O. 2012. Aptamers as potential tools for super-resolution microscopy. *Nature Methods*, 9, 938-939.
- ORGEL, J. P. R. O., IRVING, T. C., MILLER, A. & WESS, T. J. 2006. Microfibrillar structure of type I collagen *in situ*. *Proceedings of the National Academy of Sciences*, 103, 9001-9005.
- OVESNÝ, M., KRÍŽEK, P., BORKOVEC, J., ŠVINDRYCH, Z. & HAGEN, G. M. 2014. ThunderSTORM: a comprehensive ImageJ plug-in for PALM and STORM data analysis and super-resolution imaging. *Bioinformatics*, 30, 2389-2390.
- PAGEON, S. V., NICOVICH, P. R., MOLLAZADE, M., TABARIN, T. & GAUS, K. 2016. Clus-DoC: a combined cluster detection and colocalization analysis for single-

- molecule localization microscopy data. *Molecular biology of the cell*, 27, 3627-3636.
- PAL SINGH, S., DAMMEIJER, F. & HENDRIKS, R. W. 2018. Role of Bruton's tyrosine kinase in B cells and malignancies. *Molecular cancer*, 17, 57-57.
- PALACIOS, E. H. & WEISS, A. 2004. Function of the Src-family kinases, Lck and Fyn, in T-cell development and activation. *Oncogene*, 23, 7990-8000.
- PALLINI, C., PIKE, J. A., O'SHEA, C., ANDREWS, R. K., GARDINER, E. E., WATSON, S. P. & POULTER, N. S. 2020. Immobilised collagen prevents shedding and induces sustained GPVI clustering and signalling in platelets. *bioRxiv*, 2020.07.07.192435.
- PAN, Z., SCHEERENS, H., LI, S. J., SCHULTZ, B. E., SPRENGELER, P. A., BURRILL, L. C., MENDONCA, R. V., SWEENEY, M. D., SCOTT, K. C., GROTHAUS, P. G., JEFFERY, D. A., SPOERKE, J. M., HONIGBERG, L. A., YOUNG, P. R., DALRYMPLE, S. A. & PALMER, J. T. 2007. Discovery of selective irreversible inhibitors for Bruton's tyrosine kinase. *ChemMedChem*, 2, 58-61.
- PARGUINA, A. F., ALONSO, J., ROSA, I., VELEZ, P., GONZALEZ-LOPEZ, M. J., GUITIAN, E., EBLE, J. A., LOZA, M. I. & GARCIA, A. 2012. A detailed proteomic analysis of rhodocytin-activated platelets reveals novel clues on the CLEC-2 signalosome: implications for CLEC-2 signaling regulation. *Blood*, 120, e117-26.
- PARK, H., WAHL, M. I., AFAR, D. E., TURCK, C. W., RAWLINGS, D. J., TAM, C., SCHARENBERG, A. M., KINET, J. P. & WITTE, O. N. 1996. Regulation of Btk function by a major autophosphorylation site within the SH3 domain. *Immunity*, 4, 515-25.
- PASQUET, J. M., BOBE, R., GROSS, B., GRATACAP, M. P., TOMLINSON, M. G., PAYRASTRE, B. & WATSON, S. P. 1999a. A collagen-related peptide regulates phospholipase Cgamma2 via phosphatidylinositol 3-kinase in human platelets. *Biochem J*, 342 (Pt 1), 171-7.
- PASQUET, J. M., GROSS, B., QUEK, L., ASAZUMA, N., ZHANG, W., SOMMERS, C. L., SCHWEIGHOFFER, E., TYBULEWICZ, V., JUDD, B., LEE, J. R., KORETZKY, G., LOVE, P. E., SAMELSON, L. E. & WATSON, S. P. 1999b. LAT is required for tyrosine phosphorylation of phospholipase cgamma2 and platelet activation by the collagen receptor GPVI. *Mol Cell Biol*, 19, 8326-34.
- PASQUET, J. M., QUEK, L., STEVENS, C., BOBE, R., HUBER, M., DURONIO, V., KRYSTAL, G. & WATSON, S. P. 2000. Phosphatidylinositol 3,4,5-trisphosphate regulates Ca(2+) entry via btk in platelets and megakaryocytes without increasing phospholipase C activity. *The EMBO journal*, 19, 2793-2802.
- PATEL, A., KOSTYAK, J., DANGELMAIER, C., BADOLIA, R., BHAVANASI, D., ASLAN, J. E., MERALI, S., KIM, S., EBLE, J. A., GOLDFINGER, L. & KUNAPULI, S. 2019. ELMO1 deficiency enhances platelet function. *Blood advances*, 3, 575-587.
- PATEL, H. V., TZENG, S. R., LIAO, C. Y., CHEN, S. H. & CHENG, J. W. 1997. SH3 domain of Bruton's tyrosine kinase can bind to proline-rich peptides of TH domain of the kinase and p120cbl. *Proteins*, 29, 545-52.
- PATEL, V., BALAKRISHNAN, K., BIBIKOVA, E., AYRES, M., KEATING, M. J., WIERDA, W. G. & GANDHI, V. 2016. Comparison of Acalabrutinib, A Selective Bruton Tyrosine Kinase Inhibitor, with Ibrutinib in Chronic Lymphocytic Leukemia Cells. *Clin Cancer Res*.
- PATRA, R., CHANDRA DAS, N. & MUKHERJEE, S. 2020. Targeting human TLRs to combat COVID-19: A solution? *Journal of medical virology*, 10.1002/jmv.26387.
- PAYNE, H., PONOMARYOV, T., WATSON, S. P. & BRILL, A. 2017. Mice with a deficiency in CLEC-2 are protected against deep vein thrombosis. *Blood*, 129, 2013-2020.

- PAYRASTRE, B., MISSY, K., TRUMEL, C., BODIN, S., PLANTAVID, M. & CHAP, H. 2000. The integrin alpha IIb/beta 3 in human platelet signal transduction. *Biochem Pharmacol*, 60, 1069-74.
- PLEINES, I., ELVERS, M., STREHL, A., POZGAJOVA, M., VARGA-SZABO, D., MAY, F., CHROSTEK-GRASHOFF, A., BRAKEBUSCH, C. & NIESWANDT, B. 2009. Rac1 is essential for phospholipase C- γ 2 activation in platelets. *Pflügers Archiv - European Journal of Physiology*, 457, 1173-1185.
- POLLITT, A. Y., GRYGIELSKA, B., LEBLOND, B., DESIRE, L., EBLE, J. A. & WATSON, S. P. 2010. Phosphorylation of CLEC-2 is dependent on lipid rafts, actin polymerization, secondary mediators, and Rac. *Blood*, 115, 2938-46.
- POLLITT, A. Y., POULTER, N. S., GITZ, E., NAVARRO-NUNEZ, L., WANG, Y. J., HUGHES, C. E., THOMAS, S. G., NIESWANDT, B., DOUGLAS, M. R., OWEN, D. M., JACKSON, D. G., DUSTIN, M. L. & WATSON, S. P. 2014. Syk and Src family kinases regulate C-type lectin receptor 2 (CLEC-2)-mediated clustering of podoplanin and platelet adhesion to lymphatic endothelial cells. *J Biol Chem*, 289, 35695-710.
- POOLE, A., GIBBINS, J. M., TURNER, M., VAN VUGT, M. J., VAN DE WINKEL, J. G., SAITO, T., TYBULEWICZ, V. L. & WATSON, S. P. 1997. The Fc receptor gamma-chain and the tyrosine kinase Syk are essential for activation of mouse platelets by collagen. *Embo j*, 16, 2333-41.
- POULTER, N. S., KHAN, A. O., PALLINI, C. & THOMAS, S. G. 2018. Single-Molecule Localization and Structured Illumination Microscopy of Platelet Proteins. In: GIBBINS, J. M. & MAHAUT-SMITH, M. (eds.) *Platelets and Megakaryocytes : Volume 4, Advanced Protocols and Perspectives*. New York, NY: Springer New York.
- POULTER, N. S., POLLITT, A. Y., DAVIES, A., MALINOVA, D., NASH, G. B., HANNON, M. J., PIKRAMENOU, Z., RAPPOPORT, J. Z., HARTWIG, J. H., OWEN, D. M., THRASHER, A. J., WATSON, S. P. & THOMAS, S. G. 2015. Platelet actin nodules are podosome-like structures dependent on Wiskott–Aldrich syndrome protein and ARP2/3 complex. *Nature Communications*, 6, 7254.
- POULTER, N. S., POLLITT, A. Y., OWEN, D. M., GARDINER, E. E., ANDREWS, R. K., SHIMIZU, H., ISHIKAWA, D., BIHAN, D., FARNDAL, R. W., MOROI, M., WATSON, S. P. & JUNG, S. M. 2017. Clustering of GPVI dimers upon adhesion to collagen as a mechanism to regulate GPVI signalling in platelets. *J Thromb Haemost*.
- PROTTY, M. B., WATKINS, N. A., COLOMBO, D., THOMAS, S. G., HEATH, V. L., HERBERT, J. M. J., BICKNELL, R., SENIS, Y. A., ASHMAN, L. K., BERDITCHEVSKI, F., OUWEHAND, W. H., WATSON, S. P. & TOMLINSON, M. G. 2009. Identification of Tspan9 as a novel platelet tetraspanin and the collagen receptor GPVI as a component of tetraspanin microdomains. *The Biochemical journal*, 417, 391-400.
- PULIDO, R. 2018. PTEN Inhibition in Human Disease Therapy. *Molecules (Basel, Switzerland)*, 23, 285.
- QI, Q., SAHU, N. & AUGUST, A. 2006. Tec Kinase Itk Forms Membrane Clusters Specifically in the Vicinity of Recruiting Receptors. *Journal of Biological Chemistry*, 281, 38529-38534.
- QUEK, L. S., BOLEN, J. & WATSON, S. P. 1998. A role for Bruton's tyrosine kinase (Btk) in platelet activation by collagen. *Curr Biol*, 8, 1137-40.
- QUEK, L. S., PASQUET, J. M., HERS, I., CORNALL, R., KNIGHT, G., BARNES, M., HIBBS, M. L., DUNN, A. R., LOWELL, C. A. & WATSON, S. P. 2000. Fyn and Lyn phosphorylate the Fc receptor gamma chain downstream of glycoprotein VI in murine platelets, and Lyn regulates a novel feedback pathway. *Blood*, 96, 4246-53.

- RABES, A., ZIMMERMANN, S., REPPE, K., LANG, R., SEEBERGER, P. H., SUTTORP, N., WITZENRATH, M., LEPENIES, B. & OPITZ, B. 2015. The C-Type Lectin Receptor Mincle Binds to *Streptococcus pneumoniae* but Plays a Limited Role in the Anti-Pneumococcal Innate Immune Response. *PLOS ONE*, 10, e0117022.
- RAN, F. A., HSU, P. D., WRIGHT, J., AGARWALA, V., SCOTT, D. A. & ZHANG, F. 2013. Genome engineering using the CRISPR-Cas9 system. *Nat Protoc*, 8, 2281-2308.
- RAWLINGS, D. J., SCHARENBERG, A. M., PARK, H., WAHL, M. I., LIN, S., KATO, R. M., FLUCKIGER, A.-C., WITTE, O. N. & KINET, J.-P. 1996. Activation of BTK by a Phosphorylation Mechanism Initiated by SRC Family Kinases. *Science*, 271, 822-825.
- RAYES, J., JADOUI, S., LAX, S., GROS, A., WICHAIYO, S., OLLIVIER, V., DENIS, C. V., WARE, J., NIESWANDT, B., JANDROT-PERRUS, M., WATSON, S. P. & HO-TIN-NOÉ, B. 2018. The contribution of platelet glycoprotein receptors to inflammatory bleeding prevention is stimulus and organ dependent. *Haematologica*, 103, e256-e258.
- RAYES, J., LAX, S., WICHAIYO, S., WATSON, S. K., DI, Y., LOMBARD, S., GRYGIELSKA, B., SMITH, S. W., SKORDILIS, K. & WATSON, S. P. 2017. The podoplanin-CLEC-2 axis inhibits inflammation in sepsis. *Nat Commun*, 8, 2239.
- REES, J. S., LILLEY, K. S. & JACKSON, A. P. 2015. The chicken B-cell line DT40 proteome, beadome and interactomes. *Data in Brief*, 3, 29-33.
- RETH, M. 1989. Antigen receptor tail clue. *Nature*, 338, 383-4.
- RICE, P., LONGDEN, I. & BLEASBY, A. 2000. EMBOSS: the European Molecular Biology Open Software Suite. *Trends in genetics : TIG*, 16, 276-277.
- RICHARDSON, C. D., RAY, G. J., DEWITT, M. A., CURIE, G. L. & CORN, J. E. 2016. Enhancing homology-directed genome editing by catalytically active and inactive CRISPR-Cas9 using asymmetric donor DNA. *Nat Biotechnol*, 34, 339-44.
- RIES, J., KAPLAN, C., PLATONOVA, E., EGHLIDI, H. & EWERS, H. 2012. A simple, versatile method for GFP-based super-resolution microscopy via nanobodies. *Nature Methods*, 9, 582-584.
- RIGG, R. A., ASLAN, J. E., HEALY, L. D., WALLISCH, M., THIERHEIMER, M. L. D., LOREN, C. P., PANG, J., HINDS, M. T., GRUBER, A. & MCCARTY, O. J. T. 2016. Oral administration of Bruton's tyrosine kinase inhibitors impairs GPVI-mediated platelet function. *American journal of physiology. Cell physiology*, 310, C373-C380.
- ROBERT, X. & GOUET, P. 2014. Deciphering key features in protein structures with the new ENDscript server. *Nucleic Acids Research*, 42, W320-W324.
- RODRIGUEZ, R., MATSUDA, M., PERISIC, O., BRAVO, J., PAUL, A., JONES, N. P., LIGHT, Y., SWANN, K., WILLIAMS, R. L. & KATAN, M. 2001. Tyrosine residues in phospholipase Cgamma 2 essential for the enzyme function in B-cell signaling. *J Biol Chem*, 276, 47982-92.
- ROHRER, J., PAROLINI, O., BELMONT, J. W., CONLEY, M. E. & PAROLINO, O. 1994. The genomic structure of human BTK, the defective gene in X-linked agammaglobulinemia. *Immunogenetics*, 40, 319-24.
- ROLLI, V., GALLWITZ, M., WOSSNING, T., FLEMMING, A., SCHAMEL, W. W., ZÜRN, C. & RETH, M. 2002. Amplification of B cell antigen receptor signaling by a Syk/ITAM positive feedback loop. *Mol Cell*, 10, 1057-69.
- ROMAN-GARCIA, S., MERINO-CORTES, S. V., GARDETA, S. R., DE BRUIJN, M. J. W., HENDRIKS, R. W. & CARRASCO, Y. R. 2018. Distinct Roles for Bruton's Tyrosine Kinase in B Cell Immune Synapse Formation. *Front Immunol*, 9, 2027.
- ROWLEY, R. B., BURKHARDT, A. L., CHAO, H. G., MATSUEDA, G. R. & BOLEN, J. B. 1995. Syk protein-tyrosine kinase is regulated by tyrosine-phosphorylated Ig

- alpha/Ig beta immunoreceptor tyrosine activation motif binding and autophosphorylation. *J Biol Chem*, 270, 11590-4.
- RUGGERI, M. & RODEGHIERO, F. 2016. Thrombotic risk in patients with immune haemolytic anaemia. *British Journal of Haematology*, 172, 144-146.
- RUST, M. J., BATES, M. & ZHUANG, X. 2006. Sub-diffraction-limit imaging by stochastic optical reconstruction microscopy (STORM). *Nat Methods*, 3, 793-5.
- SAFFRAN, D. C., PAROLINI, O., FITCH-HILGENBERG, M. E., RAWLINGS, D. J., AFAR, D. E., WITTE, O. N. & CONLEY, M. E. 1994. Brief report: a point mutation in the SH2 domain of Bruton's tyrosine kinase in atypical X-linked agammaglobulinemia. *N Engl J Med*, 330, 1488-91.
- SAHARINEN, P., TAKALUOMA, K. & SILVENNOINEN, O. 2000. Regulation of the Jak2 tyrosine kinase by its pseudokinase domain. *Mol Cell Biol*, 20, 3387-95.
- SAITO, K., SCHARENBERG, A. M. & KINET, J. P. 2001. Interaction between the Btk PH domain and phosphatidylinositol-3,4,5-trisphosphate directly regulates Btk. *J Biol Chem*, 276, 16201-6.
- SAITO, K., TOLIAS, K. F., SACI, A., KOON, H. B., HUMPHRIES, L. A., SCHARENBERG, A., RAWLINGS, D. J., KINET, J.-P. & CARPENTER, C. L. 2003. BTK Regulates PtdIns-4,5-P2 Synthesis: Importance for Calcium Signaling and PI3K Activity. *Immunity*, 19, 669-677.
- SALIM, K., BOTTOMLEY, M. J., QUERFURTH, E., ZVELEBIL, M. J., GOUT, I., SCAIFE, R., MARGOLIS, R. L., GIGG, R., SMITH, C. I., DRISCOLL, P. C., WATERFIELD, M. D. & PANAYOTOU, G. 1996. Distinct specificity in the recognition of phosphoinositides by the pleckstrin homology domains of dynamin and Bruton's tyrosine kinase. *Embo j*, 15, 6241-50.
- SAVAGE, B., SIXMA, J. J. & RUGGERI, Z. M. 2002. Functional self-association of von Willebrand factor during platelet adhesion under flow. *Proc Natl Acad Sci U S A*, 99, 425-30.
- SAVI, P., BEAUVERGER, P., LABOURET, C., DELFAUD, M., SALEL, V., KAGHAD, M. & HERBERT, J. M. 1998. Role of P2Y1 purinoceptor in ADP-induced platelet activation. *FEBS Lett*, 422, 291-5.
- SCARFÒ, L., FERRERI, A. J. & GHIA, P. 2016. Chronic lymphocytic leukaemia. *Crit Rev Oncol Hematol*, 104, 169-82.
- SCHARENBERG, A. M., EL-HILLAL, O., FRUMAN, D. A., BEITZ, L. O., LI, Z., LIN, S., GOUT, I., CANTLEY, L. C., RAWLINGS, D. J. & KINET, J. P. 1998. Phosphatidylinositol-3,4,5-trisphosphate (PtdIns-3,4,5-P3)/Tec kinase-dependent calcium signaling pathway: a target for SHIP-mediated inhibitory signals. *The EMBO Journal*, 17, 1961-1972.
- SCHEERS, E., LECLERCQ, L., DE JONG, J., BODE, N., BOCKX, M., LAENEN, A., CUYCKENS, F., SKEE, D., MURPHY, J., SUKBUNTHONG, J. & MANNENS, G. 2015. Absorption, Metabolism, and Excretion of Oral ¹⁴C Radiolabeled Ibrutinib: An Open-Label, Phase I, Single-Dose Study in Healthy Men. *Drug Metabolism and Disposition*, 43, 289-297.
- SCHMAIER, A. A., ZOU, Z., KAZLAUSKAS, A., EMERT-SEDLAK, L., FONG, K. P., NEEVES, K. B., MALONEY, S. F., DIAMOND, S. L., KUNAPULI, S. P., WARE, J., BRASS, L. F., SMITHGALL, T. E., SAKSELA, K. & KAHN, M. L. 2009. Molecular priming of Lyn by GPVI enables an immune receptor to adopt a hemostatic role. *Proc Natl Acad Sci U S A*, 106, 21167-72.
- SCHNEIDER, C. A., RASBAND, W. S. & ELICEIRI, K. W. 2012. NIH Image to ImageJ: 25 years of image analysis. *Nature Methods*, 9, 671-675.
- SCHÜPKE, S., HEIN-ROTHWEILER, R., MAYER, K., JANISCH, M., SIBBING, D., NDREPEPA, G., HILZ, R., LAUGWITZ, K. L., BERNLOCHNER, I., GSCHWENDTNER, S., KUPKA, D., GORI, T., ZEIHNER, A. M., SCHUNKERT, H., MASSBERG, S. & KASTRATI, A. 2019. Revacept, a Novel Inhibitor of Platelet Adhesion, in Patients Undergoing Elective PCI-Design and Rationale of the Randomized ISAR-PLASTER Trial. *Thromb Haemost*, 119, 1539-1545.

- SCHWER, H. D., LECINE, P., TIWARI, S., ITALIANO, J. E., JR., HARTWIG, J. H. & SHIVDASANI, R. A. 2001. A lineage-restricted and divergent beta-tubulin isoform is essential for the biogenesis, structure and function of blood platelets. *Curr Biol*, 11, 579-86.
- SEBZDA, E., HIBBARD, C., SWEENEY, S., ABTAHIAN, F., BEZMAN, N., CLEMENS, G., MALTZMAN, J. S., CHENG, L., LIU, F., TURNER, M., TYBULEWICZ, V., KORETZKY, G. A. & KAHN, M. L. 2006. Syk and Slp-76 Mutant Mice Reveal a Cell-Autonomous Hematopoietic Cell Contribution to Vascular Development. *Developmental Cell*, 11, 349-361.
- SENIS, Y. A., MAZHARIAN, A. & MORI, J. 2014. Src family kinases: at the forefront of platelet activation. *Blood*, 124, 2013-2024.
- SENIS, Y. A., TOMLINSON, M. G., GARCÍA, Á., DUMON, S., HEATH, V. L., HERBERT, J., COBBOLD, S. P., SPALTON, J. C., AYMAN, S., ANTROBUS, R., ZITZMANN, N., BICKNELL, R., FRAMPTON, J., AUTHI, K., MARTIN, A., WAKELAM, M. J. O. & WATSON, S. P. 2007. A comprehensive proteomics and genomics analysis reveals novel transmembrane proteins in human platelets and mouse megakaryocytes including G6b-B, a novel ITIM protein. *Molecular & cellular proteomics : MCP*, 6, 548-564.
- SERIES, J., GARCIA, C., LEVADE, M., VIAUD, J., SIÉ, P., YSEBAERT, L. & PAYRASTRE, B. 2019. Differences and similarities in the effects of ibrutinib and acalabrutinib on platelet functions. *Haematologica*, 104, 2292-2299.
- SEVERIN, S., POLLITT, A. Y., NAVARRO-NUNEZ, L., NASH, C. A., MOURAO-SA, D., EBLE, J. A., SENIS, Y. A. & WATSON, S. P. 2011. Syk-dependent phosphorylation of CLEC-2: a novel mechanism of hem-immunoreceptor tyrosine-based activation motif signaling. *J Biol Chem*, 286, 4107-16.
- SHALEM, O., SANJANA, N. E., HARTENIAN, E., SHI, X., SCOTT, D. A., MIKKELSEN, T. S., HECKL, D., EBERT, B. L., ROOT, D. E., DOENCH, J. G. & ZHANG, F. 2014. Genome-Scale CRISPR-Cas9 Knockout Screening in Human Cells. *Science*, 343, 84-87.
- SHAN, X., CZAR, M. J., BUNNELL, S. C., LIU, P., LIU, Y., SCHWARTZBERG, P. L. & WANGE, R. L. 2000. Deficiency of PTEN in Jurkat T cells causes constitutive localization of Itk to the plasma membrane and hyperresponsiveness to CD3 stimulation. *Mol Cell Biol*, 20, 6945-57.
- SHARMA, S., ORLOWSKI, G. & SONG, W. 2009. Btk regulates B cell receptor-mediated antigen processing and presentation by controlling actin cytoskeleton dynamics in B cells. *Journal of immunology (Baltimore, Md. : 1950)*, 182, 329-339.
- SHATTIL, S. J. & BRASS, L. F. 1987. Induction of the fibrinogen receptor on human platelets by intracellular mediators. *J Biol Chem*, 262, 992-1000.
- SHATZEL, J. J. 2017. Ibrutinib-associated bleeding; pathogenesis, management, and risk reduction strategies. 15, 835-47.
- SHIBAHARA, J., KASHIMA, T., KIKUCHI, Y., KUNITA, A. & FUKAYAMA, M. 2006. Podoplanin is expressed in subsets of tumors of the central nervous system. *Virchows Archiv*, 448, 493-499.
- SHIN, Y. & MORITA, T. 1998. Rhodocytin, a functional novel platelet agonist belonging to the heterodimeric C-type lectin family, induces platelet aggregation independently of glycoprotein Ib. *Biochem Biophys Res Commun*, 245, 741-5.
- SHIRAI, T., INOUE, O., TAMURA, S., TSUKIJI, N., SASAKI, T., ENDO, H., SATOH, K., OSADA, M., SATO-UCHIDA, H., FUJII, H., OZAKI, Y. & SUZUKI-INOUE, K. 2017. C-type lectin-like receptor 2 promotes hematogenous tumor metastasis and prothrombotic state in tumor-bearing mice. *Journal of Thrombosis and Haemostasis*, 15, 513-525.
- SIMON, S. M. 2009. Partial internal reflections on total internal reflection fluorescent microscopy. *Trends in cell biology*, 19, 661-668.

- SMETHURST, P. A., ONLEY, D. J., JARVIS, G. E., O'CONNOR, M. N., KNIGHT, C. G., HERR, A. B., OUWEHAND, W. H. & FARNDAL, R. W. 2007. Structural basis for the platelet-collagen interaction: the smallest motif within collagen that recognizes and activates platelet Glycoprotein VI contains two glycine-proline-hydroxyproline triplets. *J Biol Chem*, 282, 1296-304.
- SMITH, C. I. E., ISLAM, T. C., MATTSSON, P. T., MOHAMED, A. J., NORE, B. F. & VIHINEN, M. 2001. The Tec family of cytoplasmic tyrosine kinases: mammalian Btk, Bmx, Itk, Tec, Txk and homologs in other species. *BioEssays*, 23, 436-446.
- SONG, F. & STIEGER, K. 2017. Optimizing the DNA Donor Template for Homology-Directed Repair of Double-Strand Breaks. *Molecular therapy. Nucleic acids*, 7, 53-60.
- SORIANI, A., MORAN, B., DE VIRGILIO, M., KAWAKAMI, T., ALTMAN, A., LOWELL, C., ETO, K. & SHATTIL, S. J. 2006. A role for PKC θ in outside-in α IIb β 3 signaling. *Journal of Thrombosis and Haemostasis*, 4, 648-655.
- SPALTON, J. C., MORI, J., POLLITT, A. Y., HUGHES, C. E., EBLE, J. A. & WATSON, S. P. 2009. The novel Syk inhibitor R406 reveals mechanistic differences in the initiation of GPVI and CLEC-2 signaling in platelets. *J Thromb Haemost*, 7, 1192-9.
- SPÄTH, P. J., GRANATA, G., LA MARRA, F., KUIJPERS, T. W. & QUINTI, I. 2015. On the dark side of therapies with immunoglobulin concentrates: the adverse events. *Frontiers in immunology*, 6, 11-11.
- SPRINGER, T. A., ZHU, J. & XIAO, T. 2008. Structural basis for distinctive recognition of fibrinogen gammaC peptide by the platelet integrin α IIb β 3. *J Cell Biol*, 182, 791-800.
- STECHA, P., GRAILER, J., CHENG, Z.-J. J., HARTNETT, J., FAN, F. & CONG, M. 2015. Abstract 5439: Development of a robust reporter-based T-cell activation assay for bispecific therapeutic antibodies in immunotherapy. *Cancer Research*, 75, 5439-5439.
- STOTHARD, P. 2000. The sequence manipulation suite: JavaScript programs for analyzing and formatting protein and DNA sequences. *Biotechniques*, 28, 1102, 1104.
- STRIJBIS, K., TAFESSE, F. G., FAIRN, G. D., WITTE, M. D., DOUGAN, S. K., WATSON, N., SPOONER, E., ESTEBAN, A., VYAS, V. K., FINK, G. R., GRINSTEIN, S. & PLOEGH, H. L. 2013. Bruton's Tyrosine Kinase (BTK) and Vav1 Contribute to Dectin1-Dependent Phagocytosis of *Candida albicans* in Macrophages. *PLOS Pathogens*, 9, e1003446.
- SUGIYAMA, T., OKUMA, M., USHIKUBI, F., SENSAKI, S., KANAJI, K. & UCHINO, H. 1987. A novel platelet aggregating factor found in a patient with defective collagen-induced platelet aggregation and autoimmune thrombocytopenia. *Blood*, 69, 1712-20.
- SUZUKI-INOUE, K., FULLER, G. L., GARCIA, A., EBLE, J. A., POHLMANN, S., INOUE, O., GARTNER, T. K., HUGHAN, S. C., PEARCE, A. C., LAING, G. D., THEAKSTON, R. D., SCHWEIGHOFFER, E., ZITZMANN, N., MORITA, T., TYBULEWICZ, V. L., OZAKI, Y. & WATSON, S. P. 2006. A novel Syk-dependent mechanism of platelet activation by the C-type lectin receptor CLEC-2. *Blood*, 107, 542-9.
- SUZUKI-INOUE, K., INOUE, O., DING, G., NISHIMURA, S., HOKAMURA, K., ETO, K., KASHIWAGI, H., TOMIYAMA, Y., YATOMI, Y., UMEMURA, K., SHIN, Y., HIRASHIMA, M. & OZAKI, Y. 2010. Essential in vivo roles of the C-type lectin receptor CLEC-2: embryonic/neonatal lethality of CLEC-2-deficient mice by blood/lymphatic misconnections and impaired thrombus formation of CLEC-2-deficient platelets. *J Biol Chem*, 285, 24494-507.
- SUZUKI-INOUE, K., KATO, Y., INOUE, O., KANEKO, M. K., MISHIMA, K., YATOMI, Y., YAMAZAKI, Y., NARIMATSU, H. & OZAKI, Y. 2007. Involvement of the

- snake toxin receptor CLEC-2, in podoplanin-mediated platelet activation, by cancer cells. *J Biol Chem*, 282, 25993-6001.
- SUZUKI-INOUE, K., OZAKI, Y., KAINOH, M., SHIN, Y., WU, Y., YATOMI, Y., OHMORI, T., TANAKA, T., SATOH, K. & MORITA, T. 2001. Rhodocytin induces platelet aggregation by interacting with glycoprotein Ia/IIa (GPIa/IIa, Integrin alpha 2beta 1). Involvement of GPIa/IIa-associated src and protein tyrosine phosphorylation. *J Biol Chem*, 276, 1643-52.
- SUZUKI-INOUE, K., TULASNE, D., SHEN, Y., BORI-SANZ, T., INOUE, O., JUNG, S. M., MOROI, M., ANDREWS, R. K., BERNDT, M. C. & WATSON, S. P. 2002. Association of Fyn and Lyn with the proline-rich domain of glycoprotein VI regulates intracellular signaling. *J Biol Chem*, 277, 21561-6.
- TAKATA, M., HOMMA, Y. & KUROSAKI, T. 1995. Requirement of phospholipase C-gamma 2 activation in surface immunoglobulin M-induced B cell apoptosis. *J Exp Med*, 182, 907-14.
- TAKATA, M. & KUROSAKI, T. 1996. A role for Bruton's tyrosine kinase in B cell antigen receptor-mediated activation of phospholipase C-gamma 2. *J Exp Med*, 184, 31-40.
- TAKATA, M., SABE, H., HATA, A., INAZU, T., HOMMA, Y., NUKADA, T., YAMAMURA, H. & KUROSAKI, T. 1994. Tyrosine kinases Lyn and Syk regulate B cell receptor-coupled Ca²⁺ mobilization through distinct pathways. *The EMBO journal*, 13, 1341-1349.
- TANAKA, K. A. K., SUZUKI, K. G. N., SHIRAI, Y. M., SHIBUTANI, S. T., MIYAHARA, M. S. H., TSUBOI, H., YAHARA, M., YOSHIMURA, A., MAYOR, S., FUJIWARA, T. K. & KUSUMI, A. 2010. Membrane molecules mobile even after chemical fixation. *Nature Methods*, 7, 865-866.
- THACHIL, J., TANG, N., GANDO, S., FALANGA, A., CATTANEO, M., LEVI, M., CLARK, C. & IBA, T. 2020. ISTH interim guidance on recognition and management of coagulopathy in COVID-19. *J Thromb Haemost*, 18, 1023-1026.
- TOCANTINS, L. M. 1938. The Mammalian Blood Platelet In Health And Disease. *Medicine*, 17, 155.
- TOMLINSON, M. G., CALAMINUS, S. D., BERLANGA, O., AUGER, J. M., BORI-SANZ, T., MEYAARD, L. & WATSON, S. P. 2007. Collagen promotes sustained glycoprotein VI signaling in platelets and cell lines. *J Thromb Haemost*, 5, 2274-83.
- TOMLINSON, M. G., HEATH, V. L., TURCK, C. W., WATSON, S. P. & WEISS, A. 2004a. SHIP family inositol phosphatases interact with and negatively regulate the Tec tyrosine kinase. *J Biol Chem*, 279, 55089-96.
- TOMLINSON, M. G., KANE, L. P., SU, J., KADLECEK, T. A., MOLLENAUER, M. N. & WEISS, A. 2004b. Expression and function of Tec, Itk, and Btk in lymphocytes: evidence for a unique role for Tec. *Mol Cell Biol*, 24, 2455-66.
- TOMLINSON, M. G., KUROSAKI, T., BERSON, A. E., FUJII, G. H., JOHNSTON, J. A. & BOLEN, J. B. 1999. Reconstitution of Btk Signaling by the Atypical Tec Family Tyrosine Kinases Bmx and Txk. *Journal of Biological Chemistry*, 274, 13577-13585.
- TOMLINSON, M. G., WOODS, D. B., MCMAHON, M., WAHL, M. I., WITTE, O. N., KUROSAKI, T., BOLEN, J. B. & JOHNSTON, J. A. 2001. A conditional form of Bruton's tyrosine kinase is sufficient to activate multiple downstream signaling pathways via PLC Gamma 2 in B cells. *BMC Immunol*, 2, 4.
- TOURDOT, B. E., BRENNER, M. K., KEOUGH, K. C., HOLYST, T., NEWMAN, P. J. & NEWMAN, D. K. 2013. Immunoreceptor tyrosine-based inhibitory motif (ITIM)-mediated inhibitory signaling is regulated by sequential phosphorylation mediated by distinct nonreceptor tyrosine kinases: a case study involving PECAM-1. *Biochemistry*, 52, 2597-608.

- TSUKADA, S., SIMON, M. I., WITTE, O. N. & KATZ, A. 1994. Binding of beta gamma subunits of heterotrimeric G proteins to the PH domain of Bruton tyrosine kinase. *Proceedings of the National Academy of Sciences of the United States of America*, 91, 11256-11260.
- TURETSKY, A., KIM, E., KOHLER, R., MILLER, M. & WEISSLEDER, R. 2014. Single cell imaging of Bruton's Tyrosine Kinase using an irreversible inhibitor. *Scientific reports*, 4, 4782.
- TURNER, M., MEE, P. J., COSTELLO, P. S., WILLIAMS, O., PRICE, A. A., DUDDY, L. P., FURLONG, M. T., GEAHLEN, R. L. & TYBULEWICZ, V. L. 1995. Perinatal lethality and blocked B-cell development in mice lacking the tyrosine kinase Syk. *Nature*, 378, 298-302.
- UNDERHILL, D. M. & GOODRIDGE, H. S. 2007. The many faces of ITAMs. *Trends Immunol*, 28, 66-73.
- UNGERER, M., ROSPORT, K., BÜLTMANN, A., PIECHATZEK, R., UHLAND, K., SCHLIEPER, P., GAWAZ, M. & MÜNCH, G. 2011. Novel antiplatelet drug revacept (Dimeric Glycoprotein VI-Fc) specifically and efficiently inhibited collagen-induced platelet aggregation without affecting general hemostasis in humans. *Circulation*, 123, 1891-9.
- VÄLIAHO, J., SMITH, C. I. & VIHINEN, M. 2006. BTKbase: the mutation database for X-linked agammaglobulinemia. *Hum Mutat*, 27, 1209-17.
- VALLANCE, T. M., ZEUNER, M.-T., WILLIAMS, H. F., WIDERA, D. & VAIYAPURI, S. 2017. Toll-Like Receptor 4 Signalling and Its Impact on Platelet Function, Thrombosis, and Haemostasis. *Mediators of inflammation*, 2017, 9605894-9605894.
- VALLES, J., SANTOS, M., AZNAR, J., MARCUS, A., MARTINEZ-SALES, V., PORTOLES, M., BROEKMAN, M. & SAFIER, L. 1991. Erythrocytes metabolically enhance collagen-induced platelet responsiveness via increased thromboxane production, adenosine diphosphate release, and recruitment. *Blood*, 78, 154-162.
- VARGA-SZABO, D., BRAUN, A. & NIESWANDT, B. 2009. Calcium signaling in platelets. *J Thromb Haemost*, 7, 1057-66.
- VARMA, R., CAMPI, G., YOKOSUKA, T., SAITO, T. & DUSTIN, M. L. 2006. T cell receptor-proximal signals are sustained in peripheral microclusters and terminated in the central supramolecular activation cluster. *Immunity*, 25, 117-127.
- VÁRNAI, P., ROTHER, K. I. & BALLA, T. 1999. Phosphatidylinositol 3-kinase-dependent membrane association of the Bruton's tyrosine kinase pleckstrin homology domain visualized in single living cells. *J Biol Chem*, 274, 10983-9.
- VIHINEN, M., IWATA, T., KINNON, C., KWAN, S. P., OCHS, H. D., VORECHOVSKÝ, I. & SMITH, C. I. 1996. BTKbase, mutation database for X-linked agammaglobulinemia (XLA). *Nucleic Acids Research*, 24, 160-165.
- VIHINEN, M., NILSSON, L. & SMITH, C. I. E. 1994a. Tec homology (TH) adjacent to the PH domain. *FEBS Letters*, 350, 263-265.
- VIHINEN, M., VETRIE, D., MANIAR, H. S., OCHS, H. D., ZHU, Q., VORECHOVSKÝ, I., WEBSTER, A. D., NOTARANGELO, L. D., NILSSON, L. & SOWADSKI, J. M. 1994b. Structural basis for chromosome X-linked agammaglobulinemia: a tyrosine kinase disease. *Proceedings of the National Academy of Sciences of the United States of America*, 91, 12803-12807.
- WADOWSKI, P. P., EICHELBERGER, B., KOPP, C. W., PULTAR, J., SEIDINGER, D., KOPPENSTEINER, R., LANG, I. M., PANZER, S. & GREMMEL, T. 2017. Disaggregation Following Agonist-Induced Platelet Activation in Patients on Dual Antiplatelet Therapy. *Journal of cardiovascular translational research*, 10, 359-367.
- WAHL, M. I., FLUCKIGER, A. C., KATO, R. M., PARK, H., WITTE, O. N. & RAWLINGS, D. J. 1997. Phosphorylation of two regulatory tyrosine residues in

- the activation of Bruton's tyrosine kinase via alternative receptors. *Proc Natl Acad Sci U S A*, 94, 11526-33.
- WANG, B., WANG, F., HUANG, H. & ZHAO, Z. 2019a. A Novel DT40 Antibody Library for the Generation of Monoclonal Antibodies. *Virology*, 34, 641-647.
- WANG, J. & RICHARDS, D. A. 2012. Segregation of PIP2 and PIP3 into distinct nanoscale regions within the plasma membrane. *Biology open*, 1, 857-862.
- WANG, J., SOHN, H., SUN, G., MILNER, J. D. & PIERCE, S. K. 2014. The autoinhibitory C-terminal SH2 domain of phospholipase C- γ 2 stabilizes B cell receptor signalosome assembly. *Sci Signal*, 7, ra89.
- WANG, Q., PECHERSKY, Y., SAGAWA, S., PAN, A. C. & SHAW, D. E. 2019b. Structural mechanism for Bruton's tyrosine kinase activation at the cell membrane. *Proceedings of the National Academy of Sciences of the United States of America*, 116, 9390-9399.
- WANG, Q., VOGAN, E. M., NOCKA, L. M., ROSEN, C. E., ZORN, J. A., HARRISON, S. C. & KURIYAN, J. 2015. Autoinhibition of Bruton's tyrosine kinase (Btk) and activation by soluble inositol hexakisphosphate. *Elife*, 4.
- WATANABE, D., HASHIMOTO, S., ISHIAI, M., MATSUSHITA, M., BABA, Y., KISHIMOTO, T., KUROSAKI, T. & TSUKADA, S. 2001. Four tyrosine residues in phospholipase C-gamma 2, identified as Btk-dependent phosphorylation sites, are required for B cell antigen receptor-coupled calcium signaling. *J Biol Chem*, 276, 38595-601.
- WATKINS, N. A., GUSNANTO, A., DE BONO, B., DE, S., MIRANDA-SAAVEDRA, D., HARDIE, D. L., ANGENENT, W. G., ATTWOOD, A. P., ELLIS, P. D., ERBER, W., FOAD, N. S., GARNER, S. F., ISACKE, C. M., JOLLEY, J., KOCH, K., MACAULAY, I. C., MORLEY, S. L., RENDON, A., RICE, K. M., TAYLOR, N., THIJSSEN-TIMMER, D. C., TIJSSEN, M. R., VAN DER SCHOOT, C. E., WERNISCH, L., WINZER, T., DUDBRIDGE, F., BUCKLEY, C. D., LANGFORD, C. F., TEICHMANN, S., GOTTGENS, B. & OUWEHAND, W. H. 2009. A HaemAtlas: characterizing gene expression in differentiated human blood cells. *Blood*, 113, e1-9.
- WATSON, A. A., BROWN, J., HARLOS, K., EBLE, J. A., WALTER, T. S. & O'CALLAGHAN, C. A. 2007. The crystal structure and mutational binding analysis of the extracellular domain of the platelet-activating receptor CLEC-2. *J Biol Chem*, 282, 3165-72.
- WATSON, A. A., CHRISTOU, C. M., JAMES, J. R., FENTON-MAY, A. E., MONCAYO, G. E., MISTRY, A. R., DAVIS, S. J., GILBERT, R. J. C., CHAKERA, A. & O'CALLAGHAN, C. A. 2009. The Platelet Receptor CLEC-2 Is Active as a Dimer. *Biochemistry*, 48, 10988-10996.
- WATSON, A. A. & O'CALLAGHAN, C. A. 2011. Molecular analysis of the interaction of the snake venom rhodocytin with the platelet receptor CLEC-2. *Toxins (Basel)*, 3, 991-1003.
- WATSON, S. P., HERBERT, J. M. J. & POLLITT, A. Y. 2010. GPVI and CLEC-2 in hemostasis and vascular integrity. *Journal of Thrombosis and Haemostasis*, 8, 1456-1467.
- WEBER, M., TREANOR, B., DEPOIL, D., SHINOHARA, H., HARWOOD, N. E., HIKIDA, M., KUROSAKI, T. & BATISTA, F. D. 2008. Phospholipase C-gamma2 and Vav cooperate within signaling microclusters to propagate B cell spreading in response to membrane-bound antigen. *J Exp Med*, 205, 853-68.
- WHITTLE, B. J., MONCADA, S. & VANE, J. R. 1978. Comparison of the effects of prostacyclin (PGI₂), prostaglandin E₁ and D₂ on platelet aggregation in different species. *Prostaglandins*, 16, 373-88.
- WIST, M., MEIER, L., GUTMAN, O., HAAS, J., ENDRES, S., ZHOU, Y., RÖSLER, R., WIESE, S., STILGENBAUER, S., HOBEIKA, E., HENIS, Y. I., GIERSCHIK, P. & WALLISER, C. 2020. Noncatalytic Bruton's tyrosine kinase activates PLC γ (2)

- variants mediating ibrutinib resistance in human chronic lymphocytic leukemia cells. *J Biol Chem*, 295, 5717-5736.
- WOLTER, K. G., HSU, Y. T., SMITH, C. L., NECHUSHTAN, A., XI, X. G. & YOULE, R. J. 1997. Movement of Bax from the cytosol to mitochondria during apoptosis. *The Journal of cell biology*, 139, 1281-1292.
- WONEROW, P., OBERGFELL, A., WILDE, J. I., BOBE, R., ASAZUMA, N., BRDICKA, T., LEO, A., SCHRAVEN, B., HOREJSÍ, V., SHATTIL, S. J. & WATSON, S. P. 2002. Differential role of glycolipid-enriched membrane domains in glycoprotein VI- and integrin-mediated phospholipase C γ 2 regulation in platelets. *The Biochemical journal*, 364, 755-765.
- WOODS, M. L., KIVENS, W. J., ADELSMAN, M. A., QIU, Y., AUGUST, A. & SHIMIZU, Y. 2001. A novel function for the Tec family tyrosine kinase Itk in activation of beta 1 integrins by the T-cell receptor. *The EMBO journal*, 20, 1232-1244.
- WOODS, V. L., JR., WOLFF, L. E. & KELLER, D. M. 1986. Resting platelets contain a substantial centrally located pool of glycoprotein IIb-IIIa complex which may be accessible to some but not other extracellular proteins. *J Biol Chem*, 261, 15242-51.
- WOYACH, J. A., FURMAN, R. R., LIU, T.-M., OZER, H. G., ZAPATKA, M., RUPPERT, A. S., XUE, L., LI, D. H.-H., STEGGERDA, S. M., VERSELE, M., DAVE, S. S., ZHANG, J., YILMAZ, A. S., JAGLOWSKI, S. M., BLUM, K. A., LOZANSKI, A., LOZANSKI, G., JAMES, D. F., BARRIENTOS, J. C., LICHTER, P., STILGENBAUER, S., BUGGY, J. J., CHANG, B. Y., JOHNSON, A. J. & BYRD, J. C. 2014. Resistance mechanisms for the Bruton's tyrosine kinase inhibitor ibrutinib. *The New England journal of medicine*, 370, 2286-2294.
- WOYACH, J. A., RUPPERT, A. S., GUINN, D., LEHMAN, A., BLACHLY, J. S., LOZANSKI, A., HEEREMA, N. A., ZHAO, W., COLEMAN, J., JONES, D., ABRUZZO, L., GORDON, A., MANTEL, R., SMITH, L. L., MCWHORTER, S., DAVIS, M., DOONG, T.-J., NY, F., LUCAS, M., CHASE, W., JONES, J. A., FLYNN, J. M., MADDOCKS, K., ROGERS, K., JAGLOWSKI, S., ANDRITSOS, L. A., AWAN, F. T., BLUM, K. A., GREVER, M. R., LOZANSKI, G., JOHNSON, A. J. & BYRD, J. C. 2017. BTK(C481S)-Mediated Resistance to Ibrutinib in Chronic Lymphocytic Leukemia. *Journal of clinical oncology : official journal of the American Society of Clinical Oncology*, 35, 1437-1443.
- WU, J., ZHANG, M. & LIU, D. 2016. Acalabrutinib (ACP-196): a selective second-generation BTK inhibitor. *Journal of Hematology & Oncology*, 9, 21.
- WU, Y. 2015. Contact pathway of coagulation and inflammation. *Thrombosis journal*, 13, 17-17.
- XIAO, L., SALEM, J.-E., CLAUSS, S., HANLEY, A., BAPAT, A., HULSMANS, M., IWAMOTO, Y., WOJTKIEWICZ, G., CETINBAS, M., SCHLOSS, M. J., TEDESCHI, J., LEBRUN-VIGNES, B., LUNDBY, A., SADREYEV, R. I., MOSLEHI, J. J., NAHRENDORF, M., ELLINOR, P. T. & MILAN, D. J. 2020. Ibrutinib-Mediated Atrial Fibrillation Due to Inhibition of CSK. *Circulation*, 0.
- XIONG, J. P., STEHLE, T., ZHANG, R., JOACHIMIAK, A., FRECH, M., GOODMAN, S. L. & ARNAOUT, M. A. 2002. Crystal structure of the extracellular segment of integrin alpha Vbeta3 in complex with an Arg-Gly-Asp ligand. *Science*, 296, 151-5.
- YANG, W. & DESIDERIO, S. 1997. BAP-135, a target for Bruton's tyrosine kinase in response to B cell receptor engagement. *Proceedings of the National Academy of Sciences of the United States of America*, 94, 604-609.
- YANG, W., MALEK, S. N. & DESIDERIO, S. 1995. An SH3-binding site conserved in Bruton's tyrosine kinase and related tyrosine kinases mediates specific protein interactions in vitro and in vivo. *J Biol Chem*, 270, 20832-40.
- YARON, J. R., RAO, M. Y., GANGARAJU, S., ZHANG, L., KONG, X., SU, F., TIAN, Y., GLENN, H. L. & MELDRUM, D. R. 2016. The oxindole Syk inhibitor OXSI-2

- blocks nigericin-induced inflammasome signaling and pyroptosis independent of potassium efflux. *Biochem Biophys Res Commun*, 472, 545-50.
- ZAHN, A., JENNINGS, N., OUWEHAND, W. H. & ALLAIN, J. P. 2006. Hepatitis C virus interacts with human platelet glycoprotein VI. *J Gen Virol*, 87, 2243-2251.
- ZEILER, M., MOSER, M. & MANN, M. 2014. Copy number analysis of the murine platelet proteome spanning the complete abundance range. *Mol Cell Proteomics*, 13, 3435-45.
- ZEKE, A., LUKACS, M., LIM, W. A. & REMENYI, A. 2009. Scaffolds: interaction platforms for cellular signalling circuits. *Trends Cell Biol*, 19, 364-74.
- ZHANG, D., EBRAHIM, M., ADLER, K., BLANCHET, X., JAMASBI, J., MEGENS, R. T. A., UHLAND, K., UNGERER, M., MÜNCH, G., DECKMYN, H., WEBER, C., ELIA, N., LORENZ, R. & SIESS, W. 2020. Glycoprotein VI is not a Functional Platelet Receptor for Fibrin Formed in Plasma or Blood. *Thromb Haemost*, 120, 977-993.
- ZHANG, M. S., TRAN, P. M., WOLFF, A. J., TREMBLAY, M. M., FOSDICK, M. G. & HOUTMAN, J. C. D. 2018. Glycerol monolaurate induces filopodia formation by disrupting the association between LAT and SLP-76 microclusters. *Science Signaling*, 11, eaam9095.
- ZHANG, N., ZHI, H., CURTIS, B. R., RAO, S., JOBALIYA, C., PONCZ, M., FRENCH, D. L. & NEWMAN, P. J. 2016. CRISPR/Cas9-mediated conversion of human platelet alloantigen allotypes. *Blood*, 127, 675-680.
- ZHONG, Y., JOHNSON, A. J., BYRD, J. C. & DUBOVSKY, J. A. 2014. Targeting Interleukin-2-Inducible T-cell Kinase (ITK) in T-Cell Related Diseases. *Postdoc journal : a journal of postdoctoral research and postdoctoral affairs*, 2, 1-11.
- ZHOU, F., HU, J., MA, H., HARRISON, M. L. & GEHLEN, R. L. 2006. Nucleocytoplasmic trafficking of the Syk protein tyrosine kinase. *Molecular and cellular biology*, 26, 3478-3491.
- ZHOU, P., MA, B., XU, S., ZHANG, S., TANG, H., ZHU, S., XIAO, S., BEN, D. & XIA, Z. 2014. Knockdown of Burton's tyrosine kinase confers potent protection against sepsis-induced acute lung injury. *Cell Biochemistry and Biophysics*, 70, 1265-1275.
- ZWOLANEK, F., RIEDELBERGER, M., STOLZ, V., JENULL, S., ISTEL, F., KOPRULU, A. D., ELLMEIER, W. & KUCHLER, K. 2014. The non-receptor tyrosine kinase Tec controls assembly and activity of the noncanonical caspase-8 inflammasome. *PLoS Pathog*, 10, e1004525.